THE ROYAL INSTITUTE OF TECHNOLOGY

HIGH POWER ELECTRONICS

HVDC and SVC

Åke Ekström

June 1990

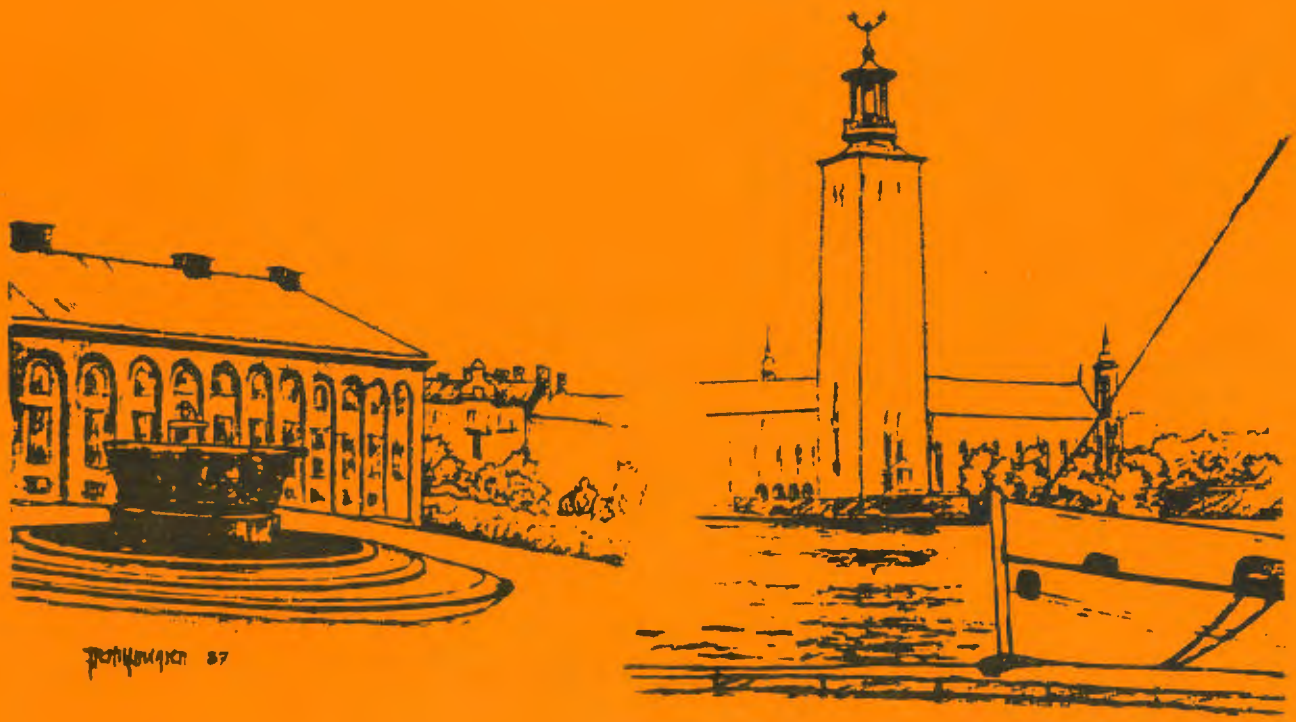

EKC – Electric Power Research Center

The Royal Institute of Technology
High Power Electronics
Teknikringen 33 – 35
S–100 44 STOCKHOLM

HIGH POWER ELECTRONICS
HVDC and SVC

CONTENTS

HIGH POWER ELECTRONICS

This text is based on a compendium in the Swedish language used for the course on "High Power Electronics" taught at the undergraduate level at the Royal Institute of Technology in Stockholm. The compendium treats power electronics applied for High Voltage Direct Current, HVDC, and Static Var Compensators, SVC. The technique used to date is mainly the line-commutated current-source converters for HVDC, thyristor switched capacitors, TSC, and thyristor controlled reactors, TCR, for SVC. However, it is expected that the forced-commutated converters will be used in the future both for HVDC and SVC, and therefore the basics of these types of converters have also been included in a final chapter.

Emphasis has been predominantly placed on the presentation of the basic theory for the line-commutated current-source converters and its control. The generation and filtering of the harmonics have also been treated in some detail. Although only the generation and filtering of harmonics for HVDC converter stations have been treated, this presentation is also to a great extent applicable to SVC-stations. This also applies to the thyristor valve, which is often designed in a similar way for both HVDC and SVC stations. The chapter overcurrents and overvoltages is, on the other hand, mainly applicable to HVDC converter stations, while the basic functions and the control of Static Var Compensators have been treated in a separate chapter.

The first chapter of the compendium provides a survey of the usage of, both, HVDC and SVC techniques and gives some illustrative information about the layout of typical HVDC and SVC stations as well. However, since the intention has been to concentrate on the theoretical basis for the techniques, the compendium provides only limited

information about the practical design of stations and equipment as well as of the protection systems.

Chapters 2 and 3 have partly been based on Ref. 2 and chapter 4 on Ref. 1. These two references are also highly recommended to be studied for a deeper understanding of the line-commutated converters and for the derivation of some of the basic equations presented in chapter 4 and 6. Further information about the Static Var Compensators can be obtained in Ref. 4 which has been prepared by a CIGRÉ Working Group WG 38-01, TF 2.

REFERENCES

[1] Kimbark E.W. (1971)
Direct Current Transmission
John Wiley & Sons.

[2] Uhlman E. (1975)
Power Transmission by Direct Current.
Springer-Verlag.

[3] Shore N.L., Andersson G., Canelhas A.P. and
Asplund G. (1988)

A THREE-PULSE MODEL OF D.C. SIDE HARMONIC FLOW IN HVDC SYSTEMS. IEEE 88. SM 599-3

[4] Static Var Compensators
CIGRÉ (1986)
Program by WG 38-01, TF 2.

[5] Erik V. Persson
Calculation of transfer functions in gride-controlled convertor systems.
With special reference to h.v.d.c. transmissions
PROC. IEE Vol. 117 No. 5 May 1970

LIST OF SUBSCRIPTS

0	at no load
N	rated value
d	direct-current or voltage
i	ideal
L	line-side of transformer
v	valve-side of transformer
f	phase-voltages
h	phase-to-phase (line-to-line voltages)
g	ground-mode
p	pole-mode
n or υ	order of harmonic
1	fundamental component
m	maximum

LIST OF LETTER SYMBOLS

Capital letters (U,I) r.m.s. or dc values.
Small letters (u,i) instantaneous values.

$\hat{U}$	peak voltage values.
U_d	direct voltage (average value)
U_{di0}	ideal no-load direct voltage.
U_{dN}	rated direct voltage.
u_{a0}, u_{b0}, u_{c0}	instantaneous values of the phase source-voltages.
u_a, u_b, u_c	instantaneous values of the phase-voltages on the valve side of the converter transformers.
I_d	direct-current (average value), bridge current
i_d	instantaneous value of the bridge current.
i_a	instantaneous value of the current in the ac-phase a.
I_1	fundamental component (r.m.s. value) of the ac-current to the converter bridge.
α	firing angle (day angle)
γ	extinction angle (commutation margin)
u	angle of overlap.
σ	conduction interval for a thyristor controlled reactor.

λ	pulse-width modulation angle.
δ	firing delay of a forced-commutated voltage-source converter.
d_r	total resistive direct voltage drop in per cent or per unit referred to U_{dio}.
d_{rN}	rated value of d_r
d_x	total inductive direct voltage drop in per cent or per unit referred to U_{dio}.
d_{xN}	rated value of d_x
p	pulse number
q	commutation number
f	frequence of the ac-network
s	Laplace operation

1. APPLICATION AND LAYOUT OF HIGH VOLTAGE DIRECT CURRENT (HVDC) POWER TRANSMISSION SYSTEM AND STATIC VAR COMPENSATORS (SVC)

1.1 Introduction

The general aspects, including application and build up, of High Voltage Direct Current (HVDC) power transmission systems and Static Var Compensators (SVC) will be described in this chapter. The HVDC and SVC techniques have very much in common since thyristors are used as switching elements in both cases. The HVDC technique can be characterized as a technique for conversion and control of active power while the SVC technique is restricted to control of reactive power.

The HVDC technique will first be treated in this chapter followed by a section covering the SVC technique. The reason for this order is partly historical, as the HVDC technique is older, and partly depends on the fact that the SVC technique can be regarded as a compliment to the traditional ac-technique as well as to the HVDC technique.

The history of HVDC goes back to the first electrical power station of 1882 as further described in Ref. [1]. However, the real breakthrough came much later in 1954, when the 20 MW, 100 kV, HVDC cable transmission system between the mainland of Sweden and the island Gotland was commissioned. The convertor valve for this scheme was a mercury-arc valve. Nine more HVDC convertor schemes were later built with this technique. The last HVDC scheme using mercury arc-valves was the Nelson River Bipole T scheme in Manitoba with a rating of 1620 MW and a voltage of ± 450 kV. This scheme was commissioned in 1973. Further details about HVDC schemes with mercury-arc valves and the technique used are given in Ref. [1].

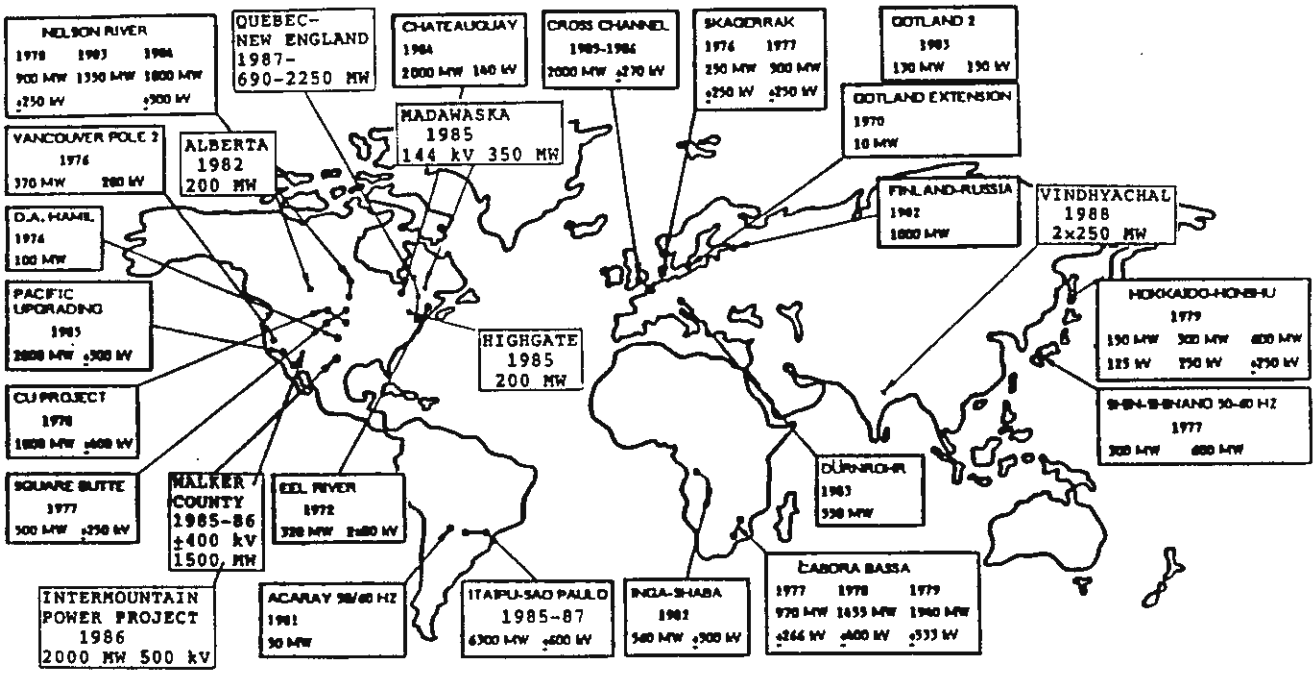

Figure 1-1 HVDC systems with thyristor valves.

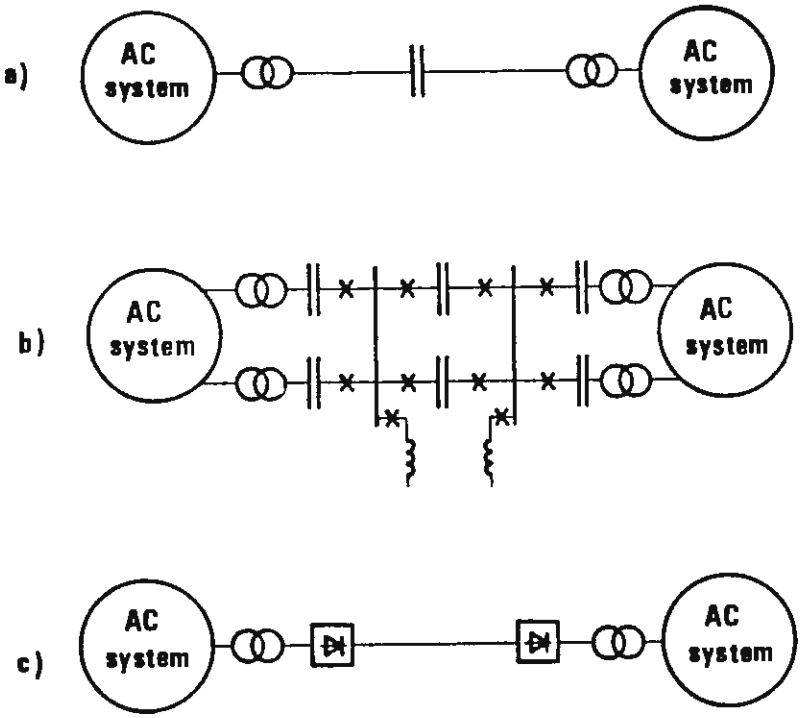

Figure 1-2 HVAC and HVDC transmission systems.
a) HVAC system with a single three-phase series compensated overhead line.
b) HVAC system using two parallel three-phase series compensated ovehead lines and two intermediate switching stations with shunt reactors.
c) HVDC transmission with a single overhead line.

At the end of 1960s the fast development of thyristor technology made it possible to design convertor valves for HVDC using thyristors. The thyristor valves had the advantage as compared to the mercury-arc valves that they did not suffer from the short-commings of occationally losing the capability of sustaining the reverse blocking capability resulting in arc-back currents.

The first HVDC convertors of thyristor valves were commissioned in 1970 (Gotland) and the first complete convertor station equipped with thyristor valves only was commissioned in 1972 (Eel River). Since then a large number of HVDC schemes using thyristor valves have been commissioned as illustrated in figure 1-1.

The modern SVC technique is also a result of the fast development of the semiconductor technology which started in the early 1970s. The SVC technique has since then been widely accepted as an effective way for reactive power and voltage control and has, for instance, almost completly replaced the use of synchronous compensators for electrical power systems. The application of SVC will mainly be restricted to electrical power transmission systems in this book, while, for instance, flicker-control in conjunction with arc-furnaces will not be discussed.

1.2 Electrical Power Transmission with HVDC

Comparison between HVAC and HVDC transmission systems

Figure 1-2 shows schematically simple transmission systems. Two electrical power systems are connected with one or two parallel HVAC-lines or a single HVDC line.

Figure 1-2a shows a case with a single HVAC-line. Often such a transmission line requires installation of

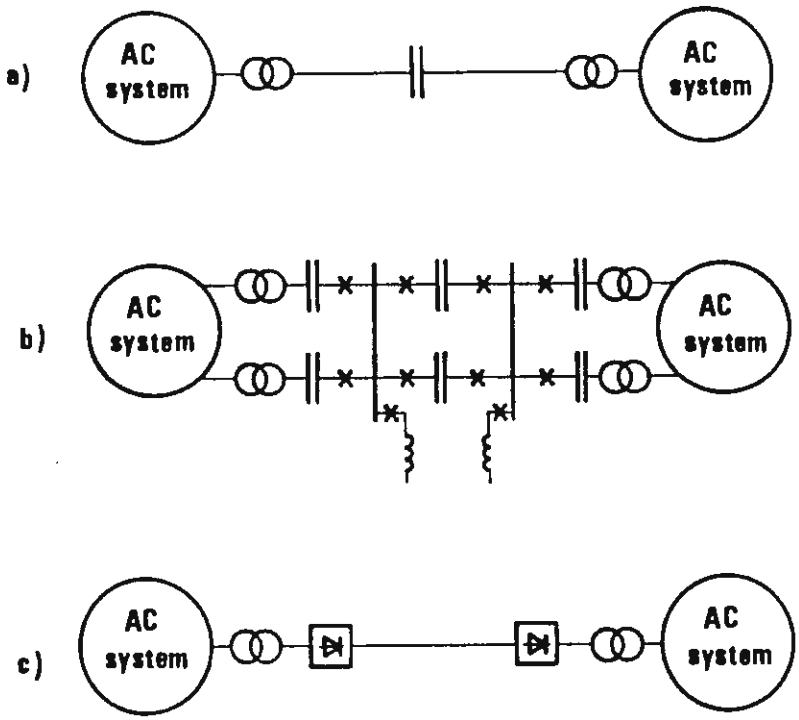

Figure 1-2 HVAC and HVDC transmission systems.
a) HVAC system with a single three-phase series compensated overhead line.
b) HVAC system using two parallel three-phase series compensated ovehead lines and two intermediate switching stations with shunt reactors.
c) HVDC transmission with a single overhead line.

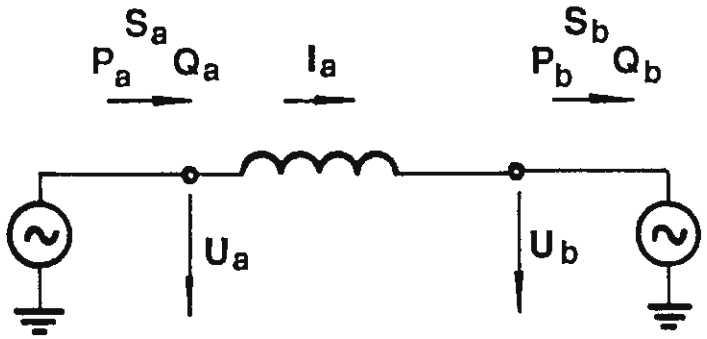

Figure 1-3 Two machines or AC-networks connected via an inductance.

transformers at both ends of the transmission line to step-up the voltage at in the sending end and to step-down at the receiving end. For most long lines with 400 kV or higher voltages the total series inductance usually has to be decreased by installation of series capacitors, as illustrated in figure 1-2a.

The importance of the total line inductance may be further illustrated by the simple two machines case as illustrated in figure 1-3. The two machines, which may represent two ac-networks, are connected together via a pure inductance, representing an overhead line. If the line is long the capacitive generation line charging has to be represented and the line may be represented by an equivalent π-link. The capacitive branches may then, in figure 1-3, be considered part of the machine representations.

In this case the line current which is the same at both ends in fig 1-3 can then be written in complex form for symmetrical voltage, as

$$\bar{I}_a = \frac{\bar{U}_a - \bar{U}_b}{j\sqrt{3} \cdot X} = -j\frac{\bar{U}_a - \bar{U}_b}{\sqrt{3} \cdot X} \qquad (1\text{-}1)$$

The line-to-line voltages at the two stations are denoted by U_a and U_b. It should be noted that we, here and in the following, if nothing else is stated, use the phase-position for the phase-voltage also for the line-to-line voltage. The line-to-line voltage is thus the phase voltage multiplied by $\sqrt{3}$.

The expression for the apparent power in station a in complex form will then be

$$\bar{S}_a = \sqrt{3} \cdot \bar{U}_a \cdot \bar{I}_a^* \qquad (1\text{-}2)$$

where $\bar{I}_a^*$ is conjugate of $\bar{I}_a$.

Insertion of $\bar{I}_a^*$, gives then:

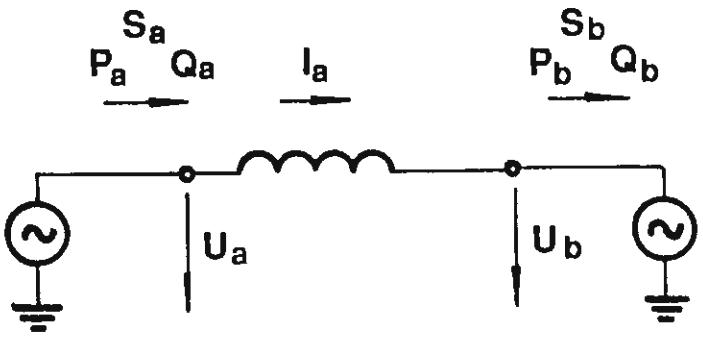

Figure 1-3 Two machines or AC-networks connected via an inductance.

$$\bar{I}_a^* = j \frac{\bar{U}_a^* - \bar{U}_b^*}{\sqrt{3} \cdot X}$$

$$\bar{U}_a \cdot \bar{U}_a^* = \left|\bar{U}_a\right|^2 ,$$

and

$$\bar{U}_a \cdot \bar{U}_b^* = U_a \cdot U_b \cdot \cos \delta + j\, U_a \cdot U_b \cdot \sin \delta_{ab}$$

where δ_{ab} is the phase angle between U_a and U_b. This gives

$$\bar{S}_a = \frac{U_a \cdot U_b \cdot \sin \delta_{ab}}{X} + j \frac{U_a \left(U_a - U_b \cdot \cos \delta_{ab}\right)}{X} \qquad (1\text{-}3)$$

Thus Eq. 1-3 represents active and reactive power components. For the generated active power in station a we obtain

$$P_a = P_b = \frac{U_a \cdot U_b \cdot \sin \delta_{ab}}{X} \qquad (1\text{-}4)$$

and for the generated reactive power in station a

$$Q_a = \frac{U_a \left(U_a - U_b \cdot \cos \delta_{ab}\right)}{X} \qquad (1\text{-}5)$$

The consumed reactive power in station b is calculated in the same way

to result:

$$Q_b = - \frac{U_b \left(U_b - U_a \cdot \cos \delta_{ab}\right)}{X} \qquad (1\text{-}6)$$

It should be noted that, as mentioned before, the capacitive generation of the line also has to be considered, which will give negative contribution to Q_a and positive contribution to Q_b.

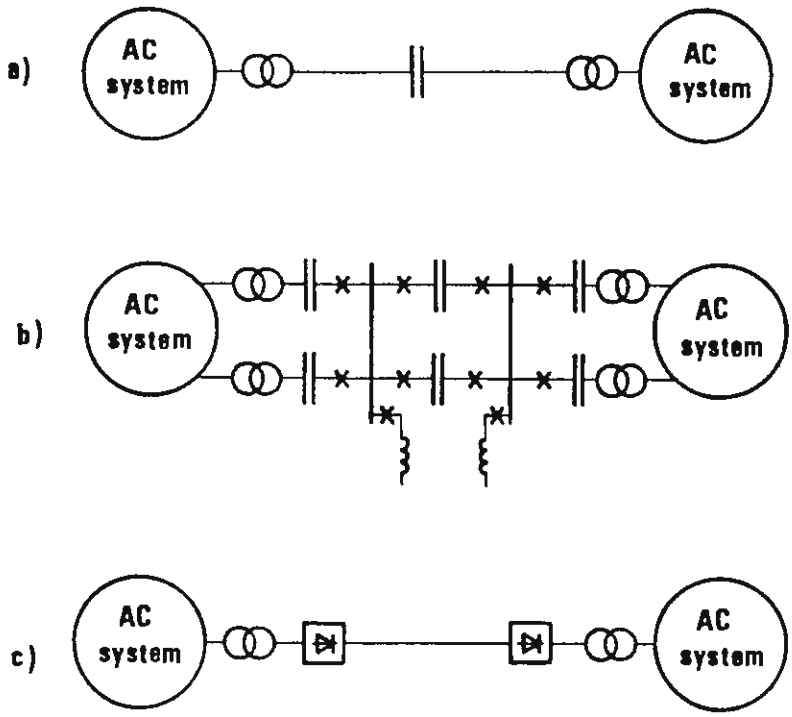

Figure 1-2 HVAC and HVDC transmission systems.
a) HVAC system with a single three-phase series compensated overhead line.
b) HVAC system using two parallel three-phase series compensated ovehead lines and two intermediate switching stations with shunt reactors.
c) HVDC transmission with a single overhead line.

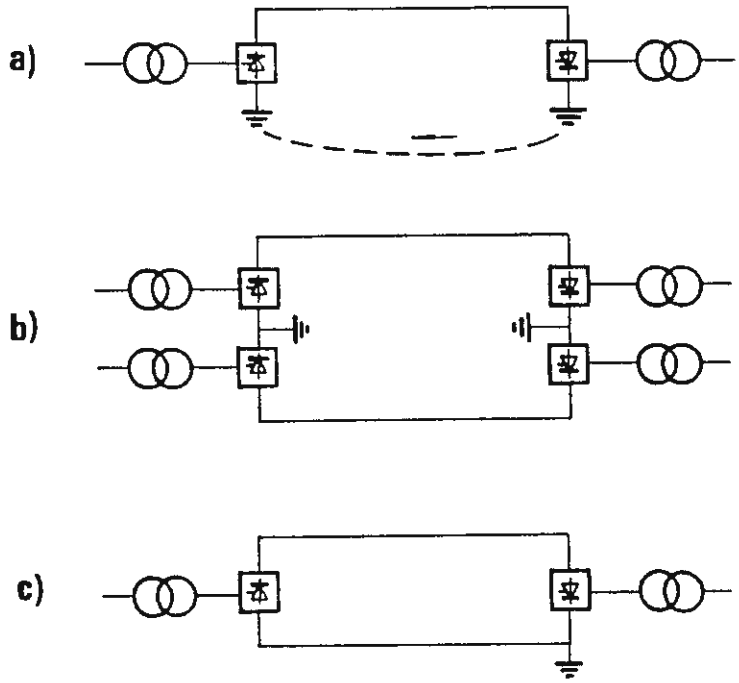

Figure 1-4 a) Monopolar HVDC transmission with earth return.
b) Bipolar HVDC transmission.
c) Monopolar HVDC transmission with metallic return.

From eq. 1-4 it is obvious that the transmitted active power is determined by the phase angle δ and the total reactance X. As the reactance X, for long lines, is mainly determined by the line reactance, the maximum transmitted power is approximately inversly proportional to the length of the line. Because of this it is common practice to reduce the inductance by the installation of capacitors connected in series for long overhead lines. For uncompensated overhead lines the length of the line is usually restricted to about 500 km. The maximum length can be increased to about 1500 km for compensated lines.

It is shown in fig 1-2b that two or more HVAC lines often are connected in parallel and split up in a number of sections with intermediate switching substations in order to increase the power transfer capacity and reliability.

A single line HVDC system, as illustrated in fig 1-2c, can either be built up of a monopolar line, as illustrated in fig 1-4a, or a bipolar line, as illustrated in fig 1-4b. When the HVDC line consists of a single conductor or a bundle conductor, as illustrated in fig 1-4a, the return current is flowing through earth. Since the earth current can have a tendency to flow in buried metallic structures, as in pipe lines, there is always a risk that earth currents can cause corrosion, if no special preventive actions are taken. Because of that monopolar operation with earth return is only permitted during short time periods in most countries. For this reason, and also to increase the power transfer capacity, HVDC lines are usually built as a bipolar transmission system that is illustrated in figure 1-4b. In case of failure of one pole power transmission can then continue on the other pole. To be able to operate for longer time periods in monopolar mode without earth return the second line conductor can be switched over to the other pole as illustrated in fig 1-4c. This operation mode is usually referred to as metallic-return operation.

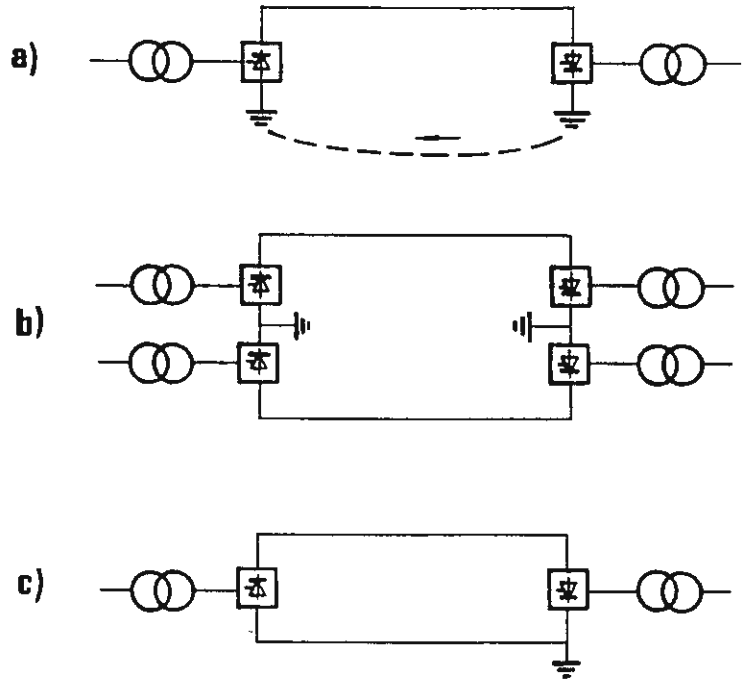

Figure 1-4 a) Monopolar HVDC transmission with earth return.
b) Bipolar HVDC transmission.
c) Monopolar HVDC transmission with metallic return.

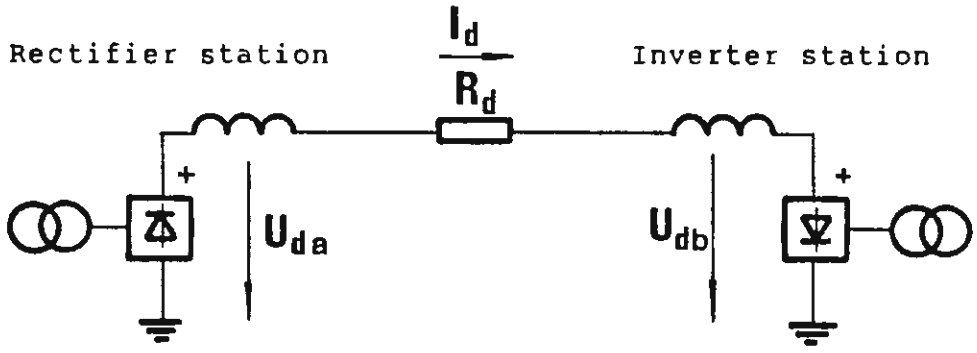

Figure 1-5 Monopolar HVDC transmission system.

From a reliability point of view a bipolar HVDC transmission can thus be considered to be built of two monopolar transmission systems and is regarded as being equivalent to a double ac line from a reliability point of view.

The two poles of a convertor station are usually built up in a similar way. Each station-pole consists of a number of current source line-commutated convertors in a two-way six pulse bridge connection. The bridges on the dc-side are connected in series and on the ac-side in parallel. What is actually meant by a line-commutated current source convertr will be further described in chapter 2. In chapter 3 the reasons for selecting the two-way six pulse bridge convertor for HVDC applications are given and its function and characteristics are further described in chapter 4.

As illustrated by the box-symbols with unidirectional thyristor elements in fig 1-4a, b, and c the direct current can only flow in one direction in the type of current source convertors used. On the other hand by means of firing angles it is possible to change the polarity of the voltage on the dc-side from a maximum positive to a maximum negative voltage. The relationship between the voltages on the dc-side and the ac-side is determined by the firing instants of the valves.

The polarities and notations of the dc-voltages and currents of a monopolar HVDC transmission system is illustrated in fig 1-5.

When the current and voltages have the same sign, with positive reference direction according to fig 1-5, the power will be transmitted from the ac-side to the dc-side. The convertor station is then said to operate in the rectifier mode. By delaying the firing instants the

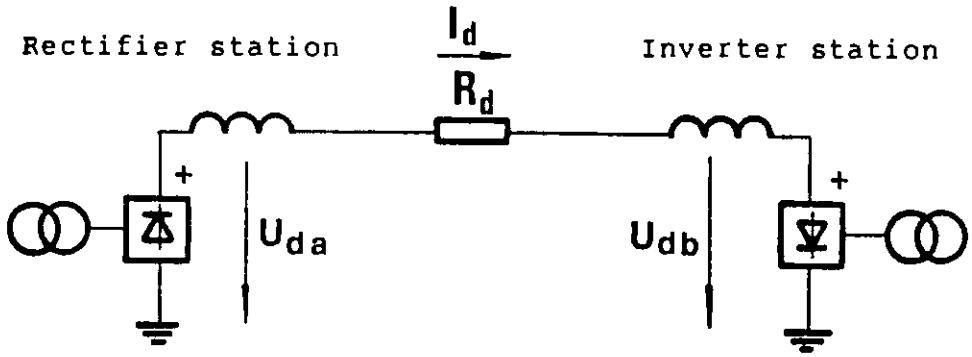

Figure 1-5 Monopolar HVDC transmission system.

polarity of the voltage on the dc-side can be reversed and the power will then be transmitted from the dc-side to the ac-side. The convertor station is then operating in the inverter mode. The direct voltage of the convertors can be changed very fast by firing-control, i.e., control of the firing instants of the valves. The voltage can be changed from a maximum positive value to a maximum negative value. The direction of the direct current can on the other hand normally not be changed for a current source convertor.

The direct current I_d is determined by the difference between the direct voltages of the rectifier (U_{da}) and inverter stations (U_{db}) and the resistence R_d according to the following relationship.

$$I_d = \frac{U_{da} - U_{db}}{R_d} \quad . \tag{1-7}$$

The active power in the inverter station is

$$P_{db} = \frac{U_{db}\,(U_{da} - U_{db})}{R_d} \quad . \tag{1-8}$$

Usually the resistive voltage drop along the dc-line is only a few percent of the rated line voltage, hence large changes of the transmitted power can be achieved by small changes of the difference voltage. Large current changes can for instance, be achieved by a small change of the voltage in the rectifier station if the direct voltage in the inverter station is assumed to be constant. A comparison between equations 1-8 and 1-4 shows that the same does not apply to an ac-transmission, for which the transmitted power is primarily determined by the phase angle difference and not by the difference of the amplitudes of the voltages for the two stations.

From eq. 1-4 it is obvious that the maximum transmitted power for an ac-transmission is inversly proportional to

the line reactance X. Because of that the maximum line length is usually, as mentioned before, limited to about 500 km for an un-compensated ac-line. The line reactance is often reduced by the connection of capacitors in series, which makes it possible to increase the line length. Another alternative is to control the voltage at the intermediate switching station using Static Var Compensators, SVC, as described in section 1-5. However, no similar limitations exist for an HVDC transmission since the total line voltage drop also for very long lines will be limited to acceptable low levels, simply by means of conductors size and their bundling.

As mentioned above the transmitted active power on ac-lines is determined by the phase angle difference betweeen the two connected ac-systems. The transmitted power can thus be considered to be selfcontrolled, which might be considered to be a merit for an ac-transmission line as compared to a dc-line. On the other hand a similar control can also be arranged for a HVDC transmission system based upon measurement of the difference of the phase angle between the two connected ac-systems. It is also rather easy to implement a more sophisticated control system for the HVDC transmission system than automatically achieved for the ac-system. Limitations of the transmitted power to the maximum overload capacity of the dc-link can then also be included. For the ac-link, on the other hand, it is always a risk that the link can be thermally overloaded resulting in the need of line to be disconnected or that the phase-difference will be too large resulting in an increase in phase-angle which will give reduced power transmitted and cause an unstable system.

The fast control of the HVDC transmission can also be used to improve the stability of the connected ac-system or systems as will be described later.

As the transmitted power in the dc-system is independent of the frequencies of the ac-systems or the phase-angle differences, HVDC systems can be used to interconnect two ac-systems having different frequencies or operating at the same frequency but without being synchronized. This is the most usual case, e.g., such as the HVDC links between Sweden-Denmark, Norway-Denmark, England-France, Canada-USA, etc.

When an HVDC link is connecting two ac-systems which are not synchronized and the power rating on the link is sufficiently large the HVDC power transmission can also be used for the frequency control of one of the ac-systems. This is for instance the case for the HVDC link to Gotland, in which case the frequency on the Gotland island is controlled by the power transmitted on the HVDC link.

For short HVAC lines reactive power is transferred from the station having the highest voltage to the station having the lowest voltage as illustrated by the equations 1-5 and 1-6. For long HVAC lines the generation or consumption of reactive power can create serious problems. At a certain transmitted power level which are referred to as the natural load, the consumption of reactive power by the series line reactance is exactly balanced by the generation of reactive power by the shunt capacitance of the line. However, the actual load is very seldom equal to the natural load, the maximum thermal load is much larger than the natural load, and the actual load varies quite widely. The ac-line will consume more reactive power when the load is larger than the natural load and generate more reactive power when the load is lower than the natural load. The amount of reactive power consumed or generated is determined by the length of the line and the level of ac-line loading.

In contrast to the ac-line the dc-line itself neither

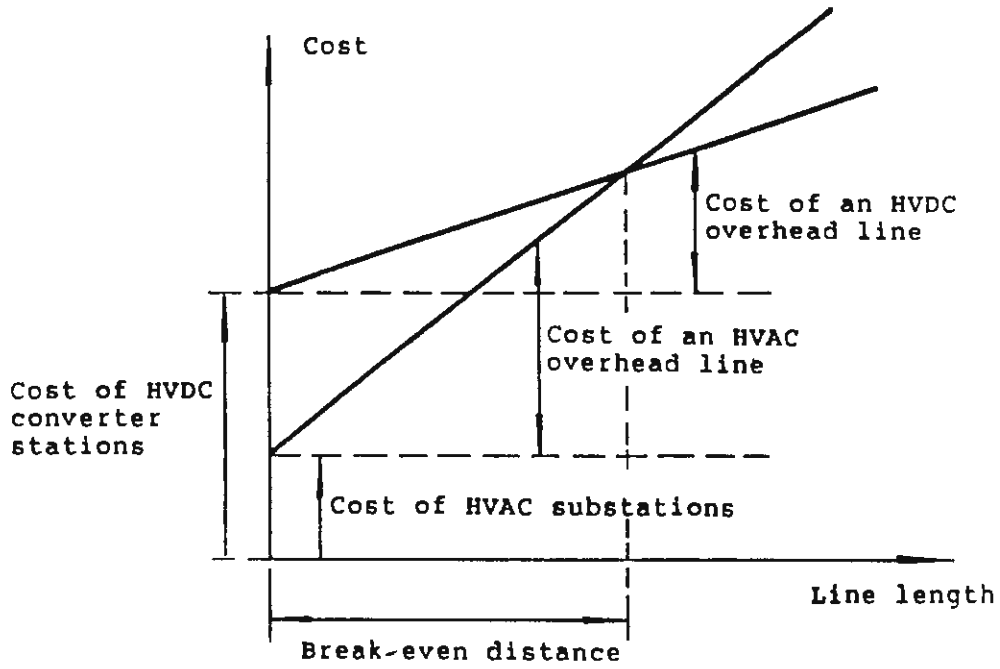

Figure 1-6 Costs of an HVDC and an HVAC transmission system as a function of the line length.

consume nor produces reactive power. However, line-commutated convertors always consume reactive power, which in practice generally amounts to about 50 percent of the active power transmitted. This is normally compensated for by the ac-filters and the shunt capacitor banks connected in each station.

We can thus conclude that reactive power control is needed, both, for ac- and dc-power stations and that in both cases a surplus of reactive power might be achieved at a lower real power level and a shortage of reactive power at a higher real power level. However, one major difference is that the line length has no influence upon the consumption of reactive power for the HVDC stations, while it is very essential for HVAC transmissions.

For HVAC cable transmissions the generation of reactive power can even for even short distances be so high that shunt reactors distributed along the lines are needed for the compensation of the generated reactive power. For sea-cables, for which it is difficult to connect shunt reactors, the maximum practical length limit for an ac-cable is about 30 km. No similar limit exists for HVDC cables.

The costs per km or mile for an overhead line or cable is lower for HVDC than for HVAC. However, as the terminal costs are considerably higher for HVDC than for HVAC a certain line length, or break even distance is needed to get lower total costs for an HVDC line than for a corresponding HVAC line. This is further illustrated in fig. 1-6. For overhead lines the break-even distance is in the range of 500 - 1000 km, while for sea-cables it is in the range of 20 to 50 km.

For the choice between HVDC and HVAC a number of other factors beside minimum line lengts and terminal costs, also

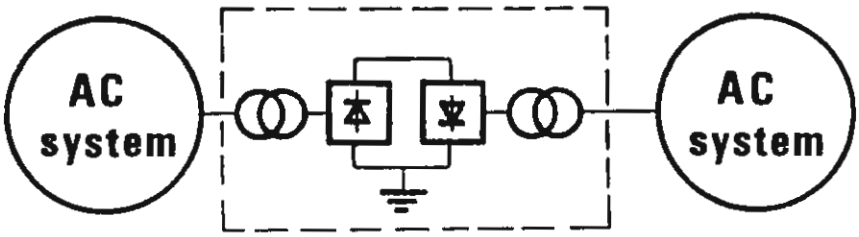

Figure 1-7 HVDC back-to-back station.

have to be considered. The possibility of connecting a ac-network, which is not synchronized or operating at different frequencies, has previously been mentioned as reasons for the selection of HVDC. HVDC has also been selected for cases where no lines are needed. As illustrated in fig. 1-7 two ac-systems may be connected together with a so called back-to-back station. Two convertors are then located in the same station, one connected to one ac-system and operating in rectifier mode and the other connected to the other ac-system and operating in inverter mode.

It should be noticed that connection of two ac-networks with an HVDC link does not increase the short-circuit capacity of the ac-network. This has sometimes been considered as an advantage of a DC connection as compared to an AC connection. However, in reality this has not been a decisive factor for the selection of HVDC. On the contrary, the fact that a certain short circuit capacity in the connected ac-network is needed for proper operation of the convertors and limitation of overvoltages has mostly been more decisive. In many of the earlier installations with weak ac-networks synchronous compensators were installed to increase the short circuit capacity of the ac-networks and at the same time generate reactive power. Today Static Var Compensators (SVC) or improved control of the HVDC convertors can often offer a less expensive alternative.

In evaluating a HVDC transmission system with a AC transmission system the reliability and availability aspects have become more and more important. Through advanced technology, simplifications, and improvements of convertor stations the reliability and availability have steadily improved to such an extent that a bipolar HVDC transmission line is properly compared with a double AC transmission line.

An important factor with regard to transmission capacity during emergency condition is the fact that today a high overload capacity can be achieved for the convertor at a marginal cost increase. This especially applies to the overload capacity of the thyristor valves. The temporary overload capacity of the IPP HVDC transmission line in USA for electrical power transmission to Los Angeles can be taken as a typical example. For this HVDC transmission the convertors have been designed with an overload capacity permitting the load to be temporarily raised to twice the rated load on one pole in case of a failure of the other pole. After six seconds the load has to be ramped down to a steady state overload capacity of 50%.

The advantages of HVDC as compared to HVAC can be summarized as follows:

- Larger power transfer capacity with practically no limitation in transmission distance.

- The earth can be used at least temporarily for the return current, allowing each pole to be operated independently of the other pole. A bipolar HVDC line can be considered equivalent to a double ac-line rising single tower construction from reliability point of view.

- Power can be transmitted between two ac-systems operating at different frequencies or at the same frequency but without being synchronized.

- The transmitted active power can be controlled in a fast and flexible way.

- The dc-line itself does not generate or consume reactive power except for the reactive power consumption of line

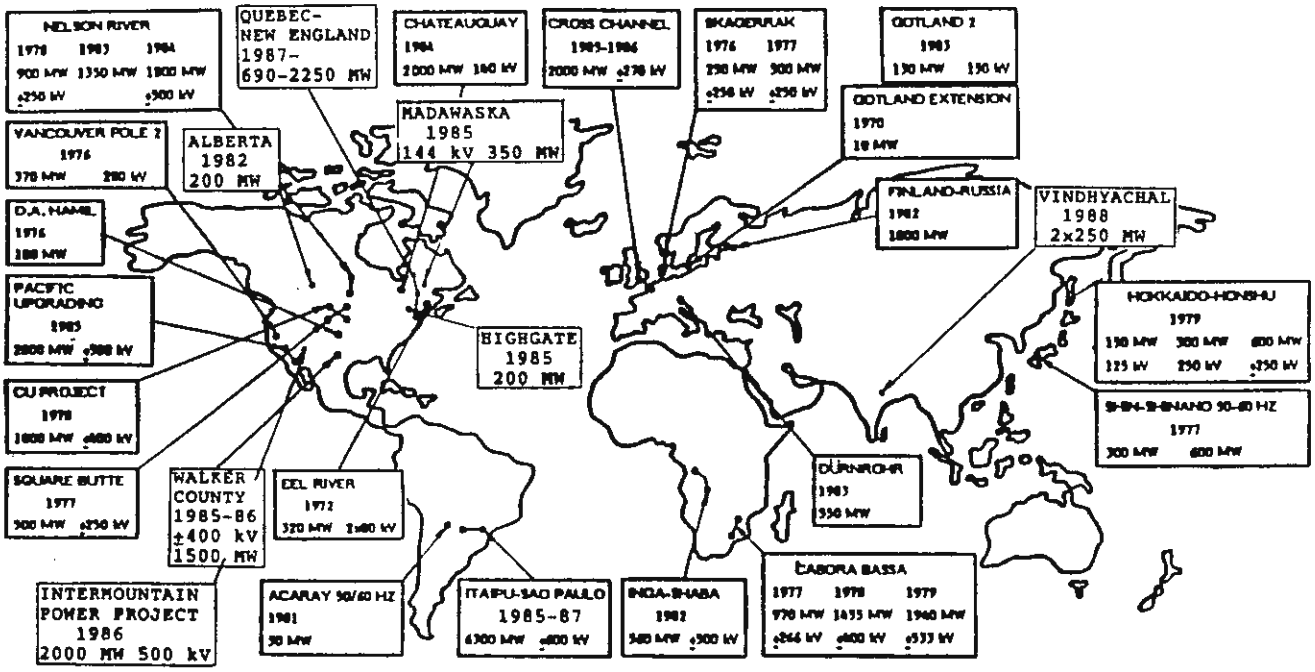

Figure 1-1 HVDC systems with thyristor valves.

commutated convertors. This means that the need for reactive power consumption is independent from the length of the line. For ac-cables the reactive power generation per line length sets a practical limit for the maximum line length.

- The costs for overhead lines and cables per line length are less for dc than for ac.

The greatest disadvantage of an HVDC transmission as compared to an HVAC transmission is the higher cost of the terminal equipment, especially the costs of the convertor and the losses in convertors. Transformers are usually needed both for HVDC and HVAC transmission, but for HVAC transmissions more simple transformers, e.g., auto-connected transformers can mostly be used. For HVDC the valves cause additional costs as well, since the filters are needed to short circuit the harmonics generated both on the ac- and the dc-sides of the convertor bridge.

Considering the above listed advantages and disadvantages HVDC transmissions have turned out to be a good alternative, especially for the following cases:

- power transmission with overhead lines over very long distances and for long sea cable transmissions.

- power transmission between ac-network operating at different frequencies or at the same frequency but without being synchronized.

- the special capability of fast and flexible control for HVDC has during recent years turned out to be an increasingly more essential factor in the choice between ac and dc.

Figure 1-1 gives a survey of existing HVDC transmission

systems in the world built up using thyristor valves.

Multiterminal HVDC transmissions

The listed HVDC transmission systems in figure 1-1 are all two terminal transmission systems. For a two terminal HVDC transmission with only one rectifier terminal and one inverter terminal per pole, no breakers are needed on the dc-side, as the current can, if needed, be reduced to zero by the firing control of the convorters. The dc-circuit can then be opened with fast operating disconnectors.

The possibility of building HVDC systems with more than two terminals has been discussed and studied since the first two terminal HVDC link to Gotland was commissioned in 1954. Until the 1970s it was argued that the availability of HVDC breakers, which could break the direct current, was required to be able to build HVDC multiterminal systems. During the 1970s different types of HVDC breakers were built and tested. Most concepts were based on the use of conventional AC breakers combined with capacitors and arresters for the dissipation of energy. However, extensive studies performed on simulators have shown that multiterminal systems of moderate size can also be built without the use of breakers having a capability to break direct currents, as the current can be controlled to zero by the convertors.

The real limiting factor, which until recently has prevented the use of multiterminal HVDC system is the high costs of the convertor terminals. At present, 1991, one multiterminal system is in operation having a 50 MW tapping station on the Corsica island on the 200 MW HVDC link between Italy and Sardinia. Another major multi-terminal HVDC system is under construction in North-America for the transmission of power between Canada and USA, the Quebeck-New England transmission system.

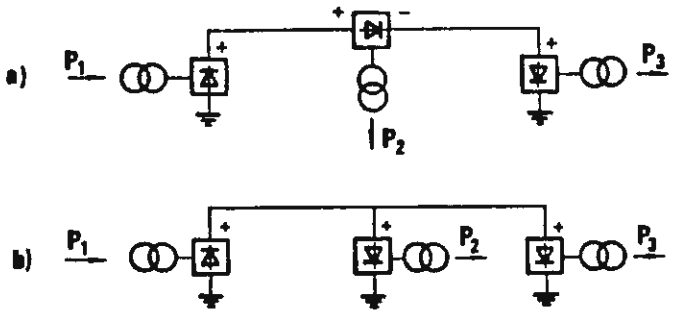

Figure 1-8 HVDC multiterminal system with three converter stations.
a) Converter stations connected in series on the dc-side.
b) Converter stations connected in parallel on the dc-side.

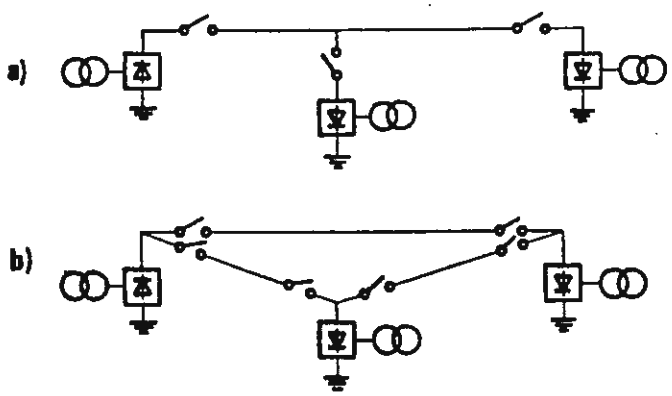

Figure 1-9 HVDC multiterminal system with three converter stations.
a) Radial network.
b) Meshed network.

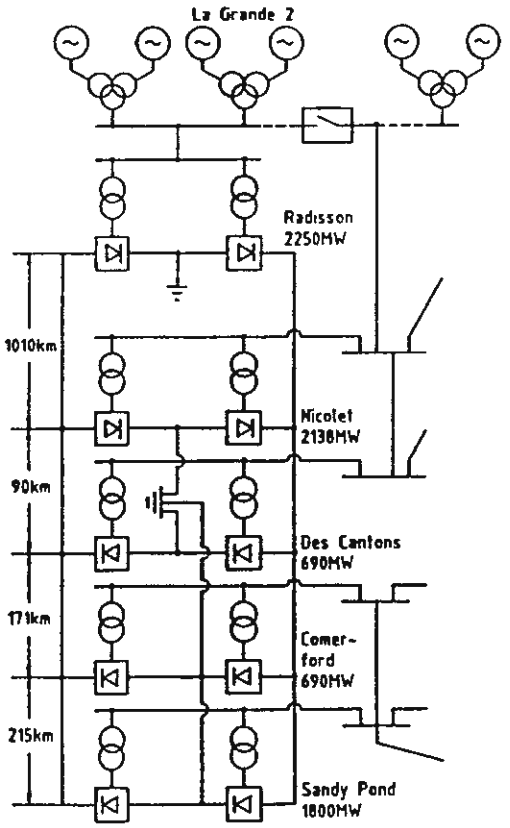

Figure 1-10 Quebec-New England multiterminal HVDC system.

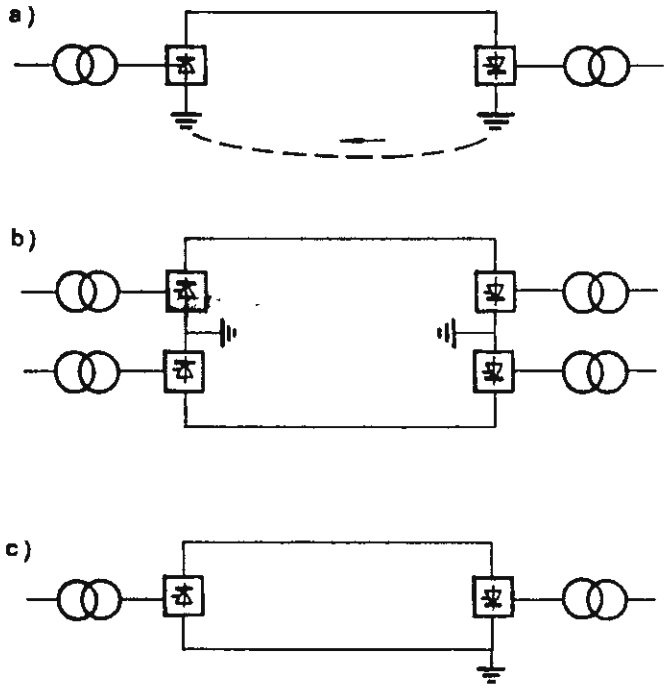

Figure 1-4 a) Monopolar HVDC transmission with earth return.
b) Bipolar HVDC transmission.
c) Monopolar HVDC transmission with metallic return.

In an HVDC multiterminal system the convertor stations can, on the dc-side, either be connected in series or in parallel, as illustrated in figure 1-8. In series connection the direct current is the same for all the convertor stations but the direct voltage will be different and will depend on the load distribution. This implies that this type of multiterminal system has been mainly considered for tapping of small amounts of power from a basically two terminal system.

The parallel connection on the dc-side, which makes it possible to keep the direct voltage in the whole system close to the rated voltages, is the system, that is most practical to use when the power to be tapped off is large or when the system consists of more than two terminals with power ratings of the same order of magnitudes. The tapping station at Corsica and multiterminal stations like the Quebeck-New England system. As shown in figure 1-9, the lines can either be connected as a radial network or in a mesh configuration. The advantage of the radial connection is that the current in the lines will be the same as the current in the convertor stations, which makes it possible to directly control the current in the line by the current control systems of the convertors. This reduces the need for HVDC circuit breakers. The meshed system will, on the other hand, result in greater flexibility to transmit power between the stations even in case of a failure of a single line, but at the same time increase the need for HVDC circuit breakers. The previously mentioned Quebeck-New England system, for which all the stations are located along the same route, is basically a multiterminal system of the radial type. Data and configuration of the system is illustrated in figure 1-10.

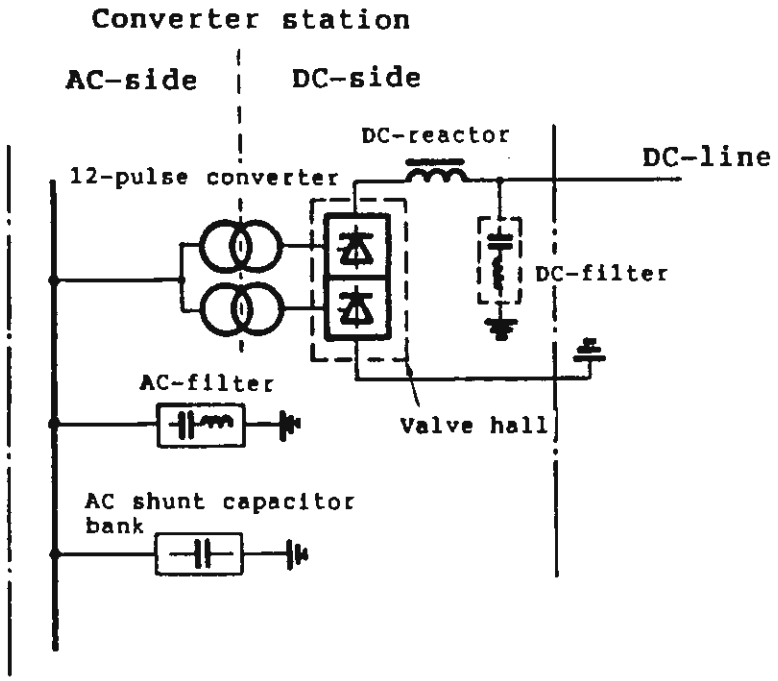

Figure 1-11 Main circuits of one pole of an HVDC converter station with one 12-pulse converter unit.

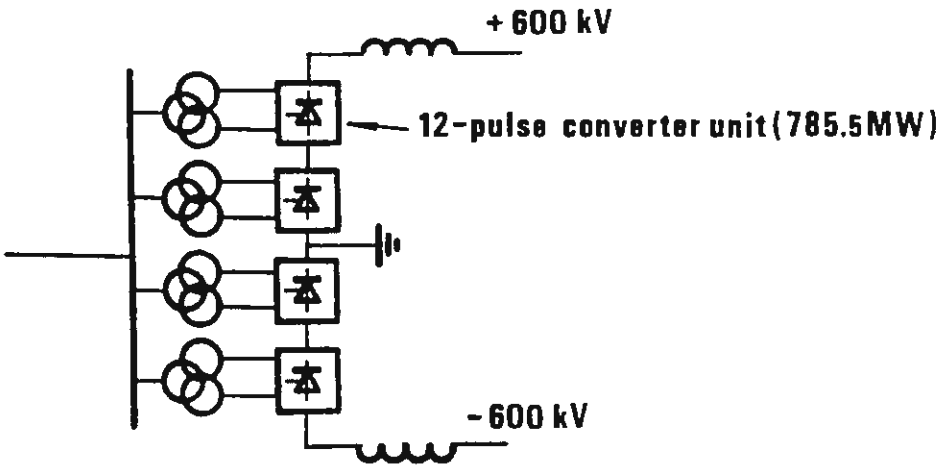

Figure 1-12 Connection of 12-pulse converter units for one bipole of the Itaipu converter station.

HVDC Convertor stations

An HVDC system is usually built up of two poles as mentioned previously and illustrated in the figures 1-4b and 1-10. The two poles are usually designed to be as independent of each other as possible in order to improve the reliability of the complete system. Each HVDC convertor station is, because of that, also split up in to two independent station poles. However some equipment is used jointly for the both poles, e.g., equipment for the connection to the earth electrode line, and to some extent filters, and equipment for reactive power supply on the ac-side.

Each station pole consists usually of at least one 12-pulse convertor for the full line voltage, as illustrated in figure 1-11. It is also possible to connect two converters in series on the dc-side in order to increase the voltage of the convertor station and its power rating. This is the case, for examples, the Itaipu HVDC system, for which each 12-pulse convertor has the rated direct voltage of 300 kV and a rated power of 787,5 MW, while the rating of the complete bipole is ±600 kV and 3150 MW, as illustrated in figure 1-12.

Each 12-pulse convertor consists of 12 thyristor valves built up as three quadruple valves, three convertor transformer(s), controls and protection equipment. Beside the convertor each station pole consists, as illustrated in figure 1-11 of a direct current reactor or smoothing reactor for reduction of ripples and transient changes of the direct current. The direct current reactor also reduces, together with the direct current filters, the harmonics generated which are injected into the dc-line.

The current harmonics generated into the ac-side are short-circuited by the ac-filters, which also together with

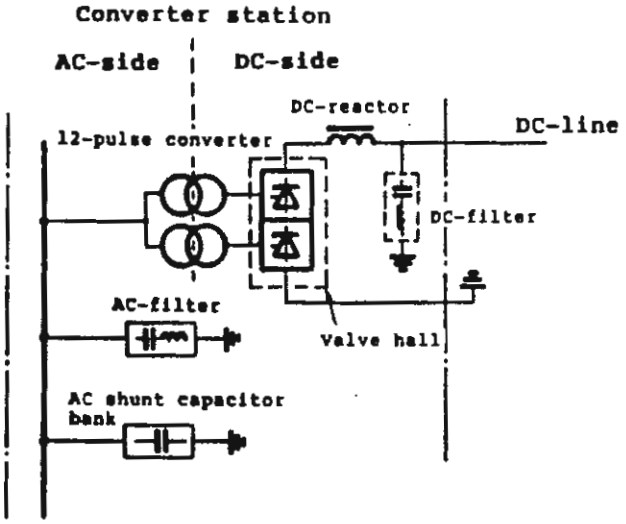

Figure 1-11 Main circuits of one pole of an HVDC converter station with one 12-pulse converter unit.

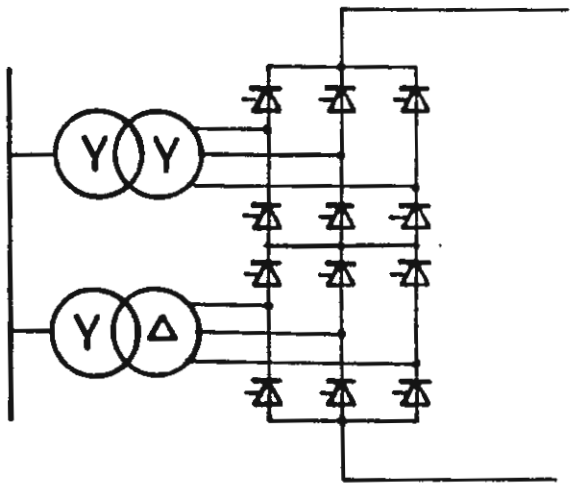

Figure 1-13 12-pulse converter.

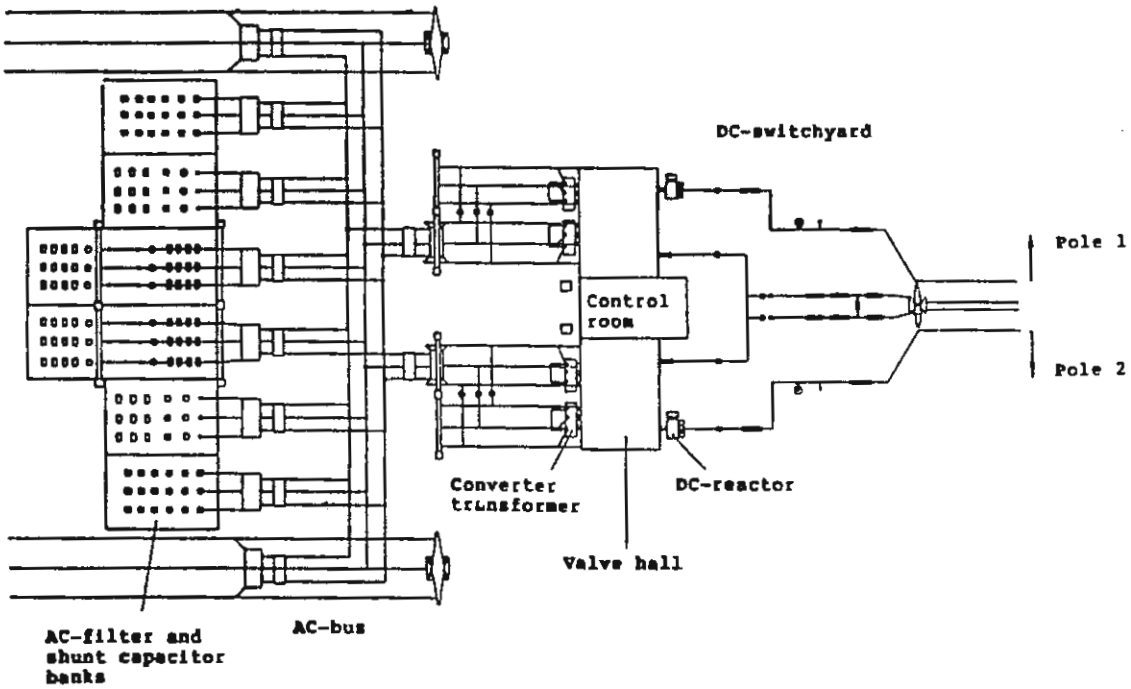

Figure 1-14 Typical layout of an HVDC converter station (500 kV dc and 400 kV ac).

shunt capacitor banks generate the necessary reactive power supply.

Beside the equipment illustrated above in figure 1-11 the convertor station pole also consists of arresters for overvoltage protection, different types of electrical switches, instrument transformers and control and protection equipment.

The equipment in a convertor station is usually referred to as main-circuits equipment, control and protection equipment and monitoring equipment.

The main circuits can be divided into an ac-side and a dc-side with the border line going right through the convertor transformer, as illustrated in figure 1-11. It should however be noted that, both, the valve windings and the valves, which belong to the dc-side, are stressed with, both, the alternating as well as direct voltages, while the ac-side equipment are only stressed with ac-voltages.

Each station pole usually consists of at least one 12-pulse convertor unit as previously mentioned. Each 12-pulse convertor unit is made up of two 6-pulse convertor units connected in series, as illustrated in figure 1-13. As further described in chapters, 3-6, the valves are connected in a two way bridge connection with one transformer Y-Y connected and the other Y-Δ connected to give a 30° phase shift between the feeding alternating voltages to balance out the 6-pulse harmonics.

The thyristor valves and the arresters for the direct protection of the valves are usually located indoors in a valve hall, but all other equipment is located outdoors in a dc-switchyard and an ac-switchyard. A control- and service building is often located between the valve halls for the two poles. Figure 1-14 demonstrates a typical

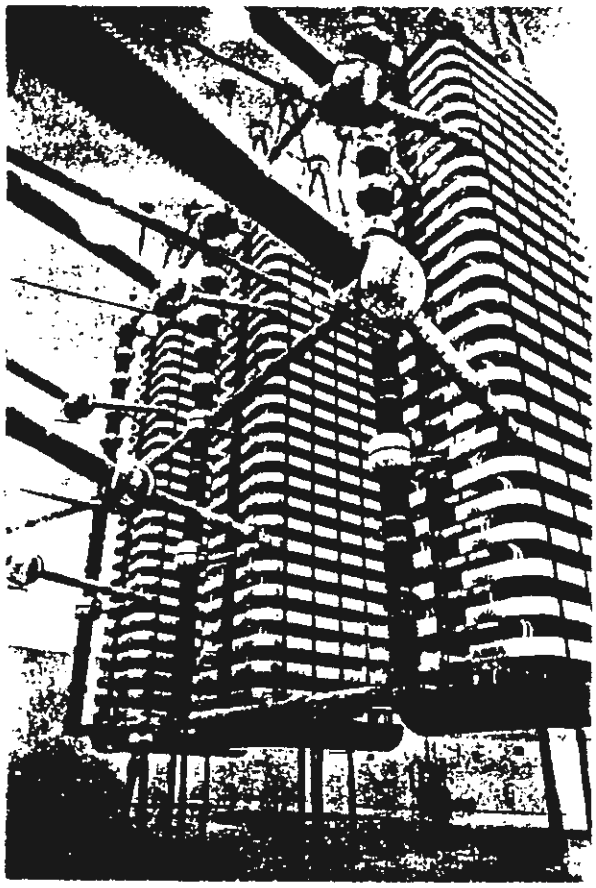

Figure 1-15 Valve hall with suspended water-cooled valves. Intermountain Power Project (IPP), 800 MW and 500 kV per pole.

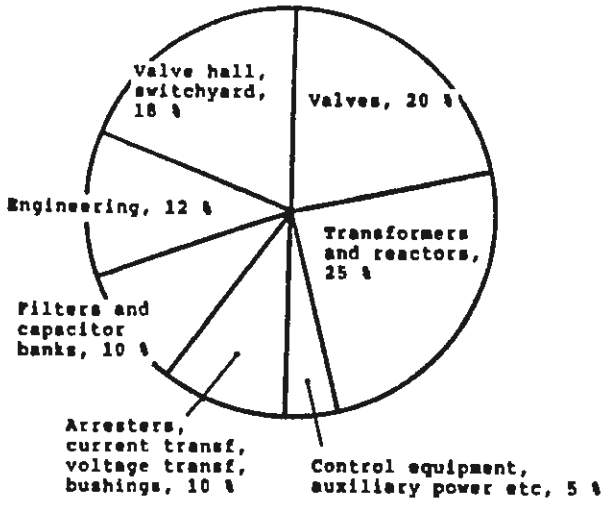

Figure 1-16 Typical distribution of costs of an HVDC converter station.

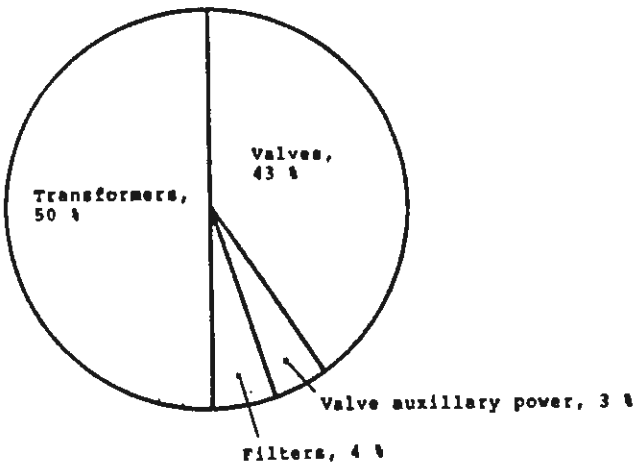

Figure 1-17 Distribution of the total power losses in an HVDC converter station.

layout of an HVDC convertor station (in this case it is shown without dc-filters). The function of the convertor bridge is described in more details in chapter 4, the function of the filters in chapter 6 and the function of overvoltage protection in chapter 8. The design and layout of the valves are further described in chapter 9. Figure 1-15 shows a view from a valve hall of water-cooled valves for a 12-pulse bridge rated 800 MW.

Costs of convertor stations

Figure 1-16 shows a typical distribution of the cost of a modern convertor station. As can be seen from figure 1-16 the cost for the convertor transformer and the dc-reactor amounts to about 25% of the total cost of the convertor station closely followed by the valves, which may cost between 15-25% of the station cost.

The cost for filters and shuntcapacitors amounts to about 10% and all other equipment: as arresters, bushings, switchers, etc., gives another 10%. The cost for control and protection equipment including auxiliary power generation, is usually smaller, say between 4-5% of the total cost.

Figure 1-17 shows the distribution of the total losses of a convertor station, which amounts to about 0.7 - 0.9% of rated real power. As can be seen from the figure the relationship between the losses in the transformer and the valves are almost the same as the relationship between the costs of the transformers and the valves. It should also be noted that thanks to the fast improved development of the semiconductor technology it is to be expected that both the costs and losses of valves will be further reduced. However, the same fast development cannot be expected for the transformers.

Convertor transformers

The convertor transformers are designed in a similar way as the transformers for ac systems. However, since the valve-windings are also stressed by a direct voltage component, the dielectric insulation, especially at the ends of the windings and at the connections to the bushings, has to be built up in a special way. It should be noted that the direct voltage distribution in the transformer is determined by the resistance while the ac voltage distribution is determined by the capacitance.

The major part of the direct voltage between the valve winding and network winding, and between valve winding and ground, will then be taken up by a barrier system of solid paper board insulation.

This implies that more solid insulation material has to be used in a convertor transformer and that the convertor transformer will be larger than an ac-transformer having the same power-rating. It should also be noted that the barrier system needed for insulation has to be designed so that the oil flow can give an efficient cooling of the windings.

Another difference between conventional ac transformers and convertor transformers is the fact that the current harmonics will cause additional losses in the windings and other parts of the transformers penetrated by the leakage fluxes. The difficulty in determining exactly the additional losses at testing shall especially be noted.

The convertor transformers can be built as single-phase or three-phase units with two or more windings on the same phase. Decisive factors in selecting the best alternative for a specific plant are transport limitations and whether spare unit are needed.

a)

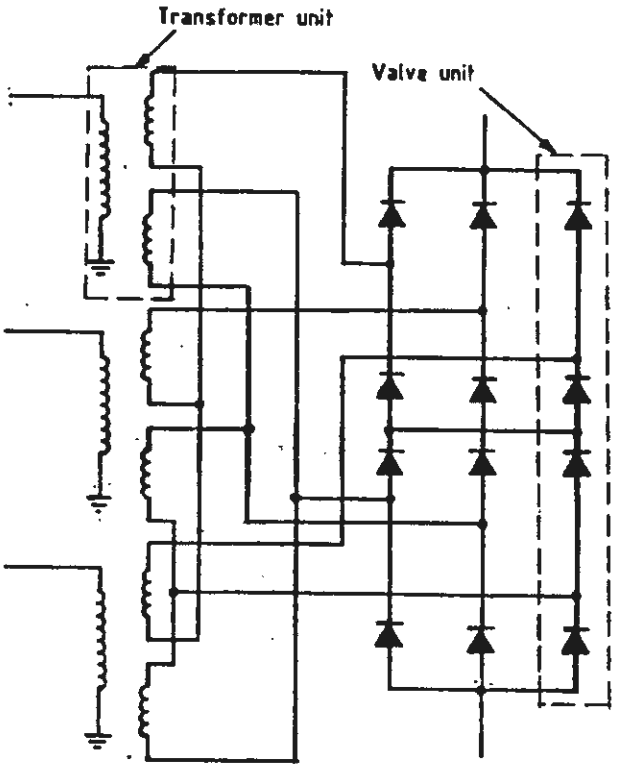

b)

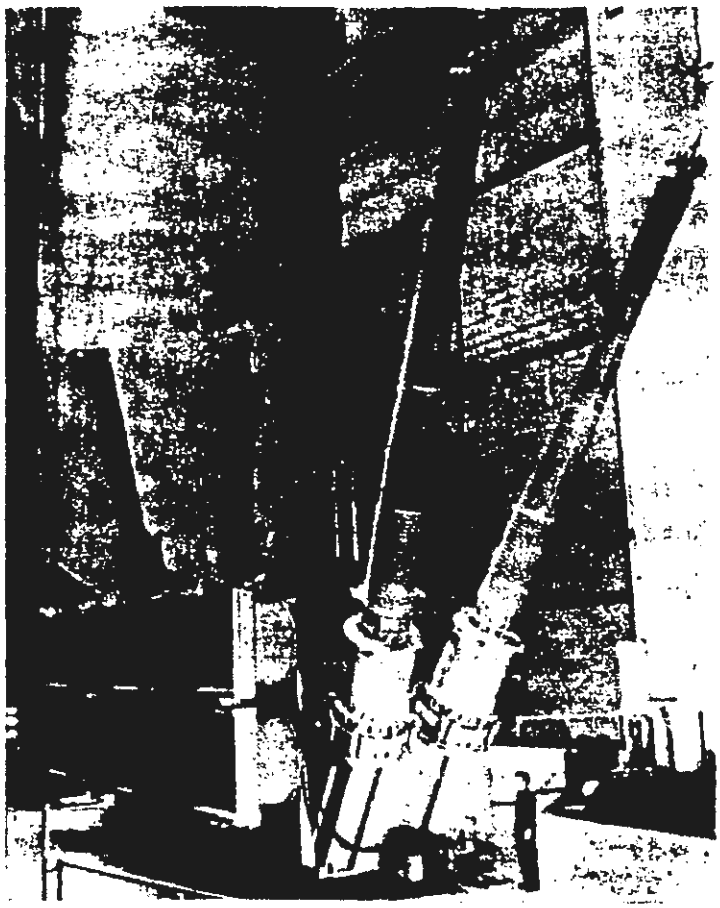

Figure 1-18 a) 12-pulse converter with three single-phase three-winding converter transformers and three quadruple valves.
b) Single-phase three-winding transformer for the Intermountain Power Project (IPP).

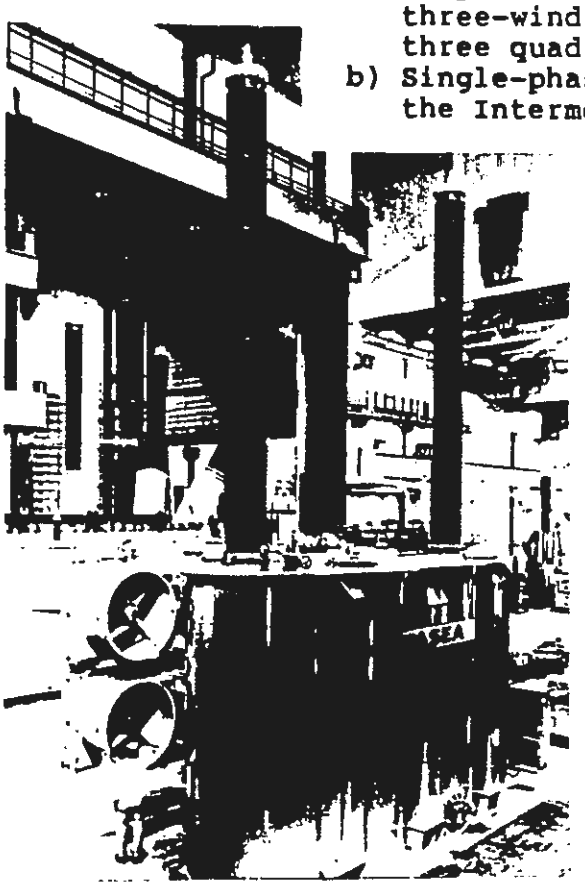

Figure 1-19 Oil immersed DC-reactor.

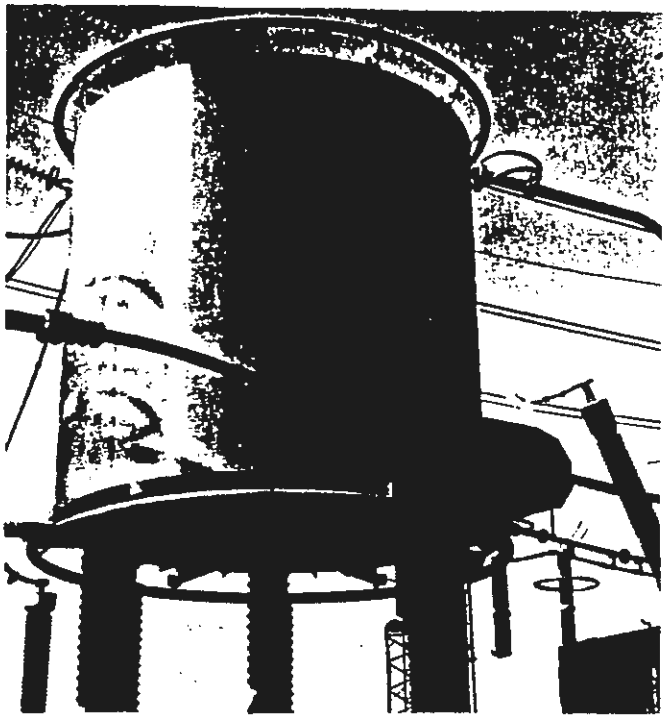

Figure 1-20 Air core DC-reactor.

As previously mentioned convertor stations are usually built up of 12-pulse units at present, with one six-pulse bridge being fed from a y-y connected transformer unit and the other bridge being fed from an Y-Δ connected unit. Both cases always have on ac-side Y grounded.

For small or medium sized convertor stations three-phase transformer units are usually chosen. The transformers are often placed close to the valve hall with the valve-winding bushings penetrating the wall of the valve hall.

For convertor stations of higher rating mostly single-phase, three windings transformer units are used connected according to figure 1-18a.

Figure 1-18b shows a picture of a convertor transformer for the IPP HVDC link in USA. The rating for this link is ± 500 kV and 1800 A.

DC-REACTOR

A reactor, which is called dc-reactor or smoothing reactor, is connected in series with the convertor bridges on the dc-side. This reactor will reduce the current ripples and will thus function as a part of the filter. The reactor also has an important function in reducing transient current changes surges at certain faults, as will be described in chapter 8. The required inductance of the reactor depends on the rated voltage and current of the convertor station and is usually in the range of 0.3-0.7 H for two-terminal transmission systems. Traditionally the reactors have been built of oil immersed type with the reactor placed in a tank like a transformer, as shown in figure 1-19. However, during the last years it has become more common to build them as air insulated reactors,

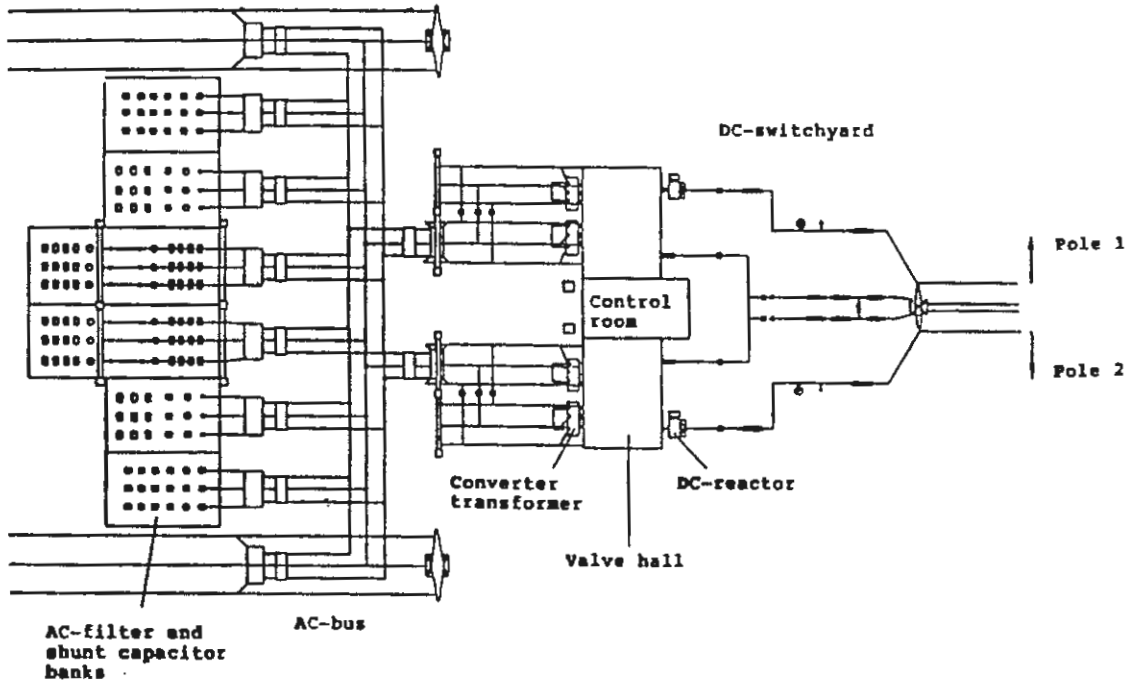

Figure 1-14 Typical layout of an HVDC converter station (500 kV dc and 400 kV ac).

Figure 1-21 AC-filters.

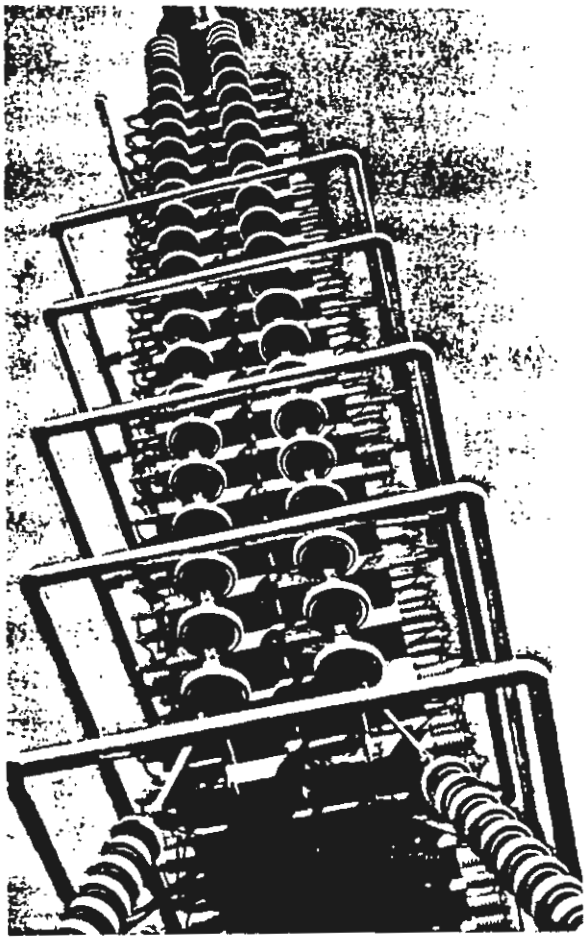

Figure 1-22 Suspended chain of capacitor cans in a DC-filter.

especially for lower voltages but sometimes also for higher voltages, see figure 1-20.

Filters

The generation of harmonics and the dimensioning of filters, both, on the ac- and dc-sides will be further described in chapter 6.
The filterbanks on the ac-side, which also have the important function of generating the reactive power, can be fairly large, as illustrated by fig 1-14, showing a typical layout of a convertor station.

Figure 1-21 shows a view of an ac-filter, which consists of banks containing a large number of capacitor cans and air core reactors.

The filters on the dc-side are considerably smaller than the filters on the ac-side. For pure cable transmissions or back-to-back stations no special dc-filters are usually used. The chain of capacitor cans are sometimes mounted and suspended as shown in figure 1-22.

Control equipment

The convertor stations are equipped with an advanced equipment for control, protection and monitoring. The major part of the equipment is placed in a control room. Small or medium sized stations are often remotely controlled from a regional control center and are usually only manned during daytime.

The basic unit of the control equipment is the firing control system which generates the firing pulses to the valves. The firing of the valves in the inverter station is usually controlled by a minimum extinction angle (commutation margin) and the firing in the rectifier

station is controlled to produce the desired magnitude of direct current. The principles for the firing control system will be further described in chapter 7.

The coordination of the control orders of the different convertor stations belonging to the same HVDC system is achieved through a telecommunication system.

The current orders are basically derived from a master control system. The control is based upon measured direct voltage and measured quantities in the connected ac-networks and is arranged according to one or more of the following options.

- constant transmitted power
- constant frequency e.g. in the ac-network connected to the inverter
- stabilizing control of the ac-networks

In order to protect the valves and the other equipment against excessive stresses each convertor station is equipped with advanced protective electronic equipment. Large overcurrents can usually be avoided by the fast action of the protection equipment, which delays or prevents the firing of the valves. Tripping of the ac-breakers is only ordered at faults requiring a permanent shut down of a convertor.

Earth faults on the dc-line are taken care of by a fast acting earth fault protection which deenergizes the line by delaying the firing pulses in the rectifier and thereby forcing it to inverter operation temporarily. The line is reenergized and brought to full operation after a preset time in the order of about 300 - 500 ms.

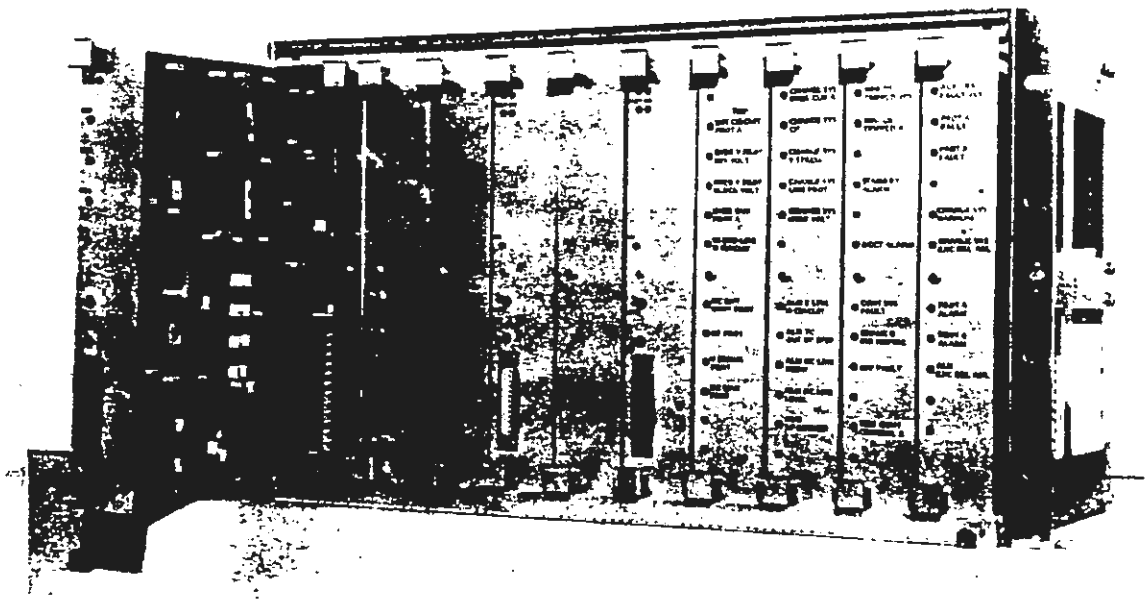

Figure 1-23 Control and protection equipment.

Figure 1-24 Control panel and computer screens in the control room in a converter station for the Itaipu HVDC system.

All essential voltages and currents and also some critical apparatus and components in the convertor station are monitored. The thyristor monitoring system will be further described in chapter 9.

The control, protection and monitoring functions are at present, to a great extent, realized by microprocessor circuits. One advantage with this technique is that the same hardware can be used for the realization of many different functions.

Figure 1-23 shows an example of a control equipment for the control and protection system.

The facilities for man-machine communication are an important part of the control equipment. Besides the conventional control panels, computer screens are at present widely used especially for the monitoring system.

Figure 1-24 shows a picture of the control panel and computer screens for the Itaipu HVDC transmission system.

1.3 Static Var Compensators

Applications of Static Var Compensators

Static Var Compensators are used for the voltage control by generation or absorption of reactive power both in power transmission systems and industrial applications. They are, in the latter case connected to a middle voltage level and are used for fast compensation of the power factor of the loads, especially at fast load changes, e.g., at steel mills and arc-furnaces (flicker-control). The following discussions of different applications will be limited to the use of Static Var Compensation in electrical power transmission systems only.

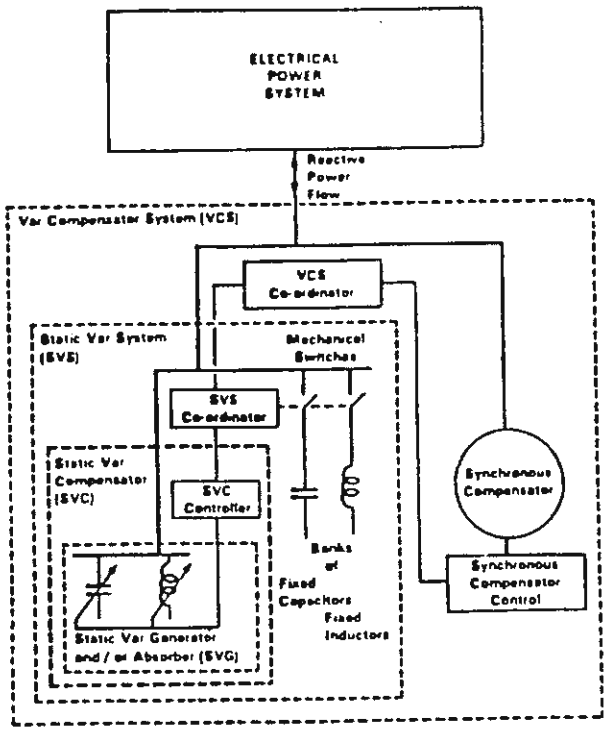

Figure 1-25 Diagram illustrating the definition of Static Var Compensator and its relationship with other reactive compensation devices (figure 1.1 in Static Var Compensators CIGRE WG 38-01 Task Force No 2 on SVC, 1986).

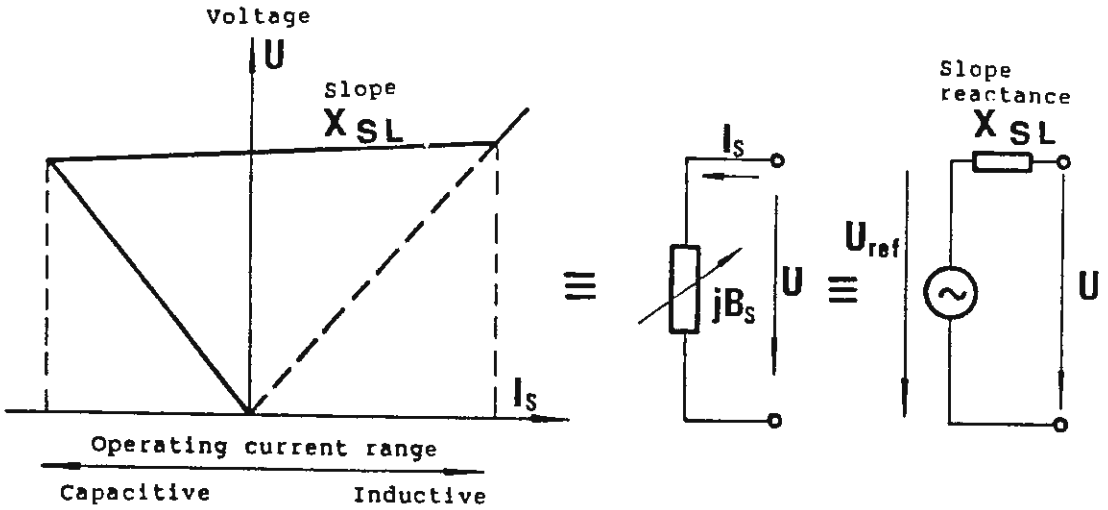

Figure 1-26 Typical steady-state voltage-current characteristics of an SVC and its equivalent representation.

Static Var Compensators (SVC) can generate and absorb reactive power in a similar way as synchronous compensators. As they lack rotating elements they are called Static Var Compensators.

Static Var Compensators can be combined with mechanically switched shunt-capacitors for the generation of reactive power or shunt-reactors for the absorption of reactive power. The total system, including control equipment, is then called Static Var System (SVS). The difference between SVC and SVS is illustrated in figure 1-25.

However, it should be noted that the two abbreviations SVC and SVS are often used without making a clear distinction between the two concepts.

A typical steady-state voltage-current characteristic for a Static Var Compensator (SVC) is shown in figure 1-26. The SVC can be controlled to keep the actual ac-voltage close to a reference value U_{ref}. At a voltage value above the voltage reference level it will absorb reactive power, i.e., it acts as an inductive load and at a voltage level below U_{ref} it generates reactive power, i.e., it acts as a capacitive load. The constant voltage control system has a limited amplification in order to obtain a stable system. The steady state amplification in the voltage control loop corresponds to a slope reactance X_{SL}. From steady state control point of view the SVC can either be regarded as a variable susceptance B_s or as a constant voltage-source connected in series with a slope reactance X_{SL}. This is illustrated in figure 1-26.

A SVC behaves like a synchronous compensator for stationary conditions with regard to the control of reactive power. However, the control of a SVC is much faster. It could also be compared with a synchronous condenser without inertia

because it can neither generate nor absorb active power transiently as it does not have any components, where large energies can be stored, corresponding to the rotating energy of the synchronous condenser.

In the following the Static Var Compensator will be treated as a load. This gives that a positive reactive power (Q>0) means absorption of reactive power, i.e., provides the same load as a shunt reactor. Negative reactive power (Q<0) corresponds accordingly to the load of a shunt-capacitor. This implies that the susceptance is negative, when the reactive power load is positive i.e.

$$B_s = - \frac{Q}{U^2} \qquad (1-9)$$

Compare also:

$$Y = G + jB, \qquad (1-10)$$

where:
$B = \omega C$

for a capacitance and

$$B = - \frac{1}{\omega L}$$

for an inductance.

The Static Var Compensators (SVC) are used for the control of reactive power and thus for the control of the ac-voltage. The SVC will offer a substantially better control of the reactive power than could possibly be obtained with mechanically switched capacitor banks and shunt-reactors, as the control can be performed very fast and continously with thyristors for Static Var Compensators. This provides a great flexibility in the

selection of control strategies. It is, for instance, possible to also attenuate mechanical oscillations in the ac-network, as the ac-voltage, which will be directly controlled, will influence both the transmitted power on the ac-lines and the loads. A Static Var Compensator, besides the faster control will also offer other advantages as compared to synchronous compensators such as lower losses, higher reliability and availability and lower cost.

The Static Var Compensators will in electrical power systems be used to

- obtain an efficient control of the ac-voltage and limit temporary overvoltage

- balance unsymmetrical loads

- increase the transmission capacity for active power

- improve the transient stability

- attenuate power oscillations

- attenuate and control reactive power of HVDC convertor stations.

Usually a number of the above listed reasons are decisive for a decision to install a Static Var Compensator. We will now briefly highlight some of the listed applications.

Voltage control and limitation of temporary overvoltages

Large load variations can result in large variations of ac-voltage in ac-networks having a low short-circuit capacity. The ac-network can approximately be represented with a Thevenin equivalent according to figure 1-27, if we

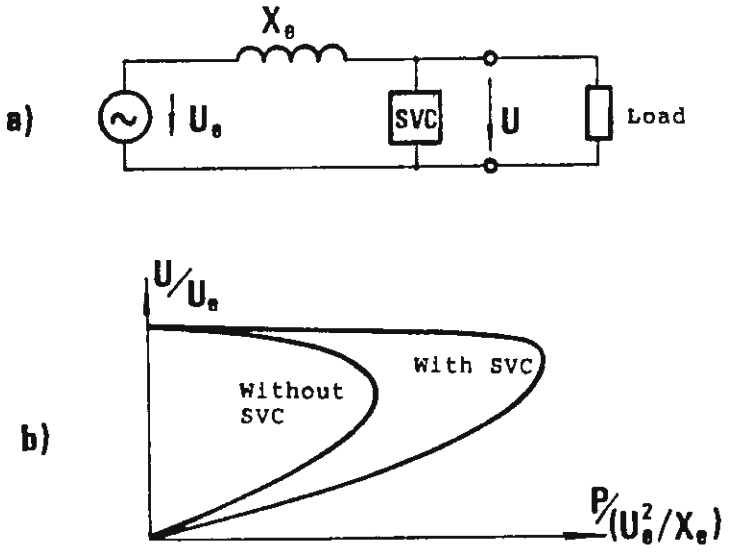

Figure 1-27 a) Equivalent circuit for a load and a SVC unit connected to an ac-power system with the short circuit capacity U_N^2/X_e.
b) Relationship between load and ac-bus voltage.

disregard the influence from the voltage control of the connected synchronous machines. This is a reasonable assumption, when the machines are not connected close to the point in the network which is studied. The reactance X_e corresponds to the short-circuit capacity and the voltage U_e is the voltage that would be obtained at a complete load-rejection.

The voltage at the ac-bus will vary with the load as illustrated in the figure 1-27b, provided that the voltage is not controlled. For a resistive load the following maximum power, P_{max}, is obtained

$$P_{max} = \frac{U_e^2}{2\ X_e} \quad \text{at} \quad \frac{U}{U_e} = \frac{1}{\sqrt{2}}$$

The ac-bus voltage can be kept almost constant over a wide power range by connecting a SVC unit at the ac-bus as illustrated in figure 1-27a. Temporary overvoltages at the disconnection of the load can be limited by the connection of a SVC unit. The magnitudes of the fundamental frequency components of the temporary overvoltages can be obtained by comparing the actual ac-voltage at a certain load with the corresponding ac-voltage at no load.

Figure 1-27 illustrates the case with a pure resistive load. Similar characteristics can be drawn for other types of loads of more inductive or capacitive character. It can thus be shown that a SVC unit can be effective in reducing the temporary overvoltages at disconnection of HVDC convertor stations or connection of long no-loaded ac-overhead lines.

Balancing of unsymmetrical loads

It has been assumed above that the loads are equal in magnitude in all phases. However, it might be even more

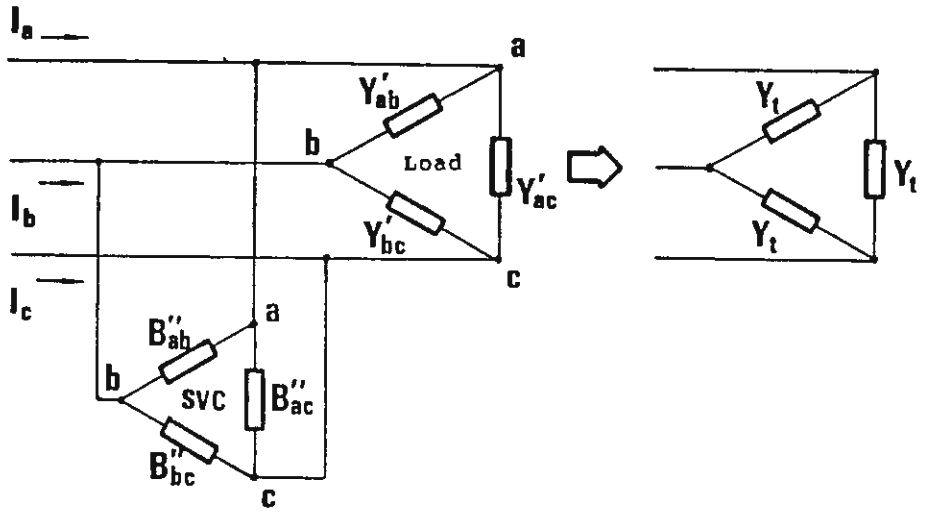

Figure 1-28 Unsymmetrical loads balanced by individual phase control of the SVC.

important to balance the loads and their variations in case the loads are different in the three phases, which can generate asymmetries between the ac-phases. It is thereby interesting to note, that it is also possible to balance out even unsymmetrical active loads in the three phases by individual compensation with only reactive power controls in the three phases. This is illustrated by figure 1-28. The total admittances (Y_t) which are determined by the admittance of the loads (Y'_{ab}, Y'_{ac} and Y'_{bc}) can be made equal in all phases by suitable control of the susceptances of the SVC (B''_{ab}, B''_{ac}, B''_{bc}). This will be treated further in chapter 10.

Increase of the transmission capacity for active power and improved transient stability

The maximum transmitting capacity of a purely inductive line is limited by the total line inductance, as illustrated in equation 1-4. The longitudinal inductance of the line is, because of that, often partly compensated for by the connection of series capacitors. The total longitudinal line impedance will then decrease and the power transmitting capacity will increase. However, too high a degree of compensation might cause other problems, e.g., resonance at lower frequencies (sub-synchronous oscillations). It is, because of that, of interest to find other ways of increasing the transmission capability. One alternative is to control the voltage close to the middle of the line by the connection of a SVC unit. If we assume that the voltages at the end of the line are constant and equal to the rated voltage U_N, and that no SVC is connected, we will obtain the following maximum transmitted power.

$$P_{max} = \frac{U_N^2}{X}$$

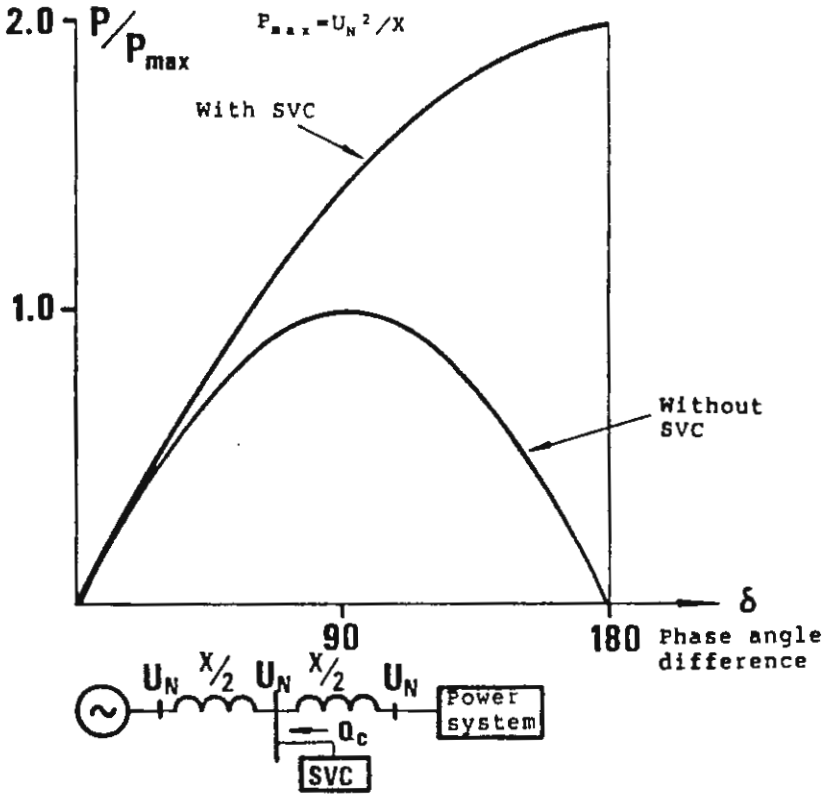

Figure 1-29 Power transmission capacity with and without an SVC unit. Note: no limitation is included because of limited rating of the SVC unit.

If we also assume that the voltage at the middle of the line is kept constant and equal to the rated voltage, we will obtain an increase of the maximum transmitted power by a factor of two. It is then assumed, that the SVC unit installed to control the voltage has a sufficient capacity, such that it can generate the needed reactive power. The SVC unit has to generate, for the assumed case, reactive power to each half of the line equal to

$$Q = \frac{2 \cdot U_N^2}{X}$$

This is obtained from equations 1-5 and 1-6 by setting $\delta = \pi/2$. The case is further illustrated by figure 1-29. However, it should be noted that a total rating of $Q = 4P_{max}$ is needed in order to transmit an active power of $2P_{max}$. The limitations of the rating of the SVC unit will, because of that, in a practical case decrease the maximum transmitted power to a lower value.

The transient stability limit can also be improved by the connection of a SVC unit in the ac-networkand thereby transiently increasing the power transmission capacity of the network.

Increased damping of power oscillations and sub-synchronous resonance

The transmitted active power on an ac-transmission can partly be controlled by the control of the voltages at certain points. It is, because of that, possible to utilize the fast control of a SVC unit to attenuate power oscillations due to sub-synchronous resonance. The risk for

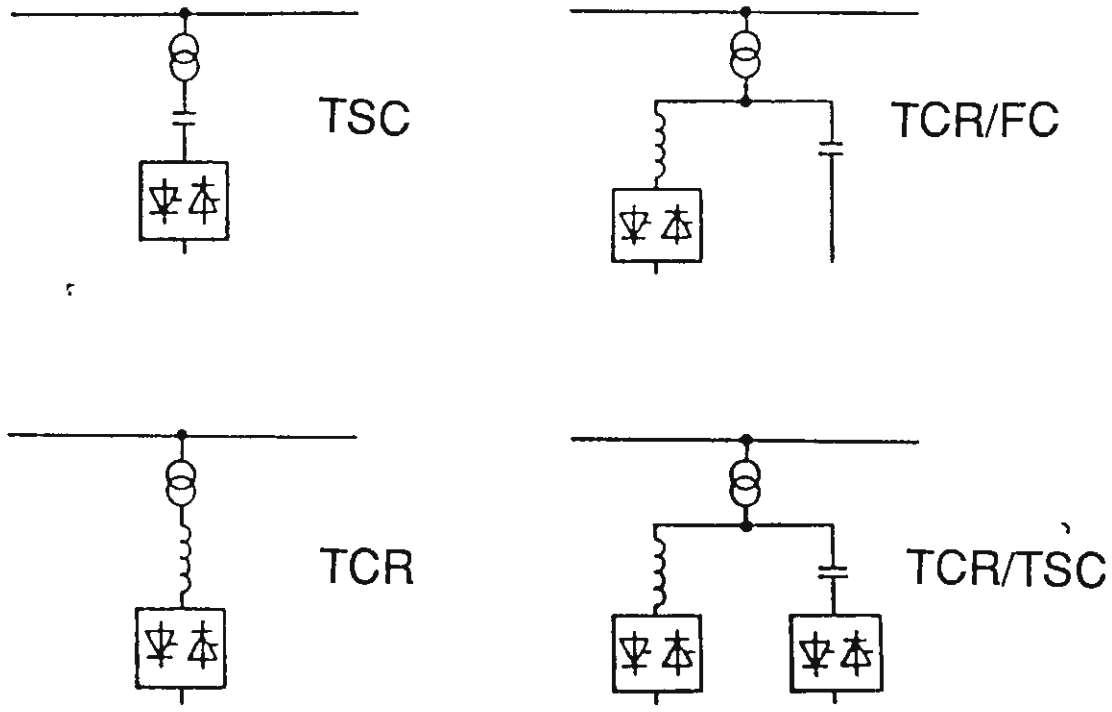

Figure 1-30 Static Var Systems with thyristors as the switching component.

sub-synchronous resonance is especially high, when long series compensated lines are connected close to power stations with turbo generators. Compensation of the line inductance by connection of capacitors in series can cause resonance at a frequency, which is lower than the network frequency. This can be understood from the fact, that at decreased frequencies the reactance of the capacitor will increase but the reactance of the inductance will decrease making them equal at resonance. If this resonance frequency coincides with a side-band, which is generated at any of the mechanical resonances of the machines, there is a risk for oscillations of increasing amplitude. Fairly small control actions are needed from a SVC unit to prevent such sub-synchronous oscillations from building up. However, to be effective the control of the SVC unit has to be fairly fast as the critical frequencies can be in the range 10-15 Hz.

Principle design of Static Var Compensators

The different types of Static Var Systems which will be described in the following are illustrated in figure 1-30. The systems will be described in the order they are presented in the figure, i.e.,:

* Thyristor Switched Capacitor — TSC
* Thyristor Controlled Reactor — TCR
* Thyristor Controlled Reactor with Fixed Capacitor — TCR/FC
* Thyristor Switched Capacitor combined with a Thyristor Controlled Reactor — TSC/TCR

All these systems are based on the use of thyristors as

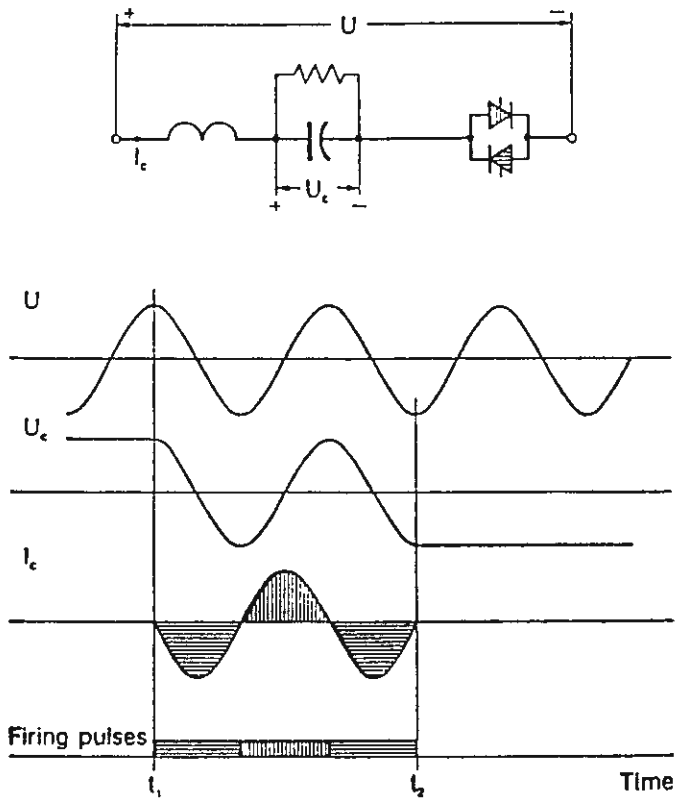

Figure 1-31 Thyristor switched capacitors (TSC) - functional principle.

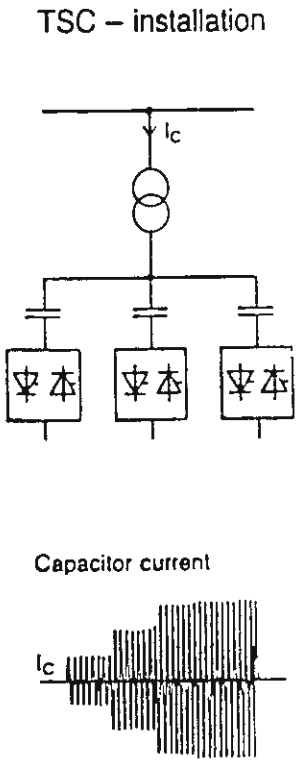

Figure 1-32 Three parallel TSC units.

switching elements. Beside these types, other types also exist, e.g., Mechanically Switched Capacitors and/or Reactors (MSC and/or MSR) and Saturated Reactors (SR). These later types will not be treated in this chapter.

Reactive power could also be absorbed and controlled by line commutated current-source convertors operating at a firing angle of 90°. However, as both the costs and losses will be higher than for thyristor controlled reactors this solution is not used. The development of forced-commutated convertors, as described and discussed in chapter 11, will provide more interesting alternatives, as it then, with the same equipment, will be possible to both generate and absorb reactive power. Some smaller prototype installations are already in operation using this technique, but it is expected, that it will take another few years, before this alternative can offer an economically attractive alternative to the types of SVC systems listed above and which will be further described below.

Thyristor switched capacitors

The functional principle of the thyristor switched capacitor is illustrated in figure 1-31. In the case shown the capacitor is connected during three half cycles by firing the thyristors at time t_1 and blocking them before t_2. It has here been assumed, that the initial voltage of the capacitor U_c is equal to the peak value of the applied voltage U and that these voltages have the same sign at the time t_1. Usually a number of TSC units are connected in parallel, as illustrated in figure 1-32, which makes it possible to change the capacitor currents in a number of steps. However, for cost reasons the number of steps is mostly limited to two or three. The voltage is usually transformed down to the range 3-20 kV in order to get the

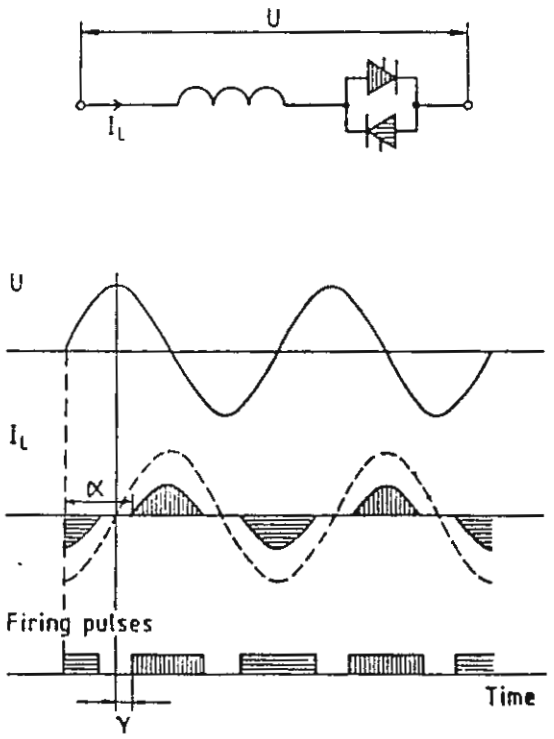

Figure 1-33 Thyristor controlled reactor (TCR) - functional principle.

lowest total costs. A single-phase diagram is shown in figure 1-32. The three phases can be connected in either Δ or Y-connection.

Thyristor controlled reactors

The main elements of a thyristor controlled reactor (TCR) are reactors connected in series with thyristors which are connected in anti-parallel as shown in figure 1-33. The maximum current is obtained through the reactors, when the thyristors are conducting during the whole cycle. The current will then be sinusoidal as illustrated by the dashed curve in the figure. The firing of the thyristors can be delayed by the delay of the firing pulses to the thyristors. The position of the firing pulses are mostly determined from the zero crossing of the voltage in a similar way as for convertors. The firing angle is denoted with α and will, for a thyristor controlled reactor have, a value between 90° and 180° or $\pi/2$ and π rad as shown in the figure 1-33.

The current will only be sinusoidal for $\alpha = 90°$. For larger values of the firing angle the current will be lower and contain harmonics, which can be especially large for the harmonics of order 3, 5 and 7. The basic relationships between the firing angle, the fundamental frequency susceptance and the magnitudes of the harmonics will be treated in chapter 10.

The high third harmonic component can easily be eliminated for a symmetrical ac-network by symmetric firing and connection of the elements for the three phases in Δ. The 5th and 7th harmonics can be eliminated either by the use of tuned filters or by the use of a 12-pulse connection, i.e., feeding one unit from a Y-Δ connected transformer and the other unit from a Y-Y connected transformer.

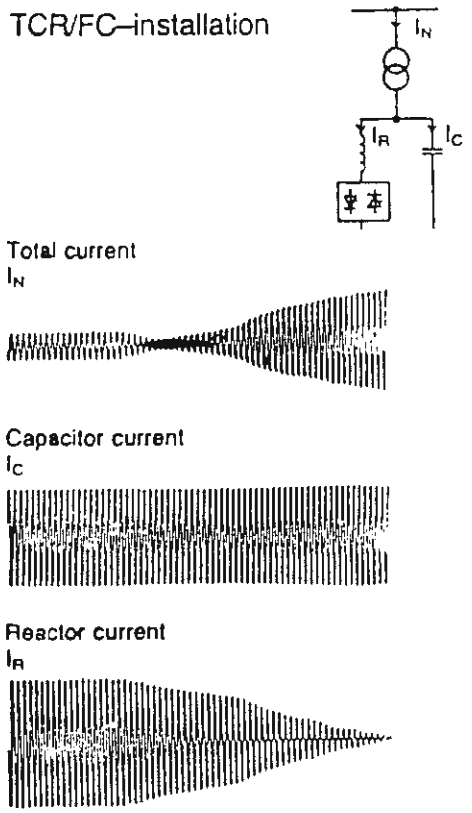

Figure 1-34 Thyristor controlled reactor combined with a fixed capacitor (TCR/FC).

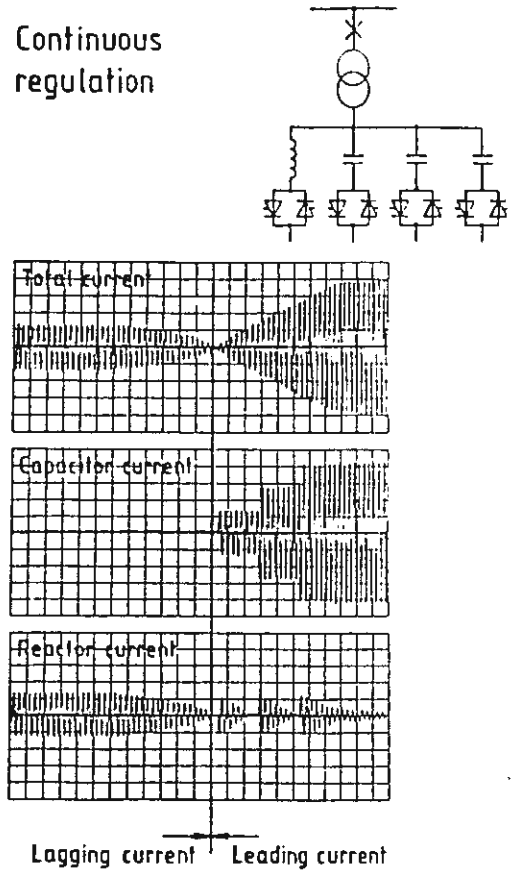

Figure 1-35 Combination of thyristor controlled reactor and thyristor switched capacitor (TCR/TSC).

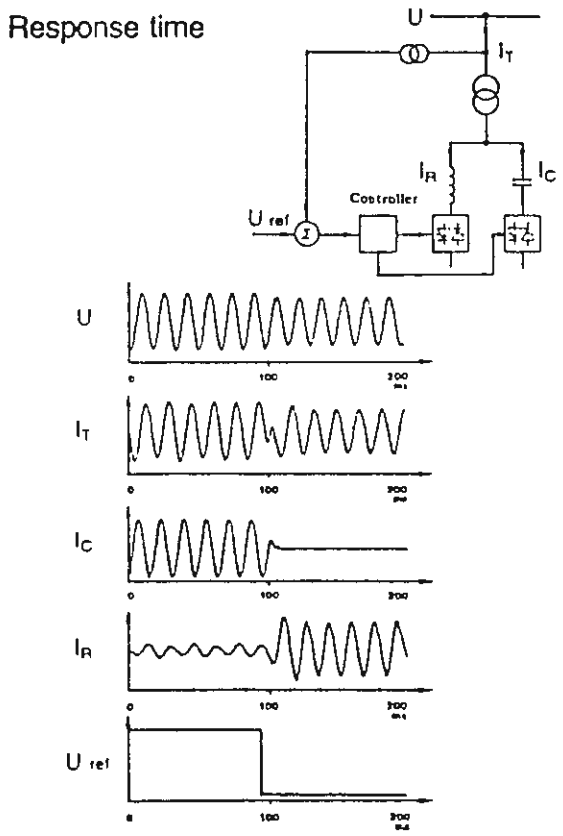

Figure 1-36 Control and step response.

The absorbed reactive power in a TCR unit can be continuously varied from its maximum value down to zero. This is an important difference as compared to the thyristor switched capacitor (TSC) for which the generated reactive power could only be varied in steps. A combination of a thyristor controlled reactor and a filter or fixed capacitor, TCR/FC, will provide the possibility of continous control and to both generate and absorb reactive power. See figure 1-34.

Combination of thyristor controlled reactors and thyristor switched capacitors TCR/TSC

The combination of a thyristor controlled reactor and a fixed capacitor (TCR/FC), according to figure 1-34, will have certain drawbacks, as the thyristor controlled reactor and the fixed capacitor counteracts each other. This will for instance both, cause higher costs and higher losses. Figure 1-35 suggests an alternative solution, where a thyristor controlled reactor is combined with three thyristor switched capacitor units. This SVC system will permit a continuous variation of the reactive power with minimum losses.

Control

The control principle of a TCR/TSC system in its simplest form is illustrated in figure 1-36. It is here assumed, that the TSC unit is conducting current at $t = 0$ and that at that time only a small current is flowing through the TCR (α close to 180°). A step-change in the reference voltage to the controller is applied at $t \simeq 90$ ms. The controller reacts by blocking the firing pulses to the TSC unit, causing the current I_C to decrease to zero within

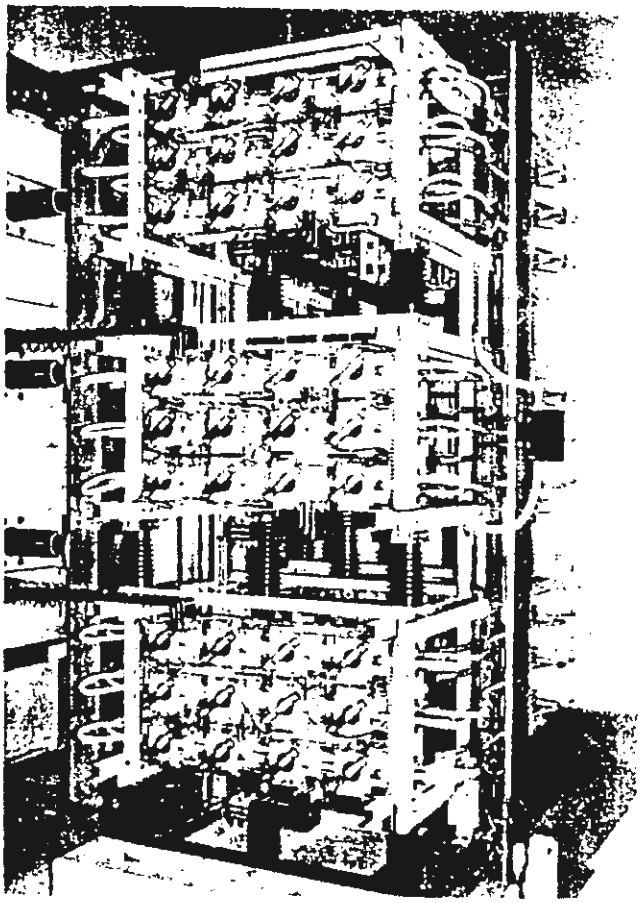

Figure 1-37 Water cooled thyristor valves for SVC.

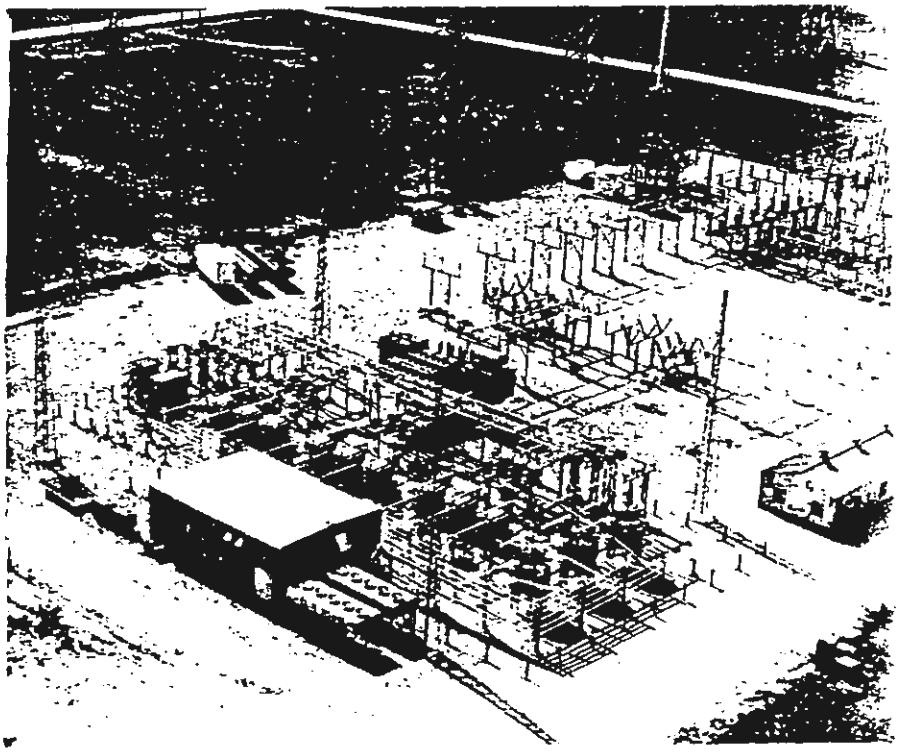

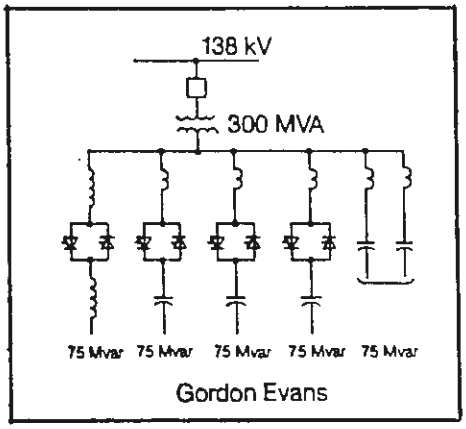

Figure 1-38 SVS station Gordon Evans.

half a cycle. The firing angle to the reactor is decreased resulting in an increase of the current through the reactor. The change from reactive power generation to reactive power absorption in the TCR/TSC unit will effect the desired reduction in ac-voltage. The basic principles of the control will be further treated in chapter 10.

Station design

A Static Var System consists of the following main circuit components.

- transformers

- reactors

- capacitor banks that can be designed as filters

- thyristor valves

The thyristor valves are usually air-insulated and placed indoor. Figure 1-37 shows a picture of a water cooled thyristor valve.

Figure 1-38 shows a view of a SVS station, Gordon Evans, in USA. Figure 1-38 shows also the circuit diagram for the station. The reactive power can in this case be varied in a continuous way in the range from 0-300 Mvar capacitive. The reactors are air-insulated and located in the right part of the picture.

2. MAIN PRINCIPLES OF CONVERTOR CIRCUITS. CURRENT-SOURCE AND VOLTAGE SOURCE CONVERTORS. LINE-COMMUTATED AND FORCE-COMMUTATED CONVERTORS.

2.1 Basic characteristics of current-source and voltage-source converteors

As already mentioned in the previous chapter the dc-lines of HVDC transmission systems are usually operated close to the rated voltage in order to minimize the line current and by that the line losses. A few of the first direct current transmission systems were built to operate at constant current but varying voltage. The basic reason for choosing a constant current system was that it provided certain advantages with regard to the possibility of limiting fault currents due to line faults.
However, as the limitation of fault currents for modern HVDC transmission systems can easily be achieved by a fast acting current control system, both the requirement to always operate close to the rated voltage and the limitation of fault currents are met. The control is arranged so, that the firing of the valves at a fault occurance is almost immediately delayed by the controls and protection system.

The circuits for conversion from ac-current and voltage to dc-current and voltage and vice versa can be arranged in different ways. In the same way as for power electronics used for other applications, e.g., electrical drives, it is feasible to distinguish between current-source (current-stiff) and voltage-source (voltage-stiff) convertors. As voltage-source convertors are usually used for the conversion of energy from the dc-side to the ac-side, i.e., inverter operation, voltage-source convertors are often referred to as Voltage-Source Inverters (VSI). However, in

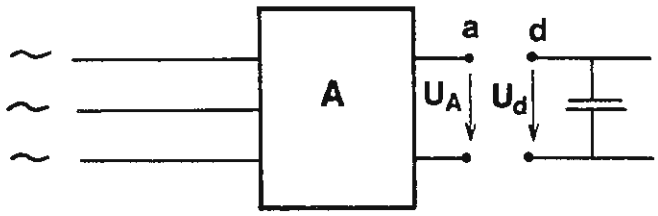

Figure 2-1 Connection of a dc-network to an ac-network by means of conversion arrangement A (Ref. [2]).

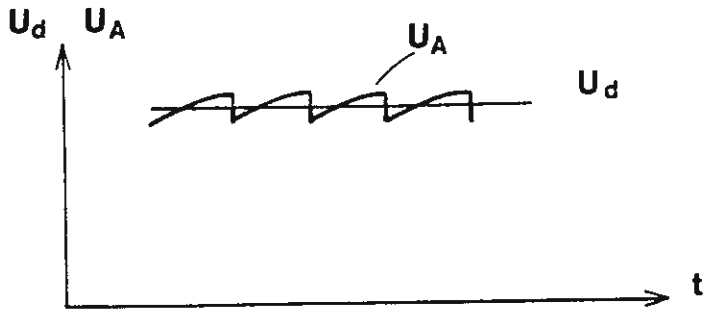

Figure 2-2 Possible waveshapes of the voltages u_a and u_d.

this text we will use the term voltage-source convertor to stress that this type of convertor might be used for conversion of energy in both directions i.e. from the ac-side to the dc-side (rectifier operation) as well as from the dc-side to the ac-side (inverter operation).

At first we will study a circuit arrangment according to figure 2-1 to illustrate the principal difference between a current source convertor (current-stiff) and a voltage-source convertor (voltage-stiff). The arrangement is used for the conversion of power from an ac-system (on the left hand side) to a dc-system (on the right hand side) or vice versa. We assume that the block A consists of a number of switching elements and transformer windings. The voltage U_A is at each moment made up of suitable portions of the three feeding ac-phase voltages, which we assume to be stiff and sinusoidal. The topology of the circuit connecting the ac-side with the dc-side will be changed at each switching instant, but will be unchanged between these instants. This means that the voltage U_A will also be a part of a sinusoidal function during this interval. By increasing the number of switching elements and transformer windings and making each time interval shorter it is possible to decrease the difference between U_A and the voltage U_d, which is assumed to be a stiff dc-voltage.

If it is assumed that all the circuits are symmetrically arranged and the switchings are performed in a periodic way the voltage U_A during each switching interval will be identical as illustrated in figure 2-2. However, as also illustrated in figure 2-2, there will be a difference between U_A and U_d during most parts of each interval.

If we now assume that both the alternating voltage on the left side of the block circuit A and the direct voltage U_d are stiff, and also assume that the internal impedance of the circuit A is very small a connection of the terminals a

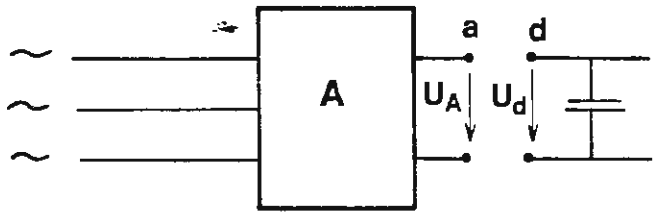

Figure 2-1 Connection of a dc-network to an ac-network by means of conversion arrangement A (Ref. [2]).

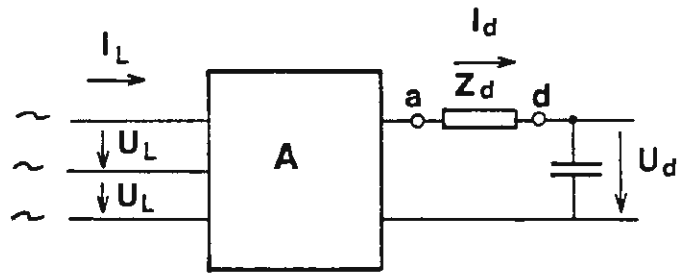

Figure 2-3 Principle of a current-source converter with the impedance Z_d on the dc-side (Ref. [2]).

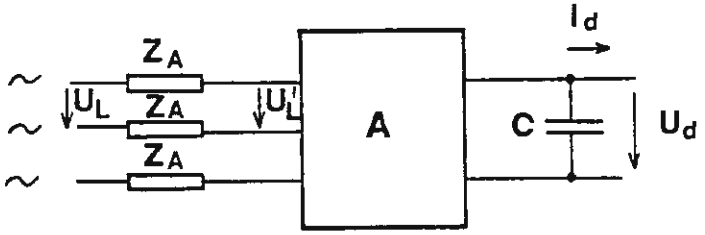

Figure 2-4 Principle of a voltage-source converter with the impedance Z_A on the ac-side.

with the terminals d of the circuit, as shown in figure 2-1, would result in very high harmonic currents. Because of that, suitable impedances have to be inserted in the system to limit these harmonic currents.

The most obvious way to do it is to insert an impedance between the terminals a and d, as illustrated in figure 2-3. From a practical point of view this impedance ought to be low for steady state direct currents in order to minimize the additional losses, but ought to be high for current harmonics of the frequencies appearing in the voltage U_A. A pure inductance will meet these requirements. As viewed from the block A the direct current side will now become current-stiff or act as a current-source. Because of that such a circuit is referred to as a "current-source convertor" or a "current-stiff convertor". Most practical circuits are arranged to permit power transfer in both directions. As will be described later the circuits are usually arranged so that the direction of the direct current is always the same. A change of the power direction is then achieved by a change in the polarity of the direct voltage U_d.

Instead of inserting the impedance as a series inductance on the direct current side according to figure 2-3 the inductances can be inserted on the alternating current side as illustrated in figure 2-4. The impedances Z_A, which are inserted in each phase, consist usually of the leakage inductances of the convertor transformer. The current on the dc-side of block A will now, besides a dc-component, also contain ripple, i.e., harmonic currents. To short-circuit these harmonics and to minimize the ripples in the voltage on the dc-side a large capacitance C usually has to be connected on the dc-side. As viewed from block A the dc-side can now be regarded as a stiff direct voltage or a voltage-source. Because of that, this type of convertor is usually referred to as a voltage-source

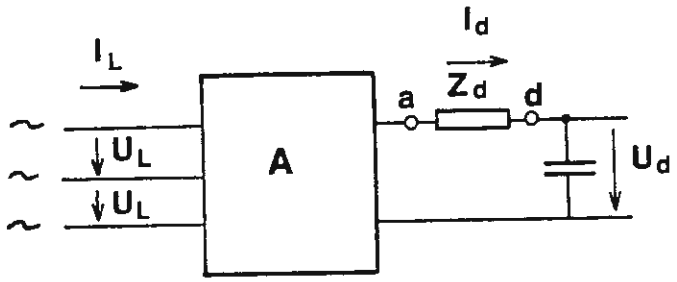

Figure 2-3 Principle of a current-source converter with the impedance Z_d on the dc-side (Ref. [2]).

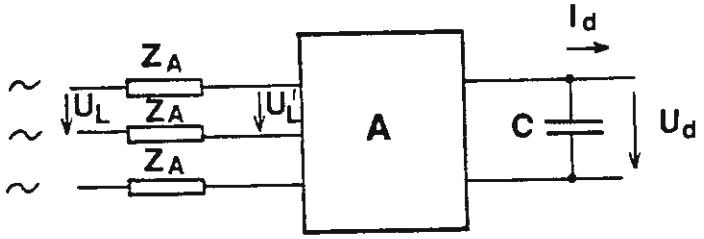

Figure 2-4 Principle of a voltage-source converter with the impedance Z_A on the ac side.

convertor (or voltage-source inverter, VSI) or voltage-stiff convertor. As for the current-source convertor the direction of power can either be from the ac-side to the dc-side or vice versa. However, in contrast to the current-source convertor case, change of power direction for the voltage source convertor is achieved by change of direction of direct current I_d, while the polarity of the direct voltage U_d is unchanged.

In chapter 11 it will be further described how the circuits for current-source or voltage-source are realized. In this chapter we will limit ourself to the fundamental characteristics and relationships between the various quantities on the ac-side and dc-side. These characteristics are valid and independent from how the circuits are realized and are sufficient for the discussion of the feasibility of the circuits for HVDC applications.

The current on the ac-side is directly proportional to the direct current for a current-source convertor, if it is assumed that the switching sequence and the intervals between switchings of the circuits A are independent of the magnitude of the direct current. The instantaneous value of the current i_L on the ac-side will then be changed in a step-wise way at the switchings in the circuit A. The following relationship is valid between the r.m.s. value of the fundamental component of i_L, which is denoted $I_{L(1)}$, and the direct current I_d.

$$\frac{\sqrt{3} \cdot I_{L(1)}}{I_d} = k \qquad (2\text{-}1)$$

As we assume that the circuit elements in the block A and the impedance Z_d are lossless the following relationship is valid for the transmitted active power:

$$P = U_d \cdot I_d = \sqrt{3}\, U_L \cdot I_{L(1)} \cdot \cos \phi_L \qquad (2\text{-}2)$$

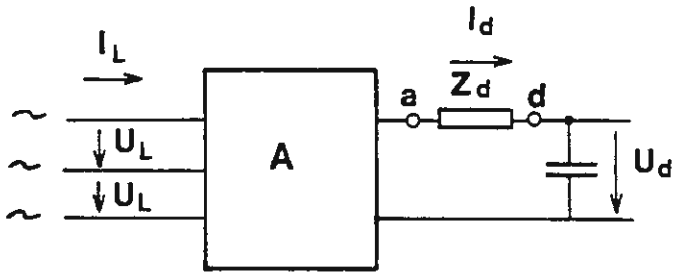

Figure 2-3 Principle of a current-source converter with the impedance Z_d on the dc-side (Ref. [2]).

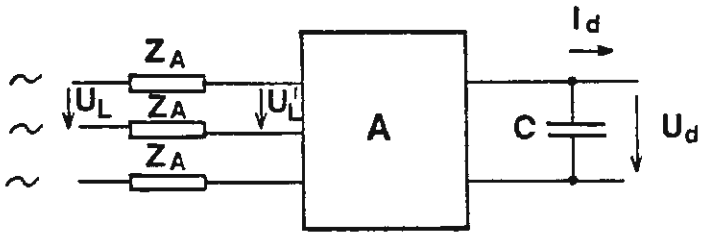

Figure 2-4 Principle of a voltage-source converter with the impedance Z_A on the ac-side.

where:

U_L is the r.m.s value of the phase-to-phase voltage (assumed sinusoidal without distortion), $I_{L(1)}$ is the r.m.s. value of the fundamental component of the ac-current, and $\cos\phi_L$ the corresponding power factor. The equations (2-1) and (2-2) result in following relationship.

$$U_d = k \cdot U_L \cdot \cos \phi_L \qquad (2-3)$$

It should be noted that $\cos \phi_L$ for a line-commutated convertor is determined, both, by the magnitude of the commutating inductances and the phase angle of the firing instants. The equation 2-3 is valid as long as equation (2-1) is valid. As the constant k is somewhat dependent upon the magnitude of the overlap, the magnitude of k is also somewhat dependent upon the magnitude of the current. However, as will be seen later in chapter 4, this influence is usually small and can usually be disregarded. The constant k, can on the other hand, be varied by an interval of the order of 15% by the tap-changers of the convertor transformers. The constant k can also be varied by firing controls for convertors of the forced-commutated types as the switching intervals can then be changed by so called pulse width modulation, PWM.

For a voltage-source convertor, according to fig 2-4, similar relationships are valid, however, with the currents replaced by voltages. According to fig 2-4, the internal voltages U_L', which are generated by the direct voltage, U_d, using various topologies of convertor transformer windings, determined by the valves as switching elements, will be changed in a stepwise way. This can be compared with the stepwise change of the current i_L in the current-source convertor, according to figure 2-3. The r.m.s. value of the fundamental voltage component of U_L' will thus be

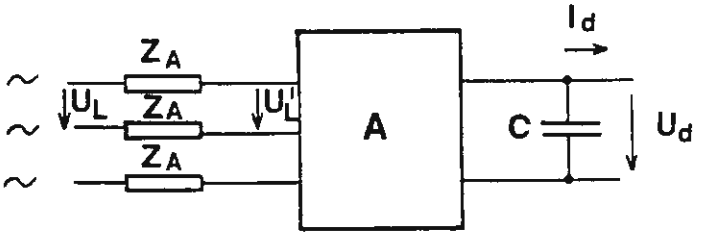

Figure 2-4 Principle of a voltage-source converter with the impedance Z_A on the ac-side.

proportional to U_d. The following relationship will apply between the r.m.s. value of the fundamental voltage component of U_L' which we denote by U'_{L1} and the direct voltage U_d

$$\frac{U'_{L1}}{U_d} = k' \qquad (2\text{-}4)$$

The constant k' can in the same way as the constant k in equation (2-1) be varied by tap-changer control. For a fixed winding turn ratio in the convertor transformer the constant k' is also fixed as long as the switching sequence and the switching intervals are not changed. However, the length of the switching intervals can be changed in a forced-commutated convertor, e.g., by Pulse Width Modulation (PWM). It will then be possible to control the magnitude of the constant k' from a certain maximum value down to zero. This will be further treated in chapter 11.

The phase position of the voltage U'_{L1} relative to the voltage U_L which is denoted by δ, can be controlled by the firing of the valves in the box A. The angle δ is positive when the voltage U_L is leading U'_{L1}. The requirement that the active power on the dc- and ac-side shall be equal effects the following relationship.

$$P = U_d \cdot I_d = \frac{U_L \cdot U'_{L1}}{X_A} \sin \delta \qquad (2\text{-}5)$$

It has here been assumed that the impedance Z_A is purely inductive thus a reactance X_A.

Equations (2-4) and (2-5) result in the following relationship:

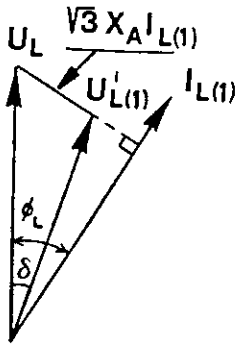

Figure 2-5 Voltage-source converter, phasor diagram for ac-side quantities, rectifier operation, $\delta>0$.

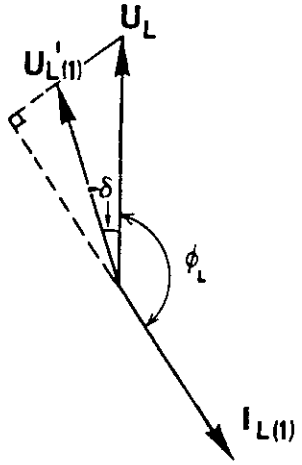

Figure 2-6 Voltage-source converter, phasor diagram for ac-side quantities, inverter operation, $\delta<0$.

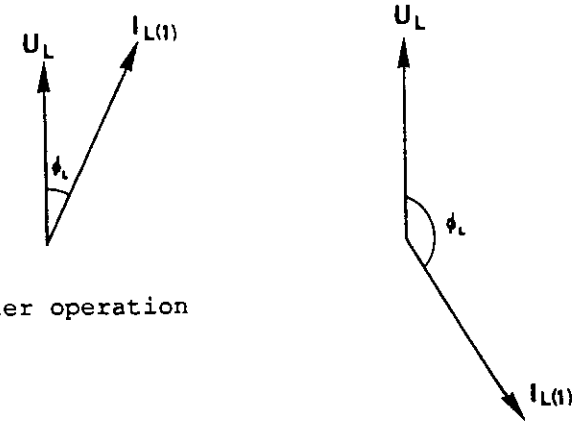

Figure 2-7 Current-source converter, phasor diagram for ac-side quantities, for rectifier and inverter operations, respectively.

$$I_d = k' \frac{U_L}{X_A} \sin \delta \qquad (2\text{-}6)$$

This equation, which is valid for the voltage-source convertor, can also be compared with the equation (2-3) for the current-source convertor.

The power direction for a voltage-source convertor is determined by the polarity of the angle δ, as can be seen from the equation (2-5).

The convertor is operating in the rectifier mode, when δ is positive, i.e., when the line voltage U_L is leading U'_{L1}. This is also illustrated in the phasor-diagram, as shown in figure 2-5. If the firing instants are advanced so that the voltage U'_{L1} is leading U_L and the angle δ becomes negative the power direction will be reversed. The convertor will then operate in the inverter mode, as illustrated in figure 2-6.

The phase angle ϕ_L between the line voltage U_L and the fundamental of the ac-current I_{L1} has also been indicated in figures 2-5 and 2-6. It can be seen from these figures that the phase-angle ϕ is increased when the firing angle is advanced and the angle δ is changed from a positive value to a negative value going from rectifier operation to inverter operation. For comparison the corresponding phasor-diagrams for a current-source convertor in rectifier mode and inverter mode operations are shown in figure 2-7. In this case the change from rectifier operation to inverter operation is obtained by an increased delay of the firing instants of the valve. The change of power direction from rectifier operation to inverter operation for the current-source convertor is obtained by a change in the

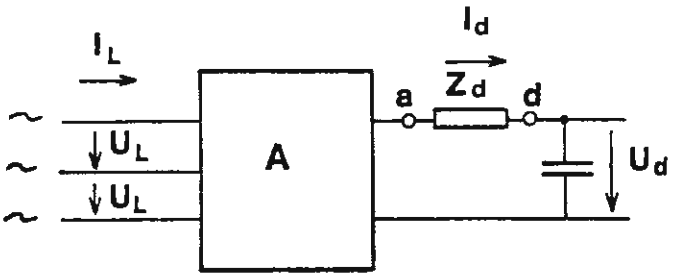

Figure 2-3 Principle of a current-source converter with the impedance Z_d on the dc-side (Ref.[2]).

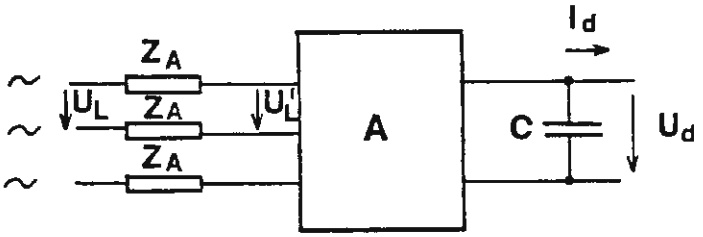

Figure 2-4 Principle of a voltage-source converter with the impedance Z_A on the ac-side.

polarity of the direct voltage as the angle ϕ_L is increased above the $\pi/2$ rad. For the voltage-source convertor the corresponding change of power direction is obtained by a change of the polarity of the direct current when the polarity of the angle δ is changed (compare equation (2-6)). Voltage-source convertors are, because of that arranged so that, the current can flow in both directions (e.g., with each valve branch consisting of one thyristors valve connected in parallel with a diode valve of the opposite polarity).

2.2 General characteristics of line-commutated and forced-commutated convertors

In the previous section the basic principles for current-source convertors and voltage-source convertors were treated as illustrated by figures 2-3 and 2-4. The basic differences are related to, whether a high impedance is placed on the ac-side or on the dc-side of the conversion arrangement A. Another aspect that has to be considered is how the switching or commutation of the current within block A is achieved.

Traditionally the commutation in most types of convertors has been performed by sending triggering signals to the valves to be fired. The commutation of the current is then performed by the line voltage, which then must have a positive polarity measured across the valve to be fired. These types of convertors are referred to as line-commutated convertors. They can, in principle be, both, of the current-source type or the voltage-source type, although, as we shall see later, almost only line-commutated current- source convertors are used.

Commutation of the current from one circuit to the following circuit configuration in A can also be performed by some artificial means without relying on a positive line voltage component. These types of convertors are at present usually realized with valves having current turn-off capabilities (e.g., GTO thyristors or power transistors). The commutation of current from one circuit to the succeeding circuit could also be performed by energies stored in capacitors. These types of convertors are often referred to as "forced-commutated convertors" or "self-commutated convertors". When GTO thyristors are used they might also be referred to as grid-commutated convertors. We will use the term "forced-commutated convertors", independent from how the commutation is achieved. As will be further described in chapter 11 forced-commutated convertors can either be of the current source type or the voltage-source type. Forced-commutated convertors have until now only been used for low and medium voltage applications, e.g., for motor drives but not yet for HVDC. A few forced-commutated convertors of the voltage-source type have recently been installed for reactive power control(SVC). However, because forced-commutated convertors can offer certain principle advantages for HVDC also such as being less vulnerable for commutation failures and making it possible to control active and reactive power independently, they might also be of interest for HVDC applications.

The fact that commutation of the current in a line-commutated convertor is achieved by the line voltage causes certain restrictions as to where the commutation can occur. Because the voltages across the valves to be fired always must be positive, the ac-voltages on the valve side must always lead the ac-current. This gives the following requirement for a current-source line-commutated convertor with no commutation reactance:

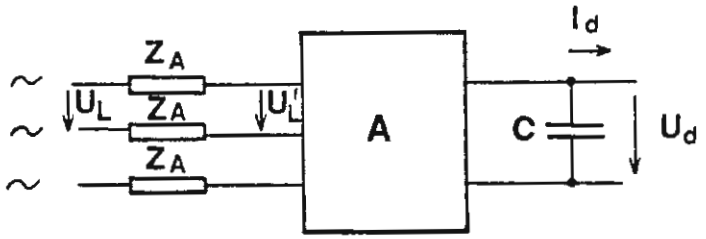

Figure 2-4 Principle of a voltage-source converter with the impedance Z_A on the ac-side.

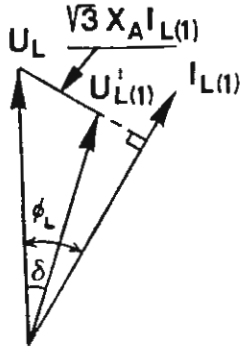

Figure 2-5 Voltage-source converer, phasor diagram for ac-side quantities, rectifier operation, $\delta>0$.

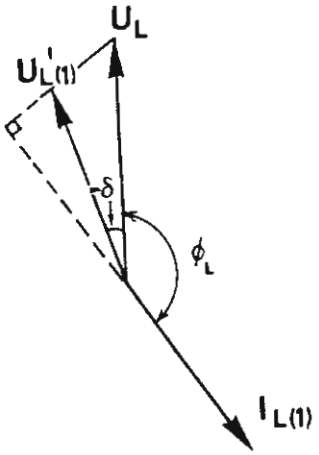

Figure 2-6 Voltage-source converter, phasor diagram for ac-side quantities, inverter operation, $\delta<0$.

$$0 < \Phi_L < \pi \qquad (2\text{-}7)$$

For a voltage-source line-commutated convertor the corresponding relationship will be

$$0 < \Phi_L - \delta < \pi \qquad (2\text{-}8)$$

In practice some additional restrictions have to be added for inverter operation to avoid making the convertor too sensitive to commutation failures.

In both cases the restriction on the phase-angles results in a condition that reactive power is consumed by the convertors.

As can be seen from figures 2-5 and 2-6 the requirement according to equation (2-8) calls for a line-commutated voltage-source convertor the modified requirement:

$$U_L \cos \delta > U'_{L1}, \qquad (2\text{-}9)$$

or by insertion of U'_{L1}, according to equation (2-4)

$$U_L \cos \delta > k' U_d \qquad (2\text{-}10)$$

The relationship between the voltages U_L and U_d therefore have to be chosen so that the reactive power always is flowing from the ac-side into the circuit A according to figure 2-4. This also makes this convertor circuit very

vulnerable to changes in the ac-voltage. The commutation process will collapse for a line-commutated voltage-source convertor at a transient reduction of the ac-voltage such that the requirement according to equation 2-10 is no longer fulfilled. Because of that line-commutated voltage-source convertors are not used. On the other hand voltage-source convertors of the forced-commutated type seem to offer greater advantages than forced-commutated convertors of the current-source type.

2.3 Current-source or voltage-source type of convertor for HVDC systems?

The basic principles of the current-source and voltage-source convertors as well as of the line-commutated and forced commutated convertors have been described in the previous section. It was also concluded that until now only line-commutated current-source convertors have been used for HVDC and that line-commutated voltage-source convertors can be disregarded as avaible alternative. However, since forced-commutated convertors can offer interesting alternatives, especially forced-commutated convertors of the voltage- source type, it is of interest to compare the characteristics of HVDC systems with convertor stations using current-source convertors with those using voltage-source convertors.

In the following lecture material the characteristics of two terminal HVDC systems will mainly be studied in which both stations are equipped with convertors of the same type. For HVDC systems in which the power direction is always the same, a mixed system could also offer an interesting alternative, e.g., with a line-commutated current-source convertor at the sending end (rectifier station) and a forced-commutated voltage-source convertor

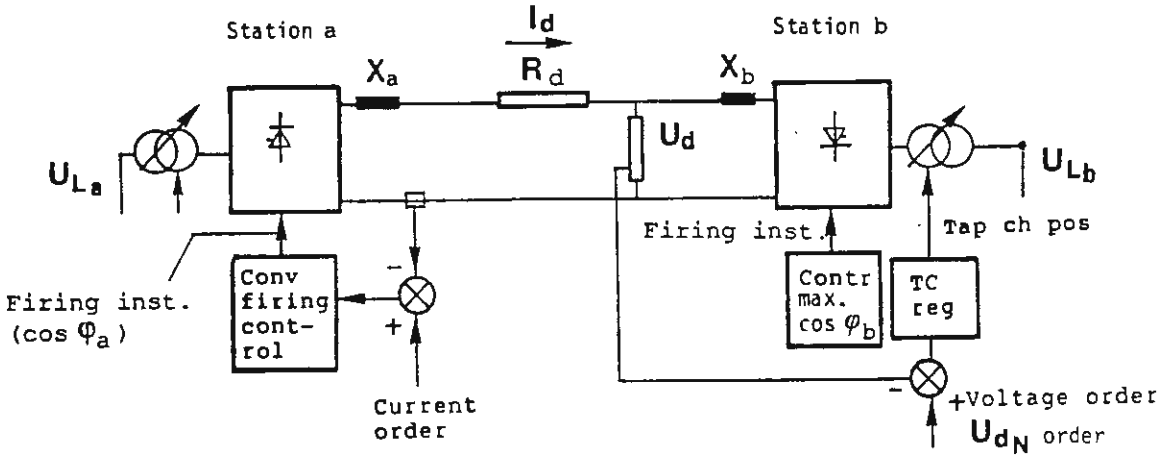

Figure 2-8 **Principle diagram of control system for a two terminal HVDC system using current-source converters.**

at the receiving end (inverter station).

HVDC systems with current-source convertors

The direct current I_d in a two terminal HVDC system is determined by the difference of the direct voltages U_{da} and U_{db} of the two stations (identified by a and b) and the total resistance of the complete dc-circuit, R_d. As the direct voltages for current-source convertors are determined by equation (2-3), we will get the following relationship:

$$I_d = \frac{|k_a \cdot U_{La} \cdot \cos\Phi_a| - |k_b \cdot U_{Lb} \cdot \cos\Phi_b|}{R_d} \qquad (2\text{-}11)$$

Thus it can be seen from this equation that we have basically four control variables at our disposal for the control of the direct current, i.e., k_a, $\cos\Phi_a$, k_b and $\cos\Phi_b$ (the ac-line voltages U_{La} and U_{Lb} are assumed not to be directly controllable and the resistance R_d is assumed to be constant) The constants k_a and k_b are determined by the windings turns ratio of the convertor transformers and can thus be controlled by the setting of the tap-changers. The tap-changer range is usually of the order $\pm$10-15% with steps of 1-1.5%. However, it should be noted that the maximum control speed is limited when conventional mechanical step-changers are used, and that a large part of the control range is used to adjust changes in the ac-line voltages and internal voltage drops in the convertors. As previously described the constants k_a and k_b can also be controlled by pulse width modulation for forced-commutated convertors.

The power factors cos Φ_a and $\cos\Phi_b$ are, besides, the

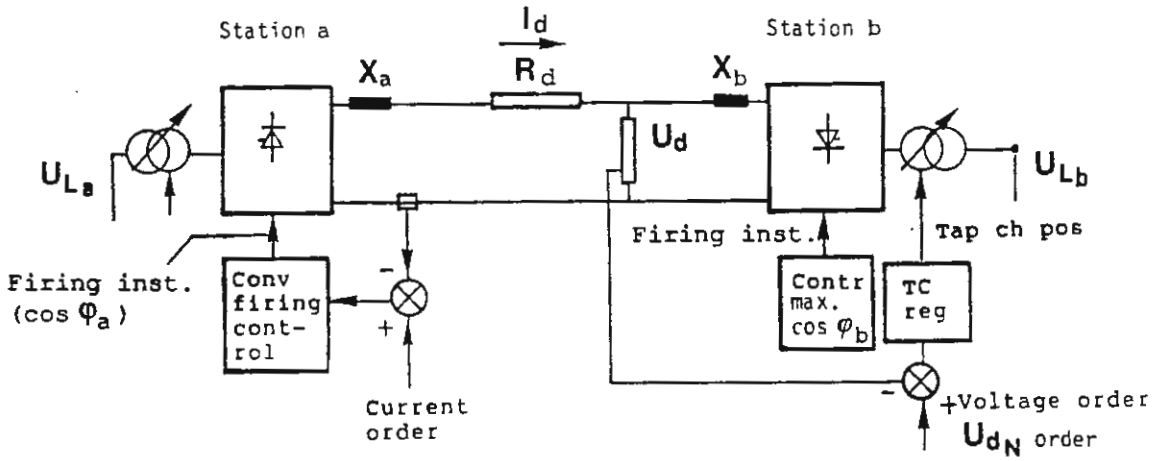

Figure 2-8 Principle diagram of control system for a two terminal HVDC system using current-source converters.

reactances of the convertor transformers, determined by the firing angles of the valves. As the firing angles of the valves can be changed continuously and this also applies for the power factors cos Φ_a and cosΦ_b.

Because the total resistive voltage drop of an HVDC line is usually only a few percent of the rated direct line voltage it is obvious, that it is impossible to achieve adequate control of the direct current by only the control of the tap-changers. Such a control system would be, both, too slow and too inaccurate.

On the other hand it is possible to get a very fast and accurate control by the control of either cosΦ_a or cosΦ_b, or a control of both variables, simultaneously.

As will be further described in a later chapter on controls, the conventional control systems for HVDC systems with current-source convertors is based on the concept that the direct voltage is controlled in one of the two stations by controlling the variable k (normally at the inverter station, station b in figure 2-8) and cosΦ is controlled at the other station to achieve the desired direct current (station a in figure 2-8).

The power factor cosΦ in the station which controls the direct voltage by the tap-changer setting (station b in figure 2-8) is adjusted to the maximum possible value in order to minimize sinΦ and by that the consumption of the reactive power. The tap-changer in the other station (station a in fig 2-8) is also adjusted to effect cosΦ at maximum value, but with the additional requirement that a certain control range of cosΦ must be available for the fast current control.

When line-commutated convertors are used, the convertors in both stations consume reactive power from the ac-systems.

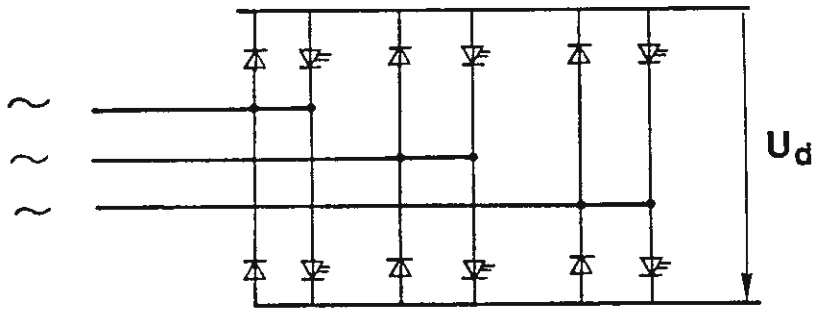

Figure 2-9 Complete two-way six-pulse valve bridge converter for current conduction in both directions.

In principle it may be possible to arrange a fast control of the reactive power in both stations by the control of $\cos\Phi_a$ and $\cos\Phi_b$. However, as long as it is not possible to arrange a simultaneous fast control of k_a and k_b, a fast control of $\cos\Phi_a$ also means that $\cos\Phi_b$ has to be changed. It should also be noted, as can be seen from equation (2-3), that the direct voltage will be adjusted at the same time. Because of that, reactive power control by control of $\cos\Phi$ has until now only been used for back-to-back stations, where keeping the direct voltage close to its rated value is not required. It has also been used for transient control of the ac-voltage in receiving stations connected to weak ac-systems.

The great advantages of fast controls in the direct current and the possibility of limit overcurrents due to faults have resulted that only current-source convertors have been used for HVDC systems. It should especially be noted, that as the power factor $\cos\Phi$ very quickly can be reduced to zero at earth faults on the dc-line, the direct current can also be reduced to zero, which indicates that no circuit breakers with direct current breaking capability are needed for two terminal HVDC systems.

Besides the advantage of limited overcurrents, which also has been of importance for the reduction of the costs of the valves, current-source convertor circuits also require a limited number of valves. Both, the current-source convertor and the voltage source convertor require a valve arrangement with valves for both current directions, if it is required for the direct current to flow in both directions. Figure 2-9 shows a valve arrangement for a three-phase bridge connection permitting the current to flow in both directions. However, as shown in figure 2-9 half of the valves in a voltage-source convertor can be diode-valves as the convertor always operates with the same polarity of the direct voltage across the bridge. For HVDC

systems with current-source convertors it is usually practical to change power direction by changing the polarity of the voltage instead of changing the polarity of the, direct current. Because of that the number of valves can be reduced by a factor of two. On the other hand all valves must be controllable and be designed to be able to sustain both forward and reverse blocking voltage.

The current-source convertors have, as described above, offered a number of advantages for HVDC applications as compared to the voltage-source convertors. Until now only line-commutated convertors have been used although different alternative schemes with forced-commutated current-source convertors have been investigated especially during the last 15 years. The major incentives for such studies have been the short-comings of a line-commutated convertor namely that of always consuming reactive power and thus the need for a certain quality of the ac-system to support the commutations. Various possible types of forced-commutated convertors will be further described in chapter 11.

One of the decisive factors for using line-commutated current source convertors has been the limited cost of the valve, which earlier was responsible for up to 40% of the total cost of a convertor station. However, the fast development of the semiconductor technology has during the last years, drastically reduced the cost for the valves. It has at the same time also increased their overcurrent capability and made it possible to design valves with turn off capabilities. This has now stimulated a new interest in studying alternatives with forced-commutated convertors and especially forced-commutated convertors of the voltage-source type. Some of the main characteristics of a possible HVDC system with forced-commutated voltage-source convertors will be discussed next. The line-commutated current-source convertor circuits used in the HVDC system

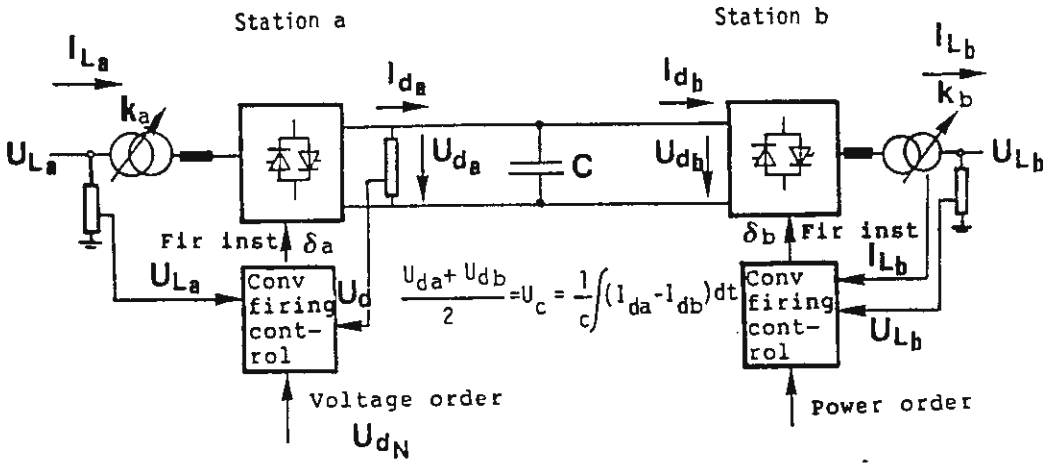

Figure 2-10 Principle layout of a control system for a two-terminal HVDC system using voltage-source converter.

until now will then be treated in some detail in the next chapters.

HVDC systems with forced commutated voltage source convertors

A characteristic feature of a voltage-source convertor is the relationship between the direct voltage U_d and the internal alternating voltage U_{L1}' according to equation (2-4). On the other hand there is no directly controllable relationship between the line voltage U_L and the direct voltage U_d corresponding to equation (2-3) for the current-source convertor. The dc line voltage for a two terminal HVDC system according to figure 2-10 will, because of that, be indirectly controlled through the time integral of the difference of the direct currents in the two stations and the total line capacitance. The direct current in each convertor station is determined by the angle δ according to equation (2-6), which is determined by the firing instants of the valves relative to the phase position of the line-voltage U_L. Figure 2-10 shows a possible way of arranging the control system. The angle δ_b at the receiving station (inverter) is controlled by received active power. The angle δ_a at the sending station is then controlled so that the desired direct voltage on the line is obtained. The control of a multiterminal scheme can be arranged in a similar way such that one station controls the direct voltage and the others are controlled by active power.

As shown in figure 2-10 the constant k_a' and k_b' can be changed by tap-changer control. These constants which determine the relationship between the internal ac-voltage U_{L1}' and the direct voltage U_d according to equation (2-4), can also be controlled in a fast and independent way if pulse width modulation is applied to the convertor. The control of the k_a' and k_b' factor is mainly used for the

control of the reactive power consumption of the convertors. At normal operation when the direct voltage is kept close to its rated value, an increase of the constant will effect decreased consumption or increased generation of reactive power. This is further described in chapter 11 providing details about the forced- commutated voltage-source convertors.
It should, however, be noted that in practice there is a limited range for the increase of the factor k'. This means that an earth fault on the dc-side will reduce the internal voltage U_L' to zero giving high overcurrents in the convertor. Compared to HVDC system equipped with current-source convertors this is definitly a great drawback, which could be decisive for the utilization of voltage-source convertors, especially for overhead line systems. Even the possible overcurrent at other types of faults on the dc-side could be decisive for the future use of voltage-source convertors for HVDC applications.

Another decisive factor is that further development of the semi-conductor and valve technology is necessary since no experience of high voltage valves with turn off capabilities exists so far.

3 OPTIMAL CONVERTOR CIRCUITS

3.1 Criteria for optimal circuit

In this chapter different possible convertor circuits will be analyzed in order to find the convertor circuit optimal for HVDC application. The analysis will be restricted to current-source line commutated convertors although the result is probably valid to, both, voltage-source and forced-commutated convertors. The influence of the reactances in the convertor transformers is neglected, i.e., the commutations are assumed to take place with no overlap.

Usually the optimization of technical equipment is made with the objective to achieve

- minimum costs
- minimum losses
- highest possible reliability and availability
- optimal performance of other characteristics

For HVDC convertor stations the magnitudes of the direct currents and the direct voltages are mainly determined based on optimization of the total costs of stations, lines and losses. Because of that, these values can be assumed to be given. Typical ratings for overhead line transmission systems are 500 kV and 1500-2000A per station and pole.

With regard to other performance characteristics, e.g., behavior at disturbances and risks for commutation failures the behavior is rather independent from the selection of a convertor circuit as long as the convertor is of the

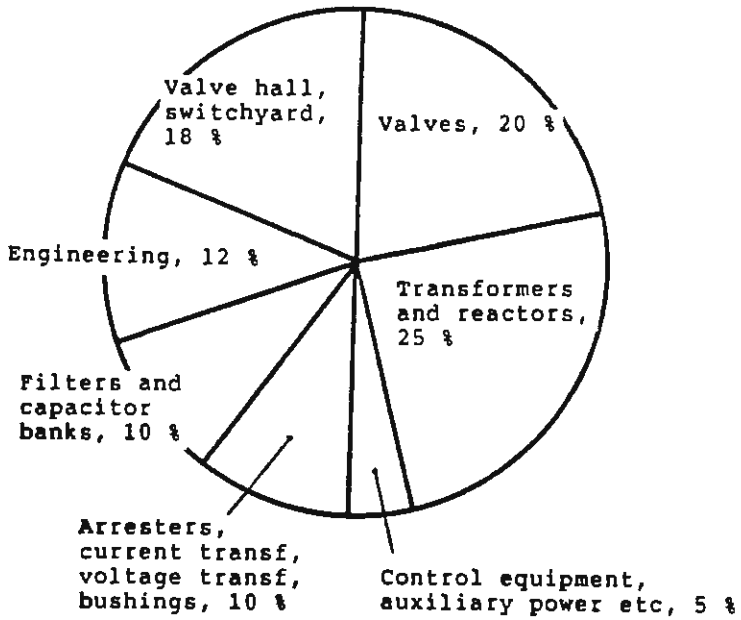

Figure 1-16 Typical distribution of costs of an HVDC converter station.

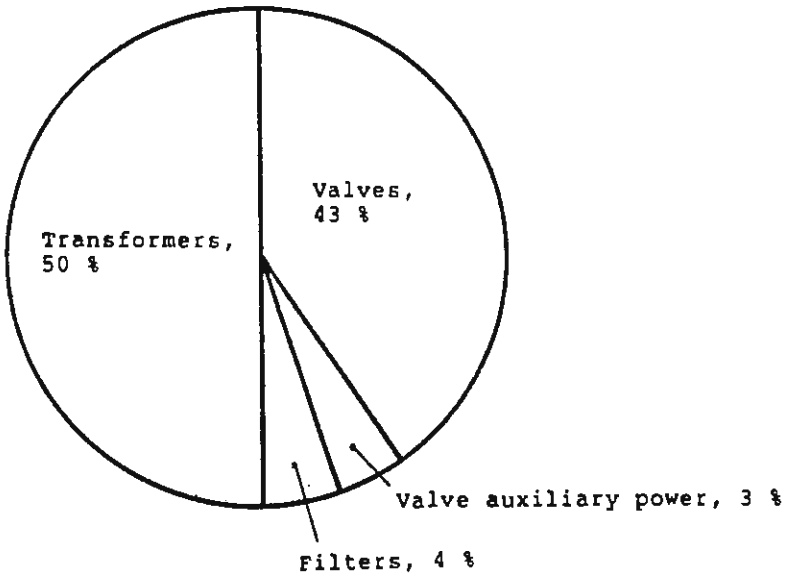

Figure 1-17 Distribution of the total power losses in an HVDC converter station.

line-commutated current-source type. This also applies to reliability and availability, provided that the simplest possible solution with a minimum number of circuit components is selected. On the other hand, to get the most simple and reliable filter solution, a high pulse number is preferred, which increases the number of valve windings and convertor valves.

What is said above implies that it basically is the requirement of minimum costs and losses that determines the choice of a convertor circuit. Figure 1-16 illustrates how the costs for a complete convertor station are typically distributed of the major items. As can be seen from the figure the convertor transformers and the valves are responsible for the major part of the total cost. As can be seen from fig 1-17 they are also responsible for the major part of the total losses. The increased loss evaluation during the past years have caused decreased losses but increased cost for the transformers. On the other hand, the costs of the valves have been steadily reduced due to the fast development of the thyristor technology resulting in increased power handling capability per thyristor. As a result the cost of the convertor transformers is presently the largest cost item as illustrated in figure 1-16.

As can be seen from figure 1-16 the valve hall and switchyard are, after the transformers and the valves, the part responsible for the next largest cost. For a current-source convertor the power factor cosΦ is independent from the convertor circuit used and the harmonics are only determined by the pulse number. This indicates that with a given pulse number, primarily the convertor circuit shall be chosen which gives the lowest transformer cost and secondly the lowest valve cost.

For the convertor transformers the minimum of the total power rating, S_T, of all transformer windings (line-winding

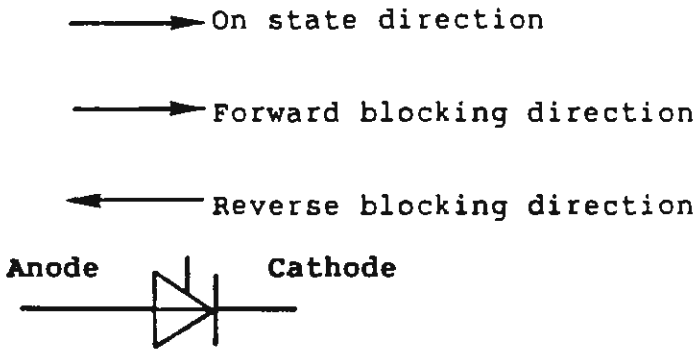

Figure 3-1 Symbol for thyristor and for controllable valve.

and valve-winding(s)) results in an acceptable optimization criteria. This takes into account, both, the investment cost as well as the losses. The real transformer cost will then be influenced by a number of factors such as transport limitations, need for spare transformers and voltage levels.

The cost and losses of the valves are usually proportional to the required voltage withstand levels for all valves, which we can assume to be proportional to the peak value of the forward or reverse blocking voltage ($\hat{U}_{rev}$) across the valves. Although the cost for the valves usually increases less than propotional to the rated current, we will in the following use the minimum rated valve power as defined below as a criteria for circuit evaluation.

$$S_v = k_v \cdot n_v \cdot \hat{U}_{rev} \cdot I_v \qquad (3\text{-}1)$$

k_v is here a constant, n_v is the number of valves and I_v is the r.m.s value of the valve current at rated operation.

3.2 Valve characteristics

The characteristics of the valve as well as the electrical and mechanical design of the valves will be treated in chapter 9. We will only here give a few characteristics essential for the function of the convertor here.

The complete thyristor valve will have basically the same characteristics as that of a single thyristor as it is built of a large number of thyristors connected in series. As can be seen from fig 3-1 the same symbols are usually used for a single thyristor as for a complete valve.

The basic characteristics of an ideal thyristor valve are:

- it can only conduct current in one direction (forward direction)

- a valve in the off-state (not conducting current) can sustain voltage in, both, a forward and a reverse blocking direction.

- a forward blocking voltage and a firing pulse have to be applied to a valve to bring an off-state valve to the on-state (conducting). The valve remains in the on-state (conducting) as long as a current is flowing in the forward direction.

- The voltage-current characteristic in the on-state can be approximated as shown in fig 3-2 i.e. a constant voltage drop plus a voltage drop which is proportional to the magnitude of the current.

- The valves are normally protected internally against overvoltages which are too high in forward blocking direction by protective firing, which brings a thyristor to the on-state before overvoltages, which are too high, will occur. The level of the protective firing is in the range 2.0-2.3 times max forward blocking voltage at rated operation (exclusive commutation overshoot).

- The valves are usually designed for a voltage withstand capability in the reverse blocking direction of about 2.5 times max reverse blocking voltage at rated operation ($\hat{U}_{rev}$).

As the operation conditions at rectifier operation and inverter operation are very similar we will restrict the

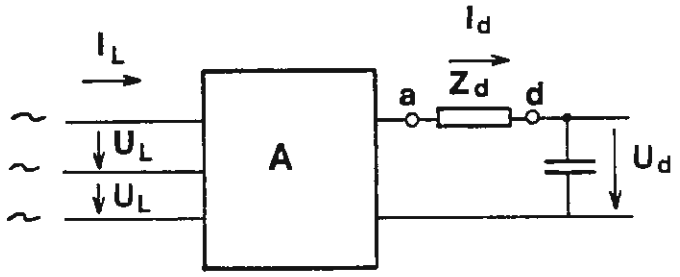

Figure 2-3 Principle of a current-stiff or current-source converter with the impedance Z_d on the dc-side (Ref. [2]).

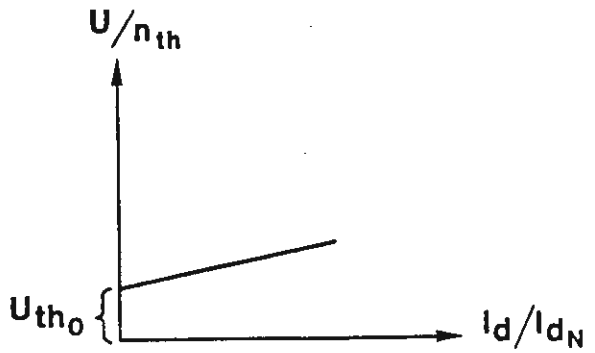

U/n_{th} = On state characteristics of individual thyristor

Figure 3-2 On state characteristics.

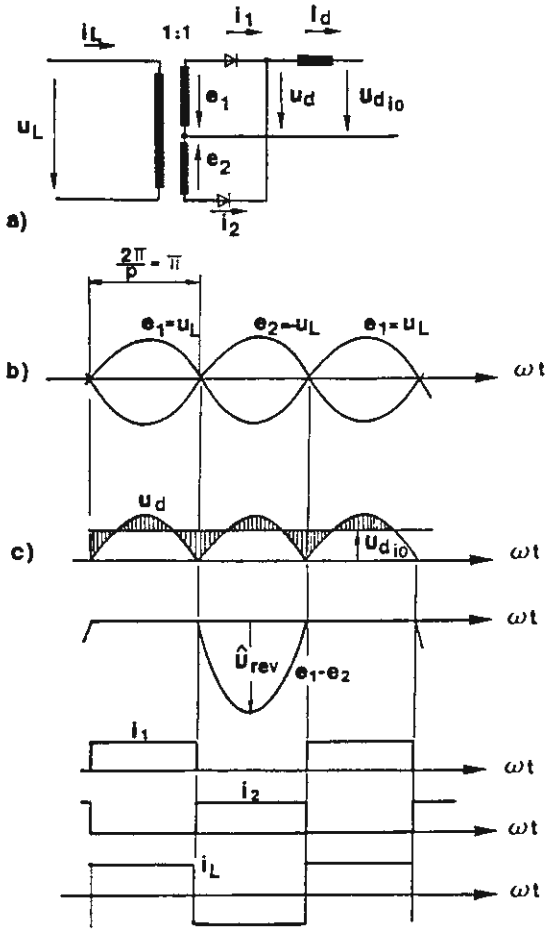

Figure 3-3 Circuit diagram and waveshapes for a single-phase full wave converter, p=2, q=2, s=1.

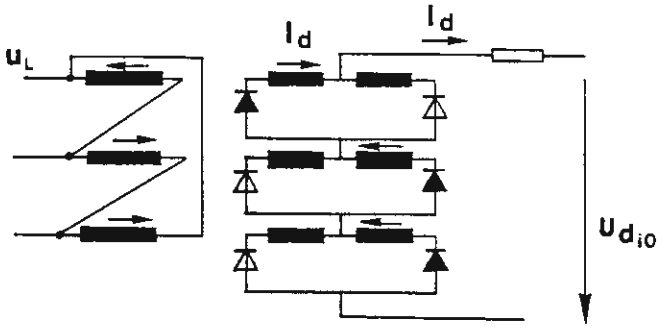

Figure 3-8 Three-phase converter circuit with p=6, q=2, s=3.

following analysis to rectifier operation with non-controlled valves, which cannot take up any forward blocking voltage (diode valves).

3.3 Convertor circuits built up of partial circuits

The block A in figure 2-3 is supposed to consist of the transformer windings and valves which, during one cycle of the network frequency, performs p switchings.

Each switching will generate a new circuit topology resulting in the voltage on the dc-side being built up from the three phases on the ac-side in a different way. As it is assumed that the three ac-voltages are sinusoidal each partial voltage must also be a part of a sinusoidal voltage. We will further assume that each partial voltage has the same waveshape and amplitude, that all the switching intervals have the same lengths and that the partial voltages are phase-shifted $2\pi/p$ rad.

As the valves are assumed to be diodes the partial voltage which has the highest amplitude will automatically be connected to the dc-side. This can be illustrated by the single phase convertor according to figure 3-3 with the pulse-number p=2. The direct current, which is assumed to be completely smoothed, flows through p=2 different circuits during one cycle. Each current circuit consists in this case, of one valve winding and one valve.

In the simple case shown in figure 3-3 each circuit consists only of one transformer winding and one valve, while in other convertor circuits each circuit can consist of a number(s) of partial circuits connected in series as shown in figure 3-8 (s=3). From fig 3-8 it is also obvious that different partial circuits may be connected together during different parts of the cycle. A number of partial

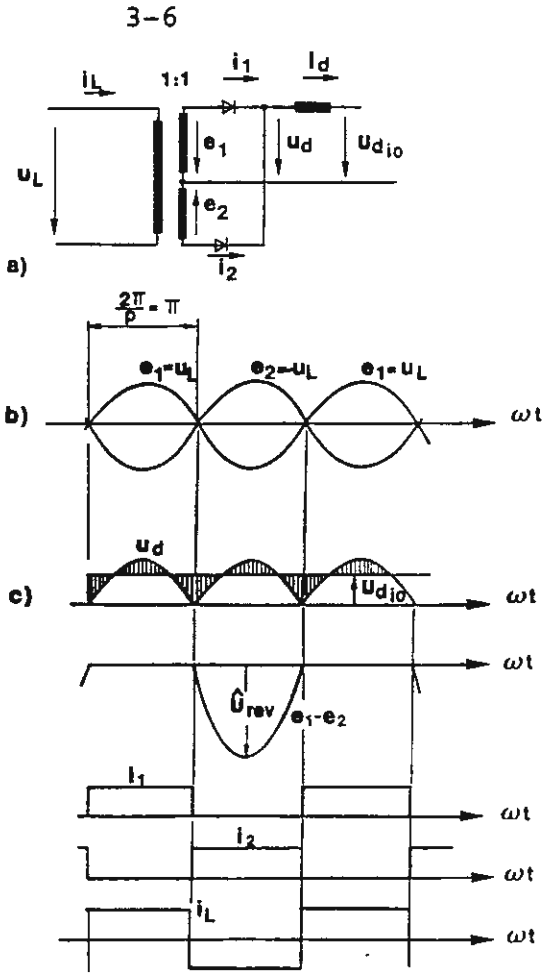

Figure 3-3 Circuit diagram and waveshapes for a single-phase full wave converter, p=2, q=2, s=1.

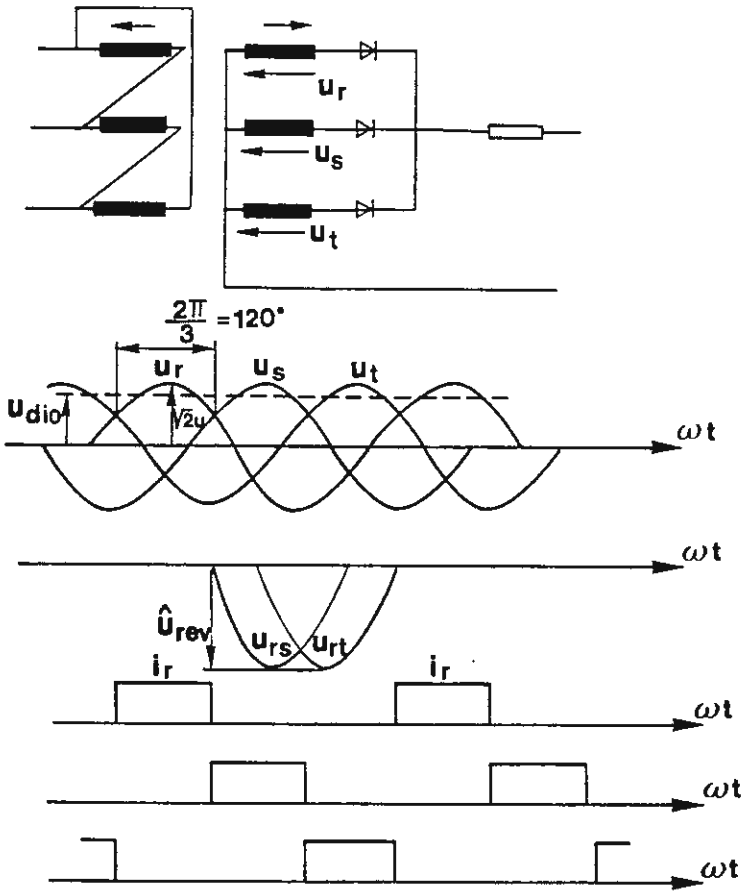

Figure 3-4 Three-phase single-way converter, p=3, q=3, s=1.

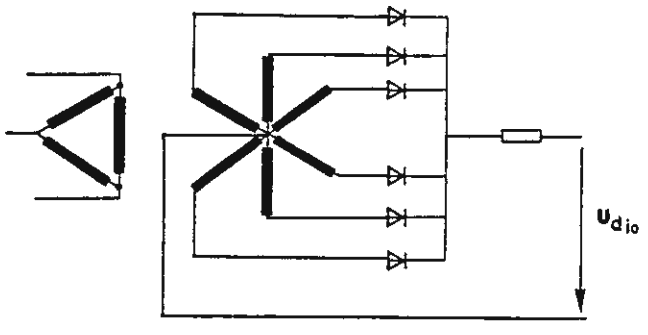

Figure 3-5 Six-phase converter, p=6, q=6, s=1, r=1.

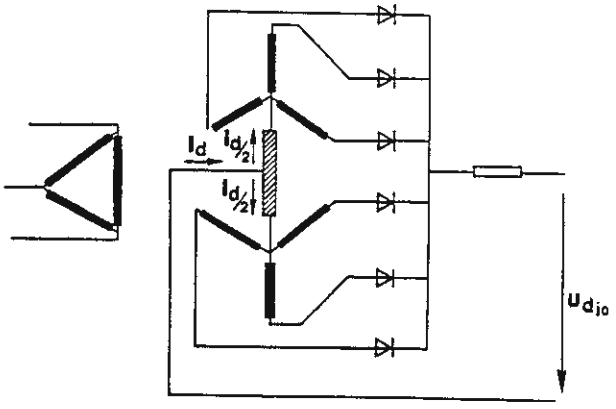

Figure 3-6 Six-pulse converter with interphase transformer, p=6, q=3, s=1, r=2.

circuits (q), which forms a group of circuits, of which only one is conducting current at each moment, is called a commutation group (q=2 in figure 3-3, q=3 in figure 3-4 and q=6 in figure 3-5).

It is possible to arrange the partial circuits so that at each moment the current is equally shared between r parallel partial circuits. This is shown in figure 3-6 in which the direct current is shared equally between two parallel circuits.

The following relationship is valid for the pulse-number, p

$$p = r \cdot s \cdot q \qquad (3\text{-}2)$$

As each partial circuit is conducting during a q-part of the cycle the average current through the valve and the corresponding convertor transformer winding will be

$$I_{vav} = \frac{I_d}{r \cdot q} \qquad (3\text{-}3)$$

The r.m.s value (I_v) of the current becomes

$$I_v = \frac{I_d}{r \cdot \sqrt{q}} \qquad (3\text{-}4)$$

The r.m.s. value of the sinusoidal voltage in each partial circuit is denoted U_v. As each partial circuit is connected during $2\pi/q$ rad the following expression is achieved for the ideal no-load direct voltage

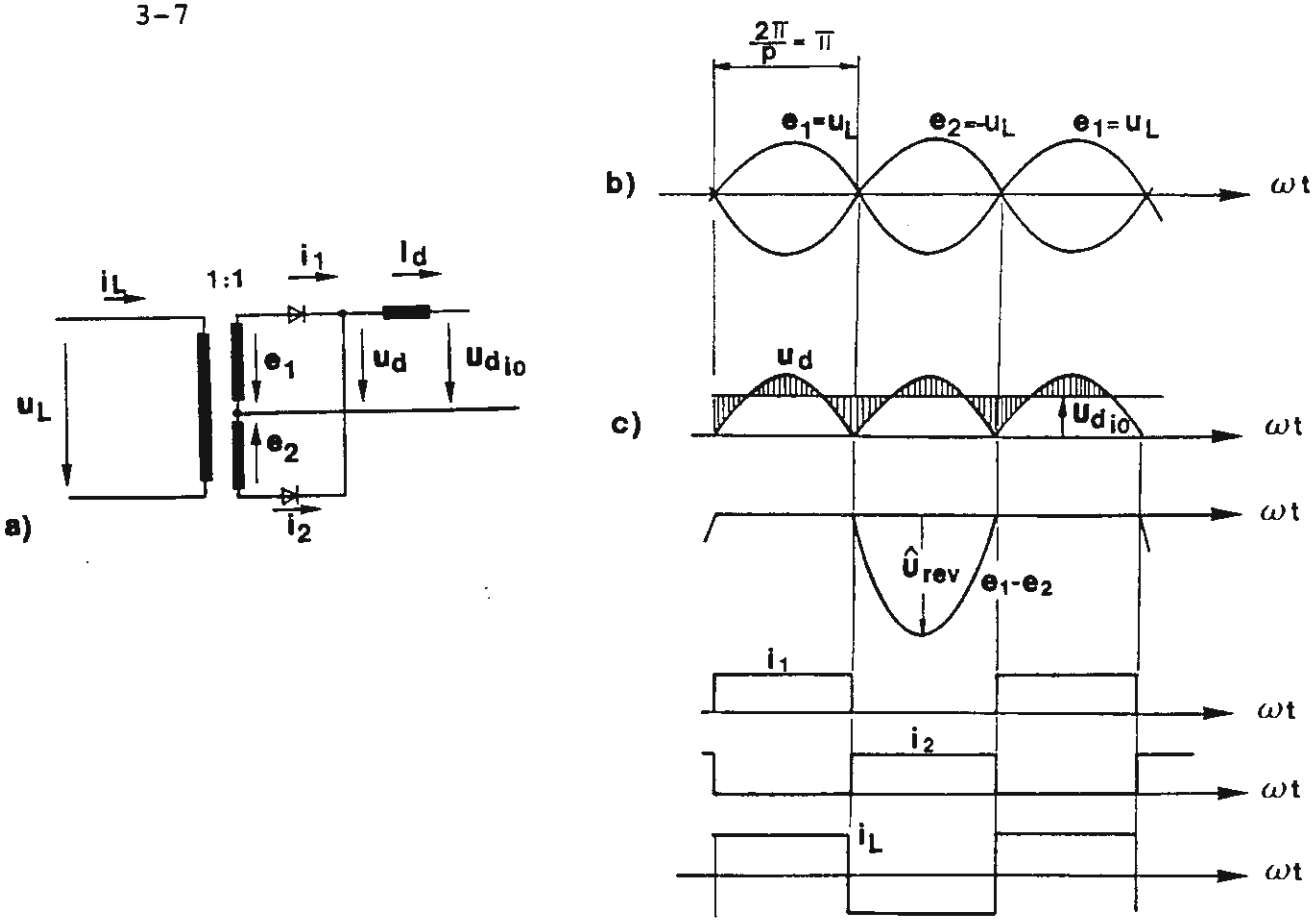

Figure 3-3 Circuit diagram and waveshapes for a single phase full wave converter, p=2, q=2, s=1.

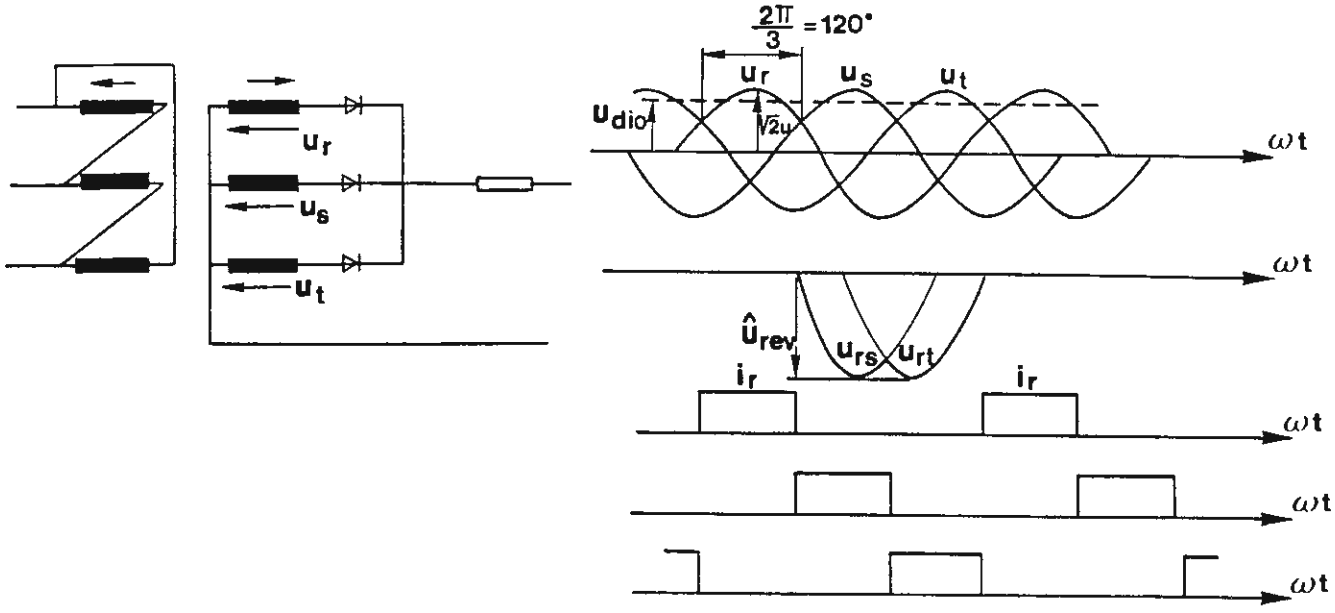

Figure 3-4 Three-phase single-way converter, p=3, q=3,s=1.

$$U_{dio} = s \cdot \frac{q}{\pi} \cdot \sqrt{2} \cdot U_v \int_0^{\frac{\pi}{q}} \cos(\omega t)\, d(\omega t) = s \cdot \frac{q}{\pi} \sin\frac{\pi}{q} \cdot \sqrt{2} \cdot U_v \qquad (3\text{-}5)$$

The peak value of the reverse blocking voltage across the valve depends on whether q is an even or an odd number. This is also obvious from a comparison between the figures 3-3 and 3-4. When q is an even number there is always another partial circuit in the same commutation group having a phase-shift of 180°. This implies that the maximum reverse blocking voltage will occur when this valve is conducting. The peak value of the reverse blocking voltage $\hat{U}_{rev}$ is

$$\hat{U}_{rev} = 2\sqrt{2}\, U_v \qquad (3\text{-}6)$$

When q is an odd number the expression for the corresponding peak value is

$$\hat{U}_{rev} = 2\sqrt{2} \cdot \cos \pi/2q \cdot U_v \qquad (3\text{-}7)$$

The equations (3-5), (3-6) and (3-7) give

$$\frac{\hat{U}_{rev}}{U_{dio}} = \frac{2\pi}{s \cdot q \cdot \sin\frac{\pi}{2q}} \quad \text{when q is even number} \qquad (3\text{-}9)$$

and

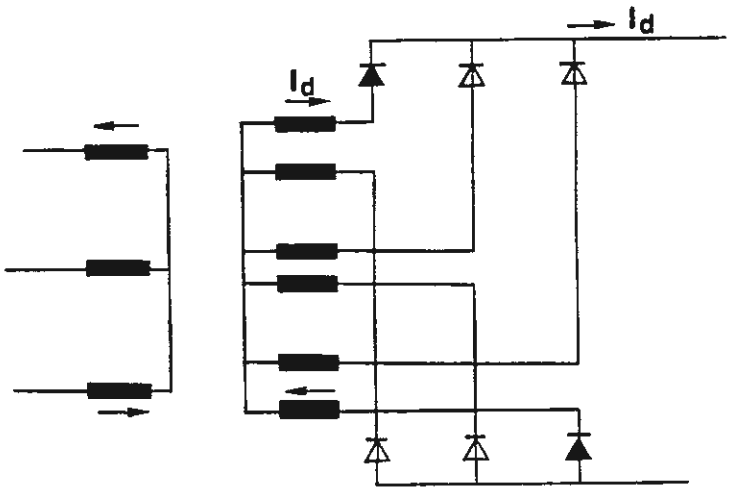

Figure 3-7 Three-phase converter circuit with p=6, q=3, s=2.

$$\frac{\hat{U}_{rev}}{U_{dio}} = \frac{\pi}{s \cdot q \cdot \sin \frac{\pi}{2q}} \quad \text{when q is an odd number} \qquad (3\text{-}9)$$

Optimal convertor circuit with regard to minimum valve costs

The equations (3-2) to (3-8) give sufficient information to evaluate different convertor circuits with regard to minimum cost for valves and transformers. A summary of the convertor circuits of interest with pulse number p=6 is shown in table 3-1.

We assume that the valve cost is proportional to S_v according to equation (3-1). As a result q=3 gives the lowest valve costs and we can either connect the two commutating groups in series or in parallel. However, it should be noted, that it is usually not quite correct to assume that the cost of the valves is proportional to $\hat{U}_{rev} \cdot I_v$ as it is more easy to design a thyristor for a high current than for a high voltage. The thyristors can be designed for the full current without the need for parallel connection for all the studied alternative circuits. As on the other hand a large number of thyristors always have to be connected in series the alternative, which gives the lowest valve voltage is preferred. This implies that the convertor circuit, according to figure 3-7 with q=3, s=2 and r=1, is optimal.

Optimal convertor circuit with regard to minimum transformer cost

The sum of the rated power of the convertor transformer valve windings is.

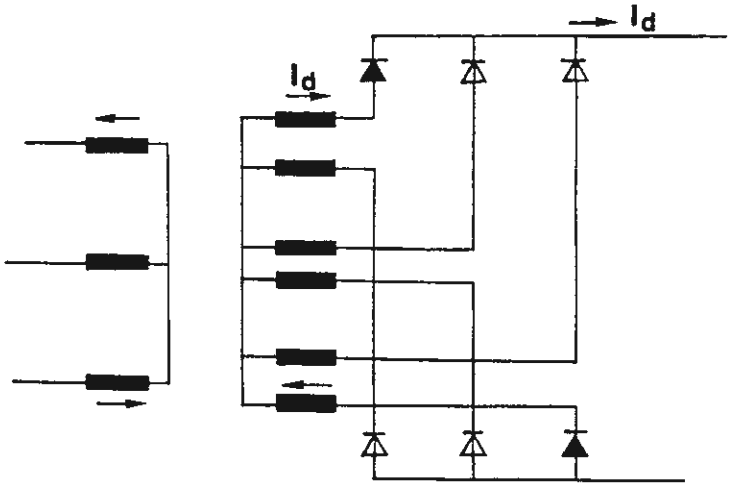

Figure 3-7 Three-phase converter circuit with p=6, q=3, s=2.

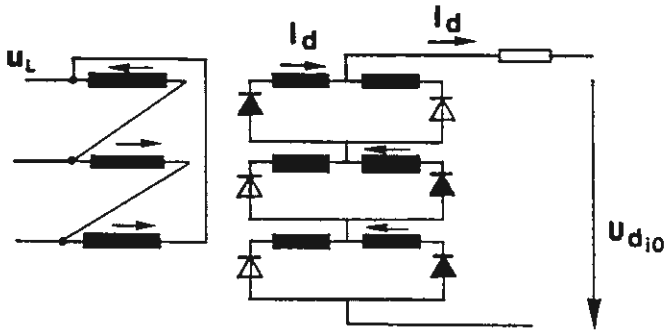

Figure 3-8 Three-phase converter circuit with p=6, q=2, s=3.

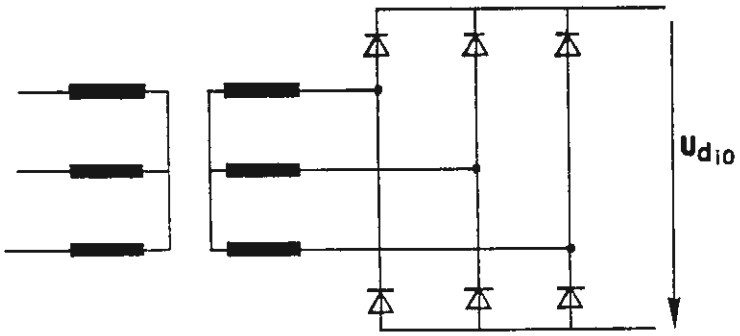

Figure 3-9 Two-way six-pulse bridge converter circuit, p=6, q=3, s=2.

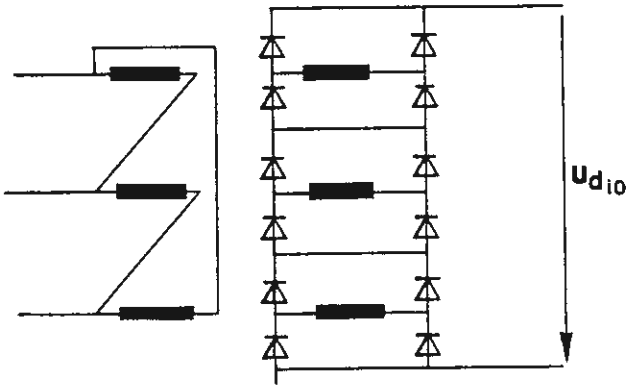

Figure 3-10 Six-phase bridge converter circuit with p=6, q=2, s=6.

$$S_{tv} = p \cdot U_v \cdot I_v \qquad (3\text{-}9)$$

Insertion of the equation (3-2), (3-4) and (3-5) in equation (3-9) gives

$$S_{tv} = p \cdot \frac{\pi \cdot U_{dio}\ I_d}{s \cdot q \cdot \sin\frac{\pi}{q}\ \sqrt{2}\ r\sqrt{q}} = \frac{\pi}{\sqrt{2}} \frac{U_{dio} \cdot I_d}{\sqrt{q} \cdot \sin\frac{\pi}{q}} \qquad (3\text{-}10)$$

This equation shows that the required total ratings of all the valve windings is a function of the the commutation number q. Here it is assumed that each of the p circuits has only one valve winding. If two series-connected windings, fed from phase shifted voltages, are used in each partial current circuit (e.g. zigzag connection) the installed ratings of the windings will be increased.

If we assume that q is a variable that can be varied in a continuous way and determines S_{tv}, according to equation (3-10) with regard to q, we will find that q=2.7 gives an optimum value. This indicates that q=3 gives an optimal solution for the integer case. This is also obvious from the top part of table 3-2 in which the circuits according to the figures from 3-7 and 3-8, have been included.

The power ratings of the line windings have also been included in the table. They are derived by dividing the power ratings of the valve windings (S_{tv}) by $\sqrt{2}$. The factor $\sqrt{2}$ is achieved as the number of line windings is half of the number of valve windings, but the line windings are stressed by current pulses both during the positive and the negative half-cycle.

The circuit according to figure 3-7, is preferred over the circuit, according to figure 3-8 also with regard to minimum cost of the convertor transformer as can be seen

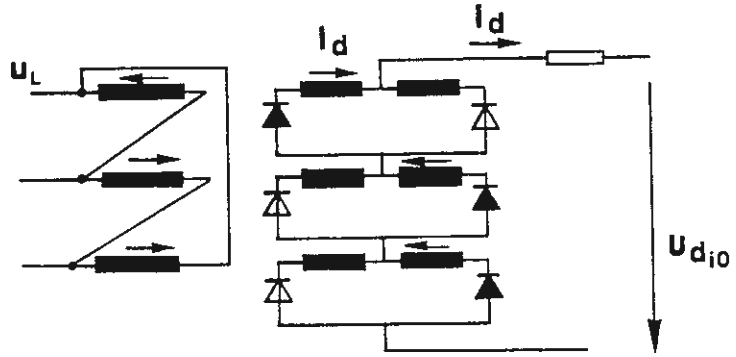

Figure 3-8 Three-phase converter circuit with p=6, q=2, s=3.

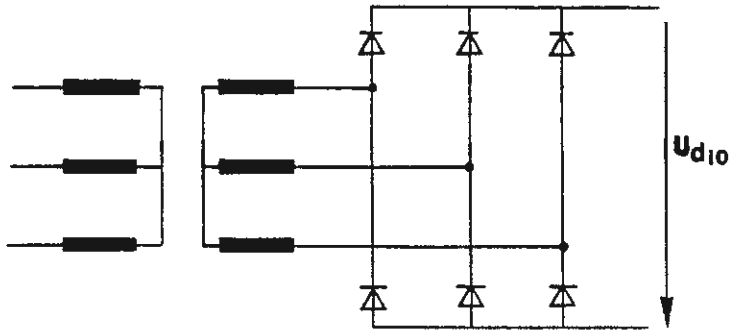

Figure 3-9 Two-way six-pulse bridge converter circuit, p=6, q=3, s=2.

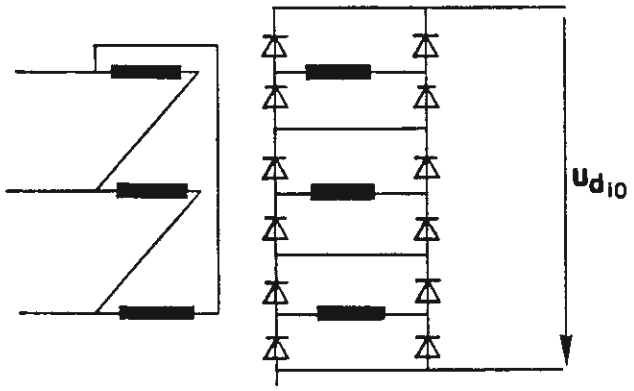

Figure 3-10 Six-phase bridge converter circuit with p=6, q=2, s=6.

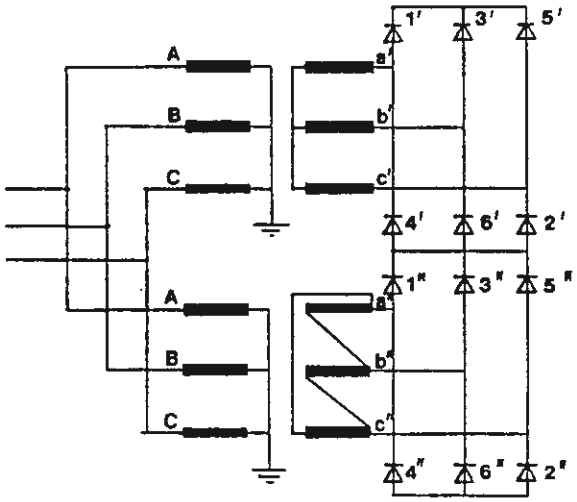

Figure 3-11 Twelve-pulse converter circuit formed by two 30° phase-shifted two-way six-pulse bridge converter circuits connected in series, p=12, q=3, s=4.

from table 3-2. This is also to be expected as q=3. Another advantage with the circuit, according to figure 3-7, is that the sum of the currents in the three phases is equal to zero. The network winding can, because of that, either be Y- or Δ-connected.

3.4 Bridge-connection

The three-phase convertor circuit, according to figure 3-7, can be simplified, as the two valve-windings for each phase can be combined in a single valve-winding for each phase giving the conventional two-way six-pulse bridge convertor circuit, according to figure 3-9. The two valve windings in each phase in the circuit, according to figure 3-8, can also be combined in joint valve-winding if each valve is split up in two valves connected in series according to figure 3-10. The total power rating of the valve windings will be reduced by a factor of $\sqrt{2}$ as the number of valve-windings is reduced by a factor of two, but the current pulses are flowing both during the positive and negative halfcycle. This implies that the same power rating is achieved for both the line windings and the valve windings.

As the number of phases is three, which is close to the optimal calculated commutation number q, only convertor circuits having pulse-numbers with a multiple of three are of interest to be studied. We have seen above that the two-way six pulse bridge convertor is optimal with regard to minimum cost for valves and transformers. Today two such circuits are usually combined by series connection on the dc-side, which gives a circuit, according to figure 3-11, with p=12, q=3 and s=4. The installed relative ratings of valves and convertor transformers will be the same for two six-pulse bridges as for the single bridge because the two bridges usually are operating independent of each other.

The twelve-pulse connection, according to figure 3-11, usually results in higher transformer costs than for the six-pulse connection, according to figure 3-9, as the number of windings will increase. However, the increase in pulse number gives certain savings in the cost for filtering on, both, the ac- and dc-sides, which has been the decisive factor for the choice of this convertor circuit.

The use of convertor circuits with a higher pulse number than twelve for HVDC have also been discussed. Such convertors have, for instance, been used for other applications. However, as this will lead to more complicated and more expensive transformers without resulting in corresponding savings for filtering, it has not been found to be economical attractive so far.

Table 3-1 Convertor circuits and parameters for p = 6

Fig	q	s	r	$\frac{I_{vav}}{I_d}$	$\frac{I_v}{I_d}$	$\frac{U_{dio}}{U_v}$	$\frac{\hat{U}_{rev}}{U_{dio}}$	$\frac{6 \cdot \hat{U}_{rev} \cdot I_v}{U_{dio} \cdot I_d}$
3-5	6	1	1	$\frac{1}{6}$	$\frac{1}{\sqrt{6}}$	$\frac{3\sqrt{2}}{\pi}$	$\frac{2\pi}{3}$	$\frac{2\sqrt{2}\cdot\pi}{\sqrt{3}} = 5{,}13$
3-6	3	1	2	$\frac{1}{6}$	$\frac{1}{2\sqrt{3}}$	$\frac{3\sqrt{6}}{2\pi}$	$\frac{2\pi}{3}$	$\frac{2\pi}{\sqrt{3}} = 3.62$
3-7	3	2	1	$\frac{1}{3}$	$\frac{1}{\sqrt{3}}$	$\frac{3\sqrt{6}}{\pi}$	$\frac{\pi}{3}$	$\frac{2\pi}{\sqrt{3}} = 3.62$
-	2	1	3	$\frac{1}{6}$	$\frac{1}{3\sqrt{2}}$	$\frac{2\sqrt{2}}{\pi}$	π	$\sqrt{2}\cdot\pi = 4.44$
3-8	2	3	1	$\frac{1}{2}$	$\frac{1}{\sqrt{2}}$	$\frac{6\sqrt{2}}{\pi}$	$\frac{\pi}{3}$	$\sqrt{2}\cdot\pi = 4.44$

Table 3-2 Rated power in the convertor transformer windings

Fig	q	s	r	$\frac{S_{tv}}{U_{dio}\cdot I_d}$	$\frac{S_{tL}}{U_{dio}\cdot I_d}$
3-7	3	2	1	$\frac{\pi}{3}\sqrt{2} = 1.48$	$\frac{\pi}{3} = 1.05$
3-8	2	3	1	$\frac{\pi}{2} = 1.57$	$\frac{\pi}{2\sqrt{2}} = 1.11$
3-9	3	2	1	$\frac{\pi}{3} = 1.05$	$\frac{\pi}{3} = 1.05$
3-10	2	3	1	$\frac{\pi}{2\sqrt{2}} = 1.11$	$\frac{\pi}{2\sqrt{2}} = 1.11$

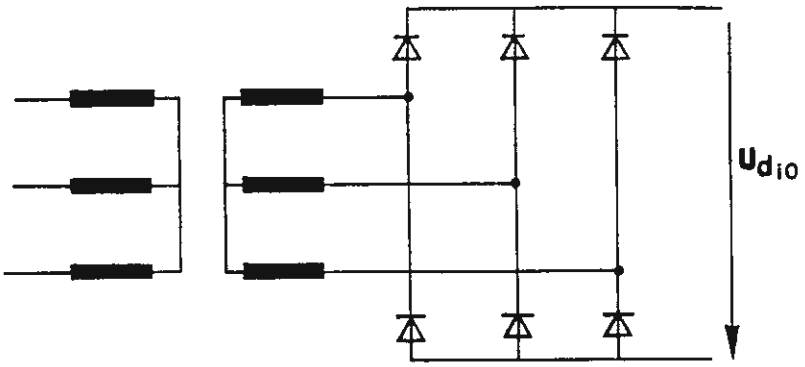

Figure 3-9 Two-way six-pulse bridge converter circuit, p=6, q=3, s=2.

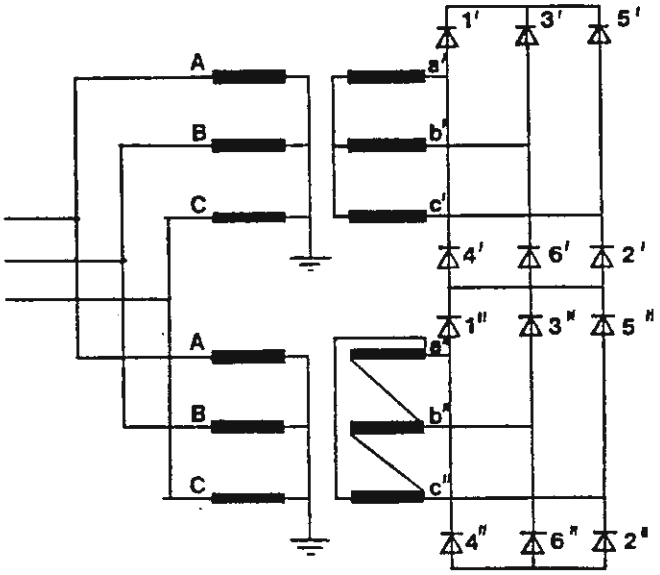

Figure 3-11 Twelve-pulse converter circuit formed by two 30° phase-shifted two-way six-pulse bridge converter circuits connected in series, p=12, q=3, s=4.

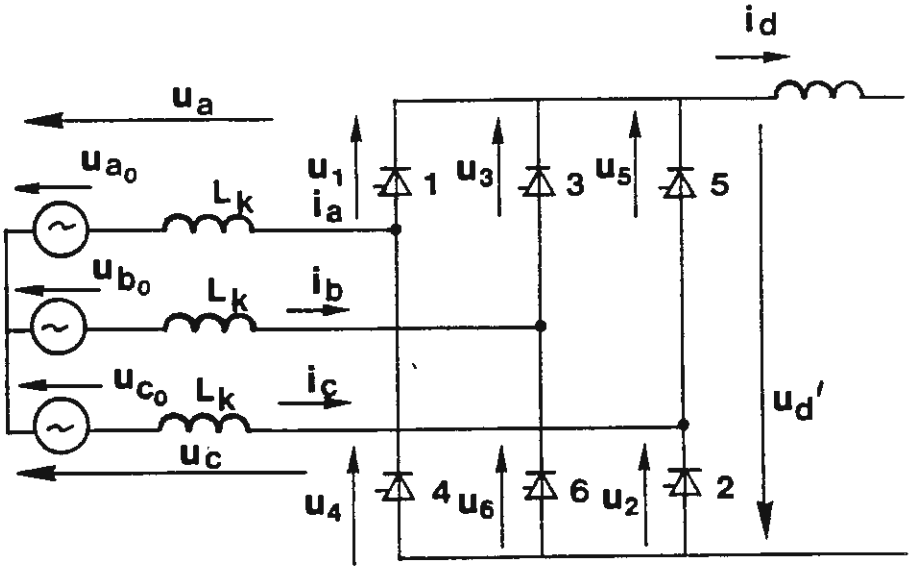

Figure 4-1 Two-way six-pulse converter bridge.

4 CHARACTERISTICS OF A CURRENT-SOURCE LINE-COMMUTATED TWO-WAY SIX-PULSE BRIDGE CONVERTOR

4.1 General, assumptions

As described in chapter two only current-source line-commutated convertors have so far been used for HVDC applications. Different convertor circuits were analysed in the previous chapter and it was found that the two-way six-pulse bridge convertor according to figure 3-9, resulted in lowest costs, both, for convertor transformers and convertor valves.

Two six-phase convertors fed by ac-voltages, which are 30° phase shifted, are usually connected in series on the dc-side to achieve twelve-pulse convertor units according to figure 3-11.

The analyses of the convertor characteristics in the steady state operation can, for the twelve-pulse unit, according to figure 3-11, be restricted to the operation of the six-pulse convertor when it is assumed that the feeding ac-voltages are stiff, symmetric and sinusoidal. This analysis will in the following presentation be based on the circuit, according to figure 4-1. The following assumptions will be valid if nothing else is stated:

- The feeding ac-voltages are symmetric, stiff and sinusoidal,

- The convertor transformers are represented with their leakage inductances (commutating inductance per phase, L_k), which are assumed to have the same magnitude in all phases. The transformer I^2Rt losses are usually neglected.

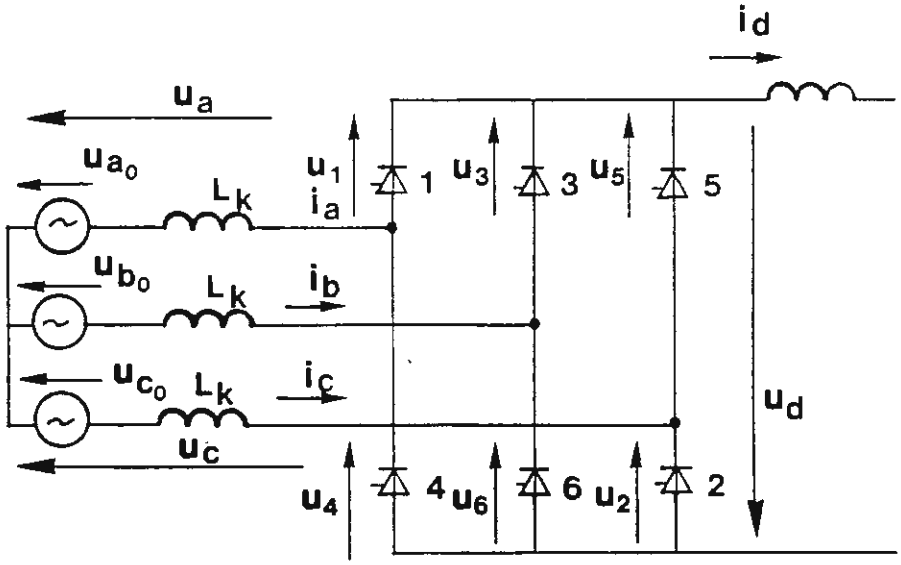

Figure 4-1 Two-way six-pulse converter bridge.

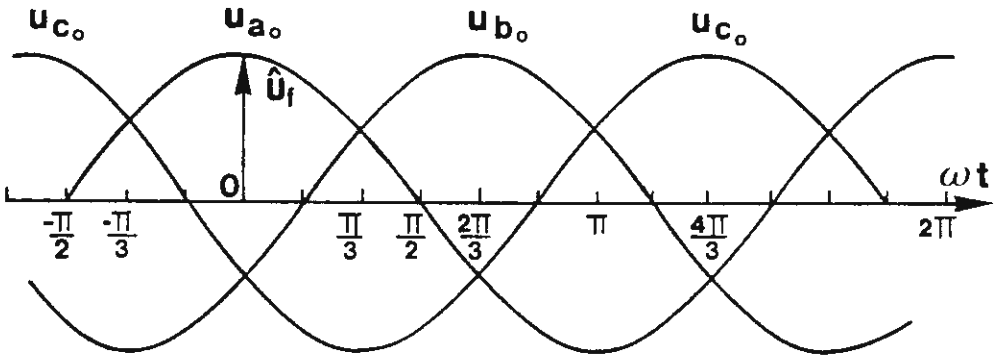

Figure 4-2 Source phase voltages.

- The inductance L_d on the dc-side is assumed to be infinitily large, e.g., the direct current is completly smoothed (no ripples).

- The valves are assumed to be controllable and ideal, i.e., without losses.

- The firings of the valves are assumed to occur at intervals of exactly 60° or $2\pi/6$ rad. (Equidistant firing apart)

The instantaneous values of the feeding alternating voltages are

$$u_{ao} = \hat{U}_f \cos \omega t \qquad (4\text{-}1)$$

$$u_{bo} = \hat{U}_f \cos(\omega t - \frac{2\pi}{3}) \qquad (4\text{-}2)$$

$$u_{co} = \hat{U}_f \cos(\omega t - \frac{4\pi}{3}) \qquad (4\text{-}3)$$

The voltages u_{a0}, u_{b0} and u_{c0} are shown in figure 4-2.

The valves in the convertor bridge function as switching units, which periodically switch in different ac-phases to the dc-side. The valves are numbered in figure 4-1 in the sequence according to which they conduct. In normal operation at least one of the valves in the upper half of the bridge (1,3 and 5) is conducting and one of the valves in the lower half bridge (2, 4 and 6). Each such group is also called a commutation group (See chapter 3, q=3), as the valves 1, 3 and 5 usually commutate independently of the commutations of the valves 2, 4 and 6. The conduction or on-state intervals are illustrated in figure 4-3, which for each time instant shows the valves, which are

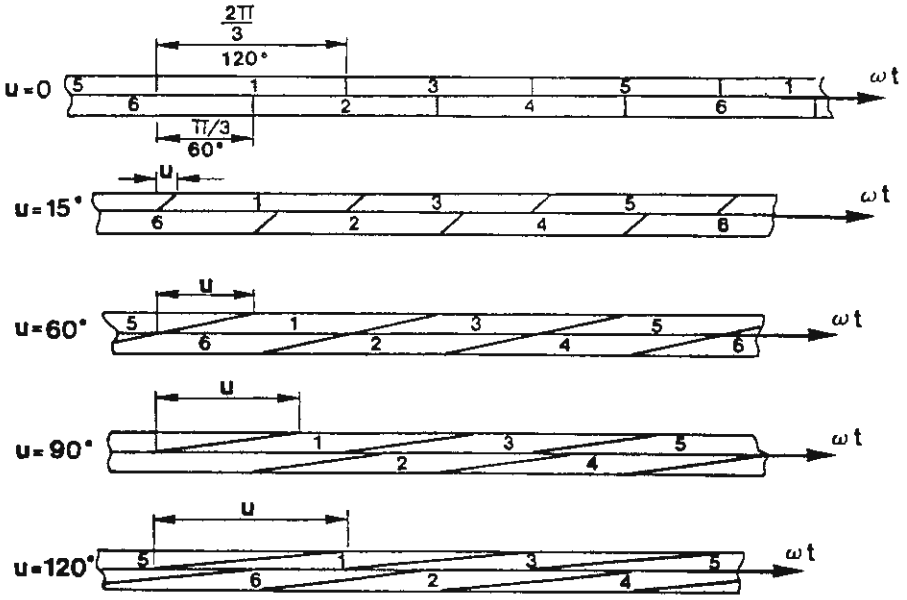

Figure 4-3 Conducting intervals of the valves at different angles of overlap, u.

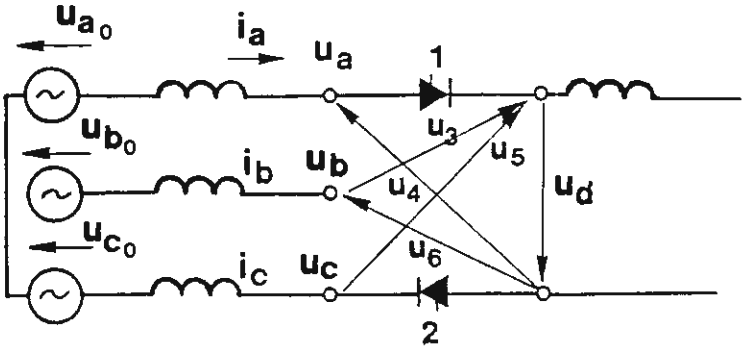

Figure 4-4 Circuit configuration with the valves 1 and 2 conducting.

conducting.

The commutation or switching between two succeeding outgoing and incomming valves will, for small currents occur almost instantanously resulting in an angle of overlap, u, close to zero. When the angle of overlap is zero, only one valve in each commutation group is conducting at any time.

For larger direct currents the commutation will take a certain time because of the commutation inductance. The angle of overlap will then be larger than zero. This implies that two and alternatively three valves will be conducting provided that the angle of overlap is less than 60°.

When the angle of overlap is equal to 60° three valves are always conducting simultaneously. In the case where the angle of overlap is larger than 60° three and alternatively four valves are conducting, as illustrated in figure 4-3. In practice the case with the angle of overlap between zero and 60° is almost always valid.

Since the case with zero overlap angle is the most simple to analyse and provides a good basis for the treatment of the case with the overlap angle larger than zero, we will first analyse the behavior of the convertor at operation with zero overlap angle.

4.2 Analysis of operation at zero angle of overlap, i.e. zero commutation inductance.

$L_k = 0$ and $u = 0$

Analysing the operation of the convertor bridge is

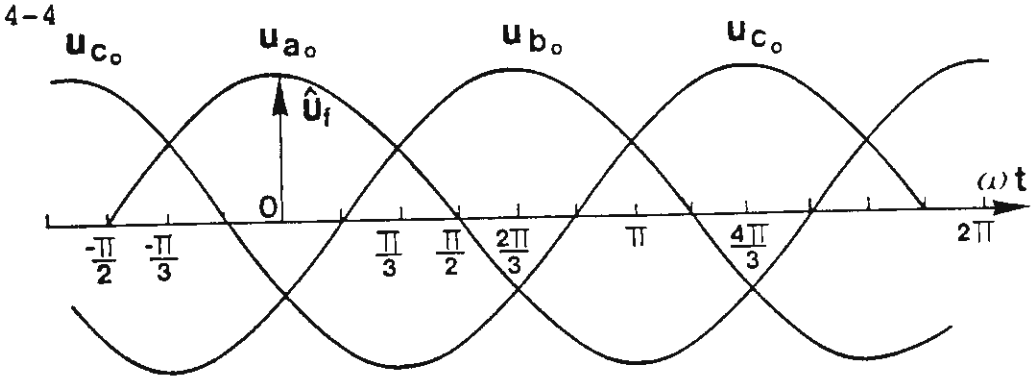

Figure 4-2 Source phase voltages.

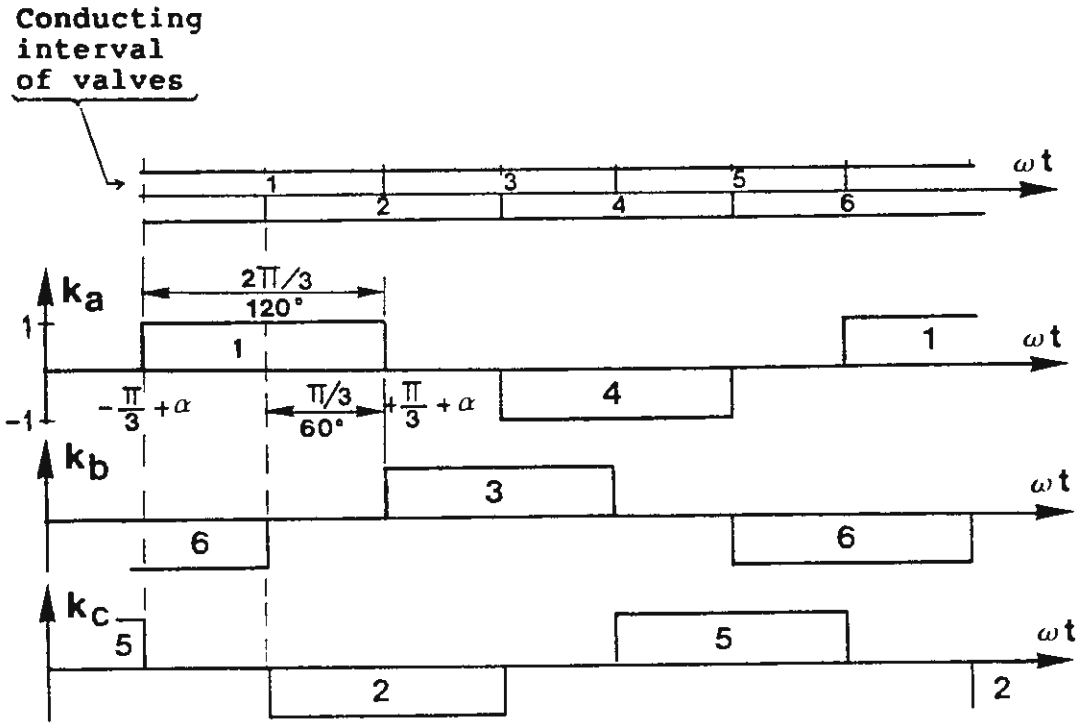

Figure 4-5 Conversion function at two-way six-pulse converter.

substantially simplified, when the angle of overlap is equal to zero. Two of the ac-phases will then, as illustrated in figure 4-4, at each moment be connected to the dc-terminals of the bridge. The third phase is left open. This can also be illustrated by the switching or conversion functions k_a, k_b and k_c, according to figure 4-5. The conversion functions can have the values +1, 0 or -1.

The instantaneous value of the bridge voltage u_d can now be achieved by multiplying the phase voltages with the corresponding conversion function, i.e.,:

$$u_d = u_{ao} \cdot k_a + u_{bo} \cdot k_b + u_{co} \cdot k_c \qquad (4-4)$$

The instantaneous values of the currents in the ac-phases can, in a similar way, be achieved by multiplying the instantaneous value of the bridge current i_d with the conversion functions i.e.

$$i_a = k_a \cdot i_d \qquad (4-5)$$

$$i_b = k_b \cdot i_d \qquad (4-6)$$

$$i_c = k_c \cdot i_d \qquad (4-7)$$

It should be noted that equations (4-4) to (4-7) are valid for an arbitrary waveshape (time-function) of the phase-voltages and the bridge current.

The valves will start to conduct (fire) as soon as the voltages across the valves are positive, provided the valves are non-controllable, i.e., diode valves. This means that valve 1 will start to conduct at $\omega t = -\pi/3$ and will continue to conduct until $\omega t = \pi/3$ with the phase voltages according to figure 4-2. Symmetric phase-voltages, according to figure 4-2, will then also result in

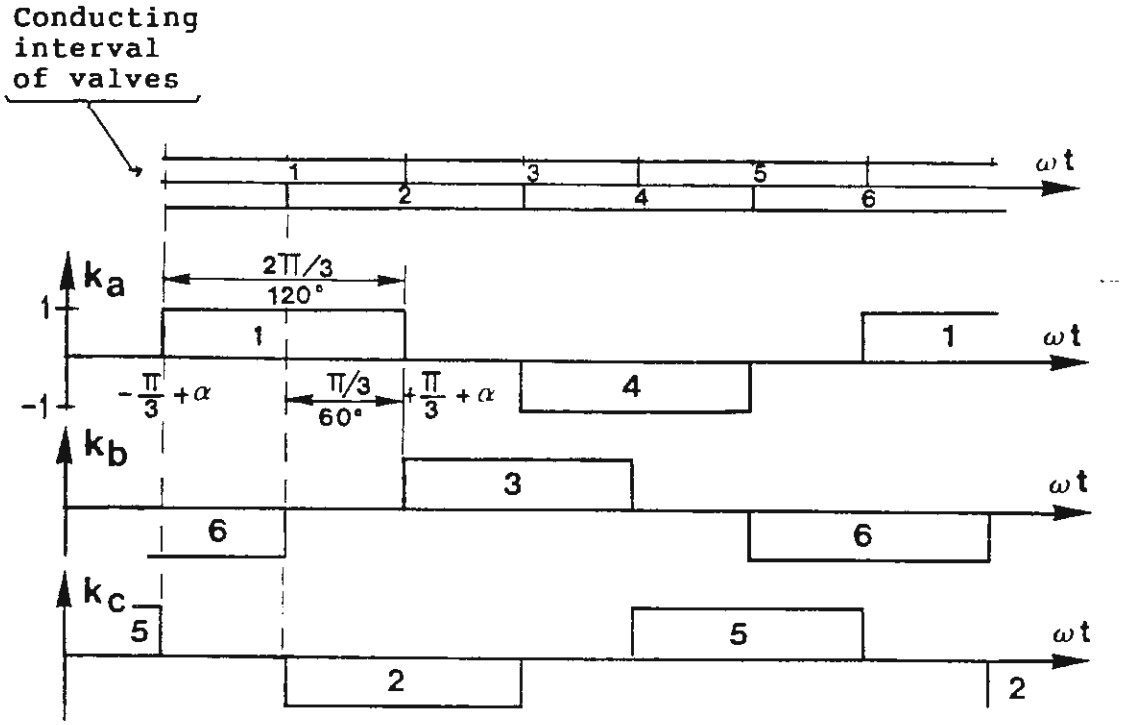

Figure 4-5 Conversion function at two-way six-pulse converter.

symmetrical conversion functions.

The firing of controllable valves (thyristor valves) can be delayed, and it is then required that, both, the voltage across the valve is positive and a firing pulse is sent to the valve before the valve will conduct. The delay in the firing instant for a controllable valve measured in °el or radians, as compared to the non-controllable case, is called the delay angle or firing angle and is denoted with α. The firing angle is thus measured relative to the zero-crossing of the line-to-line voltage (valve voltage).

The firing-control system is usually designed to provide equal time intervals between consecutive firing pulses, i.e., equidistant firing. This means that the conversion function, according to figure 4-5, will be completely symmetrical for the case of $u = 0$. A delay of the firing instants of α rad means that the conversion function is also delayed α rad.

For unsymmetrical line voltages the firing angle can either be measured from the zero crossings of the voltages for each individual valve to the firing instants or alternatively from the zero crossings of the positive sequence component of the line-to-line voltages. The last alternative is more often preferred. The following equations derived for the symmetrical case will then also be valid for the unsymmetrical case provided that the firing isequidistant and angle of overlap is zero.

The direct voltage component of the bridge voltage U_d can be derived either from integration of the line-to-line voltages or phase voltages during one cycle. As the contribution from each phase and from each half-cycle is the same the direct voltage can, for instance, be calculated from equations (4-1) and (4-4) giving:

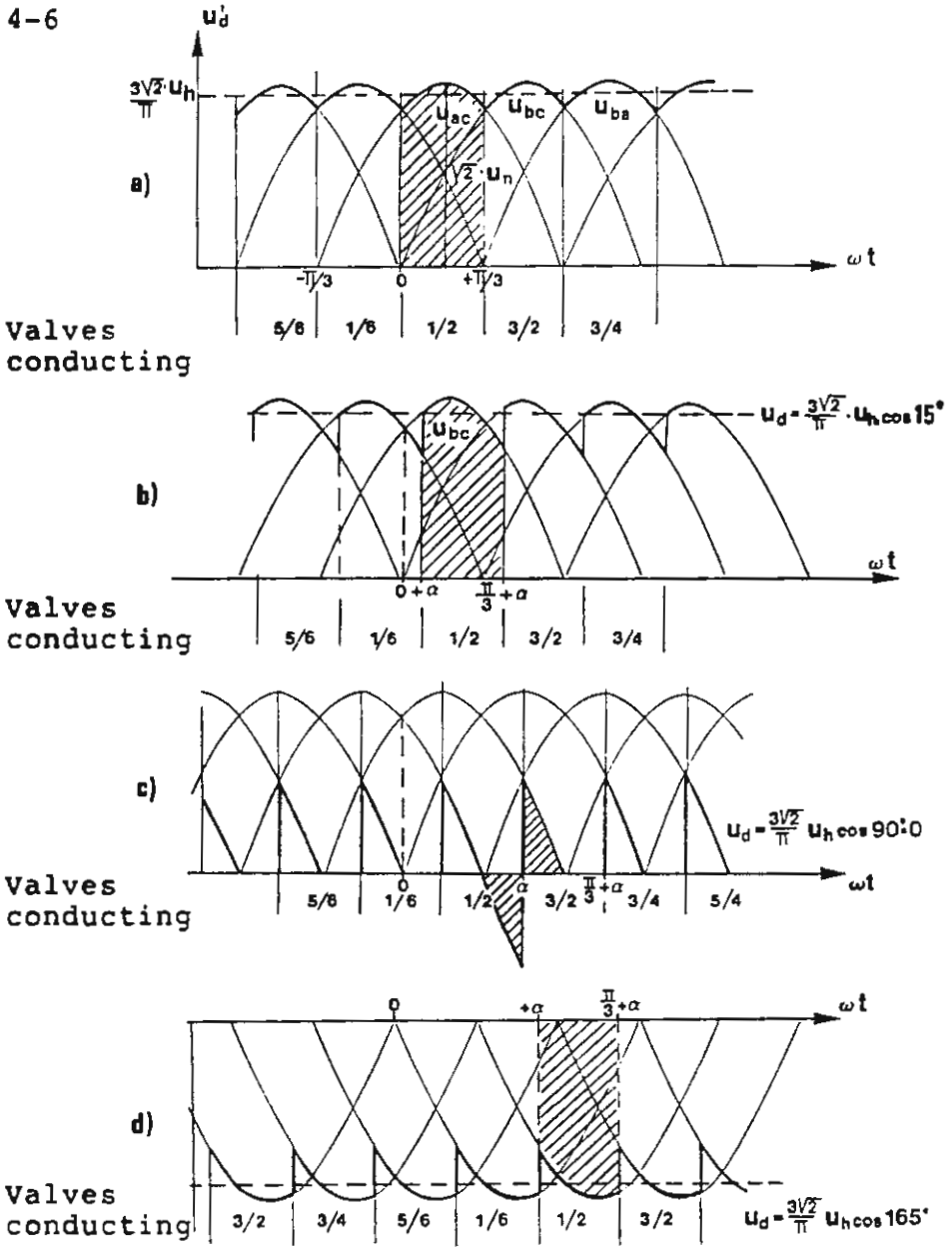

Figure 4-6 Converter bridge voltages, instantaneous values at $L_k=0$, $u=0$ and a) $\alpha=0°$ b) $\alpha=15°$ c) $\alpha=90°$ d) $\alpha=165°$

$$U_d = \frac{6\hat{U}_f}{2\pi} \int_{-\frac{\pi}{3}+\alpha}^{\frac{\pi}{3}+\alpha} \cos \omega t \cdot d(\omega t) =$$

$$= \frac{3\hat{U}_f}{\pi} \cdot \sin(\omega t) \Big|_{-\frac{\pi}{3}+\alpha}^{\frac{\pi}{3}+\alpha} = \frac{3\sqrt{3}}{\pi} \hat{U}_f \cdot \cos \alpha \qquad (4\text{-}8)$$

Usually, the relationship between the direct voltage and the r.m.s. value of the line-to-line voltage is given, i.e.

$$U_d = 3\sqrt{2}/\pi \cdot U_h \cdot \cos\alpha \qquad (4\text{-}9)$$

The value of the direct voltage at zero angle of overlap, no losses and zero firing angle is called the ideal no-load direct voltage and is denoted U_{di0}.
The equation (4-9) gives:

$$U_{dio} = 3\sqrt{2}/\pi \cdot U_h \qquad (4\text{-}10)$$

Insertion in eq. (4-9) gives:

$$U_d = U_{dio} \cos\alpha \qquad (4\text{-}11)$$

The firing angle α can theoretically be varied within the whole interval from 0 degrees or radians to 180 degrees or π radians.

This means that the direct voltage can be changed from $+U_{di0}$ to $-U_{di0}$.

Operation at $U_d > 0$ is referred to as rectifier operation and at $U_d < 0$ as inverter operation. Figure 4-6 illustrates the instantanous values of the bridge voltage at different

firing angles.

As can be seen from figure 4-6 each line-to-line voltage is during, $\pi/3$ radians, connected to the dc-side. This makes it very simple to calculate the bridge-voltage directly from the line-to-line voltage by integration from $-\pi/6 + \alpha$ to
$+\pi/6 + \alpha$.

An alternative to calculating the direct voltage using the conversion functions will now be presented. This may seem to be unnecessarily complicated but has the advantage of giving, both, the voltage harmonics as well as the most general relationships for the interaction between the ac-side and dc-side, which is of interest, e.g., for studying the behaviour of operation with unsymmetrical ac-voltages.

The conversion function for phase a may be expressed as a Fourier series.

$$k_a(\omega t) = \sum_{n=-\infty}^{+\infty} K_{an} \cdot e^{jn\omega t} \qquad (4\text{-}12)$$

in which:

$$K_{an} = \frac{1}{2\pi} \int_{-\pi}^{\pi} k_a(\omega t) \cdot e^{-jn\omega t} \, d(\omega t) \qquad (4\text{-}13)$$

Lower case letters are used for the instantaneous values of the time-function, e.g., $k_a(\omega t)$.

The integration of equation (4-13) can be limited to the interval from $-\pi/3 + \alpha$ to $\pi/3 + \alpha$, for which, interval $k_a(\omega t) = 1$.

$$K_{an} = \frac{1}{\pi} \int_{-\frac{\pi}{3}+\alpha}^{\frac{\pi}{3}+\alpha} e^{-jn\cdot\omega t}\, d(\omega t) = \frac{2 \sin\left(n\cdot\frac{\pi}{3}\right)}{n\cdot\pi} \cdot e^{-jn\alpha} \quad (4\text{-}14)$$

Taking into account that $\sin(n\cdot\pi/3) = -\sin(-n\cdot\pi/3)$ and insertion in equation (4-12) gives:

$$k_a(\omega t) = \frac{2}{\pi} \cdot \sum_{n=1}^{+\infty} \frac{\sin\left(n \cdot \frac{\pi}{3}\right)\left(e^{jn(\omega t-\alpha)} + e^{-jn(\omega t-\alpha)}\right)}{n}$$

or

$$k_a(\omega t) = \frac{4}{\pi} \sum_{n=1}^{+\infty} \frac{\sin\left(n \cdot \frac{\pi}{3}\right) \cos n(\omega t-\alpha)}{n}$$

As $k_a(\omega t) = -k_a(\omega t+\pi)$ we will get $K_{an}=0$ for n being an even number.

From equation (4-14) it can also be seen that $K_{an}=0$ for n being a multiple of three. We will thus only get contributions for n=1,5,7,11,13 and so on, i.e. when $n\geq 1$ and $n=6m\pm 1$, where m is a positive integer 0,1,2 etc. For these harmonics we get

$$k_a(\omega t) = \frac{2\cdot\sqrt{3}}{\pi} \cdot \sum_{n=1}^{+\infty} \pm \frac{\cos n\,(\omega t-\alpha)}{n} \quad (4\text{-}15)$$

(The positive sign is obtained for n=6m+1 and the negative sign for n=6m-1)

We will get $k_b(\omega t)$ and $k_c(\omega t)$ by replacement of α by $\alpha+2\pi/3$ and $\alpha+4\pi/3$ respectively and insertion in equation (4-15) will result:

$$k_b = \frac{2\sqrt{3}}{\pi} \sum_{n=1}^{+\infty} \pm \frac{\cos n\left(\omega t - \frac{2\pi}{3} - \alpha\right)}{n} \qquad (4\text{-}16)$$

and

$$k_c = \frac{2\sqrt{3}}{\pi} \sum_{n=1}^{+\infty} \pm \frac{\cos n\left(\omega t - \frac{4\pi}{3} - \alpha\right)}{n} \qquad (4\text{-}17)$$

where $n \geq 1$, $n = 6m \pm 1$ and $m = 0,1,2$ etc.

The conversion functions can also be looked at as a three-phase system in which harmonics having a positive sign in the equations above have a positive sequence and those with a negative sign have a negative sequence.

If we now apply the equations (4-15) to (4-17) to equation (4-4) using equations (4-1) to (4-3) we will get:

$$u_d = \frac{2\sqrt{3}\cdot\hat{U}_f}{\pi} \sum_{n=1}^{\infty} \pm\frac{1}{n}\left[\cos \omega t \cdot \cos n(\omega t-\alpha)+\cos(\omega t- \tfrac{2\pi}{3}) \cdot \right.$$

$$\left. \cdot\cos n(\omega t- \tfrac{2\pi}{3} -\alpha)+ \cos(\omega t- \tfrac{4\pi}{3})\cdot\cos n(\omega t- \tfrac{4\pi}{3} - \alpha)\right] \qquad (4\text{-}18)$$

or simplified

$$u_d = \frac{3\sqrt{3}}{\pi} \hat{U}_f \sum_{n=1}^{\infty} \pm \frac{1}{n} \left[\cos\left[(n+1)\ \omega t - n\alpha\ \right] + \cos\left[(n-1)\omega t - n\alpha\right]\right] \qquad (4\text{-}19)$$

Contributions to u_d are achieved for values of (n+1) and (n-1) equal to $\nu = 6m$ and $m = 0,1,2,\ldots$.

Equation (4-19) can now be rewritten

$$u_d = \frac{3\sqrt{3}}{\pi} \hat{U}_f \sum_{\nu=6}^{\infty} \left\{ - \frac{\cos[\nu \cdot \omega t - (\nu-1)\alpha]}{\nu-1} + \right.$$
$$\left. + \frac{\cos[\nu \cdot \omega t - (\nu+1)\alpha]}{\nu+1} + \cos \alpha \right\} \qquad (4\text{-}20)$$

in which $\nu = 6 \cdot m$ and $m = 1,2,3.....$

From equation (4-20) it is seen that the direct voltage component of u_d is

$$U_d = \frac{3\sqrt{3}}{\pi} \hat{U}_f \cos \alpha$$

which is in agreement with equation (4-8). The voltage u_d also contains a number of harmonic components of the order $6 \cdot m$. This will be further discussed in chapter 6, which deals with harmonics and filters.

The direct voltage component of u_d is derived from the fundamental ($n=1$) component of the conversion function in equations (4-15) to (4-17) multiplied by the fundamental component of the phase-voltage, which has the same phase-sequence. If the phase-sequences would have been different, which is valid for a negative-sequence ac-voltage components, a second order harmonic component but no direct voltage would have been generated. It should be noted that asymmetries on the ac-side only give negative sequence components but no zero sequence component on the valve side of the convertor transformer.

At zero overlap angle the currents in the ac-phases are determined by the current on the dc-side multiplied by the conversion functions for the three phases. As a result the ac-currents will, at constant and completly smoothed direct

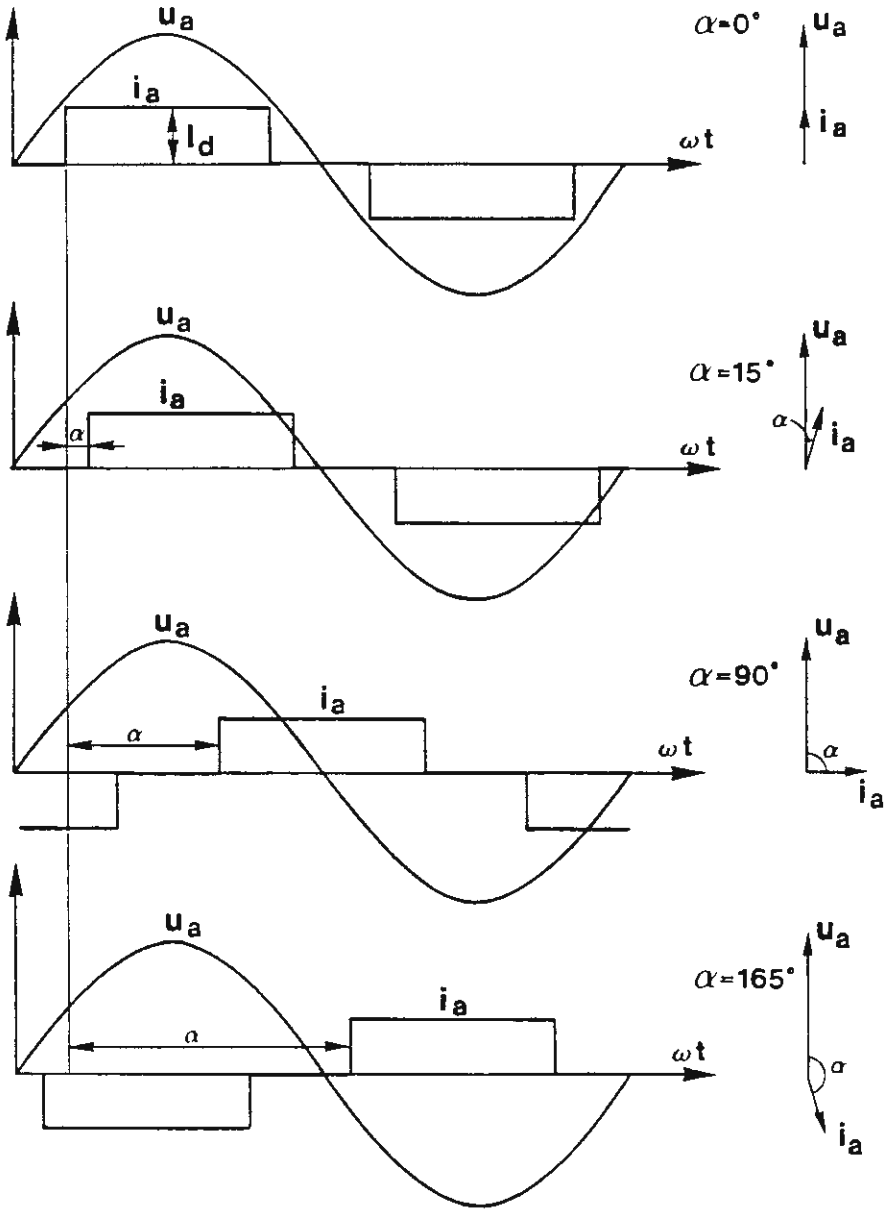

Figure 4-7 Phase-voltages and phase-currents at different values of the firing angle α. Commutation inductance L_k=0 and angle of overlap u=0.

current, have exactly the same wave-shapes as the conversion functions, as can be seen from figure 4-7. This figure shows both the waveshape and phase position in a phasor diagram for the fundamental frequency current component in phase a. The amplitude and phase position of the fundamental frequency component of the phase current is achieved from equation (4-15), which is:

$$i_{a1} = \frac{2\sqrt{3}}{\pi} \cdot I_d \cos(\omega t - \alpha) \qquad (4\text{-}21a)$$

Equation (4-21a) results in the following relationship between the direct current and the r.m.s. value of the fundamental of the phase-current on the valve side of the convertor transformer.

$$I_1 = \frac{\sqrt{6}}{\pi} \cdot I_d \qquad (4\text{-}21b)$$

The subscript a has been dropped because the current is the same in all the three phases. The phase-lag of the fundamental of the phase-current relative to the phase-voltage is equal to the firing angle i.e., $\phi=\alpha$.

The fact that the ac-current is directly proportional to the magnitude of the direct current is a characteristic feature of a current-source convertor (compare equation (2-1)).

It should be noted that equations (4-21a) and (b) can be directly derived by Fourier analyses of the ac-currents without using conversion functions.

The apparent power related to the fundamental of the ac-voltage and current is defined as

$$S_1 = \sqrt{3} \cdot U_h \cdot I_1$$

Equations (4-10) and (4-21b) result in:

$$S_1 = U_{dio} \cdot I_d \qquad (4\text{-}22a)$$

The active power on the ac-side has to be equal to the active power on the dc-side as the losses in the convertor have been neglected. This gives:

$$P = S_{(1)} \cdot \cos\phi = U_d \cdot I_d = U_{dio} \cdot I_d \cdot \cos\alpha \qquad (4\text{-}23)$$

Insertion of equation (4-22) in equation (4-23) gives:

$$\cos\phi = \cos\alpha$$

and

$$\cos\phi = U_d / U_{dio} \qquad (4\text{-}24)$$

As $S_1^2 = P^2 + Q_1^2$, we will also obtain:

$$Q_1 = P\sqrt{\left(\frac{S_1}{P}\right)^2 - 1} = P\sqrt{\left(\frac{U_{dio}}{U_d}\right)^2 - 1} \qquad (4\text{-}25)$$

where S_1 and Q_1 are the apparent power and reactive power related to the fundamental frequency components of the voltages and currents on the ac-side.

Equation (4-24) and (4-25) are also valid as good approximations for overlap angles larger than zero although $\cos\phi \neq \cos\alpha$

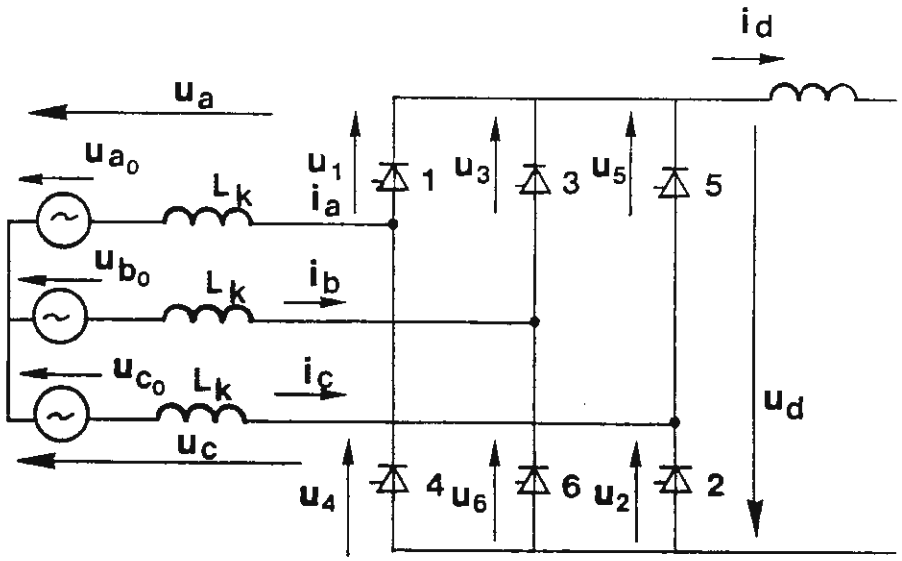

Figure 4-1 Two-way six-pulse converter bridge.

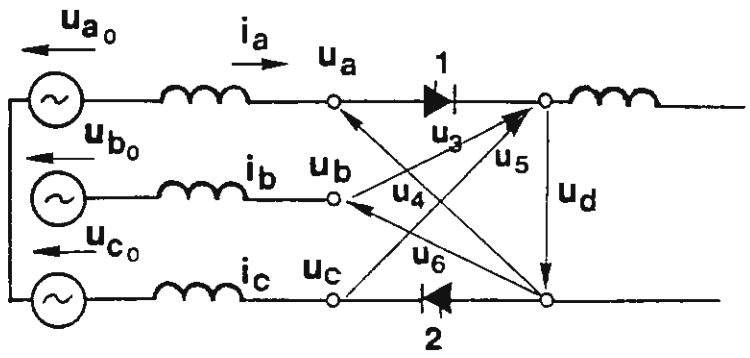

Figure 4-4 Circuit configuration with the valves 1 and 2 conducting.

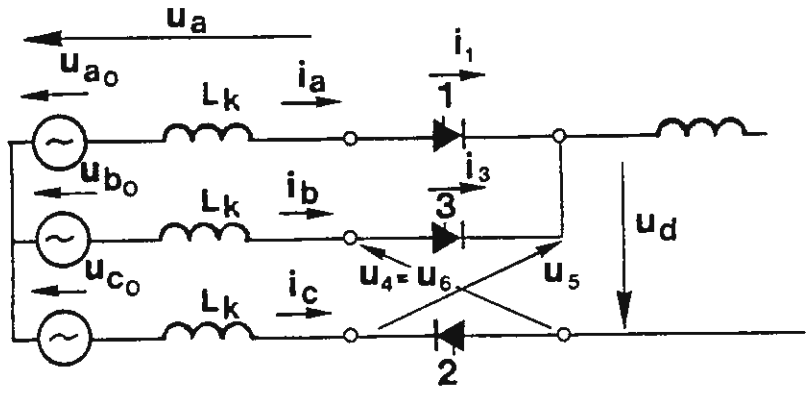

Figure 4-8 Converter bridge with the valves 1, 2 and 3 conducting.

4.3 Analysis of operation at non-zero commutation inductance and finite angle of overlap. Rectifier operation.

In the analysis of the operation characteristics of the line-commutated convertor presented above it was assumed that the influence of the commutation inductance could be neglected, i.e., the commutation from one valve to the succeeding valve is assumed to occur immediatly with a zero angle of overlap. However, a real line-commutated current-source convertor with a circuit diagram, according to figure 4-1, has always a non-zero commutation inductance of the convertor transformer. The commutation of the current from one phase to the succeeding phase will because of that always take a certain time, as it is not possible to change the current in an inductance instantaneously. The duration of the commutation time measured in degrees or radians is called the angle of overlap and denoted by u. The angle of overlap is at normal operation less than 60° el.

With an overlap angle in the range $0 < u < 60°$ the circuit topology will periodically shift between a topology with two conducting valves, illustrated by figure 4-4, and a topology with three conducting valves, illustrated by figure 4-8.

Figure 4-8 gives the circuit configuration for the time interval, when valve 3 has been fired and both valve 1 and 3 are conducting in the upper commutation group. The commutation of the current from valve 1 to valve 3 is, during this interval, determined both by the total commutation inductance in the circuit, $2 L_k$, and the commutation voltage u_k. The commutation voltage is the voltage, which at constant direct current would have occurred across the valve 3, if this valve had not been fired. In the actual case:

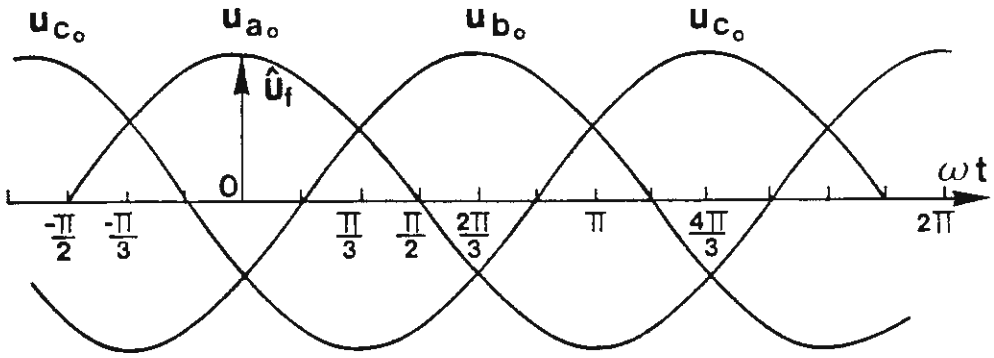

Figure 4-2 Source phase voltages.

$$u_{k3} = u_{b0} - u_{a0} \qquad (4\text{-}26a)$$

Insertion of u_{b0} and u_{ac} according to equations (4-2) and (4-1) gives:

$$u_{k3} = \sqrt{3}\,\hat{U}_f \cdot \sin(\omega t - \pi/3) \qquad (4\text{-}26b)$$

The firing angle α is measured relative to the time instant where $u_{k3}=0$, which occurs at $\omega t=\pi/3$. Equation (4-26b) shows that the instantaneous values of the commutation voltage at the firing are equal to

$$u_{k3\alpha} = \sqrt{3}\hat{u}_f \cdot \sin\alpha$$

The time t in equation (4-26b) is counted from the time instant, when the phase voltage u_{a0} has its maximum value, as illustrated in figure 4-2. To simplify the equations, when studying the commutation process it is more conventional to refer to the time from the zero crossing of the commutation voltage. We will in the following discussions denote this time with t'.

By insertion of $\omega t' = \omega t - \pi/3$ and $\sqrt{3}\cdot\hat{u}_f = \sqrt{2}\cdot U_h$ in equation (4-26b) results:

$$u_{k3} = \sqrt{2} \cdot U_h \cdot \sin \omega t' \qquad (4\text{-}26c)$$

The current in valve 1 (i_1) is at the beginning of the commutation interval, i.e., when $\omega t' = \alpha$, equal to the convertor bridge current i_d. The current in valve 3(i_3) is then zero. At the end of the commutation interval, i.e., when $\omega t' = \alpha+u$, the following equations are valid: $i_1 = 0$ and $i_3 = I_d$.

The current i_3 is, during the commutation interval, i.e.,

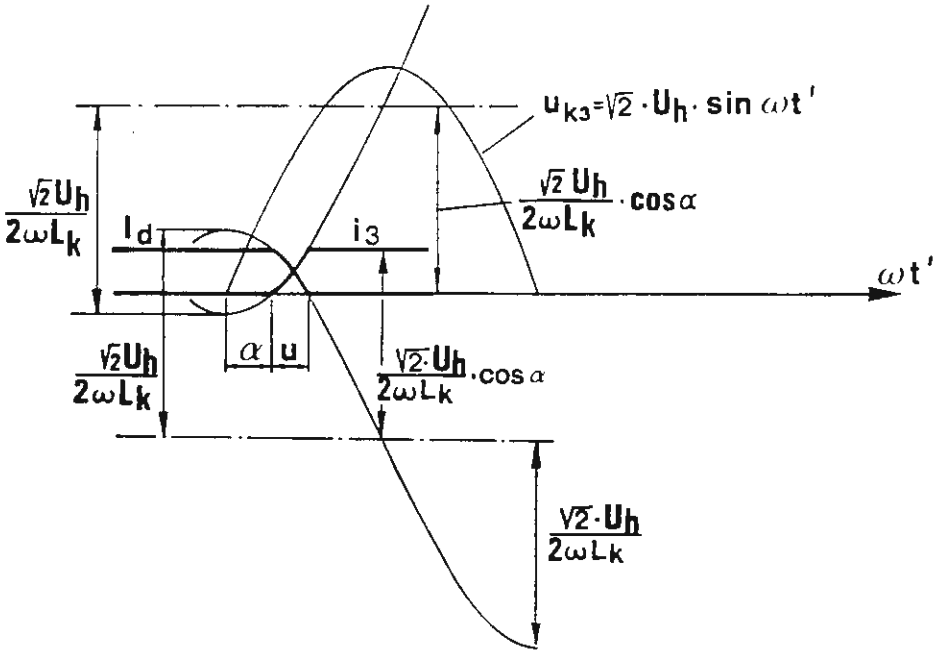

Figure 4-9 Commutation currents.

for $\alpha<\omega t'<\alpha+u$, equal to the commutation current i_{k3}. The commutation current i_{k3} is determined by the commutation voltage u_{k3} and the total commutation inductance $2\ L_k$. If we assume, that the convertor bridge current i_d is constant and equal to I_d and that the resistive losses are neglected, we will get

$$\frac{di_{k3}}{dt} = \frac{\sqrt{2}\cdot U_h \cdot \sin\ \omega t'}{2L_k}$$

Integration gives:

$$i_{k3} = \frac{\sqrt{2}\cdot \hat{U}_h}{2L_k} \int_{\alpha/\omega}^{t'} \sin\ \omega t \cdot dt$$

or

$$i_{k3} = \frac{\sqrt{2}\cdot U_h}{2\ \omega\ L_k} (\cos\ \alpha - \cos\ \omega t') \qquad (4\text{-}27)$$

When the convertor bridge current is not constant but varies during the commutation interval, the current in valve 3 is determined by the commutation current i_{k3}, according to equation (4-27), and a superimposed component proportional to the change in bridge current. As both valves 1 and valve 3 are conducting and as the inductances in series with each valve are equal, the superimposed change in bridge current will be equally shared between valves 1 and 3. If we denote the change in the bridge current from the instant, when valve 3 was fired, by Δi_d, we will get

$$i_3 = i_{k3} + \frac{1}{2}\ \Delta i_d \qquad (4\text{-}28)$$

The waveshape of the currents in valves 1 and 3 at constant bridge current ($\Delta i_d=0$) is illustrated in figure 4-9. The commutation-voltage u_{k3} is also shown. The

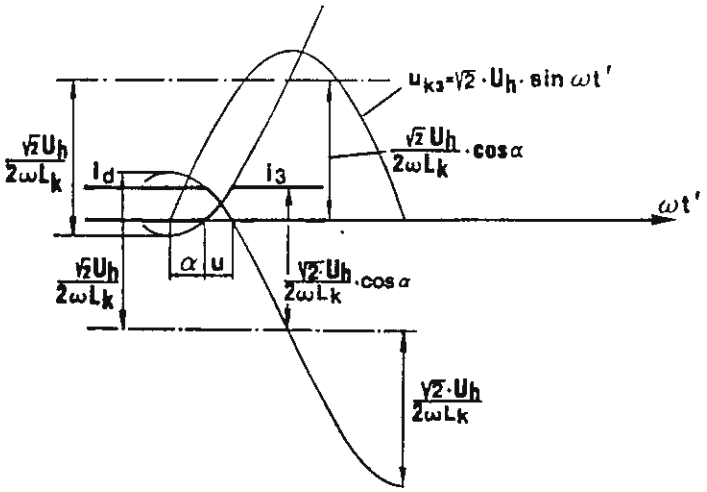

Figure 4-9 Commutation currents.

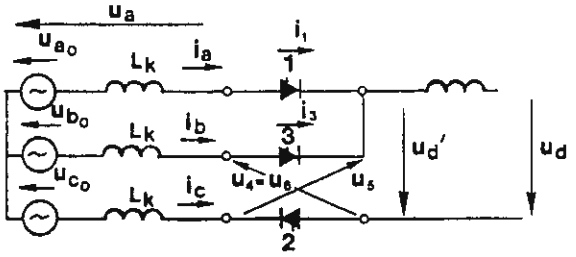

Figure 4-8 Converter bridge with the valves 1, 2 and 3 conducting.

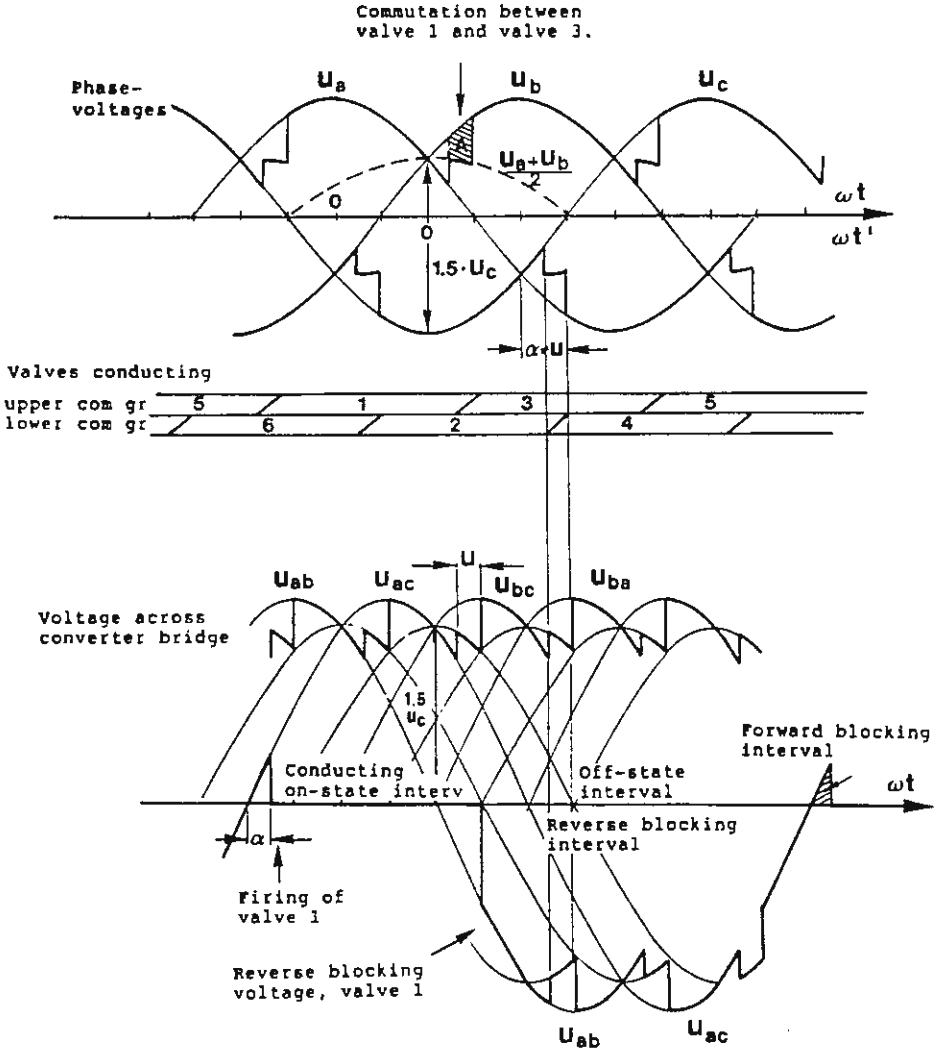

Figure 4-10 Rectifier operation. Phase-voltages, voltage across the converter bridge and voltage across valve 1 at α=15° and u=15°.

commutation-current at commutation from valve 1 to valve 3 can also be regarded as a superimposed short-circuit current, which is limited to:

$i_{k3}=I_d$ at $\omega t'=\alpha+u$ and then $i_1=I_d-i_{k3}=0$.

Insertion of $i_{k3}=I_d$ and $\omega t'=\alpha+u$ in equation (4-27) gives:

$$\cos\alpha-\cos(\alpha+u) = \frac{2\omega \cdot L_k I_d}{\sqrt{2}\cdot U_h} \qquad (4-29)$$

Equation (4-29) can also be used for the case, when the bridge current varies during the commutation, if $2I_d$ is replaced by $I_{d\alpha}+I_{d(\alpha+u)}$ where $I_{d\alpha}$ is the value of the bridge current at the firing instant and $I_{d(\alpha+u)}$ is the value at the end of the commutation interval.

The different voltages illustrated in figure 4-8 can be calculated taking into account that:

$$u_a = u_b = \frac{u_{ao} + u_{bo}}{2}$$

which gives:

$$u_d = -1.5 \cdot U_{co}$$

The phase-voltages, bridge-voltage and the voltage across valve 1 are further illustrated in figure 4-10. The bridge voltage in the lower part of the figure is derived from the difference between phase-voltages shown in the upper part of the figure.

The reduction in the direct voltage component of the bridge voltage due to the overlap can be calculated in different

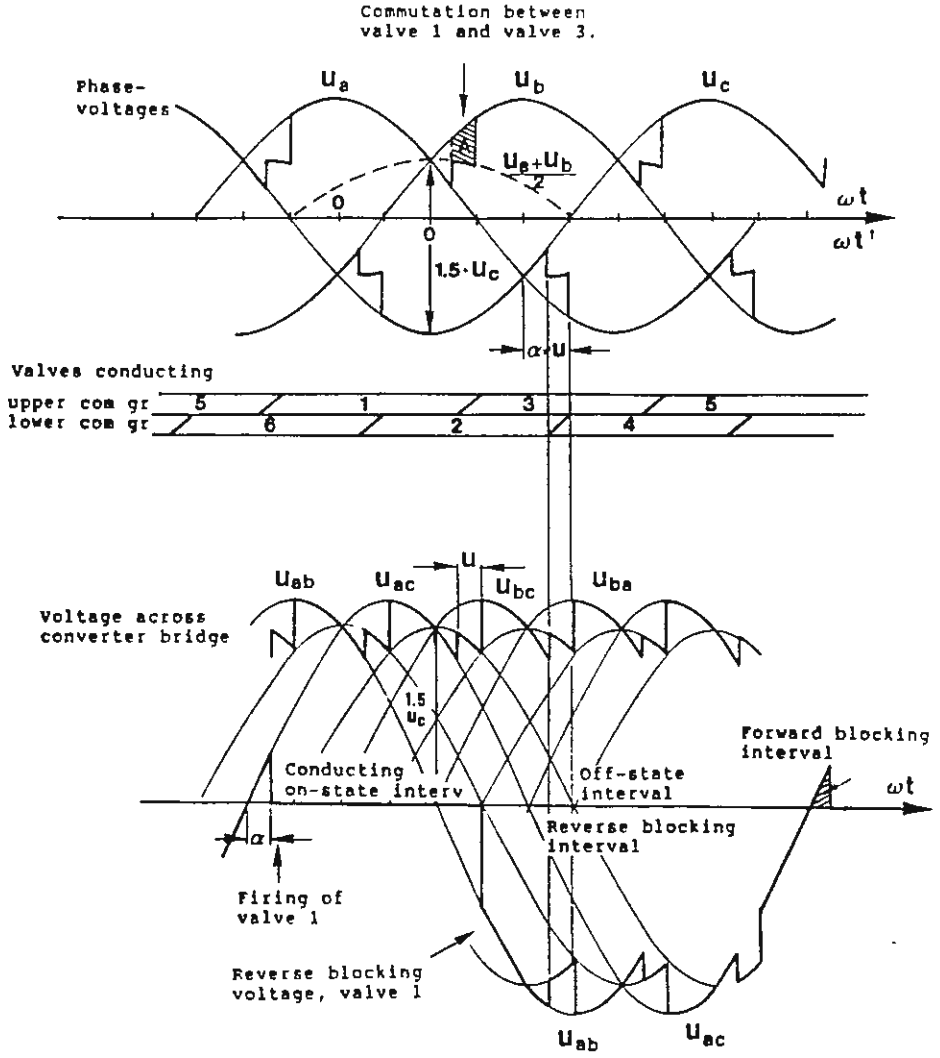

Figure 4-10 Rectifier operation. Phase-voltages, voltage across the converter bridge and voltage across valve 1 at α=15° and u=15°.

ways. One way is to calculate the "voltage-time area" A according to figure 4-10, with the time given in radians. This is achieved by integration of half the commutation voltage u_k from $\omega t'=\alpha$ to $\omega t'=\alpha+u$. The total reduction in the bridge "voltage-time area" during one cycle of the feeding ac-voltage will be equal to six times A. This gives:

$$\Delta U_{dx} = \frac{6}{2\pi} \cdot \frac{\sqrt{2}\, U_h}{2} \int_{\alpha}^{\alpha+u} \sin \omega t' \, d(\omega t') = \frac{3\sqrt{2}\, U_h}{2\pi} \left[\cos\alpha - \cos(\alpha+u)\right] \qquad (4\text{-}30a)$$

The drop in voltage time area during one cycle can also be directly calculated by multiplying the total current I_d with the value of the inductance L_k times six. This gives the following equation for the voltage drop

$$\Delta U_{dx} = 6 \cdot f \cdot L_k \cdot I_d = \frac{3}{\pi} \omega L_k \cdot I_d = \frac{3}{\pi} \cdot X_k \cdot I_d \qquad (4\text{-}30b)$$

An expression for the relative inductive voltage drop which is denoted d_x is obtained by dividing ΔU_{dx}, in equation (4-30a), by U_{dio} according to equation (4-10). This gives:

$$d_x = \frac{\Delta U_{dx}}{U_{dio}} = \frac{1}{2} \left[\cos\alpha - \cos(\alpha+u)\right] \qquad (4\text{-}31)$$

The relative inductive voltage drop can also be expressed as a function of the direct current I_d, the commutation reactance X_k and the ideal no-load direct voltage U_{dio}. Equation (4-30b) gives:

$$d_x = \frac{3}{\pi} \frac{I_d \cdot X_k}{U_{dio}} \qquad (4\text{-}32a)$$

The relative inductive voltage drop at the rated direct

current and the no-load direct voltage is denoted d_{xN},

$$d_{xN} = \frac{3}{\pi} \frac{I_{dN} \cdot X_k}{U_{dioN}} \qquad (4\text{-}32b)$$

It should be noted that the relative inductive voltage drop at rated operation is sometimes denoted with d_x instead of d_{xN}. Some caution is, because of that, recommended with regard to the definition of d_x in the actual case.

The expression for the voltage drop according to equation (4-31) is more general than the expression according to equation (4-32a) as the first expression also is valid for a not constant direct current. The notation ε is, in some literature, used instead of d_x for the expression according to eq. (4-31) (see Ref 2).

The following relationships are further valid for the rated power of the convertor transformer S_{tN} and for the relative short circuit voltage e_{kN}:

$$S_{tN} = \sqrt{3} \cdot U_{hN} \cdot I_N \qquad (4\text{-}33a)$$

$$e_{kN} = \frac{\sqrt{3} \cdot I_N \cdot X_k}{U_{hN}} \qquad (4\text{-}33b)$$

The rated r.m.s value of the ac current on the valve side has here been denoted I_N and the corresponding no-load line-to-line voltage U_{hN}.

In chapter 3 it was shown that for the case of zero overlap angle the following relationship is valid for a two-way six pulse bridge connection:

$$I = \sqrt{\frac{2}{3}} I_d \qquad (4\text{-}33c)$$

(valid for u=0).

The r m s value of the valve current is:

$$I_v = \frac{I_d}{\sqrt{3}}$$

according to equation (3-4) and the r.m.s. value of the current in one transformer phase, $I = \sqrt{2} \cdot I_v$).

As will be seen later, equation (4-33c) is also approximately valid for the case with non-zero overlap angle.

This suggests that equation (4-33a) with the use of (4-10) and (4-33c) can be rewritten.

$$S_{tN} = \frac{\pi}{3} \cdot U_{dioN} \cdot I_{dN} \qquad (4\text{-}33d)$$

(valid for u=0 and approximately for u≠0)

It should be noted that S_{tN} in equation (4-33d) refers to the rated power defined by the product of the voltage and the r.m.s value of the current, while S_1 in equation (4-22b) refers to the product of the voltage and the fundamental component of the ac-current.

The equations (4-32b), (4-10), (4-33b) and (4-33c) now result

$$d_{xN} \simeq \frac{1}{2} e_{kN} \qquad (4\text{-}33e)$$

The relationship according to (4-33e), which is approximately valid, is very essential, since e_{kN} usually is specified for the convertor transformers.

The direct voltage across the convertor bridge can now be determined from equation (4-9) or (4-11), which takes into account the effect of the firing angle control, and either equation (4-30) or (4-31) giving the voltage drops due to the commutating inductance.

The ideal convertor bridge voltage, neglecting the contribution from resistive voltage drop, will be denoted by U_{di}. The following relationship applies for this voltage:

$$U_{di}=U_{dio}\left(\cos\alpha-\frac{\Delta U_d}{U_{dio}}\right) \qquad (4\text{-}34)$$

Insertion of equation (4-31) in (4-34) gives:

$$U_{di}=U_{dio}\frac{\cos\alpha+\cos(\alpha+u)}{2} \qquad (4\text{-}35a)$$

Insertion of equation (4-32a) and (4-32b) in (4-35a) gives:

$$U_{di}= U_{dio}\left[\cos\alpha - d_{xN}\frac{I_d}{I_{dN}}\cdot\frac{U_{dioN}}{U_{dio}}\right] \qquad (4\text{-}35b)$$

Equations (4-10) and (4-30b) give an alternative expression for U_{di} i.e.

$$U_{di} = \frac{3\sqrt{2}}{\pi}U_h\cdot\cos\alpha - \frac{3}{\pi}X_k\cdot I_d \qquad (4\text{-}35c)$$

It should be noted that although the voltage drop due to

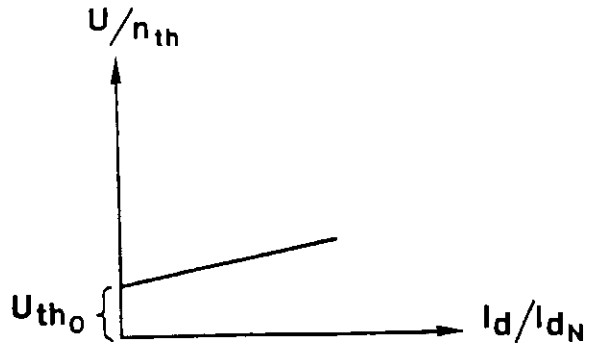

U/n_{th} = On state characteristics of individual thyristor

Figure 3-2 On state characteristics.

the commutation inductance in the above equations has the characteristics of a resistive voltage drop it does not give any active power losses. As pointed out previously, both the voltage drop and the firing angle α, due to the commutation inductance, cause on the other hand, a reduction of the power factor, according to equation (4-24).
As we will see later, this equation is also approximately valid for non-zero overlap angles.

The resistive losses in the transformers and the valves result in an additional voltage drop, ΔU_{dr}. This resistive voltage drop at rated operation is denoted by d_{rN}, i.e.,:

$$d_{rN} = \frac{\Delta U_{dr}}{U_{dio}} \qquad (4\text{-}36a)$$

The resistive voltage drop can also be calculated by dividing the actual losses with $U_{dioN} \cdot I_{dN}$, i.e.,:

$$d_{rN} = \frac{P_{CuN} + P_{thN}}{U_{dio} \cdot I_{dN}} \qquad (4\text{-}36b)$$

The current dependent losses in the transformer are here denoted by P_{CuN} and the current dependent losses in the thyristors with P_{thN}. The non-current dependent voltage drop in the thyristor valves, corresponding to U_{tho} in figure 3-2, is represented by a constant voltage drop U_T. Equation (4-35b) can now be modified to:

$$U_d = U_{dio}\left[\cos\alpha - \left(d_{xN} + d_{rN}\right)\frac{I_d}{I_{dN}} \cdot \frac{U_{dioN}}{U_{dio}}\right] - U_T \qquad (4\text{-}37)$$

It should be noted that the difference between U_d,

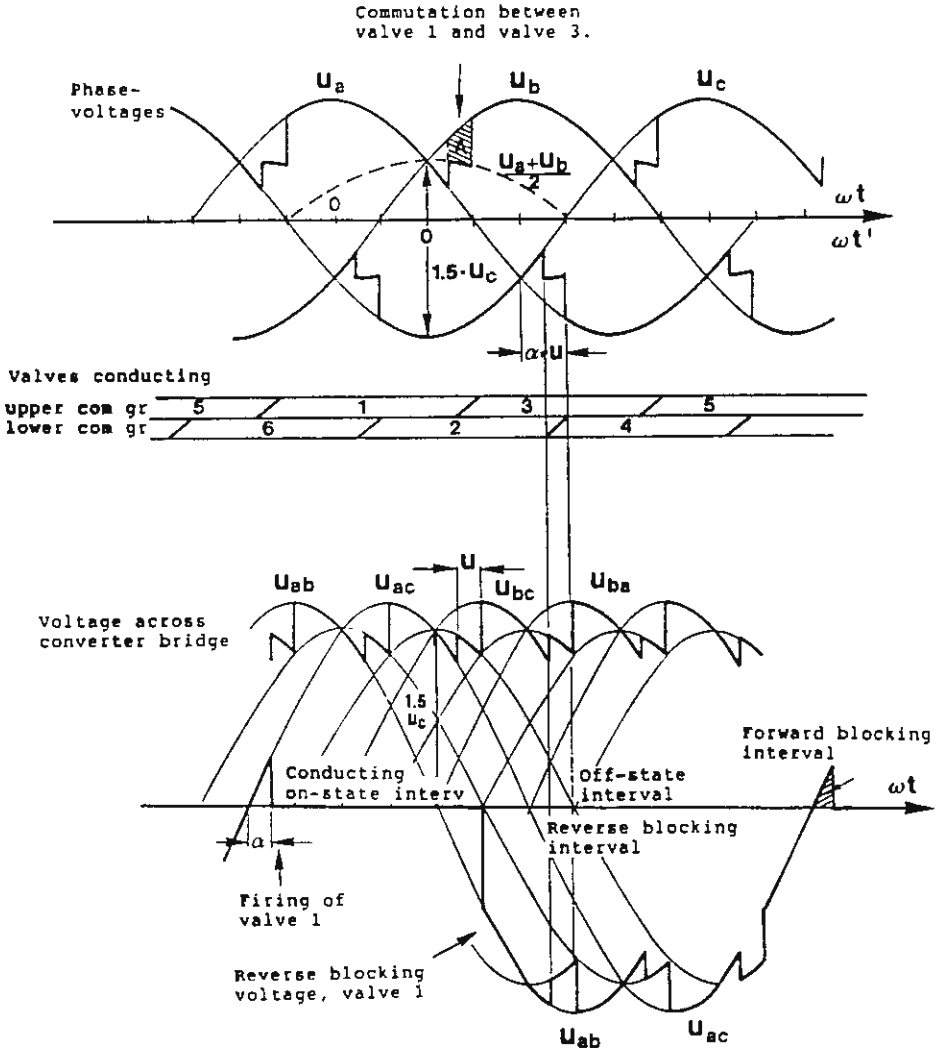

Figure 4-10 Rectifier operation. Phase-voltages, voltage across the converter bridge and voltage across valve 1 at α=15° and u=15°.

in eq. (4-37), and U_{di}, in eq. (4-35b) is usually fairly small since the total losses in a convertor is in the order of 4-6 per thousand, while the inductive voltage drop d_{xN}, on the other hand, is of the order 5-10 per cent.

4.4 Inverter operation

The description of the convertor operation presented above is valid for both rectifier and inverter operation, although it has been illustrated only for rectifier operation, e.g., figure 4-10. The time instants of the firing of the valves have been defined by the firing angle α, which for rectifier operation is less than 90° or $\pi/2$ rad. If the firing angle is further delayed, so that the firing angle will be larger than 90°, the operation of the convertor continues as described above. This is valid as long as the commutation voltage is sufficient for the commutation of the current from one valve to the succeeding valve. The polarity of the bridge current will be unchanged since the valves can only carry current in one direction. However, the polarity of the voltage across the bridge will be changed at a firing angle slightly more than 90°, as can be seen from equation (4-37). The power direction will then also change and the operation of the convertor is changed from rectifier operation to inverter operation.

The normal inverter operation will occur at firing angles considerably larger than 90°. Because of that, it is convenient to define an angle from the end of the commutation to the succeeding zero crossing of the commutation voltage. This angle is denoted by γ and is called extinction angle or commutation margin. The firing angle α, the angle of overlap u, and the extinction angle

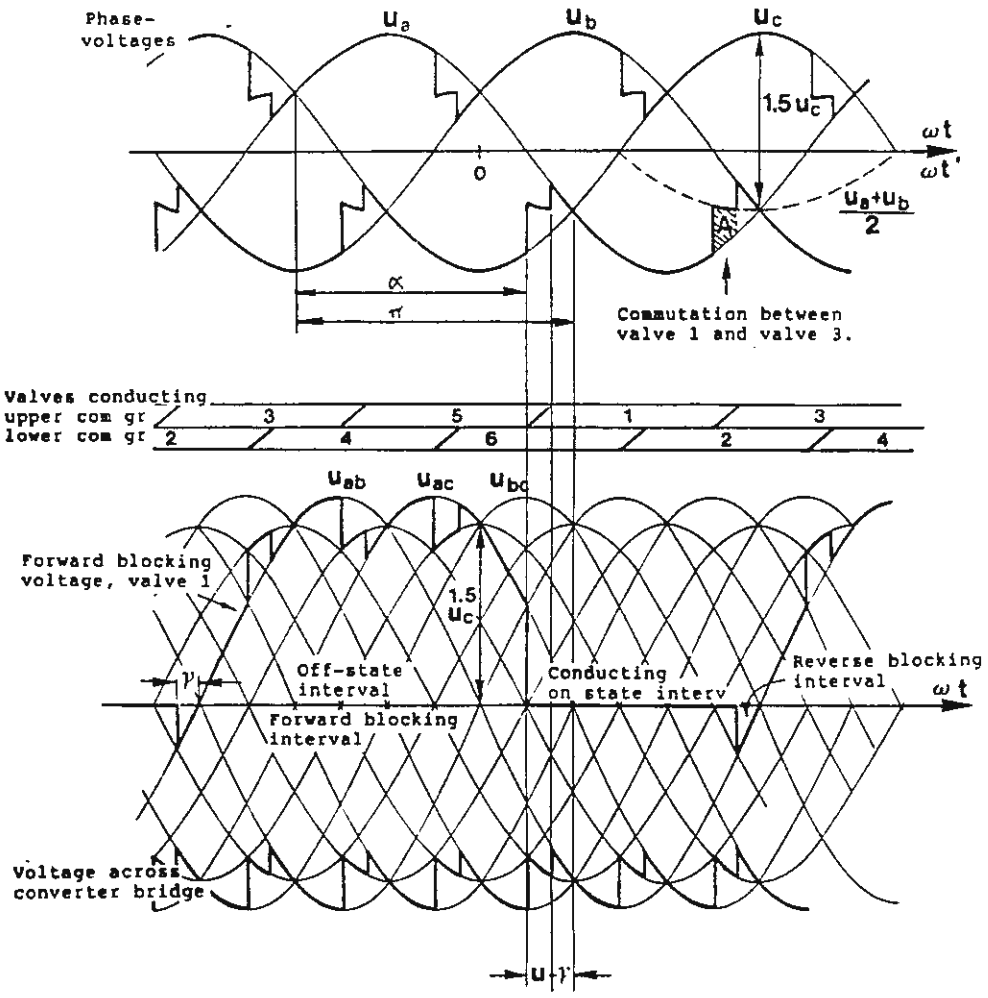

Figure 4-11 Inverter operation. Phase-voltages, voltage across valve bridge and voltage across valve 1 at γ=15° and u=15°.

γ, are illustrated for the commutation between valves 1 and 3 in figure 4-11. The figure also shows the phase-voltages, the voltage across the convertor bridge and the voltage across valve 1 for u=15° and γ=15°. As can be seen from figure 4-11 the following relationship exists between α, u and γ:

$$\alpha+u+\gamma=180°(\text{or } \pi \text{ rad}) \qquad (4-38)$$

Since the previously presented equations for the convertor are valid independent from the magnitude of α they are also valid for inverter operation. The equations can be rewritten using equation (4-38), with γ replacing α as independent variable.

Insertion of equation (4-38) in equation (4-31) gives:

$$d_x = \frac{1}{2}\left[\cos\gamma-\cos(\gamma+u)\right] \qquad (4-39)$$

Insertion of eq. (4-38) in eq. (4-35a) gives:

$$U_{di} = - U_{dio}\,\frac{\left[\cos\gamma+\cos(\gamma+u)\right]}{2} \qquad (4-40a)$$

Insertion in the equations (4-35a) and (4-35c) taking into account equation (4-32b) and (4-39) gives:

$$U_{di} = - U_{dio}\left(\cos\gamma - d_{xN}\cdot\frac{I_d}{I_{dN}}\cdot\frac{U_{dioN}}{U_{dio}}\right) \qquad (4-40b)$$

and:

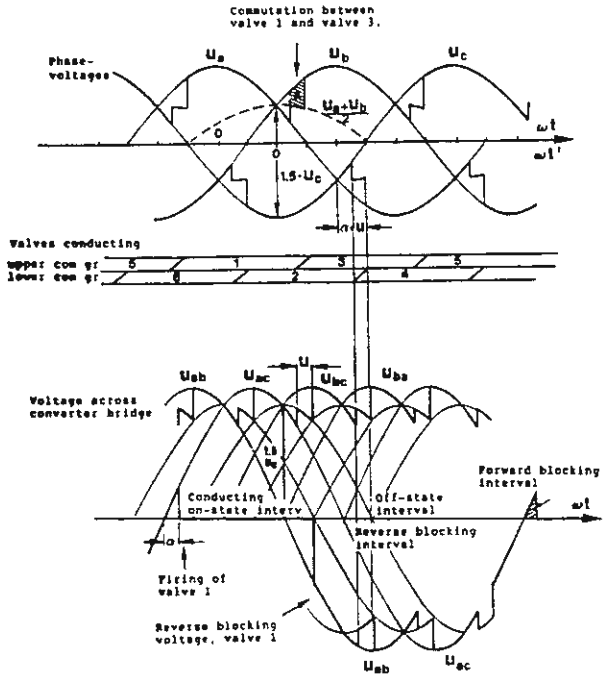

Figure 4-10 Rectifier operation. Phase-voltages, voltage across the converter bridge and voltage across valve 1 at α=15° and u=15°.

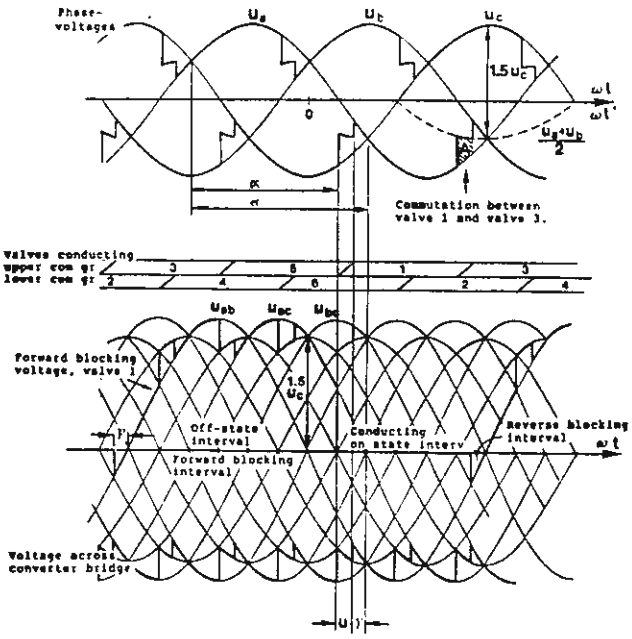

Figure 4-11 Inverter operation. Phase-voltages, voltage across valve bridge and voltage across valve 1 at γ=15° and u=15°.

$$U_{di} = -\left(\frac{3\sqrt{2}}{\pi} U_h \cdot \cos\gamma - \frac{3}{\pi} X_k \cdot I_d\right) \qquad (4\text{-}40c)$$

Positive voltage polarity for inverter operation is usually defined in the opposite direction compared to positive voltage polarity at rectifier operation. With the reversed polarity convention the minus signs before the paranthesis in the three (4-40) equations have to be replaced by positive signs. This indicates that the same equations are achieved for inverter operation, as for rectifier operation if the angle α is replaced by the angle γ. However, this is no longer valid if the resistive voltage drop is also taken into account. Equation (4-37), valid for rectifier operation, is in inverter operation replaced by:

$$U_d = U_{dio}\left[\cos\gamma - \left(d_{xN} - d_{rN}\right)\frac{I_d}{I_{dN}}\frac{U_{dioN}}{U_{dio}}\right] + U_T \qquad (4\text{-}41)$$

The waveshape of the voltage across the bridge as well as the valves will, in inverter operation, be the same as in rectifier operation with the polarity and direction of the time-axis reversed.

This is illustrated by comparing figure 4-10 with figure 4-11. In this case the same definition of positive voltage polarity has been used resulting in the bridge voltage showing negative for inverter operation. It should also be noted that the valve voltage is essential negative in rectifier operation (reverse blocking direction) while being positive in inverter operation (forward blocking direction).

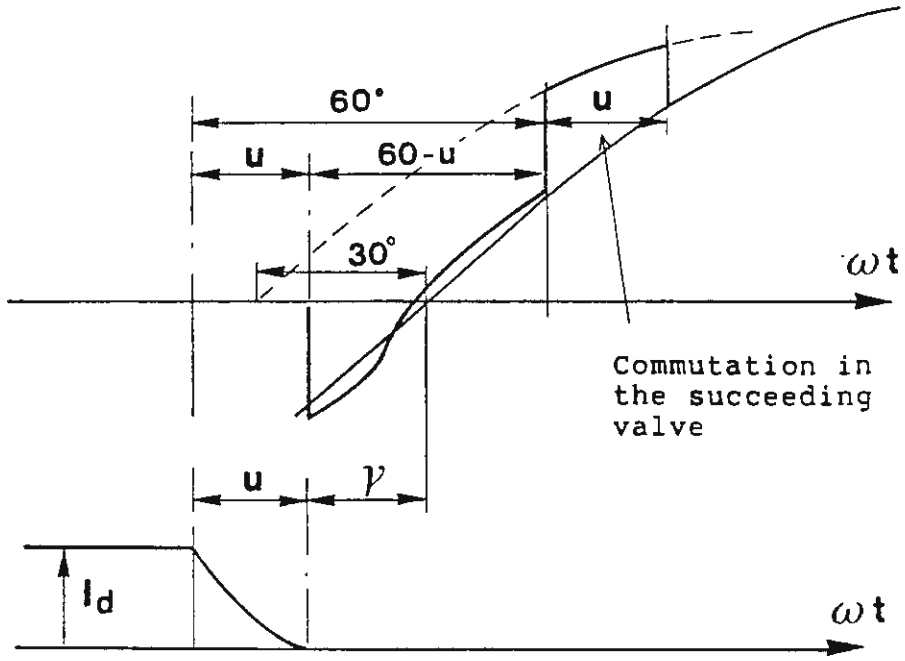

Figure 4-12 End of commutation at inverter operation u=20° and γ=20°.

Commutation margin

The firing angle in rectifier operation can be decreased to a minimum value of about 5°el. This value is only limited by the requirement that the voltages across the valves at firing must have a sufficient high positive value and that it often requires equal distances between succeeding firings and also at small unsymmetries in the feeding ac-voltage. The commutation margin in inverter operation must, on the other hand, be no less than 17-18° in order to secure safe operation with sufficient small risks for commutation failures. The commutation process at inverter operation is further illustrated in figure 4-12, which shows the valve current at the end of the conduction interval and the voltage across the same valve.

The definition of the angle of overlap u and the commutation margin angle γ is also illustrated. As shown in the figure, the angle γ is in the case of a distorted waveshape referred to the zero-crossing of an ideal sinusoidal waveshape. As illustrated in the figure distortions in the feeding ac-voltage can also reduce the real time to the zero crossing of the voltage.

Thyristor valves require a certain minimum time interval with negative blocking voltage before the voltage polarity is reversed in order to recover. This interval can be as long as corresponding to 10°el. In this chapter it has further been assumed that the thyristor valves act as ideal switches with the reverse voltage appearing as soon as the current reaches zero. However, as will be described in chapter 9, the voltage in reverse direction will occur with a certain delay due to the recovery charge of the thyristors. Since the commutation margin shall be measured from the zero-crossing of the current this will further decrease the available time for the recovery of the valves.

The discussion above has been limited to steady state operation. During transients and disturbances it must also be taken into account that there is always a certain delay in the action of the firing control system and that the firing control system can only determine the firing instant but cannot take into account disturbances occuring during the commutation interval. Events that can cause transient changes of the commutation voltages are for instance switchings of large loads or earth faults in the ac-network.

The choice of an optimal value for the commutation margin is rather delicate. A smaller commutation margin angle reduces the costs for most equipment such as valves, transformers, filters and capacitor banks for generation of reactive power. Too small a commutation margin angle will, on the other hand, increase the risk for commutation failures. Experience from plants in operation has shown that only a small increase from 17 to 19° can drastically reduce the frequency of commutation failures. Improvement in firing control and valve design as well as the trend to reduce the commutation inductances has resulted in reduced the angle of overlap which reduces the risk for commutation failures.

4.5 Current - voltage characteristic

The current-voltage characteristics for rectifier operation are given by equation (4-35b) and for inverter operation by equation (4-40b). The resistive voltage drops have been neglected in these cases. The polarity of the voltages have been defined positive for rectifier operation. These characteristics are illustrated by straight lines in figure 4-13.

The characteristics for constant overlap angle of u=45° and

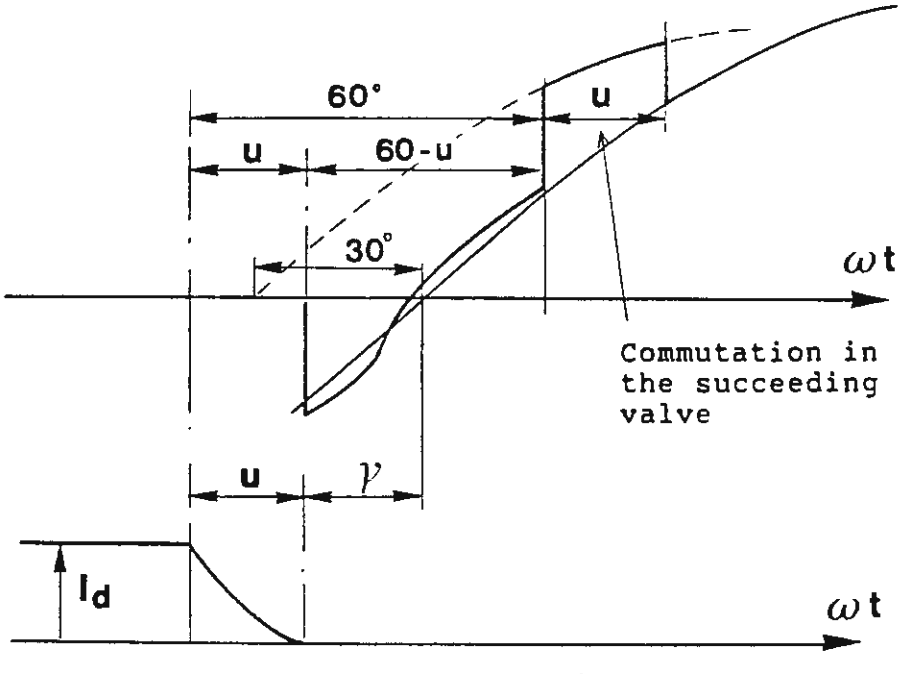

Figure 4-12 End of commutation at inverter operation u=20° and γ=20°.

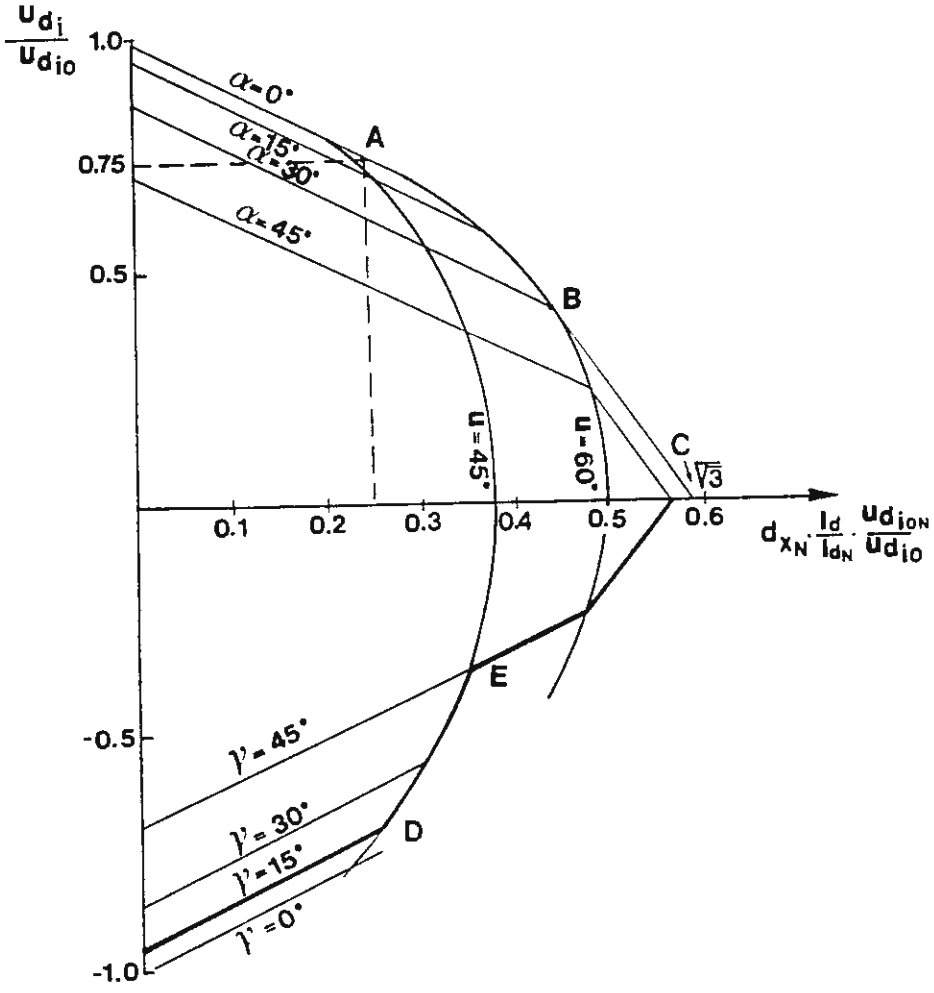

Figure 4-13 Current-voltage characteristics of a 6-pulse converter.

u=60° are also shown in the diagram. These characteristics have the form of ellipses.

Usually, only the left part of the diagram for $d_x<0.25$ is of interest since the maximum value of d_{xN} is of the order of 0.1. This means that high values of d_x can only occur at high direct currents and low ac-voltages (low values of U_{dio}). Further, only the region above $\gamma=15°$ is of interest with regard to the risk for commutation failures at smaller values of γ.

It should also be noted that equations (4-35b) and (4-40b) are only valid for the overlap angles less than 60°. This can also be seen from figure 4-12, which shows the valve current and valve voltage at the end of the conduction interval in inverter operation. However the same figure placed upside down is also valid for the beginning of the conduction interval at rectifier operation. From this figure it is obvious that the angle of overlap cannot be larger than 60° unless the firing angle α or the extinction angle γ is larger than 30°.

This explains why the limitation curve between point A and point B follows the ellipse for u=60°.

For inverter operation the ellipse for u=45° is more relevant as operation along this ellipse, between point D and E in the diagram, gives 15° with reverse blocking voltage across the valve.

For overlap angles larger than 60°, commutations will take place simultaneously in both the upper and lower commutation group during a part of the cycle. This operation mode is called double overlap. During the part of the cycle, when four valves are conducting in the bridge, the bridge voltage will be zero, resulting in that the direct voltage across the bridge will decrease steeply for

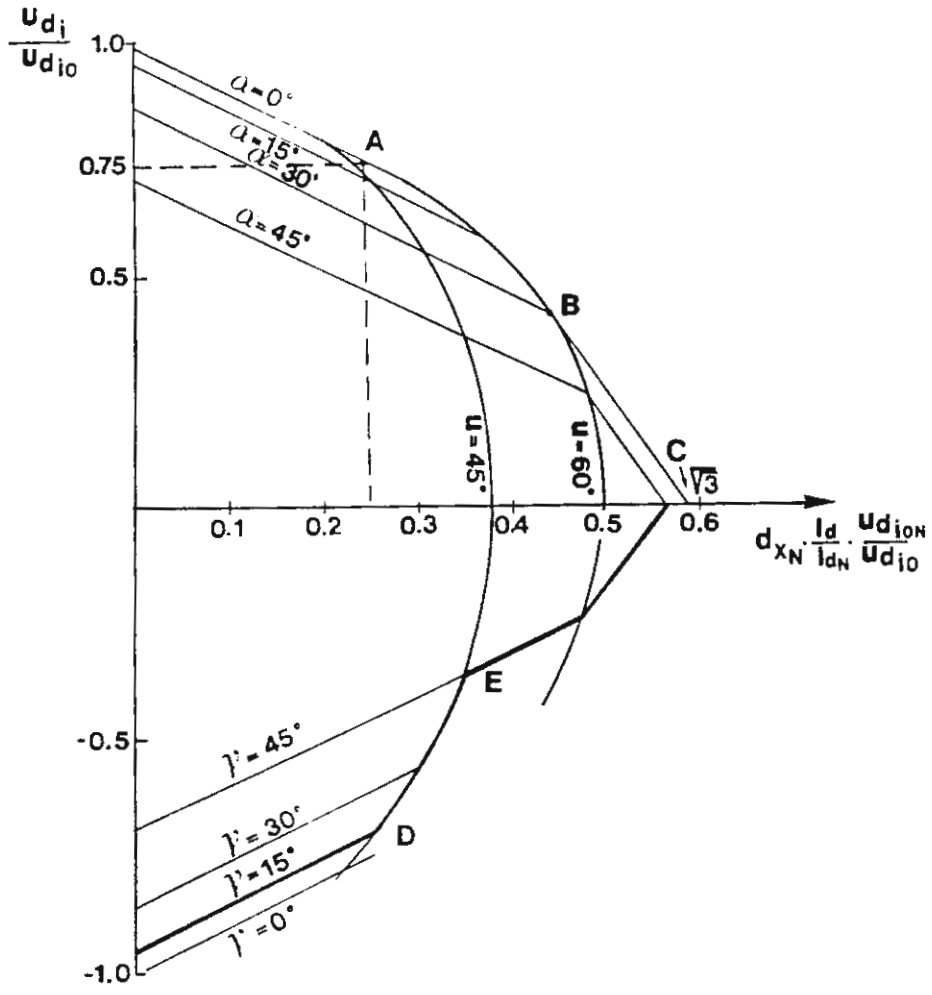

Figure 4-13 Current-voltage characteristics of a 6-pulse converter.

increased current for the part of diagram giving double overlap, e.g., the straight line between B and C in the figure 4-13.

4.6 Fundamental and r.m.s. values of ac-currents

The commutation sequence for rectifier and inverter operation and the basic relationship between dc-voltage and ac-voltage with the direct current as independent variable have been treated above. For the case with zero overlap-angle simple relationships were also derived between dc- and ac-currents. It was also shown, that it could be feasible to use conversion functions for converting ac-quantities to dc-quantities and vice versa.

However, it will be much more complicated to use the technique with conversion functions for u>0 as the topology of the circuit will be different during the commutation process and as the duration of the commutation will be a function of the value of the direct current. As a result a linear relationship no longer exists between the current on the dc-side and on the the ac-side.

However, it may still be feasible to use a technique with conversion functions similar to the one described for the case with u=0 also for u>0 when studying small superimposed oscillations and the interaction between the ac- and the dc-side. See ref [5]

The fundamental of the ac-current is for the case u=0 proportional to the dc-current as shown in equation (4-21b). This was also assumed to be generally valid for a current source system according to chapter 2 equation (2-1). The question now is to what extent equation (4-21b) can also be used for the case u≠0.

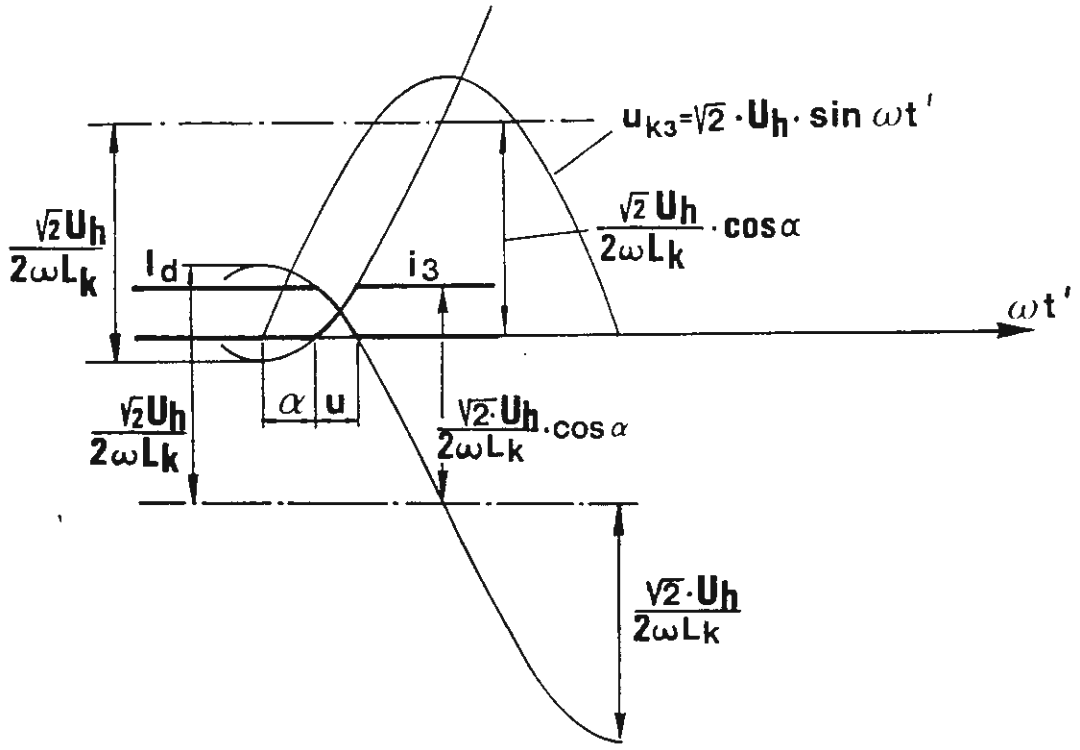

Figure 4-9 Commutation currents.

Equations for the instantaneous value of the valve currents during the commutation have previously been derived in eq. (4-26). The valve current is also illustrated in figure 4-9. At the remaining intervals the valve current is either zero or equal to the convertor bridge current I_d.

The current in an ac-phase of the convertor transformer is determined from the currents in the two valves connected to the phase. A Fourier analysis to determine the fundamental component of ac-phase currents causes relative extensive calculations, which will not be presented here. See Ref. 1 Appendix B. The result shown in complex r.m.s. value form and with the corresponding phase-voltage as phase refernce is:

$$I_1 = \frac{\sqrt{6}}{4\pi} \cdot \frac{(e^{-j2\alpha} - e^{-j\,2(\alpha+u)} - j\,2u)}{\cos\alpha - \cos(\alpha+u)} \cdot I_d \qquad (4\text{-}42)$$

Equation 4-42 gives for u=0 equation (4-21b).

The complex fundamental power can be written:

$$P + jQ_1 = 3 \cdot U_f \cdot I_1^* \qquad (4\text{-}43)$$

The ideal no load voltage U_{dio} written as a function of the phase voltage U_f is (compare eq. (4-10):

$$U_{dio} = \frac{3\sqrt{6}}{\pi} \cdot U_f$$

Equation (4-42) inserted in equation (4-43) and taking into account that:

$$e^{jx} = \cos x + j \sin x$$

gives:

$$\frac{P}{U_{dio} \cdot I_d} = \frac{\cos 2\alpha - \cos 2(\alpha+u)}{4[\cos\alpha - \cos(\alpha+u)]} = \frac{\cos\alpha + \cos(\alpha+u)}{2} \qquad (4\text{-}44)$$

This can also be directly achieved from equation (4-35a) since:

$$P = U_{di} \cdot I_d$$

The fundamental reactive power Q, is derived in the corresponding way. This gives:

$$\frac{Q_1}{U_{dio} \cdot I_d} = \frac{\sin 2\alpha - \sin 2(\alpha+u) + 2u}{4[\cos\alpha - \cos(\alpha+u)]} \qquad (4\text{-}45)$$

The apparent fundamental power is derived from equation (4-44) and (4-45) which gives:

$$\frac{S_1}{U_{dio} \cdot I_d} = \sqrt{\frac{P^2 + Q_1^2}{U_{dio}\ I_d}} = \sqrt{\frac{u^2 + \sin^2 u - 2u \cdot \sin u \cdot \cos(2\alpha+u)}{2[\cos\alpha - \cos(\alpha+u)]}} \qquad (4\text{-}46)$$

The right part of equation (4-46) will be approximately equal to one in the operation range of major interest. For $u=15°$ and $\alpha=15°$ the expression is equal to 0.9973. This indicates that equations (4-21b), (4-22b) and (4-24) are approximately valid also for $u>0$. Equation (4-25) can also be used as a first approximation although equation 4-45 is recommended for a more accurate calculation of reactive power.

The r.m.s. value of the phase current has previously been derived for the case of zero overlap angle, see equation 4-33c:

$$I=\sqrt{\frac{2}{3}}\ I_d \qquad (4\text{-}33c)$$

This relationship is also valid as a good approximation for u>0, see Ref 1. Appendix A. As an example, it can be mentioned that for $\alpha=15°$ and $u=15°$ the exact calculation gives:

$$I=0.98\sqrt{\frac{2}{3}}\cdot I_d$$

However it should be noted that it is primarily the fundamental component of the phase current that is of interest when studying the cooperation between the ac- and dc-side of the convertor station. The relationships between the fundamental component of the phase-current, the phase-voltage and the phase-angle are further illustrated in the phasor-diagrams figure 4-14 and 4-15 for rectifier and inverter operation. Equation (4-21b) can be used to determine the phase-current from the direct current and equation (4-42) can be used if more accurate determination is desireable. Usually the approximate relationships valid for u=0 are satisfactory. The convertor transformer is represented by the commutation reactance per phase X_k in the diagram.

In rectifier operation active power is fed from the ac-network to the convertor bridge. In inverter operation the power direction is opposite. Reactive power is in both

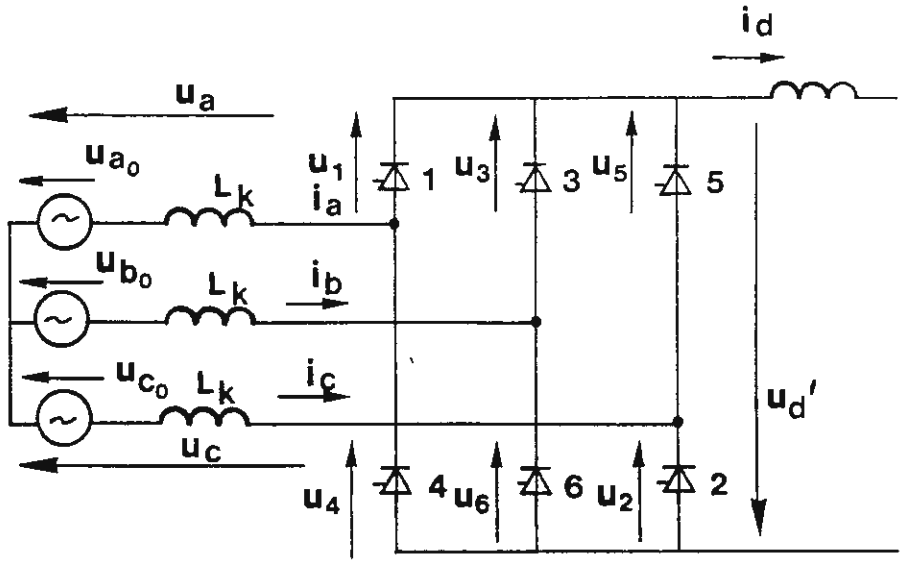

Figure 4-1 Two-way six-pulse converter bridge.

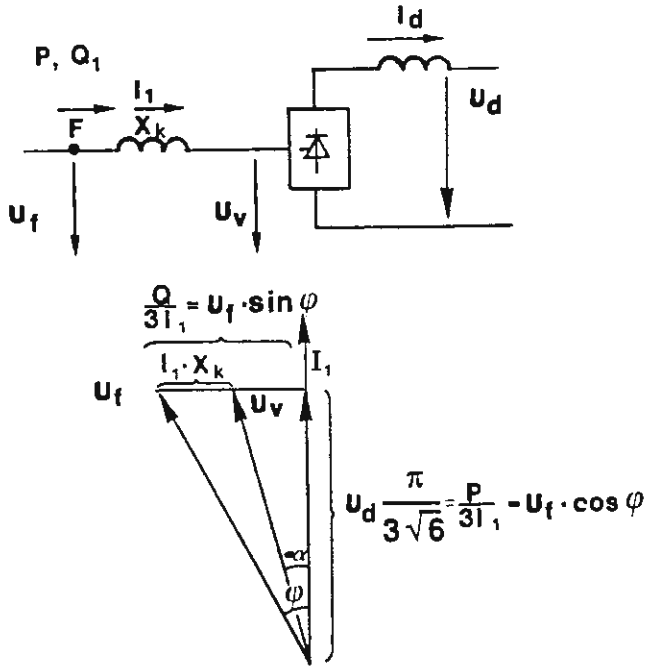

Figure 4-14 Simplified circuit diagram and phaser diagram for a rectifier, phase-voltage.

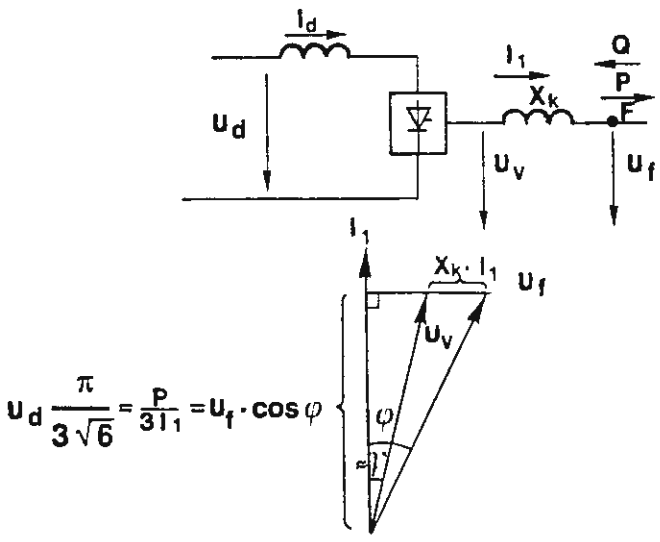

Figure 4-15 Simplified circuit diagram and phaser diagram for an inverter, phase-voltage.

The ac-voltage on the line side, transformed to the valve side of the convertor transformer, has been denoted U_f. This voltage is here assumed to be sinusoidal. Usually filters are connected on the line side of the convertor transformer to short-circuit all generated harmonic currents. The voltage U_f can be regarded as the commutation voltage (Compare u_{ao}, u_{bo} and u_{co} in figure 4-1). The reactive power at point F in figure 4-15 will thus be given by equation (4-45). The resistive voltage drop has been disregarded in this diagram. It should be noted that this type of phasor- diagram is often shown for line-to-line voltages instead of phase-voltages as shown in figures 4-14 and 4-15.

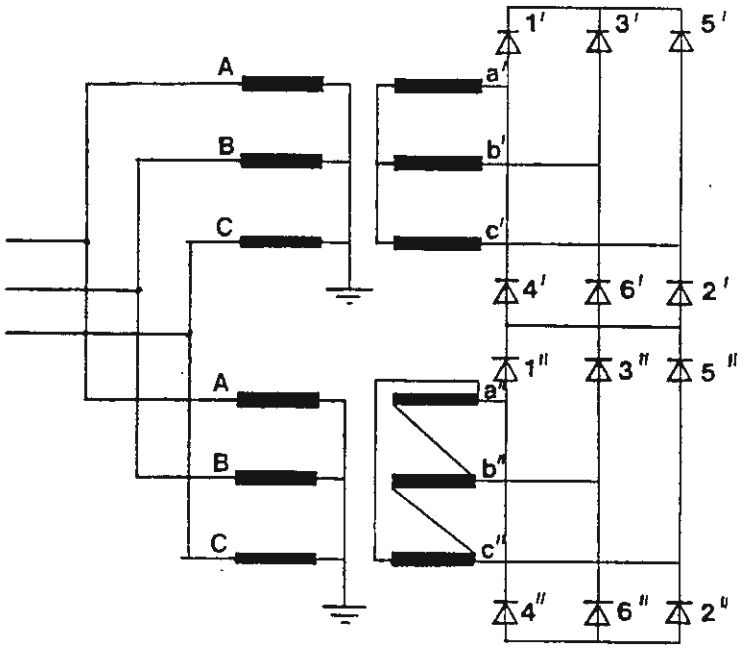

Figure 3-11 Twelve-pulse converter circuit formed by two 30° phase-shifted two-way six-pulse bridge converter circuits connected in series, p=12, q=3, s=4.

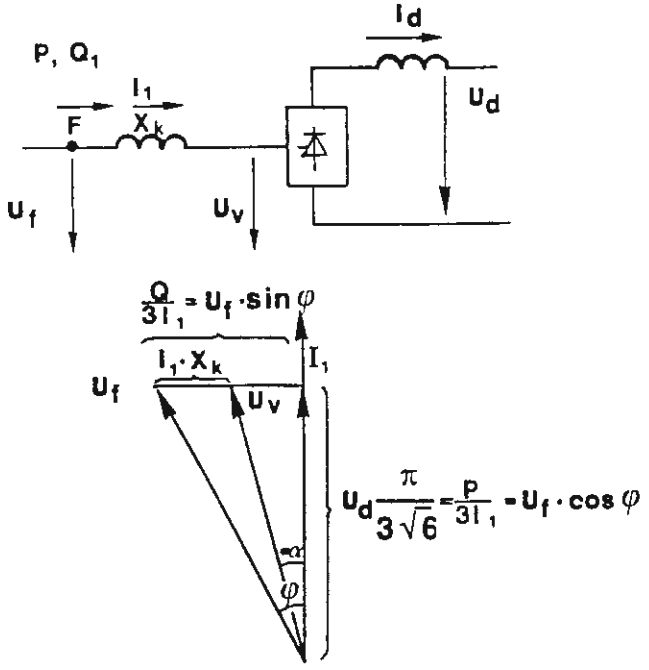

Figure 4-14 Simplified circuit diagram and phasor diagram for a rectifier, phase-voltage.

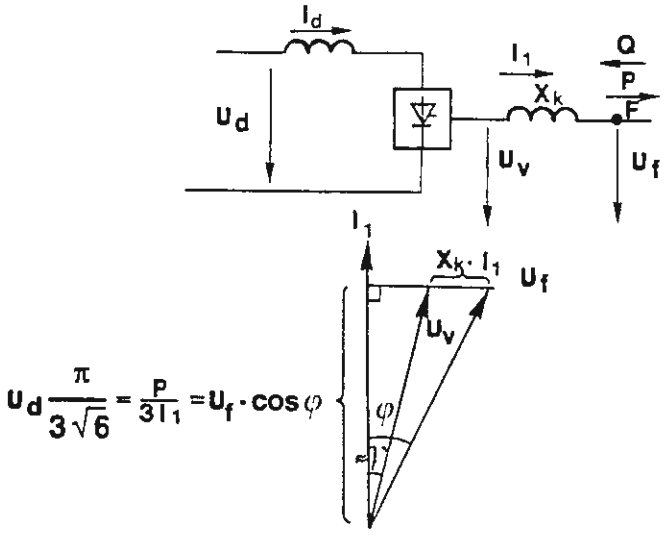

Figure 4-15 Simplified circuit diagram and phasor diagram for an inverter, phase-voltage.

5 CONNECTION OF 6-PULSE CONVERTOR BRIDGES TO AN AC-NETWORK, 12-PULSE CONNECTION

5.1 Interaction between convertors with filters connected at the ac-bus

Usually, pairs of two 6-pulse convertors are connected together to form 12-pulse convertor units. (See figure 3-11). They are connected in parallel but 30° phase-shifted on the ac-side and connected in series on the dc-side. Usually, filters, which short-circuit the generated harmonics, are connected at the ac-bus to which the convertors are connected. The ac-voltage will be sinusoidal because of the filters and there will be no interaction from one convertor to the other at commutations in the convertors, which, due to the different transformer connections, will not occur simultaneously. The commutation in one convertor will, because of that, occur independently of the commutation in the other convertor. The operation of the individual convertor, will at steady-state operation, be the same as for a six-pulse convertor fed from a stiff sinusoidal voltage, as described in the previous chapter. All the equations derived in this chapter are then valid and the operation can, as seen from the ac-network, be described by the phasor-diagrams according to the figures 4-14 and 4-15.

5.2 Interaction between 6-pulse convertors with a partly common commutation reactance

As a comparison to the previous case, where the two phase-shifted convertors were assumed to be decoupled on the ac-side through the ac-filters connected to the ac-bus, we will now study the case without filters connected at the

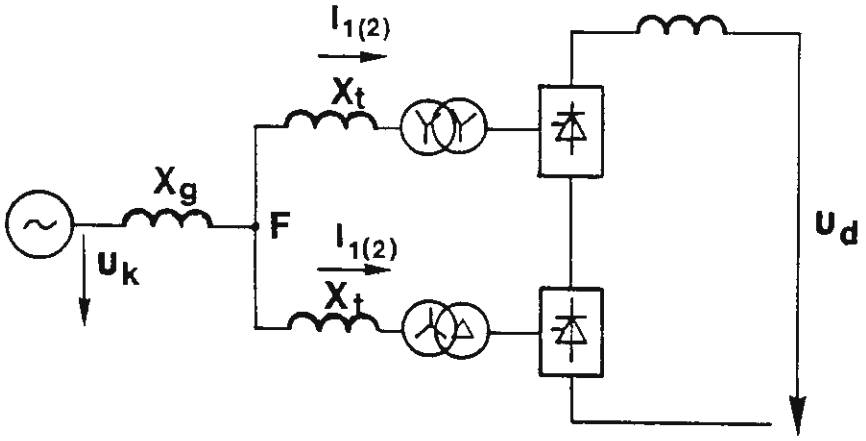

Figure 5-1 12-pulse converter with the commutation reactance partly in commmon for the two 6-pulse converters.

connection point F as illustrated in figure 5-1. The commutation reactance will then have a common part x_g, e.g., the reactance of a generator and its transformer feeding the convertors.

The reactances in the convertor transformers, which are assumed to be Y-Y and Y-Δ connected to give the 30° phase-shift, are assumed to be X_t. The commutations in the two bridges will take place independent of each other as long as the angle of overlap is less than 30°. The commutations will now be determined by the commutation voltage U_k (the internal voltage of the generator) and the commutation reactance, namely:

$$X_k = X_g + X_t \tag{5-1}$$

The fundamental of the ac-phase current to each convertor bridge can be calculated from equation (4-42). This current multiplied by the commutation voltage U_k gives the active and reactive power. From this it is obvious that the previously derived equations for direct voltage, e.g., equations (4-34), (4-35) are still valid for the individual convertor and that the total direct voltage, active and reactive power are derived by multiplication by the factor two.

It should be noted that the voltage at point F will get commutation notches at commutations in either one of the two bridges because of the common reactance X_g. The magnitude of these notches will be determined by the factor.

$$k = \frac{X_g}{X_g + X_t} \tag{5-2}$$

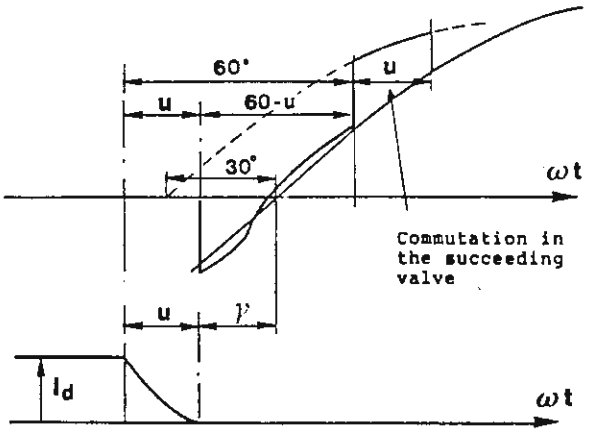

Figure 4-12 End of commutation at inverter operation u=20° and γ=20°.

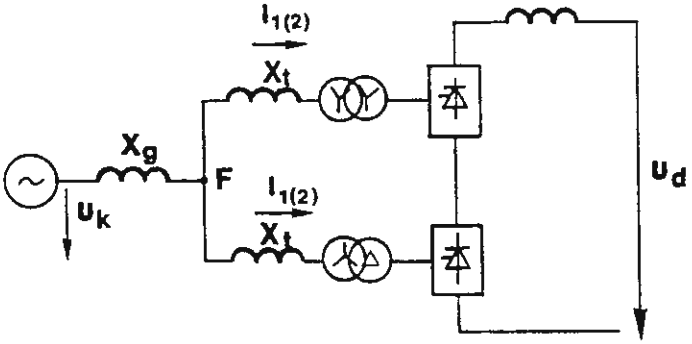

Figure 5-1 12-pulse converter with the commutation reactance partly in commmon for the two 6-pulse converters.

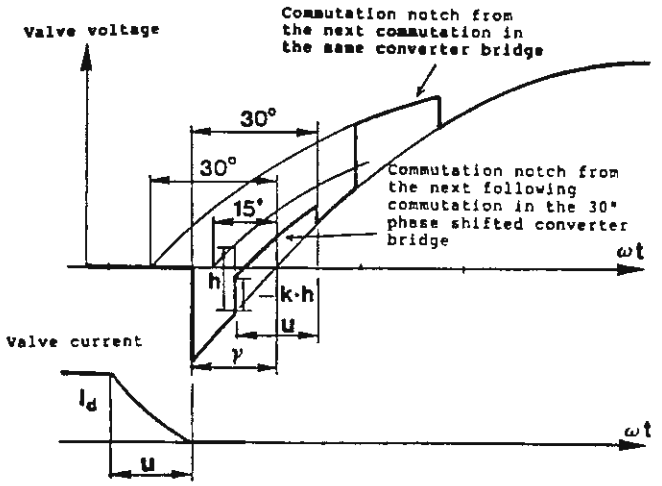

Figure 5-2 Interaction between two 30° phase-shifted six-pulse converter bridges with the commutation reactance partly in common.

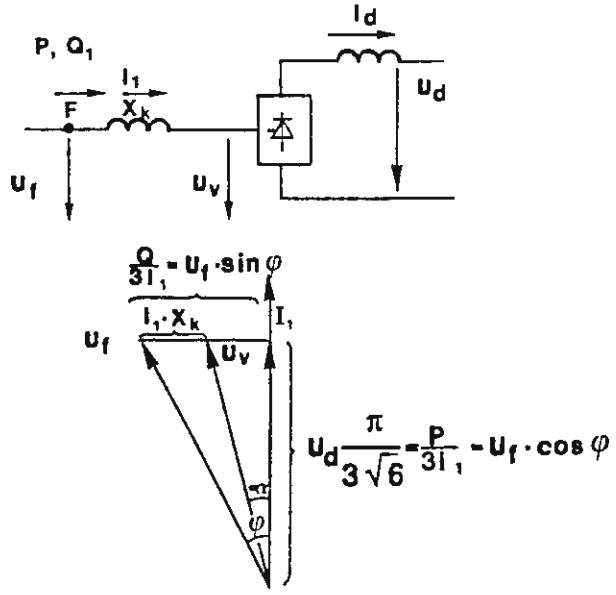

Figure 4-14 Simplified circuit diagram and phasor diagram for a rectifier, phase-voltage.

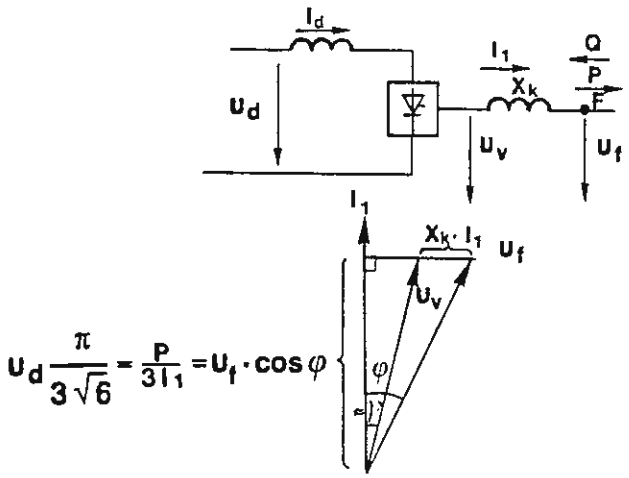

Figure 4-15 Simplified circuit diagram and phasor diagram for an inverter, phase voltage.

These commutation notches should be specially considered at inverter operation. The firing of the succeeding valve in the other phase-shifted convertor bridge will then usually decrease the available real commutation margin. This is further illustrated by figure 5-2, which shows how figure 4-12 will be modified for the case according to figure 5-1 with a common part X_g of the commutation reactance.

5.3 The influence of the ac-network impedance. Short-circuit capacity, short-circuit ratio and effective short circuit ratio

It is usually sufficient to limit the studies to the fundamental components of the ac-currents and voltages illustrated by figure 4-14 and 4-15, when studying the cooperation between the convertor station and the ac-network. The different phase-shifts in the Y-Y and Y-Δ connected transformers will not influence the ac-currents on the line side of the convertor transformers. The diagrams according to figures 4-14 and 4-15 are thus valid independent from the connection of the transformer. From the ac-side it is thus only the number of convertors and the total power that is of interest. Because of that it is convenient to represent all convertors, which are controlled in the identical way, just with a single six-pulse convertor having the same power rating as the total sum of all the convertors. A bipolar convertor station, with two six-pulse convertors in each pole, can then be represented by a single convertor as seen from the ac-side, when studying the effect on the ac-side of complete blocking of both poles.

A simplified circuit diagram for an HVDC station is shown in figure 5-3a (next page). The convertor station is connected to an ac-network, which is represented by an

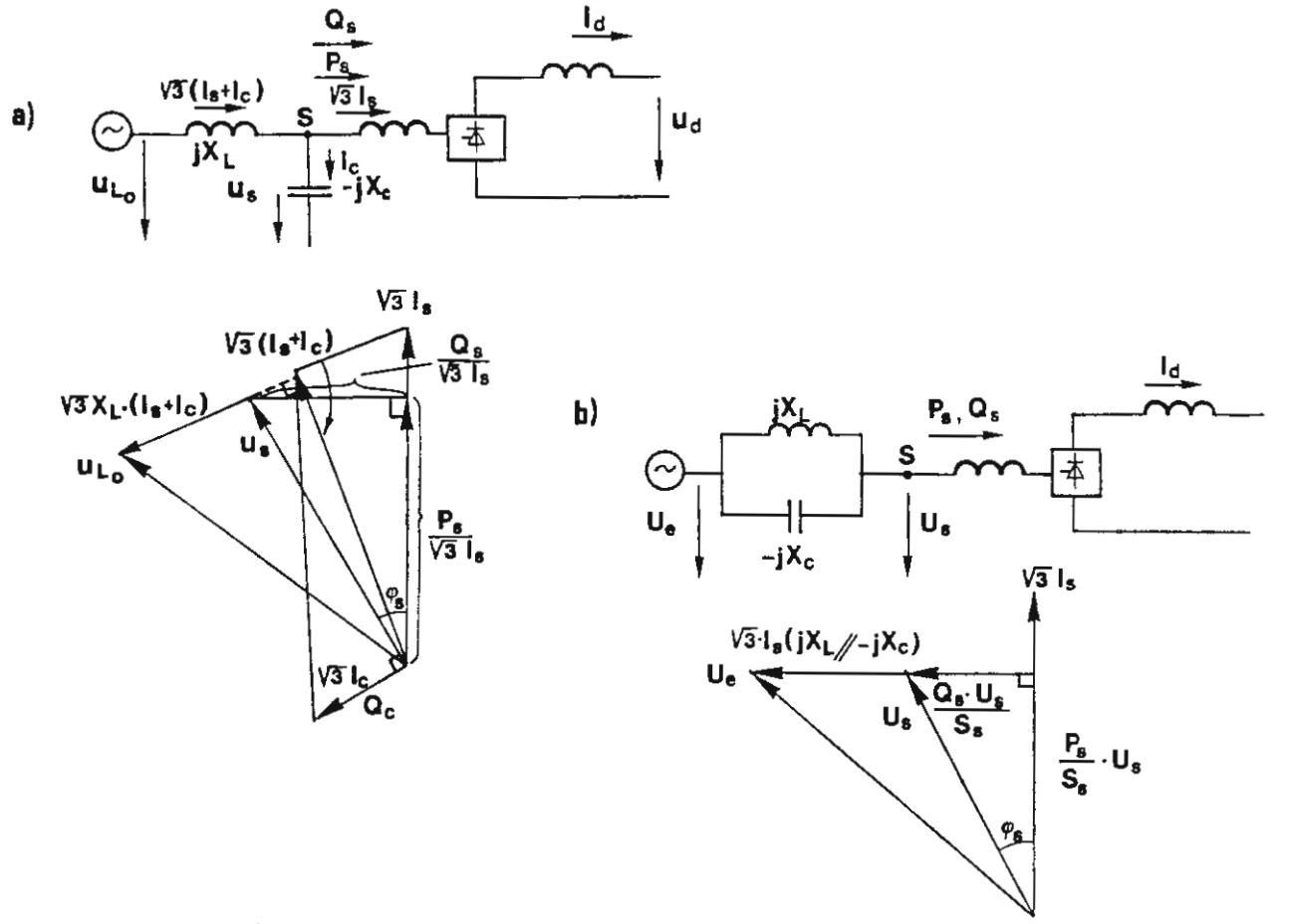

Figure 5-3 Circuit diagram and phasor diagram for a converter station.

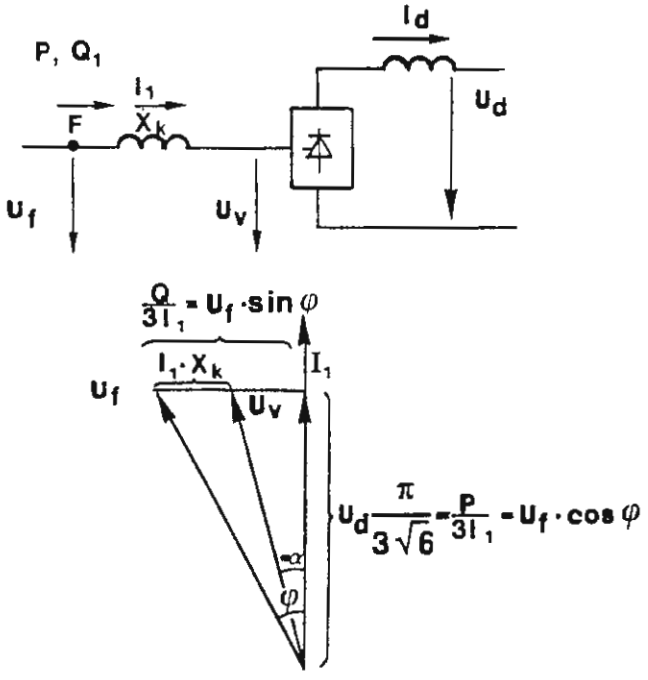

Figure 4-14 Simplified circuit diagram and phasor diagram for a rectifier, phase-voltage.

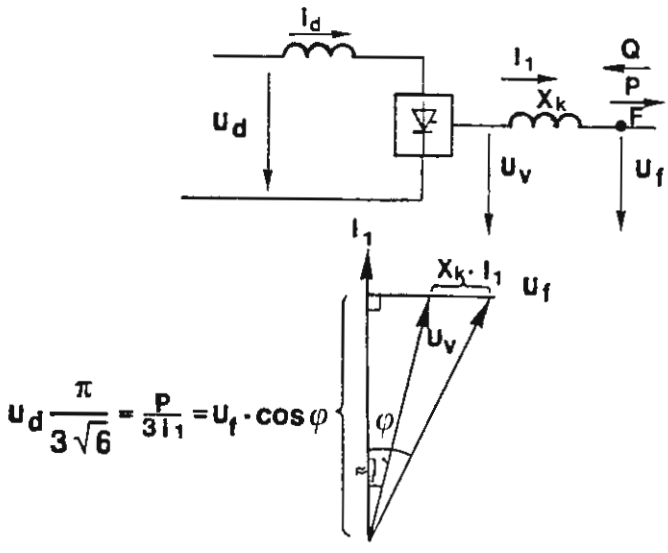

Figure 4-15 Simplified circuit diagram and phasor diagram for an inverter, phase-voltage.

internal voltage U_{LO} behind a pure inductive impedance $j\omega L$. The convertor station is further equipped with a filter and shunt capacitor bank having a total fundamental frequency reactance X_C which is negative. The voltages on the ac-side are here used as line-to-line voltages in contrast to the figures 4-14 and 4-15, where they are used as phase voltages. The convertor quantities are identified by the subscript s.

It is common practice and convenient to express the internal impedance of the ac-network as the network short-circuit capacity. We will define the short-circuit capacity for a pure inductive network as:

$$S_{LN} = U_N^2/X_L \qquad (5-3)$$

The voltage U_N is here the rated voltage of the ac-network. It should be noted that the source voltage U_{L0} is usually different and higher than the rated voltage U_N. The actual short-circuit capacity directly proportional to the admittance of the ac-network, with the proportionality constant being U_N^2 according to equation (5-3).

The ratio between the short-circuit capacity of the ac-network and the rated active power of the convertor station is for HVDC expressed as the "Short Circuit Ratio", SCR. In the following presentation we will denote SCR by k_S, with the definition:

$$k_S = S_{LN}/P_{SN} \qquad (5-4)$$

(It should be noted that in other applications of power electronics, e.g., for motor drives, a different definition

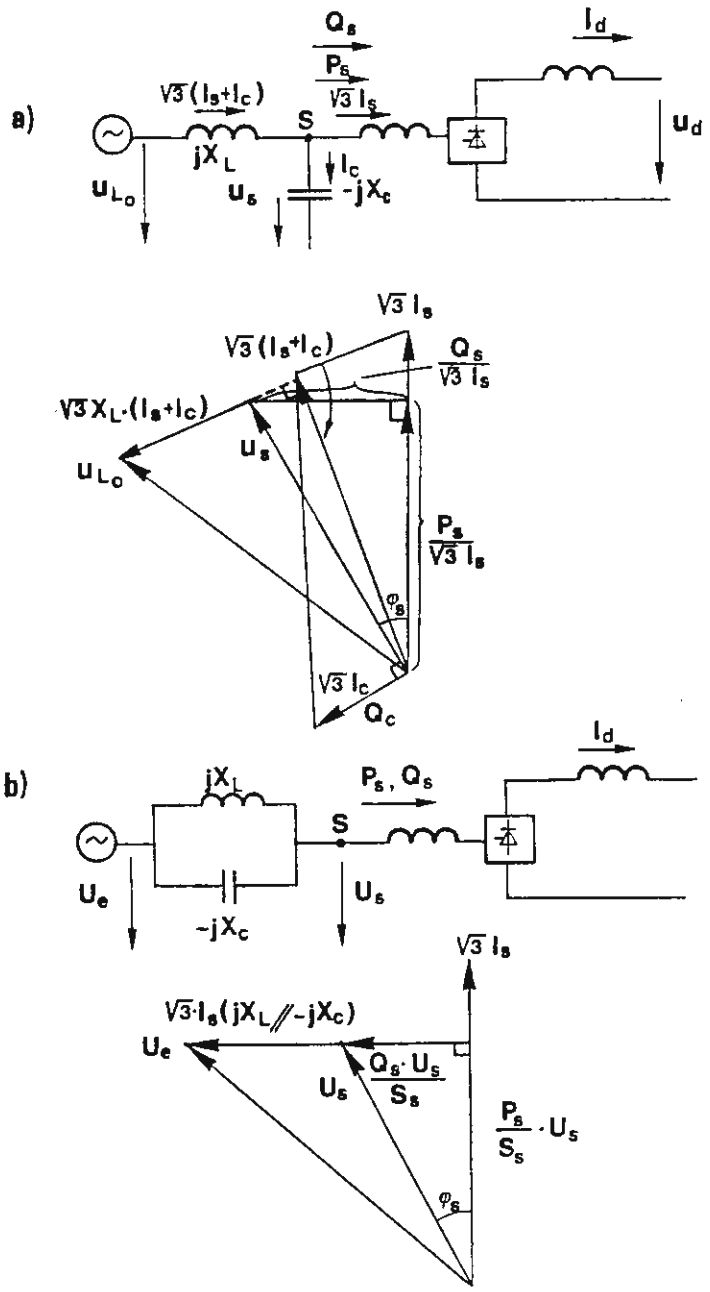

Figure 5-3 Circuit diagram and phasor diagram for a converter station.

of SCR is used. The apparent power S_{SN} is then used as a base instead of the active power P_{SN} as used for HVDC according to equation (5-4).

It is often practical to modify the circuit diagram of figure 5-3a as shown in figure 5-3b. The total network reactance X_e is determined by the network reactance X_L in parallel with the filter reactance X_C. This then gives the following equation for the total reactance X_e:

$$1/X_e = 1/X_L + 1/X_C \qquad (5-5)$$

The corresponding short-circuit capacity is then called "effective short circuit capacity" which we will denote by S_{eN}

$$S_{eN} = \frac{U_N^2}{X_e} = S_{LN} - Q_{CN} \qquad (5-6)$$

when the following equation applies for the rated generated reactive power of the filter and shunt capacitor bank

$$Q_{CN} = U_N^2/X_C$$

The ratio between S_{eN} and P_{SN} is called "Effective Short Circuit Ratio", ESCR, and will in the following be denoted k_e, i.e.,:

$$k_e = S_{eN}/P_{SN} \qquad (5-7)$$

The voltage drop across the effective network reactance X_e will now be:

$$\sqrt{3} \cdot I_S \cdot X_e = S_S/U_S \cdot U_N^2/S_{eN} \qquad (5-8)$$

The apparent fundamental power into the convertor is here denoted by S_S. Figure 5-3b results in the following equations:

$$U_e^2 = \left(\frac{S_s}{S_{eN}} \cdot \frac{U_N^2}{U_s} + \frac{Q_s \cdot U_s}{S_s}\right)^2 + \left(\frac{P_s}{S_s} U_s\right)^2 \qquad (5\text{-}9)$$

Division by U_S gives

$$\frac{U_e}{U_s} = \sqrt{\left(\frac{S_s}{S_{eN}} \cdot \left(\frac{U_N}{U_s}\right)^2 + \frac{Q_s}{S_s}\right)^2 + \left(\frac{P_s}{S_s}\right)^2} \qquad (5\text{-}10)$$

Since $S_S^2 = P_S^2 + Q_S^2$ equation 5-10 can, for the case $U_S = U_N$, be rewritten:

$$\frac{U_e}{U_s} = \sqrt{\left(1 + \frac{Q_s}{S_{eN}}\right)^2 + \left(\frac{P_s}{S_{eN}}\right)^2} \qquad (5\text{-}11)$$

or by utilization of equation 5-7

$$\frac{U_e}{U_s} = \sqrt{\left(1 + \frac{Q_s}{P_{sN}} \cdot \frac{1}{k_e}\right)^2 + \left(\frac{P_s}{P_{sN}} \cdot \frac{1}{k_e}\right)^2} \qquad (5\text{-}12)$$

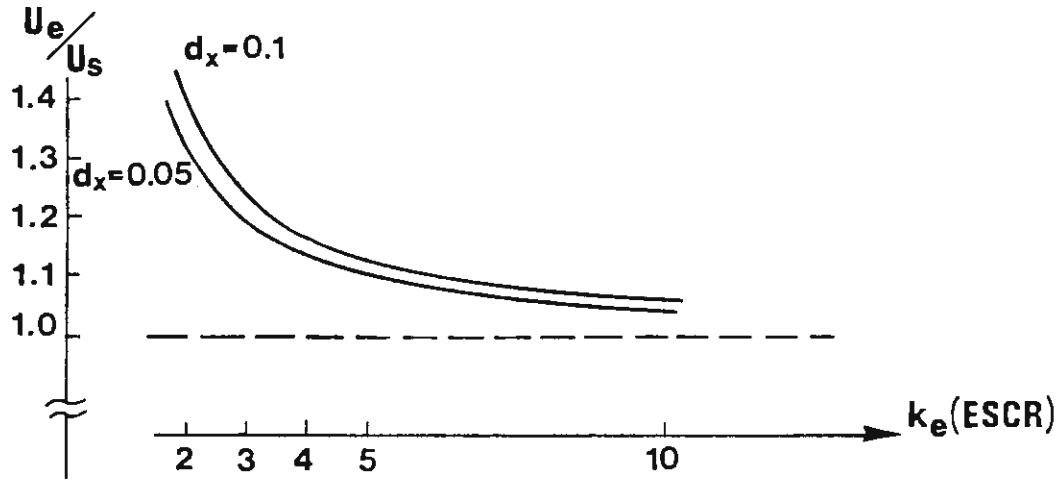

Figure 5-4 Transient voltage rise on load rejection, α=15°, d_x=0.05 and 0.1. u_e and u_s are as shown on figure 5-3b.

At an instantaneous blocking of all the convertors the convertor power will be transiently reduced to zero and the voltage U_s will increase to U_e. Equation 5-12 will thus indicate a measure of the voltage increase at sudden load rejection as a function of the effective short circuit ratio ESCR (k_e). If we assume that $P_s=P_{sN}$, $Q_s=Q_{sN}$, $\alpha_N=15°$ and $d_{XN}=15°$ and 10% respectively, we will, by using equation (4-35) get $U_{di}/U_{dio}=0.916$ and 0.866 respectively and by insertion into equation (4-25), $Q_{SN}/P_{SN}=0.438$ and 0.578 respectively. Insertion into equation (5-12) results in relationships between U_e/U_s and the effective short circuit ratio, as illustrated in figure 5-4.

It should be noted that the curves in the figure 5-4 only illustrate the transient increase in the fundamental frequency component of the filter bus voltage. At a sudden blocking transient voltages of higher frequencies can also be superimposed on this voltage.

The transient increase of the fundamental frequency component of the ac-bus voltage can be substantial at low values of the effective short-circuit ratio (ESCR=k_e) as illustrated in figure 5-4. This is one of the reasons, why the system is usually designed so that $k_e \geq 2.5$-3. However, it should be noted that the calculations presented are approximate because a simplified representation of the ac-network neglecting the resistive losses has been used. The resistive losses will increase the voltage U_e in rectifier operation and decrease the voltage U_e in inverter operation.

It should also be noted that the value of the network impedance is partly determined (affected) by the impedances of connected synchronous machines. For the transient voltage increase at a sudden load rejection, the transient

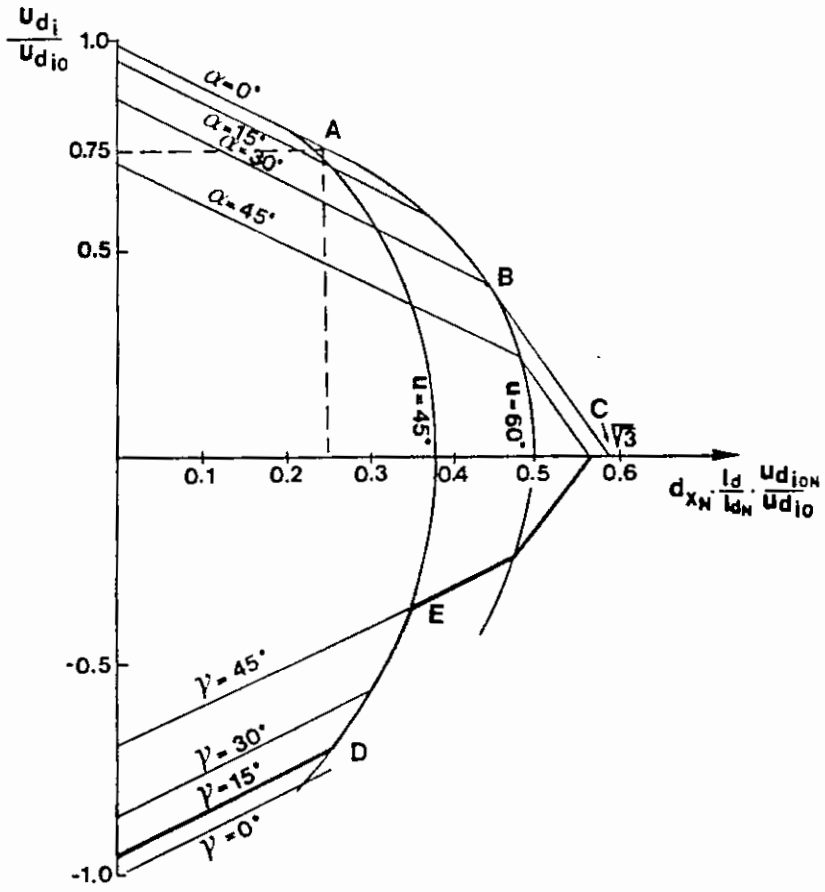

Figure 4-13 Current-voltage characteristics of a 6-pulse converter.

reactances of the synchronous machines usually result the most adequate representation.

The transient increase of the voltage is usually of fairly limited duration as the voltage control of the synchronous machines after a few seconds will reduce the voltage increase and eliminate the major part of the voltage change. This especially applies when synchronous machines are directly connected to the convertor ac-bus.

The network impedance will also influence the current-voltage characteristics as viewed from the dc-side. A fast increase in the direct current will transiently decrease the ac-bus voltage. This reduction will add to the voltage reduction in the convertor, as illustrated by the current-voltage characteristics, according to figure 4-13.

The most efficient way to reduce the voltage variations on the ac-bus at sudden load changes is to connect static var compensators (SVC) directly to the ac-bus. However, it should be noted that, although it is possible in this way to stabilize the ac-bus voltage at sudden load variations, a too high network impedance, which is too high, can still be critical. The impedance of the ac-network will, together with the total capacitance of the filters and shunt banks for reactive power control, determine the resonance frequency of the ac-system. Connection of synchronous compensators for reactive power generation and voltage control on the ac-bus has the advantage of decreasing the total reactance and increasing the resonance frequency. A connected SVC unit will, on the contrary, usually increase the total capacitance and by that decrease the resonance frequency. On the other hand, with regard to costs, losses and need for maintenance, installations of SVC-units are preferred compared to installations of synchronous compensators.

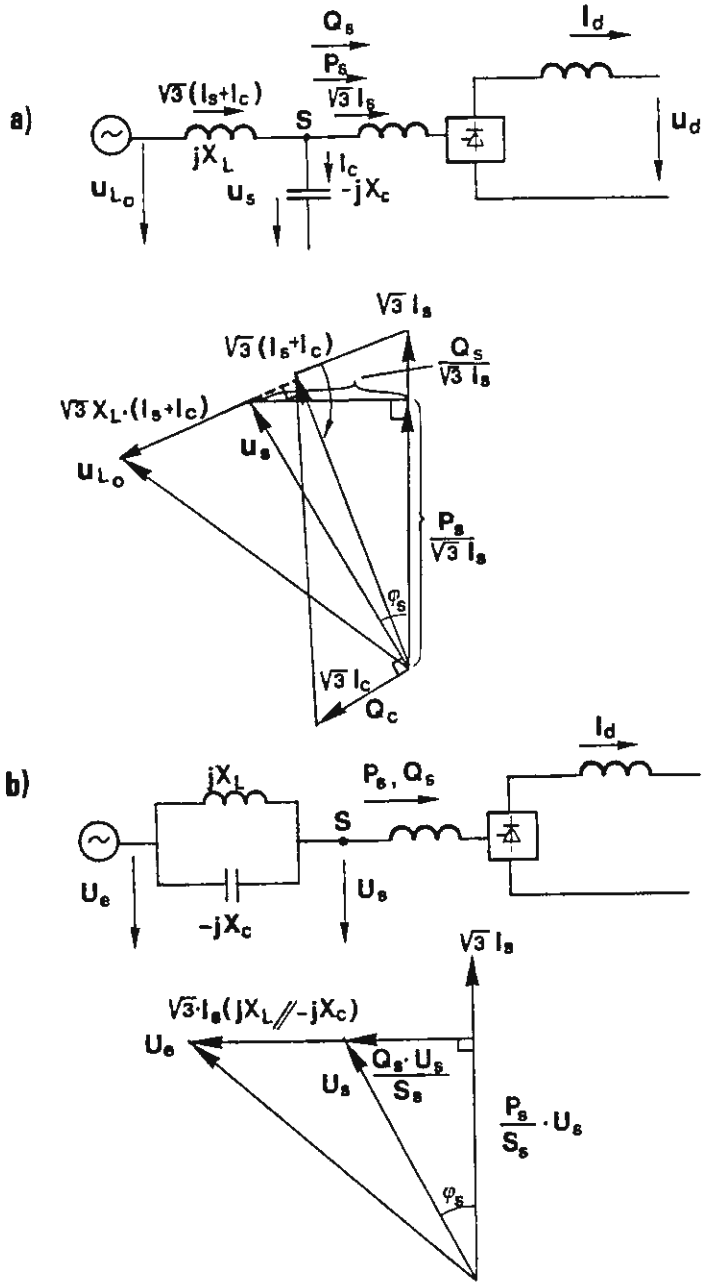

Figure 5-3 Circuit diagram and phasor diagram for a converter station.

For a system according to figure 5-3 the expression for the resonance frequency of the ac-system, expressed as an angular frequency, in rad/sec, will be:

$$\omega_0 = \frac{1}{\sqrt{L_L \cdot C}} \qquad (5\text{-}13)$$

Insertion of

$$S_{LN} = \frac{U_N^2}{X_L} = \frac{U_N^2}{\omega_1 \cdot L_L}$$

and

$$Q_{CN} = \frac{U_N^2}{X_C} = U_n^2 \, \omega_1 C$$

gives

$$\frac{\omega_0}{\omega_1} = \sqrt{\frac{S_{LN}}{Q_{CN}}} \qquad (5\text{-}14)$$

If we assume that $Q_C = 0.5\ P_{SN}$ and insert k_S according to equation 5-4 we will get

$$\frac{\omega_0}{\omega_1} = \sqrt{2 \cdot k_s}$$

This shows that a short circuit ratio of two, in this case, gives an ac-system resonance at the second harmonic. Theoretically second harmonic resonance could be avoided by installation of special filters tuned to this frequency. However, in practice it turns out that such filters can be very expensive and that a second harmonic resonance can result in a number of problems and should be avoided if possible. To avoid this and other problems associated with a too high network impedance the convertor stations and the system are usually designed with a short circuit ratio (SCR) that is well above two and often three or larger.

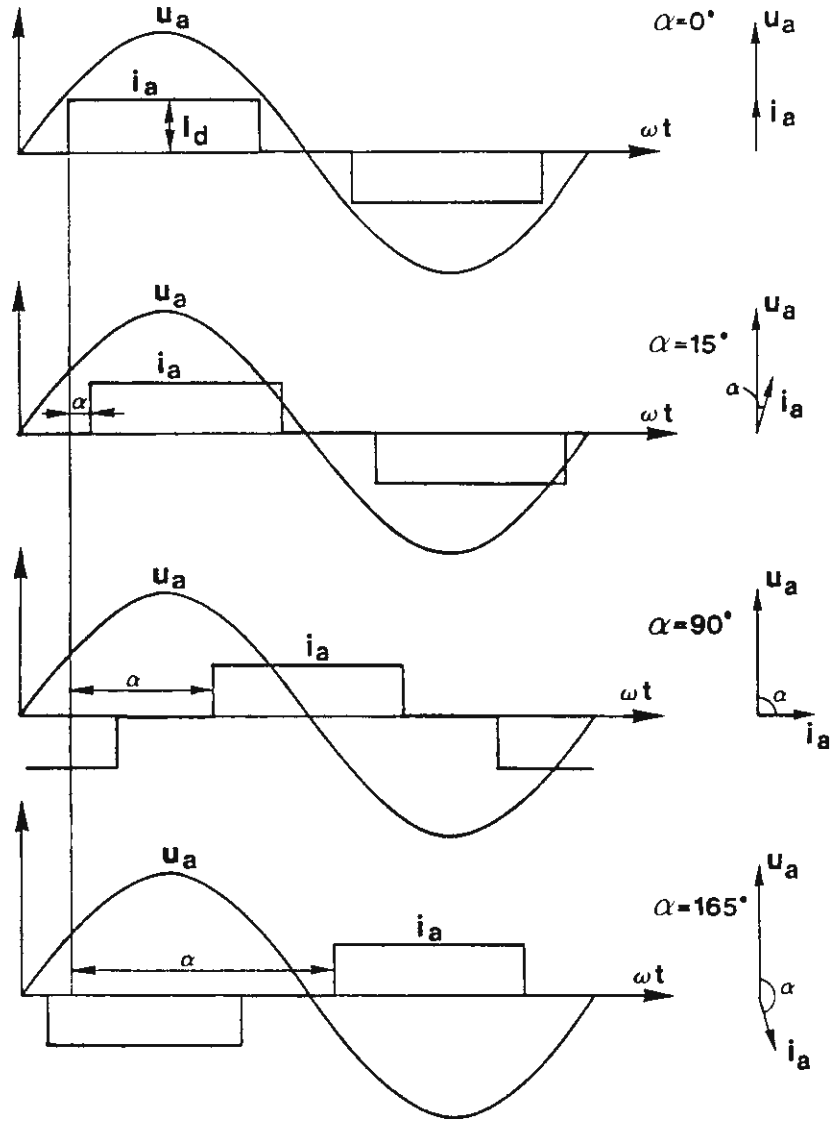

Figure 4-7 Phase-voltages and phase-currents at different values of the firing angle α. Commutation inductance L_k=0 and angle of overlap u=0.

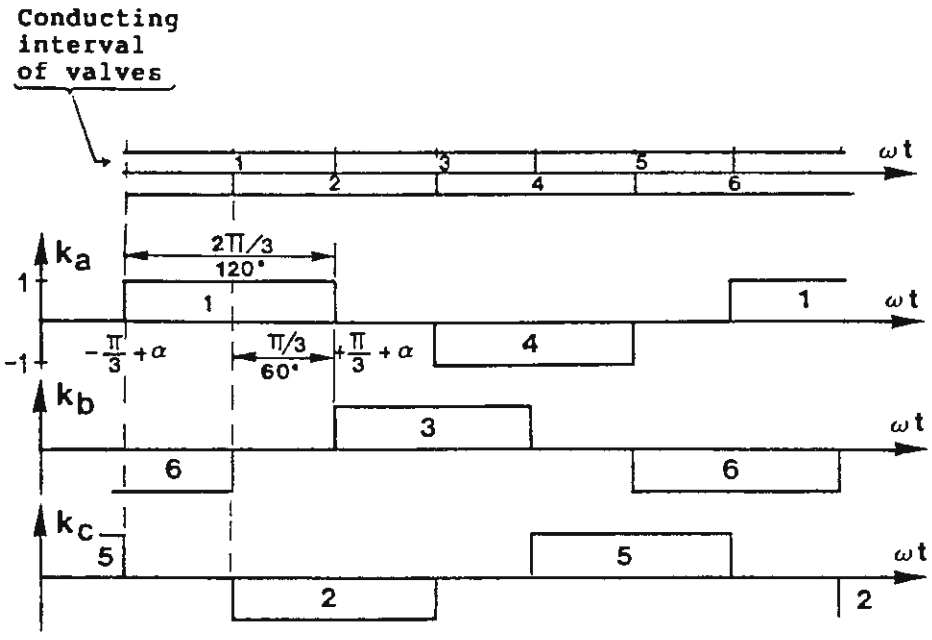

Figure 4-5 Conversion function at two-way six-pulse converter.

6 HARMONICS AND FILTERS

6.1 Generation of characteristic harmonics Six-pulse convertor with zero overlap angle (u=0)

In chapter 4 the 6-pulse convertor with zero overlap angle was treated in section 4-2, and the convertor with non-zero overlap angle in section 4-3. For zero overlap angle and constant bridge current with no ripple the phase current on the valve side of the convertor transformer, figure 4-7, will have the same waveshape as the conversion function, figure 4-5. This points out that the fundamental frequency component of the ac-current ($I_{(1)}$) is directly proportional to the bridge current I_d. The instantaneous value of the current in phase a, i_a according to equation (4-21a), was derived through Fourier-analysis of the conversion function.

The harmonics of the ac-current can be derived correspondingly by multiplication of the conversion function, according to equation (4-15), by the constant bridge current I_d. This then gives the following expression for the harmonics in phase a at zero overlap angle (u=0).

$$i_{a(n)0} = \pm \frac{2\sqrt{3}}{\pi} \cdot I_d \frac{\cos n(\omega t-\alpha)}{n} \qquad (6-1)$$

where $n = 6\,m \pm 1$

and $m = 1,2,3,$ etc

The r.m.s. value of the harmonics will be:

$$I_{(n)0} = I_{(1)}/n \qquad (6\text{-}2)$$

The equation (6-2) is valid for all phases. Because of that, subscript a has been deleted. The phase-shift for the harmonics in phase b and c will be such that harmonics with plus-signs (7,13, etc) will get a positive phase sequence and harmonics with minus-signs in eq. (6-1) (5,11, etc.) will get a negative phase sequence. This is directly obtained from equations (4-16) and (4-17).

The ac-current harmonics can be regarded as being generated by the stiff harmonic current sources.The magnitude of the current harmonics are directly proportional to the direct current I_d, which is assumed to be stiff and completly smoothed. This is a typical feature of a current source convertor.

An expression for the instantaneous voltage across the convertor bridge, U_d, was derived (4-20) in (section 4-2) equation. This expression was derived by multiplying the feeding ac-phase voltage by the conversion function for each phase and adding up the contributions for the three phases. The bridge-voltage consists of a direct voltage component and the superimposed harmonics. The following equation is valid for the harmonics (The subscript 0 indicates that the overlap angle u=0).

$$u_{d(\nu)0}(t) = \frac{3\sqrt{3}}{\pi}\hat{U}_f\left\{\frac{\cos[\nu\cdot\omega t-(\nu+1)\alpha]}{\nu+1} - \frac{\cos[\nu\omega t-(\nu-1)\alpha]}{\nu-1}\right\} \qquad (6\text{-}3)$$

where $\nu = 6\cdot m$ and $m = 1,2,3,.....etc$

It should also be noted that,

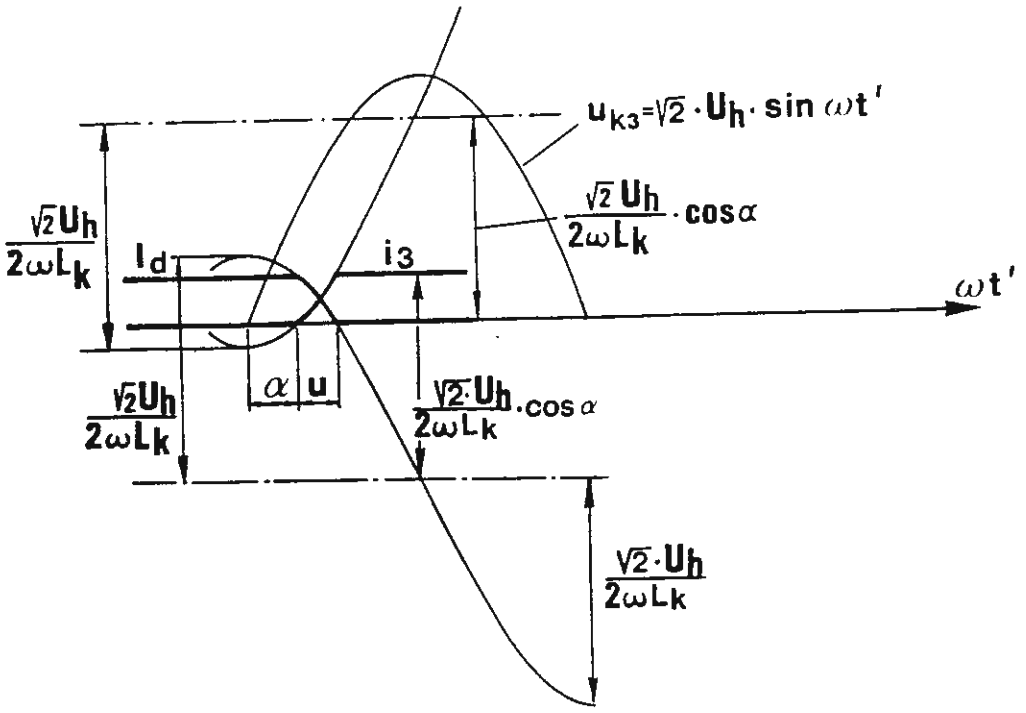

Figure 4-9 Commutation currents.

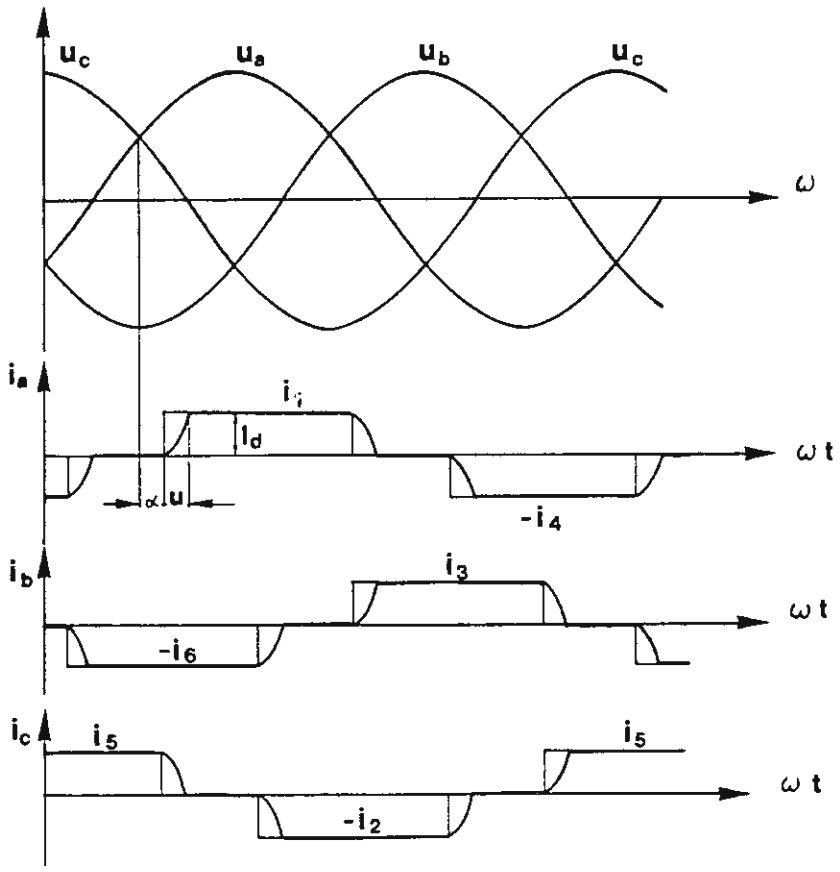

Figure 6-1 6-pulse converter with u>0. Phase-voltages and phase-currents.

$U_{dio} = 3\sqrt{3}\hat{U}_f/\pi$, according to equation (4-8) and (4-10).

Harmonic voltages of the order n=υ can, according to equation 6-3, be split up into two components with the amplitudes $U_{dio}/(n+1)$ and $U_{dio}/(n-1)$, respectively. The two components are phase-shifted by the angle, $(180-2\alpha)$ °el. The following expression can be derived for the r.m.s. value of the harmonic of the order n from equation (6-3) by the use of the cosine rule:

$$\frac{U_{d(n)o}}{U_{dio}} = \frac{1}{\sqrt{2}} \sqrt{\left(\frac{1}{n+1}\right)^2 + \left(\frac{1}{n-1}\right)^2 - \frac{2\cos 2\alpha}{(n+1)(n-1)}} \qquad (6\text{-}4)$$

Equation 6-4 can also be written, as:

$$\frac{U_{d(n)o}}{U_{dio}} = \frac{\sqrt{2}}{n^2-1} \sqrt{1+(n^2-1)\sin^2\alpha} \qquad (6\text{-}5)$$

As the feeding commutation voltages have been assumed to be stiff and sinusoidal the feeding harmonic voltages according to equations (6-3) to (6-5) will have the characteristic of a stiff voltage source.

Six-pulse convertor with non-zero angle of overlap (u>0)

The currents in the ac-phases will get a more curved wave-shape for overlap angles larger than zero than for the assumed ideal case with u=0. This is further illustrated by figure 4-9, showing the valve current at commutation, and figure 6-1 showing the phase currents. The voltage across the convertor bridge will also, at large firing angles, get a somewhat more smoothed wave-shape at larger overlap angles than at zero overlap angles. From this it is obvious that the amplitudes of the harmonic currents will

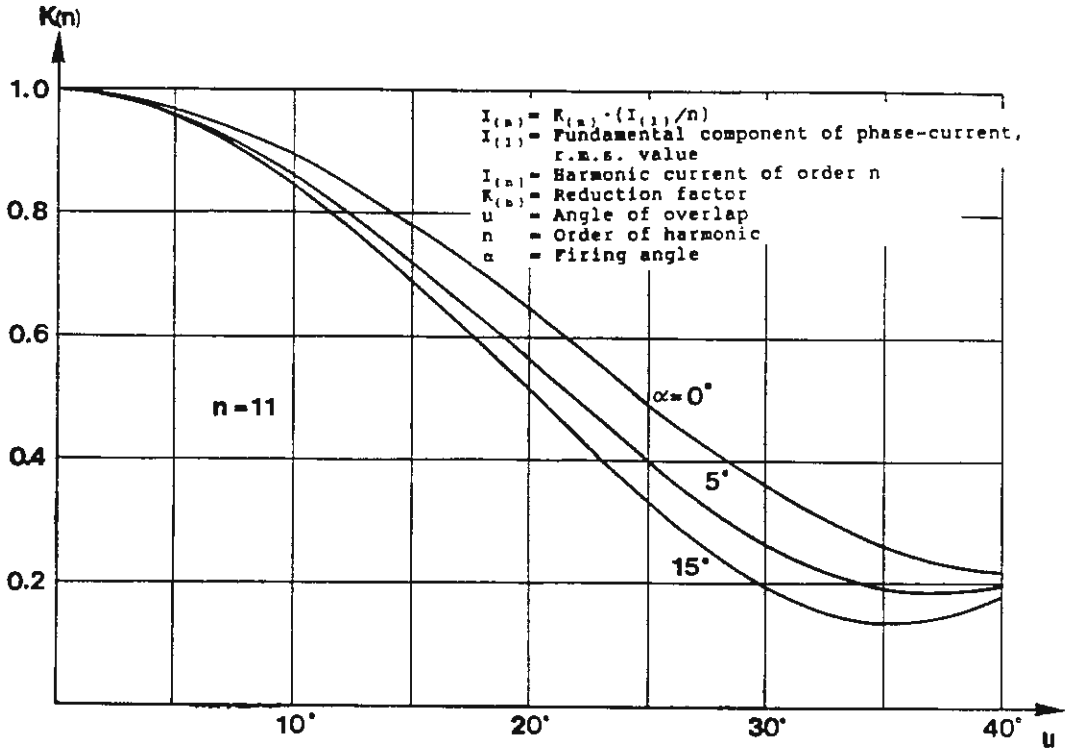

Diagram 6.1 AC phase-current harmonics as a function of the overlap angle u.

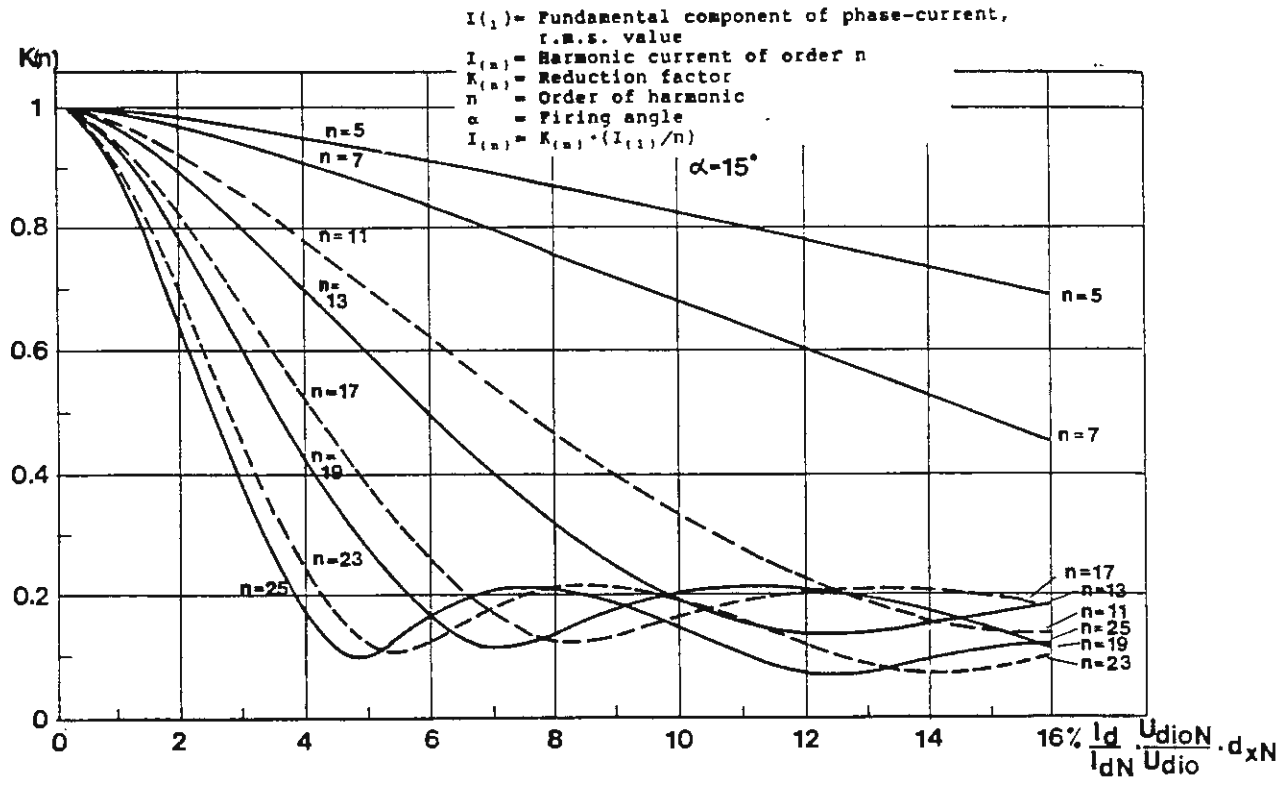

Diagram 6.2 AC phase-current harmonics as a function of the relative inductive voltage drop.

especially be reduced at increased overlap angles. However, for the calculation of the amplitude of the harmonics it is no longer practical to use the conversion functions. The actual wave-form of the current and voltages as calculated in chapter 4 has to be used and Fourier-analyzed. These calculations are relatively volumneous and will not be presented here. See Ref [1]. We will only present the results here. The ratio between the magnitude of the harmonic currents of order n on the ac-side with and without overlap (subscript o) is denoted by K_n. The following expression can be derived for K_n under the assumption that the bridge current is completely smoothed.

$$K_{(n)} = \frac{I_{(n)}}{I_{(n)o}} = \sqrt{\frac{A^2+B^2-2AB\ \cos(2\alpha+u)}{\cos\alpha - \cos(\alpha+u)}}$$

where

$$A = \frac{\sin[(n+1)u/2]}{n+1} \qquad (6\text{-}6)$$

$$B = \frac{\sin[(n-1)u/2]}{n-1}$$

The relationship between K_n and the angle of overlap u is further illustrated for n=11 and α=0°, 5° and 15° in diagram 6.1. However, for practical calculations it is often more convenient to calculate K_n as a function of d_x than as a function of the overlap angle u. Diagram 6.2 shows these relationships for α=15° and for harmonics between n=5 and n=25. The influence of u and d_x upon the factor K_n is substantial as can be seen from the diagrams 6.1 and 6.2. The value of d_{xN} varies between 5 and 10% for HVDC convertor stations.

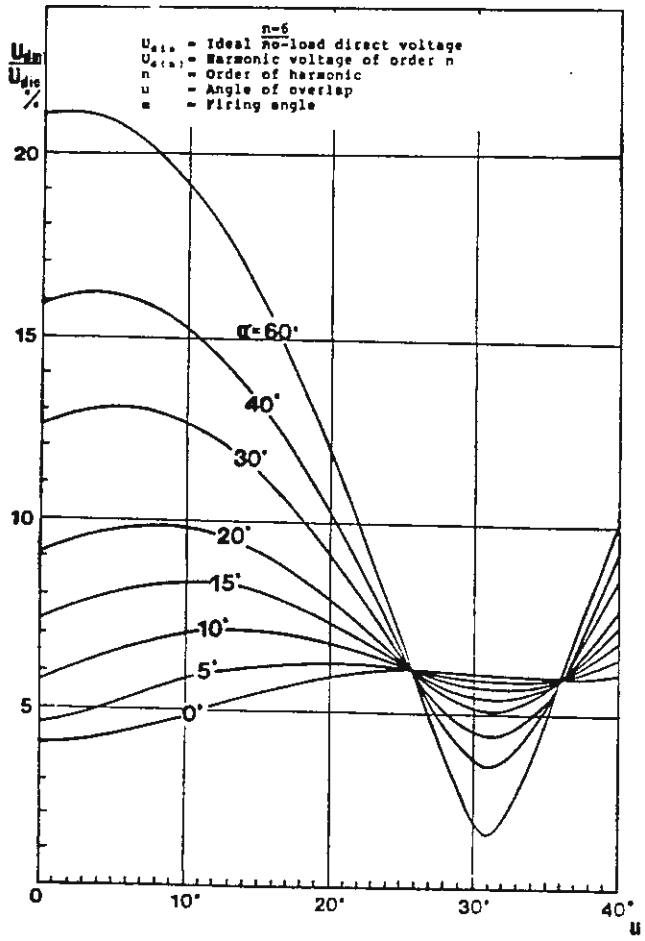

Diagram 6.3 Converter bridge voltage harmonics, n=6.

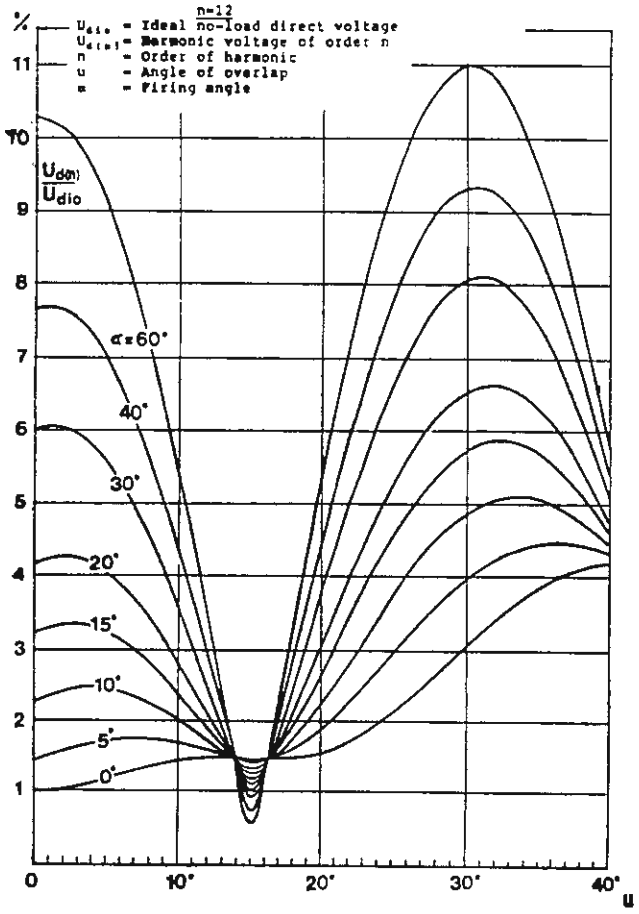

Diagram 6.4 Converter bridge voltage harmonics, n=12.

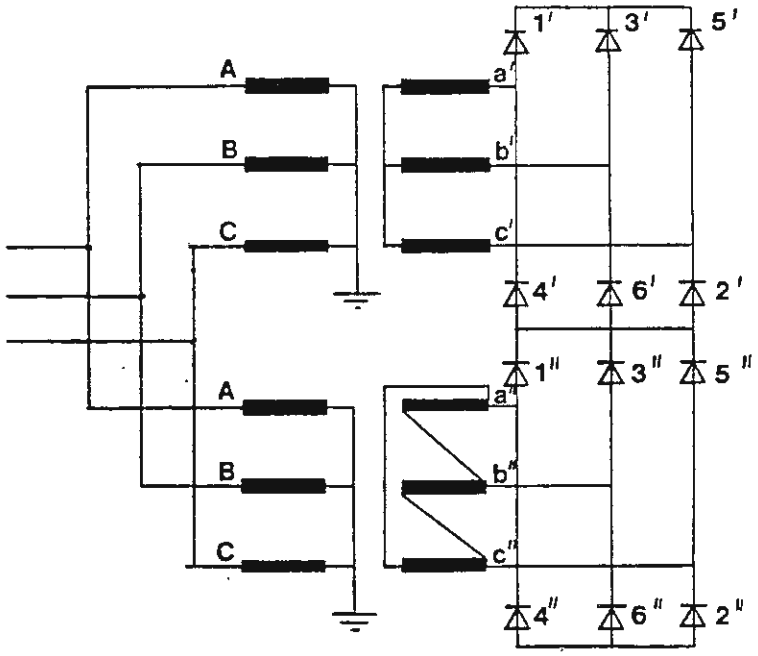

Figure 3-11 Twelve-pulse converter circuit formed by two 30° phase-shifted two-way six-pulse bridge converter circuits connected in series, p=12, q=3, s=4.

For overlap angles larger than zero equation 6-4 has to be replaced by the following expression. It is here assumed that the size of the dc-reactor is infinitely large resulting in no ripples of the dc-current.

$$\frac{U_{d(n)}}{U_{dio}} = \frac{1}{\sqrt{2}} \sqrt{C^2+D^2-2C\cdot D\cdot\cos(2\alpha+u)} \qquad (6\text{-}7)$$

where $C = \frac{\cos[(n+1)\ \frac{u}{2}]}{n+1}$

and $D = \frac{\cos[(n-1)\ \frac{u}{2}]}{n-1}$

Equation (6-7) will be converged to equation (6-4) when the angle of overlap approaches zero. The relationships according to equation (6-7), are illustrated in the diagrams 6.3 and 6.4 for n=6 and n=12, respectively.

12-pulse convertor

The harmonic currents in each phase according to equations (6-1) and (6-6) are referred to the valve side of the convertor transformer. When the transformers are Y-Y or Y-Δ connected the corresponding harmonic current on the line side is achieved by multiplication with the turn-ratio κ of the transformer. (Number of turns on the valve side divided by the number of turns on the line side).

This shows that the contribution to the instantaneous value of the harmonic current in phase A from the upper bridge in a 12-pulse connection according to figure 3-11 as derived from equation (4-15) will be (u=0)

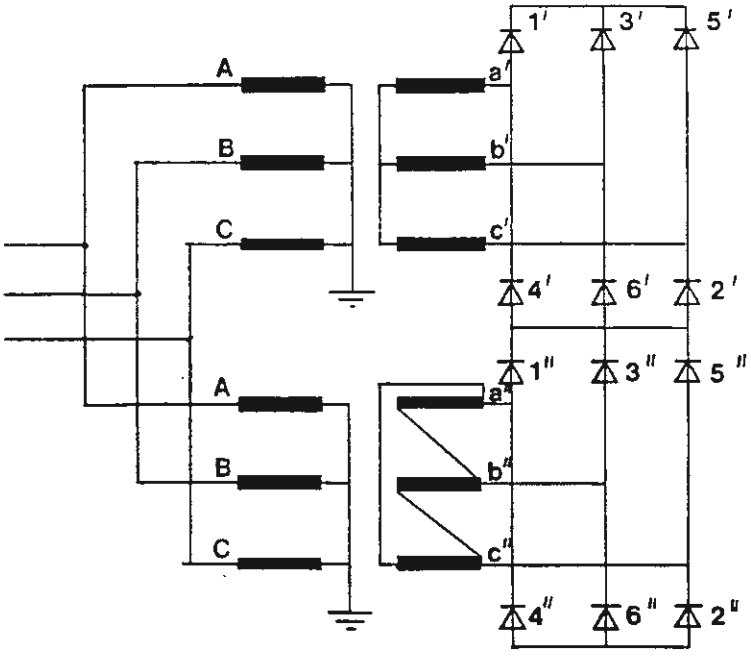

Figure 3-11 Twelve-pulse converter circuit formed by two 30° phase-shifted two-way six-pulse bridge converter circuits connected in series, p=12, q=3, s=4.

$$i'_A = \frac{2\sqrt{3}}{\pi} \kappa \cdot I_d \sum_{n=1}^{\infty} \pm \frac{\cos\, n(\omega t-\alpha)}{n} \qquad (6\text{-}8)$$

The transformers to the two bridges in figure 3-11 have different connections to give a 30° phase-shift between the ac-voltages on the valve-side. The voltages for the phases a", b" and c" are lagging the voltages for the phase a', b' and c' by 30°. This indicates that the firing of the valves in the lower bridge is delayed by $\pi/(6\cdot\omega)$ sec. compared to the firing of the corresponding valves in the upper bridge. It is here assumed that the firing is equidistant, i.e., having equal time intervals between successive firings. This also means that the corresponding conversion functions according to equations (4-15) to (4-17) will be delayed by $\pi/(6\cdot\omega)$ sec.

The contribution to the current on the line side of the convertor transformer in phase A from the lower bridge is given by the difference between the current in the phases a" and b" multiplied by $\kappa/\sqrt{3}$. Insertion in equations (4-15) and (4-16) gives the contribution to the phase current i_A from the lower bridge to be:

$$i''_A = \frac{2}{\pi} \kappa \cdot I_d \sum_{n=1}^{\infty} \pm \left[\frac{\cos\, n(\omega t-\alpha-\pi/6)}{n} - \frac{\cos\, n(\omega t-\alpha-2\pi/3-\pi/6}{n} \right] \qquad (6\text{-}9a)$$

where $n \geq 1$, $n = 6m \pm 1$ and $m = 0,1,2,3.....$

Equation (6-9a) can be simplified to

$$i''_A = \frac{2\sqrt{3}}{\pi} \kappa \cdot I_d \sum_{n=1}^{\infty} \pm \frac{\cos\cdot n(\omega t-\alpha)}{n} (-1)^m \qquad (6\text{-}9b)$$

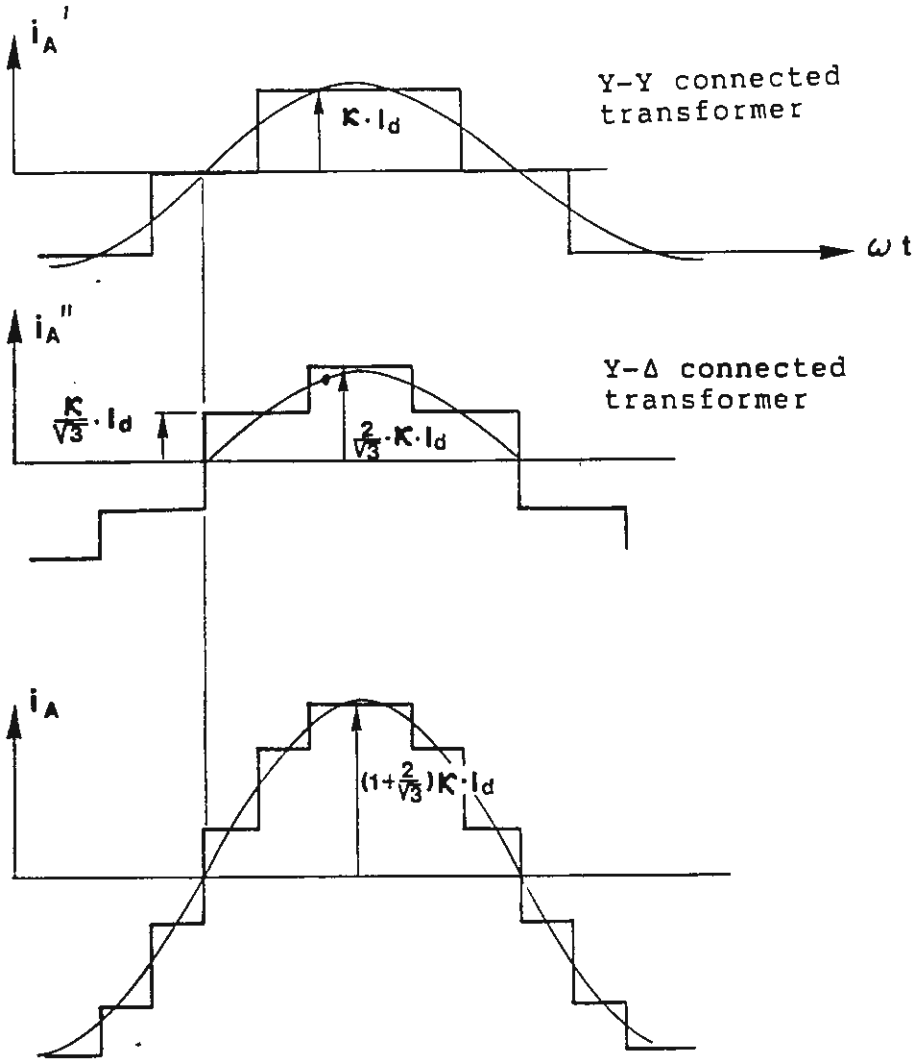

Figure 6-2 AC current at the network side of a 12-pulse converter at a voltage ratio of κ in each converter transformer, overlap u=0°.

Comparing equations (6-8) and (6-9b) shows that all harmonics, for which m is an odd number, have different signs in equations (6-8) and (6-9b). As a result they will disappear when they are added up, i.e.,:

$$i_A = i_A' + i_A'' = \frac{4\sqrt{3}}{\pi} \kappa \cdot I_d \sum_{n=1}^{\infty} \pm \frac{\cos n(\omega t - \alpha)}{n} \qquad (6\text{-}10)$$

where $n \geq 1$, $n = 12m \pm 1$ and $m = 0, 1, 2$, etc.

The superposition of the currents i_A' and i_A'' to form i_A is further illustrated in figure 6-2.

Superposition of the voltage harmonics on the dc-side from the two bridges connected in series, will correspondingly show that harmonics of the order $n = 6 \cdot m$, where m is an odd number, will cancel, as they have the same magnitude but different signs.

6.2 Generation of non-characteristic harmonics

We have in the previous sections assumed completely symmetrical conditions i.e. symmetric voltages, equal commutation inductances in all phases and exactly the same time-intervals between consecutive firing pulses i.e. equidistant firing. The harmonics generated under these conditions are usually referred to as characteristic harmonics. Beside these harmonics additional harmonics will be generated when the conditions are not quite symmetric. The dominant asymmetry are usually asymmetries in the feeding ac-voltage(s), but differences in the commutation reactances between the different phases and non-equidistant

firing also have to be considered. Such asymmetries can give additional harmonics of any frequency being an integer multiple of the network frequency. These additional harmonics are referred to as non-characteristic harmonics.

Modern firing control systems are usually designed to effect equidistant firing to the valves. The asymmetry in the firing can, because of that, often be neglected. However, asymmetries in the feeding ac-voltages and differences between the commutation phase reactances can produce in differences in the overlap angles. The extinctions (discontinuely of conduction) of consecutive valves might because of that, no longer be equidistant. As a result the phase-currents besides the characteristic harmonics will also contain odd non-characteristic harmonics. The amplitude of the non-characteristic harmonics is usually much smaller than that of the characteristic harmonics. The influence of the non-characteristic current harmonics on the ac-side can, because of that, usually be neglected.

Non-characteristic voltage harmonics of even order are obtained on the dc-side due to asymmetric ac-voltages or differences in phase commutation reactances. It should be noted that asymmetries in the ac-voltage will result in non-characteristic voltage harmonics on the dc-side, and also for the case of a perfectly symmetrical conversion function (at equidistant firing and zero overlap angle) To analyze this case it is convenient to resolve up the ac-voltage in symmetrical components. In case of non-symmetric ac-voltages we will also get an ac-voltage component having a negative phase-sequence, i.e., or negative-sequence component. Ac-networks having a negative-sequence voltage component of less than 2% of the positive sequence component are usually classified as being symmetric.

Let's now assume that the negative-sequence component has a phase-position such that the negative-sequence component in each phase can be written according to equations (4-1) to (4-3) but with positive signs before the angles $2\pi/3$ and $4\pi/3$. The amplitude will be denoted $\hat{U}_{f-}$. Equation (4-18) can now be used for the superimposed components in the internal bridge voltage caused by the negative sequence component in the ac-voltage, provided that $\hat{U}_f$ is replaced by $\hat{U}_{f-}$ and the signs in front of the angles $2\pi/3$ and $4\pi/3$ in the first cosine-term are changed.

The following contribution to the bridge voltage from the negative-sequence voltage component will then be achieved after certain calculations.

$$u_{d-} = \frac{3\sqrt{3}}{\pi}\,\hat{U}_{f-}\left[\sum_{\upsilon=2}^{\infty}\frac{\cos[\upsilon\cdot\omega t-(\upsilon-1)\alpha]}{\upsilon-1} - \sum_{\upsilon=4}^{\infty}\frac{\cos[\upsilon\cdot\omega t-(\upsilon+1)\alpha]}{\upsilon+1}\right] \qquad (6\text{-}11)$$

$\upsilon = 6\,m + 2$ and $m = 0,1,2,3$, etc., for the first summation term and
$\upsilon = 6\,m - 2$ and $m = 1,2,3$ etc for the second summation term.

Comparing equation (6-11) with (4-20), which applies for an ac-voltage component of positive phase-sequence, shows that the two expressions are fairly similar. It can be seen that the negative sequence components in the feeding ac-voltage result in all the even harmonics, which were not generated by the positive-sequence voltage component i.e. of the order $\upsilon=2,4,8,10$ etc. A non-characteristic harmonic of greatest interest is the second order harmonic. The amplitude of this harmonic is:

$$\hat{U}_{d2} = 3\sqrt{3}/\pi \; \hat{U}_{f-} \qquad (6\text{-}12a)$$

This can be compared with the ideal no-load direct voltage generated by the positive sequence voltage component with the amplitude $\hat{U}_{f+}$ for which we have:

$$U_{dio} = 3\sqrt{3}/\pi \; \hat{U}_{f+} \qquad (6\text{-}12b)$$

This gives

$$\hat{U}_{d2} = \frac{U_{dio} \cdot \hat{U}_{f-}}{\hat{U}_{f+}} \qquad (6\text{-}12c)$$

The r.m.s value of the second harmonic will thus be

$$U_{d2} = \frac{U_{dio}}{\sqrt{2}} \cdot \frac{\hat{U}_{f-}}{\hat{U}_{f+}} \qquad (6\text{-}12d)$$

Equation (6-12d) shows that a negative-sequence component of 2%, which is not unreasonable for a so called symmetric ac-voltage, could result in a second harmonic component on the dc-side of about 1.4% of the ideal no-load direct voltage.

6.3 Interference caused by the harmonics General filtering requirement

Harmonic currents and voltages in electric power systems can cause interferences and various troubles. Because of that strict requirements are usually set for limitation of the generated harmonics from HVDC convertor stations. The increased use of power electronics during the past years

have caused a tendency to increase the harmonic contents in the power systems, especially at low or medium voltage levels. The following types of inconveniences and interferences caused by the harmonics should especially be considered.

a) **Harmonics of lower frequencies**, up to 500-600 Hz, can cause additional thermal stresses on machines and capacitors. They can also increase the voltage stresses on capacitor banks, especially in the case of resonances. The low frequency harmonics can also interfere with the operation of certain equipment. Electric power systems using superimposed pulses of certain frequencies for control of certain loads, e.g., for switching in and out of loads, e.g.,heaters (ripple control), are especially sensitive to the injected harmonics.

For these low frequency harmonics resulting in a distorted waveform of the feeding ac-voltage, harmonic currents and voltages of positive, negative and zero sequence can be critical.

b) **Harmonics of higher frequencies** are usually mainly critical with regard to the risks of telephone interference. Open telephone lines of older types which are not properly balanced are most sensitive. It is mainly the magnetic coupling between the electric power lines and the telephone lines that is critical. Because of that, it is primarily the zero sequence harmonic currents on the power lines that can interfere with parallel running telephone lines. Harmonic currents of positive and negative-phase sequence can also cause telephone interference, especially when the telephone lines are running very close to the power lines, e.g., on the same towers, or are crossing a power line.

It should also be noted that injected harmonic currents of

positive- and negative-phase sequence at one point of the power system, can result in zero-sequence harmonic currents in other parts of the systems through unbalances between the three phases e.g., due to not sufficiently transposed lines. This shows that the harmonics generated by an HVDC convertor station can cause interference in the telephone network although the injected harmonics from the convertors are only of the positive- and negative-sequence character. Unbalances in the filters might also result in zero-sequence harmonic currents that are generated to the ac-system.

The distribution of the harmonic currents from the convertor station into the ac-network is usually not analyzed in detail for each project. The ac-network can usually be connected in many different ways with different loads connected, which makes it very difficult to analyze all the critical cases. Because of that it is common pratice to only specify maximum permitted harmonic voltages at the connection point of the convertor station to the ac-network. This could be combined with requirements on maximum injected harmonic currents to the lines or to synchronous machines connected at the convertor station.

The situation is quite different for the HVDC line. The line is well defined with only convertor stations connected to the line. It will thus be less complicated to calculate the harmonic current along the dc-line. The filtering requirement for the dc-side is because of that usually specified as maximum permitted harmonic currents of zero-sequence characteristics along the dc-line.

6.4 Specification of filtering requirement On the ac-side

The requirement for maximum harmonic voltages on the ac-bus is usually specified partly as a maximum permitted voltage distortion and partly as the root sum square of the harmonic voltages weighted by a frequency dependent factor. This factor takes into account the sensitivity of the telephone lines and the sensitivity of the human ear for various frequencies.

Distortion

The maximum permitted distortion of the ac-voltage is usually specified, both, as max relative amplitude for each individual harmonic and as a max. permitted total distortion.

The distortion related to the individual harmonic is specified as

$$D_{(n)} = U_{(n)}/U_{(1)} \cdot 100\% \qquad (6\text{-}15)$$

where $U_{(1)}$ is the fundamental frequency component of the voltage and $U_{(n)}$ is the magnitude of the voltage harmonic of order n. A typical requirement for high voltage networks ($\geq$130 kV) is that $D_{(n)} \leq 1\%$. Usually higher values are accepted for medium voltage networks.

The accumulated or total distortion is specified as either arithmetic distortion:

$$D = \sum_{n=2}^{m} D_{(n)} \qquad (6\text{-}16)$$

where m usually is 50 and the required limit is 3-5% or as the root sum square of the distortions for the individual

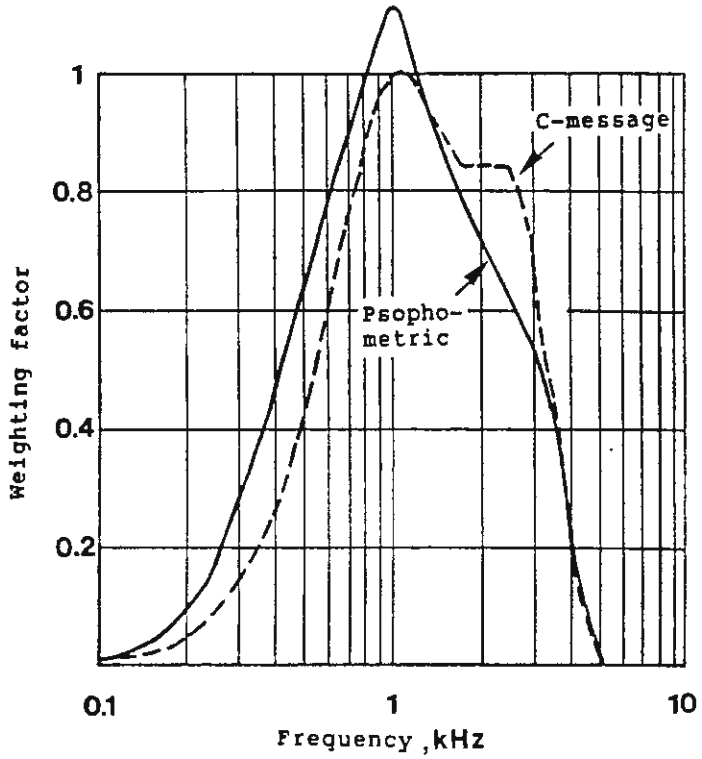

Diagram 6.5 C-message and Psophometric weighting factor.

harmonics i.e.

$$D_{rss} = \sqrt{\sum_{n=2}^{m} D_{(n)}^2} \qquad (6\text{-}17)$$

Specified limit values of D_{rss} is 2-3%.

Since it usually is the thermal stresses, caused by the low frequency harmonics, that can be critical, it is therefore recommended to specify D_{rss} rather than D.

Telephone interference

High frequency harmonics are usually mainly critical with regard to the risk of telephone interference. The frequency is here critical as, both, the mutual coupling to telephone lines and the sensitivity of the telephones and the human ear depends very much upon the frequency of the harmonic.

The following standardized definitions have been developed in North America and Europe.

a) Telephone influence factor, TIF (America)

$$TIF = \sqrt{\sum_{n=2}^{m} \left(F_n \cdot U_{(n)} U_{(1)}\right)^2} \qquad (6\text{-}18)$$

where $F_n = C_n \cdot 5 \cdot n \cdot f_1$

C_n is the "C-message weighting factor" as shown in diagram 6-5.

b) Telephone harmonic form factor, THFF (Europe)

$$THFF = \sqrt{\sum_{n=2}^{m} \left(F_n \cdot U_{(n)} / U_{(1)}\right)^2} \qquad (6\text{-}19)$$

where $F_n = P_n \cdot n \cdot f_1/800$

P_n is the psophometric weighting factor from the diagram 6-5.

Typical requirement on TIF is 25-40 and on THFF about 1% which corresponds to TIF 30-40

c) Beside requirements due to distortion and telephone interference as specified above, requirements are sometimes also specified for max generated weighted harmonic currents to the ac-lines. This is identified as max IT values specified as below.

$$IT = \sqrt{\sum_{n=2}^{m} \left(I_{(n)} \cdot F_n\right)^2} \qquad (6\text{-}20)$$

$I_{(n)}$ is the r.m.s. value in amperes of the current harmonic of order n, and F_n is the weighting factor according to equation (6-18).

Since the harmonic currents generated and injected into the ac-system are limited by shunt-filters, primarily limiting the harmonic voltages but not the currents, it is fairly difficult to specify and verify requirements on harmonic currents. The harmonic currents injected in the ac-system will depend very much on the actual ac-line impedance. It is especially very important that the min. ac-network impedances are correctly determined, when max IT values are specified. Values of IT in the range 20,000 - 50,000 have

been used.

6.5 Specification of the filtering requirement on the dc-side

In principle the requirement on the filtering, with limitation of the distortion in voltage and current, as used for the ac-side, could also be used for the dc-side. However, as already mentioned, it is often more practical to specify a maximum level for the harmonic currents along the line or a section of the line which might be most critical with regard to interference of adjacent telephone lines. It should be noted that the amplitude of the harmonic currents will vary along the lines. For lower frequencies the reflections at the end of the lines will influence the current distribution along the lines. This implies that the maximum amplitude must not necessarily occur close to the terminals where the harmonics are injected.

It is primarily the ground-mode component (corresponding to zero-sequence component in a three phase ac-system) that will have a mutual coupling to the telephone lines. It is difficult to directly measure the ground-mode component of the harmonics in the overhead line. Because of that, the requirement on filtering has often been specified as maximum weighted harmonic voltages measured in a test line having a length of 1 km and running in parallel to the power line at a distance of 1 km. The mutual coupling between the overhead line and the test line depends on the resistivity of the earth. The following approximate formula is often used for the mutual impedance.

$$Z_{kt} = \frac{k \cdot 1 \cdot \rho}{d^2} \qquad (6\text{-}21)$$

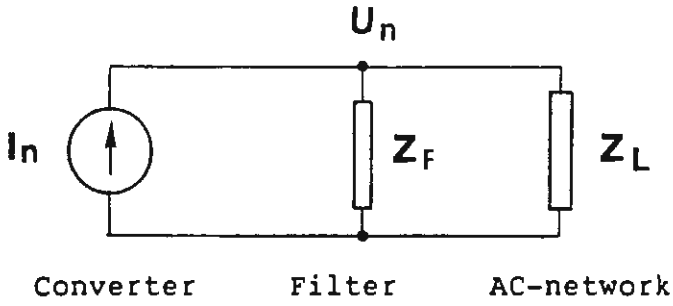

Figure 6-3 Simplified circuit diagram for the calculation of the generated and injected harmonic currents into the ac-network.

k is a constant factor
l is the length of the test line
(or the telephone line)
ρ is the resistivity of the earth (ground)
d is the distance between the overhead line and the telephone line.

The critical parameter here is the earth resistivity, which can vary along the line and also vary as a function of time and depth. The best way to determine the earth resistivity ρ is usually to measure Z_{kt} and use equation (6-21). One end of the test line is then directly grounded and the harmonic voltages are measured at the other end. The measured harmonic voltages are weigthed with the factor C_n and summed as the root sum square according to equation (6-18).

6.6 Calculation of the harmonics generated and injected into the ac-network and different methods for reducing them.

The harmonics generated and injected into the ac-network can be calculated using the simplified circuit diagram shown in figure 6-3. It is here assumed that the internal impedance of the convertor is so large that the generated harmonic currents from the convertor are independent from the external impedance (Z_F in parallel with Z_L in figure 6-3). The convertor may then be represented as a current source for harmonics (note current-source convertor). The ac-network is represented by an impedance Z_L, which is determined by the positive- and negative-sequence impedance of the network for the actual (operating) frequencies. These impedances are usually the same for higher frequencies. It should be noted that the current source only generates harmonics of positive- or negative-sequence but no components of zero-sequence as long as the convertor transformer is ideal. The impedance of the ac-filter and

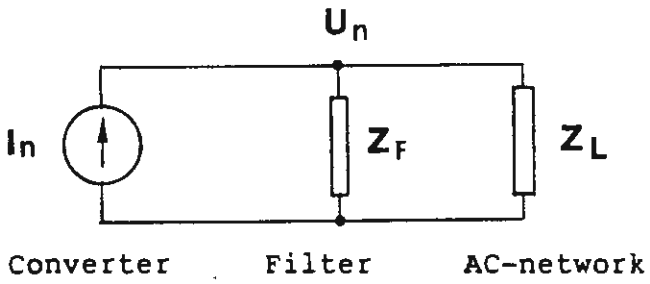

Figure 6-3 Simplified circuit diagram for the calculation of the generated harmonic currents injected into the ac-network.

shunt capacitor banks connected to the convertor ac-bus is represented by the impedance Z_F. When synchronous compensators are connected to the ac-bus, their impedances might be considered to be included in the ac-network impedance Z_L. This also applies for the impedances of possible transformers connected between the convertor station and the ac-network.

The harmonic currents generated and injected into the ac-network will now be determined by:

$$I_{(n)L} = \frac{Z_F}{Z_F + Z_L} \cdot I_n \qquad (6\text{-}22)$$

The harmonic voltages measured at the connection point of the filters will be

$$U_{(n)} = \frac{Z_F \cdot Z_L}{Z_F + Z_L} \cdot I_{(n)} \qquad (6\text{-}23)$$

or

$$U_{(n)} = \frac{1}{Y_F + Y_L} \cdot I_{(n)} \qquad (6\text{-}24)$$

where $Y_F = 1/Z_F$ and $Y_L = 1/Z_L$

The most efficient way to limit the generated harmonics and injected into the network would be to limit the harmonics generated from the convertor. An increased pulse-number will be the most efficient way to achieve this. During the 1960s, when mercury-arc valves were used for the convertors, the convertor stations were built up of 6-pulse

convertors. When the mercury-arc valves were replaced by thyristor-valves in the 1970th it was found advantageous to build up the convertor stations of 12-pulse convertor units instead. The major reason for the choice of 6-pulse convertors, when mercury-arc valves were used, was that the convertor bridges had to be temporarily disconnected in case of arc-backs.

The great advantage of using 12-pulse units instead of 6-pulse units is that harmonics of the order 5, 7, 17 and 19, disappear or at least can be drastically reduced. The filters for the 5th and 7th harmonics are large and expensive for 6-pulse convertors. The lower the harmonics order the larger the filter required which is also more expensive.

As we will see later, all filters are almost purely capacitive at the fundamental frequency. The requirement for total installed capacitance in ac-filters and shunt capacitor banks is usually determined by the requirement to generate and supply a certain amount of reactive power. The fact that large filters for the 5th and 7th harmonics are no longer needed for 12-pulse convertors does not mean that the total amount of reactive power generated in filters and shunt capacitor banks can be reduced. However, this has made it possible to simplify the design of the filters for the other harmonics and it has also made it easier to control the reactive power at light loads.

A further increase of the pulse number, e.g. from 12 to 24, would, from a filtering point of view, result in certain advantages. A possible way to build a 24-pulse convertor would be to connect four 6-pulse convertors in series on the dc-side. Two of them could then be fed from transformers connected in Y/Y and Y/Δ as used for the 12-pulse convertor. The phase shift in these transformers is 0° and 30°. The other two transformers could on the

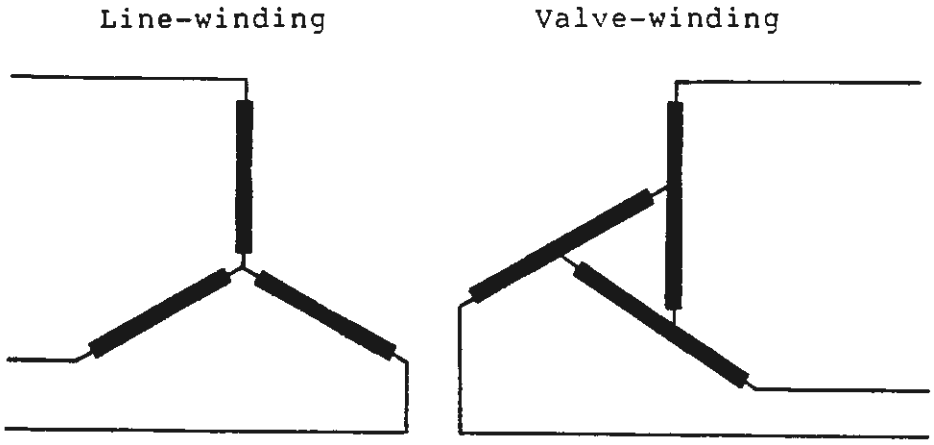

Figure 6-4 Three-phase transformer with extended delta connection of the valve-windings.

valve side be connected in a so called extended delta connection as shown in figure 6-4 producing a phase shift of ±15°. This transformer connection has already been used for back-to-back stations for 12-pulse convertors. The reason for the choice of this transformer connection then was that a single spare transformer could be used for both 6-pulse convertors.

The main reason why, a 24-pulse convertor has not been used for HVDC, is rather economical than technical, since the possible cost savings in the filters has not out-weighted the increased cost for transformers, bushings, arrestors and other equipment. It must also be taken into account that the non-characteristic harmonics due to asymmetries will not decrease with an increased pulse-number.

We will now in the following presentation assume that the pulse number and the generation of harmonics are given. The harmonic voltages on the filter-bus are determined by the filter impedance Z_F and the network impedance Z_L as can be seen from equations (6-23) and (6-24).

The following alternative simplified assumptions are often made regarding the impedance of the ac-network as the real network impedance can vary within a wide range.

a) The network impedance is assumed to be infinitely large, which gives $U_{(n)} = Z_F \cdot I_{(n)}$.

b) It is assumed that parallel resonance between the ac-network and the filter can occur, i.e., the network impedance has a value, which gives a minimum of $|Y_F+Y_L|$.

To be able to judge if case b, which is the most critical case, can occur, we need more information about the ac-network impedance.

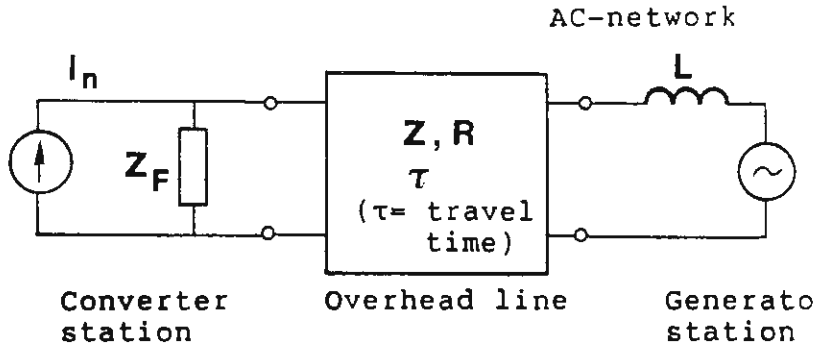

Figure 6-5 Simplified representation of the ac-network with one overhead line connected to a generator station.

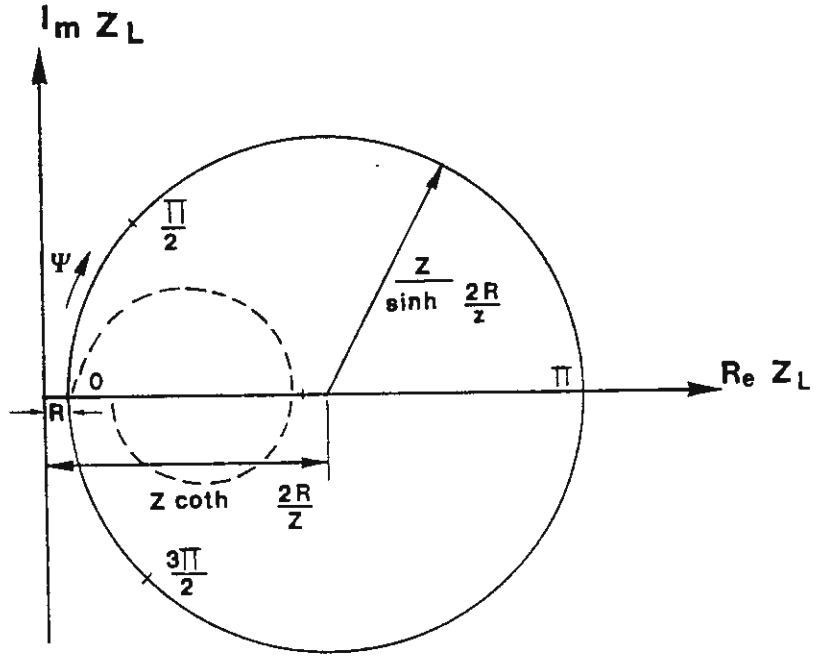

Figure 6-6 The impedance diagram of the ac-network according to figure 6-5.

Ac-network impedance

At first we will study a very simplified representation of the ac-network as shown in figure 6-5 to become familar with how the impedance in a real ac-network may vary. We assume that the convertor station is connected to a long distortion free overhead line. See Ref. [2], p 362. The wave-impedance is Z, travel time τ, and total longitudinal resistance R. It is further assumed, that the other end is terminated with an impedance, which can be represented by a pure inductance L. We define the following parameters so that:

$$\omega_n = 2\pi \cdot n \cdot f_1$$
$$T = L/Z, \text{ then}$$
$$tg\lambda = \omega_n \cdot T \qquad (6\text{-}25)$$
$$\psi = 2(\omega_n \cdot \tau + \lambda)$$

We will then get the following expression for the impedance Z_L of the line as viewed from the convertor station (see Ref. [2], page 363):

$$Z_L = Z \frac{\sinh \frac{2R}{Z} + j \sin \psi}{\cosh \frac{2R}{Z} + \cos \psi} \qquad (6\text{-}26)$$

For $\psi = 0, 2\pi, 4\pi$, etc., and $R/Z << 1$ we will get $Z_L \approx R$. As can be seen from figure 6-6 the locus of the impedance Z_L will, in an impedance diagram, fall on a circle. The center of the circle is on the real axis at a distance M from origin.

$$M = Z \cdot \coth (2R/Z) \qquad (6\text{-}27)$$

The radius r of the circle is

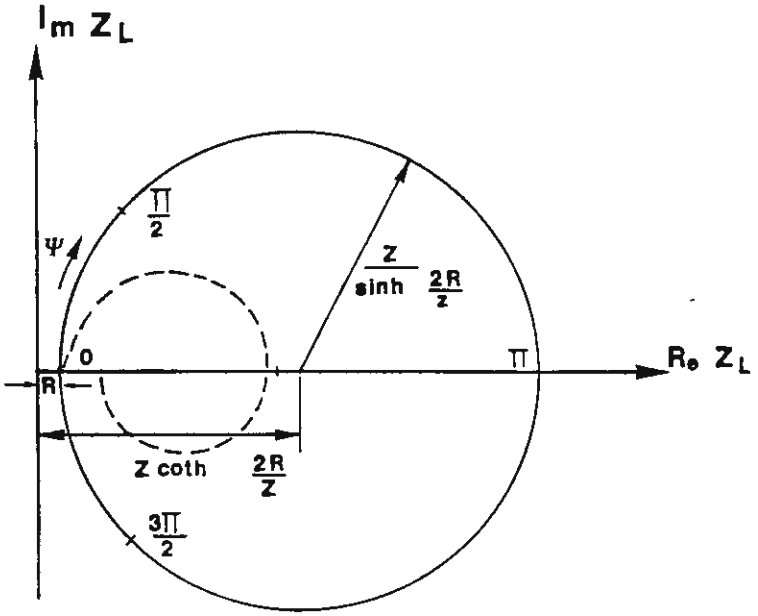

Figure 6-6 The impedance diagram of the ac-network according to figure 6-5.

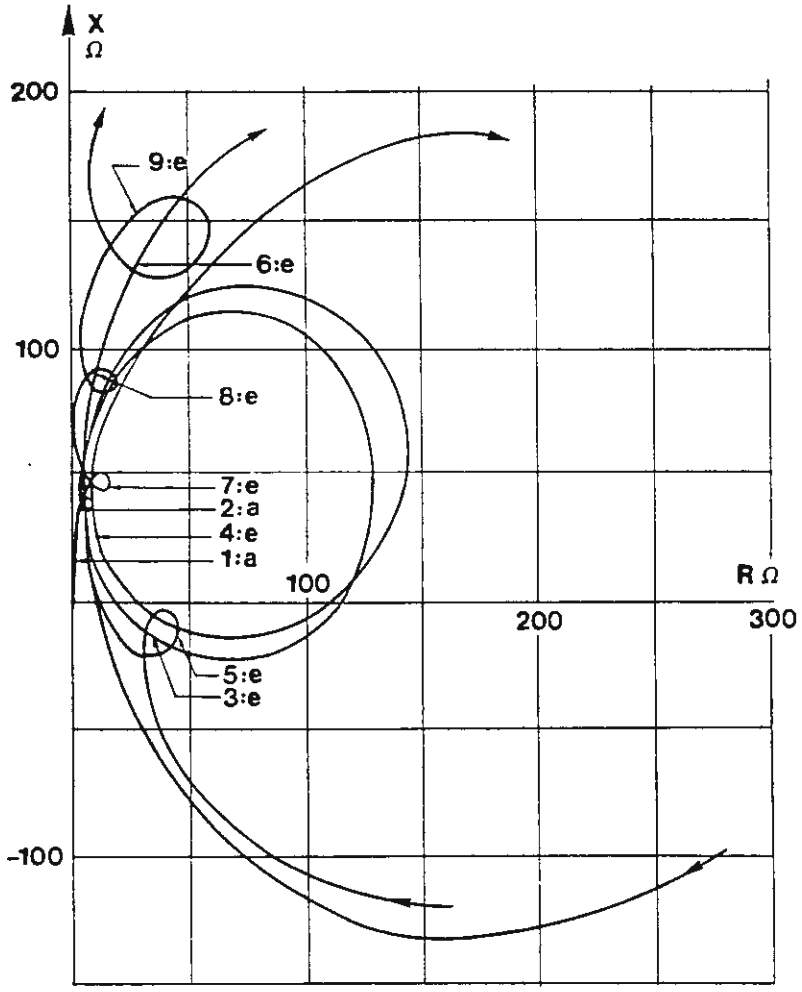

Figure 6-7 A typical calculated impedance diagram for an ac-network.

$$r = \frac{Z}{\sinh \frac{2R}{Z}} \qquad (6\text{-}28)$$

It is of interest to note that the radius of the circle depends only upon the damping of the line. We will approximately get $r = Z^2/2R$ for $R/Z << 1$.

We will get a curve with a smaller radius, as shown by dashed line in figure 6-6, if the line is not assumed to be distortion free or if attenuation is achieved at the end of the line.
The impedance diagram for a real ac-network can be calculated with suitable computer programs. However, the correct representation of the loads at the ends of the lines is usually very critical, as illustrated by the above simplified calculations. Figure 6-7 shows an example of such a computer calculated impedance diagram for a real ac-network.

Measurements of the ac-network impedances have also been made in real ac-networks with varying success. Relatively large signal-amplitudes and high power are then needed to get an acceptable signal to noise ratio. The measurements ought also to be performed with a three-phase signal generator in order to determine the positive- sequence impedance. Accurate measurements, if they could be performed, would also be of limited value for an actual optimization of the filters, as the network-impedance would change with the actual configuration of the network. However, such measurement would certainly be of value for the verifications of the models used.

A detailed impedance curve shown figure 6-7 is hardly usuable for the optimization of ac-filters. The normal practice is to instead use limitation curves defining

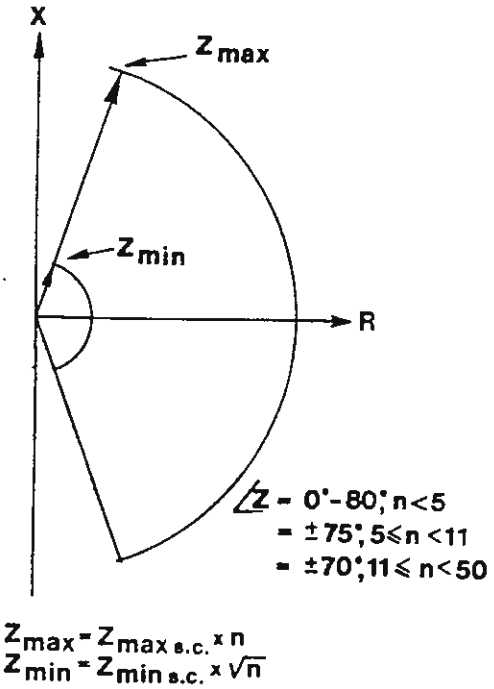

Figure 6-8 Boundaries for ac-network impedance. The general sector model.

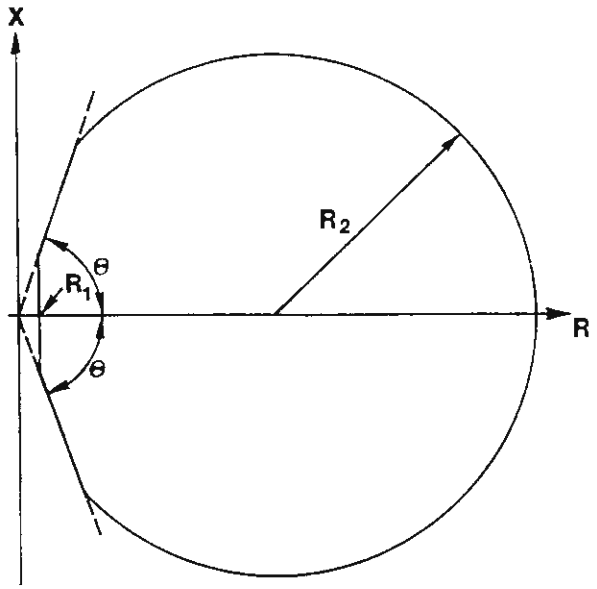

Figure 6-9 Boundaries for ac-network impedance. The general circle model.

possible regions for the real expected impedances. Figures 6-8 and 6-9 show two examples of such limiting curves. In the first case the max. magnitude of the phase angle of the impedance is specified as well as the maximum and minimum value of the magnitude of the impedance. The limiting values are given as a function of the harmonic number. In the latter case the limiting curve is given as a circle with additional limitations on the phase-angle and the minimum resistance.

6.7 Ac-filters

As described above ac-filters are connected to the ac-bus of the convertor station in order to:

- reduce harmonics generated and injected into the ac-network
- generate reactive power

The ac-filters are usually connected at the ac-bus between the ac-phases and ground. The ac-filters shall offer a low impedance for the generated harmonics and are usually referred to as either one of the following two types.

- Band-pass filters or tuned filters which offer a low impedance for one or a limited number of harmonics. They are usually designed as the single-tuned or the double-tuned resonance filters.

- High-pass filters or damped filters which usually a low impedance for higher frequencies.

Modern convertor stations are usually equipped with band-pass filters for the 11^{th} and 13^{th} harmonics and high-pass filters for higher harmonics. The connected shunt-capacitor banks will also offer a low impedance for

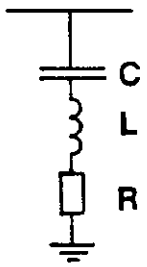

Figure 6-10 Single-tuned band-pass filter.

higher frequencies. The ratings of the filters are usually determined by the amount of reactive power generated at rated ac-voltage. The ratings of the (installed) capacitors in the filters will usually be somewhat larger as they are connected in series with reactors.

Single-tuned band-pass filters

A single-tuned band-pass filter is built up of a series resonance circuit as shown in figure 6-10.

A resistor is often connected in series to give the required band-width of the filter. The resistance of the reactor, which is usually air-insulated, is often too small to give the required damping. The impedance of the band-pass filter is given by:

$$Z_{fn} = R + j(\omega L - 1/\omega C) \qquad (6\text{-}29)$$

The filter is purely resistive at the resonance angular-frequency

$$\omega_{(n)} = 1/\sqrt{LC} = n \cdot \omega_{(1)} \qquad (6\text{-}30)$$

The relative frequency deviation from the resonance frequency is defined as

$$\delta = \frac{\omega - \omega_{(n)}}{\omega_{(n)}} \qquad (6\text{-}31)$$

The reactance of the reactor is, at resonance frequency equally large, but of opposite sign of the reactance of the capacitor. The magnitude of the reactance is Q times larger than the total series resistance R, i.e.,:

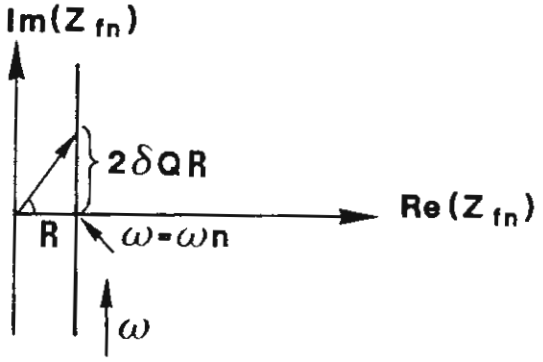

Figure 6-11 Single-tuned band-pass filter. Impedance diagram.

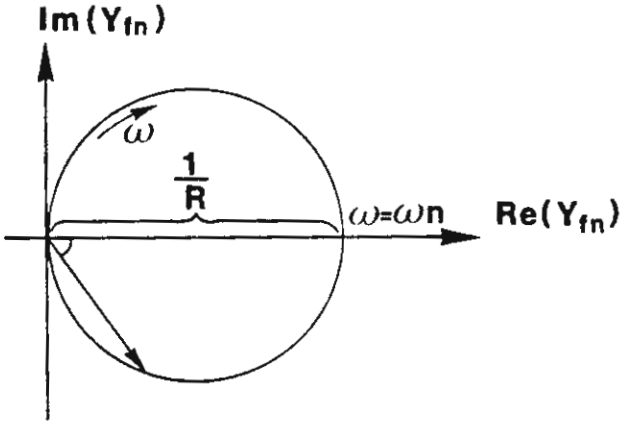

Figure 6-12 Single-tuned band-pass filter. Admittance diagram.

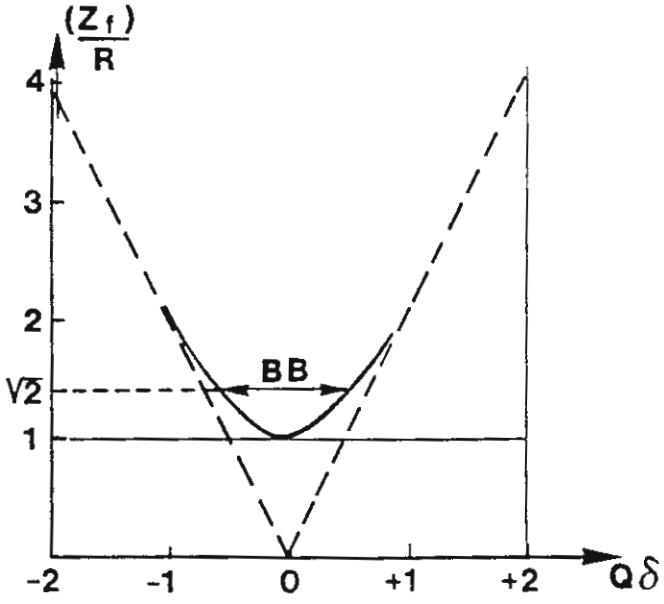

Figure 6-13 Single-tuned band-pass filter. Magnitude of the impedance as a function of δ·Q.

$$Q = \frac{\sqrt{\frac{L}{C}}}{R} = \frac{\omega_{(n)} \cdot L}{R} = \frac{1}{R \cdot \omega_{(n)} C} \qquad (6\text{-}32)$$

The number Q is called the Q-value of the filter or quality-factor, which is a measure of the sharpness of the tuning of the filter. Equation (6-29) can now be rewritten with assistance of equations (6-30), (6-31) and (6-32) to result:

$$Z_{fn} = R\left(1 + j\, Q\, \delta\, \frac{2 + \delta}{1 + \delta}\right) \qquad (6\text{-}33a)$$

Since the Q-value for tuned filters is fairly high (50-100), it is of interest to study how the filter impedance Z_{fn} varies close to the resonance frequency. Equation (6-33a) can now be rewritten, as $\delta << 1$:

$$Z_{fn} \approx R\left(1 + j\, 2\, \delta\, Q\right) \approx \frac{1}{n \cdot \omega_{(1)} \cdot C}\left(-\frac{1}{Q} + j\, 2\, \delta\right) \qquad (6\text{-}33b)$$

The phase-angle of the filter is ± 45° at a frequency deviation giving $2\delta \cdot Q = \pm 1$. These limits define the band-width of the filter. This gives:

$$BB = \omega_n / Q \qquad (6\text{-}34)$$

The admittance of the filter is derived from equation (6-33b) and is

$$Y_{fn} \approx \frac{1}{R(1+j\ 2\delta \cdot Q)} = \frac{1-j\ 2\delta Q}{R\left(1+4\delta^2 Q^2\right)} = \frac{n \cdot \omega_{(1)} \cdot C \cdot Q\left(1-j2\delta Q\right)}{1 + 4\delta^2\ Q^2} \qquad (6\text{-}35)$$

The impedance and admittance characteristics of the filters

are shown in figures 6-11 and 6-12, respectivly. The magnitude of the filter impedance is obtainedas a function of $Q \cdot \delta$ from figure 6-13, which also illustrates the definition of the band-width BB.

Tuning

The filter impedance is very sensitive to the tuning of the filter as illustrated in equation (6-33b) and figure 6-13. The phase-angle is especially very sensitive to the tuning at large values of the quality-factor Q. The filters are almost always more or less detuned, caused by:

a) The network frequency deviates from the rated frequency, e.g., max ± 0.5Hz or ± 1%.

b) The capacitance C of the capacitor units depends on the temperature, e.g., the value will change 3% for a temperature change of 100°C. The capacitance can also change because of aging and failures of capacitor elements (or capacitor cans).

c) Inaccuracy in the tuning. Tuning can be achieved through change of the inductance of the reactor (connections to different terminals) or different connections of the capacitor cans.

Equations (6-30) and (6-31) show the following relationship between the relative detuning δ and the above mentioned factors.

$$\delta = \frac{\Delta f_1}{f_n} + \frac{1}{2}\left(\frac{\Delta C}{C} + \frac{\Delta L}{L}\right) \qquad (6\text{-}36)$$

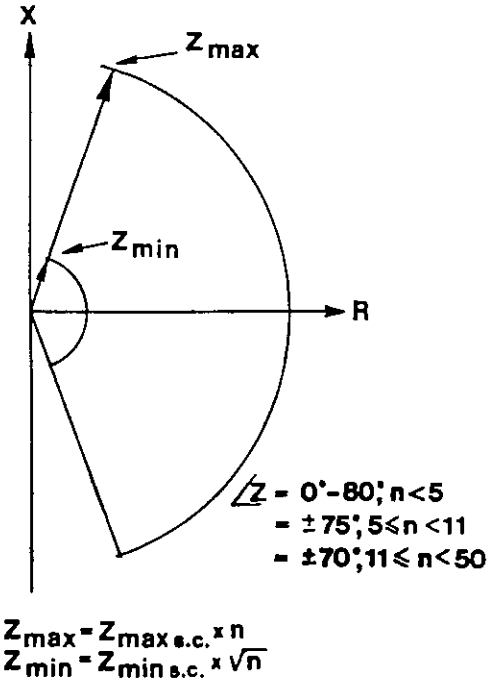

Figure 6-8 Boundaries for ac-network impedance. The general sector model.

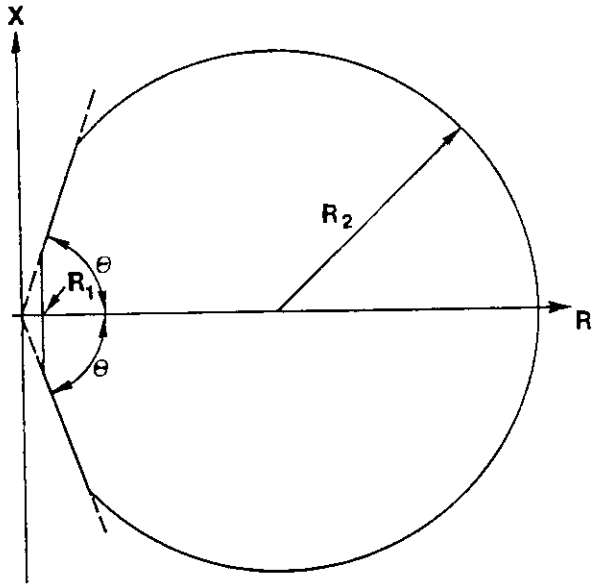

Figure 6-9 Boundaries for ac-network impedance. The general circle model.

Choice of optimal Q-value

An optimal Q-value for a tuned filter is determined with regard to requirement of lowest possible power losses and the requirement of maximum permitted generation of harmonics to the ac-network. Equation (6-24) shows the relationship between the generated harmonic currents the convertor $I_{(n)}$ and the harmonic voltages at the ac-bus, $U_{(n)}$. Equation (6-35) shows an expression for the filter admittance. The admittance of the ac-network can be calculated from the specified limiting curves provided in figures 6-8 and 6-9.

The admittance of the other branches of the total filter and of the connected shunt capacitor bank should also be considered. However, if we assume that the fundamental frequency admittance of the other branches are of the same order of magnitude as that of the tuned filter and that the Q-value is at least fifty, we will find that the influence of the other branches are rather small, as the admittance Y_{fn} is proportional to Q (compare equation (6-35))

Let's now consider the following two cases.

a The network admittance is substantially less than the admittance of the filter, i.e. $Y_{fn} >> Y_L$. We will then get the minimum harmonic voltage U_n if Q is chosen as large as possible.

b The maximum phase-angle of the network impedance is ± 90°, and the magnitude of the network impedance can achieve arbitrary values. The maximum harmonic voltage U_n will then occur, when the susceptance of the ac-network is equal to that of the filter but have opposite sign. Equations (6-24) and (6-35) result in the following expression for the maximum harmonic voltage.

$$U_{nmax} = \frac{1 + 4\,\delta^2_{max}\,Q^2}{n \cdot \omega_{(1)} \cdot C \cdot Q} \cdot I_{nmax} \qquad (6\text{-}37)$$

The optimal Q is:

$$Q_{opt} = 1/2\delta_{max} \qquad (6\text{-}38)$$

If the max phase-angle of the network is less than 90° the minimum of U_{nmax} is derived at a slightly lower Q-value. According to Ref. [1] the following optimal Q-value is then achieved.

$$Q_{opt} = \frac{\cot\left(\Phi_m \frac{1}{2}\right)}{2\delta_{max}} \qquad (6\text{-}39)$$

Typical Q-values fall in the range 30-90. The power losses have then also to be considered.

Example of simplified calculation of band-pass filters

Assumptions

$d_{xN} = 6\%$
$\alpha_N = 15°$
$\delta_{max} = \pm 1\%$
Max phase-angle of the ac-network $\pm$ 90°

Requirement

$U_{(n)}/U_{(1)} < 0.5\%$

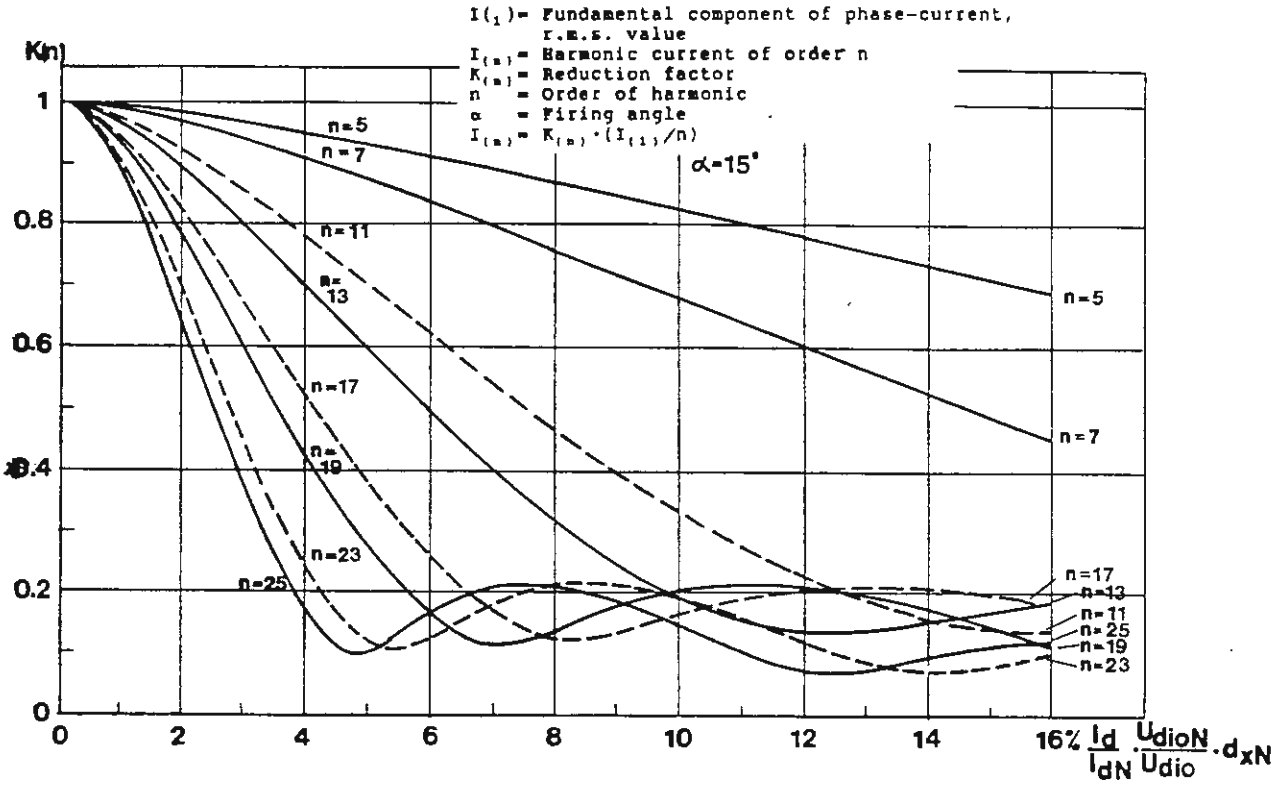

Diagram 6.2 AC phase-current harmonics as a function of the relative inductive voltage drop.

Calculations

Equation (6-38) results:

$Q = 50$

Diagram 6.2 gives:

$I_{(11)}/I_{(1)} = 0.62/11 = 0.056$

Equation (6-37) results:

$$0.005 \cdot U_{(1)} = \frac{2 \cdot 0.056 \cdot I_{(1)}}{11 \cdot \omega_{(1)} \cdot C \cdot 50}$$

The apparent fundamental frequency power of the convertor $S_{(1)} = 3 \cdot U_{(1)} \cdot I_{(1)}$ and the rated reactive power of the 11^{th} harmonic filter-branch $Q_{c11} = 3 \cdot U_{(1)}^2 \cdot \omega_{(1)} \cdot C$. The above relationships results:

$$Q_c = 0.04 \cdot S_{(1)}$$

This indicates, that at the assumptions given above the required harmonic levels could be fulfilled with a rather small filter-branch for the 11th harmonic. We have here assumed, that the firing angle $\alpha = 15°$. Usually the filters are designed for larger firing angles, which will increase the harmonics. The conservative assumptions of the ac-network have resulted in a fairly low Q-value. A slightly larger filter than 4% of the apparent rated power of the convertor and a higher Q-value, would probably be more optimal with regard to the power losses.

Double-tuned resonance filters

A single double-tuned band-pass filter tuned to the 11^{th} and 13^{th} harmonic is often an interesting alternative to two separate single tuned filters for the 11^{th} and 13^{th} harmonics. The circuit diagram and the impedance

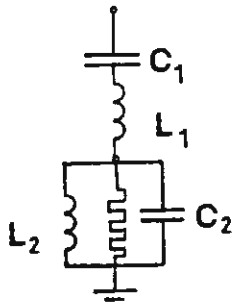

Figure 6-14 Double-tuned band-pass filter.

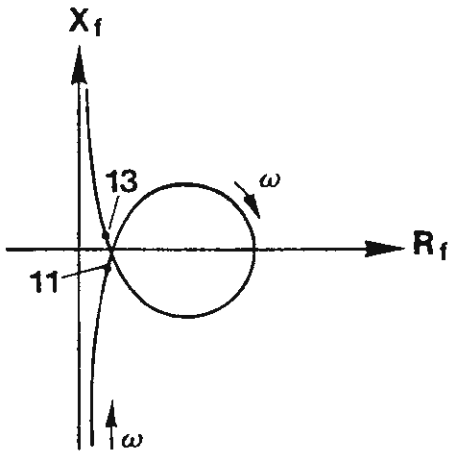

Figure 6-15 Impedance characteristics of the double-tuned band-pass filter.

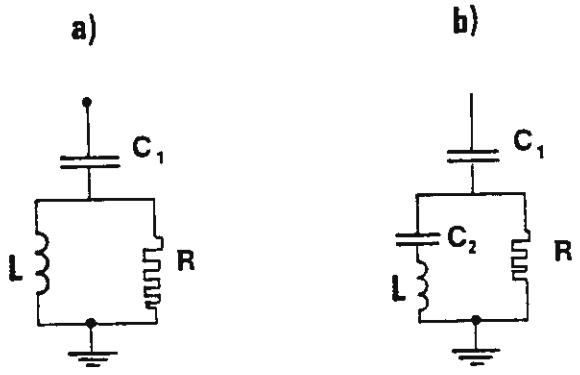

Figure 6-16 High-pass filter
a) High-pass filter of the 2nd order
b) Modified high-pass filter for reduced fundamental frequency losses.

characteristic for a double-tuned filter is shown in figures 6-14 and 6-15.

The total rating of the installed capacitors has to be roughly the same for a double-tuned filter as for the two single-tuned filters together in order to get the same impedance at the 11^{th} and the 13^{th} harmonics for the two alternatives.

The great advantage with the double-tuned filter is that the main capcitance C_1 can be realized in one unit, which at high ac-voltages and small filters can be especially essential. The disadvantage with the double-tuned filter as compared to two single-tuned filters is that the tuning is more difficult.

High-pass filters

High-pass filters are usually installed for the higher frequencies. Figure 6-16 shows two alternative designs of high-pass filters. The 2^{nd} order filter shown as alternative (a) is the filter most often used. As shown in alternative (b) an additional capacitance C_2 may be installed in order to reduce the fundamental frequency losses. The value of C_2 is then chosen such that:

$$\omega_1 = 1/\sqrt{LC_2}$$

The following is valid for the impedance of the circuit shown in alternative (a):

$$Z_a = \frac{1}{j\omega C_1} + \left(\frac{1}{R} + \frac{1}{j\omega L}\right)^{-1} \qquad (6\text{-}40)$$

A resonance frequency ω_n and a Q-value are defined in

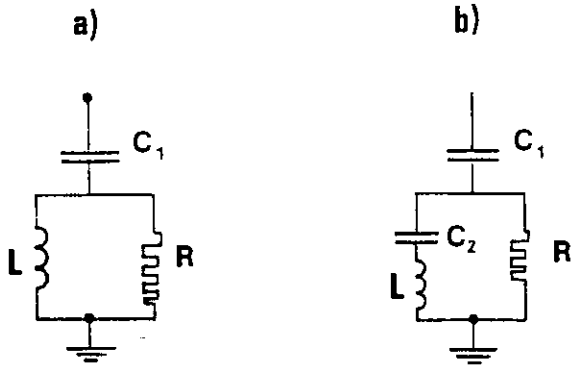

Figure 6-16 High-pass filter
a) High-pass filter of the 2nd order
b) Modified high-pass filter for reduced fundamental frequency losses.

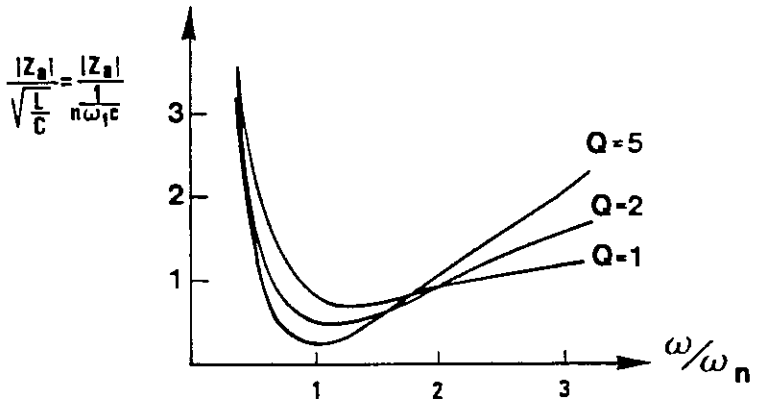

Figure 6-17 Magnitude of the impedance for high-pass filter alt. a).

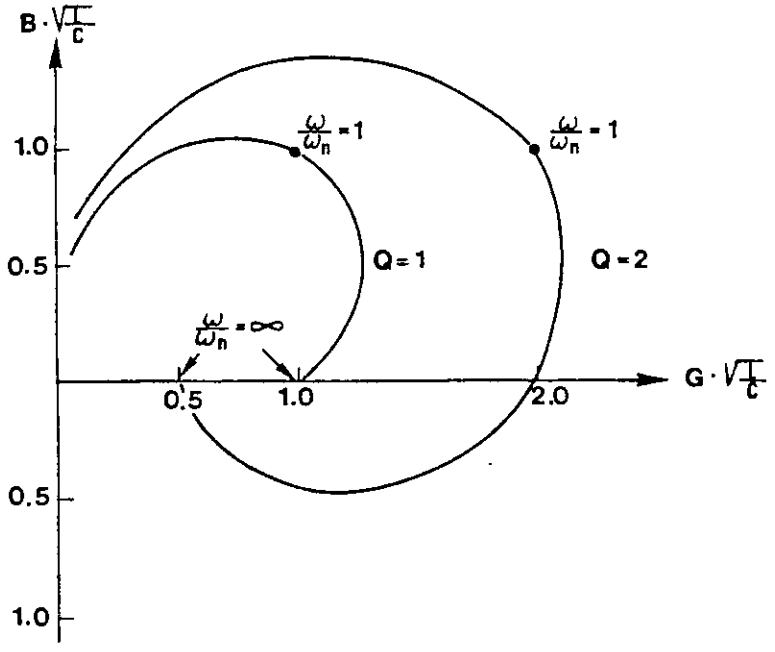

Figure 6-18 Admittance diagram for high-pass filter of 2nd order shown on fig 6-16 a).

similar ways as for the band-pass filter, i.e.,:

$$\omega_{(n)} = 1/\sqrt{LC_1} = n \cdot \omega_{(1)} \qquad (6\text{-}41)$$

and:

$$Q = \frac{R}{\sqrt{\frac{L}{C}}} = \omega_{(n)} \cdot R \cdot C \qquad (6\text{-}42)$$

The Q-value is much lower for a high-pass filter than for a band-pass filter and is usually chosen in the range 2 to 5. This will also result in a limited phase-shift in the frequency range of interest. The characteristics of the filter-impedance and filter admittance are shown in figure 6-17 and 6-18, respectively.

Example of simplified calculation of a high-pass filter

Assumptions

$f_1 = 50Hz$
$d_{xN} = 6\%$
$\alpha_N = 15°$

High-pass filter with Q=2 and $\omega_n/\omega_1 = 24$. The impedance of the ac-network is assumed to be substantially larger than that of the filter.

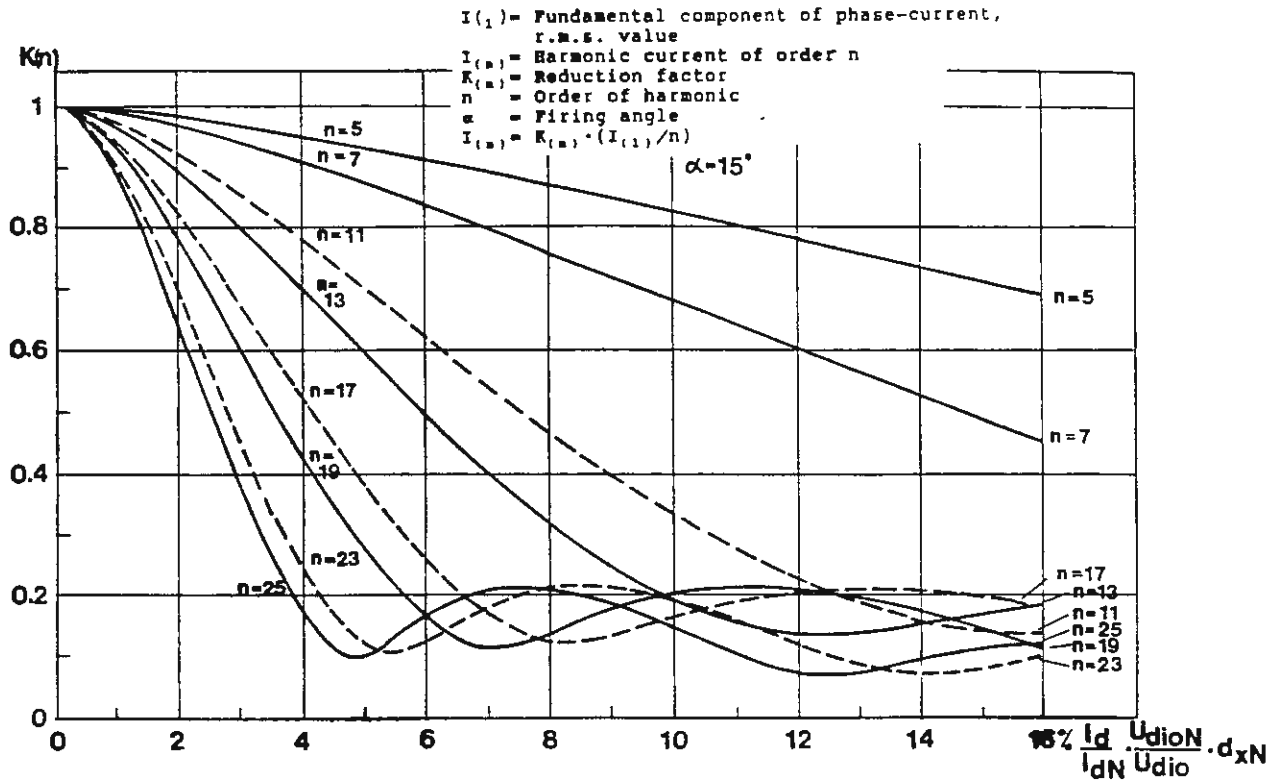

Diagram 6.2 AC phase-current harmonics as a function of the relative inductive voltage drop.

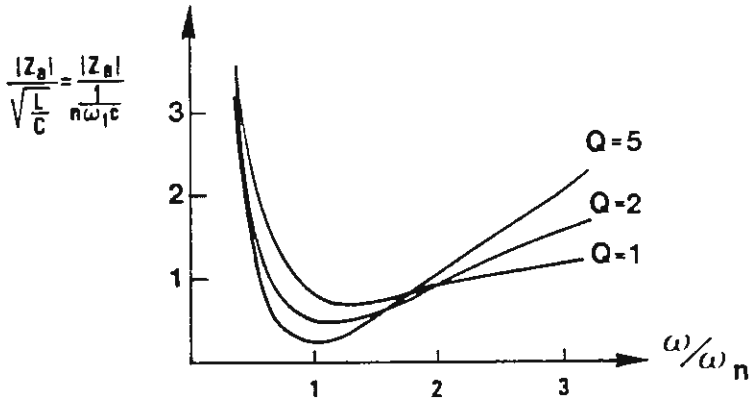

Figure 6-17 Magnitude of the impedance for high-pass filter alt. a).

Requirement

Determine the minimum relative rating of the high-pass filter which limits the contribution to the THFF value for the 23rd harmonic to 0.2%.

Calculations

Equation 6-19 results:

$F_n \cdot U_{(n)}/U_{(1)} \leq 0.002$

where $F_n = P_n \cdot 1150/800 = 1.035 \cdot 1150/800 = 1.49$ i.e.

$U_{(n)}/U_{(1)} \leq 0.00134$

Diagram 6-2 shows maximum generation of the 23rd harmonic at $I_d/I_{dN} = 0.33$, i.e. $I_d/I_{dN} \cdot d_{xN} = 2\%$ and

$I_{23}/I_{1N} = 0.33 \cdot 0.7/23 = 0.010$

Figure 6-17 shows for Q=2 and $\omega_n/\omega_1 = 24$ that:

$$|Z_a| \cdot n \cdot \omega_1 \cdot C = 0.4$$

This gives:

$$\frac{U_{(23)}}{U_{(1)}} = \frac{I_{(23)} \cdot Z_a}{U_{(1)}} = \frac{I_{(23)} \cdot Z_a \cdot I_{(1)N}}{I_{1N} \cdot U_{(1)}} = \frac{0.010 \cdot 0.4 \cdot I_{(1)N}}{24 \cdot \omega_{(1)} C \cdot U_{(1)}} < 0.00134$$

The rated reactive power at the fundamental frequency of the high-pass filter $Q_{cHP} = 3 \cdot U_1^2 \cdot \omega_1 \cdot C$ and the apparent fundamental frequency power of the convertors $S_{(1)N} = 3\, U_{(1)} \cdot I_{(1)N}$

(Note! $U_{(1)}$ is the phase-voltage)

The above relationships results:

$$Q_{c(24)}/S_{(1)N} \geq 0.12$$

In the previous example it was found, that the

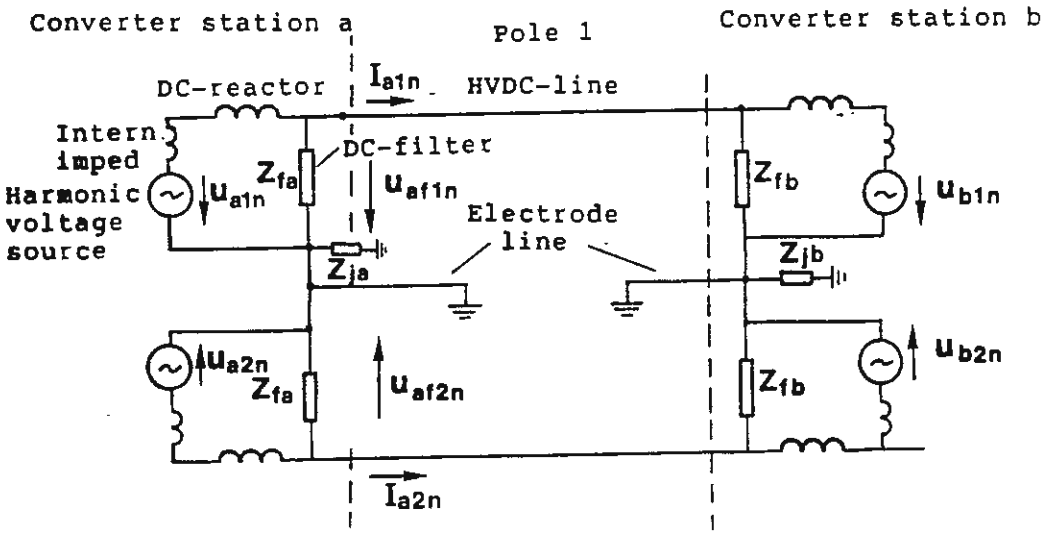

Figure 6-19 Circuit diagram for calculations of harmonics on the dc-line.

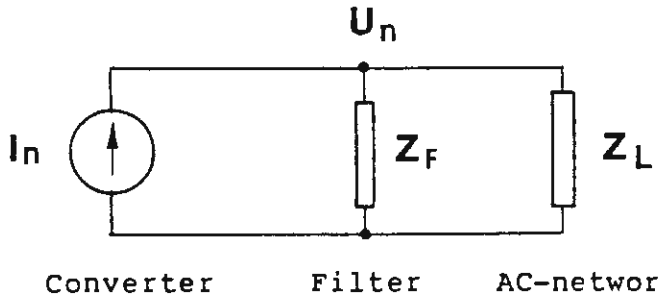

Figure 6-3 Simplified circuit diagram for the calculation of the generated and injected harmonic currents into the ac-network.

corresponding size of the 11^{th} harmonic filter was 4%. If we assume that the 13^{th} harmonic filter has the same size as that of the 11^{th} harmonic filter, we will get the required minimum size of the total filter equal to 4 + 4 + 12 = 20% for the total filter. It is often required that reduntant (spare) filters be installed, which then results in a total filter capacity of 40% of the apparent ac-power of the convertor station. This can be compared with a total reactive power normally absorbed by the convertor which is of the order of 50%. The remaining reactive power is usually generated by pure shunt-capacitor banks. The shunt capacitor banks can also be combined with some other and smaller filters for other harmonics, which might be critical, e.g., for the 3^{rd} harmonic.

6.8 Calculation of harmonics generated and injected into the dc-line

The filters needed to take care of the harmonics generated and injected into the dc-side, are usually considerably smaller and less expensive than the filters on the ac-side. Usually no filters are at all needed for pure cable transmission lines, or so called back-to-back stations, i.e., convertor stations where both the rectifier and inverter are located in the same station without any dc-line. The following treatment of the harmonics on the dc-side will, because of that, be restricted to HVDC systems with overhead lines on the dc-side.

We will base the treatment on the circuit diagram in to figure 6-19, showing a two terminal bipolar HVDC system with an overhead line. As compared to the corresponding very simplified diagram in figure 6-3, we will note the following differences for the harmonics generated to the ac-side:

- A convertor can, as viewed from the dc-side, be represented as a harmonic voltage-source (compared to current-source on the ac-side) connected in series with the internal impedance of the convertor and the inductance of the dc-reactor.

- The HVDC line is well defined making it possible to calculate the harmonic currents along the whole line. The mutual coupling between the two poles should then be considered as well as the generation of harmonics from both poles and both stations.

- Harmonic currents will also flow in the ground return when only one pole is in operation or if the generated harmonic voltages from the two poles are not exactly 180° phase-shifted and of equal magnitude

This can be compared with the situation on the ac-side where, both, harmonic currents of positive and negative phase-sequence will be generated but no zero-sequence harmonic currents are generated, since the neutral points of the convertor transformers will not be grounded on the valve side.

The treatment of the harmonics on the dc-side, to be presented in the following presentation, may be referred to as the classical way of calculation. During the last years it has been found that the leakage capacitances to ground in the convertor transformers must also be taken into account sometimes when calculating the ground mode currents on the dc-side. See Ref. [3] for further information.

Ground-mode and pole-mode

The voltages and currents in one pole can not be calculated independent of the voltages and currents in the other pole because of the mutual coupling impedance between the poles. It is because of that, more convenient to transfer the voltages and the currents in the individual poles to ground-mode component and pole-mode components. These components can then be treated independently, as there is no coupling between them on a symmetric overhead line. This should be compared with the use of symmetrical components of a three-phase ac-system. The ground-mode for the bipolar dc-system corresponds to the zero-sequence component of the ac-system and the pole-component to the positive-sequence component.

We will by analogy of the definition of the zero-sequence component define the ground mode of the voltage, U_g, as:

$$U_g = \frac{U_1 + U_2}{2} \qquad (6\text{-}43)$$

where U_1 and U_2 are the voltages to ground in pole 1 and pole 2.

In a similar way we will define the pole-component, U_p, as:

$$U_p = \frac{U_1 - U_2}{2} \qquad (6\text{-}44)$$

Concequently, we will get the corresponding definition for the ground- mode current, I_g, and pole-mode current, I_p, i.e.,

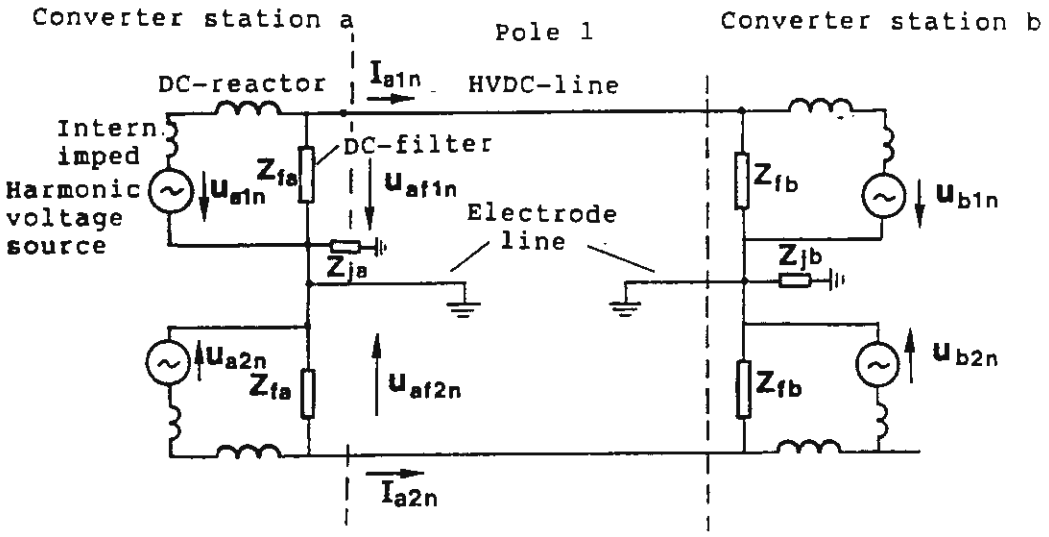

Figure 6-19 Circuit diagram for calculations of harmonics on the dc-line.

$$I_g = \frac{I_1 + I_2}{2} \qquad (6\text{-}45)$$

and

$$I_p = \frac{I_1 - I_2}{2} \qquad (6\text{-}46)$$

The corresponding transformation can also be performed for the harmonic voltage-sources in the two poles of station a, according to figure 6-19. This then gives:

$$U_{ag(n)} = \frac{U_{a1(n)} + U_{a2(n)}}{2} \qquad (6\text{-}47)$$

and:

$$U_{ap(n)} = \frac{U_{a1(n)} - U_{a2(n)}}{2} \qquad (6\text{-}48)$$

The ground-mode component of the harmonic source-voltage will be zero, if we assume that each pole consists of a 12-pulse convertor, each having the same firing angle, the same turn-ratio in the transformer (same tap-changer position) and the same commutating reactances. The characteristic harmonics in the two poles will then be 180° phase-shifted using the reference directions as shown in figure 6-19. The pole-mode components will then be equal to the characteristic harmonics in each pole. Asymmetries between the two poles will however also generate

ground-mode harmonics. As mentioned before the leakage capacitances in the convertors also have to be taken into account for a more accurate calculation of the ground mode components. (See Ref. [3]). This especially applies at high values of the impedance to ground in the stations, Z_{ja} and Z_{jb}.

The ground-mode impedance Z_g and the pole-mode impedance Z_p are defined in a similar way as the ground-mode and the pole-mode voltages and currents. The ground-mode and pole-mode impedances in the stations are equally large, if the impedances Z_{ja} and Z_{jb} are small and could be neglected.

On the other hand the ground-mode impedance of the overhead line differs from the pole-mode impedance, both, with regard to magnitude and character. This is illustrated by the following relationships derived for the longitudinal differential voltage drops ΔU_1 and ΔU_2 in pole 1 and 2 of the line, respectively.

$$\begin{vmatrix} \Delta U_1 \\ \Delta U_2 \end{vmatrix} = \begin{vmatrix} Z_{11} & Z_{12} \\ Z_{21} & Z_{22} \end{vmatrix} \cdot \begin{vmatrix} I_1 \\ I_2 \end{vmatrix} \qquad (6\text{-}49a)$$

We can here for a symmetrical line set $Z_{12} = Z_{21}$ and $Z_{11} = Z_{22}$, which results:

$$\frac{\Delta U_1 + \Delta U_2}{I_1 + I_2} = Z_{11} + Z_{12} = Z_g \qquad (6\text{-}49b)$$

and:

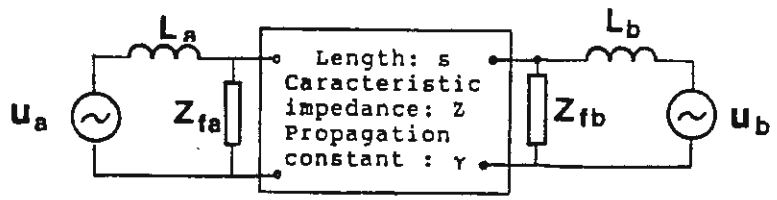

Figure 6-20 Simplified circuit diagram for the calculation of the ground-mode component.

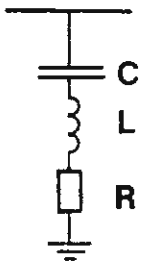

Figure 6-10 Single-tuned band-pass filter.

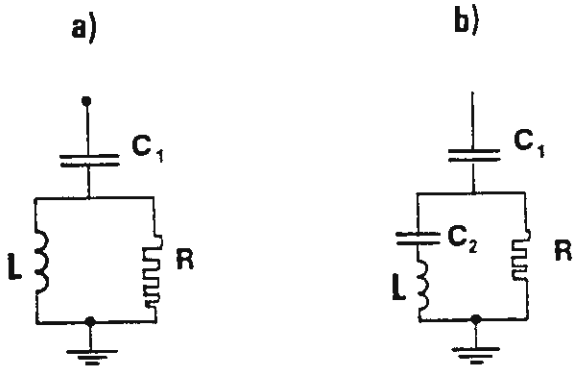

Figure 6-16 High-pass filter
a) High-pass filter of the 2nd order
b) Modified high-pass filter for reduced fundamental frequency losses.

$$\frac{\Delta U_1 - \Delta U_2}{I_1 - I_2} = Z_{11} - Z_{12} = Z_p \qquad (6\text{-}49c)$$

The calculation of the harmonic voltages and currents along the line can now be performed separately for the ground-mode and the pole-mode system by using the simplified circuit diagram as shown in figure 6-20. We have here assumed that $Z_{ja} = Z_{jb} = 0$. The influence of the electrode-line has also been neglected. The inductances L_a and L_b are determined by the sum of the inductances of the dc-reactors and the internal inductances of the convertors.

The filter-impedances Z_{fa} and Z_{fb} are usually designed in a similar way as on the ac-side, i.e., to provide low impedances for the characteristic harmonics. It is common practice to install a single-tuned band-pass filter for the 12^{th} harmonic as shown in fig 6-10 and a high-pass filter for the 24^{th} and higher harmonics, as shown in figure 6-16. These filters are primarily designed for the characteristic harmonics. However, it should be noted that the ground-mode components have a much larger mutual coupling to adjacent telephone lines than the pole-mode components. At normal bipolar operation the characteristic harmonics are usually well balanced and thus cause only a limited contribution to the interference. Unsymmetrical operation conditions have however also to be considered, e.g., operation with different firing angles or tap-changer positions in the two poles. The highest unbalance is of course achieved at single-pole operation.

The characteristics of the ground-mode and pole-mode of the overhead line can be described by the longitudinal impedance and admittance components per km, i.e. resistance r, inductance l, conductance g and capacitance c as well as

the total length of the line s. As an alternative to impedance and admittance components the characteristics can be determined by transmission constant, defined as:

$$\gamma = \alpha + j\beta = \sqrt{(r + j\omega l)\ (g + j\omega c)} \qquad (6\text{-}50)$$

and the characteristic-impedance, or wave-impedance Z, defined as:

$$Z = \sqrt{\frac{r + j\omega l}{g + j\omega c}} \qquad (6\text{-}51)$$

The following relationship is valid for a thin lossless single line above an ideal ground with no earth resistivity

$$\gamma = j\omega \sqrt{\mu_o \cdot \varepsilon_o} = \frac{j\omega}{c_o} \qquad (6\text{-}52)$$

The constant c_o is here the velocity of light in vacuum, i.e., about $3 \cdot 10^5$ km/sec. Equation (6-52) is approximately valid for the pole-component, while the transmission velocity of the ground-mode components is a function of frequency and the earth resistivity. This is due to the fact that the equivalent return current, which at zero earth resistivity will flow at a depth equal to the height of the overhead line above ground, will flow at a larger depth at higher earth resistivities especially at lower frequencies. A typical value of the transmission velocity for the ground-mode component is in the order of $2 \cdot 10^5$ km/sec.

The injected harmonic voltage into the line can be directly

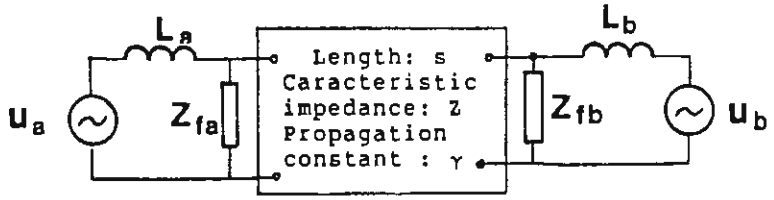

Figure 6-20 Simplified circuit diagram for the calculation of the ground-mode component.

derived from figure 6-20, if we assume that no reflection will occur at the other end (e.g., terminated by the line-characstic impedance Z). We will then obtain:

$$U_{af(n)} = \frac{\frac{Z_{fa} \cdot Z}{Z + Z_{fa}}}{\frac{Z_{fa} \cdot Z}{Z + Z_{fa}} + j\omega La} \cdot U_{a(n)} \qquad (6\text{-}53)$$

The impedance relationship according to equation (6-53), in station (a) will be denoted by G_a and will, in the following, be called transmission factor for station a. The transmission factor shows how much of the generated harmonic voltage is transmitted to the line.

We can now rewrite equation (6-53):

$$U_{afn} = G_a \cdot U_{an} \qquad (6\text{-}54)$$

The harmonic voltage at the distance x from station (a) will, provided that no reflections occur at station (b), be:

$$U_{ax(n)} = G_a \cdot e^{-\gamma x} \cdot U_{a(n)} = G_a \cdot e^{-(\alpha + j\beta)x} U_{a(n)} \qquad (6\text{-}55)$$

The corresponding harmonic current is derived through division by the characteristic impedance, Z, i.e.,:

$$I_{ax(n)} = \frac{G_a \cdot e^{-\gamma x}}{Z} \cdot U_{a(n)} \qquad (6\text{-}56)$$

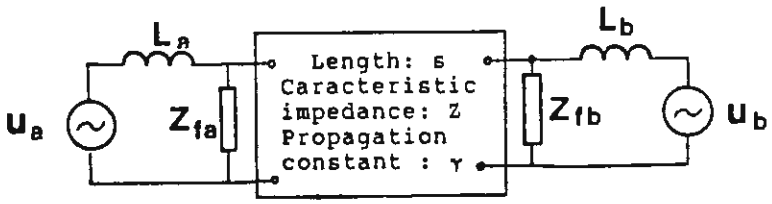

Figure 6-20 Simplified circuit diagram for the calculation of the ground-mode component.

The arriving voltage-current wave at station (b) will now see an impedance Z_b which is derived from figure 6-20 to be:

$$Z_b = \frac{Z_{fb} \cdot j\omega L_b}{Z_{fb} + j\omega L_b} \qquad (6\text{-}57)$$

The voltage-current wave arriving at station (b) will now be reflected and generate a voltage wave travelling from station (b) to station (a). The magnitude of this voltage wave will be:

$$U_{asr(n)} = \frac{Z_b - Z}{Z_b + Z} \cdot U_{as(n)} \qquad (6\text{-}58)$$

As can be seen from equation (6-58) no reflection will occur if $Z_b = Z$. For this case equations (6-55) and (6-56) will also result in the voltage and current distribution along the line. However, this case will seldom occur in practice. Usually either $Z_b << Z$ in case filters are connected giving a low impedance for the harmonic, or $Z_b >> Z$ in case no filters are connected.

We will then get reflections at both ends of the line. Equations (6-55) and (6-56) can then no longer be used directly for the calculation of the harmonics along the line, as the harmonics along the line might be considered to be superimposed on waves travelling in both directions, which are reflected a number of times. We will use the following modified expression for the reflection factor, as shown in equation (6-58), to get it in the same form as equation (6-55) for the transmission along the line.

$$e^{-(A_b+jB_b)} = \frac{Z_b - Z}{Z_b + Z} \qquad (6\text{-}59)$$

Index (**b**) is here used for the reflection factor in station (**b**).

Superposition of the contributions on the waves travelling in both directions gives the following expression for the harmonic voltages at a distance x from station (a) where it is assumed that the harmonic voltage U_{an} is generated.

$$U_{ax(n)} = G_a \cdot e^{-\alpha x} \left| \frac{1 + e^{-(A_b+2\alpha(s-x)\ -j\left(B_b\ +\ 2\beta(s-x)\right)}}{1 - e^{-(A_a+A_b+2\alpha\cdot s)\ -\ j(B_a+B_b+2\beta s)}} \right| \cdot U_{a(n)} \qquad (6\text{-}60)$$

The following expression is then derived for the harmonic current along the line

$$I_{ax(n)} = \frac{G_a \cdot e^{-\alpha x}}{Z} \left| \frac{1 - e^{-\left(A_b+2\alpha(s-x)\right)-\ j\left(B_b+2\beta(s-x)\right)}}{1 - e^{-(A_a+A_b+2\alpha s)\ -\ j(B_a+B_b+2\beta s)}} \right| \cdot U_{a(n)} \qquad (6\text{-}61)$$

The denominators are the same in both equations (6-60) and (6-61) except for Z. A low value of the denominator will cause a risk for high amplitude of the harmonics. This will occur if $B_a + B_b + 2\beta \cdot s = 2\pi \cdot m$ where m is an integer number. Frequencies for which this applies are called

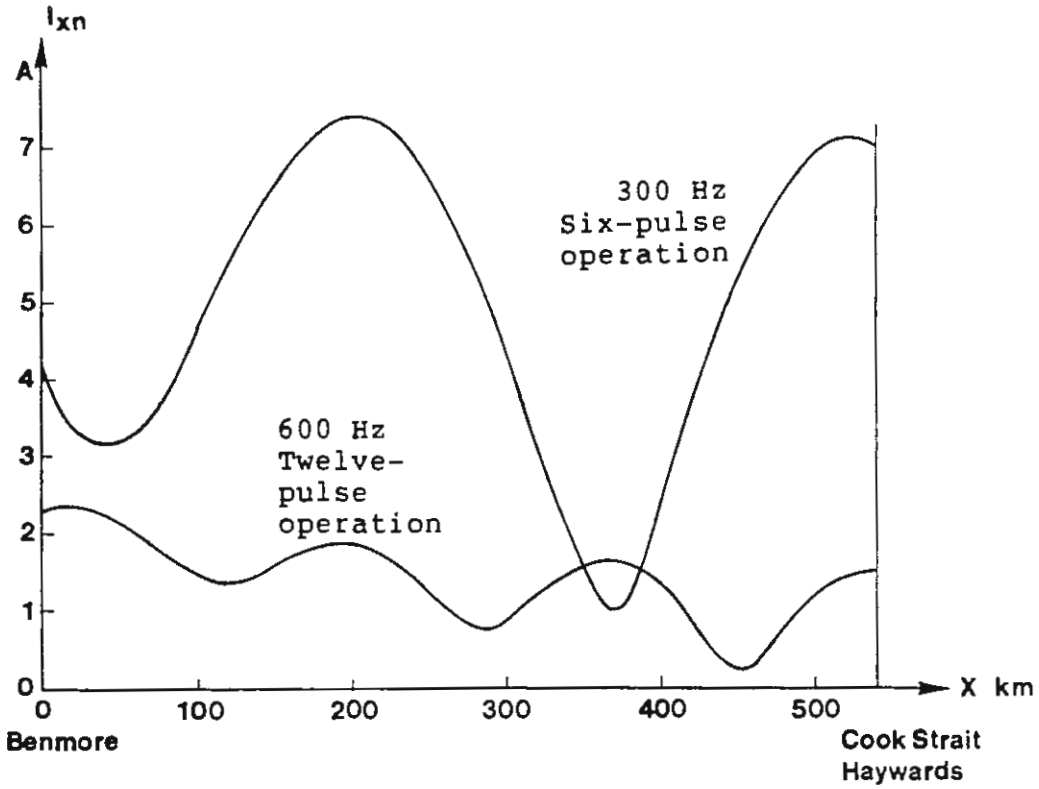

Figure 6-21 Harmonic currents with ground-return operation on the overhead HVDC-line between the converter station at Benmore and the cable termination at Cook Strait (New Zeeland). Harmonic voltage injected at Benmore.

resonance frequencies.

Equations (6-60) and (6-61) show that a resonance frequency can give high amplitudes if the total attenuation is low (low values of $A_a + A_b + 2\alpha \cdot s$). However, the attenuation at higher frequencies is usually fairly high for the ground-mode component. It is, because of that, no longer critical whether resonance will occur or not.

It should be noted that the nominators are different in the expression for voltage and current when comparing equation (6-60) and (6-61). This means that the current normally has a maximum value for a location, where the voltage has a minimum value and vice versa.

Fig 6-21 shows an example of the calculated harmonic currents along an overhead line terminated by a cable at the far end. (New Zeeland). The harmonics are injected at Benmore and the cable is located at Cook Strait. The injected harmonics have, in this case, been assumed to occur between parallel connected poles and ground. A current maximum is, of course, achieved close to the cable, as $Z_b << Z$ at the cable, which gives $B_b = \pi$ rad., according to equation (6-59). It could also be seen that the attenuation is higher at 600 Hz than at 300 Hz.

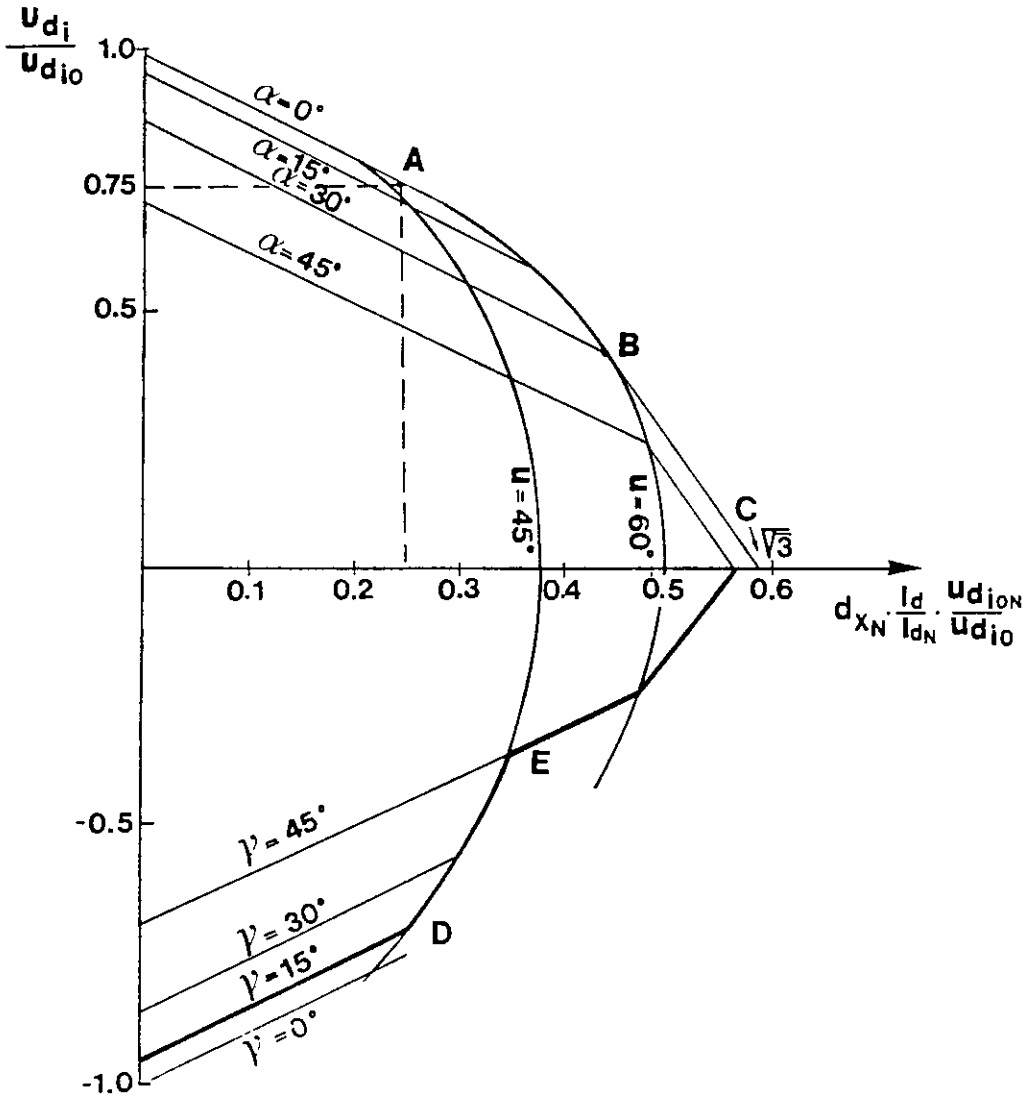

Figure 4-13 Current-voltage characteristics of a 6-pulse converter.

7 CONTROL DYNAMIC CHARACTERISTICS

7.1 Basic control principles

The basic characteristics of a six-pulse convertor have been treated in chapter 4. The current-voltage characteristic was also determined and is summarized in figure 4-13. It is shown that the direct voltage will be negative if the firings of the valves are delayed so that the firing angle is larger than 90°. The convertor will operate in inverter mode. It is then more convenient to use the extinction angle or commutation margin angle, γ, instead of the firing angle α. The extinction angle γ is measured from the zero crossing of the current at the end of the conduction or on-state interval to the next zero crossing of the voltage across the valve. Equation (4-38) shows the relationship between the firing angle α, the angle of overlap u, and the extinction angle γ.

$$\alpha + u + \gamma = \pi \qquad (4\text{-}38)$$

In rectifier operation the firing control to be arranged so that the firing angle will not be decreased below a certain minimum value, α_{min}, in order to secure a certain positive voltage across the valve at firing instant. Normal min. values of the firing angle are 3-5°. The firing control system has further, in inverter operation, to be arranged so that the extinction angle γ will never decrease below a certain min. value, which usually is set to be 17-19°. Too small value will make the convertor too vulnerable for commutation failures (See section 4.3).

With regard to stresses and ratings of the main-circuit components at steady state operation it would be advantageous to operate with the smallest possible values of α and γ. This would decrease the consumption of reactive power, reduce the amplitude of the harmonics, and minimize

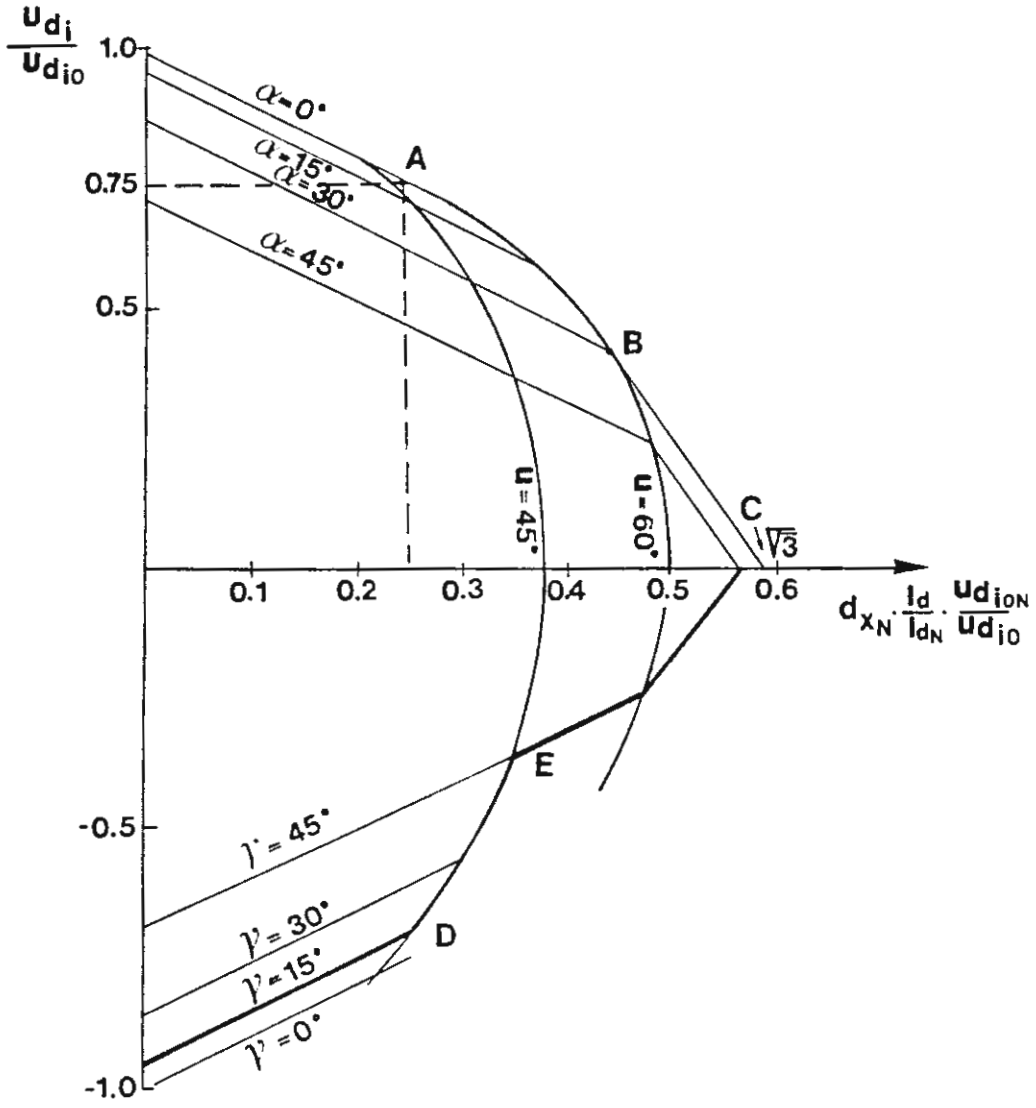

Figure 4-13 Current-voltage characteristics of a 6-pulse converter.

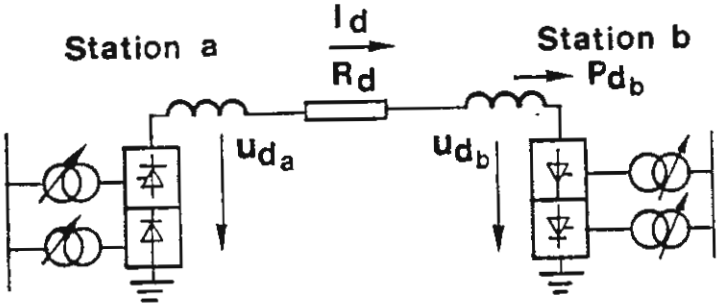

Figure 7-1 Monopolar two terminal HVDC-transmission.

the stresses on the valves and the transformers. The control system will, because of that, be arranged so that at least one of the convertor stations will operate either at minimum firing angle or minimum extinction angle (or commutation margin). The control systems for most terminal HVDC schemes are arranged so that at normal operation the inverter is operating at its γ_{min} limit. The direct voltage of the inverter will then be determined by the ac-voltage on the valve side of the convertor transformer and the direct current according to equation (4-41) and figure 4-13. The magnitude of the direct voltage can be controlled by the tap-changer setting in the inverter station. The direct current and the transmitted active power can be controlled by the control of the voltage in the rectifier terminal.

With notations as shown in figure 7-1 we will get the following relationships:

$$I_d = \frac{U_{da} - U_{db}}{R_d} \qquad (7\text{-}1)$$

and

$$P = \frac{U_{db}(U_{da} - U_{db})}{R_d} \qquad (7\text{-}2)$$

The firing angle in the rectifier station has now to be chosen so that it will be possible to, both, increase and decrease the direct voltage U_{da} in the rectifier terminal in order to be able to control the direct current. However, as the voltage drop in the dc-circuit is rather small and usually much less than 10%, the voltage range, which is needed for the current control, is also fairly small. A firing angle of 15° is usually sufficient to get an adequate margin of $\alpha_{min} \simeq 3°$. This gives $\Delta U/U_d \simeq \cos 3° -$

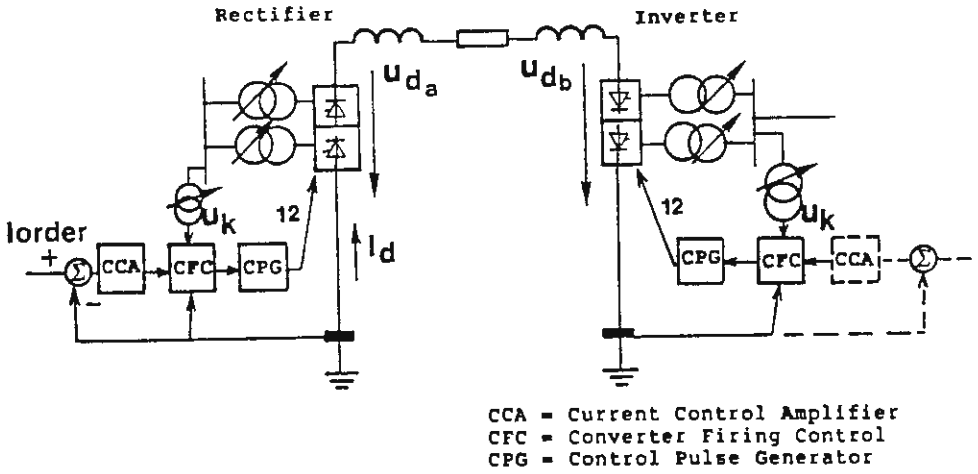

Figure 7-2 Monopolar two terminal HVDC-transmission with basic control system.

cos 15° = 0.033.

The magnitude of the direct voltage can be changed very fast with the firing control of the valves. New firing pulses are generated twelve times per cycle for a twelve-pulse convertor. The average time-lag τ from a change in the output signal of the firing control to the execution can be set to

$$\tau = \frac{1}{2 \cdot 12 \cdot f} = \frac{1}{24 \cdot f} \quad \text{sec.} \qquad (7\text{-}3)$$

where f is the ac-network frequency in Hz.

The current control system is arranged, as a feed-back control system, as illustrated in figure 7-2. The control system will be further described below. Both convertor stations are usually equipped with identical control systems, which can operate in different modes, depending upon whether they operate at the α_{min} or the γ_{min} limits, or if the firing angle α is controlled to achieve the desired current.

The current feed-back control loop is drawn dashed in the inverter- station, as it is assumed that this loop is inactive and the inverter is operating at the γ_{min} limit.

The current feedback control loop is assumed to be active in the rectifier station. A disturbance which causes the direct current I_d to be less than the current order, I_{order} will result in the control amplifier generating a signal, which decreases the firing angle. This increases the direct voltage in the rectifier which increases the direct current.

The dynamic characteristic of the current control system is primarily determined by the transfer function of the

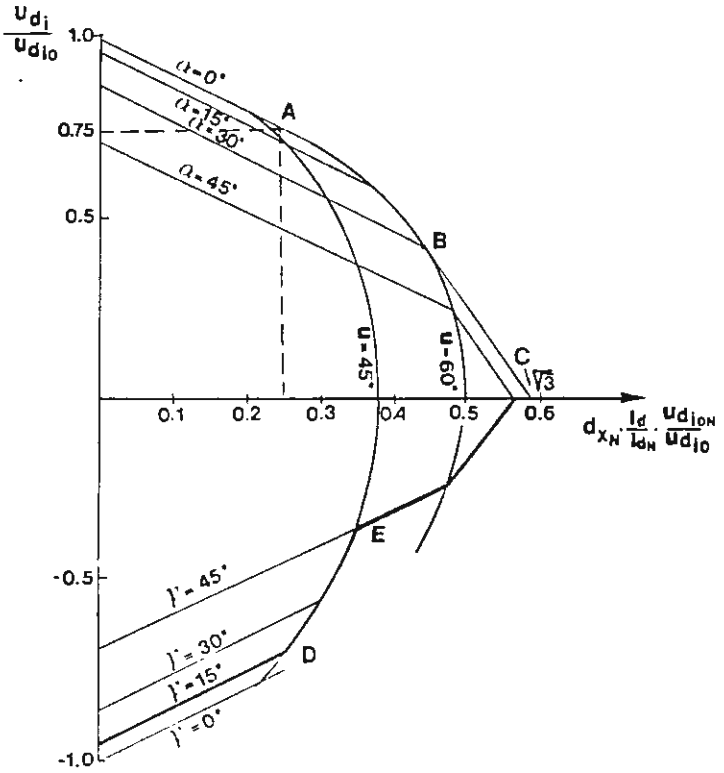

Figure 4-13 Current-voltage characteristics of a 6-pulse converter.

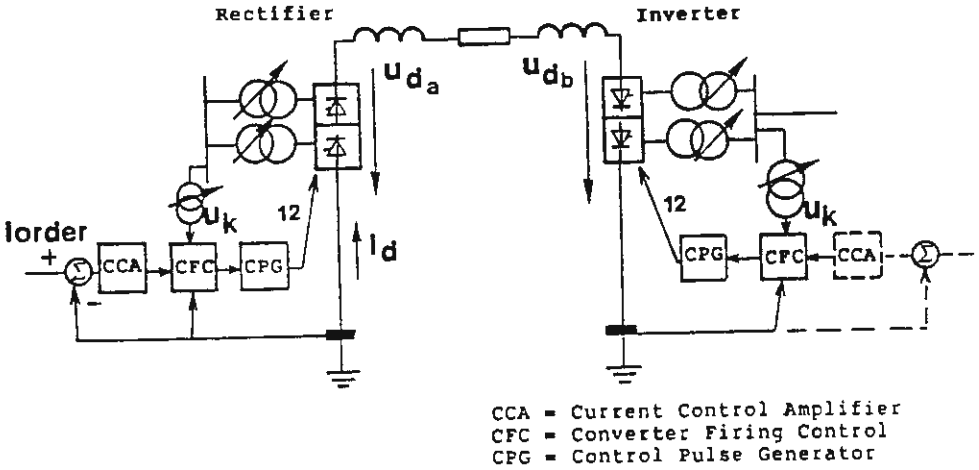

Figure 7-2 Monopolar two terminal HVDC-transmission with basic control system.

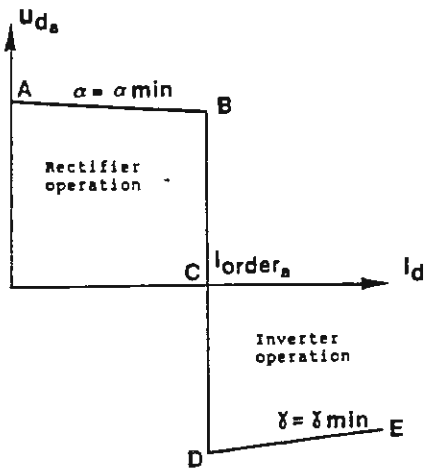

Figure 7-3 Steady state U_d/I_d characteristics.

current control amplifier CCA. The amplification can be chosen very high for low frequencies ($\leq$ 10 Hz). The current control system can in this way secure that $I_d = I_{order}$ as long as $\alpha > \alpha_{min}$, for steady state and quasi-stationary conditions.

7.2 Current-voltage characteristic

The current-voltage characteristic for a six-pulse convertor is illustrated in figure 4-13. It should be noted that only the left part of the diagram is usually of interest, as usual, with good margins, the following applies

$$d_{xN} \cdot \frac{I_d}{I_{dN}} \cdot \frac{U_{dioN}}{U_{dio}} \leq 0.25$$

This characteristic could be modified to also take into account the control system, as illustrated in figure 7-2.

If we assume that the ac-source voltage is constant (commutation voltage U_k according to figure 7-2 and U_{dio} in figure 4-13 is constant) we will get the modified steady state characteristics according to figure 7-3.

For direct currents, which are less than the current order, I_{order}, the convertor will try to increase the current by decreasing the firing angle. The convertor will because of that, operate against the α_{min} - limit for current smaller than the current order (part A-B of the characteristic in figure 7-3). A reduced counter voltage from the inverter will cause the operating point to move along the line A - B in direction towards B. At operating point B the current is equal to the current order. A further decrease of the voltage of the inverter station will not give a further

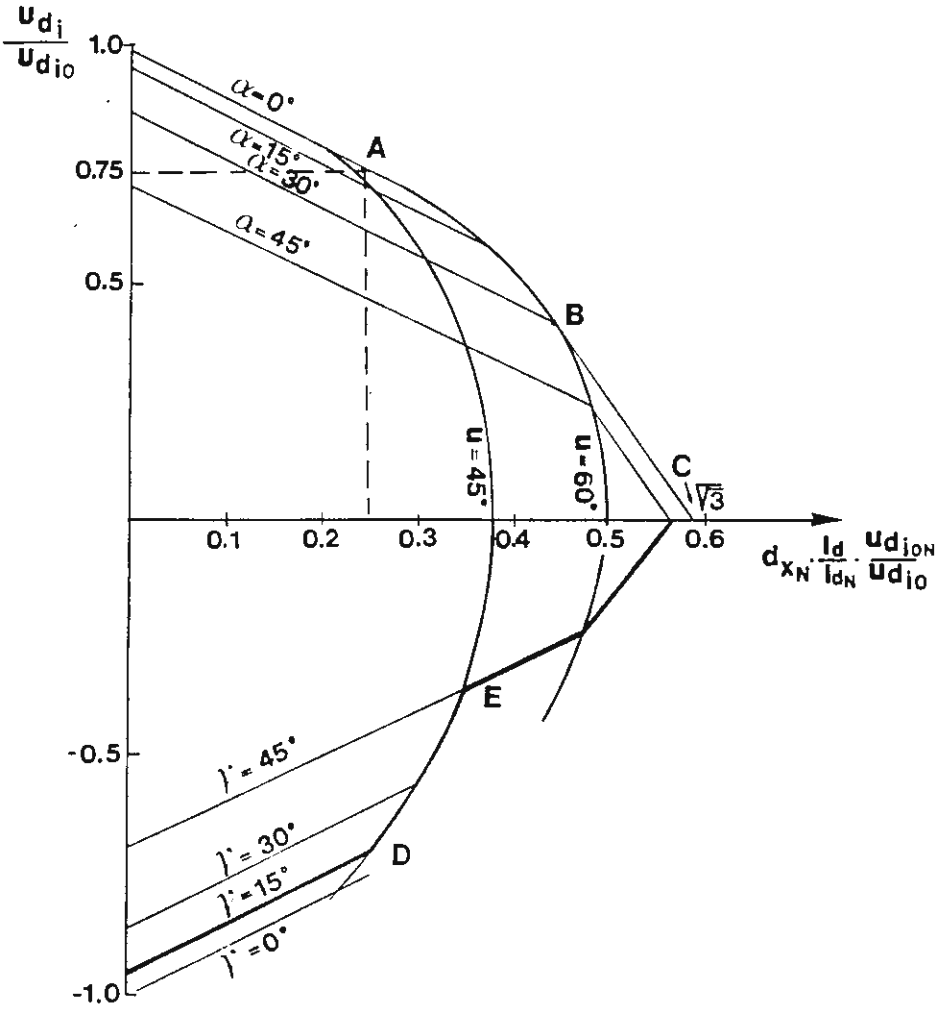

Figure 4-13 Current-voltage characteristics of a 6-pulse converter.

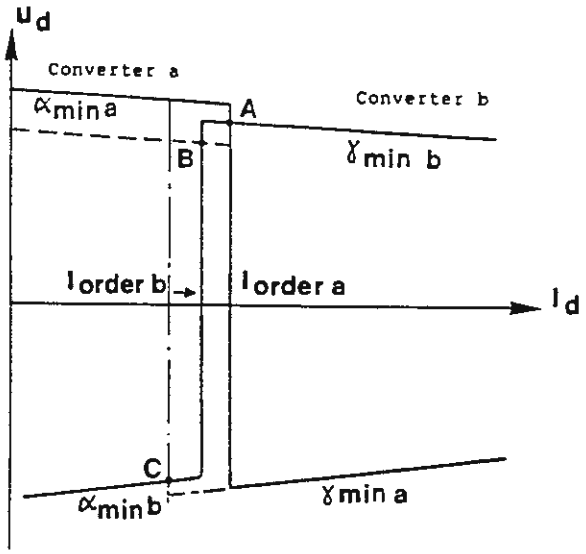

Figure 7-4 Steady state U_d/I_d characteristics for station (a) and station (b). Positive voltage reference direction, power transmission a→b.

increase of the direct current. The current control system will now increase the firing angle in the rectifier in order to keep the actual direct current equal to the current order. The operation point will now fall along line B - C and the operation point will move in direction towards C at a decreasing voltage from the inverter station.

The power direction will be reversed when the direct voltage changes sign at point C. If the direct voltage is increased in the reversed direction the operation point will move along part C - D in direction towards D. The firing angle is now larger than 90° and the extinction angle γ decreases. The operation point D is reached when the extinction angle has decreased to its minimum value γ_{min}. The current control feedback loop will now be deactivated. The direct-current can now increase and the operation point is moving in direction from D to E.

Operation in the region ABC is usually referred to as rectifier operation and operation in the region CDE as inverter operation. The linear parts A -B for rectifier operation and D - E for inverter operation corresponds to the lines for $\alpha = \alpha_{min}$ and $\gamma = \gamma_{min}$ in figure 4-13.

To illustrate the co-operation between the two convertor terminals it is convenient to draw the current-voltage characteristics for both stations in the same diagram. It is then practical to change the positive reference direction of the voltage in one of the stations to make it possible to directly compare the voltages. Let us define positive power direction when power is transmitted from station (a) to station (b), i.e., station (a) is operation as rectifier and station (b) as inverter. We will define positive reference direction for the dc-voltage such that both stations have positive voltages at this power direction. Figure 7-4 shows an example with both the

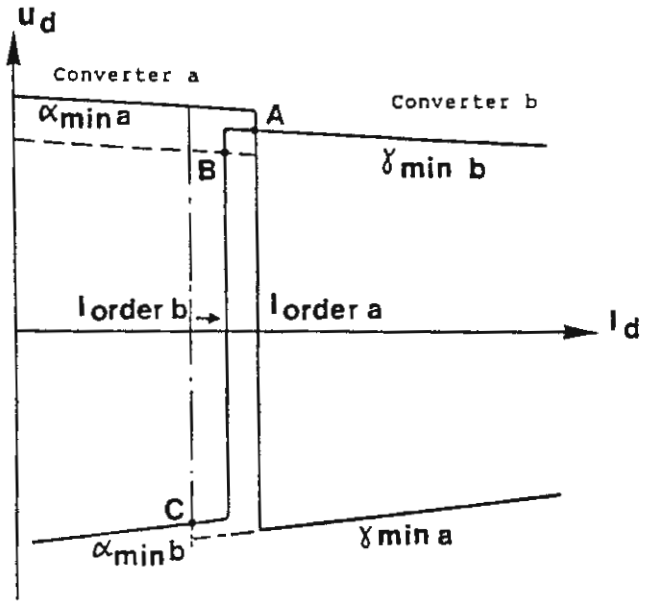

Figure 7-4 Steady state U_d/I_d characteristics for station (a) and station (b). Positive voltage reference direction, power transmission a→b.

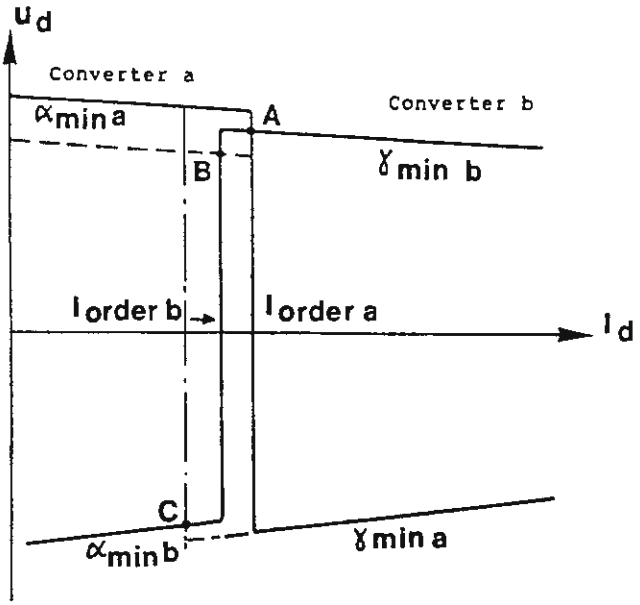

Figure 7-4 Steady state U_d/I_d characteristics for station (a) and station (b). Positive voltage reference direction, power transmission a→b.

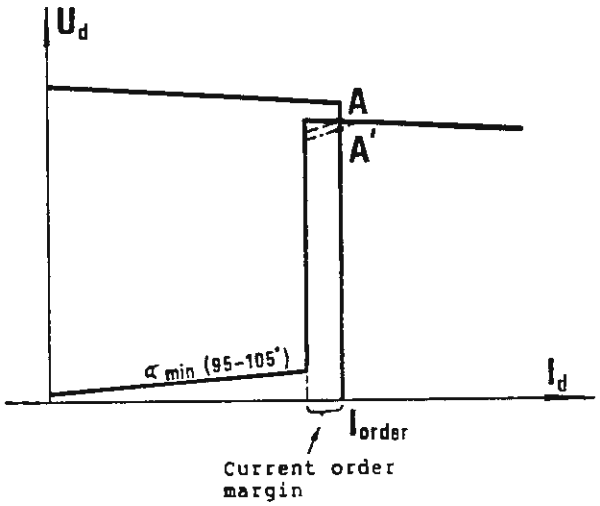

Figure 7-5 Steady state U_d/I_d characteristics for rectifier and inverter with special α_{min}-limit and cutting off the corner of the U_d/I_d characteristic in the inverter.

characteristics for station (a) and station (b) drawn in the same diagram. The crossing point between the two characteristics shows the actual operation point provided the voltage drop along the dc-line can be neglected (point A in figure 7-4).

It can be seen from figure 7-4 that the current order at the rectifier always has to be larger than the current order in the inverter. If the current order in station (b) is increased so that its current order will be larger than the current order in station (a) a new crossing point would be achieved for negative voltages, i.e., with an opposite power direction.

The rectifier (station (a)) is at point A operating at a firing angle, which is larger than its min value, which means that the current control system is active in station (a). The inverter (station (b)) is operating at the minimum extinction angle ($\gamma = \gamma_{min}$) and its current feedback control loop is deactivated. The mode of operation as illustrated by point A, is the usual operating mode at steady state operation.

A transfer of the operation mode from A to B can occur if either the feeding ac-voltage in station (a) is decreased or if the α_{min} limit is increased (dashed line), This means that station (b) will take over the control of the direct current, which will now be equal to the current order in station (b).

A third case with the operation point C is also illustrated in figure 7-4. It is here assumed that the current order in station (a) has been decreased to be less than the current order in station b. The direct voltage and power direction will be reversed. It has here been assumed that the ac-voltage of the station (a) is sufficiently large to let this station still control the current.

The convertor having the largest current order will, as seen above, operate as rectifier. The difference in current orders between the two stations is called current margin and is usually chosen to be about 10% of the rated current. The control systems in the two stations are usually designed identical with a joint and equal current-order which is decreased by the current margin in the station designated to operate as inverter.

A reversal of the power direction could in principle be obtained by switching only the current margins between the stations. In practice it is desirable to control a change of the power direction in a better way than just changing the current margins. Special protections are also included to prevent an unintentional change of the power direction. One precaution is to introduce a special α_{min} - limitation in the inverter station. This limit is usually chosen in the range $\alpha_{min} \simeq 95 - 105°$ (see figure 7-5). By the introduction of this additional limitation it is also possible to prevent the inverter in case of an earth fault on the dc-line feeding current to the earth fault.

A decrease of the ac-voltage can result in the operation point being changed from point A to point B, as illustrated in figure 7-4. This will also show that the actual direct current is decreased with an amount equal to the current margin. To avoid a small decrease in voltage from resulting in large current fluctuation and a not well defined operation point, especially at equal slopes of the characteristics, the corner of the characteristics of the inverter is usually cut-off as shown with the short dashed line in figure 7-5. This modification of the current-voltage characteristics will also give certain other advantages as it will change the dynamic characteristics of the inverter as seen from the dc-line. This is especially valid if the characteristics according

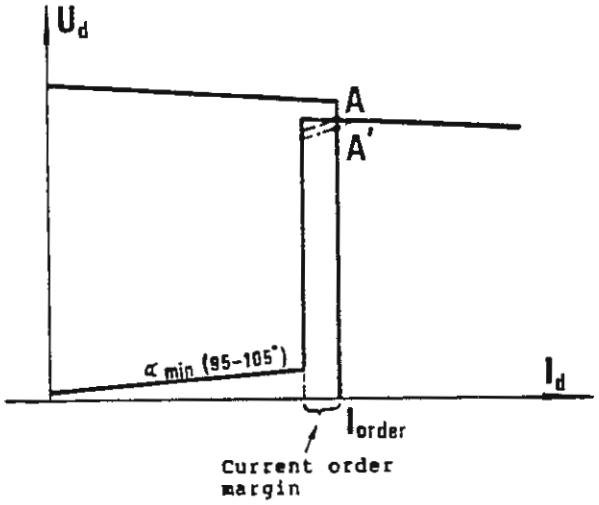

Figure 7-5 Steady state U_d/I_d characteristics for rectifier and inverter with special α_{min}-limit and cutting off the corner of the U_d/I_d characteristic in the inverter.

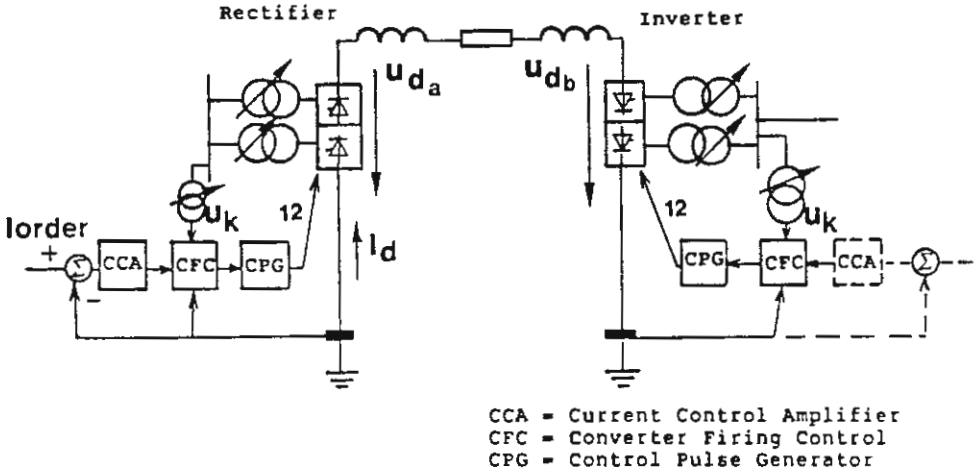

Figure 7-2 Monopolar two terminal HVDC-transmission with basic control system.

to the dash-dotted line is chosen, which results in the operation at point A'.

The current-voltage characteristics, according to figure 7-5, is primarily valid for steady state operation. However, they are also valid for dynamics of lower frequencies. This will be further treated in section 7-4. A current-voltage characteristic for an inverter operating at γ_{min} shows that the inverter voltage will decrease at increased direct current. As seen from the dc-side this corresponds to a constant counter voltage connected in series with a negative resistance. The negative slope of the characteristic will result in a less damped system and can in certain cases, result in instabilities. Cutting of the corner of the characteristic as shown in figure 7-5, results in the slope being positive for superimposed oscillations of small amplitudes around the operation point **A** or **A'**. This will give additional damping of the system and is the basic reason for the selection of this type of characteristics.

7.3 Convertor firing control system

The control system which determines the firing instants of the valve will in the following be called convertor firing control system. The convertor firing control system (CFC) is connected to a control pulse generator (CPG in figure 7-2), which generates the firing control pulses to the valves. A firing pulse must always be generated to one valve in each commutation group to secure that current can flow in the convertor bridge. At operation with very low direct currents the bridge current can intermittently be extinguished. It is then important that at least one valve in each commutation group always has a firing pulse and is ready to fire, when a forward blocking voltage appears across the valve. Similar conditions will appear at the

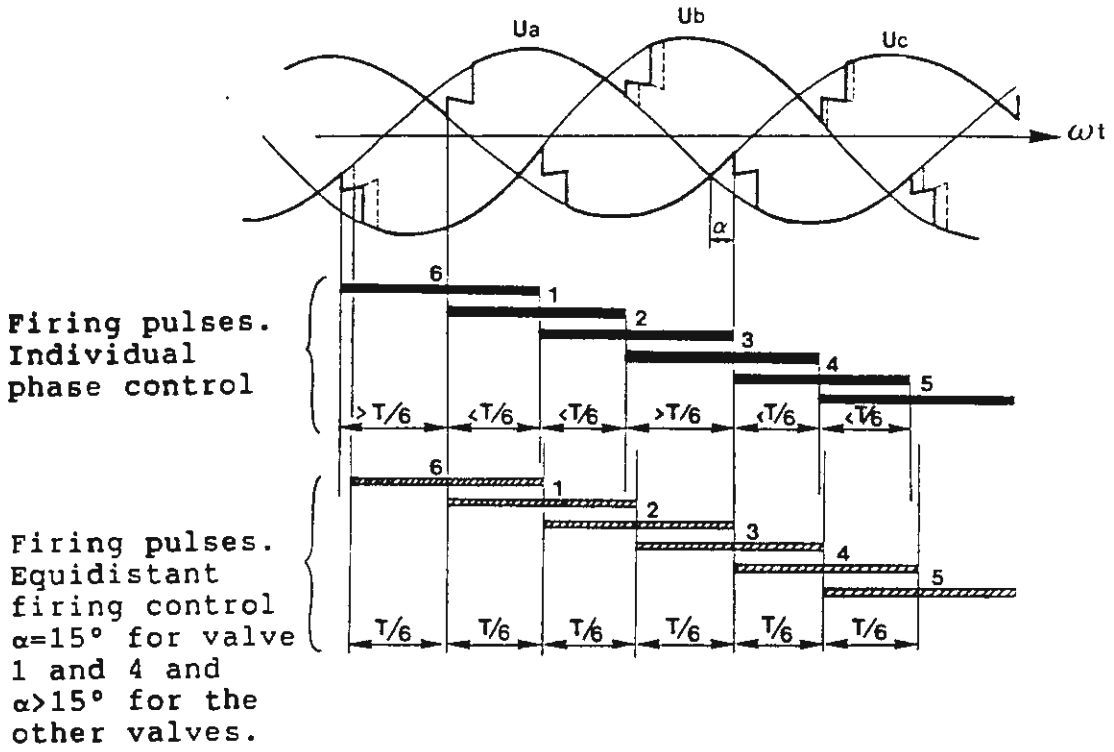

Figure 7-6 Firing pulses generated by individual-phase and equidistant firing control system at asymmetrical ac-voltages.

start of the convertor bridge. Because of this it is not sufficient to only generate short firing pulses at the instances, when the valves will start to conduct at normal operation, which will not occur simultaneously in the two commutation groups of a six-pulse bridge.

The active input signal to the firing control system is either the output signal from the current control amplifier, provided the current control is active, or the measured commutation voltage and direct current, when the firing is determined by the α_{min} limit. Firing control systems are designed according to one of the following two alternative basic principles:

1 Individual-phase control or phase-to-phase control.

2 Equidistant firing control.

Firing control systems provided according to any one of the above principles will result in the same performance at symmetrical ac-voltages. However, they will behave different at asymmetrical ac-voltages. A firing control system of the individual-phase control type will, at constant input signal from the current control amplifier, give equal firing angles α or alternatively equal extinction angles γ at operation on γ_{min} in inverter operation. This means that at asymmetrical ac-voltages the time intervals between firings of successive valves will normally be different and not be equal to 60° for a six-pulse convertor (see figure 7-6).

The same asymmetrical condition will, on the other hand, result in equal time intervals between the firing of successive valves for an equidistant firing control system. This means that the firing angles might be different for valves connected to different phases (see figure 7-6).

An advantage with a firing system, which provides the same firing angle α or the same extinction angle γ_{min} for all the valves is that such a firing system will give the maximum possible direct voltage across the convertor bridge. An equidistant firing control system will, on the other hand, result in $\gamma = \gamma_{min}$ only for the valves connected to one phase and that $\gamma > \gamma_{min}$ for the other valves. This will give a lower direct voltage across the convertor bridge.

A great advantage with a firing system of the equidistant type is that this will result in lower amplitudes of the generated non-characteristic harmonics on the ac-side. This is easily understood if we study the case with zero overlap angle. An equidistant firing system will then give a symmetric conversion function and thus no non-characteristic harmonics in the ac-current.

An individual phase-control system will, on the other hand, at asymmetrical ac-voltages result in different time intervals between firings and a non-symmetric conversion function. Such a firing control system will, because of that, result in a higher content of non-characteristic harmonics, especially harmonics of odd order, e.g., the 3rd and 9th harmonics.

The firing instants are, for firing control systems of the individual-phase type, determined by a control function generated from the measured commutation voltages. Since the control functions are individually adjusted for each phase, such a control system will often result in additional asymmetries in the firing. A more critical factor is that an additional feedback loop is achieved, as the control function is generated from the measured commutation voltages, which in turn will be effected by the firing instants.

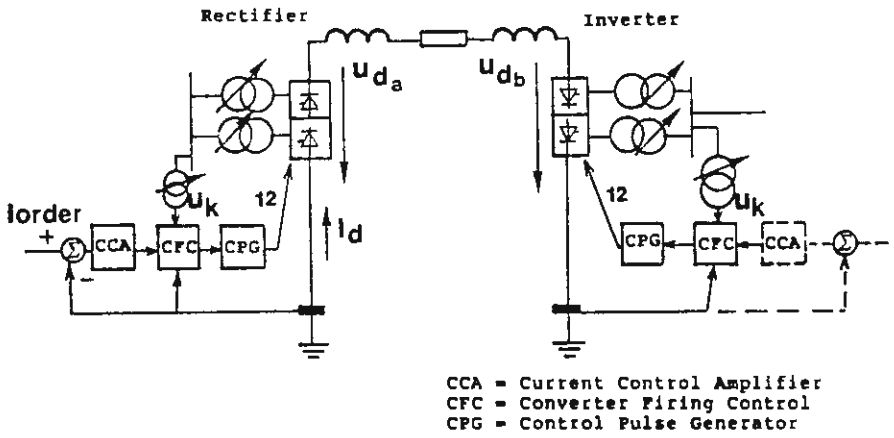

Figure 7-2 Monopolar two terminal HVDC-transmission with basic control system.

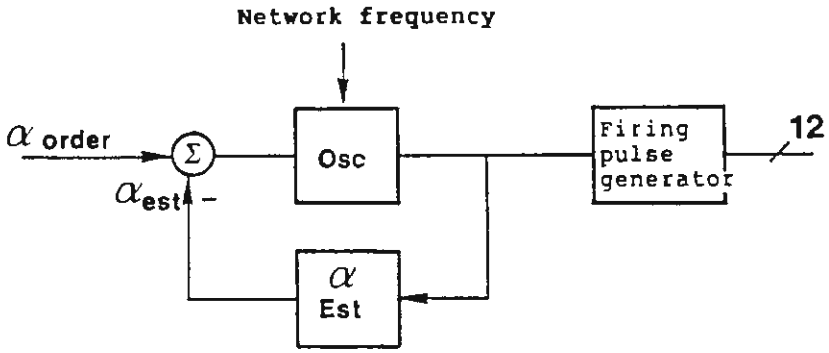

Figure 7-7 Part of an equidistant converter firing control. Phase-locked (phase-controlled) oscillator and α-estimator.

The HVDC systems, which were built during the 1960s, were equipped with firing control systems of the individual phase control type. Because of the short-commings of such systems as discussed above, almost all later HVDC systems have been equipped with firing control systems of the equidistant type. These newer systems are sometimes designed to have equidistant firing up to a certain limit of the asymmetry in the ac-voltages. An increased asymmetry above this limit will give a corresponding asymmetry in the firing. The idea is to achieve a minimum amount of non-characteristic harmonics at normal asymmetries but to achieve the advantage of maximum direct voltage at larger asymmetries, which can only last for a limited time-period.

In the following only the principles of the pure equidistant firing control system will be presented.

Equidistant firing-control system

Firing control systems of the equidistant firing type can be designed in several different ways. It should also be noted that modern microprocessors make it possible to implement a number of special functions. The following description will be limited to the basic principles of one widely used system.

Let's assume that the current control amplifier CCA, as shown in figure 7-2, generates an output signal which is a function of the firing angle order α_{order}. The part of the firing control system, which is activated at current control, can in a simplified way be represented as shown in figure 7-7. The main part is an oscillator. The frequency of the oscillator is controlled by the input voltage supplied from the ac network. It is further arranged so that the switching of the oscillator is only permitted at certain time-intervals, or phase-positions, related to the

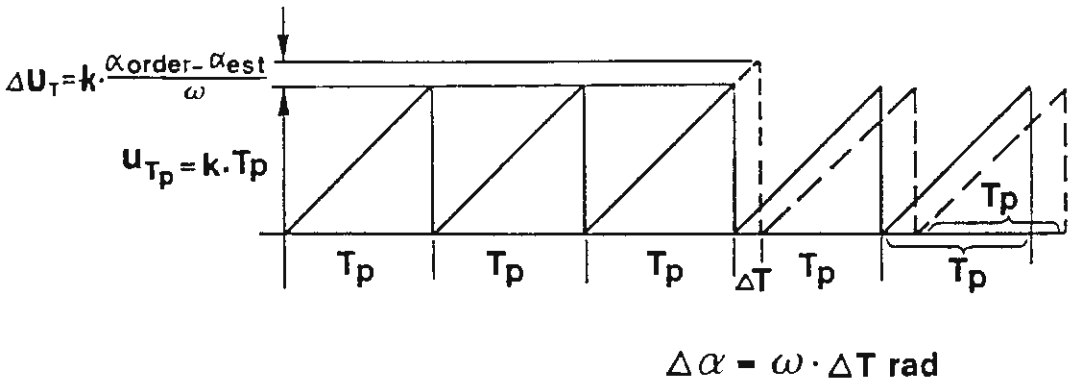

Figure 7-8 Phase-controlled (phase-locked) oscillator.

timing of the ac-voltages. This type of oscillator is, because of that, often called a phase-locked or phase-controlled oscillator. At steady state operation the oscillator will generate pulses at a frequency equal to p x f, where p is the pulse-number of the convertor (usually 12 for HVDC) and f is the ac-network frequency.

The phase-locked oscillator can operate, as illustrated in figure 7-8. The oscillator is arranged to give pulses at the time-intervals

$$T_p = \frac{1}{p \cdot f}$$

When the oscillator is realized by analog circuits, the voltage from a ramp-generator with constant slope is compared with a voltage U_{Tp}, which is made proportional to the measured cycle time of the ac-network. The same function is realized by counters in digital circuits. As a result at zero input signal, corresponding to steady state operation, the firing pulses will be generated at equidistant time intervals. This also means that at steady state operation the firing angle for a specific valve will be constant. However, as described further above the firing angles might be different for different valves at asymmetries between the ac-voltages.

The actual average value of the firing angles for all the valves will be estimated (determined) in a special circuit, (α_{est}). When the estimated α, (α_{est}), deviates from the ordered firing angle, a signal proportional to the difference is added to U_{Tp}, as shown in figure 7-8. The addition of $\kappa \cdot \Delta \alpha/\omega$ will cause the time-interval between two successive firings to increase by:

$$\Delta T = \frac{\Delta\alpha}{\omega} \quad , \quad \text{where} \quad \frac{\Delta\alpha}{\omega} = \frac{\alpha_{order} - \alpha_{est}}{\omega}$$

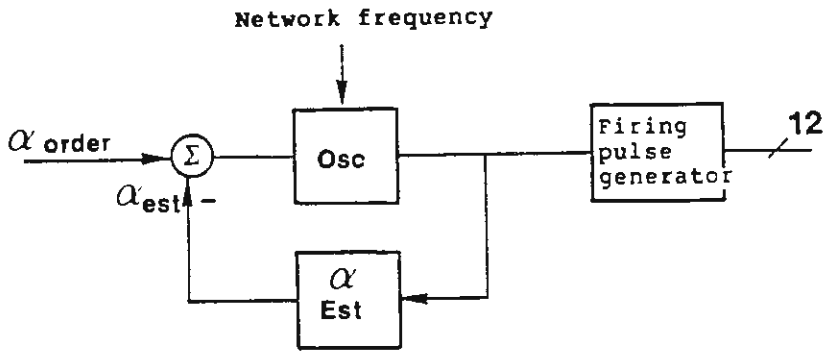

Figure 7-7 Part of an equidistant converter firing control. Phase-locked (phase-controlled) oscillator and α-estimator.

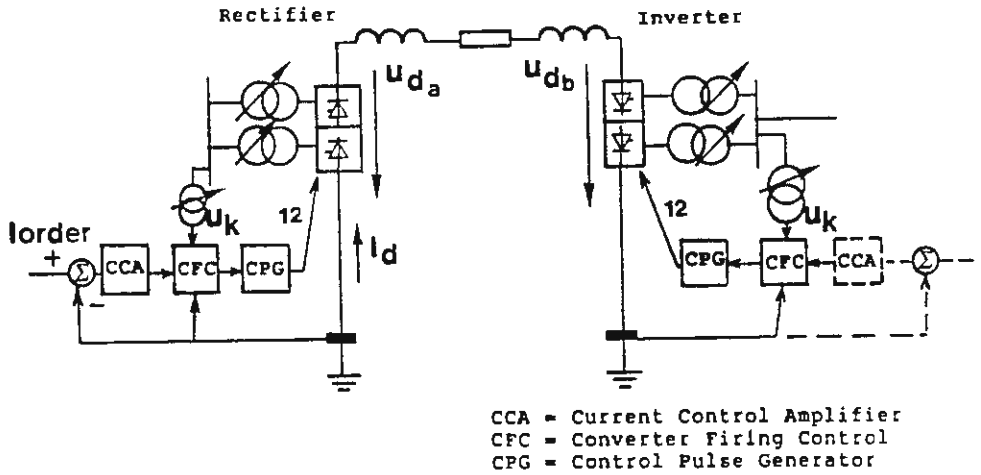

Figure 7-2 Monopolar two terminal HVDC-transmission with basic control system.

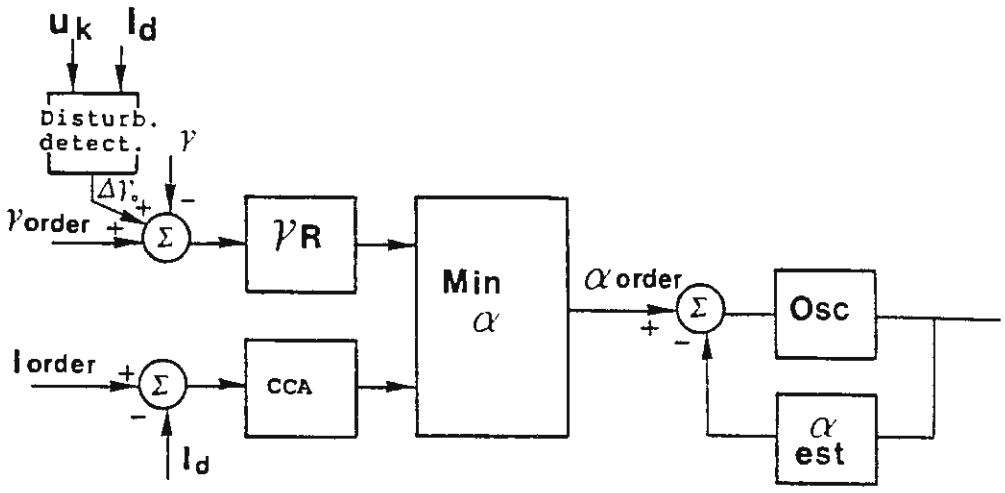

Figure 7-9 Converter firing control system with a feedback control of γ.

This means that the next valve will be fired ΔT seconds later. In order to avoid the situation such that the next valve to fire after that will not get an additional increase in the firing equal to $\Delta\alpha$, i.e., that the total change in α will be equal to $2\Delta\alpha$, it is essential that block α_{est} is updated by the performed adjustment, as soon as the firing has occurred. Overshoots in the control can in this way be avoided.

Signal α_{order}, into current control, in figure 7-7, is derived from the output of the current control amplifier CCA in figure 7-2. However, since even with equidistant firing but asymmetric ac-voltages, the current in the dc-circuit will contain second-order harmonics, the output from the amplifier CCA will also contain a small component of this second order harmonic. The current control feedback loop can thus generate some asymmetries in the firing also at an equidistant firing control system.

The control at minimum extinction angle or commutation margin γ_{min}, can either be determined by feed-back control, or by feed-forward or predictive control. A possible way of arranging a feed-back control system for γ_{min} is illustrated in figure 7-9. The signal α_{order} is selected from either the output of the γ-regultor, γ_R, or from the current control amplifier.

A drawback of a pure feedback control system for minimum commutation margin is that the response of the system will be rather relatively slow at disturbances. A transient change of the ac-voltage or the direct current, which would normally require an earlier firing, will not result in any action before a too small commutation margin is measured. As shown in figure 7-9, a disturbance detector may be added to the system, which effects an increase of γ_{order} as soon as a disturbance is detected.

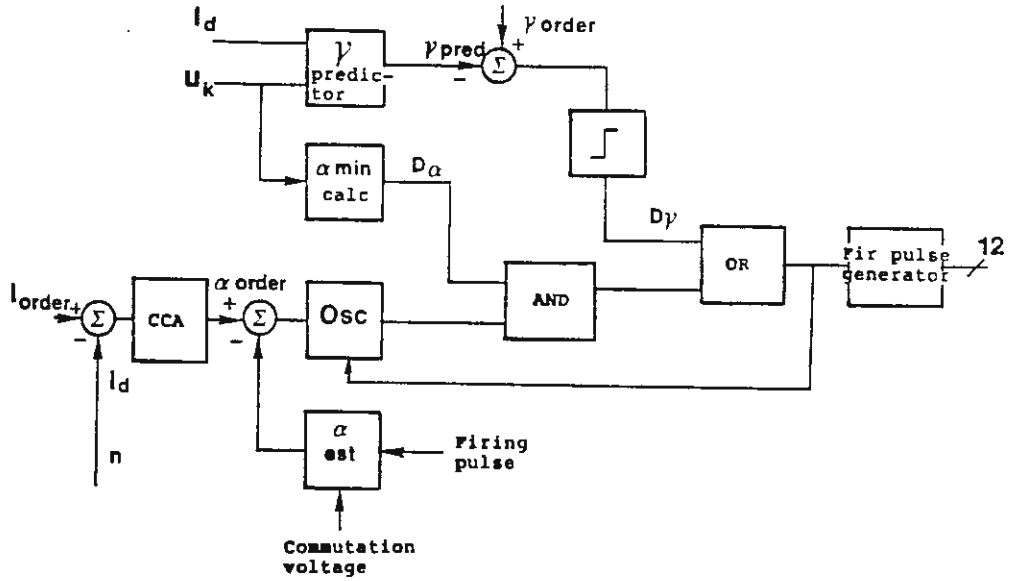

Figure 7-10 Converter firing control with predictive γ_{min}-control.

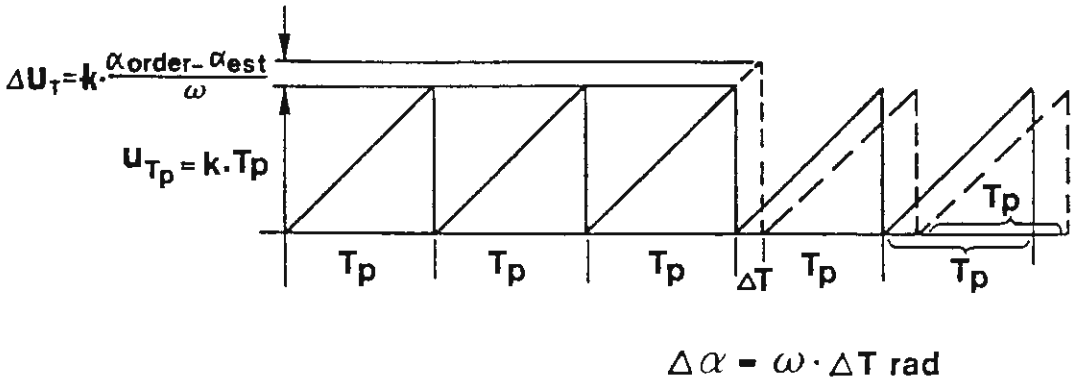

Figure 7-8 Phase-controlled (phase-locked) oscillator.

A predictive firing control on γ_{min}

A firing control-system based on prediction of γ will now be described. The possibilities of avoiding commutation failures at disturbances in the ac-voltages are at least theoretically better with this type of control than with a feedback type of system. The system will be described with the use of figure 7-10.

Firing pulses at rectifier operation are generated, when a signal is received from the AND circuit. The following two conditions have then to be fullfilled.

- The firing angle α or instantaneous value of the commutation voltage u_k has to be sufficiently large to secure correct firing. This is indicated by the signal D_α.

- The current regulator requests firing via a pulse from the phase-locked oscillator (osc). It should be noted, that the ramp (analog) or counter (digital) according to figure 7-8, will not restart until the firing pulse generator has been ordered to generate a new firing pulse. Because of that, as also illustrated in figure 7-10, both, the AND and the OR block are in fact integral parts of the phase-locked oscillator function.

An additional function, not shown here in figure 7-10, is also included in order to achieve equidistant firing for operation at the α_{min}-limit. This is arranged so that the valve, which at equidistant firing gets the smallest firing angle, will be decisive for (initiating) the firing instants of all the other valves, i.e. by instant shifting of the successive firing of the valves. The input voltage to the oscillator will, during the firings of the eleven succeeding valves at twelve pulse operation, be limited in

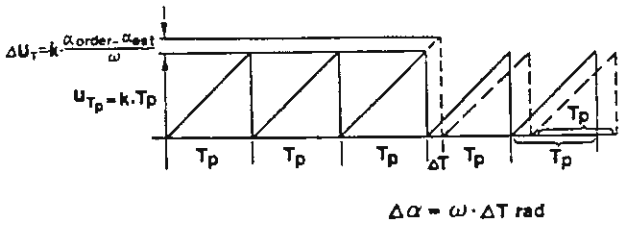

Figure 7-8 Phase-controlled (phase-locked) oscillator.

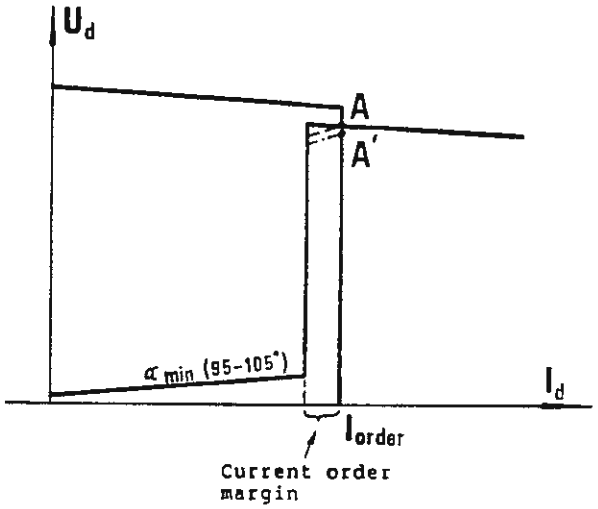

Figure 7-5 Steady state U_d/I_d characteristics for rectifier and inverter with special α_{min}-limit and cutting off the corner of the U_d/I_d characteristic in the inverter.

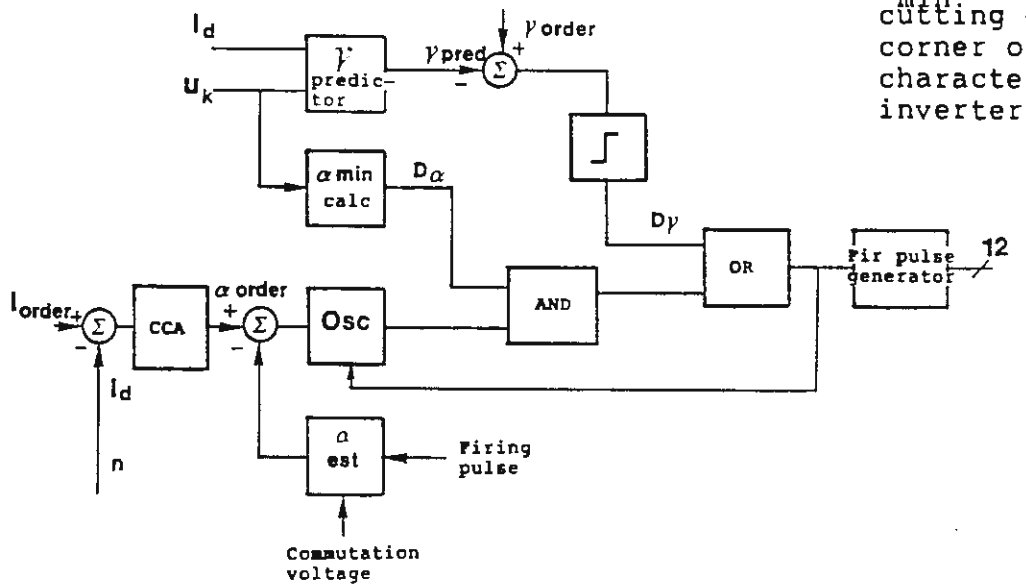

Figure 7-10 Converter firing control with predictive γ_{min}-control.

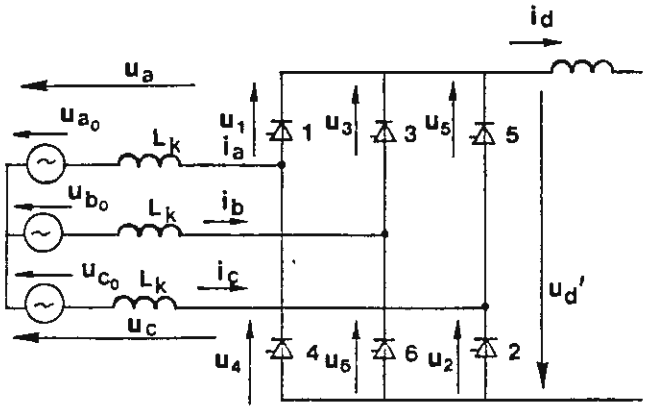

Figure 4-1 Two-way six-pulse converter bridge.

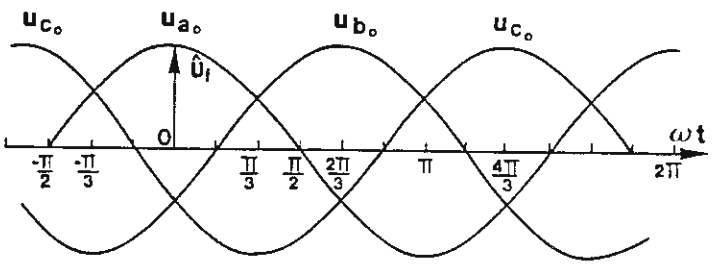

Figure 4-2 Source phase voltages

such a way, that the time-intervals between the successive firings will be at least T_p according to figure 7-8. These limitations will not prevent an increase of the firing angle, if needed, e.g., if the measured direct current is larger than the ordered current.
At inverter operation fairly high values of α_{min} are used (α_{min} = 95 - 105°), as can be seen in figure 7-5. This function is included in the α_{min}-block as can be seen in figure 7-10.

An additional requirement for the timing of the firing pulses are added in inverter operation, i.e. $\gamma \geq \gamma_{min}$. The γ-predictor and the OR-block secure that this condition is fullfilled.

The function of the γ-predictor is based on the measured commutation voltage and the direct current for the next valve to be fired. It calculates at each moment the predicted commutation margin in case firing would take place at that moment. Let's assume that valve 3 is the next valve to be fired. The commutation from valve 1 to valve 3 will then be determined by the commutation voltage $u_{ba} = u_b - u_a$, as can be seen in figures 4-1 and figure 4-2. The length of the commutation interval will also be determined by the actual direct current and half the estimated current change during the commutation interval.

The measured commutation voltages u_k and the direct current on the dc-side are, because of that, input signals to the γ-predictor. Information about the time-instants for the previous zero-crossings of the commutation voltages are also stored in the γ-predictor. As soon as the predicted commutation margin, γ_{pred}, is equal to the ordered commutation margin, γ_{order}, the signal D_γ is generated, which triggers the firing of the valve via the OR-gate.

Special limitations are included on the input side of the

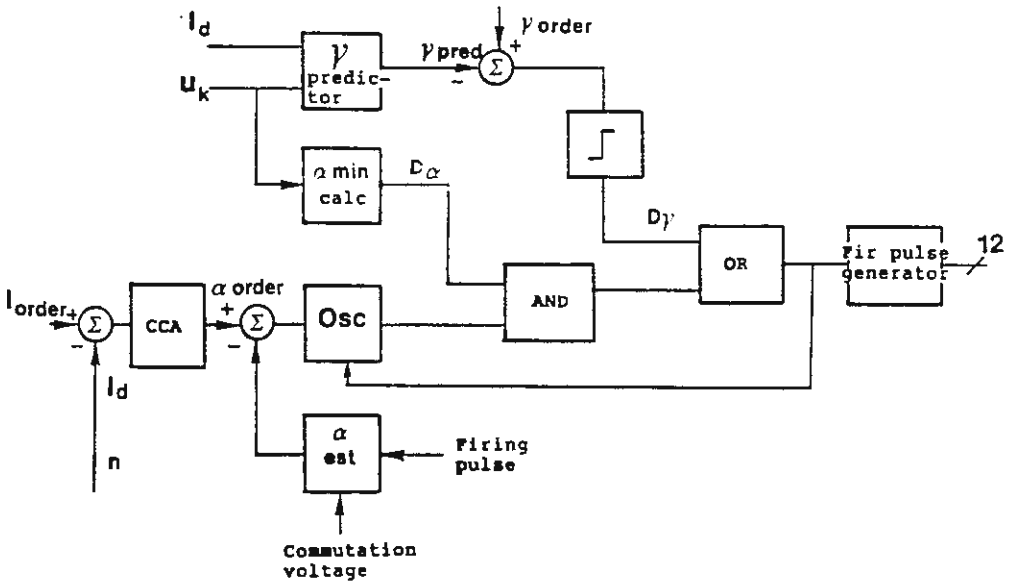

Figure 7-10 Converter firing control with predictive γ_{min}-control.

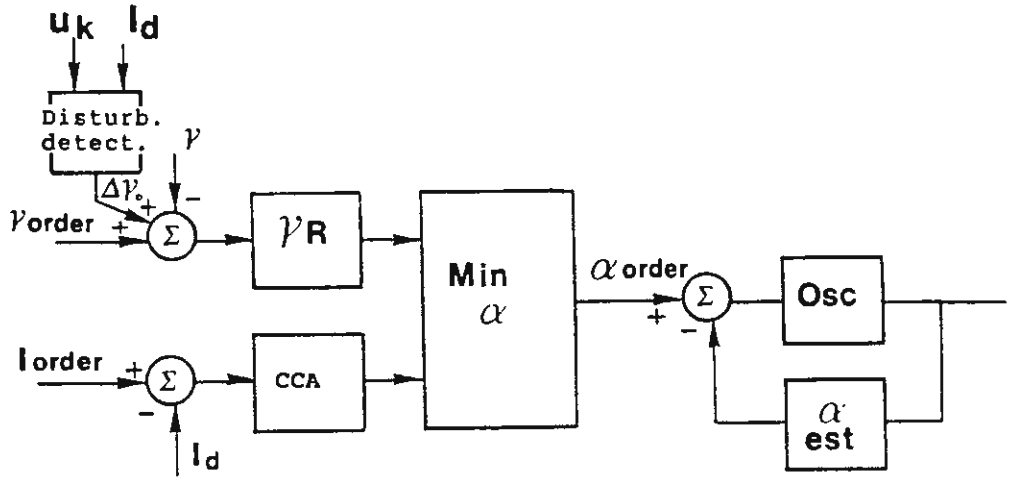

Figure 7-9 Converter firing control system with a feedback control of γ.

oscillator, OSC, to secure equidistant firing for operation at γ_{min}. These circuits are similar to those previously described for operation at α_{min}, but here are arranged so that the current regulator can order an earlier firing than the one corresponding to $\gamma = \gamma_{min}$.

It should be noted, that most of the circuits, according to figure 7-10, are used in common for all valves of a convertor, i.e., for twelve valves in a twelve-pulse convertor circuit. The firing pulse generator generates the firing pulses to the correct valves and works on the principle of a ring-counter. It will also generate control pulses to the α_{min}- and γ-predictor block so that the performed calculations are based on the commutation voltage for the valve in turn to fire. The commutation voltages u_k are determined from the measured voltages on the filter bus and the actual convertor transformer tap-changer position.

It should finally be noted, that since some parameters in the γ-predictor, according to figure 7-10, are continuously up-dated based on actual measured commutation margins, and since the γ-feedback system, according to figure 7-9, also contains a disturbance detector, the difference in performance of firing control system utilizing both principles simultaneously, is not as great as could be expected.

The modern micro-processor based firing control system offers a great flexibility in realizing various advanced control strategies. The very high requirement for speed in the calculation and resolution, especially with regard to time, will however also give very high requirement on computing capacity. It could, for instance, be mentioned that a requirement on equidistant firing of $\pm$ 0.02° el corresponds to a maximum deviation of about $\pm$ 1 μs.

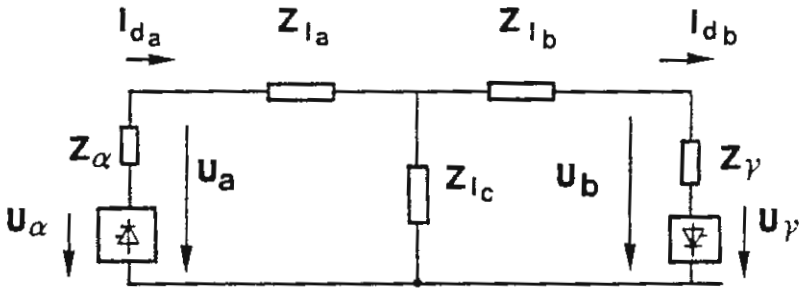

Figure 7-11 Simplified circuit diagram for an HVDC-transmission between the stations a and b.

7.4 The current control amplifier (CCA) Dynamic characteristics

The dynamic characteristics of a HVDC convertor in the frequency range 10-100Hz are to a large extent determined by the dynamic characteristic of the current control amplifier. The dynamic characteristics at lower frequencies are mainly determined by the dynamic characteristics of the higher level control, which generates the current order, or by the voltage dependent current order limit (VDCOL). The dynamic characteristics at lower frequencies are of special interest with regard to the operation of the HVDC transmission in the total power transmission system. This will be treated later.

The following cases have to be considered for the optimization of the dynamic characteristic of the current amplifier:

- the step response at current order changes
- current order changes at short-circuits on the dc-side
- influence on the attenuation of oscillations on the dc-side at different disturbances, especially those resulting in injection of voltages of fundamental frequency to the dc-side.

Representation of convertors and main-circuits

We will now study the dynamic behaviour of an HVDC transmission system represented by the simplified circuit diagram, as shown in figure 7-11. The intention is to provide a basic understanding, as to how the current control system will affect the dynamic behaviour of the

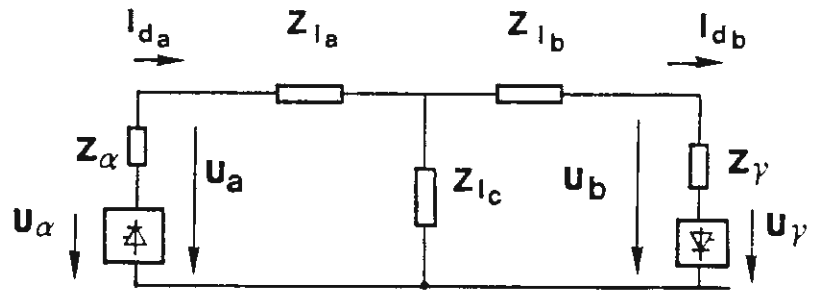

Figure 7-11 Simplified circuit diagram for an HVDC-transmission between the stations a and b.

HVDC link and which possibilities and limitations then exist. We will assume, that station (a) is operating as rectifier controlled by constant current and that station (b) is operating as inverter controlled by γ_{min}. The convertor stations, as viewed from the dc-side are represented by the internal voltages U_α and U_γ and the internal impedances Z_α and Z_γ. It is assumed that the internal voltages are only determined by the firing instants of the valves as long as the commutation voltages are constant. The current dependencies on the convertor voltages are represented by the internal impedances. We will denote the convertor voltages in a complex form with U_a and U_b (superimposed harmonic voltages due to the commutations are neglected). We will get:

$$U_a = U_\alpha - Z_\alpha \cdot I_a \qquad (7\text{-}4)$$

$$U_b = U_\gamma + Z_\gamma \cdot I_b \qquad (7\text{-}5)$$

The impedance of the line can be represented as a T-equivalent, as shown in figure 7-11. The impedances of the dc-reactor are here assumed to be included in the impedances Z_{la} and Z_{lb} respectively. No dc-filters are assumed.

We can base the determination of U_α and U_γ and the real parts of Z_α and Z_γ i.e. R_α and R_γ on the steady state characteristics of the convertors, according to the equations (4-37) and (4-41). It can be shown that these equations are also valid for quasi-stationary conditions. Comparison to equations (7-4) and (7-5) will, for a constant U_{dio}, result (U_T is neglected).

$$U_\alpha = U_{dio} \cdot \cos \alpha \qquad (7\text{-}6)$$

$$R_\alpha = (d_{xN} + d_{rN}) \cdot \frac{U_{dioN}}{I_{dN}} \qquad (7\text{-}7)$$

$$U_\gamma = U_{dio} \cdot \cos \gamma \qquad (7\text{-}8)$$

$$R_\gamma = -(d_{xN} - d_{rN}) \cdot \frac{U_{dioN}}{I_{dN}} \qquad (7\text{-}9)$$

Equation (7-6) can now, for small superimposed oscillations in the firing angle α, be written:

$$\Delta U_\alpha = - U_{dio} \cdot \sin \alpha \cdot \Delta\alpha \qquad (7\text{-}10)$$

Equation (7-10) is valid as a good approximation as long as the oscillation frequency is considerably lower than the pulse-number times the network frequency. At higher frequencies it is necessary to take into account that the control is not continuous but can only influence the output voltage at the firing instants of the valves. The control system can thus be treated as a sampled control system. However, only superimposed oscillations usually having a frequency up to the second harmonic are of interest, as the amplification in the current control system for higher frequencies is lower than one. Because of that, it is often sufficient to consider the limited pulse-number in an approximate way by including an additional time delay equal to half of the time between two consequtive commutations. Equation (7-10) will then be multiplied by the transfer function

$$G_s = e^{-\frac{sT_P}{2}} \qquad (7\text{-}11)$$

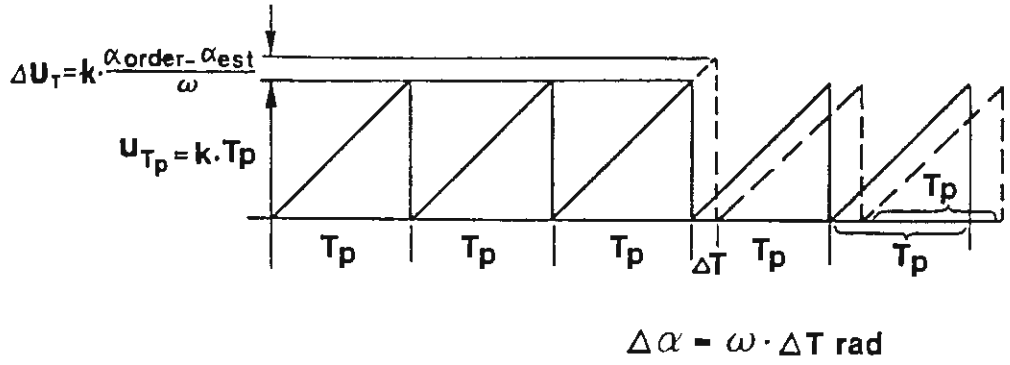

Figure 7-8 Phase-controlled (phase-locked) oscillator.

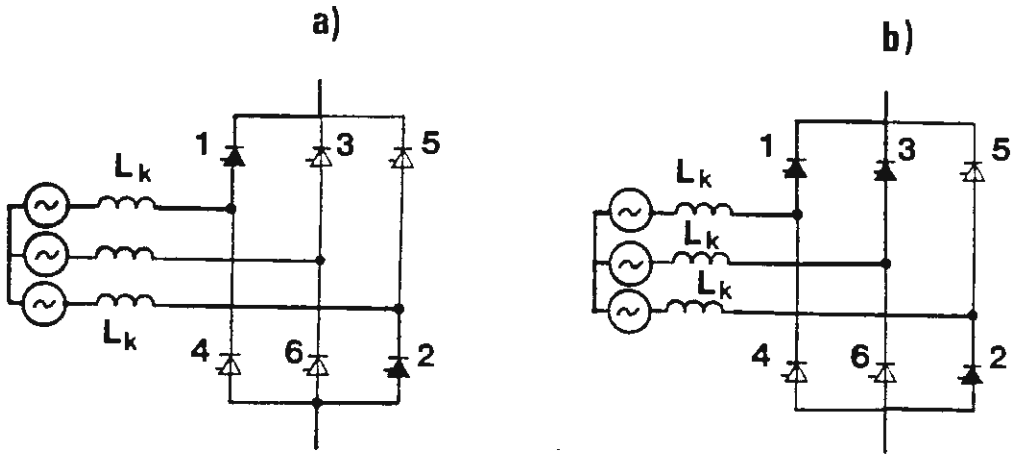

Figure 7-12 The two alternative types of typology for a converter bridge.
a) Two valves conducting. No commutation.
b) Three valves conducting. Commutation interval.

The quantity T_p is the time in seconds between two consequtive commutations, according to figure 7-8.

Equation (7-7) can be considered to describe the voltage drop due to the voltage-time area needed for the commutations plus the real resistive voltage drop. It is then obvious that equation (7-7) is also approximately valid for superimposed current oscillations, provided that the cycle time is substantially longer than the angle of overlap.

Equations (7-7) and (7-9) were derived from the steady state characteristics of the convertors. It is thus obvious that these equations cannot give any information regarding any additional drop of the convertor voltage due to the time derivative of the convertor current.

To calculate this voltage drop we have to take into account the different types of circuit topologies applicable during the operation of the convertor. This is illustrated by figure 7-12, showing the topology with two conducting valves during an interval with no commutation, and the topology with three conducting valves during the commutation interval. As viewed from the dc-side the convertor can be represented by an inductance equal to $3L_k/2$ when three valves are conducting. The average inductance is derived by taking into account the total duration per cycle for each topology. This shows that the average inductance for a 6-pulse bridge is:

$$L_{i6} = \frac{\left(\frac{\pi}{3} - u\right) \cdot 2L_k}{\frac{\pi}{3}} + \frac{u \cdot 3L_k}{\frac{\pi}{3} \cdot 2}$$

or

$$L_{i6} = \left(2 - \frac{3}{2\pi} \cdot u\right) L_k \qquad (7\text{-}12)$$

The average inductance for a 12-pulse convertor unit will be derived by multiplication by a factor of two, i.e.,:

$$L_{i12} = \left(2 - \frac{3}{2\pi} u\right) 2 \cdot L_k \qquad (7\text{-}13)$$

A more complex current dependency than the one presented above will be achieved for the case when the commutation voltage is not a stiff voltage. This will usually give a more positive impedance in the rectifier, since a small transient increase of the convertor current will decrease the commutation voltage.

The ac-network impedance will, in the inverter, give an additional contribution in the negative direction, as an increased convertor current will decrease the commutation voltage and thus decrease the counter voltage as viewed from the dc-side. (Note the opposite definition of the positive reference voltage in the rectifier and the inverter).

The internal resistance, due to the inductive voltage drop d_{xN}, is for an inverter operating at constant commutation margin γ, according to equation (7-9), negative. This is valid for superimposed oscillations of lower frequencies, for which it can be assumed that the commutation margin γ is kept constant. However, at superimposed oscillations of higher frequencies the equidistant control system will try to keep the firing angle rather than the commutation margin γ constant. This means that the internal resistance will be positive at higher frequencies as shown by equation (7-7).

As mentioned above the ac-network impedance will result in

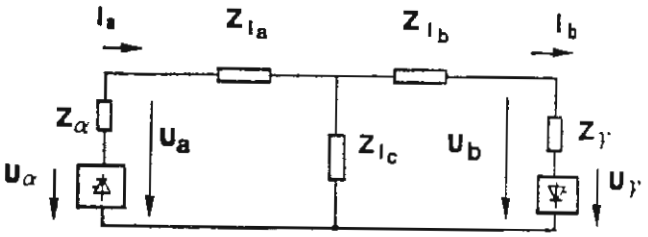

Figure 7-11 Simplified circuit diagram for an HVDC-transmission between the stations a and b.

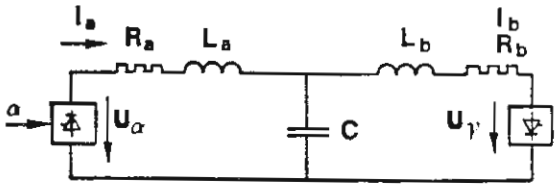

Figure 7-13 Simplified circuit diagram for small superimposed oscillations.

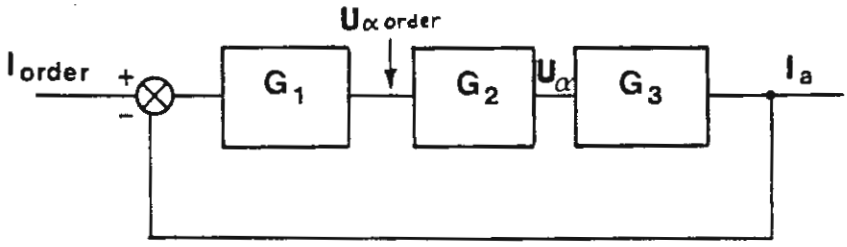

Figure 7-14 Block diagram for the current control.

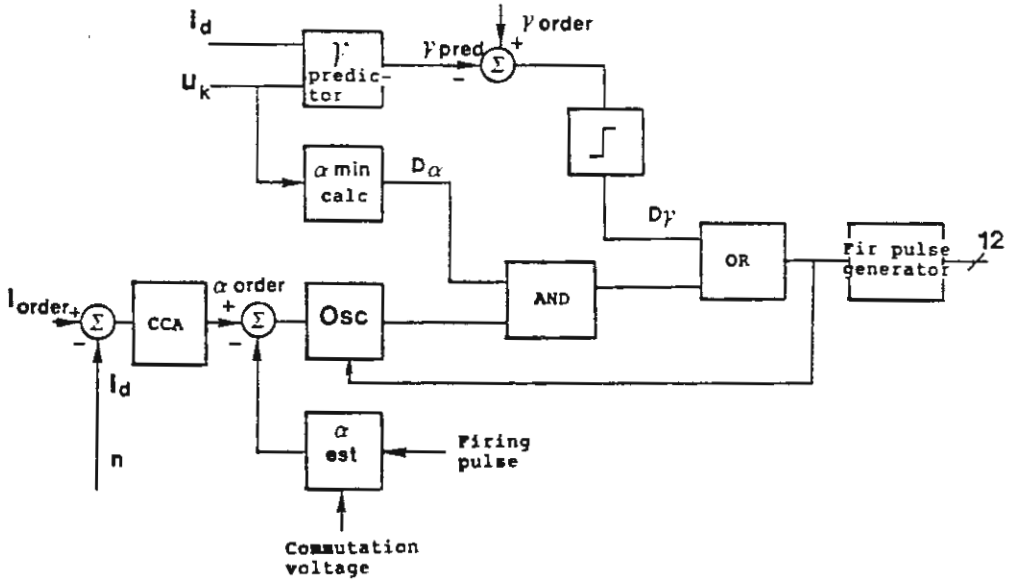

Figure 7-10 Converter firing control with predictive γ_{min}-control.

a contribution in the negative direction also for higher frequencies. This contribution will usually increase at increased ac-network impedances, i.e., weaker ac-systems.

The circuit diagram, according to figure 7-11, can be further simplified, when we assume that the HVDC transmission is a cable transmission system. This is shown in figure 7-13. The diagram is also approximately valid for an overhead line transmission at lower frequencies. The resistances R_a and R_b are determined by the internal equivalent resistances of the convertors and half of the line resistance. The inductances L_a and L_b are determined by the internal inductances of the convertors, the inductances of the dc-reactors and half of the line inductance. The capacitance is the total capacitance of the cable (or approximately of the whole overhead line).

Block diagram for the current control system

The current control system can be represented with a simplified block diagram, according to figure 7-14, for superimposed oscillations of small amplitudes, provided the station (a) is controlled by constant current. The block G_1 is determined by the transfer function of the current control amplifier (CCA in figures 7-2, 7-9 and 7-10). Block G_2 represents the transfer function of the convertor firing control system and the convertor with the output voltage U_α. The block G_3 represents the transfer function of the dc-circuit from the voltage U_α to the convertor current I_a according to figure 7-13.

The transfer function G_2 is a non-linear function of α, providedthe signal U_α is made proportional to the firing angle α, refer to equation (7-10). Because of that a linear-rization function has to be included in the control loop in order to avoid getting a non-linear control system with an amplification being dependent upon the value of the

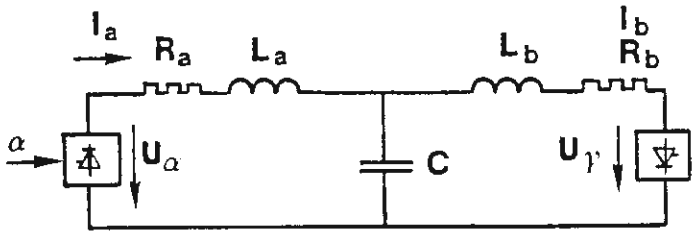

Figure 7-13 Simplified circuit diagram for small superimposed oscillations.

firing angle. This can be obtained by making the amplification of the current control amplifier for small signals proportional to $1/\sin\alpha$. We will, in the following, assume that such a feature is included in either G_1 or G_2, so that the closed loop amplification is then independent on the value of the firing angle α.

Normalization

It is often practical to normalize all quantities and refer them to suitable base units (p.u.) in order to simplify the treatment. Thus we will, in the following express voltages, impedances, currents and angular frequencies in p.u. of the following quantities:

Voltage: U_{dioN} of the convertor (Usually 12-pulse)

Impedance: $Z = \sqrt{\frac{L}{C}}$ (7-14a)

To simplify the calculations we will set
$L_a = L_b = L$ (see figure 7-13)

Current: $\frac{U_{dioN}}{Z}$ (7-14b)

Angular frequency: $\omega_o = \frac{1}{\sqrt{LC}}$ (7-14c)

Transfer function of the current control amplifier G_1

The characteristics of the current control amplifier are usually chosen so that the transfer function G_1 can be written in the following form:

$$G_1 = \frac{k'(1+sT_2)}{sT_3\,(1+sT_1)} \qquad (7\text{-}15)$$

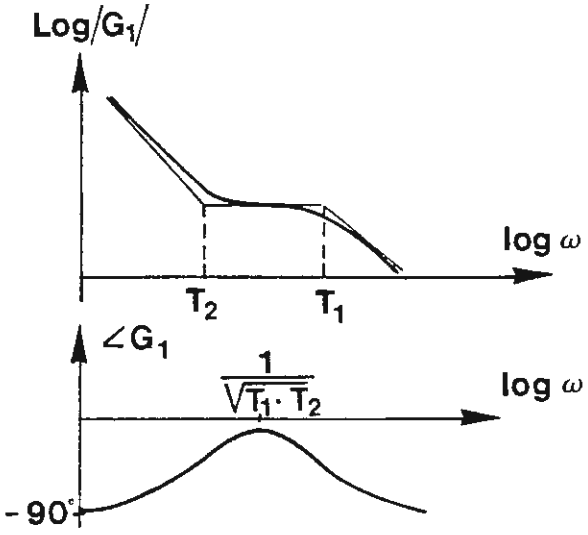

Figure 7-15 Bode diagram for a typical transfer function G_1.

where $T_1 > T_2$

The Bode-diagrams for amplification and phase-shift of G_1 areshown in figure 7-15.

For high frequency oscillations, for which $\omega T_2 >> 1$, we can simplify G_1 to

$$G_1 \simeq \frac{k' \cdot T_2}{T_3(1+sT_1)} \qquad (7\text{-}16)$$

We will in the following set

$$G_1 = \frac{k_1}{1+sT_1} \qquad (7\text{-}17)$$

The constant k_1 is assumed to be normalized. The input current is expressed in p.u., a the base according to eq. 7-14b. This implies that a current error equal to U_{dioN}/Z results in the voltage change across the convertor equal to $k_1 \cdot U_{dioN}$.

The transfer function for the convertor G_2

The transfer function of the convertor from $\sin\alpha \cdot \Delta\alpha$ to ΔU_α can, approximately, be represented by a time-delay, according to equation (7-11), as previously described. This means that the transfer function expressed in p.u. will be

$$G_2 = e^{\frac{-sT_p}{2}} \qquad (7\text{-}18)$$

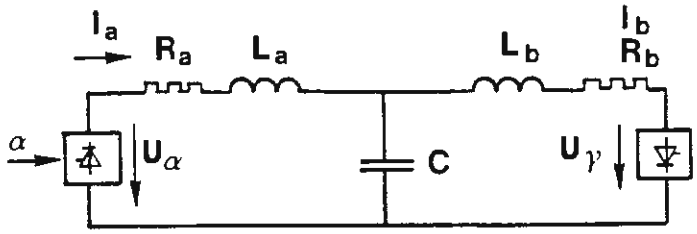

Figure 7-13 Simplified circuit diagram for small superimposed oscillations.

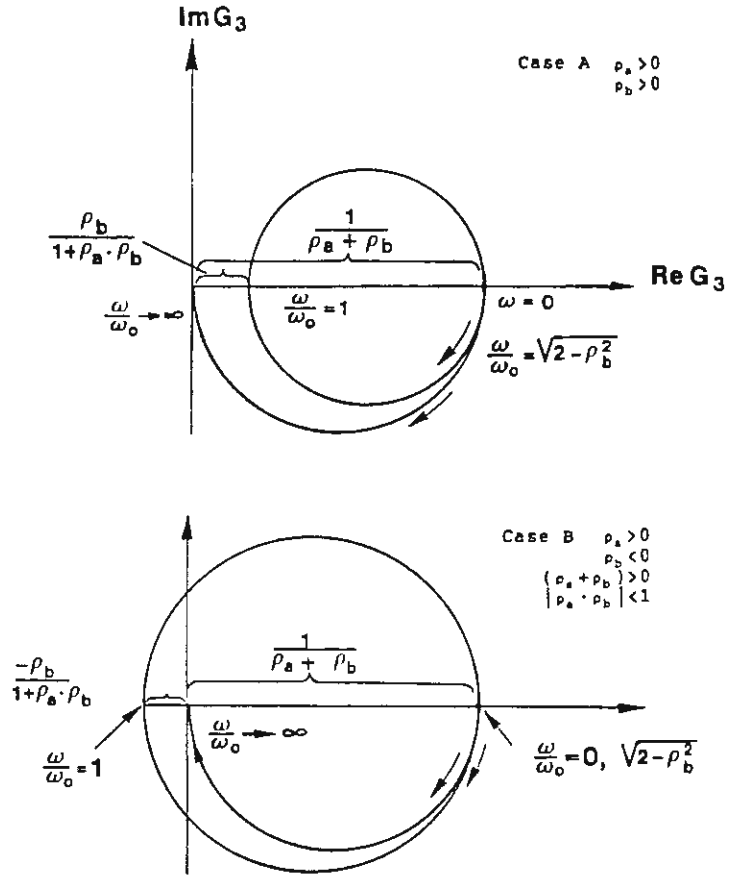

Figure 7-16 Transfer function G_3 in the complex plane (Impedance diagram) in p.u. Base $Z=\sqrt{(L/C)}$, $L_a=L_b=L$, $\rho_a=R_a/Z$, $\rho_b=R_b/Z$.

The transfer function of the dc-circuit G_3

We will get the following transfer function G_3 for the circuit, according to figure 7-13, provided U_γ is assumed to be constant.

$$G_3(s) = \frac{\Delta I_a}{\Delta \alpha}$$

or

$$G_3(s) = \frac{1+s\cdot R_b\cdot C + s^2\cdot L_b\cdot C}{R_a+R_b+s\left(L_a+L_b+R_a\cdot R_b\cdot C\right)+s^2\left(R_a\cdot L_b+R_b\cdot L_a\right)\cdot C+s^3\cdot L_a\cdot L_b\cdot C} \qquad (7\text{-}19)$$

The transfer function G_3, expressed in p.u. will have the characteristics as shown in figure 7-16, provided $s = j\omega$, $L_a = L_b = L$, $\omega_o = 1/\sqrt{LC}$ and $Z = \sqrt{L/C}$. We have here used the normalized resistances $\rho_a = R_a/Z$ and $\rho_b = R_b/Z$.

The transfer function is shown for two different typical cases of interest.

In case A it has been assumed that both R_a and R_b are positive, while in case B it has been assumed, that R_b is negative and $\rho_a + \rho_b > 0$. The later case could be a typical one if it is assumed that $\Delta\gamma = 0$ also at higher frequencies. It should be noted that the impedance of the ac-network in the inverter station will give contribution to the negative resistance. The line resistance, the symmetrizing, the equidistant control, and the cutting of the corner in control characteristic will, on the other hand, provide contributions for decreasing the negative resistance. However, for weak ac-networks at the receiving end, the net-effect will often be that the total equivalent

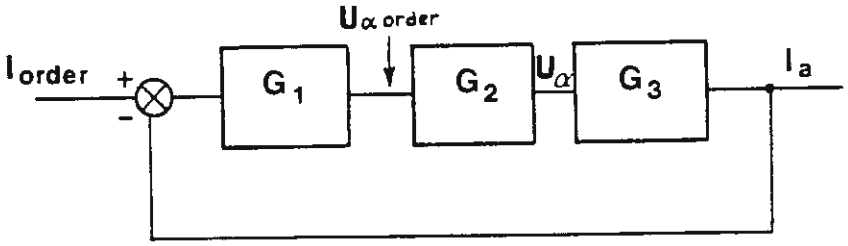

Figure 7-14 Block diagram for the current control.

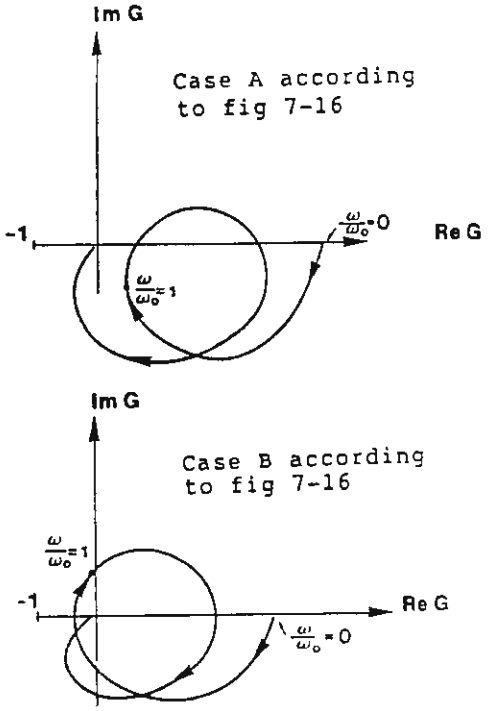

Figure 7-17 Nyquist diagram for $G=G_1 \cdot G_2 \cdot G_3$. G_1 according to equation 7-17 and G_3 according to figure 7-16.

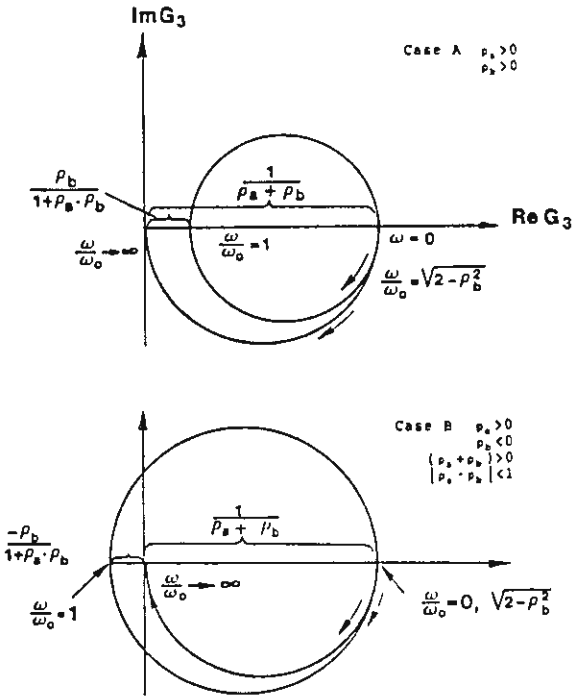

Figure 7-16 Transfer function G_3 in the complex plane (Impedance diagram) in p.u. Base $Z=\sqrt{(L/C)}$, $L_a=L_b=L$, $\rho_a=R_a/Z$, $\rho_b=R_b/Z$.

resistance is negative i.e., $R_b < 0$ and case B will apply.

Transfer function for the closed current control system

We will get the following overall transfer function for the closed loop current control system.

$$I_a = \frac{G}{1+G} \cdot I_{order} \qquad (7\text{-}20)$$

$G = G_1 \cdot G_2 \cdot G_3$, according to figure 7-14. We can usually approximately set $G_2 = 1$ as $1/\omega_0 >> T_p/2$. The amplification in the open circuit is usually very high for lower frequencies ($|G| >> 1$) as the amplification of the current control amplifier is very high, refer to equation (7-15). This implies that $I_a \approx I_{order}$.

To achieve a fast current control system it is further desirable that the following condition is valid for as high frequencies as possible.

$$1 < \left| \frac{G}{1+G} \right| < \sqrt{2}$$

The Nyquist diagram for the current control system will have the characteristics as shown in figure 7-17, that the transfer function of the dc-circuit G_3 can be represented as shown for case A and B in figure 7-16 resoectively and the transfer function of the current control amplifier can be represented by equation (7-17).

It is obvious from figure 7-17, that a dc-circuit having a transfer function corresponding to case B in figure 7-16 will make it more difficult to design a fast and stable current control system than a dc-circuit with a transfer

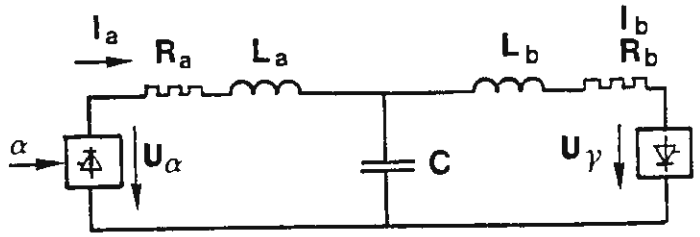

Figure 7-13 Simplified circuit diagram for small superimposed oscillations.

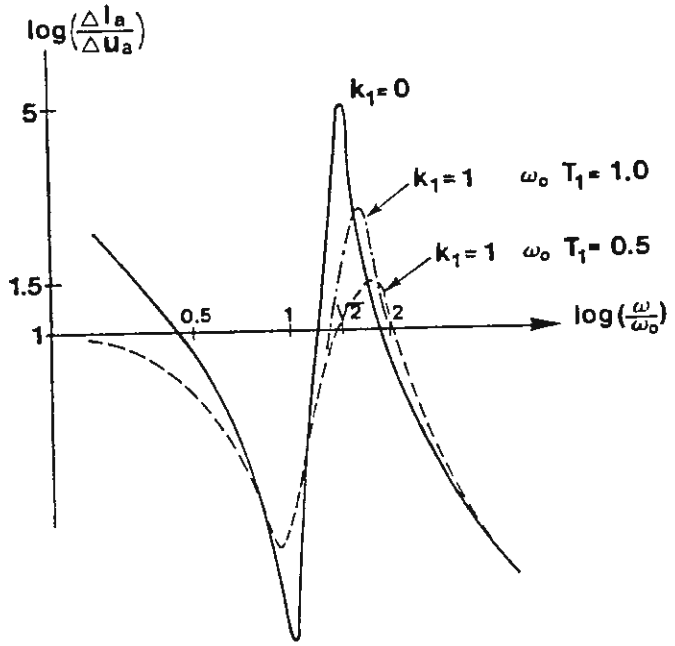

Figure 7-18 Relationship between small superimposed oscillations in current I_a and injected disturbance voltages in series of the converter in station (a). Circuit according to figure 7-13 with $L_a = L_b = L$, $Z = \sqrt{(L/C)}$, $R_a/Z = 0.1$ and $R_b/Z = 0.1$.

function of the type illustrated in case A. The essential difference is that the real part of G_3 will be negative, when $\omega/\omega_0 = 1$.

Another way of illustrating that case B is more critical than case A is to assume that the amplification of the current control amplifier is independent of the frequency, i.e. $G_1 = k_1$. If the value of k_1 is chosen above a certain critical value making the current I_a almost stiff and constant the circuit R_b, L_b and C will start to oscillate at a frequency close to $\omega_0 = 1/(\sqrt{L_b} \cdot \sqrt{C})$. These oscillations are generated by the negative resistance R_b.

However, it is usually possible to design a fast and stable current control system even for case B, by a suitable design of the transfer function G_1.

The influence of the current control system on superimposed oscillations on the dc-side

The current control system will result in a contribution of ΔU_α to the internal convertor voltage U_α as a function of the measured change ΔI_a in the current I_a. The current control system will thus result in a contribution to the circuit, according to figure 7-13 equivalent to the connection of an additional damping circuit. A current control system with constant amplification, which is independent upon the frequency, i.e., with no time constant, corresponds to insertion of an additional resistance in the circuit, while a transfer function, according to equation (7-17), is equivalent to the insertion of a resistance connected in parallel with a capacitance giving a time-constant T_1.

The influence of the current control system is illustrated in figure 7-18. This figure shows the ratio between the

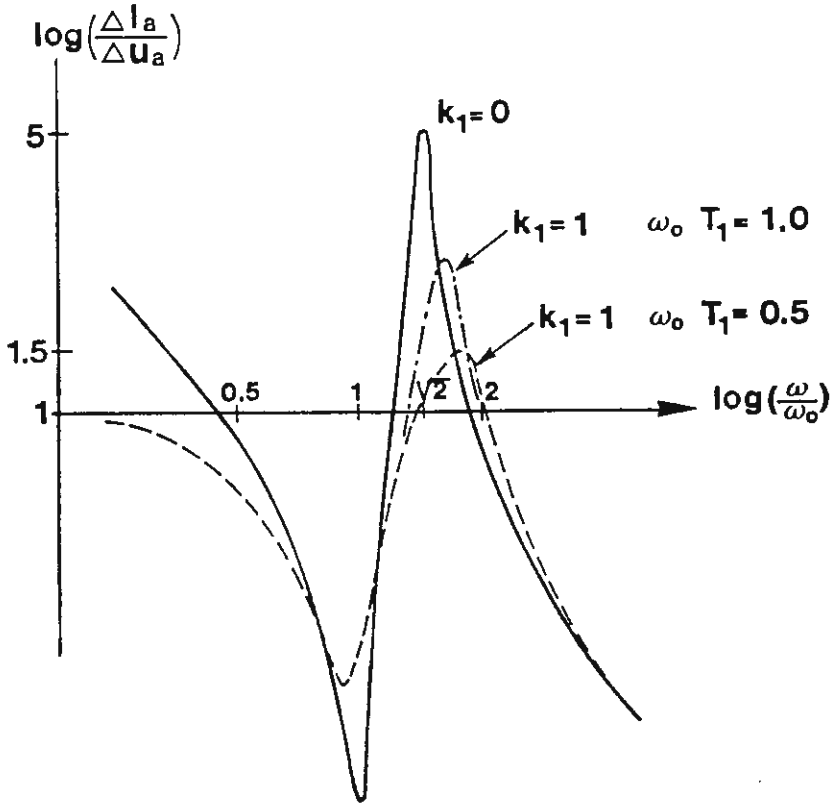

Figure 7-18 Relationship between small superimposed oscillations in current I_a and injected disturbance voltages in series of the converter in station (a). Circuit according to figure 7-13 with $L_a=L_b=L$, $Z=\sqrt{(L/C)}$, $R_a/Z=0.1$ and $R_b/Z=0.1$.

amplitudes of the superimposed oscillations in the convertor current, ΔI_a, and the amplitude of the injected disturbance voltages in series with the convertor, ΔU_a, as a function of the frequency for different values of the amplification in the oscillations. The diagram illustrates the influence of three different values of the amplification in the current control systems, k_1 (p.u. base Z) and of two different values of the time constant T_1. It has been assumed that $R_b > 0$. A negative value of R_b would mainly result in a higher resonance peak value at $\omega/\omega_0 = \sqrt{2}$ for the case $k_1 = 0$.

It should be noted that the amplification in the current control system will, both, change the magnitude of resonance peak as well as the resonance frequency. This shows that the current control system will influence the resonance frequency of the circuit. This is also true for disturbances injected from station (b). The resonance frequency will, for this case, approach $\omega_0 = 1/\sqrt{LC}$ for large values of k_1 and approach $\sqrt{2} \cdot \omega_0$ for small values of k_1.

We have so far assumed that the amplitudes of the superimposed oscillations have been small. The current control system will of course also have an essential influence upon oscillations of higher amplitudes. Such oscillations can, for instance, be generated by commutation failures in the inverter or large asymmetries in any of the ac-networks. A theoretical analysis will be much more difficult for oscillations of large amplitudes than for small amplitudes as the non-linear characteristics of the convertor as well as limitation, e.g., of α_{min} then can have an essential influence on the behavior of the convertor and the current control system. Because of that, it is recommended to study such cases on a real time simulator or by computer programs with adequate representation of, both, the control systems and the

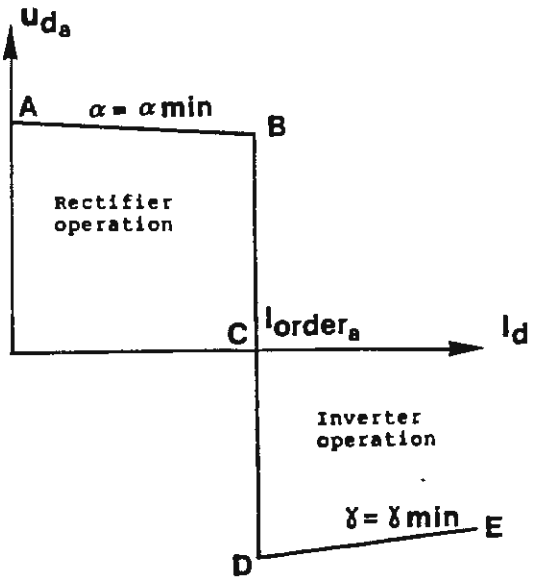

Figure 7-3 Steady state U_d/I_d characteristics.

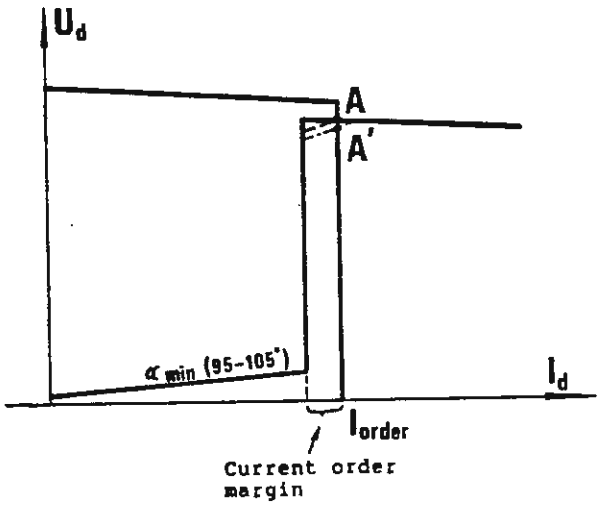

Figure 7-5 Steady state U_d/I_d characteristics for rectifier and inverter with special α_{min}-limit and cutting off the corner of the U_d/I_d characteristic in the inverter.

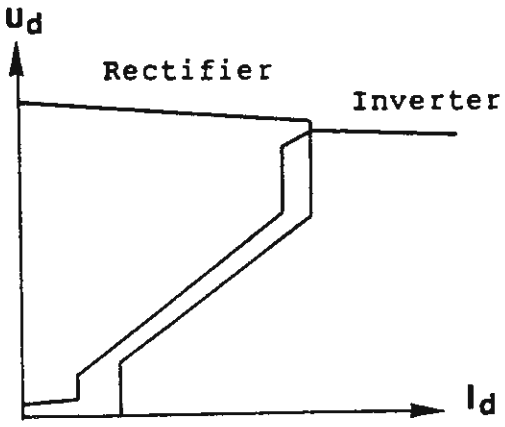

Figure 7-20 Complete U_d/I_d characteristics.

convertors.

7.5 Voltage dependent current order limit (VDCOL)

We have until now, in the treatment of the current control system, assumed that the current order is independent upon the direct voltage. See characteristic B-D in figure 7-3. However, it is for many reasons desirable to reduce the current order at large reductions of the direct voltage. Because of that all HVDC control systems are equipped with, so called, Voltage Dependent Current Order Limit, VDCOL. The main reasons for the VDCOL are:

- A reduction of the dc-line voltage requires higher firing angles, which at constant direct current results in increased reactive power consumption. This could, especially for weak ac-networks, cause too large reduction of the ac-voltages if the current is not decreased.

- A reduced dc-line voltage is often caused by commutation failures in the inverter e.g. due to a phase-to-ground fault in the ac-network connected to the inverter. It is then advantageous to reduce the current order in order to reduce the stresses on the valves and speed up the recovery after disconnection of the earth fault.

The VDCOL will usually reduce the current order quickly at a decrease of the dc-voltage but increase the current order more slowly at an increase of the dc-voltage. This will effect a more smoothed restart of the convertor after a fault.

A typical steady state characteristic for both stations, which, without the VDCOL have the shape, according to figure 7-5, will now be modified, as shown in figure 7-20.

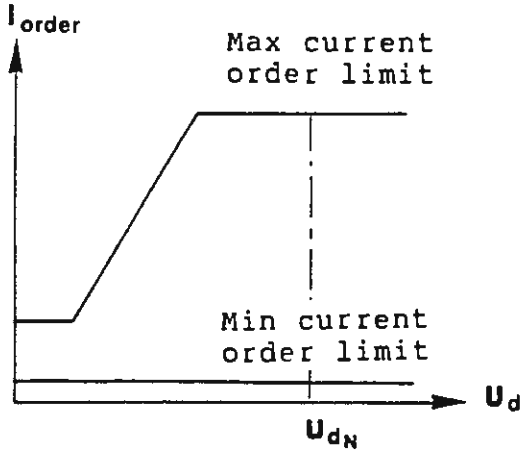

Figure 7-19 Max. and min. current order limits and voltage dependent current order limit (VDCOL).

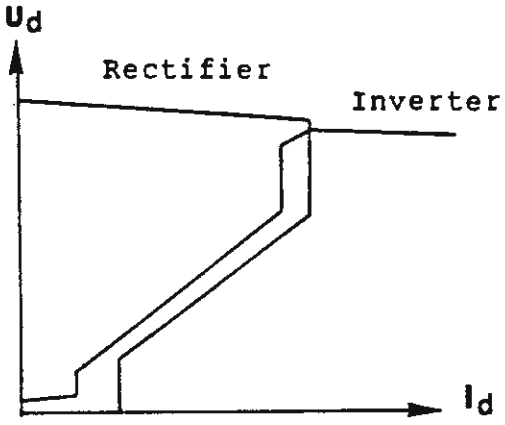

Figure 7-20 Complete U_d/I_d characteristics.

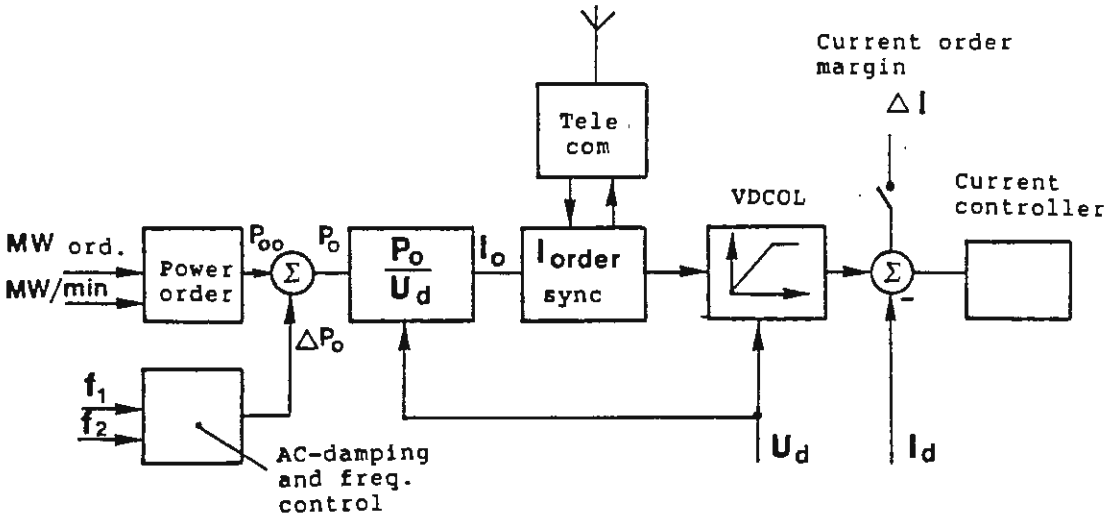

Figure 7-22 Pole master control system.

Note, that the current and voltage axes have been reversed between figures 7-19 and 7-20. The VDCOL is usually included as a seperate block in the master control system as shown in figure 7-22.

7.6 Tap-changer control system

An HVDC transmission is usually operated at a direct voltage close to the maximum operating voltage in order to reduce the resistive line losses as much as possible. It is further desirable to operate the inverter at minimum commutation margin γ_{min} in order to reduce the amount of reactive power consumption in the inverter. A constant direct voltage and constant γ_{min} requires that the commutation voltage be varied with the current.

For the rectifier station it is desirable to operate with the smallest possible firing angle and still keep a sufficient control margin in α. This implies that a suitable operation range for the firing angle is 12 - 17.5°. The commutation voltage must then, also in the rectifier, be a function of the direct current, as the direct voltage shall be kept as close as possible to the maximum permitted dc-line voltage.

The above requirement for the inverter and the rectifier requires that the transformers in both stations have to be provided with tap-changers for the control of the commutation voltages. The normal ac-voltage variations also have to be considered at the selection of the tap-changer range. The total tap-changer range has to be rather large, e.g., $\pm$ 15%, which with the maximum possible steps gives the size of each step in the range of 1 - 1.3%.

Although some tests have been performed with tap-changers using thyristors the switching is still performed by

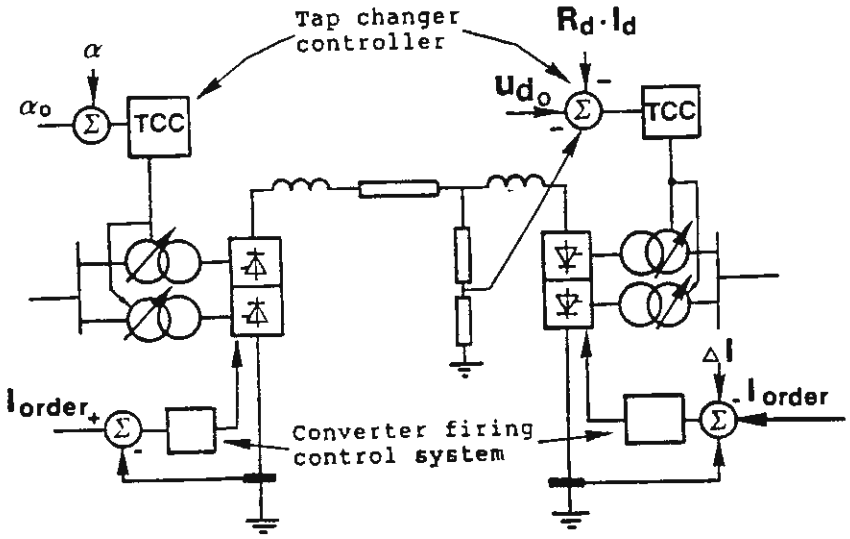

Figure 7-21 Converter transformer tap-changer control system.

mechanical switches in modern tap-changers. The speed of the tap-changers setting will because of that, be substantially slower than the speed of the convertor firing control system. As the speed of the tap-changer control and the convertor-firing control are very different the cooperation between the two control systems will not cause any problems.

The function of the tap-changer control in normal operation with the inverter controlled at minimum commutation margin, γ_{min} and the current controlled at the rectifier is illustrated in figure 7-21. Since the direct line voltage is measured at the inverter terminal and the line voltage has to be controlled to its maximum permitted value at the rectifier terminal, a compensation for the line drop, $R_d \cdot I_d$, is included in the tap-changer controller at the inverter station.

The tap-changer controllers are provided with dead-bands. The magnitudes of the dead-bands have to be chosen usually larger than twice the change in voltage or firing angle caused by one tap-changer step. The desired values are normally set in the middle between the two limit values.

7.7 Pole master control

The convertor firing control system and the tap-changer control system can be considered to be the basic system for a convertor station. The design of those systems is only slightly dependent on the actual requirements of a specific HVDC transmission, if we disregard the actual setting of the parameters.

The pole-master control system or master control system, which will be described below, is on the other hand, to a large extent designed with regard to the specific

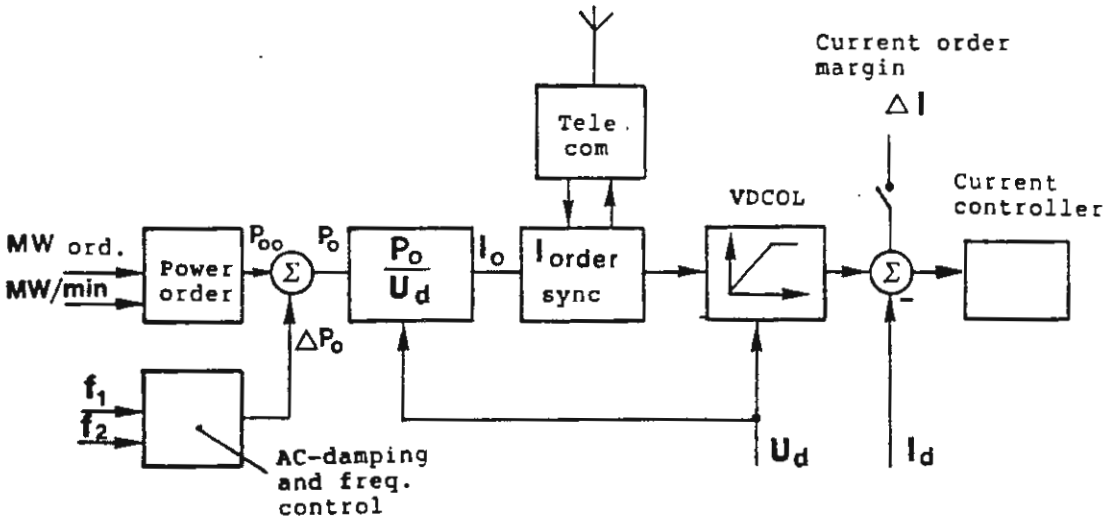

Figure 7-22 Pole master control system.

requirements for a specific HVDC transmission. Today it is possible to obtain a great flexibility in the design and meet a great variety of requirements, still using almost the same hardware, since modern pole-control systems are realized with micro-processors and the actual design and performance are determined by the programs, or software, of the micro-processors.

The telecommunication system between the two stations forms an important part of the master control. It is essential to have a fast and safe telecommunication system in order to be able to utilize the fast control features of the convertors in an optimal way as will be described later.

Figure 7-22 shows a typical layout of the master control system in one station and one pole. The master control system is usually built up separatly for each pole in order to minimize the risk that a failure in the system can effect the operation of both poles. Because of that, the master control system, according to figure 7-22, is usually called the pole master control system.

The voltage dependent current order limit, VDCOL, and the current control amplifier for the current control system are shown as two blocks in the upper right part of the figure. These two functions are as previously mentioned almost independent from the specific requirement of the plant. The other blocks are usually specially designed for each application. The functional blocks are often the same in both stations, but they are usually mainly activated in one of the stations, the master station or leading station, which is in control of the current order. The master station can either be the rectifier or the inverter station.

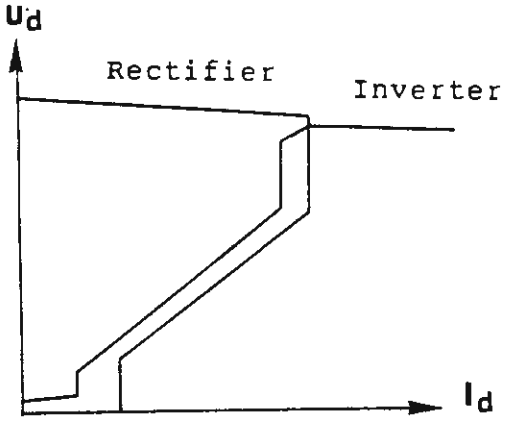

Figure 7-20 Complete U_d/I_d characteristics.

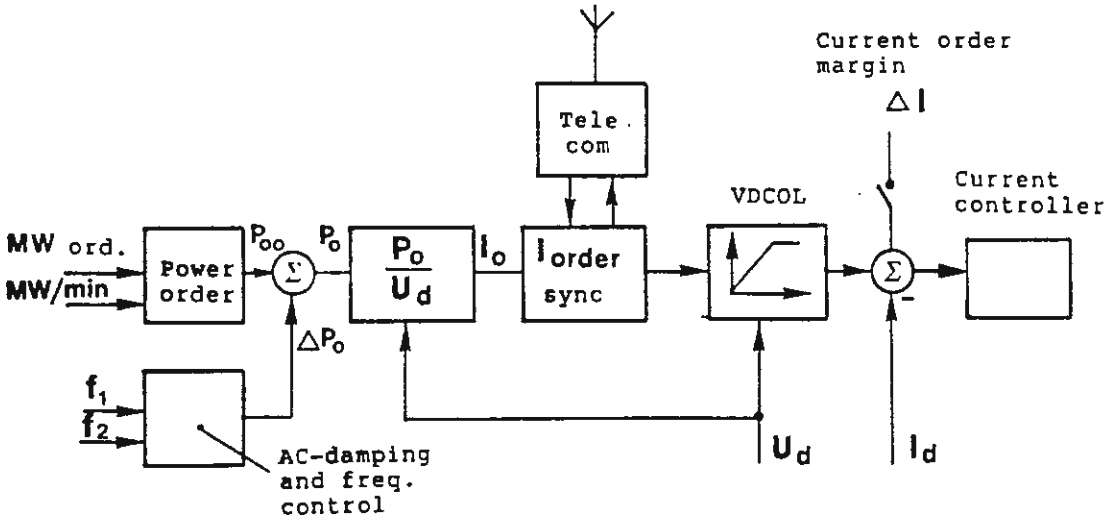

Figure 7-22 Pole master control system.

Current order setting and synchronization Telecommunication

In the previous discussions on the cooperation between the rectifier and inverter stations and the presentation of the steady state characteristics it was presumed, that, both, the rectifier and the inverter stations were supplied with the same current order. A steady state operating point was derived by substracting a current order margin in the inverter station, which results in an intersection point between the steady state characteristics of the rectifier and the inverter station. See figure 7-20 and 7-22. The speed of the current order setting will now determine the speed of the power control system for the transmission. It also has to be taken into account then, that it is essential, that the effective current order including current order margin always have to be larger in the rectifier than in the inverter to secure stable operation. This will set certain requirements on the current order setting and synchronization with regard to the speed and safety. As illustrated in figure 7-22 the current order setting and synchronization is achieved via a telecommunication system.

The requirement on the bandwith of the telecommunication channel depends on the requirement on the speed of the master control system and the resolution in the power order setting. Usually telecommunication channels having a bandwidth of 1200-2400 baud (binary digits per second) are used.

The telecommunication has to be two-way, as indicated in figure 7-22, in order to secure that the synchronization between the two stations will not be lost. The current order setting can be arranged so that a requested order change, which should result in a decrease of the current order at the rectifier station, will not be executed before

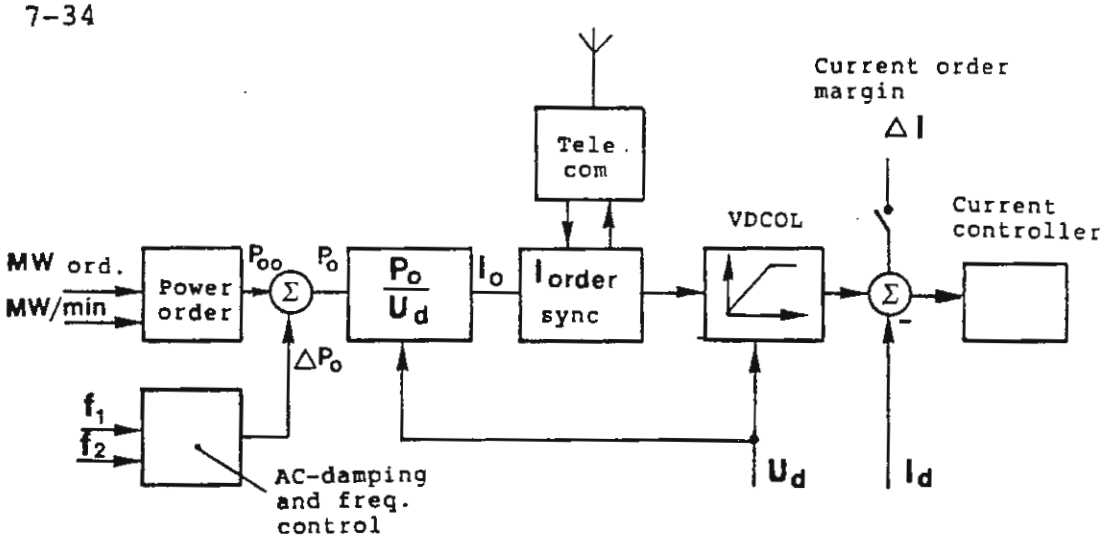

Figure 7-22 Pole master control system.

a telecoms has been received from the inverter station confirming that the corresponding change has first been executed in that station. An increase of the current order is in a similar way first executed at the rectifier station. A temporary shut-down of the telecommunication link, resulting in no appropriate telecoms being received from the other station, will result in, the current orders in both stations being temporarily frozen to the last current order value valid before the shut-down of the telecoms link. To avoid erroneous signals from being received due to disturbances and interferences on the telecommunication link special fail-safe coding techniques are used.

The requirements on the telecommunication links are especially high, when it is required to have a fast control of the transmitted power. It should be noted that, both, the time for sending each telecom as well as the total transmission delay of the link have to be considered and that these times will effect the dynamics of the control system.

Current order calculation and power order setting

The current order I_0 is derived from the ordered active power and the measured direct voltage. Figure 7-22 shows one possible principle for the current order calculation. The desired dynamics could be implemented in the block P_0/U_d.

Additional current order limits can also be implemented in this block to take into account that the transmission capacity is often higher at lower environmental temperatures giving higher cooling capacity, and that the convertors have a short time overload capacity. The thermal time-constants in the valves and transformers can then be simulated or the specified short time overload capacity can

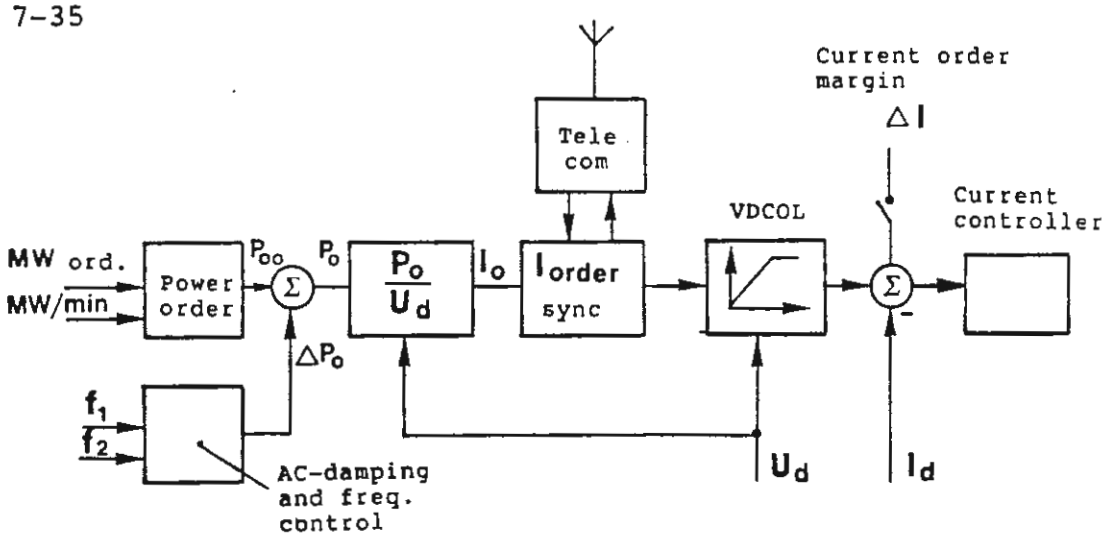

Figure 7-22 Pole master control system.

be used.

The power order setting can in the most simple way be performed manually, e.g., by setting the new power order and the desired rate of change on thumb-wheels. The orders can also be received from some dispatch center through telecommunication links.

Damping control and frequency control

The power order can also partly or completly be generated from some variables measured in the ac-network, e.g., the ac-frequency. Figure 7-22 shows an example, in which a contribution to the power order is generated from the measured frequencies f_1 and f_2. Completly different dynamic characteristics can be achieved for the system depending on the dynamic of this control block.

It is thus possible to control the frequency of the ac-network, provided the amplification in the controller is sufficiently high with a high integral part. This is the case for the HVDC transmission link between the mainland of Sweden and the island Gotland, which is supplied by the power via a bipolar HVDC transmission system of 260 MW. The transmitted power to Gotland, controlled to the frequency on the island, is keep constant at 50 Hz.

In other cases it might be more appropriate to mainly control the HVDC transmission at constant power but letting the measured frequency only influence the power transmitted in case of large frequency deviations. This type of control is often called power/frequency control. It might also be advantageous to use the fast dynamic properties of the HVDC link for the damping of oscillations in the ac-network at disturbances. Transient changes of the measured frequencies will then affect the transmitted power. This is called

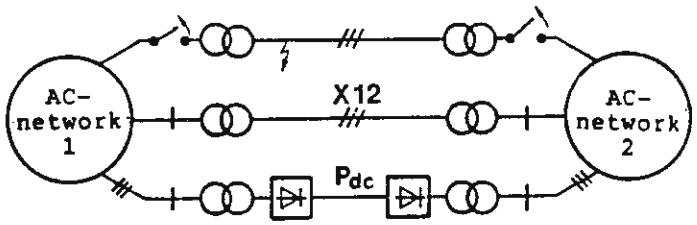

Figure 7-23 Stabilization of ac-lines with a parallel running dc-line.

damping control.

Possibilities to improve the stability of the ac-networks with HVDC transmission systems

Due to a great flexibility and speed of the control in HVDC transmission systems they can be used to improve the stability of the connected ac-networks.

Figure 7-23 illustrates a simple case with two ac-lines connecting two ac-networks 1 and 2. It is assumed, that a temporary disconnection of one of the ac-lines could result in a situation where the synchronization between the two ac-systems will be lost due to a too high transmitted power and phase angle difference on the remaining ac-line. The transmitted power on the ac-line is determined by the following relationship:

$$P = \frac{U_1 \cdot U_2 \cdot \sin \phi_{12}}{X_{12}}$$

The phase-angle difference between the ac-systems 1 and 2 is here denoted by ϕ_{12} and the total line reactance X_{12}.

The transient stability of the system can be increased by the parallel running dc-line since the power on this line can be increased very quickly. It is here assumed that the dc-line has sufficient short-time overload capability, such that the dc-line can take over the major part of the power from the disconnected ac-line. The remaining ac-line can also be more optimally used, when a dc-line is running in parallel, since it is possible to operate an ac-line closer to a phase-angle of 90°, resulting in maximum transfer transmitted power, provided that the power can always be increased on the dc-link if needed.

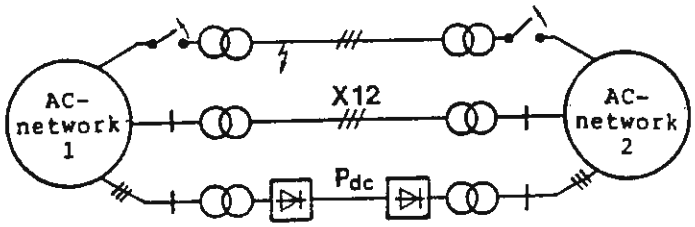

Figure 7-23 Stabilization of ac-lines with a parallel running dc-line.

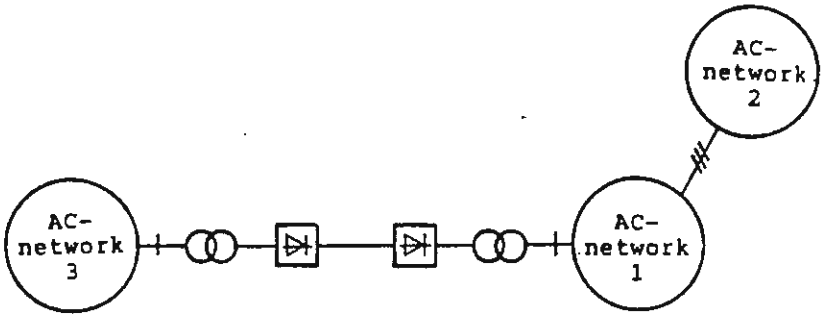

Figure 7-24 Stabilization of a weak ac-line between network 1 and 2 by a dc-line connected to network 3.

It would also be possible to transmit power between the two ac-systems on the dc-link, when both ac-lines are disconnected, since it is then no longer necessary to operate the two ac systems in synchronism and since the power on the dc-link can be accurately controlled without risk for overload.

The limit for dynamic stability for the system according to figure 7-23 can be improved by the dc-link by arranging the control of the dc-link to damp oscillations between the two ac-networks.

In most cases the dc-links are not connected in parallel with any ac-links, since the main reason for building the dc-line was the fact, that the two ac-networks connected via the dc-link are not synchronized. The dc-link can also for this case be of definite value to improve the stability of one of the connected ac-networks, primarily for the dynamic stability.

Figure 7-24 illustrates a case, where the networks 1 and 2 are connected with an ac-line and the networks 1 and 3 via an HVDC transmission line. It is then possible to damp oscillations between the networks 1 and 2 with the dc-link if the transmitted power on the dc-link to network 1 is partly based on the measured frequency deviation between network 1 and network 2.

It is fairly easy to understand that it is possible to improve, both, the transient and dynamic stabilities by the control of active power as the stability is related to mechanical oscillations between rotating machines. However, as the ac-voltages will influence the loads and by that the consumption of active power and also the transmitted power between machines it will also be possible to improve the dynamic stability by control of the ac-voltage.

Control of the ac-voltage is incorporated in some inverter called γ-control. The ac-voltage can here, to some degree, be controlled by control of the reference of the commutation margin γ, which influences the reactive power consumption in the inverter.

OVERCURRENTS AND OVERVOLTAGES. DISTURBANCES.

8.1 General

We have, in the previous chapter, treated stationary (steady state) operation and transients at the blocking (stopping) of the HVDC-transmission. However, the rating and design of the convertor equipment such as thyristor valves, transformers, dc-reactors and arrestors are to a great extent determined by the stresses at disturbances and various faults. Because of that this has to be studied in conjunction with the specification of the equipment. We will below treat some of the more typical disturbances and fault cases resulting in high overcurrents and overvoltages below. For more accurate determination of the stresses it is often necessary to perform studies on either real time HVDC simulators or with special digital computer programs permitting detailed simulation of the convertor stations. It is thereby often necessary to correctly represent the convertor firing control system as the timing of the firing pulses to the valves can be critical for the stresses.

The fault and disturbance cases resulting in high overcurrents will first be treated followed by the cases causing high overvoltages and high stresses on the arrestors.
There is a great difference between these two types of stresses with regard to protection. Beside suitable design of the main circuit and selection for inductance of the convertor transformer and dc-reactor, protection against current stresses which are too high are mainly offered indirectly by the electronic protection, controlling the timing or blocking of the firing pulses to the valves. Because of the high voltages it is not possible to directly protect equipment against too high overcurrents with fuses

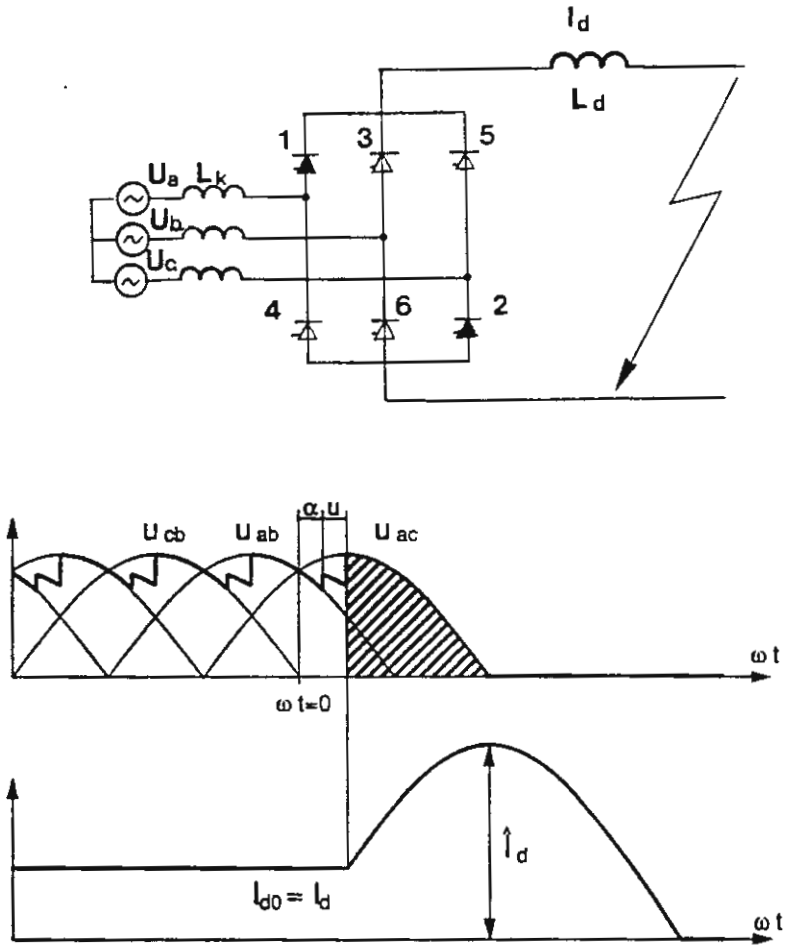

Figure 8-1 Short circuit on the line side of the dc-reactor. Immediate blocking of the firing pulses.

which are too high.

Protection against overvoltages which are too high are, on the other hand more direct, as it is provided by the arresters, which are often connected directly between the terminals, where the overvoltages have to be limited.

8.2 Overcurrents

We will, in this chapter, only treat three types of disturbances or fault cases giving overcurrents i.e.

- short-circuit between a dc-line pole and ground
- short-circuit across a thyristor valve
- commutation failure

Short-circuit between a dc-line pole and ground

The short-circuit between a dc-line pole and ground will be treated using the simplified circuit as shown in figure 8-1.

We make the simplified assumption that the convertor consists of only one six-pulse bridge, which is directly grounded at one end and connected in series with a dc-reactor at the other end. The inductance of the dc-reactor is L_d. We assume that the current in the dc-circuit before the ground fault occurs is equal to the rated dc-current I_{dN}, that the no-load direct voltage has its rated value U_{dioN}, and that $\alpha + u = 30°$.

We assume that the ground fault occurs at $\omega t = 30°$ or $\pi/6$ rad ($\omega t = 0$ is defined as shown in figure 8-1). This means

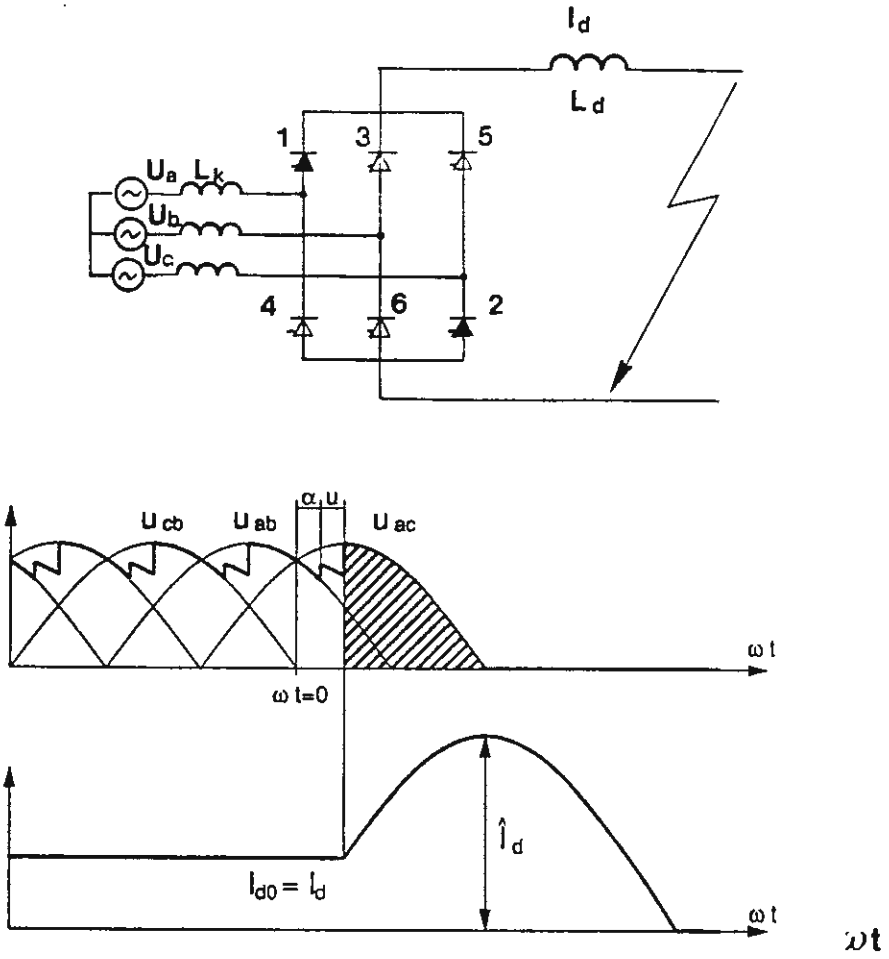

Figure 8-1 Short circuit on the line side of the dc-reactor. Immediate blocking of the firing pulses.

that the ground fault occurs at the instant when the commutation from valve 6 to valve 2 has been finished. We will also assume that no new valve will fire. This could either be obtained by the blocking of the firing pulses by the protection system or delaying the firing pulses from the current control systems, which then has to be sufficiently fast to delay the firing of the succeeding valves. The increase of the current in the dc-circuit will be determined by the dashed voltage-time area and the total inductance in the circuit, which is $L_d + 2L_k$. The peak value of the current will occur at
$\omega t = \pi/6 + \pi/2$.

We assume that the ac-source voltage is stiff and sinusoidal with a peak value of:

$$\frac{\pi}{3} U_{dioN}$$

The instantaneous value of the ac-source voltage is

$$u_{ac} = \frac{\pi}{3} \cdot U_{dioN} \cdot \cos\left(\omega t - \frac{\pi}{6}\right) \qquad (8\text{-}1a)$$

We will also get

$$\frac{di_d}{dt} = \frac{u_{ac}}{L_d + 2L_k} \qquad (8\text{-}1b)$$

This results

$$i_d(t) = I_{dN} + \frac{\pi \cdot U_{dioN}}{3(L_d+2L_k)} \int_{\frac{\pi}{6\cdot\omega}}^{t} \cos\left(\omega t - \frac{\pi}{6}\right) \cdot dt \qquad (8\text{-}1c)$$

The magnitude of the current peak at the time
$\omega t = \frac{\pi}{6} + \frac{\pi}{2}$

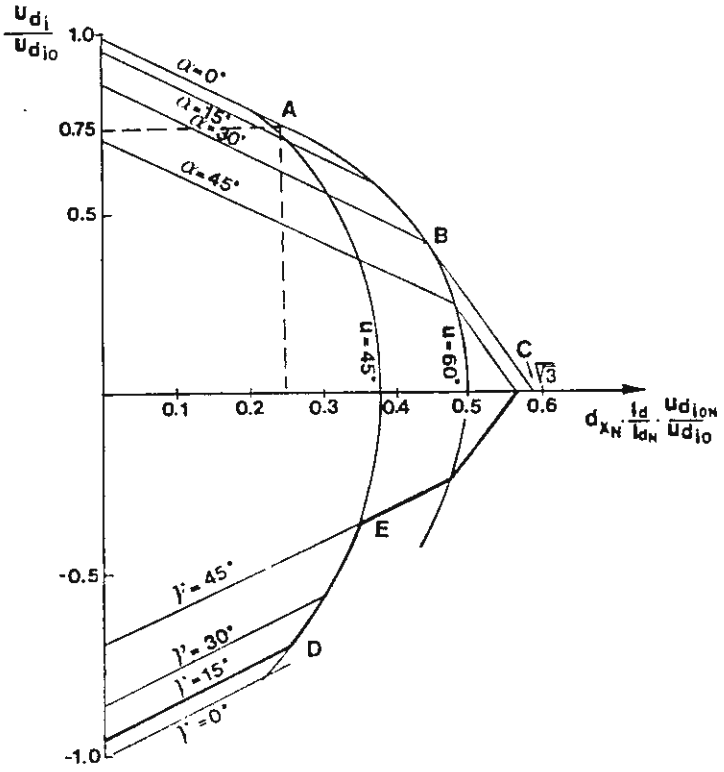

Figure 4-13 Current-voltage characteristics of a 6-pulse converter.

is obtained from equation (8 - 1c) to be:

$$\hat{I}_d = I_{dN} + \frac{\pi \cdot U_{dioN}}{3\ \omega(L_d + 2L_k)} \qquad (8\text{-}2)$$

Insertion of d_{xN} according to equation (4-32) gives:

$$\frac{\hat{I}_d}{I_{dN}} = 1 + \frac{L_k}{(L_d + 2L_k)\ d_{xN}} \qquad (8\text{-}3)$$

Example:
Typical values are $d_{xN} = 0.06$ and $L_d = 8\ L_k$.
Insertion in equation 8-3 gives:

$$\frac{\hat{I}_d}{I_{dN}} = 1 + 1.67 = 2.67$$

We will thus find that the peak of the overcurrent is limited to a fairly low value. The assumed fast action from the control, or protection system, is here an essential factor. If we, instead, had assumed that the convertors were non-controlled, we would, instead, have obtained a steady state short-circuit current corresponding to the operating point C in figure 4-13, i.e.,:

$$\frac{\hat{I}_d}{I_{dN}} = \frac{1}{\sqrt{3} \cdot d_{xN}}$$

This gives for $d_{xN} = 0.06$ $\quad I_d/I_{dN} = 9.62$

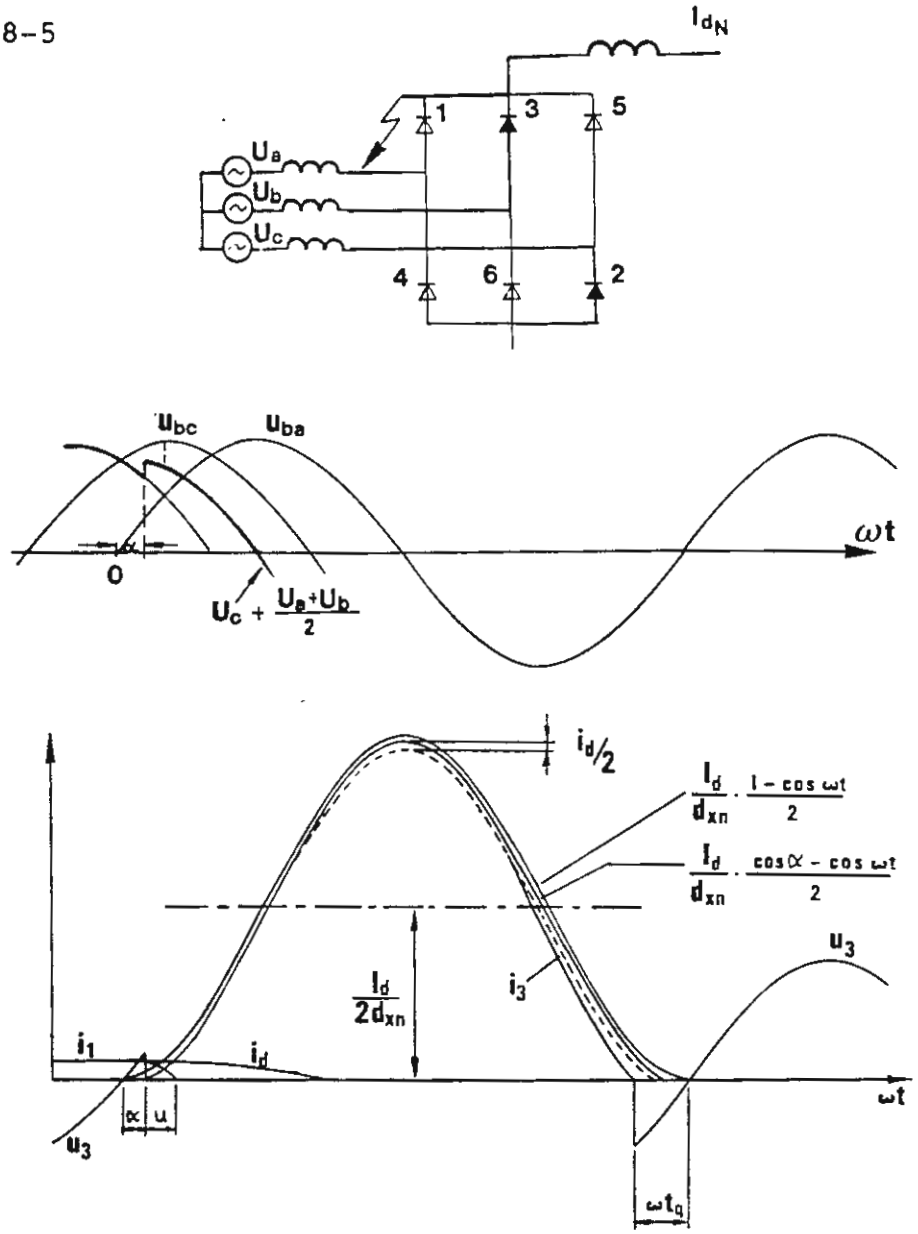

Figure 8-2 Short circuit across a valve. Immediate blocking of the firing pulses.

Short-circuit across a valve

The fault case which is usually decisive for the over-current rating of the valve is a short-circuit of another valve in the same commutating group (valve 1 in figure 8-2).

One possible case that could cause this fault is a voltage collapse of the arrester across valve 1 at the current extinction of this valve at the end of the commutation.

The same current stresses on valve 3 will occur when valve 1 cannot sustain the recovery voltage at the end of the commutation, but starts to conduct current in reverse direction. This happened now and then when mercury arc-valves were used. The phenomenon was called arc-backs. The highest current stresses could then occur in the valve suffering an arc-back and occurs, when both of the other valves in the same commutating group conduct current during parts of the cycle. For a short-circuit across valve 1 the highest short-circuit current in valve 1 would be obtained if valve 5 also starts to conduct 120° later. However, as this case is of minor interest for convertors with thyristor valves, it will not be treated further here.

It is usually assumed that the convertor is operating with maximum current when the fault occurs as this will give the most severe thermal stresses on the valves. We will, in the following simplified calculation, assume that the prefault convertor current is equal to the rated current, I_{dN}. The influence of the ac-network impedance is often neglected when calculating the recovery voltage because the maximum short-circuit current is obtained for operational cases with the ac-network having its maximum short-circuit capacity, i.e., the smallest impedance.

We will get the following expression for the current in

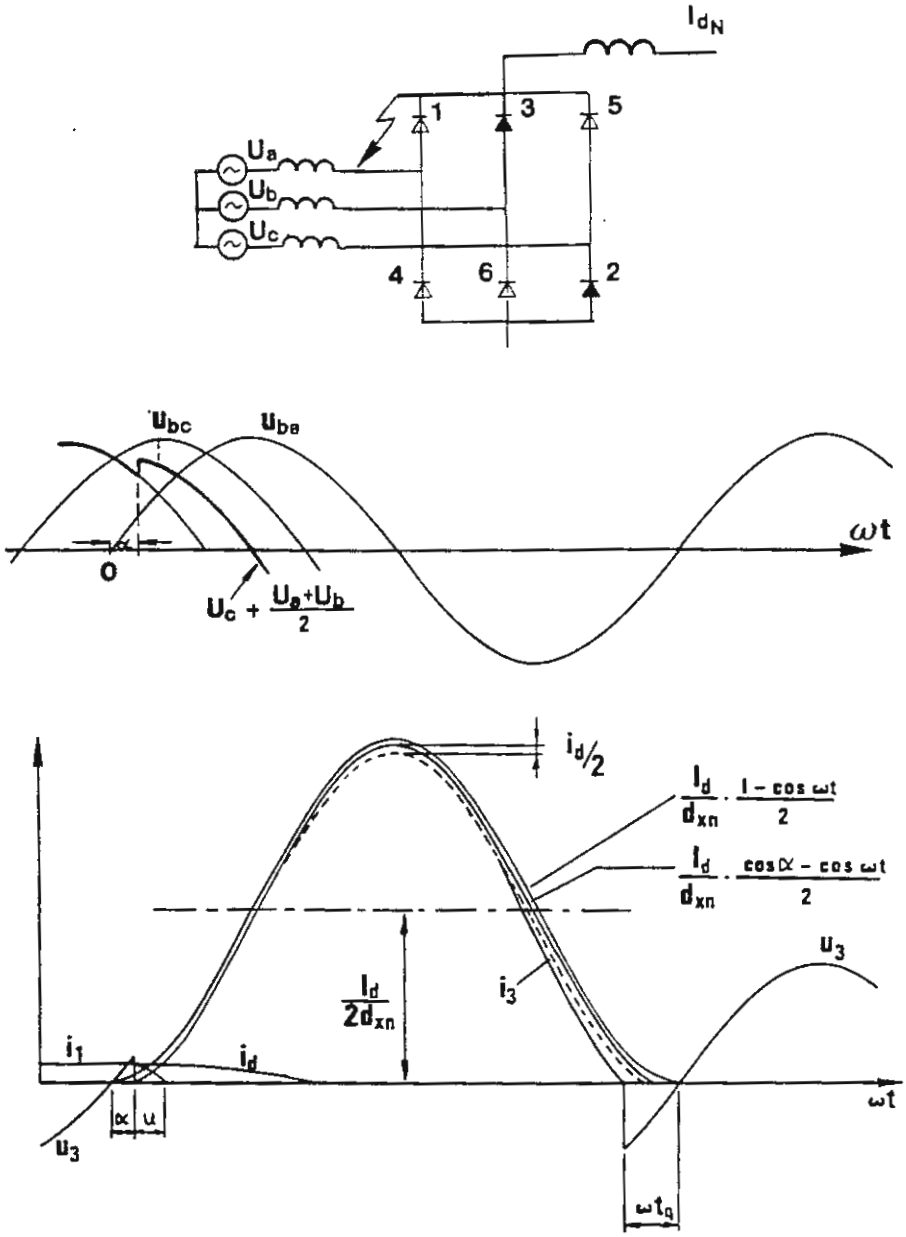

Figure 8-2 Short circuit across a valve. Immediate blocking of the firing pulses.

valve 3, if we assume that the dc-circuit current is constant during the studied time-interval, the amplitude of the ac-source voltage is constant, stiff and equal to:

$\frac{\pi}{3} \cdot U_{dioN}$ and the inductance in the circuit equal to $2L_k$

$$i_3(t) = \frac{\pi \cdot U_{dioN}}{3 \cdot 2\, L_k} \int_{\alpha/\omega}^{t} \sin \omega t \, dt \qquad (8\text{-}4a)$$

Equation (8-4a) can be rewritten as a function of I_{dN} and d_{xN} after insertion of d_{xN}, according to equation (4-32):

$$i_3(t) = \frac{I_{dN}}{2\, d_{xN}} (\cos \alpha - \cos \omega t) \qquad (8\text{-}4b)$$

The current, according to equation (8-4b), is shown in figure 8-2 for $\alpha = 0°$ and $\alpha = 15°$. The peak value will occur at $\omega t = \pi$ and is derived from equation (8-4b) to be:

$$\hat{I}_3 = \frac{(\cos\alpha + 1)\, I_{dN}}{2\, d_{xN}} \qquad (8\text{-}5b)$$

The convertor bridge voltage will decrease to zero, as shown in figure 8-2, for constant current in the dc-circuit. The instantaneous value of the voltage will be determined by:

$$u_c + \frac{u_a + u_b}{2}$$

The decrease of the convertor bridge voltage will usually cause the current in the dc-circuit to be reduced to zero before the current in valve 3 will reach its peak value. Half of this current decrease will then affect the current in valve 3. Because of that the peak value of the current

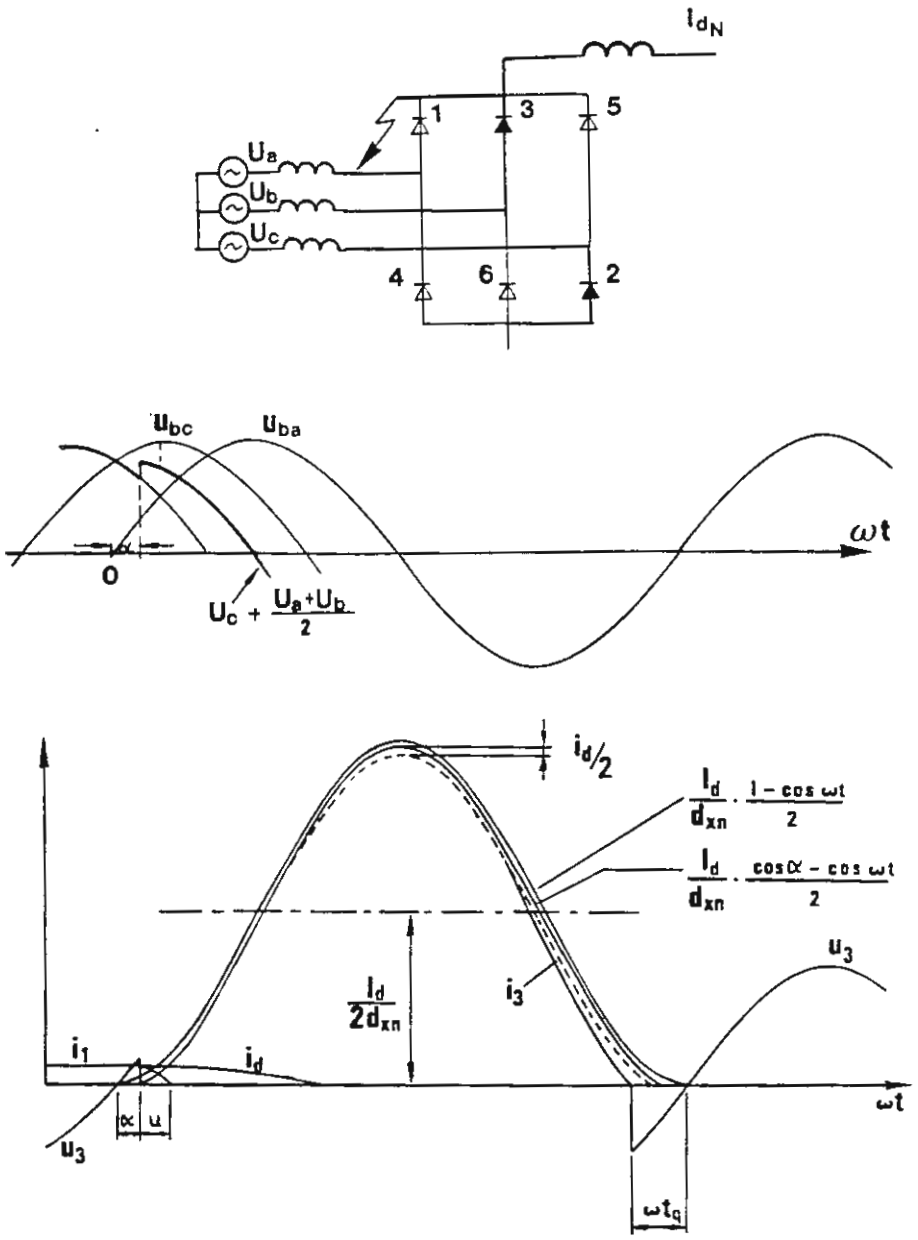

Figure 8-2 Short circuit across a valve. Immediate blocking of the firing pulses.

$\hat{I}_3$ has to be reduced by $I_{dN}/2$. (Dashed curve in figure 8-2). The resistive losses in the circuit will give a certain additional reduction of the maximum short-circuit current according to the solid line curve in figure 8-2.

The reduction in the short-circuit current caused by the decrease of the dc-circuit current and the resistive losses are essential, as they will increase the time interval t_q with reverse blocking voltage as shown in figure 8-2. (The valve has here been assumed to be ideal without recovery charge. See chapter 9.) An increased time t_q will make it easier for the valves to recover and sustain the forward blocking voltage without refiring. If valve 3 refires when the forward blocking voltage is applied, new short-circuit current pulses will stress the valves and it will not be possible to block the valve until the ac-convertor breaker clears the fault. The valves are usually designed and tested to sustain single short-circuit pulses with a requirement to be able to sustain the recovery voltage and also to sustain, without being damaged, the stresses caused by three or four succeeding short-circuit pulses. The number of pulses depends on the speed of the convertor breaker used.

Commutation failures

A failure of the commutation of the current from one valve to the succeeding valve causes a disturbance, which usually only last for a number of cycles. As described in chapter 4 too small a commutation margin makes the inverter vulnerable to commutation failures. The commutation failures are usually initiated by some disturbance in the ac-voltage, e.g., phase-to-ground faults. However, even minor voltage distortions caused by energization of transformers or capacitor banks can sometimes cause or trigger commutation failures.

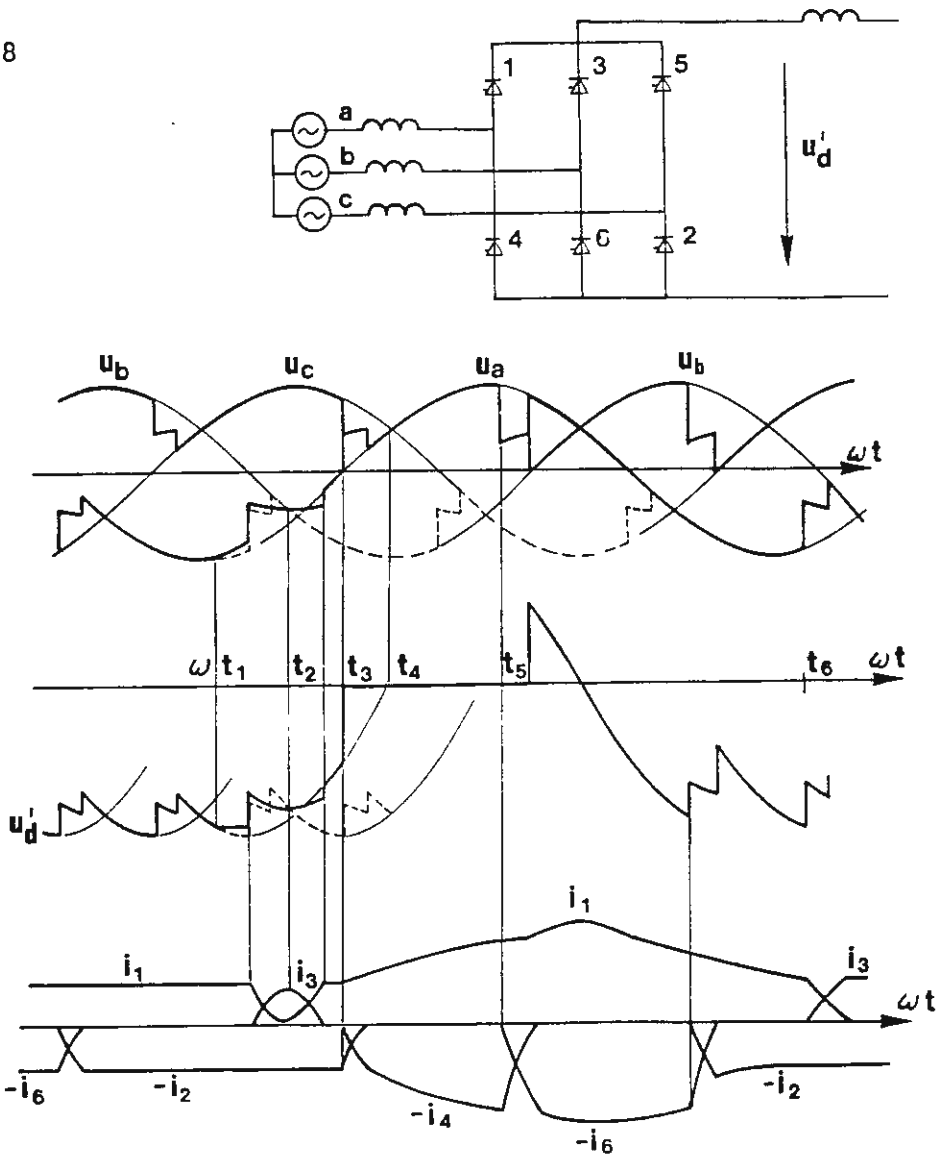

Figure 8-3 Commutation failure.

We will in the following analyze the commutation sequences at a commutation failure under some assumed ideal conditions. We will thus assume that the commutation voltages are stiff, i.e., they will be sinusoidal also during the commutation failure sequence. The commutation voltages will usually be distorted in a real plant, especially if the ac-network impedance is high.

The commutation failure will be illustrated with figure 8-3 showing phase-voltages, the voltage across the convertor bridge U_d', and the valve currents. The current in the valves in the lower commutation group has been shown with a negative sign.

A transient reduction of the phase-voltage u_a is assumed to occur at time t_1. It is assumed that the action of the control system is not sufficiently fast to initiate an earlier firing of valve 3. The commutation of the current from valve 1 to valve 3 will, because of that, fail as the commutation voltage u_{ba} will change signs at time t_2 before the current i_1 has reached zero. It is assumed that the convertor firing control system will advance the firing of the succeeding valves. This will cause substantially larger commutation margins for these valves.

When valve 4 fires at time t_3, the voltage across the convertor bridge will decrease to zero resulting in the convertor current starting to increase. Valve 5 cannot fire after the time t_4, as the commutation voltage u_{ca} is now negative. Valve 1 will because of that continue to conduct the convertor current. On the other hand it has in this case been assumed, that the commutations in the lower commutation group with valves 2,4 and 6 will continue in the correct sequence. However, it should be noted that the possibility for a commutation failure in this commutation group is also fairly high. This was avoided in this ideal

case by the advanced firing of valve 4.

The voltage across the convertor bridge is reversed at time t_5 when valve 4 extinguish. The counter voltage of the inverter will then start to build up again resulting in the convertor current also starting to decrease. The action of the current control system in the rectifier is also assumed to assist in reducing the convertor current. Valve 3 fires at time t_6 and a normal commutation of the current from valve 1 to valve 3 will take place. It should be stressed that the sequence of events at a commutation failure as described above assumes idealized conditions and stiff commutation voltages. Often the ac-voltages will be distorted due to the commutation failure and as a result it will take a few cycles to recover. Despite that, of disturbances discussed here a commutation failure is the operation disturbance that the disturbances discussed, has the smallest influence on the operation of the HVDC transmission.

However also the first fault discussed in this chapter i.e. a short circuit of the dc-line or dc-line fault can often be limited to a disturbance of short duration. The line-protection at the rectifier station will quickly increase the delay angle resulting in the line being de-energized. The line will automatically be energized after a preset time, e.g., 300 ms. The protection is often arranged to effect a number of restart attempts if the first ones are not successful. Restart can also be made at reduced line voltages, which could increase the possibility for the line to easier withstand the voltage, e.g. at unfavourable weather conditions.

The short-circuit across the valve is the most severe fault case of those discussed here. This fault will require permanent blocking of the pole. On the other hand, this fault is extremly rare, but it can be feasible to design

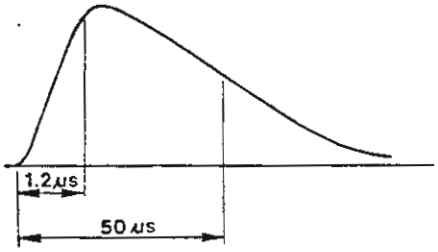

Lightning surge (impulse) 1.2/50 µs

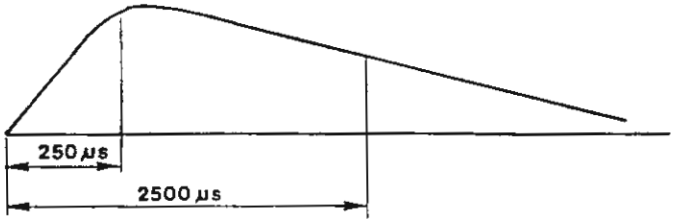

Switching surge (impulse) 250/2500 µs

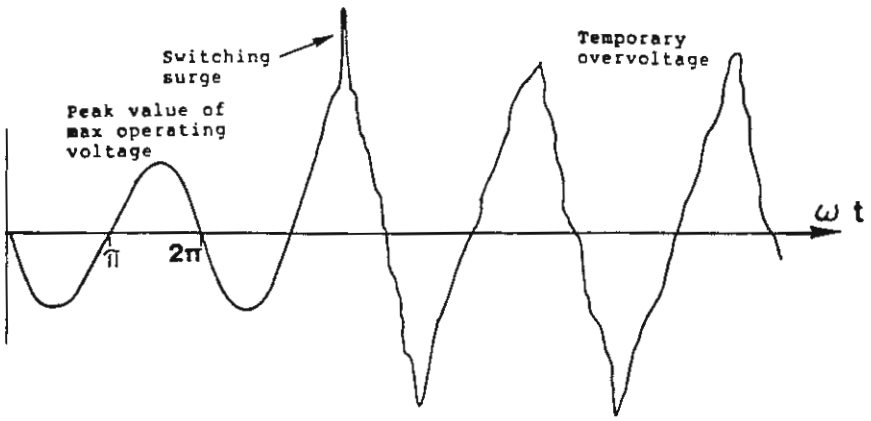

Figure 8-4 Transient and temporary overvoltages. Note! Different time scale.

for then a large number of less severe but more probable faults will automatically be covered.

8.3 Overvoltages and insulation coordination

Classification of overvoltages

The overvoltages for HVDC convertor stations might as for ac-substations, be classified either based on their wave-shape, or on the events by which they are generated. Certain standards and practices have for many years been developed for the classification of overvoltages and for the testing of equipment based on overvoltages that can occur in ac-substations. Because of that, it has been found convenient to apply the same classification of overvoltages for HVDC convertor stations as well.

The overvoltages will be classified as transient overvoltages or temporary overvoltages. A transient overvoltage will consist of one single overvoltage peak while a temporary overvoltage has a repetitive oscillatory character. We will distinguish between the following three types of standardized wave-shapes for transient overvoltages.

- Steep front surge (Steep front impulse). The front time can be very short. The steep-pulse is specified, e.g., with the steepnes of the front 1000kV/μs.

- Lightning surge (Lightning impulse). The front time is 1.2 μs and the half-value time of the tail is 50 μs (see figure 8-4)

- Switching surge (Switching impulse). The front time is

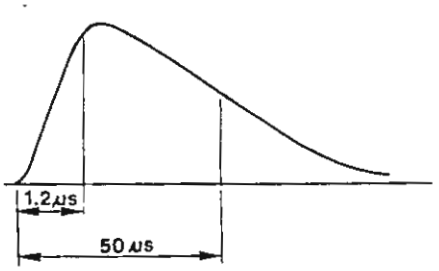

Lightning surge (impulse) 1.2/50 μs

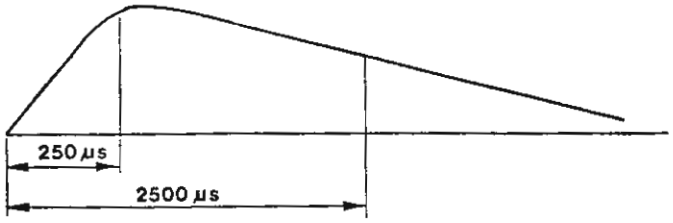

Switching surge (impulse) 250/2500 μs

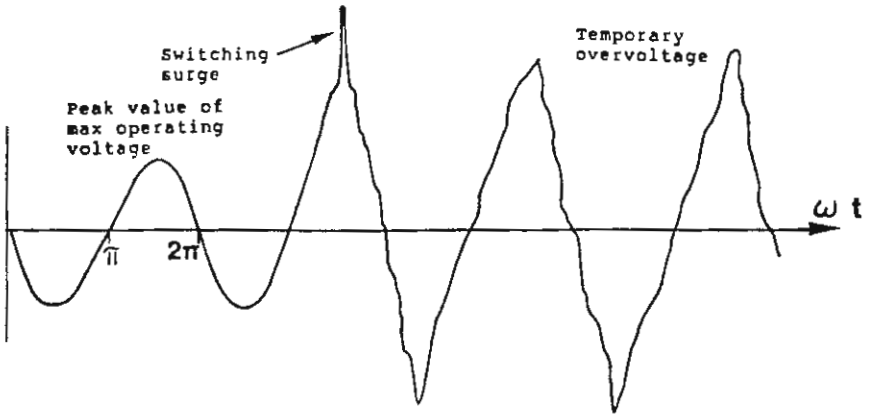

Figure 8-4 Transient and temporary overvoltages. Note! Different time scale.

250 μs and the half-value time of the tail is 2500 μs. (see figure 8-4)

The above transient overvoltages measured or calculated at site are referred to as surges. When the voltage testing is performed with the same wave-shape they are called impulses. The names lightning and switching come from the events, which usually generate overvoltages of a wave-shapes similar to the standardized wave-shapes for ac-substations. However, it should be noted that a number of other faults at HVDC convertor stations can also generate overvoltages having similar wave-shapes as lightning and switching surges.

Overvoltages of a repetitive oscillatory character, which can last for a number of cycles are called temporary overvoltages. Such overvoltages can be generated at energization of transformers, or in conjunction with ground faults, specially if such faults result in saturation of the transformers. Temporary overvoltages are specified by their peak values. As illustrated in figure 8-4 single peak overvoltages in conjunction with the faults and switching operation may be classified as transient overvoltages or switching surge voltages.

Faults and events resulting in high temporary overvoltages will often also result in an increase of the fundamental frequency component of the voltage. This overvoltage is sometimes called dynamic overvoltage and specified with its maximum r.m.s. value.

Overvoltages at a convertor station can also be classified according to the fault events generating the overvoltages. We can then classify the overvoltages in the following groups:

- overvoltages generated from the ac-side

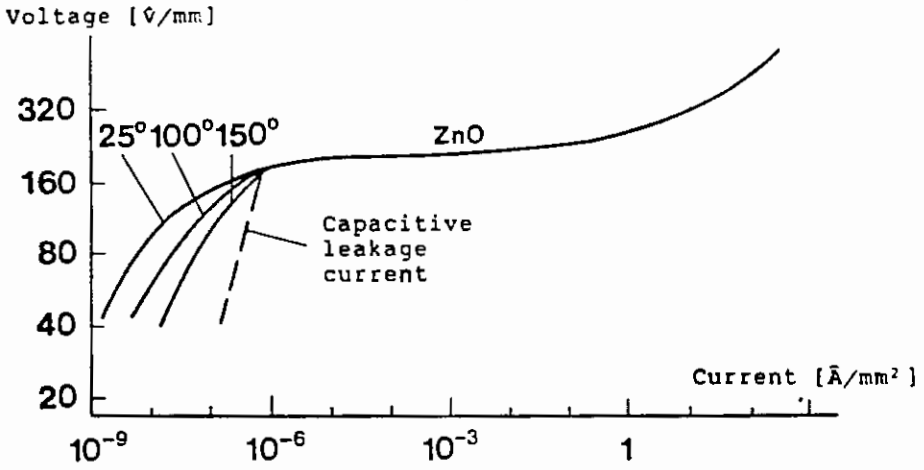

Figure 8-5 Typical current-voltage characteristics for ZnO-blocks.

- overvoltages generated in the convertor station

- overvoltages generated from the dc-line

We will treat a number of typical overvoltage cases for convertor stations below. Overvoltages generated by lightning will not be covered, as they could be treated in a similar way as for conventional ac-substations.

Overvoltage protection - arresters

The magnitudes of the overvoltage will be limited by arresters. The most critical equipment like transformers and the thyristor valves will be directly protected by arresters, which are connected as close to the protected equipment as possible, to avoid or limit the possibility of steep front surges generating overvoltages across the equipment, which are substantially higher than across the arresters due to distance effects

The arresters are nowadays usually built up of zink-oxide blocks without gaps. The zink-oxide blocks have a very non-linear current-voltage characteristic (as shown in figure 8-5).

The voltage characteristics of the blocks and of the complete arresters are partly specified with their reference voltages. These are the amplitudes of the voltages, which when applied across the blocks or the arrester respectively, will generate current pulses of a specified amplitude, the reference current. The reference current is chosen with a certain margin above the capacitive current and is usually specified by the manufacturer.

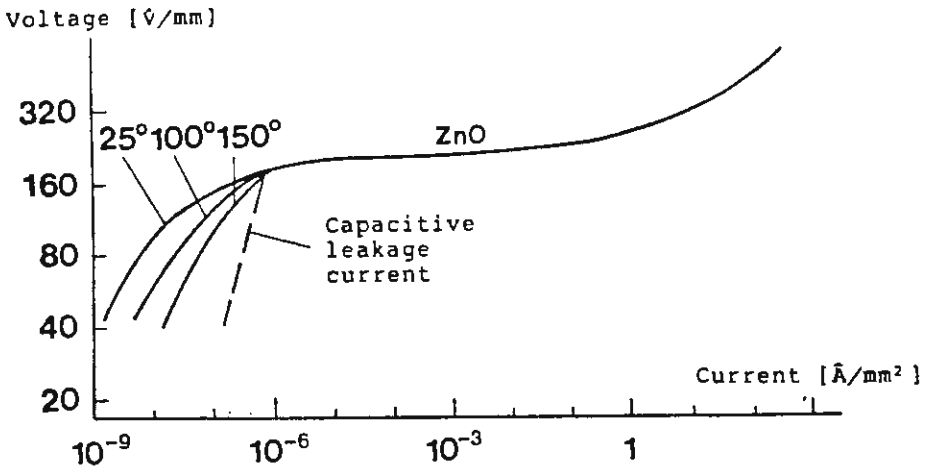

Figure 8-5 Typical current-voltage characteristics for ZnO-blocks.

The peak value of the maximum operating voltage for the arrester is lower than the reference voltage, e.g. 80% of the reference voltage. A higher voltage could cause continuous currents, which are too high through the blocks resulting in thermal instability of the arrester. High anticipated overvoltages across the arrester, i.e., the overvoltages that would have occurred across the arrester terminals, if the arrester was not installed, could result in high overcurrents through the arrester. The arrester is then operating at its flat current-voltage characteristic where the voltage level is rather independent upon the magnitude of the currents.

The peak values of the currents in the arrester close to the values obtained at the decisive fault cases are called the coordinating currents. Usually some standardized value like 2 or 10 kA is chosen for the coordinating current. The corresponding voltage across the arrester is called the protective level. It should also be noted that the protective level is dependent upon the wave-shape of the coordinating current and that the protective level usually increases for steep surges. The protective levels are specified for certain standardized surge current wave-shapes, e.g., current surges having a front time of 8μs and a half value time of the tail of 20 μs (corresponds to lightning impulse) and current surges with a longer front time than 30 μs.

Typical values of the protective level of an arrester are 1.8 - 2.5 times the maximum voltage stress (peak value) at normal operation. The lower values applyes to the arresters across the valves.

The minimum test voltage or withstand voltage level for an apparatus is based upon the protective level plus a certain insulation margin. The insulation margin is usually at

least 25% for lightning impulses and 20% for switching impulses. Certain standard values are selected for the voltage withstand level except for the thyristor valves. As the cost and the losses for the thyristor valves are almost proportional to the specified test-voltage of the valve and the voltage withstand of the valves is better monitored, it is often accepted to choose a lower insulation level for the valves than for other equipment, e.g. 20% and 15% respectively. The test voltage levels for the valves are usually not limited to standard levels.

The protective levels of the arrester are determined by:

- Maximum overvoltage peaks across the arrester at normal operation.

- Maximum dissipated energy in the arrester and the subsequent voltage stresses at certain fault cases.

- Maximum current stresses at the overvoltage events.

It should be noted that the maximum temporary overvoltages will usually not be limited by arresters. Temporary overvoltages can, despite that, be an essential factor in the specification of the arrester as they might be decisive for the minimum protective level that can be chosen for the arrester. A sufficiences high number of zinkoxide blocks have to be connected in series in the arrester in order to avoid that too high energy dissipation will be dissipated in the arrester at temporary overvoltages. However, in some cases it might be possible and feasible to limit the temporary overvoltage by arresters. This will usually result in arresters consisting of a large number of parallel columns of arrester blocks or in parallel arresters.

The overvoltage peaks generated at the end of each

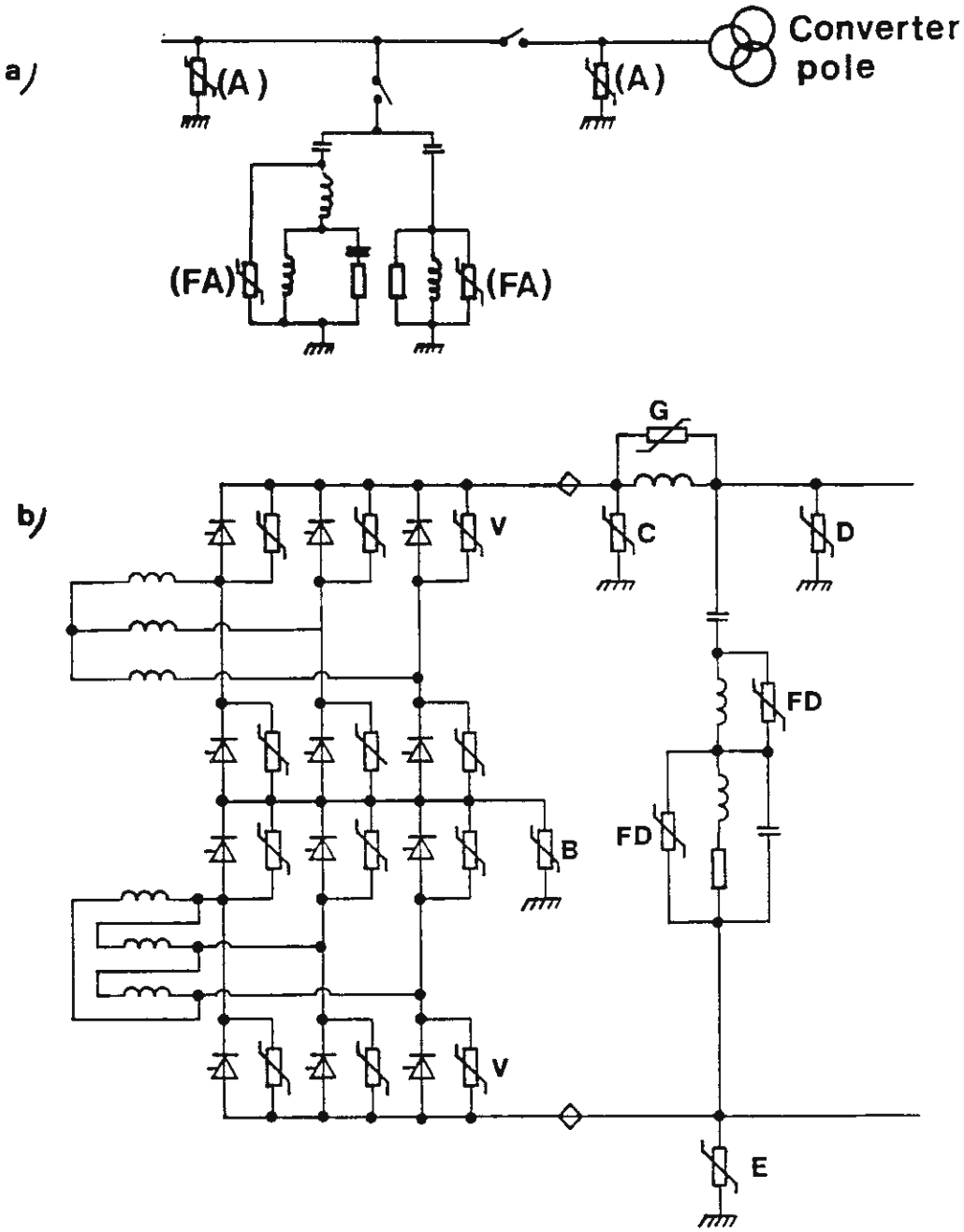

Figure 8-6 Typical arrester arrangement for one pole of an HVDC converter station.
a) AC-side
b) DC-side

commutation are often decisive for the choice of the minimum protective levels for the arresters across the valves.

A typical arrester arrangement for one pole of a HVDC convertor station is shown in figure 8-6. As can be seen from the figure, the arresters on the ac-side are usually connected between phase and ground. The arresters connected across each valve will provide an essential part of the overvoltage protection on the dc-side. They will for instance, together with the arrester B in figure 8-6, provide the overvoltage protection between each phase and ground on the valve side of the convertor transformer.

A fairly large number of different fault cases have to be considered at the specification of all the arresters with regard to maximum currents, energies and protective levels. We will in the following, treat some typical overvoltage events in order to provide some understanding for the overvoltage stresses, which are typical and different for HVDC convertor stations as compared to conventional ac-substations.

Overvoltages on the ac-bus

The ac-bus of an HVDC convertor station can, in the same way as the buses in conventional ac-substations, be stressed with overvoltages due to lightning and due to switching of transformers. However, the large filters and capacitor banks connected to the ac-buses of HVDC convertor stations, will often give lower resonance frequencies on the ac-side than for ac-substations. This can give high temporary overvoltages and more severe stresses on the arresters for an HVDC station than for conventinal ac-substations at energization of transformers and filters

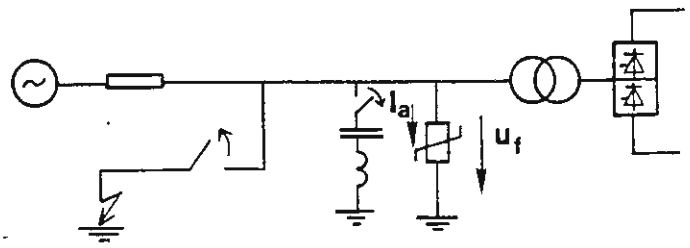

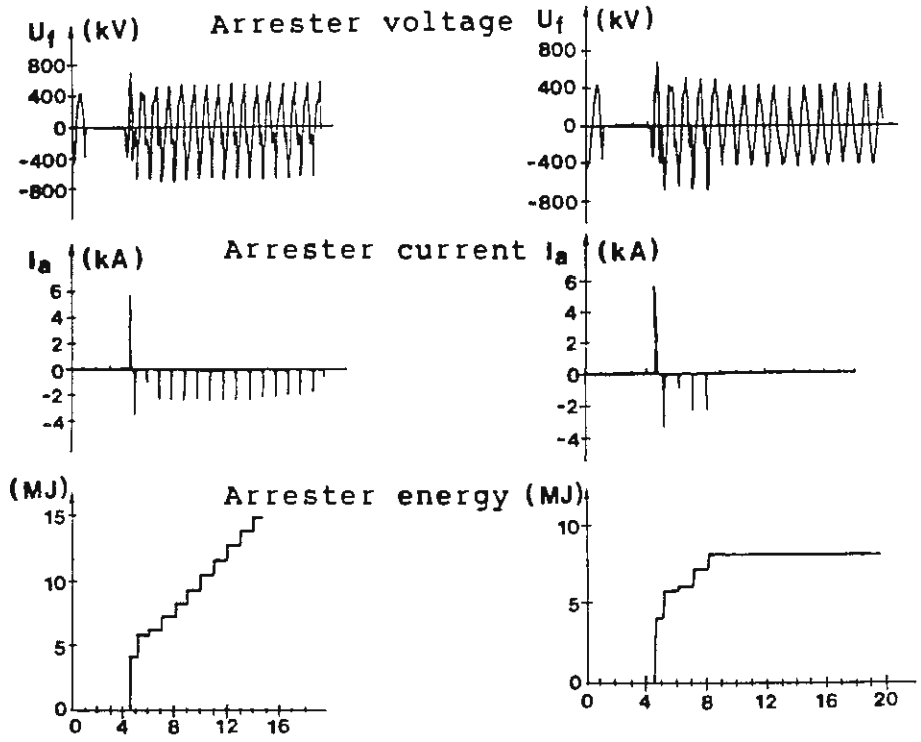

a) No disconnection of the ac-filter.

b) Disconnection of the ac-filter 4 cycles after the clearing of the three-phase to ground fault.

Figure 8-7 Temporary overvoltage and arrester stresses at clearing of a three-phase to ground fault.

or at temporary ground faults. The large filters and capacitor banks could also result in high transient overvoltages at energization. To avoid this and also avoid distortion of the ac-voltage, which could result in commutation failures at the switching, the breakers are usually provided with pre-insertion resistors.

The case that often leads to the most extensive studies and also to increased ratings of the arresters are temporary ground faults on the ac-side.

The ground fault will usually not generate any high overvoltages, when it occurs, but high temporary overvoltages can be generated at the clearing of the ground fault. One reason for this is that the transformers are left with an unfavourable magnetization, when the fault occurred as compared to the phase-position of the recovering voltage. This will cause the transformer to temporarily saturate. The worst case is obtained, if the convertor is blocked as a result of the ground fault and if the filters are still connected, when the ground fault is cleared. This can generate high dynamic overvoltages at weak ac-systems causing the transformers to saturate.

The combination of saturation of the transformers, low damping in the ac-network and resonance in the circuit consisting of the ac, the filters, and the saturation inductance of the transformer for a harmonic, which is generated by the saturation, can give high temporary overvoltages lasting for many seconds. This case is illustrated in figures 8-7a and 8-7b. These figures show the calculated arrester voltage, the arrester current and the arrester energy disipation, when a three-phase ground fault is disconnected and combined with a blocking of the convertor. Figure 8-7a illustrates the case with no disconnection of the filters and figure 8-7b the case where the filters are not disconnected until four cycles after

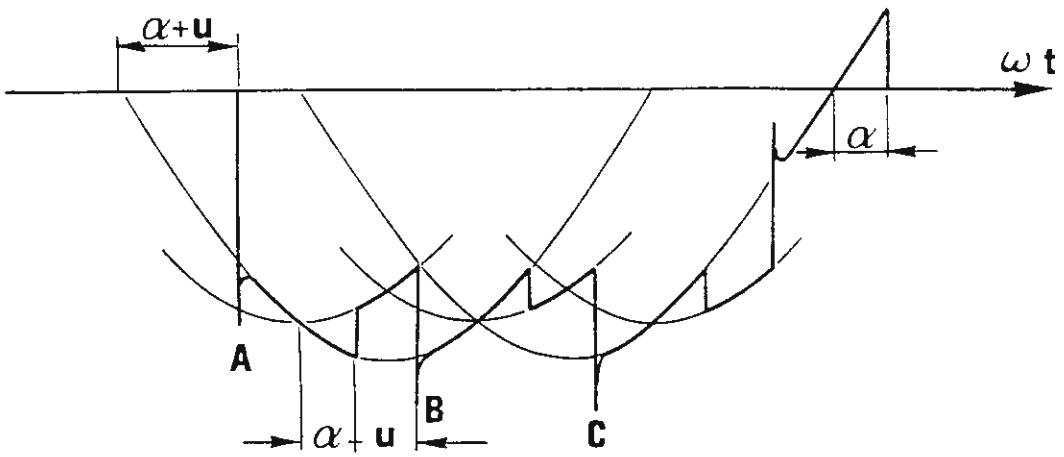

Figure 8-8 Voltage across a thyristor valve in rectifier operation.

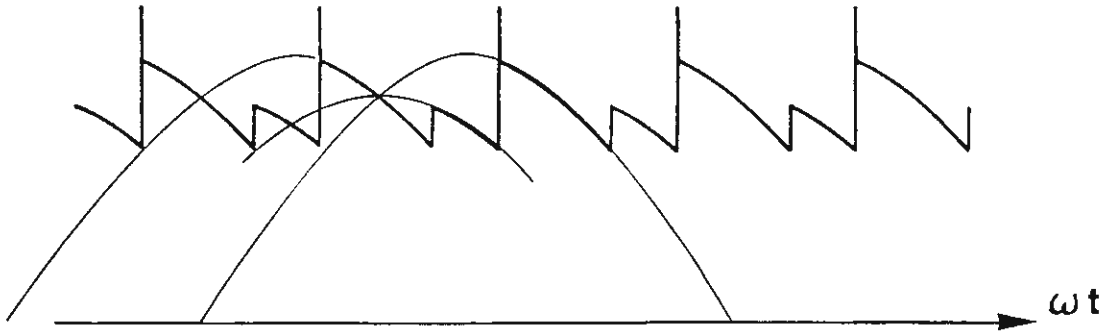

Figure 8-9 Voltage across a 6-pulse converter bridge.

the clearing of the ground fault. It should be noted, that in many cases it is difficult to determine exactly the duration of the temporary overvoltages and, because of that, the energy dissipated in the arresters, as this can depend very much on the damping of the ac-network.

Commutation overshoots across the valve and across the convertor bridge

The lower limit for the reference voltage and protective levels of the arresters across the valves and the convertor bridges are often determined by the maximum voltage stresses at steady state operation. The wave-shapes of the voltages across a valve and a convertor bridge are illustrated in figures 8-8 and 8-9. If we disregard the leakage capacitances in the convertor and assume that the valves are ideal without recovery charge, the transient voltage changes at the turn-off at the end of the on-state interval will be $\hat{U}_K \cdot \sin(\alpha+u)$. The recovery charge in the thyristors, which will be further treated in chapter 9, and the leakage capacitances will however cause transient overshoots, as illustrated in figure 8-8 (time A). These are called commutation overshoots and are in the order of 25 - 30%. Similar overshoots are also obtained at the commutation of the succeeding valves, as can be seen in figure 8-8 (time points B and C). The highest voltage peaks at normal operation are obtained at B and C, while at operation with large firing angles ($\alpha+u \geq 60°$) the highest peak can occur at the time point A.

We will now perform a simplified analysis to determine the commutation overshoots for ideal valves with no recovery charge. It will be discussed in chapter 9 how these calculations have to be modified to also take into account the recovery charge, which will increase the magnitude of the overshoots. The calculations have to be performed with

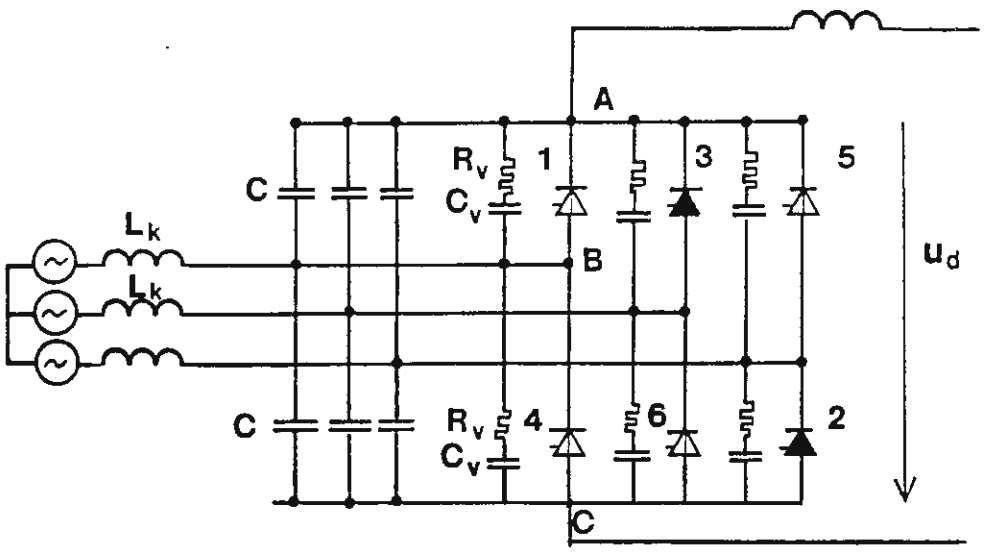

Figure 8-10 Simplified circuit diagram for a 6-pulse converter with leakage inductances and snubber circuits across each valve.

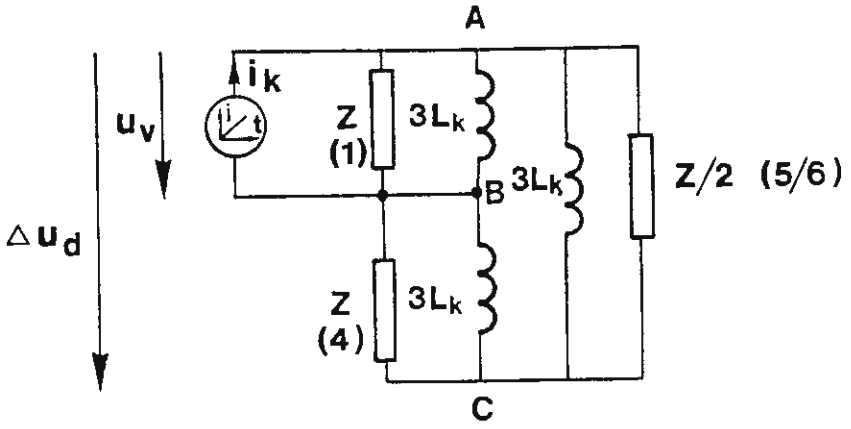

Figure 8-11 Simplified circuit diagram for the calculation of the commutation voltage transients after finished commutation from valve 1 to valve 3. (See Ref. [2] fig 5.13).

fairly extensive digital computer programs with detailed representation of, both, the valves and transformers to be able to more exactly determine the magnitude of the overshoots.

We will base our analysis on the simplified circuit diagram according to figure 8-10. Each thyristor valve is represented by an ideal thyristor, which cannot conduct current in the reverse direction and a parallel connected snubber-circuit with the resistance R_v and the capacitance C_v.

A pure capacitance C is also connected in parallel with each valve. The magnitude of this capacitance is in a real plant mainly determined by the leakage capacitances in the convertor transformer and the bushings. The capacitances will in a real plant be mainly connected to ground. In the simplified circuit according to figure 8-10 they are, on the other hand, connected across the valves and are the same for both the upper and lower part of the bridge.

The circuit diagram can be further simplified by replacing all impedances in parallel with a valve with one common impedance Z. The following expression is obtained for this impedance

$$Z(s) = \frac{s \cdot C_v \cdot R_v + 1}{s^2 \, C \, C_v \, R_v + s\left(C + C_v\right)} \qquad (8\text{-}6)$$

The circuit diagram, according to figure 8-10, can be further simplified, when studying the commutation overshoot after the finished commutation of the current from valve 1 to valve 3. See figure 8-11 and Ref. [2]. Valves 2 and 3 are then conducting and short-circuiting the corresponding parallel connected impedances. The commutation inductances L_k, which are connected in Y in figure 8-10, has been

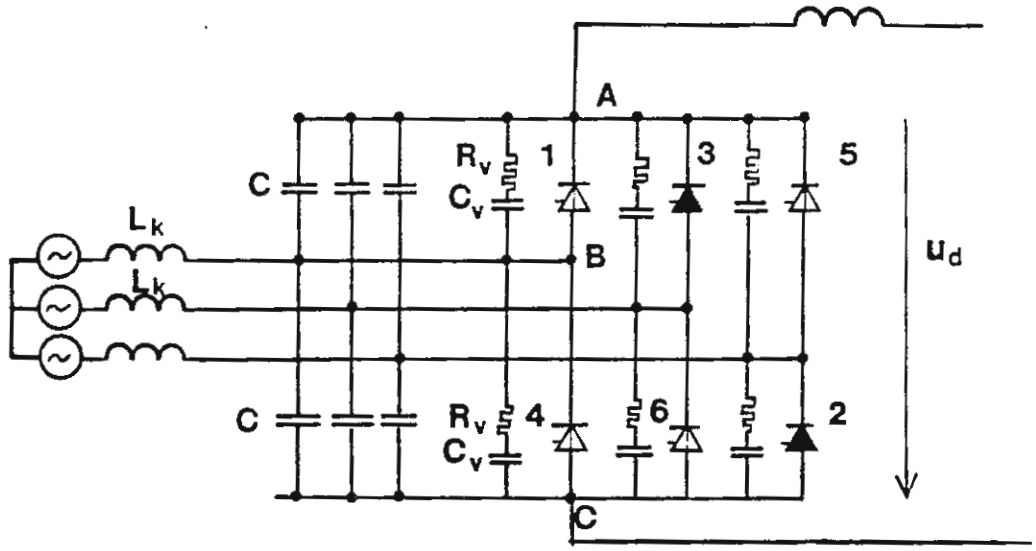

Figure 8-10 Simplified circuit diagram for a 6-pulse converter with leakage inductances and snubber circuits across each valve.

transformed to a Δ connection, and the values thereby increased to $3L_k$. The impedances in parallel with valves 5 and 6 are connected in parallel giving the magnitude Z/2. The extinction of the current in valve 1 can be represented with a superimposed ramp current i_k having a constant slope, since the commutation voltages is assumed to be constant during the time-interval of interest. This results:

$$\frac{di_k}{dt} = \frac{\hat{U}_k \cdot \sin(\alpha+u)}{2L_k} \qquad (8\text{-}7a)$$

or in Laplace-form

$$I_k(s) = \frac{\hat{U}_k \cdot \sin(\alpha+u)}{2\, s^2 \cdot L_k} \qquad (8\text{-}7b)$$

$I_k(s)$ according to equation (8-7b) and the circuit diagram according to figure 8-10, results in the following expression for the voltage across the valve:

$$\frac{U_v(s)}{\hat{U}_k \cdot \sin(\alpha+u)} = \frac{1}{4}\left[\frac{3\, Z(s)}{s(3sL_k + Z(s))} + \frac{Z(s)}{s(5sL_k + Z(s))}\right] \qquad (8\text{-}8)$$

and for the voltage across the convertor bridge.

$$\frac{\Delta U_d}{\frac{1}{2}\hat{U}_k \cdot \sin(\alpha+u)} = \frac{Z(s)}{s(5\, sL_k + Z(s))} \qquad (8\text{-}9)$$

Equations (8-8) and (8-9), as expected, result in voltages across the valve and across the convertor bridge approaching the following values when the transient

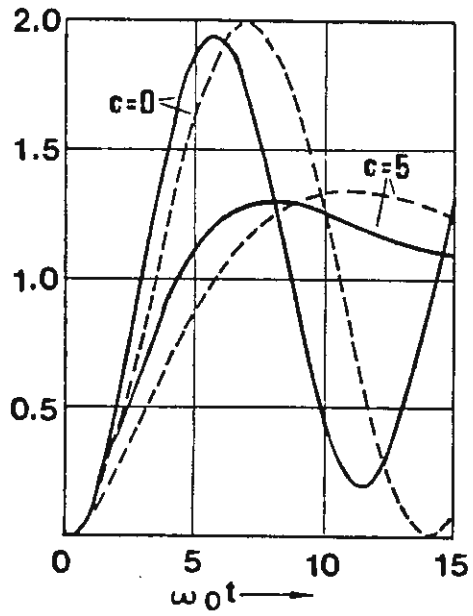

Solid curves = Recovery voltage across the valve after extinction($u_v(t)/\hat{u}_k \cdot \sin(\alpha+u)$)
Dashed curves = Transient voltage across the other valves and across the converter bridge ($\Delta u_d/(0.5 \cdot \hat{u}_k \cdot \sin(\alpha+u))$)

Figure 8-12 Unattenuated and attenuated voltage oscillation at the end of a commutation (Ref. [2], figure 5.14).

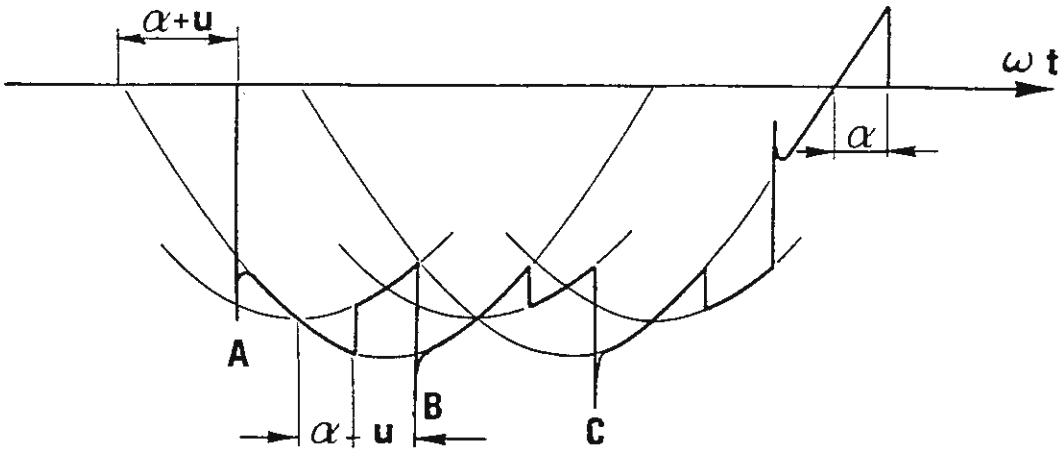

Figure 8-8 Voltage across a thyristor valve in rectifier operation.

overshoots are damped out:

$$U_v \rightarrow \hat{U}_k \sin(\alpha + u)$$

and

$$\Delta U_d \rightarrow 1/2 \cdot \hat{U}_k \cdot \sin(\alpha + u)$$

This case is further treated in Ref. 2, pp. 63-69, where the following parameters are introduced:

$$\omega_o = \frac{1}{\sqrt{L_k \cdot C}}$$

$$c = \frac{C_v}{C}$$

and

$$T = R_v \cdot C$$

The recovery voltage across the valve, $u_v(t)$ and the superimposed commutation voltage across the other valves, and across the convertor bridge $\Delta u_d(t)$, will now get a wave-shape according to figure 8-12. Two cases are illustrated, namely with no snubber circuits (c=0) and with a fairly large snubber circuit (c=5) with $\omega_0 T = 2(1+c)^{3/4}$.

It could be of interest to note that the recovery voltage across the valve $u_v(t)$ will contain two oscillation frequencies, $\omega_0/\sqrt{3}$ and $\omega_0/\sqrt{5}$, for the undamped case while the transient voltage across the other valves and the convertor bridge, $\Delta u_d(t)$, will only oscillate with one single angular frequency $\omega_0/\sqrt{5}$. In this case the voltage transients appearing across the convertor bridge will also appear across valve 5 and 6. (Compare the voltage peaks at B and C in figure 8-8).

As was already pointed out it is not correct to represent the valves existing today with ideal valves, since the

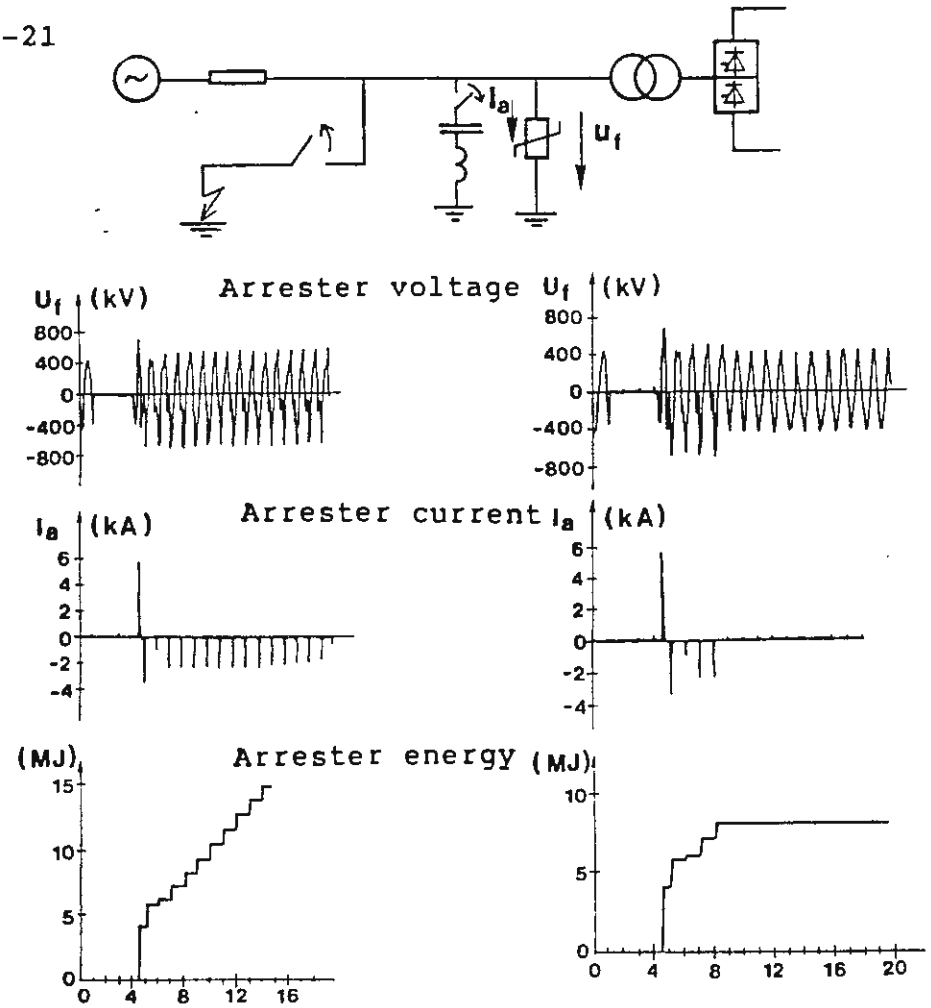

a) No disconnection of the ac-filter.

b) Disconnection of the ac-filter 4 cycles after the clearing of the three-phase to ground fault.

Figure 8-7 Temporary overvoltage and arrester stresses at clearing of a three-phase to ground fault.

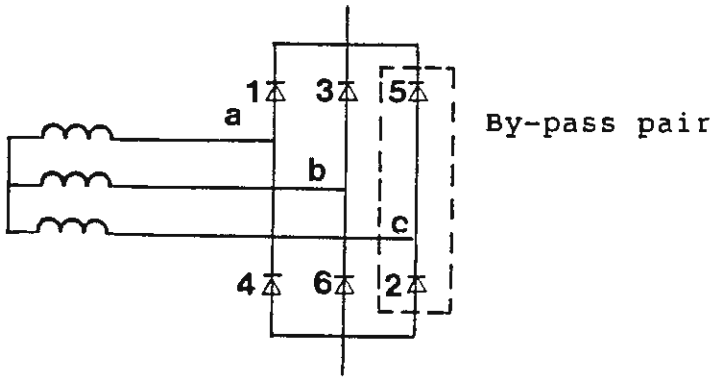

Figure 8-13 Blocking of a converter bridge with deblocking of a by-pass pair.

recovery charge of the thyristors can cause a substantial increase of the commutation overshoots. The recovery charge will, because of that, be decisive for the choice of R_v and C_v in the snubber circuits.

Maximum overvoltage and current stresses on the arresters across a valve

The commutation voltage peaks will usually be decisive for the choice of the lower limit for the reference voltage of the arresters and will in this way be decisive for the choice of the protective level. Temporary operation at large firing angles have especially to be considered then as this can give the highest commutation overshoots.

Fault cases, which can generate high overvoltages and energies in the arresters, are

- Switching surges from the ac-network, e.g., caused by clearing of ground faults and blocking of the firing pulses to the valves, according to figure 8-7.

- A ground fault on an ac-phase on the valve side of the convertor transformer

- Fault cases resulting in current oscillations and current extinction in only one commutation group.

It should be noted that the first case can give also high overvoltages, when a convertor bridge is blocked, provided a so called by-pass pair is deblocked. By-pass pair operation is illustrated in figure 8-13, in which case the ordinary firing pulses are blocked to valves 1, 3, 4 and 6 but firing pulses are generated to valves 2 and 5 forming a by-pass pair, which will short circuit the bridge. An

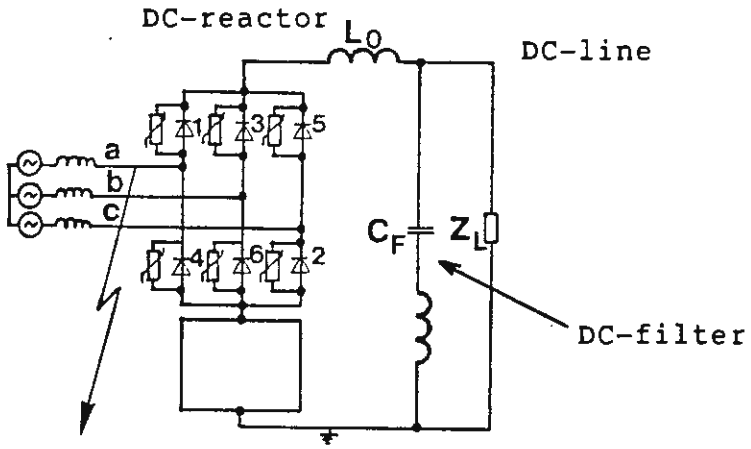

Figure 8-14 Phase to ground fault between the converter transformer and the valve-bridge.

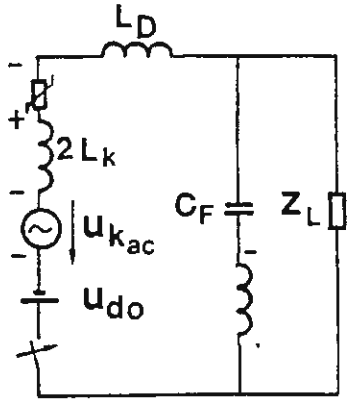

Figure 8-15 Simplified circuit diagram for a phase-to-ground fault on phase (a) and calculation of the stresses on the arrester across valve 5, according to figure 8-14.

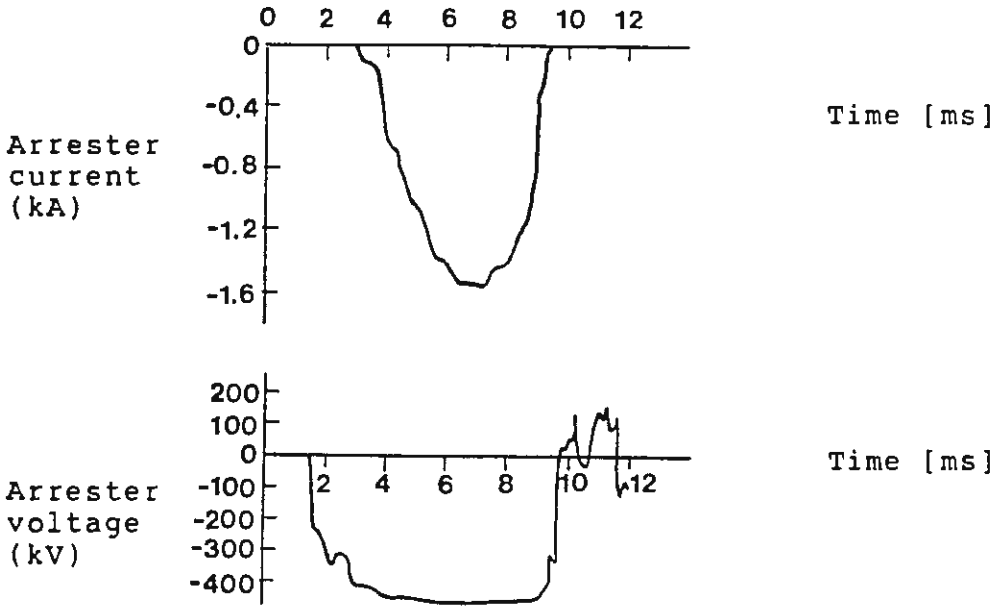

Figure 8-16 Current and voltage stresses for the arrester across valve 5 at the fault case according to figure 8-14.

incoming switching surge in the phase-to-phase voltage u_{ac} can stress valve 1 and/or valve 4 as valves 2 and 5 are conducting or can conduct current in forward direction.

However, as a phase-to-ground fault on the valve side of the transformer will usually turn out to be the decisive case for arresters connected across the valves in the upper commutation group, we will here only treat this case.

We assume, that the ground fault occurs on phase (a), according to figure 8-14. The flashover will usually first generate a steep front current surge of short duration through the arrester, which is stressed by the highest overvoltage. This current peak will only last for a few μs, as the leakage capacitances will be discharged. The discharge current of the dc-line which has to pass through the dc-reactor, will be decisive for the maximum energy stresses on the arresters. The arrester across valve 5 will have the highest voltage and get the highest surge current when the fault occurs with a fault as shown in figure 8-14. It is assumed here that phase (a) has the highest and phase (c) the lowest voltage potential, when the fault occurs. Current will flow mainly through the arrester across valve 5 as long as $u_{ac} > u_{ab}$. We will also assume that all the valves will be blocked immediatly. We will then get the simplified circuit diagram, according to figure 8-15. The battery voltage U_{do} corresponds to the pre-fault dc-line voltage. The dc-line is represented with the wave-impedance.

Figure 8-16 shows the result obtained by a computer simulation of this case. All the circuit elements were then represented. In this case it was assumed that U_{do} = 600 kV. The total dissipated energy in the arrester across valve 5 during the first current surge from the dc-line was 2.9 MJ, which can be compared to 0.03 MJ and 0.41 MJ in the arrester across valves 1 and 3 respectively.

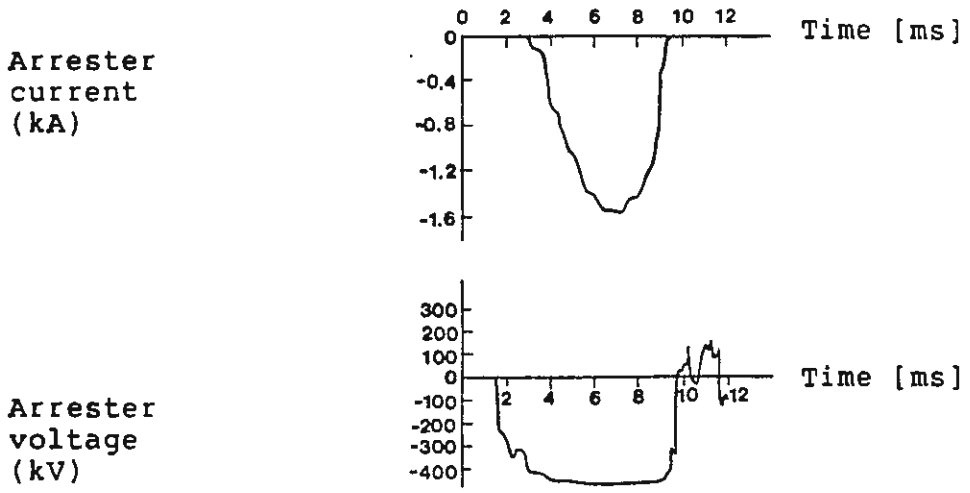

Figure 8-16 Current and voltage stresses for the arrester across valve 5 at the fault case according to figure 8-14.

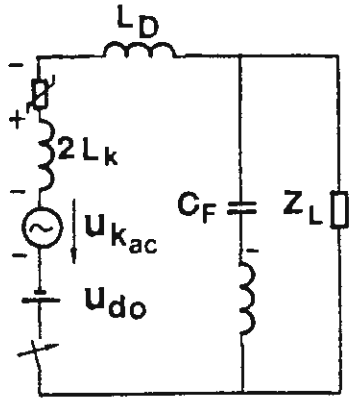

Figure 8-15 Simplified circuit diagram for a phase-to-ground fault on phase a and calculation of the stresses on the arrester across valve 5 according to figure 8-14.

The magnitudes of the succeeding current pulses are considerably lower. We will also find from figure 8-16, that the average voltage across the arrester is 450 kV, which is the protective level of the arrester at current 1 kA. The inductance of the dc-reactor was 0.34 H and the capacitance of the filter 2.1 μF.

It might now be of interest to make a simplified calculation of the energy dissipated in the arrester based on the circuit diagram, according to figure 8-15. The wave-impedance of the line for the pole-mode is 260 Ω and for the ground-mode 507 Ω, which gives 383,5 Ω as an average value. The travelling time of the line is 2.7 ms for the pole-mode and 3.8 ms for the ground mode, which result in an average value for twice the travelling time equal to 6.5 ms. The peak value of the phase-to-phase voltage is 300 kV, which gives an average voltage value of approx. 215 kV for the time from the occurance of the ground fault until the reflected wave arrives after 6.5 ms. This gives us the following average value for the current through the arrester, provided the influence from the dc-filter is neglected, $(600 + 215 - 450)/383.5 = 0.95$ kA

The corresponding energy dissipated in the arrester will be

$$0.95 \cdot 450 \cdot 6.5 \cdot 10^{-3} \text{ MJ} = 2.8 \text{ MJ}$$

We ought to add a contribution of 0.2 MJ from the dc-filter to this value, which gives a total dissipated energy of 3 MJ. This agrees almost too well with the more accurately calculated value of 2.9 MJ. This case illustrates the value of simplified calculation, as it can provide the order of magnitude of currents and energies. It is usually advisable to perform similar calculation to check as to whether the results from the more accurate calculation using sophisticated computer programs are reasonable.

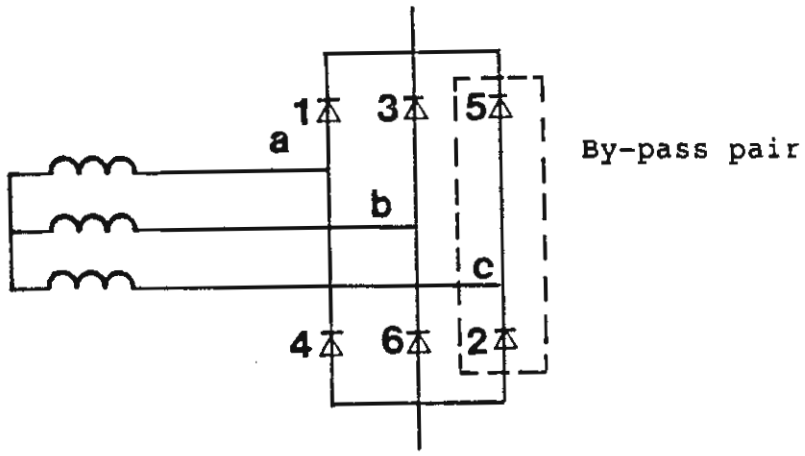

Figure 8-13 Blocking of a converter bridge with deblocking of a by-pass pair.

Other fault cases that can give high energies in the arresters across the valves, are faults resulting in the generation of ac-voltages to the dc-side. One such fault is the blocking of all the firing pulses to the valves in the inverter without the deblocking of a by-pass pair. See figure 8-13. The oscillations of the current in the dc-circuit might then result in the current extinction being obtained in only the valve in one commutation group, without causing current extinction in the other valves connected in series. The current in the dc-circuit will then be forced through the arrester connected across this valve, which could cause very high energy dissipation. It is, because of that, essential that oscillations of fundamental frequencies on the dc-side are well damped. It could also be advantageous to choose, if possible, the protective firing level of the valve lower than the protective level of the arresters connected across the valve. A voltage which is too high across the valve in forward direction will then result in that the valve being turned-on, which prevents overstressing the valve arrester. This is described in chapter 9.

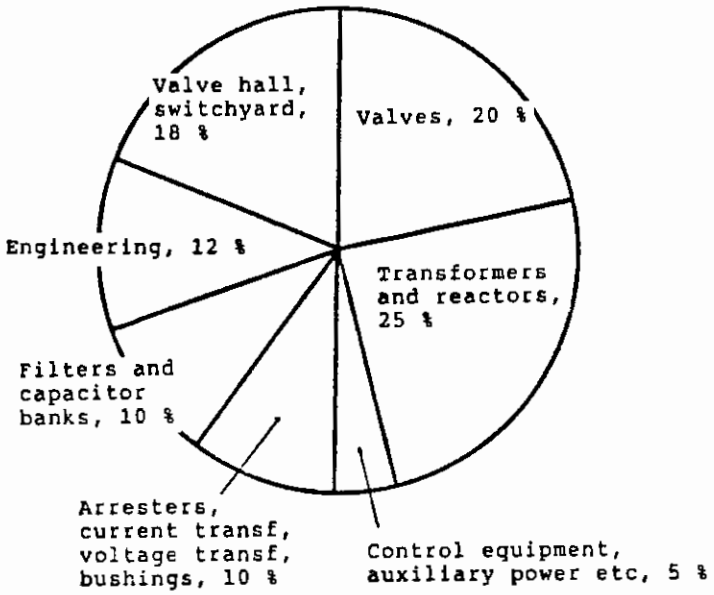

Figure 1-16 Typical distribution of costs of an HVDC converter station.

9 THYRISTOR VALVES

9.1 General

The thyristor valves and the convertor transformer are the key components of a HVDC convertor station. The cost of thyristor valves represented earlier the largest single cost item of an HVDC convertor station. The relative cost of thyristor valves has, due to the fast development of the semiconductor technology, been steadily reduced. One major factor has been the large increase of the power handling capacity of each thyristor resulting in much fewer thyristors per MW. The convertor transformers now usually represent the highest cost item, as illustrated by figure 1-16. The thyristor valves will, despite that, be treated in more detail than the convertor transformers, as their function is so vital for the function of a convertor.

The general requirements of a thyristor valve and its principle design will be treated first. Some of the most important characteristics of the thyristor will then be treated, which will be decisive for the design of the valves including snubber circuits, valve reactors, firing and protection system and the cooling system.

9.2 Fundamental requirements

We will in the following, if nothing else is stated under a valve, understand a single valve, which is connected between an ac-phase of a convertor transformer and one terminal of the convertor bridge.

The general requirement on the valves, at normal operation, was treated in chapter 3, and the requirement with regard

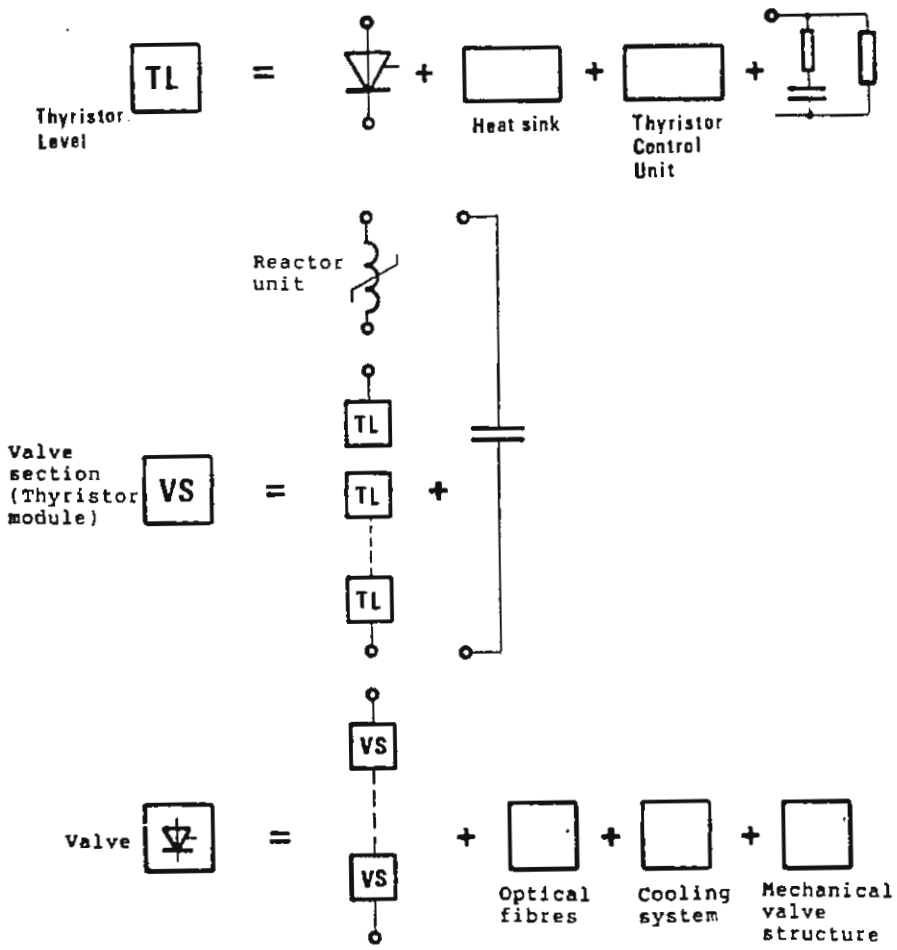

Figure 9-1 The major components and parts of a thyristor valve.

to overcurrent and overvoltage stresses was treated in chapter 8.

9.3 General valve design

The design of the valves supplied by different manufactures can be different especially if different principles for cooling are used. The basic general design can however be described according to figure 9-1, which shows the main components of a valve.

The key components of the valve are of course the thyristors. Each thyristor is mounted between two heat-sinks or coolers, which both have the function to transport the heat away which was generated due to the losses in the thyristors, and to conduct the current.

The thyristors are usually electrically triggered thyristors (ETT), and that is why they have to be provided with thyristor control units. The most important function of the thyristor control unit is to convert the received light firing pulses into electrical gate pulses. The thyristor control unit also has important protective and monitoring functions as will be described later.

Each thyristor is also provided with RC-circuits to attenuate the commutation overshoots and to secure a proper voltage division in the valve. These circuits are referred to as snubber circuits, damping circuits, or sometimes voltage dividing circuits.

A thyristor including auxiliary components is called a thyristor level, which functions as a complete valve. See figure 9-1. A large number of thyristor levels have to be connected in series in order to achieve an adequate voltage withstand level for the complete valve.

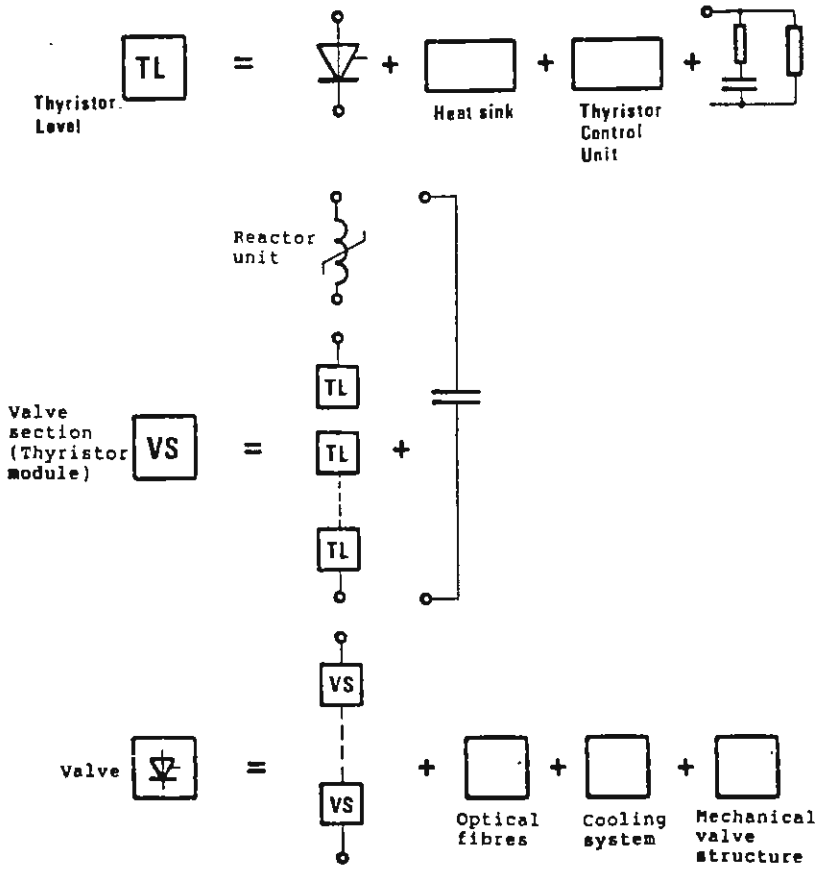

Figure 9-1 The major components and parts of a thyristor valve.

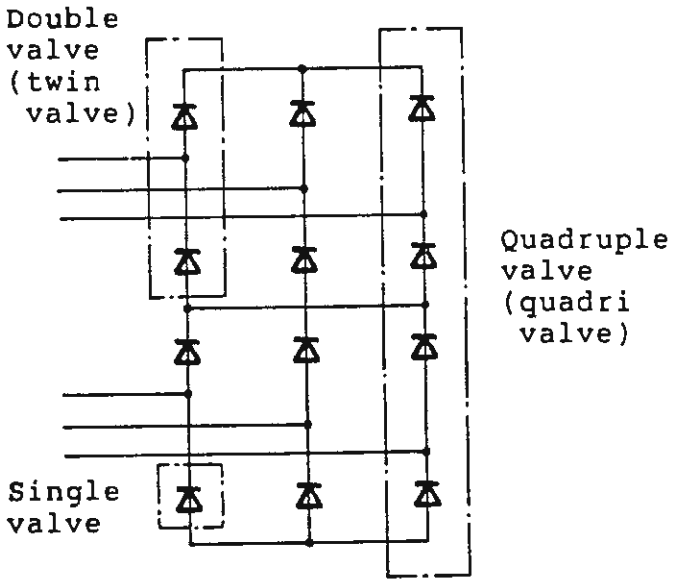

Figure 9-2 Single valve, double-valve (twin-valve) and quadruple-valve (quadri-valve).

A number of thyristor levels, e.g., 6-12, are usually connected in series together with a common reactor unit, as shown in figure 9-1. When the series connected thyristor units are built together as one unit, this unit is usually called a thyristor module. The reactor unit and the thyristor module connected in series are called a valve section. A low impedance capacitor is sometimes connected across the valve section to improve the voltage distribution across the valve at fast voltage transients.

The whole valve is built up of a number of valve sections in order to achieve a proper voltage withstand capability. The valve consists also of optical fibres for signal transmission, a cooling system, and a mechanical structure.

A valve control unit located at ground potential is also an important component of the valve.

It has usually been found feasible to mechanically combine two or four single valves in one mechanical structure or valve tower, as illustrated in figure 9-2. The corresponding valves are called double- or twin-valves, and quadruple- or quadri-valves respectively. A twelve-pulse convertor bridge then consists of three qudruple-valves.

9.4 The thyristor

The characteristics of the thyristor valve are to a very large extent determined by the characteristics of the thyristors. Below will briefly treat the basic characteristics of the thyristor and how these characteristics will influence the requirement on the thyristors, control units, reactor units, snubber circuits and cooling system. The active part of the thyristor is a silicon disc, which is about 1 mm thick. The silicon disc

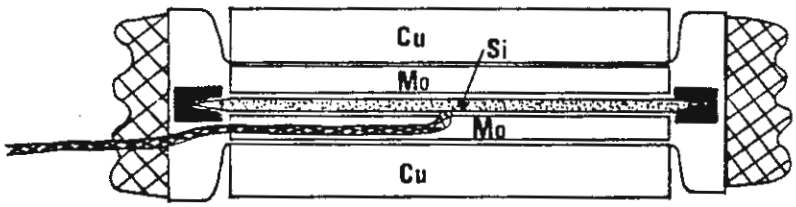

Figure 9-3 Design of a thyristor. Cross-section.

is p-n-p-n^+ doped with the cathode connected to the n^+ doped side, and the gate connected to the adjacent p-layer. The area of modern power thyristors for HVDC is usually 35-60 cm^2.

The silicon disc is located between the two molybdenum discs and two copper discs, as shown in figure 9-3. Both materials have good thermal and electrical conductance properties. Molybdenum also has a coefficient of expansion, which is fairly close to that of silicon, and will thus neutralize the large thermal movement of the copper discs due to its higher expansion coefficient.

The thyristor is mounted between two heat sinks of aluminium, which are pressed together with a fairly high pressure to get electrical and thermal junction resistance between the different discs.

As already mentioned the thyristors are usually electrically triggered. Energy in the form of an electrical pulse is applied to the gate of an electrically triggered thyristor, when it is be turned on or fired. Thyristors could also be designed to be fired through light pulses applied directly to the silicon disc. However, fairly high light intensities are then needed in order to get good turn on characteristics combined with a low sensitivity for unintentional firing at steep voltage transients. These are some of the reasons why direct light triggered thyristors (LTT) have not yet been widely used for HVDC applications, even though light is used for the transmission of the firing signals from the valve control unit to the thyristor control units. Because of that, the following treatment will be restricted to electrically triggered thyristors (ETT).

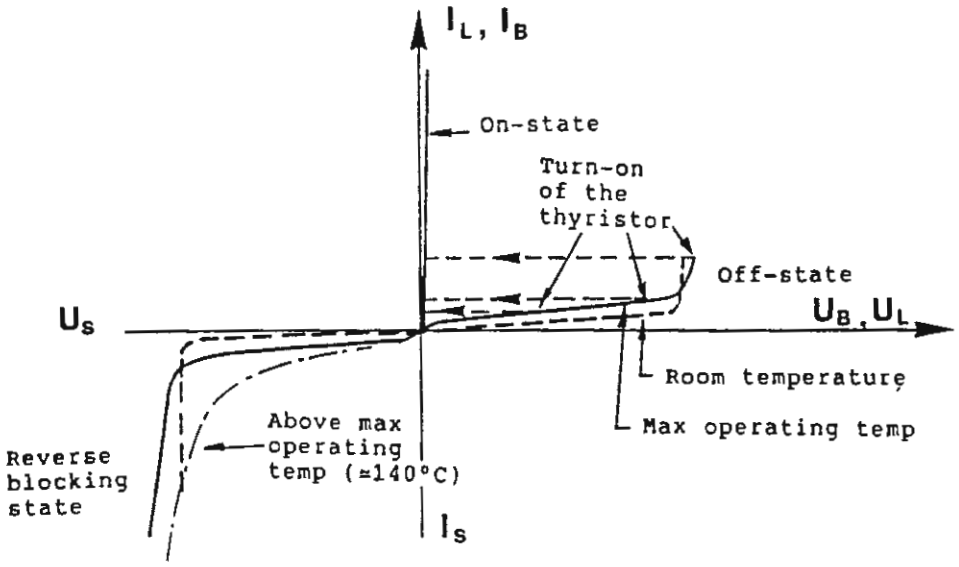

Figure 9-4 Stationary voltage-current characteristics of a thyristor.

9.5 Static voltage-current characteristic for the thyristor

The thyristor has the capability to sustain voltage in, both, the forward blocking direction (positive voltage between anode and cathode) and reverse blocking direction (negative voltage between anode and cathode). Figure 9-4 shows a typical voltage-current characteristic for a non-conducting (off-state) thyristor. The characteristics are shown for, both, a thyristor disc at room temperature (dashed curve) and for maximum operating temperature (solid curve.). It can be seen from figure 9-4 that, both, the current in forward and reverse blocking direction will increase with the temperature for voltages below the knee-point. An increased temperature will, however, give a slight increase of the maximum forward and reverse blocking voltages. It should be noted that the thyristor can sustain higher transient reverse blocking voltages than forward blocking voltages of short durations. A current which is too high in forward direction can cause the thyristor to turn-on. The thyristor can then be destroyed if the firing does not take place in the gate regions. A current, which is too high in reverse direction, can on the other hand destroy the thyristor thermally.

An increase of the thyristor temperature above the maximum operating temperature will cause the current in the reverse direction to rapidly increase resulting in reduced voltage withstand capability. The maximum operating temperature for HVDC thyristors is usually chosen in the region of 100°C, which provides a certain margin in temperature until the voltage withstand capability starts to decrease at about 125°C.

Usually, a maximum continuous reverse blocking voltage (U_R), maximum peak value of a repetitive reverse blocking voltage (U_{RRM}), and maximum non-repetitive reverse blocking voltage are specified. This takes into account that the

thyristor can sustain a higher reverse blocking voltage for a short time than during steady-state operation.

The non-repetitive reverse blocking voltage per thyristor multiplied by the total number of thyristors connected in series in a valve provides the basis for the voltage withstand capability of the valve in reverse direction. The possible non-linear voltage distribution between the thyristors and possible number of short-circuited thyristors in the valve also have to be considered.

The specified voltage withstand capability of the valve is verified at the type-test with switching impulse as well as lightning impulse tests. The voltage withstand test level is usually chosen with a margin of 15-25% above the protective level of the arrester across the valve for the corresponding type of voltage stress.

The thyristor is also specified for different voltage withstand levels in the forward blocking direction depending upon the wave-shape and if the stresses are of transient nature or repetitive. The thyristor is beside the arrester across the valve, also protected in forward direction with protective firing. Protective firing implies a direct protection of each individual thyristor against voltage, which is too high in forward direction, by firing of the thyristor, if the voltage across the thyristor increase above a certain critical level. The gate pulses for the protective firing are usually generated in the thyristor control unit, but it is also possible to design the thyristor so, that this protection is built as an integral part of the thyristor, generating turn-on in the gate region in case of a forward blocking voltage which is too high.

The voltage across the thyristor will be drastically reduced at the turn-on of the thyristor, as illustrated in

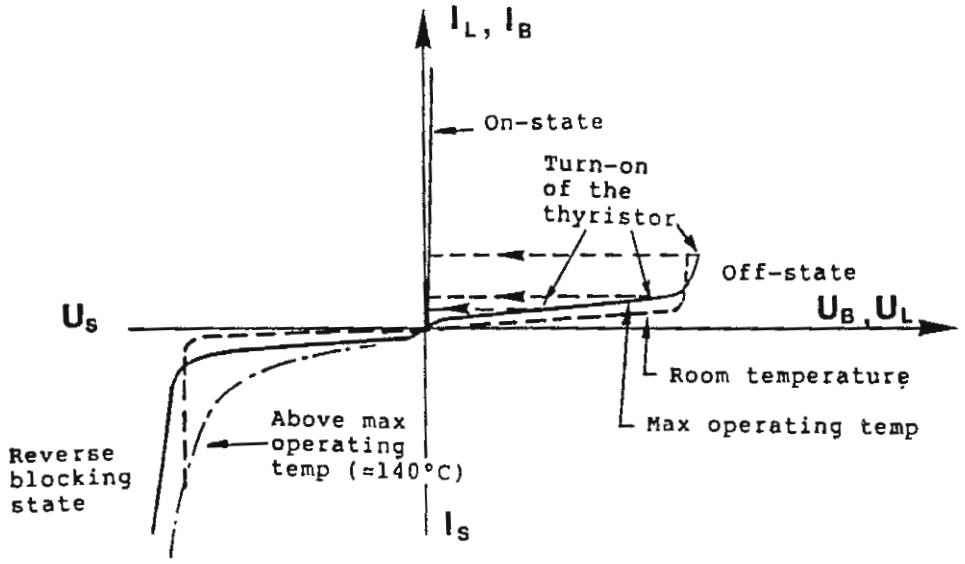

Figure 9-4 Stationary voltage-current characteristics of a thyristor.

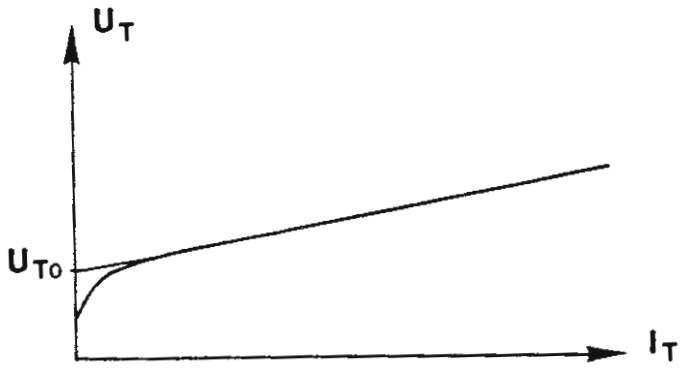

Figure 9-5 Stationar current-voltage characteristics for a thyristor in on-state.

figure 9-4. The thyristor will, in the on-state have a current-voltage characteristic, as illustrated in figure 9-5. This characteristic can be approximately represented by a constant voltage drop ($U_{TO} \approx 1V$) and a constant slope (resistance).

The current dependent part of the voltage drop depends on the resistivity in the silicon and the carrier lifetime. A thyristor for a higher blocking voltage will usually a higher resistivity and require a thicker silicon disc. This means that a high voltage component will require a higher voltage drop for a given current density. One way to reduce the voltage drop is to reduce the current density by increasing the active area of the thyristor wafer.

The on-state voltage of the thyristor can also be reduced by increasing the carrier lifetime. However, an increase of the thyristor area and the carrier lifetime will cause an increase of the recovery charge at the turn-off of the thyristor. An increased recovery charge will result in increased commutation overshoots and increased losses in the snubber circuits as well as increased turn-off losses in the thyristor.

The optimization of the thyristor voltage, the thyristor area and carrier lifetime is an important part of the thyristor valve design optimization. The optimization of the thyristor data are usually done for each separate HVDC transmission to obtain an optimal design. This is contrary to the practice for industrial applications for which standard thyristors are used.

9.6 TURN-ON OF THE THYRISTOR, OPTIMIZATION OF THE VALVE REACTOR

The turn-on of the thyristor will now be described with

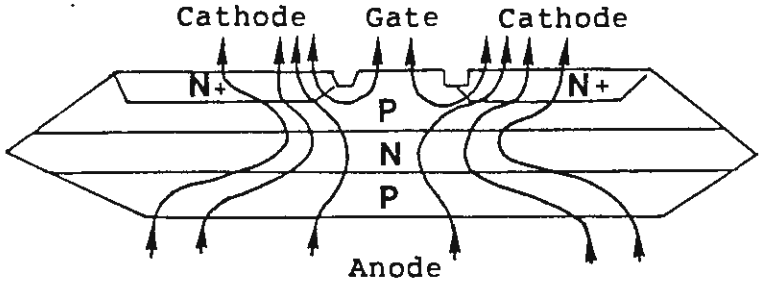

Figure 9-6 Turn-on of a thyristor. Principle figure illustrating spread of conductive plasma.

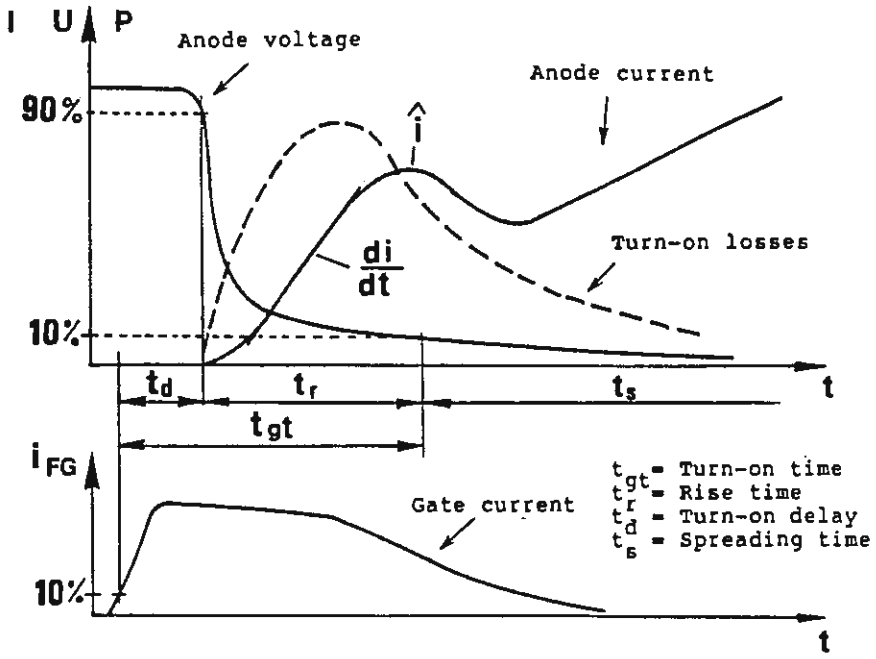

Figure 9-7 Turn-on characteristics.

help of figures 9-6 and 9-7. The thyristor is assumed to have a positive voltage between the anode and the cathode, i.e., a forward blocking voltage, before the thyristor is turned on. The major part of this voltage will be taken up by the n-layer and the pn-junction close to the gate and the cathode. A gate current starts to flow between the gate and the cathode when the gate current pulse is applied.

After a certain delay time, t_d, when the region between the cathode and the gate has been filled up with carriers, the anode current starts to increase and the voltage across the thyristor to fall. The delay time, t_d, which is about 1 μs, is defined as illustrated in figure 9-7. The current is still after the time t_d flowing through narrow firing channels close to the gate. The current density will now drastically increase and the voltage across the thyristor will drop as can be seen in figure 9-7. The time until the thyristor voltage has dropped to 10 % of its initial value is called rise time t_r and the total time is called the turn-on time t_{gt}.

The conduction plasma close to the gate will now spread to the entire area of the thyristor. The speed is, however, rather limited, 0,05 - 0,1 mm/μs, while for larger thyristor (e.g. 60 cm^2) it can take up to some ms before the whole thyristor is fully conducting. This time is called the spreading time.

The gate-current pulses should have sufficient amplitudes, e.g. 5 A, and duration (> 10μs) to get a short turn-on time. This is specially critical if the external snubber circuits and leakage capacitances can give a high time-derivate and amplitude of the anode current through the thyristor during the turn-on time.

As illustrated in figure 9-7, both, the maximum amplitude, and time derivate of the first anode current surge, have to

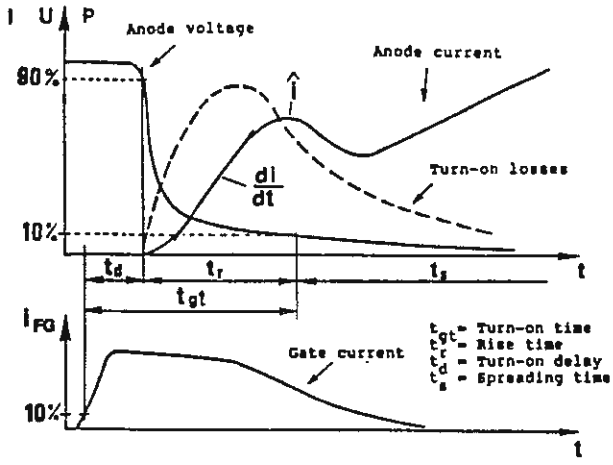

Figure 9-7 Turn-on characteristics.

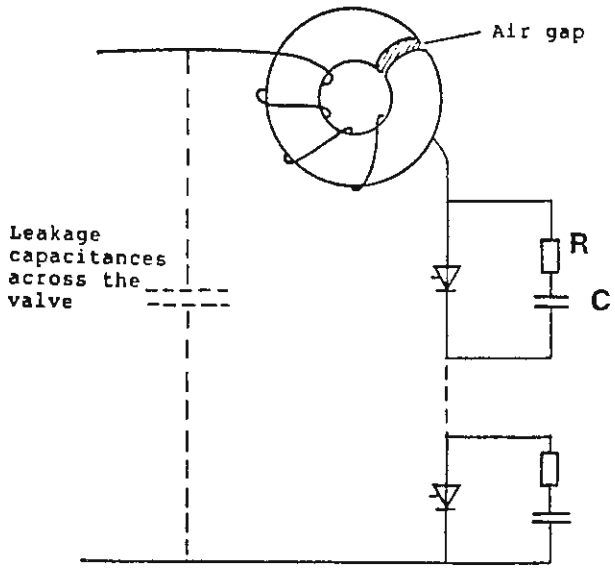

Figure 9-8 Limitation of the inrush-current at turn-on with a reactor.

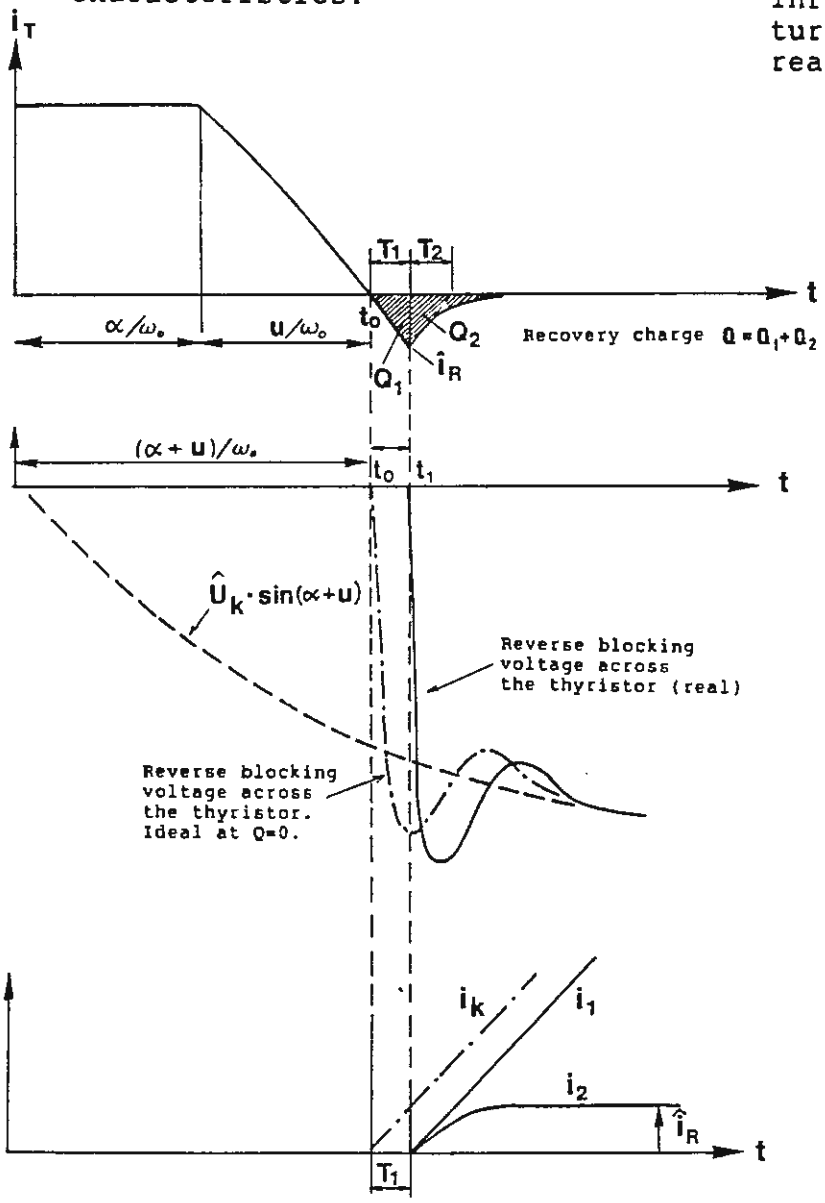

Figure 9-9 Turn-off of a thyristor.

be specified.

The turn-on losses in the thyristor have also been indicated in figure 9-7 by a dashed curve. These losses are derived by multiplications of the anode-voltage by the anode current.

The steepness and amplitude of the first peak of the anode current surge at turn-on can be limited by the connection of reactors in series with the thyristors, according to figure 9-8. The reactors are usually built of ring-cores. They are designed to limit the surge current during the turn-on of the thyristor when only a small part of the thyristor is conducting. The iron core will then saturate. The reactors are provided with an air gap which will prolong the time to saturation and avoid that effect of the reactor being limited to a delay of the current peak.

The contribution to the turn-on current from the snubber circuit connected directly in parallel with the thyristor also have to be considered. The discharge current from the snubber circuit will provide a valuable contribution to the turn-on current and is often essential in order to avoid a zero-crossing in the turn-on current after the first current surge.

9.7 Turn-off of the thyristor Design of snubber circuits

The turn-off of the thyristor at the end of the on-state interval will not occur instantaneously but take a certain time. The thyristor will not extinguish the current at the zero-crossing of the current at time t_o, as illustrated in figure 9-9. The thyristor will neither immediately take up any reverse blocking voltage at t_o but continue to conduct

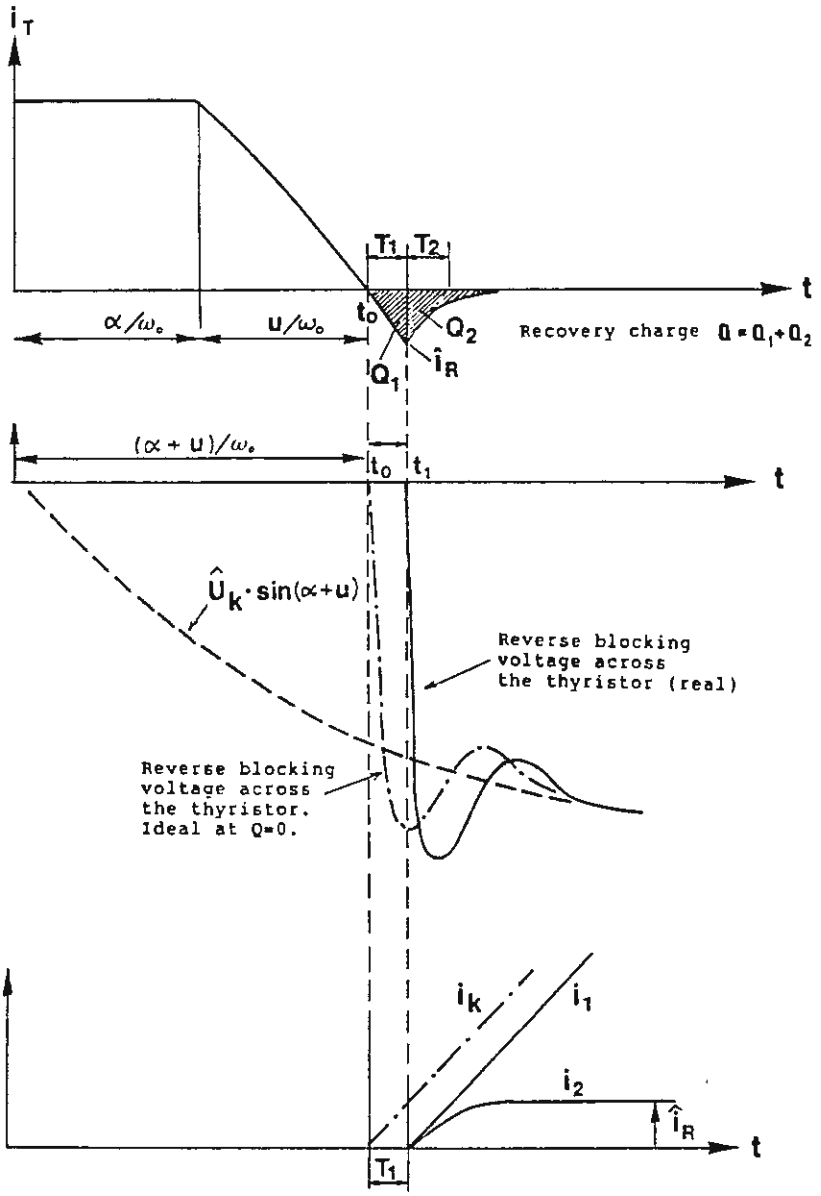

Figure 9-9 Turn-off of a thyristor.

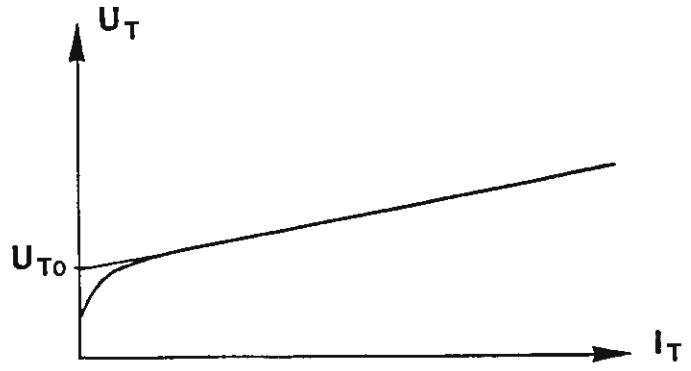

Figure 9-5 Stationar current-voltage characteristics for a thyristor in on-state.

current in the reverse direction. The thyristor will start to take up reverse blocking voltage at time t_1, when a sufficient recovery charge has been removed from the thyristor. The thyristor then starts to build up a reverse blocking voltage at the pn-junction adjacent to the anode. The current through the thyristor, which is now flowing in the reverse direction, decreases towards zero after the time t_1. The decrease of the current during this interval can, as a first approximation, be described as an exponential function with the time constant T_2, as illustrated in figure 9-9.

The total electrical charge $Q = Q_1 + Q_2$ is called the recovery charge of the thyristor. The magnitude of the recovery charge is a function of the temperature, the current and the rate of change of the current through the thyristor. The recovery charge will increase with the carrier lifetime. It is nowadays possible to be fairly exact in controlling the carrier lifetime, which is essential, as the spread in Q between different thyristors causes a non-linear voltage distribution between the thyristors connected in series. The spread in recovery charge during the 1970s was one of the decisive factors for the determination of the minimum size of the capacitors in the snubber-circuits during the 1970s while nowadays it is of minor importance. The magnitude of the recovery charge is, on the other hand, as will be described below, decisive for the choice of snubber circuits.

The current in the reverse direction after time t_1 will together with the reverse blocking voltage generate losses in the thyristor. These losses, which are called turn-off losses, have to be added to the losses determined during the on-state interval based on the steady state on-state characteristic, according to figure 9-5.

The transient overshoot of the reverse blocking voltage

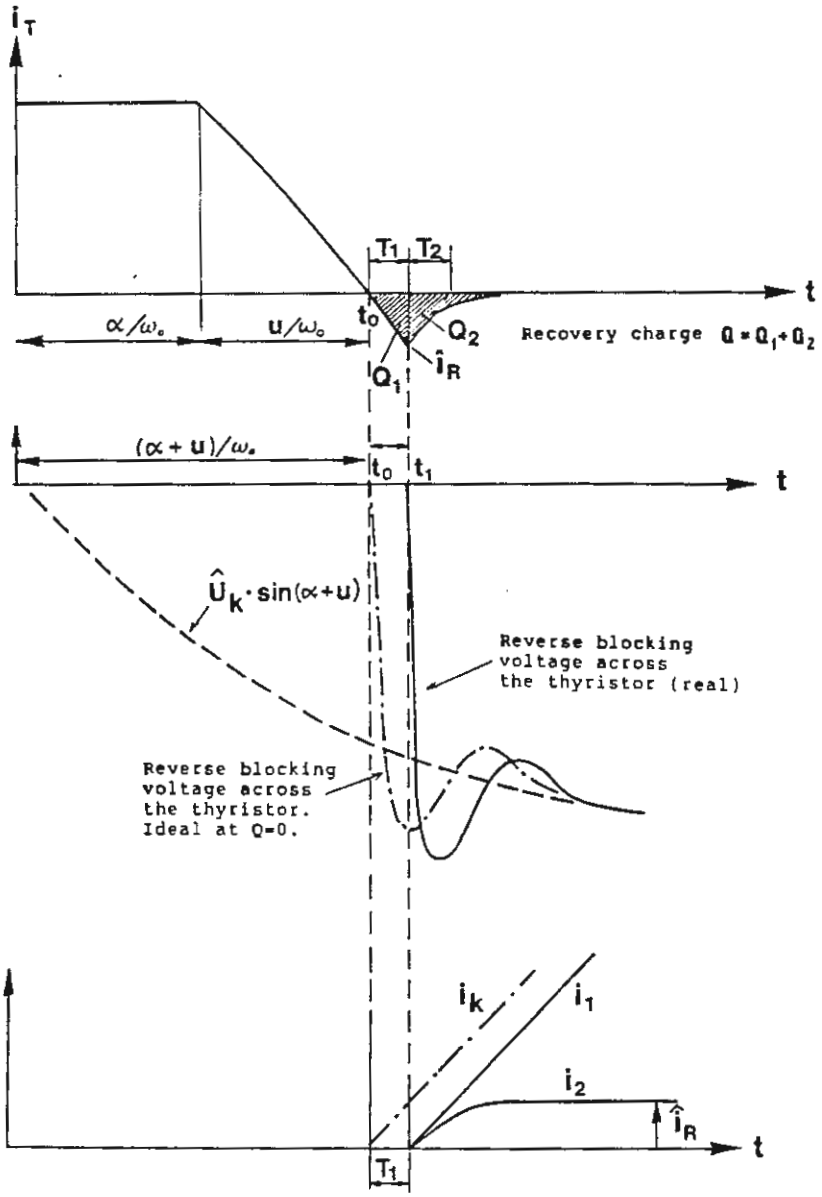

Figure 9-9 Turn-off of a thyristor.

after turn-off of the valves was calculated in the previous chapter under the assumption that the valves were ideal and equipped with thyristors without recovery charge, i.e., the current was extinguished at the zero crossing at time t_0, according to figure 9-9. This case is represented in the figure by the dash-dotted curve. The commutation overshoot was in chapter 8, determined by equation (8-8). The turn-off of the valve was then represented by a superimposed ramp current as illustrated by the dash-dotted line in the lowest diagram of figure 9-9 and in mathematical form by equations (8-7a) and (8-7b).

We can now calculate the recovery voltage across the valve for the real case with recovery charge in a similar way as for the ideal case by replacing i_k, according to the dash-dotted line, by injection of the currents i_1 and i_2, according to figure 9-9. Equations (8-7a) and (8-7b) are still valid for the current $i_1(t)$ if the time is counted from t_1 instead of from t_0 and sin $(\alpha+u)$ is replaced by $\sin(\alpha+u+t_1 \cdot \omega_0)$. We get the following expression for the current component $i_2(t)$:

$$i_2(t) = \hat{I}_R \left(1 - e^{-\frac{t}{T_2}}\right) \qquad (9\text{-}1)$$

The corresponding Laplace expression is

$$I_2 = \frac{\hat{I}_R}{s\left(1 + sT_2\right)} \qquad (9\text{-}2)$$

We denote the ideal step in recovery voltage without overshoot with ΔU for which we get the expression:

$$\Delta U = \hat{U}_k \cdot \sin\left(\alpha + u + \omega_0 T_1\right) \qquad (9\text{-}3)$$

The corresponding expression for the current $\hat{I}_R$ will be:

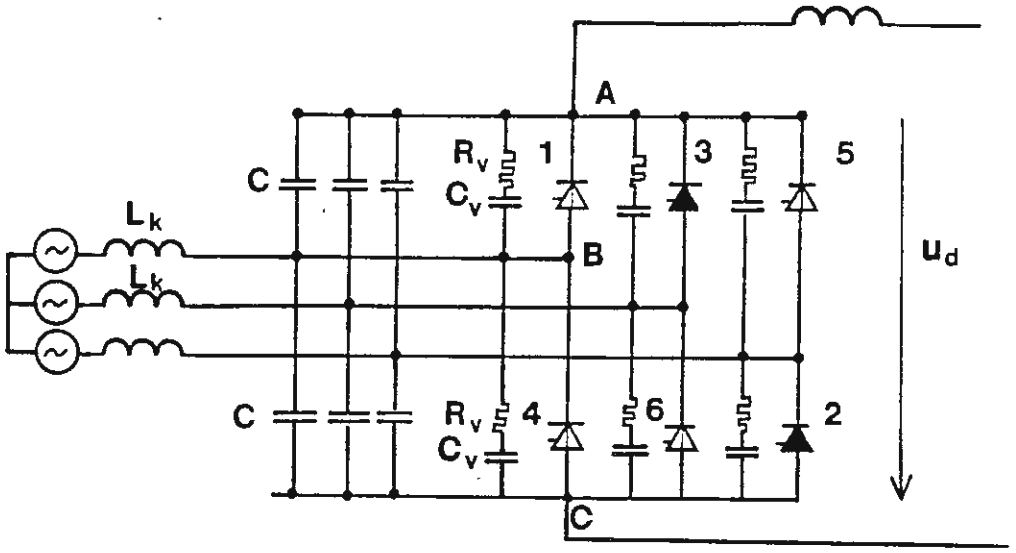

Figure 8-10 Simplified circuit diagram for a 6-pulse converter with leakage inductances and snubber circuits across each valve.

$$\hat{I}_R = \frac{\Delta U \cdot T_1}{2\ L_K} \qquad (9\text{-}4)$$

The current $i_1(t)$ will now generate a corresponding increase in the voltage across the valve. We will now get the following expression for voltage U_2 corresponding to equation (8-8) by replacing (8-7b) with (9-2) and $\hat{I}_R$ according to equation (9-4)

$$\frac{U_2(s)}{\Delta U} = \frac{T_1}{4\left(1 + sT_2\right)} \left[\frac{3\ Z(s)}{3\ sL_k + Z(s)} + \frac{Z(s)}{5\ sL_k + Z(s)}\right] \qquad (9\text{-}5)$$

The time-function, which corresponds to eq. (9-5), will be rather complex for the real case, when the impedance Z consists of a pure capacitor in parallel with an RC circuit according to figure 8-10. Because of that we will limit the treatment here to some simplified cases in order to get some understanding of how the snubber circuit parameters can affect the commutation overshoots.

We will first assume that the impedance Z is so high that it can be neglected.
Setting $C \Rightarrow 0$ and $C_v \Rightarrow 0$ gives $U_1 = \Delta U_1$,

and:

$$u_2(t) = \frac{T_1\ \Delta U}{T_2} \cdot e^{-\frac{t}{T_2}}$$

The voltages, $u_1(t)$ and $u_2(t)$, are of course for this case proportional to the time-derivates of the currents $i_1(t)$ and $i_2(t)$, respectively, as the impedances in the circuit are determined by the inductances L_k. If we assume that T_1

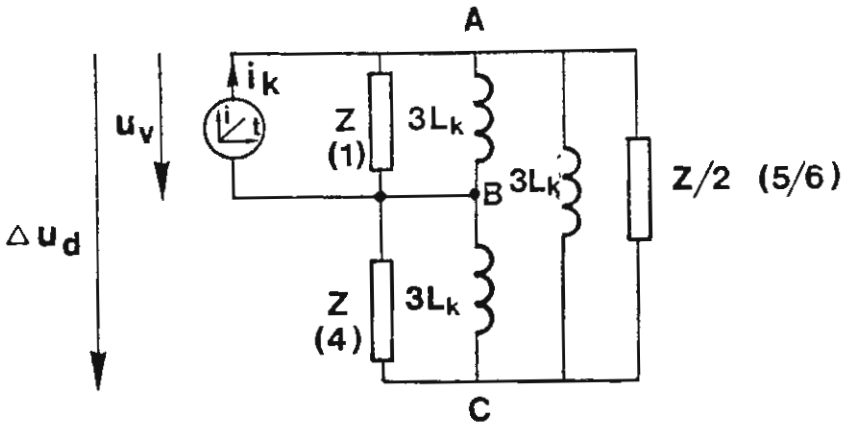

Figure 8-11 Simplified circuit diagram for the calculation of the commutation voltage transients after finished commutation from valve 1 to valve 3. (See Ref. [2], fig 5.13).

$= T_2$, which is usually approximately valid, we will find that the recovery charge will give a commutation overshoot of 100%, although the leakage capacitance C has been set to zero.

This simple case illustrates that the recovery charge will increase the commutation overshoot. Increasing the leakage capacitance C would help to decrease the contribution from $i_2(t)$. However, we learned in the previous chapter that the leakage capacitance C had to be attenuated by a parallel RC circuit. Because of that, it is more feasible to increase C_v to compensate for the contribution from the superimposed current $i_2(t)$.

The next simplified case, which we will study is to represent Z(s) with a pure capacitor i.e. $Z(s) = 1/sC$. To further simplify the calculation we will make the modification, such that the impedance between point A and point C in figure 8-11 is set to Z(s) instead of Z(s)/2. In practise this means that either the influence of the snubber circuit across valve 5 or across valve 6 is neglected. We can now simplify equation (9-5) to

$$\frac{U_2}{\Delta U} = \frac{T_1}{\left(1+sT_2\right)} \cdot \frac{Z(s)}{\left(3sL_k + Z(s)\right)} \qquad (9\text{-}6)$$

Insertion for $Z(s) = \frac{1}{sC}$ and $\omega_0 = \frac{1}{\sqrt{3L_k\ C}}$

gives

$$\frac{U_2}{\Delta U} = \frac{\omega_0^{\,2}\ T_1}{T_2 \left(s + \frac{1}{T_2}\right) \left(s^2 + \omega_0^{\,2}\right)} \qquad (9\text{-}7)$$

The corresponding time function is

$$u_2(t) = \frac{\Delta U \quad T_1 \cdot T_2 \ \omega_0^2}{\left[1 + \left(\omega_0 T_2\right)^2\right]} \cdot \left[e^{-\frac{t}{T_2}} - \cos \omega_0 t + \frac{\sin \omega_0 t}{t_2 \cdot \omega_0}\right]$$

(9-8)

If we assume that $T_1 \simeq T_2$, we will find that the condition $(\omega_0 T_2)^2 << 1$ has to be fullfilled to give a contribution not too large from $u_2(t)$ to the total commutation overshoot. We can approximately set

$$u_2(t) \simeq \Delta U \cdot T_1 \cdot \omega_0 \cdot \sin \omega_0 t \qquad (9\text{-}9)$$

If we now set the amplitude of the voltage $u_2(t)$, i.e., $\hat{U}_2$ to $\hat{U}_2 = k \cdot \Delta U$, we find from equation (9-9) that:

$$\omega_0 T_1 = k \qquad (9\text{-}10)$$

Equation (9-10) provides a rough idea about the needed capacitor in the snubber circuit, since T_1 is determined by the recovery charge, ω_0 by the size of the capacitor, and k by the magnitude of the overshoot.

The relationship, according to equation (9-10), can also be derived in a quite different way by considering the stored energy in the leakage inductance $2L_k$ at time t_1. This energy will, for an undamped system oscillate between the inductances and the capacitances and is stored in the capacitances at the peak voltage. Two thirds of the total energy will in the studied case be stored in the capacitances across the valve, which has been turned off, and one third in the other capacitances. This result in the following relationship

$$\frac{1}{2} \cdot 2L_k \cdot \hat{I}_R^2 = \frac{1}{2} \ \frac{3}{2} \ C \ (\Delta U \cdot k)^2$$

Insertion for $\hat{I}_R$, according to equation (9-4) and

further simplification, gives:

$$\frac{T_1^2}{3L_k \cdot C} = k^2$$

or

$$T_1 \cdot \omega_0 = k$$

which is the same as in equation (9-10).

A pure undamped capacitor connected across a valve will, as described in chapter 8, cause a high overshoot from the superimposed current component $i_1(t)$. Because of that, it is feasible to connect a resistor in series with the capacitor. An optimal value of R_v is in order of:

$$R_v \approx \sqrt{\frac{L_k}{C_v}}$$

It must be stressed, that the very simplified calculations presented above cannot be used for a real optimization of the snubber circuits. They have been included in order to provide a certain insight in the relationships between various parameters. The optimization of snubber circuits is usually performed with digital computer simulation programs, which also can consider other factors, such as the correct representation and damping of the convertor transformers.

The losses in the snubber circuits, which can be substantial, is another important factor that has to be considered at the optimization of the circuit parameters. As the losses will increase with the size of the capacitor,

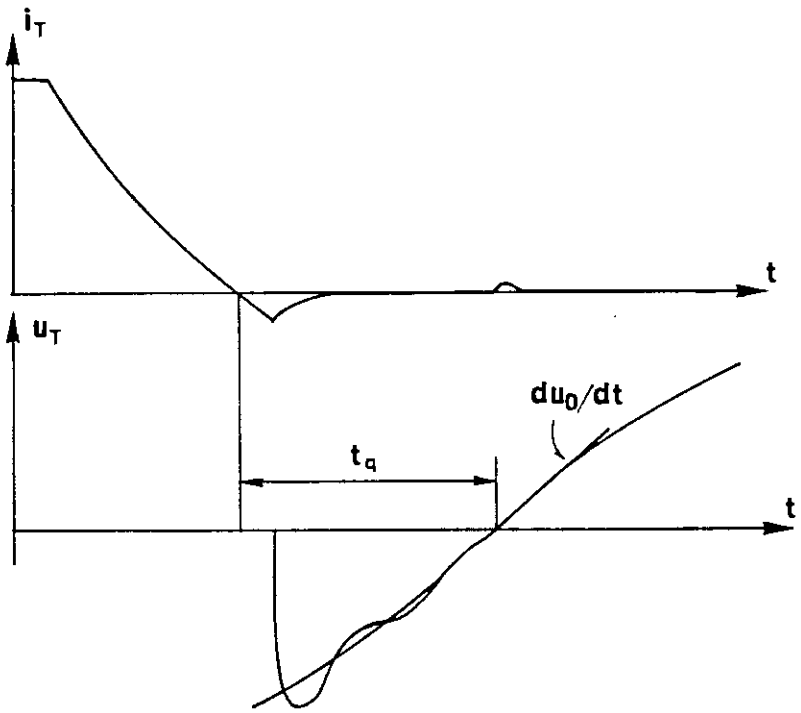

Figure 9-10 Recovery time t_q.

it is essential to limit the capacitance. The major part of the losses is generated at the charging and discharging of the capacitors at the commutations. The losses, which will be generated in the resistors connected in series with the capacitors, will at each step change in the voltage with the magnitude ΔU be approximately $1/2C_v(\Delta U)^2$. This also shows that the losses in the snubber circuit will increase substantially at operation with large firing or extinction angles. They will also depend on the magnitude of the convertor current.

9.8 The recovery of the thyristor

The thyristor cannot sustain a forward blocking voltage as soon as the current through the thyristor has decreased to zero. A certain time with reverse blocking voltage is needed for the thyristor to recover, which is called recovery time. The recovery time (t_q) is defined from the zero crossing of the thyristor current until the zero crossing of the voltage as illustrated in figure 9-10. The recovery time will increase with increased junction temperature of the thyristor and depends also on the magnitude of the reverse blocking voltage and the rate of rise of the on-state voltage.

Power thyristors for HVDC and SVC usually have a considerably longer recovery time than thyristors for many other applications. The reason for this is that it is essential to minimize the losses during the on-state interval, which means that it is optimal to use thyristors with longer carrier lifetimes. Typical recovery time values for HVDC and SVC applications are 300-400 μs.

In figure 9-10 it has been indicated that the thyristor gets a small current in forward direction, when the off-state voltage starts to build up. If this current is

sufficienly large the thyristor will turn-on again. A turn-on of the thyristor outside the gate-region can cause a current concentration which is too high in a small channel resulting in that the thyristor being destroyed.

Each thyristor is usually provided with a special recovery protection to protect the thyristor against too short recovery times. This protection is usually integrated in the thyristor control unit. One possible functional principle is to sense the time during which the thyristor is stressed with reverse blocking voltage. If this time is not long enough the protection will generate a new gate pulse to secure that the thyristor is turned-on in the gate-region. This protection might also take into account the amplitude and rate of rise of the off-state voltage. It should also be noted that the spread in recovery charges between different thyristors will cause a spread in the voltages between different thyristors with a result in that they will not get off-state voltages at the same moment. It is because of that, recommended to arrange the recovery protection individually for each thyristor.

9.9 Valve control

Valve control equipment is usually understood to be all the electronic equipment in a valve, which handles the firing, monitoring, and protection of the valve and the individual thyristors. The most essential requirements on this equipment are:

- To generate simultaneous gate pulses with adequate power for proper turn-on to all the thyristors in a valve when a valve control pulse is received from the converter firing control, provided that the off-state voltage is sufficiently high for proper turn-on.

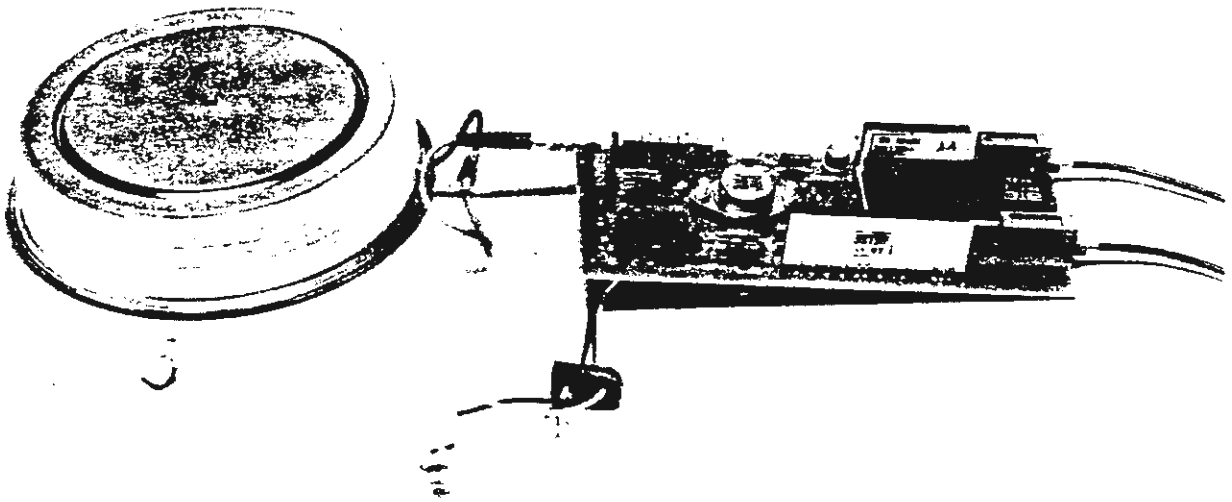

Figure 9-11 Thyristor with thyristor control unit, TCU.

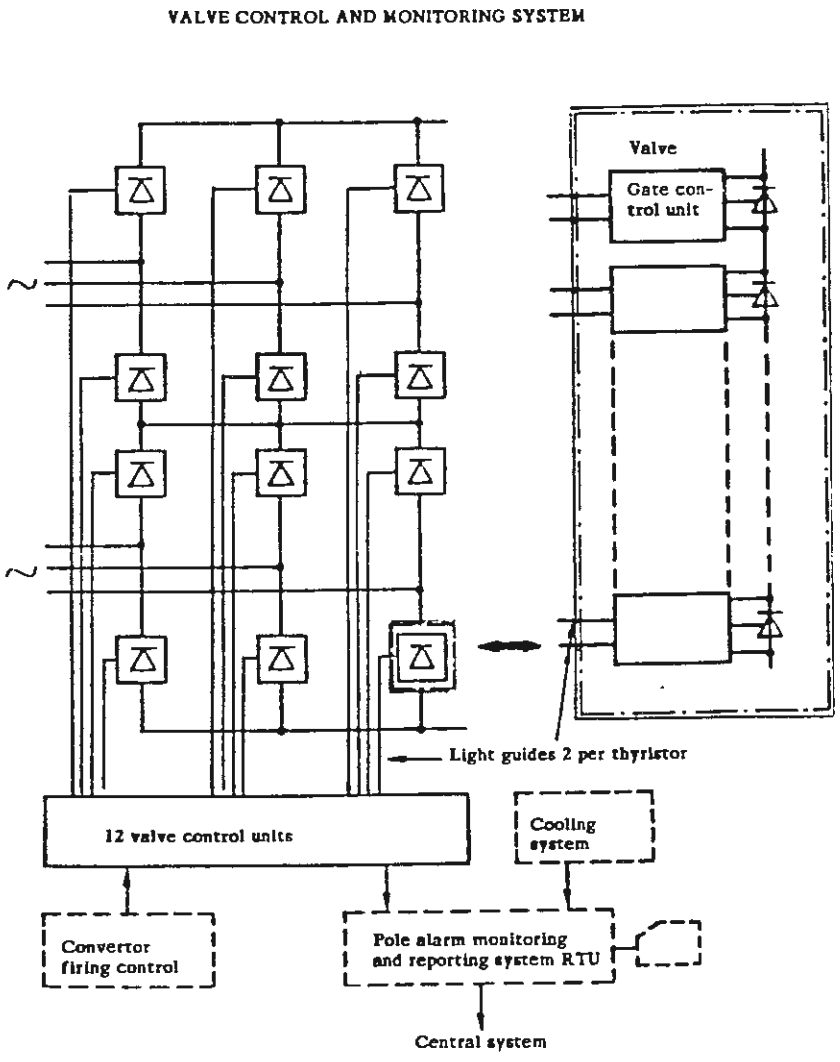

Figure 9-12 Valve control and monitoring system for a 12-pulse converter unit.

- At intermittent current operation secure that thyristors, which have temporarily been turned-off due to a current below the latching current will immediately be turned-on again, as soon as the valve has a sufficiently high off-state voltage, provided that a valve control pulse is still supplied to the valve.

- To turn-on thyristors, which have not been given a sufficiently long recovery time (Recovery protection)

- To turn-on thyristors, which are stressed with too high off-state (forward blocking) voltage. (Protective firing)

- Monitor the thyristors and present information of any short-circuited thyristors.

Most suppliers of thyristor valves will nowadays offer technical solutions which meet these requirements. The technical solution presented below has been used by ABB during the 1980s.

Each thyristor is equipped with an electronic thyristor control unit (TCU). The auxiliary power for the electronic circuit of the thyristor is supplied from the snubber circuit connected across the thyristor. The stored energy is discharged when a gate pulse is generated to the thyristor. This implies a severe requirement on a very fast recharging of TCU as soon as the thyristor takes up voltage in reverse or forward direction. The TCU is connected to the gate of the thyristor, as shown in figure 9-11. The communication with the central valve control unit, which is located at ground potential, is provided through two optical fibers.

The communication between the TCU's and the valve control unit is also illustrated in figure 9-12, which shows a

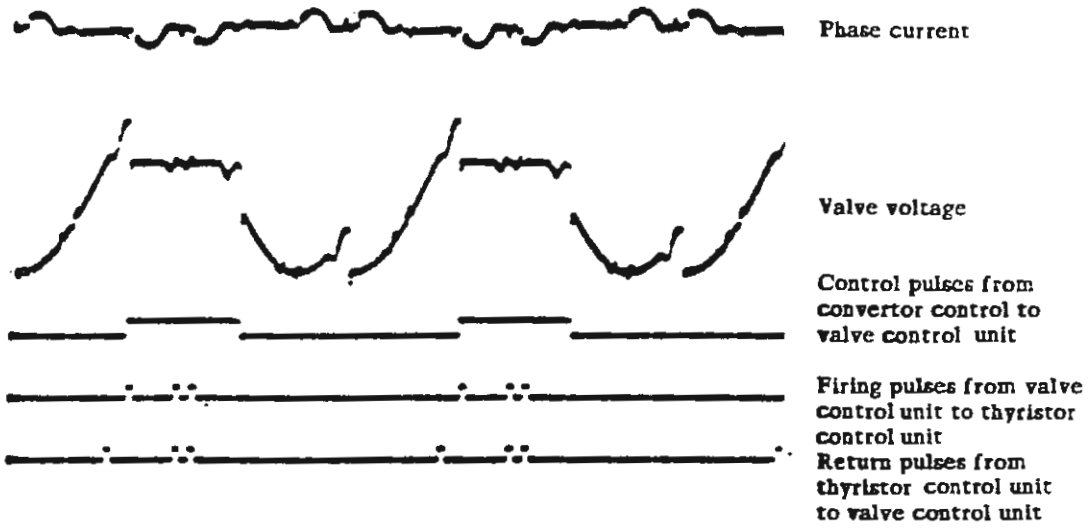

Figure 9-13 Valve firing at intermittent current operation.

principle basic layout of the valve control for a 12-pulse converter unit. The two-way communication system, with two optical fibres for each TCU, was introduced to meet the requirement, such that thyristors will always be prepared to turn-on when the valve is ordered to be in the on-state. It was also required that the communication should be performed with short light pulses in order to save the lifetime of the light-emitting diodes. These requirements were met by the two-way communication system.

A short light pulse (return pulse) is generated in the TCU as soon as a sufficiently high off-state (forward) voltage is measured across the thyristor provided enough energy is stored in the TCU for generation of a gate pulse to the thyristor. When the central valve control unit has received these pulses it will generate firing pulses to all the TCU's in a valve as soon as firing of a valve is ordered through a valve control pulse from the converter firing system. In case any thyristor would stop to conduct current and take up an off-state voltage, e.g., at the intermittent current operation it will send a new return-pulse to the valve control unit, which immediately responds with new firing pulses to all the TCU's. This function is further illustrated through figure 9-13.

The two-way communication system was thus required for the design of the short-pulse system and to provide this system the same performance as a system with long firing pulses. However, it has been found very valuable to use the information provided by the return pulses for the monitoring of the thyristors. A failure of a thyristor will result in the thyristor being short-circuited. The only consequence this will have on the performance of the valve is that the voltage withstand capability of the valve will be reduced correspondingly. This means that a couple of thyristors can usually be permitted to be short-circuited without affecting the operation of the converter. However,

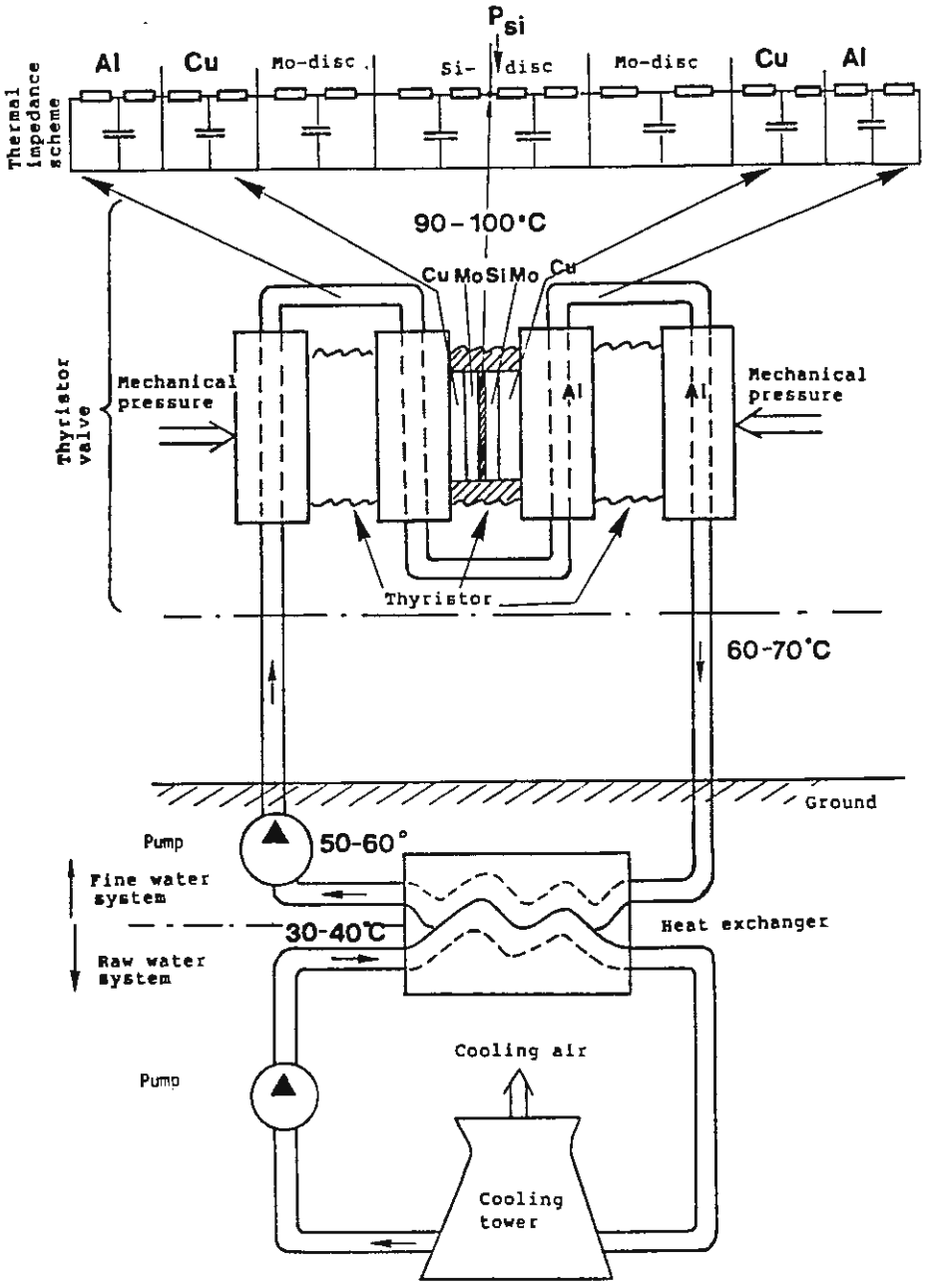

Figure 9-14 Principle build-up of the valve cooling system.

it has been found very valuable to monitor all the thyristors automatically and to get information if any thyristor has failed and where it is located. It was very easy to design such a monitoring system, as a short-circuited thyristor would result in that no return pulses are being generated from this thyristor.

9.10 Valve cooling

The on-state voltage of a thyristor, which is between 1.5 - 2.0 V at rated current, will generate power losses. These losses will also increase due to the additional losses at turn-on and turn-off of the thyristor. The total losses in the thyristor wafer will be between 0.5 - 1.5 kW depending on the rated current and thyristor size. These losses will result in a temperature increase in the silicon disc, which has to be limited, as a number of thyristor characteristics will detoriate when the temperature increases above 100 -125°C. The silicon disc has to, because of that, be cooled in a very efficient way.

The thyristor is mounted between two heat sinks, usually made of aluminium. The heat sinks, or coolers, are cooled by some cooling media, e.g., air or water, which transport the loss energy via heat exchangers towers. Nowadays water is usually used as cooling media, since water has a substantially better heat capacity than air, and makes it possible to design a very efficient and compact cooling system.

The principles of a water cooling system is illustrated in figure 9-14. The thyristor valve has been drawn in a very simplified way with only three thyristors, which are cooled in series. The cooling in a complete valve is usually

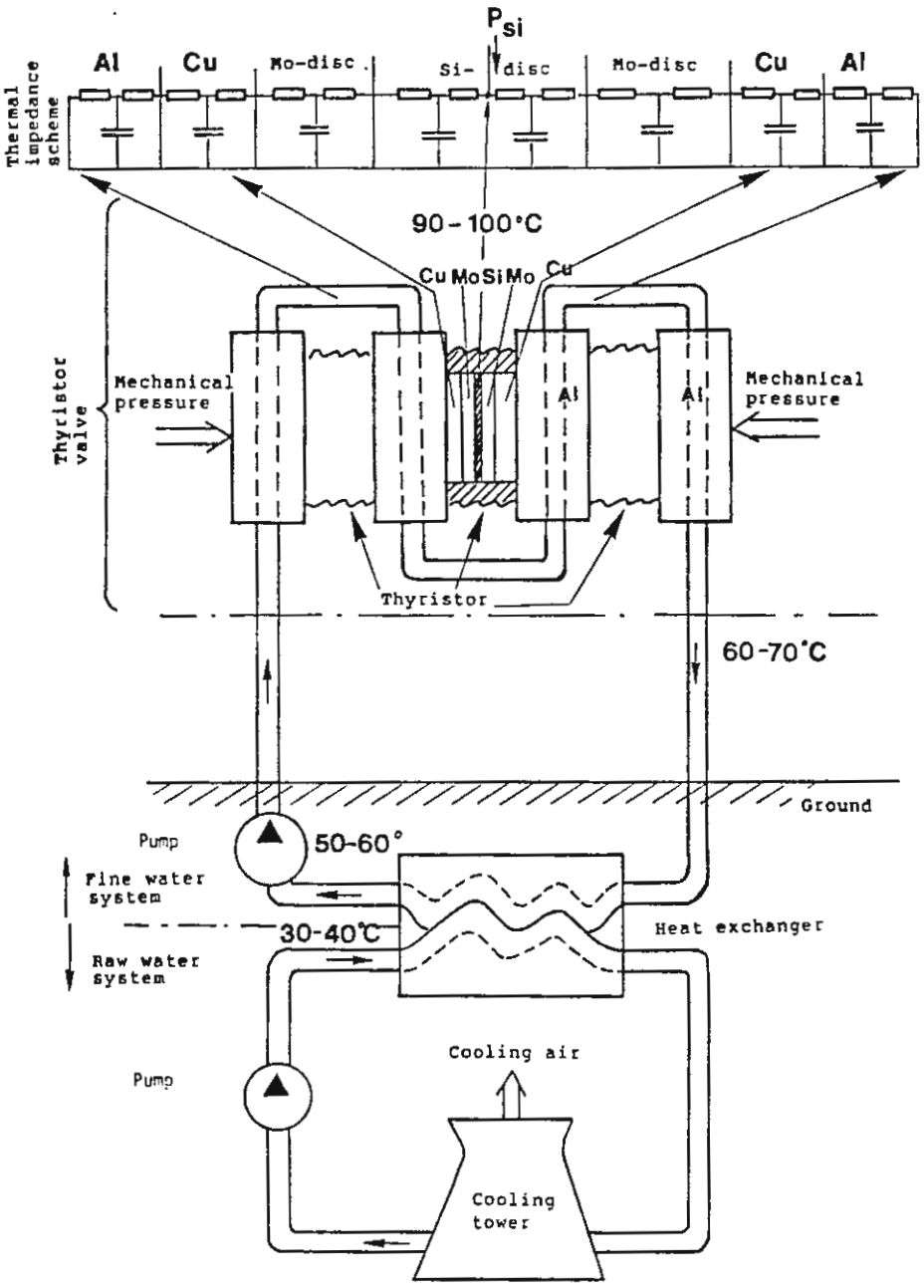

Figure 9-14 Principle build-up of the valve cooling system.

arranged in such a way that all the thyristors are cooled equally efficient as far as possible. This means that it is not acceptable to cool thyristor in series as shown in figure 9-14, where the most left side thyristor is cooled with water having an average temperature of about 55°C and the most right side one with water having an average temperature of about 65°C.

The water tube system has to be made of a material having good electrical insulation properties and the length of the tubes has to be sufficient to obtain proper voltage withstand properties. The dc-voltages to ground can, as an extreme, be up to 600 kV. The water must also have sufficient high electric resistivity, which is obtained by cleaning and deionization of the water.

The water cooling system is usually designed with two separate cooling loops, a fine deionized water cooling system and a raw-water cooling system as illustrated in figure 9-14. The two systems are connected together with a heat exchanger. Some typical water temperatures are presented in figure 9-14.

It is of special interest to study the temperature distribution internally in the thyristor and how this could vary at transient conditions. The temperature increase in K is derived from the generated heat in W multiplied by a thermal resistance in K/W, i.e,:

$$\Delta\Theta = R_{th} \cdot P \qquad (9\text{-}11)$$

This could be compared with the conditions for an electrical circuit for which the voltage in volt is derived from the current in ampere multiplied by the resistance in ohm. For the thyristor it is often most practical to express the thermal resistance in K/kW and the generated heat in kW.

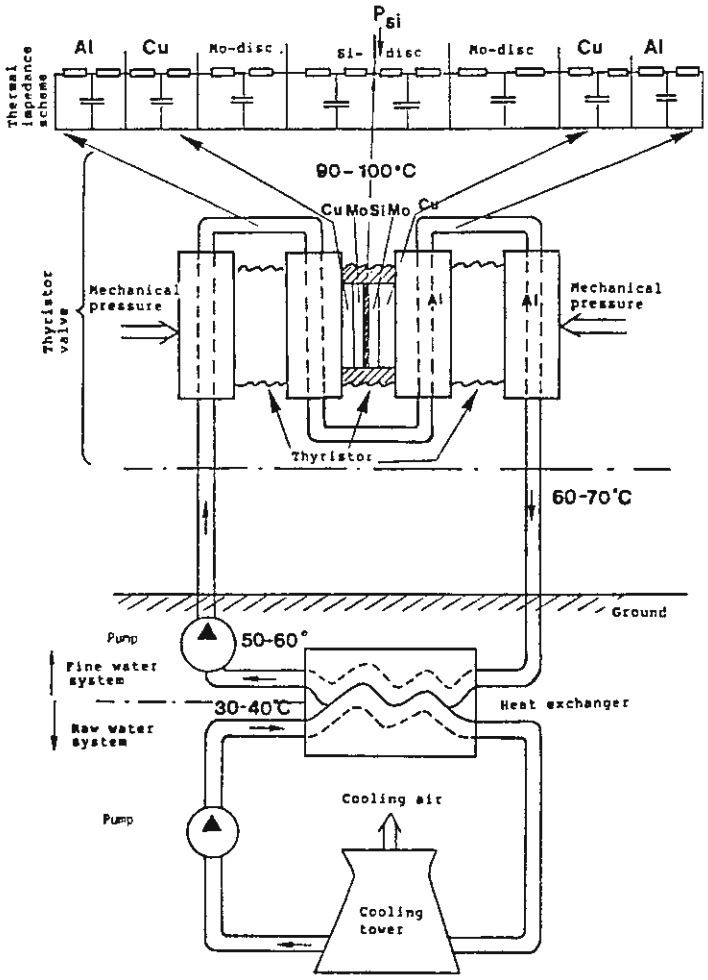

Figure 9-14 Principle build-up of the valve cooling system.

The heat transmission and the heat capacity of the different parts of the thyristor and the heat sinks for transient conditions will also be of decisive importance. It is often convenient to represent the thyristor and the two heat sinks with an electrical equivalent of the thermal system as shown in figure 9-14. The capacitances here represent the heat capacities of the different components. The heat losses are generated in the silicon wafer. The temperature in this region is often referred to as the thyristor junction temperature.

The thermal impedance for the two halfs of the thyristor will be connected in parallel as the thyristor is cooled from both sides. We can then assume that the temperature of the water is equal to the average water temperature.

It should also be noted that a temperature drop is obtained at every junction between two elements, e.g., between the molybdenum disc and the copper disc and between the thyristor and the heat sink. It is because of that, very essential that each surface is plane grinded and properly cleaned and that a sufficient high mechanical pressure is applied on the heat sinks.

The temperature drop between the heat sink and the water is determined by the velocity of the water and the design of the water cooling channels in the heat sink. The thermal resistance of the thyristor is almost inversely proportional to the area of the thyristor as the heat transport mainly takes place in the axial direction.

The transient characteristic of the thyristor and the cooling system can be described by a chain of thermal impedances as shown in figure 9-14. One way to specify the thermal impedance is in the form of the increase in the

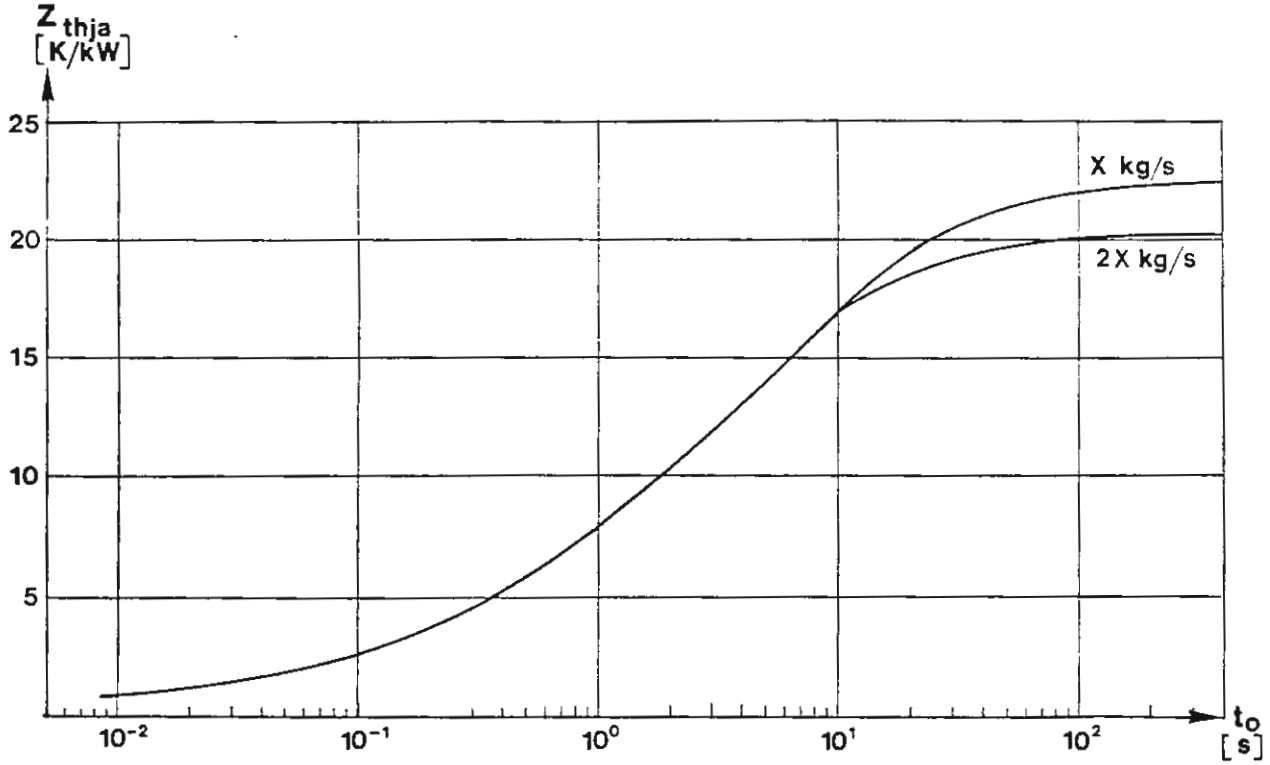

Figure 9-15 Thermal impedance. Thyristor junction temperature as a function of time at a step change in heat dissipation in the thyristor.

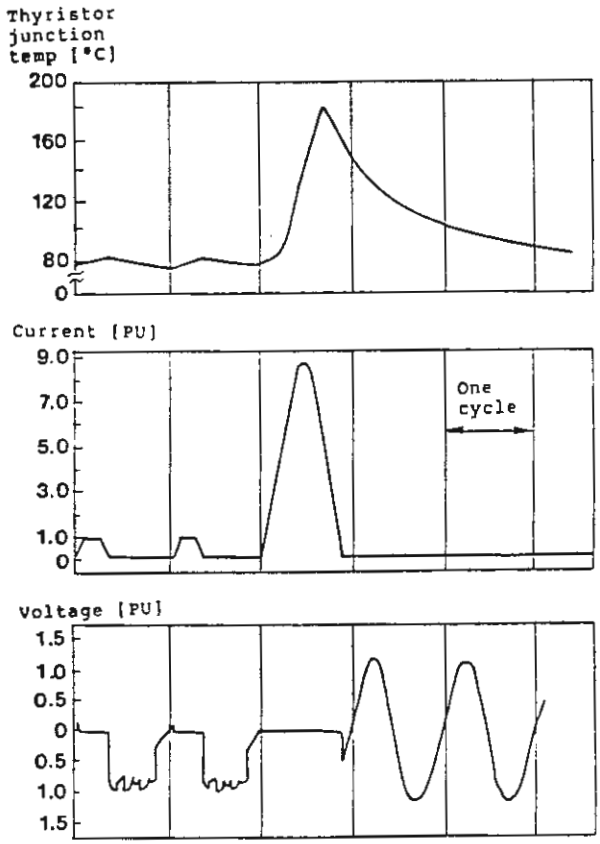

Figure 9-16 Short-circuit across a thyristor valve. Thyristor junction temperature, thyristor current and thyristor voltage.

temperature of the silicon disc as a function of time at a step change in the generated heat in the silicon disc. Figure 9-15 shows a typical shape of such a step response, i.e., the increase in the temperature of the silicon disc as a function of time at a step change in the generated heat in the silicon disc. The thermal impedance is low for short energy pulses as the thermal impedance will then be mainly determined by the heat transport within the thyristor and as the copper discs have a fairly high heat capacity. For times longer than about 10 seconds the cooling of the water will also influence the temperature, which explains why the water velocity will influence the temperature. See figure 9-15.

The junction temperature of the thyristor can be determined by the use of thermal impedance step-response diagrams as shown in figure 9-15 and also for cases when the heat generation varies in arbitrary ways. The heat generation curve is then approximated by a number of superimposed step changes of the heat generation and the step-response for each step is calculated from the step-response curve and added together.

The maximum operating temperature for HVDC thyristors is usually chosen lower than for industrial applications. The main reason for this is, that the requirements to sustain short-circuit currents as treated in chapter 8 are more severe for HVDC applications. Figure 9-16 illustrates calculated thyristor junction temperature, valve current and valve voltage for a short-circuit across another valve in the same commutation group. The junction temperature at the moment, when the off-state (forward blocking) voltage starts to build up across the valve, is most critical for this case.

The proper design and manufacturing of the thyristor and the heat sinks is also verified by testing the thyristor

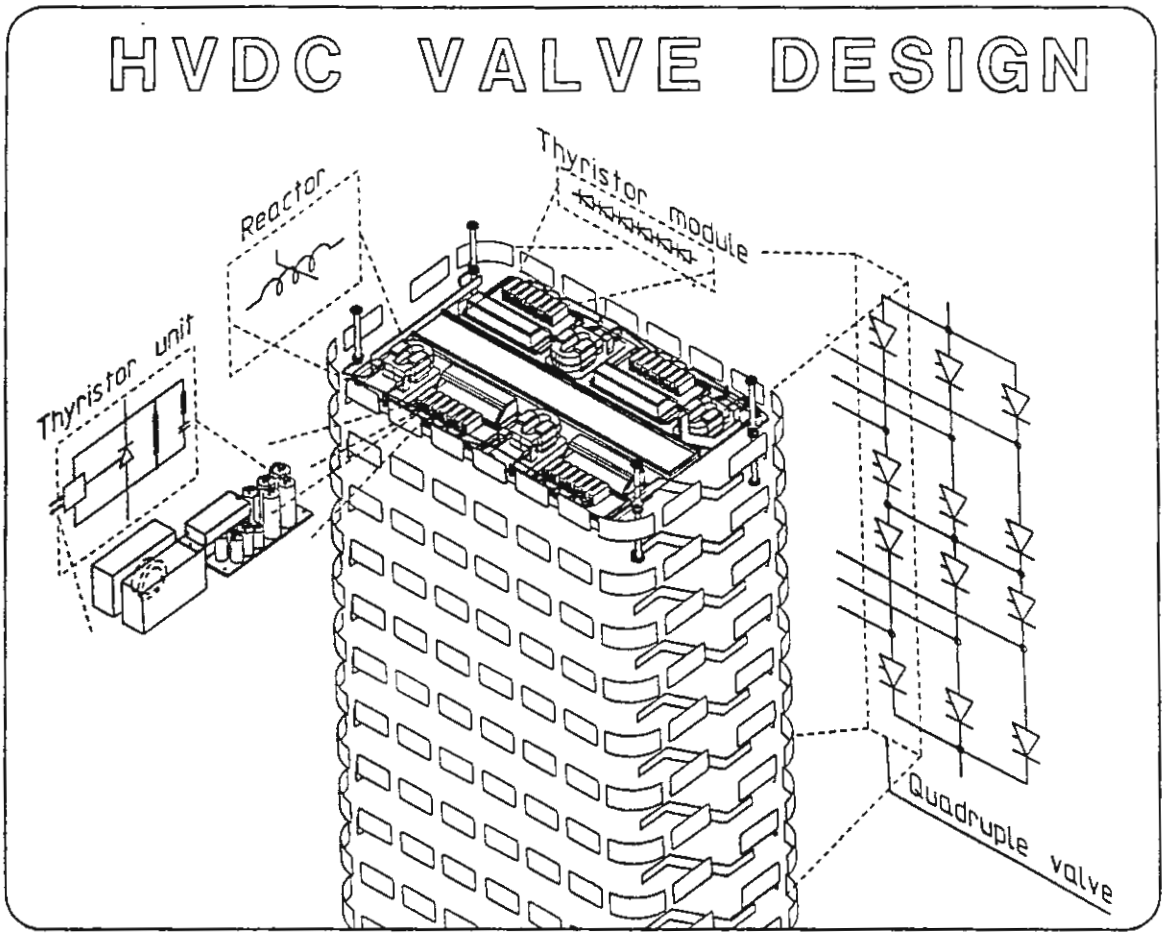

Figure 9-17 Mechanical design of a thyristor valve.

modules for this case. If the thyristors are not properly cleaned and mounted in the module it is very probable that the failure of doing so could give a junction temperature too high resulting in the thyristor not being able sustain the recovering off-state voltage.

9.11 Mechanical design of a thyristor valve

The valves are usually placed indoors in a special valvehall. This means that they are mainly air-insulated and designed for an environment with cleaned air and controlled humidity. It has also been considerd the design of more compact valves by encapsulation in SF_6 gas under high pressure. However, such valves have not yet been offered commercially. The air-insulated valves supplied by different manufacturers are in principle built up in similar ways. The design used by ABB can, because of that, be considered to be fairly representative and will be described below.

The design of a quadruple-valve, which is built up of four single valves placed on top of each other, is illustrated in figure 9-17. Each single valve consists of a number of thyristor modules and reactor units connected in series to obtain the desired number of series connected thyristors. In the design shown in figure 9-17 six thyristors are mounted together in each thyristor module. Each layer of the valve consist of four thyristor modules and four reactors connected in series, i.e. 24, thyristors per layer.

Each thyristor unit, as shown to the left in figure 9-17, function as an independent unit. It consists of a thyristor mounted between two heat sinks, a thyristor control unit (TCU) and snubber circuits. The heat sinks are used in

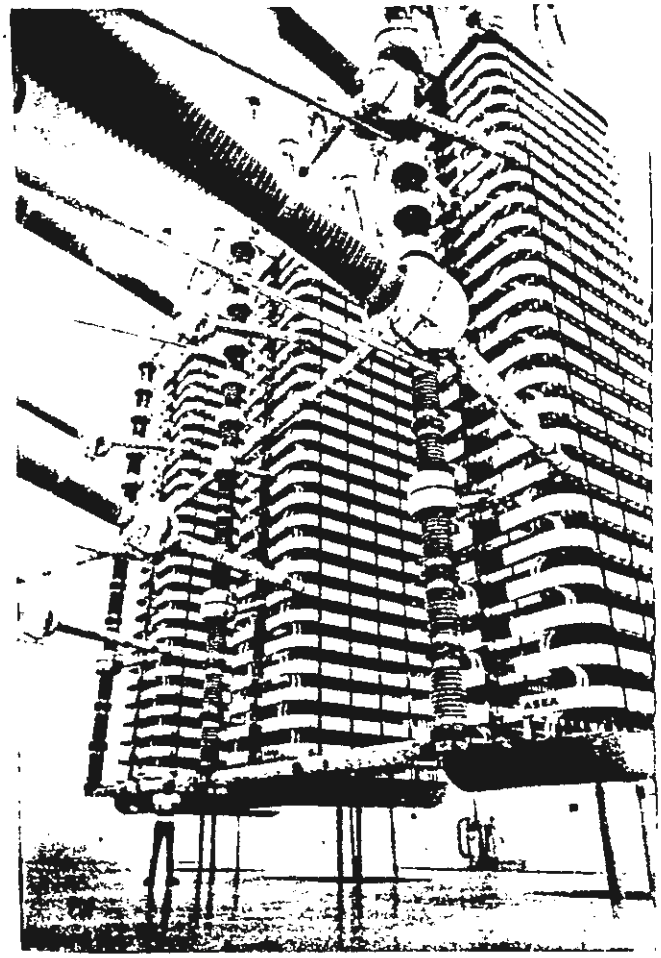

Figure 1-15 Valve hall with suspended water-cooled valves. Intermountain Power Project (IPP), 800 MW and 500 kV per pole.

common with the two adjacent thyristor units.

The valves can either be designed to be mounted on the floor of the valve hall or be suspended from the ceiling of the valve hall.

A suspended design was originally introduced in order to meet the severe seismic requirements for some HVDC converter stations in Western USA. Since the suspended design also turned out to result in lower total cost for the valve-hall and the valves, this design is now commonly also used also for converter stations with no seismic requirements. Figure 1-15 shows a view from a valve hall for the Intermountain Power Project in USA. The three quadruple valves for one 12-pulse converter unit are suspended from the ceiling.

The central valve control and the valve cooling equipment are in this case placed beneath the floor in the basement. The tubes for the cooling water and the optical fibers for control can be seen between the valves and the floor.

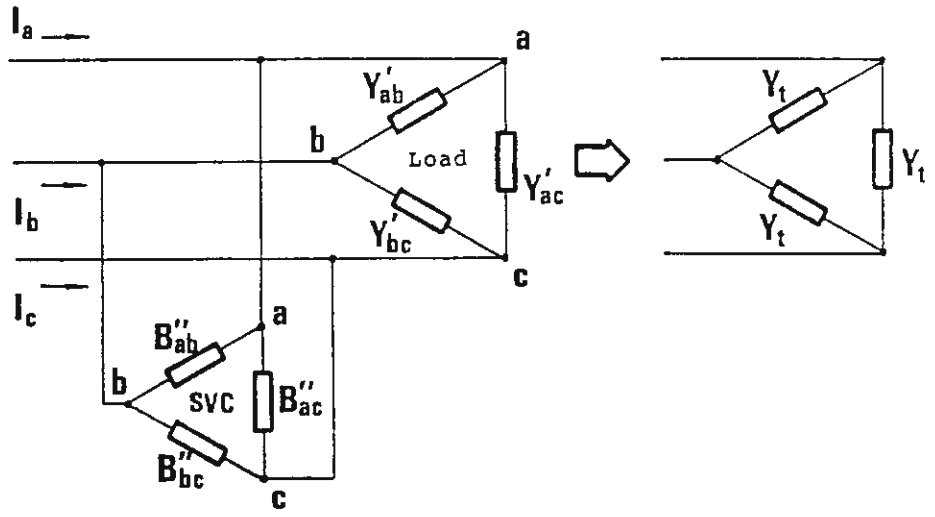

Figure 1-28 Unsymmetrical loads balanced by individual phase control of the SVC.

10 STATIC VAR COMPENSATORS

10.1 General

The basic principles of static var compensators and their applications were treated in chapter 1. A more detailed description of the basic principles including the principles for control will be treated in this chapter. Comparison will be made between the principles used for SVC and for the convertors for HVDC applications. It should be noted that the information presented in chapter 6 for harmonics and filters and in chapter 9 for thyristor valves for HVDC to a great extent also applies for filters and valves for SVC stations with thyristors as switching elements.

10.2 Unsymmetrical operation

A static var compensator of the TCR or TSC type behaves quite different from a convertor at unsymmetrical ac-voltages. An important feature of a TCR and TSR is that each phase can be individually controlled without directly influencing the operation of the units in the other phases. This is not possible for a convertor, for which the operation of the three phases are more inter-dependent. As illustrated in figure 1-28, it is possible to control the susceptances B_{ab}, B_{ac} and B_{bc} for the static var compensator individually in each phase-to-phase unit. The reactive power in each phase-to-phase unit corresponds to the stored energy in capacitors (TSC) or the stored energy in reactors (TCR). For a convertor no equivalent stored energy in the convertor exist. It should be noted, that in principle, the total stored energy in the dc-reactor for a

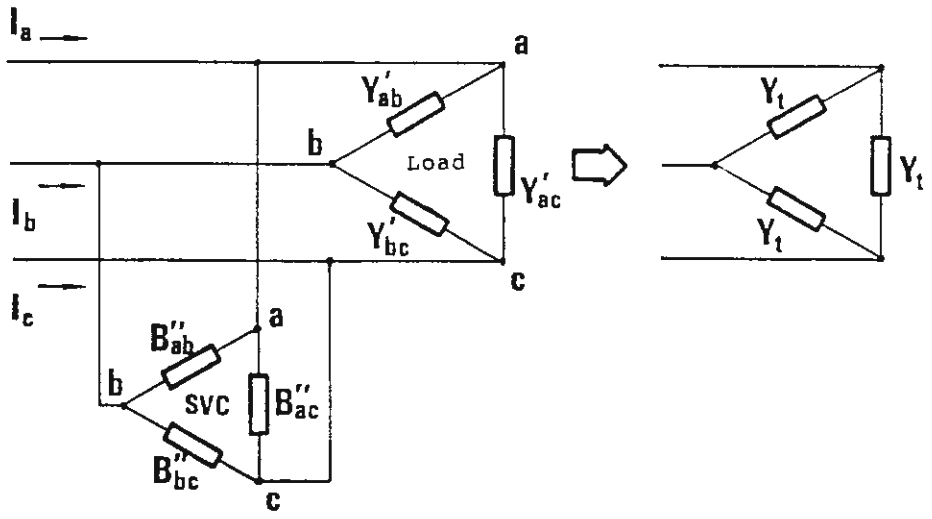

Figure 1-28 Unsymmetrical loads balanced by individual phase control of the SVC.

current-source convertor can be very small, provided a sufficiently high pulse number is used. The current-source convertor can despite that, absorb a high amount of reactive power when operating at $\alpha = 90°$ and a symmetrical ac-voltage. However, it should be noted that the sum of the instantaneous power in the three phases in this case is constant and independent upon the reactive power consumption.

The capabilities of a static var compensator of the TSC or TCR type to control the reactive power individually in each phase can be used to balance out asymmetries, both, in the active and reactive loads, as mentioned in chapter 1. Arc-furnaces and railways could generate such asymmetrical loads.

We will illustrate the balancing of asymmetrical load with figure 1-28. We introduce the following notations:

$$G_{ab} + j\ B_{ab} = G_{ab} + j(B_{ab}' + B_{ab}'') \qquad (10\text{-}1)$$

We will get the corresponding relationships for the other phase-to-phase admittances. We now obtain the following relationship between the phase currents and phase-to-phase voltages.

$$I_a = U_{ab}(G_{ab} + j\ B_{ab}) + U_{ac}\ (G_{ac} + j\ B_{ac}) \qquad (10\text{-}2)$$

Similar equations are obtained for I_b and I_c.

We assume that the ac-voltage will become symmetrical when the total load will be equally large in all phases, as shown in figure 1-28. We can then set:

$$U_{ab} = \sqrt{3} \cdot U_a \cdot e^{j\frac{\pi}{6}} \qquad (10\text{-}3)$$

$$U_{ac} = \sqrt{3} \cdot U_a \cdot e^{-j\frac{\pi}{6}}$$

Insertion of the equations (10-3) into equation (10-2) results:

$$I_a = \sqrt{3}\, U_a \left[(G_{ab} + jB_{ab})\, e^{j\frac{\pi}{6}} + (G_{ac} + j\, B_{ac})\, e^{-j\frac{\pi}{6}} \right] \qquad (10\text{-}4)$$

The corresponding expressions are derived for I_b and I_c through cyclic permutation a ⇒ b ⇒ c ⇒ a etc.

Insertion of

$$e^{\pm j\frac{\pi}{6}} = \frac{\sqrt{3}}{2} \pm j\,\frac{1}{2}$$

into equation (10-4) results:

$$I_a = \frac{\sqrt{3}}{2}\, U_a \left\{ \sqrt{3}\,(G_{ab} + G_{ac}) - B_{ab} + B_{ac} + j\left[\sqrt{3}\,(B_{ab} + B_{ac}) + G_{ab} - G_{ac} \right] \right\} \qquad (10\text{-}5)$$

If we set real components equally large and the imaginary component to zero for I_a, I_b and I_c, we will obtain:

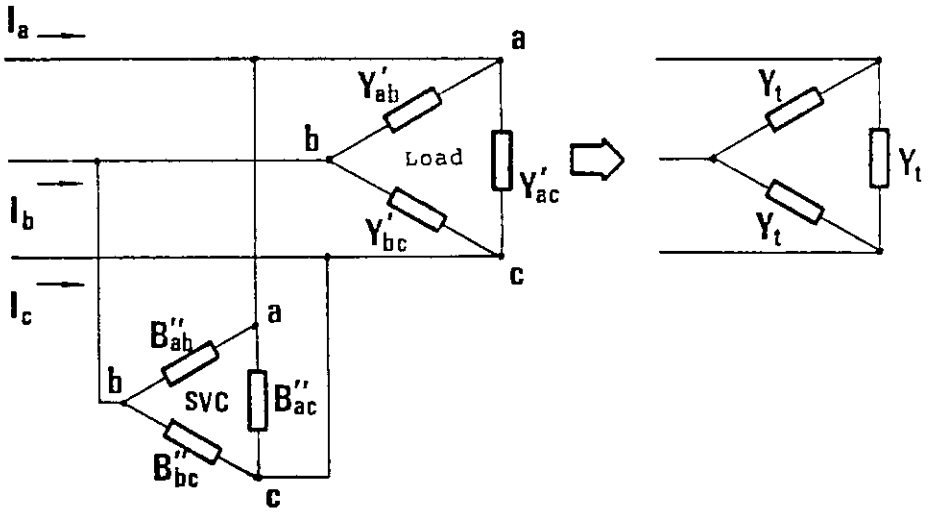

Figure 1-28 Unsymmetrical loads balanced by individual phase control of the SVC.

$$B_{ab} = \frac{G_{ac} - G_{bc}}{\sqrt{3}}$$

$$B_{bc} = \frac{G_{ab} - G_{ac}}{\sqrt{3}} \qquad (10\text{-}6)$$

$$B_{ca} = \frac{G_{bc} - G_{ab}}{\sqrt{3}}$$

When the conditions, according to (10-6) are met, the expression for the phase current I_a, according to equation (10-5), can be modified to

$$I_a = U_a(G_{ab} + G_{ac} + G_{bc})$$

This results in the total phase-to-phase admittances

$$Y_{tab} = Y_{tbc} = Y_{tca} = \frac{G_{ab} + G_{ac} + G_{bc}}{3} \qquad (10\text{-}7)$$

The equations (10-1) and (10-6) that the conditions below have to be met to obtain a symmetrical resistive total load for the circuit, as shown in figure 1-28.

$$\begin{aligned} B_{ab_{"}}^{"} &= -B_{ab,}^{'} + (G_{ac,}^{'} - G_{bc,}^{'})/\sqrt{3} \\ B_{bc_{"}}^{"} &= -B_{bc,}^{'} + (G_{ab,}^{'} - G_{ac,}^{'})/\sqrt{3} \\ B_{ca}^{"} &= -B_{ca}^{'} + (G_{bc}^{'} - G_{ab}^{'})/\sqrt{3} \end{aligned} \qquad (10\text{-}8)$$

It will of course not be necessary to compensate for the reactive loads in order to obtain a symmetrical total load. We will still get a balanced total load if all the susceptances, according to equation (10-8), are increased or decreased with the same amount.

10.3 Thyristor switched capacitors

The basic principles for the thyristor switched capacitor

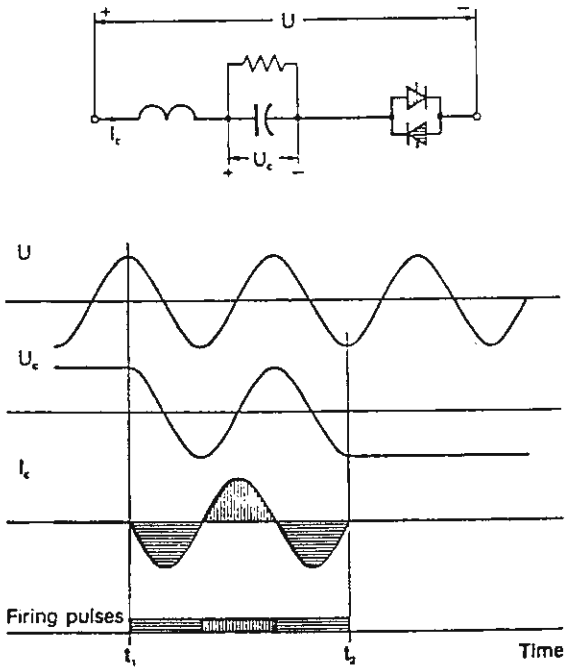

Figure 1-31 Thyristor switched capacitors (TSC), functional principle.

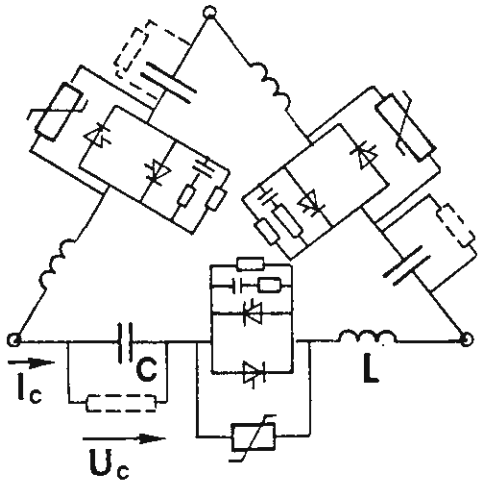

Figure 10-1 Thyristor Switched Capacitor. Δ-connection.

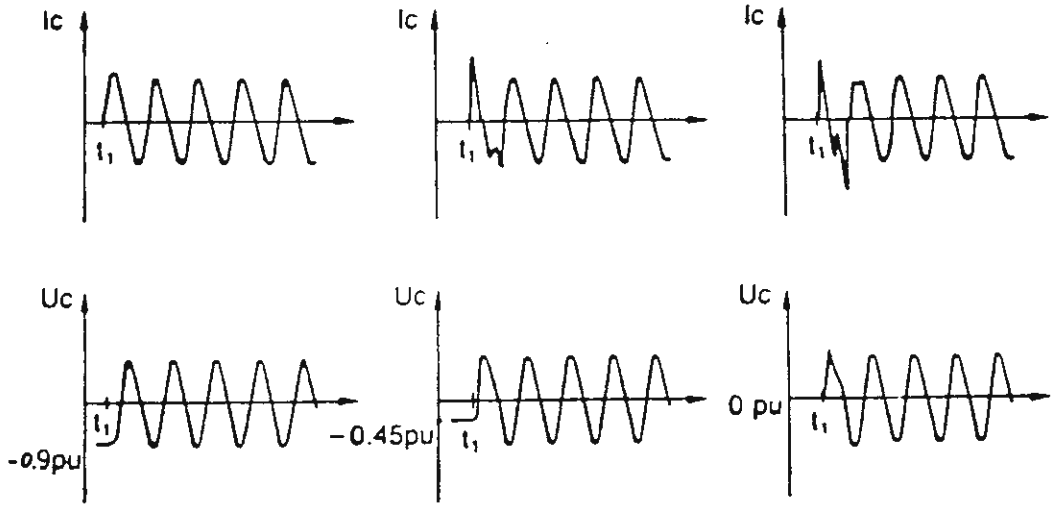

Figure 10-2 Turn-on of the thyristors of a TSC unit of different phase-positions.

was presented in chapter 1 and figure 1-31. The TSC units are usually connected in a Δ-connection, as shown in figure 10-1. Discharge resistors across the capacitors as well as damping circuits and arresters across the valves are also shown in the figure. Reactors are connected in series with the capacitors and the valves to limit the turn-on currents in case the initial voltages of the capacitors differ from the ac-voltage at the turn-on of the thyristors. This is further illustrated in figure 10-2, showing the capacitor current, when the turn-on takes place at different phase-positions. It is here assumed that the capacitance before turn-on is pre-charged to an ac-voltage, which is almost equal to the amplitude of the ac-voltage.

The control system of the TSC is arranged for firing of the thyristor valves at the correct time. However, the thyristors and the capacitors have to be rated for energization at the most unfavourable phase-position.

The magnitude of the reactor connected in series with the capacitor is chosen such, that resonance at the 5th harmonic is avoided and the maximum surge currents at unfavourable energization are limited. This usually implies that a resonance frequency is chosen close to $4.5 \cdot \omega_1$ where ω_1 is the ac-network fundamental angular frequency i.e.

$$\frac{1}{\sqrt{LC}} = 4.5 \cdot \omega_1$$

The thyristor switched capacitor is usually connected to the ac-network through a transformer in order to limit the rated voltage across the capacitor to about 10 kV (max. 30 kV).

The thyristors are of a similar design as those used for

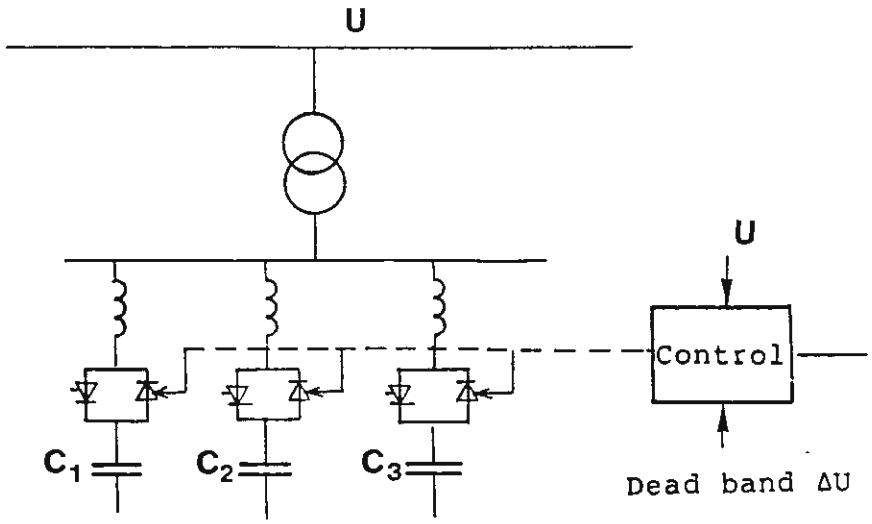

Figure 10-3 Static var compensator consisting of three thyristor switched capacitor units.

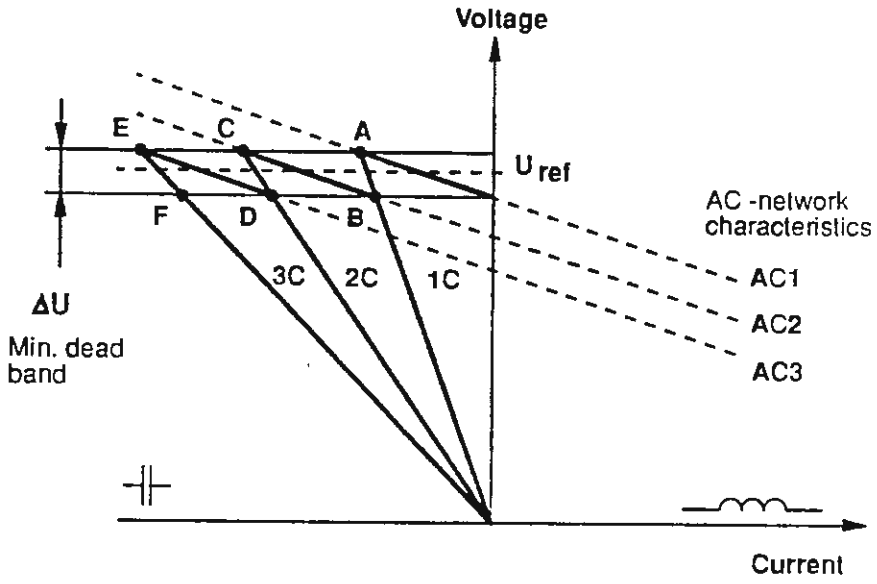

Figure 10-4 Voltage-current characteristics for a static var compensator of the TSC type.

HVDC valves. Minimization of the losses are important also for this application. However, as the thyristors are turned-off at the normal zero-crossing of the current, the stresses at recovery are less critical and thyristors with high recovery times and recovery charges can be used in order to reduce the on-state losses.

The gate-pulses to the thyristors can usually be generated via transformers (magnetic firing) since the maximum voltage to ground is limited. This could be compared to the optronic system used for HVDC valves for which the voltage to ground is mostly much higher.

It might in principle be possible to protect the thyristors against voltage stresses, which are too high, by protective firing as two thyristors are connected in parallel with reverse polarity, i.e. there is always one thyristor that can be turned-on and protect both thyristors against voltages, which are too high. However, in practice this is not feasible for thyristor switched capacitors as a protective firing of the thyristors at a too high overvoltage would cause a high risk for the turn-on of the thyristors at the wrong phase-position. The thyristors are, because of that, protected with zinc-oxide arresters connected across the thyristors.

A static var compensator of the TSC type is built up of a limited number of TSC units, e.g., three, as illustrated in figure 10-3. An increased number of units would improve the control of the reactive power but would also result in increased cost. This shows the output characteristic of the switched capacitor, as shown in figure 10-4. The actual operating point (A-F) will be determined by the crossing point between the voltage-current characteristic of the ac-network and the voltage-current characteristic of the TSC. In figure 10-4 three different characteristics for the ac-network have been assumed, all having the same slope but

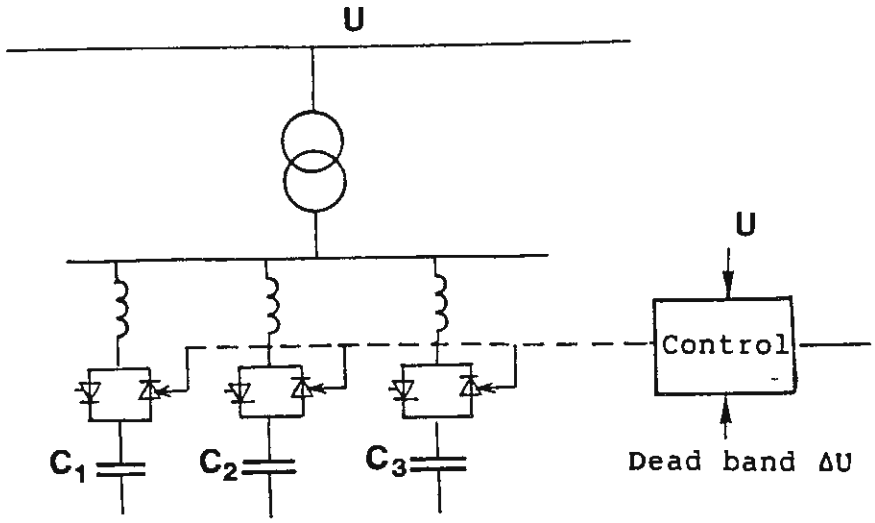

Figure 10-3 Static var compensator consisting of three thyristor switched capacitor units.

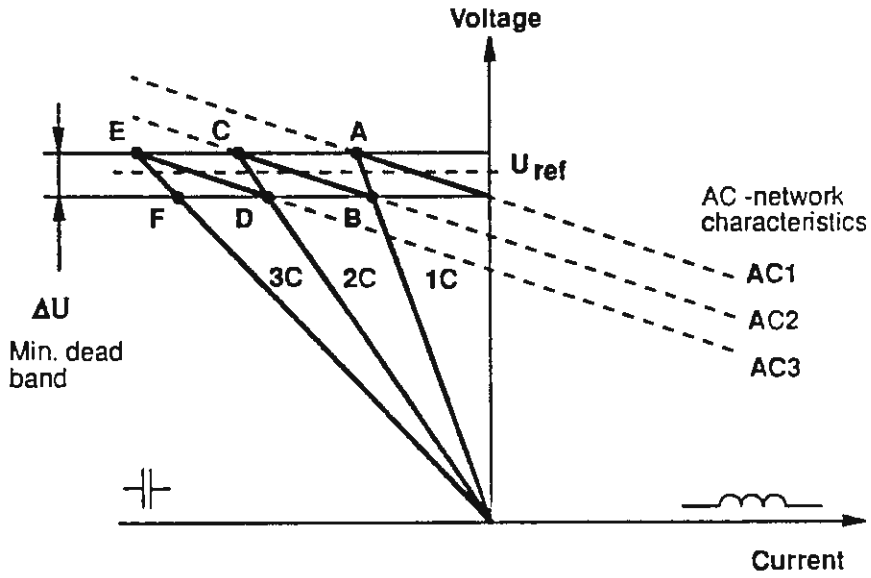

Figure 10-4 Voltage-current characteristics for a static var compensator of the TSC type.

different voltage levels. Since the impedance of the ac-network is normally inductive, an increase in the capacitive current from the compensator will cause an increase of the ac-bus voltage. We will get the operating point A, if we now assume that only one TSC unit is connected and the ac-network has a characteristic according to ac 1. A drop in the ac-network, e.g., caused by an increased load, that causes the ac-network characteristic to be changed to ac 2, will result in a new operating point at B, if only one TSC unit is still connected. When the voltage now drops further, the control might order the next TSC unit to be connected, which results in the new operating point.

The change in reactive power generation will occur in steps, implying that the voltage control also will also be performed in steps. A dead-band (ΔU) has to be introduced in the control to avoid hunting.

The speed of the control might, in principle, be performed very quickly with a delay of only half a cycle. However, in practice a somewhat slower control system has to be used to also take the measuring time into account and to get a stable system.

A thyristor switched capacitor will not generate any harmonics, as the capacitor is connected during an integer number of half-cycles. However the risk for resonance between the capacitors and the inductances in the network however has to be considered.

The losses are fairly small for a TSC unit and are mainly determined by the losses in the thyristors and to some extent by the losses in the transformers, if used. The losses in the capacitors are with modern full-film capacitors very small. The losses are, because of that, almost proportional to the generation of reactive power.

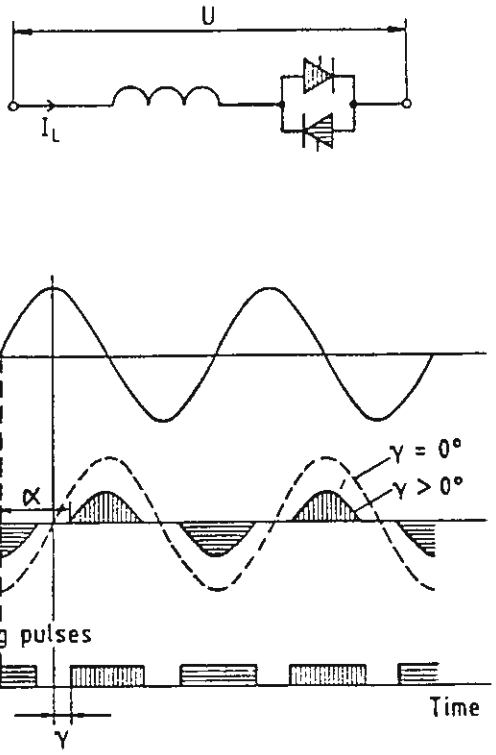

Figure 1-33 Thyristor controlled reactor, functional principle.

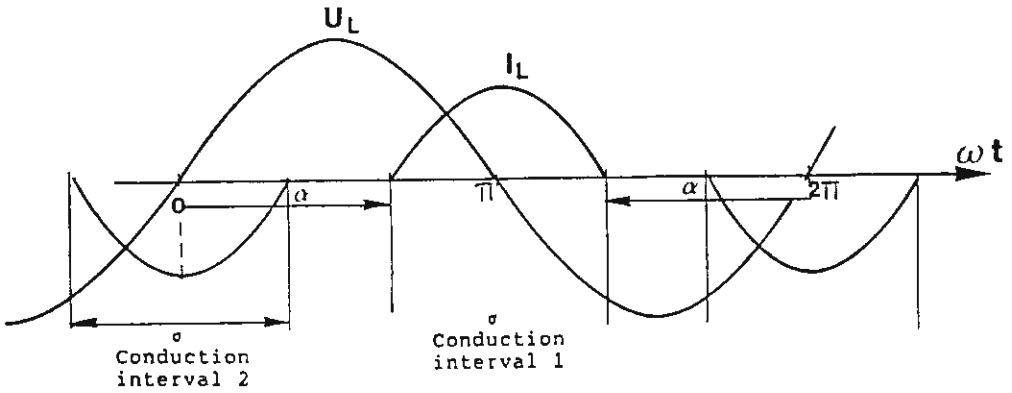

Figure 10-5 Voltage and current for a thyristor controlled reactor, TCR.

10.4 Thyristor controlled reactor. TCR

The basic principles of the thyristor controlled reactor was described in chapter 1 and figure 1-33. The possibility of continuously controlling the susceptance is mostly utilized. The firing angle α is defined relative to the zero-crossing of the voltage. This implies an operation range for α equal to $90° \leq \alpha \leq 180°$ or $\pi/2 \leq \alpha \leq \pi$ rad. The maximum current or maximum susceptance is achieved at $\alpha = 90°$ resulting in a susceptance $B_s = -1/X_L$ where $X_L = \omega L$. The current and the susceptance will decrease at larger values of α. Instead of giving the firing angle α i.e.the conduction angle σ, the length of the conduction or on-state interval is specified as shown in figure 10-5. The following relationship then applies:

$$\alpha + \sigma/2 = \pi \qquad (10\text{-}9)$$

Calculation of the fundamental frequency current and the harmonic currents

The calculation of the fundamental frequency current and the harmonic currents, as a function of the firing angle α, will be based on figure 10-5. The zero-crossing of the voltage $U_L(t)$ used as the zero reference for the angular ωt. The following expression is derived for the voltage:

$$u_L(t) = \hat{U}_L \cdot \sin \omega t \qquad (10\text{-}10)$$

During the two conduction or on-state intervals of the thyristor valves:

1) $\alpha < \omega t < 2\pi - \alpha$, and 2) $\pi + \alpha < \omega t < 3\pi - \alpha$,

the following relationship is valid:

$$L \cdot di_L/dt = \hat{U} \cdot \sin \omega t \qquad (10\text{-}11)$$

This results for interval (1):

$$i_L(t) = \frac{\hat{U}_L}{\omega L} (\cos \alpha - \cos \omega t) \qquad (10\text{-}12)$$

and for interval (2):

$$i_L(t) = - \frac{\hat{U}_L}{\omega L} (\cos \alpha + \cos \omega t) \qquad (10\text{-}13)$$

A Fourier analysis will only result in odd harmonics since $i(t) = - i(t + 1/2\ T)$ and only cosine-terms since $i(t) = i(-t)$. It is thus sufficient to integrate from $\omega t = \alpha$ to $\omega t = \pi$ in order to determine the Fourier coefficients. This results:

$$a_n = \frac{4}{\pi} \int_{\alpha}^{\pi} i_L \cdot \cos(n\omega t) \cdot d(\omega t) \qquad (10\text{-}14)$$

Insertion of $i_L(t)$, according to equation (10-12) gives:

$$a_n = \frac{2\ \hat{U}_L}{\pi \cdot \omega L} \int_{\alpha}^{\pi} \left[2 \cos\alpha \cdot \cos(n\omega t) - \cos[(n+1)\omega t] - \cos[(n-1)\omega t]\right] d(\omega t) \qquad (10\text{-}15)$$

Insertion of $n = 1$ in equation (10-15) gives

$$a_1 = - \frac{\hat{U}_L}{\pi\omega L} \left[\sin 2\alpha + 2(\pi - \alpha)\right] \qquad (10\text{-}16)$$

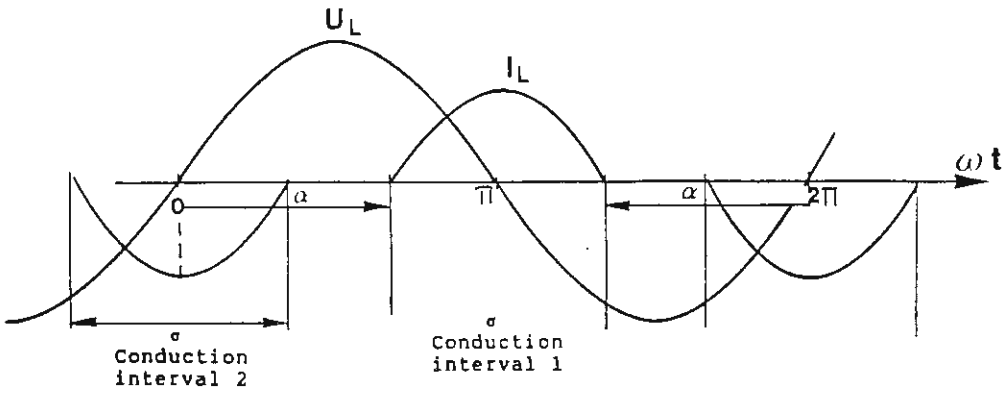

Figure 10-5 Voltage and current for a thyristor controlled reactor, TCR.

This results in the amplitude of the fundamental current being:

$$\hat{I}_{L1} = |a_1|$$

and that the susceptance is

$$B(\alpha) = - \frac{2(\pi-\alpha) + \sin 2\alpha}{\pi \cdot X_L} \qquad (10\text{-}17a)$$

This equation could alternatively be written as a function of the conduction angle σ, according to figure 10-5, and equation (10-9), which gives:

$$B(\sigma) = - \frac{\sigma - \sin\sigma}{\pi \cdot X_L} \qquad (10\text{-}17b)$$

Insertion of $\alpha = \pi/2$ or $\sigma = \pi$ in equation (10-17a) and (10-17b), respectively, will of course result:

$$B = - 1/X_L$$

Equation (10-15) will for $n > 1$ result:

$$\hat{I}_{Ln} = \frac{2\hat{U}_L}{\pi \cdot \omega L} \left\{ - \frac{2 \cos\alpha \cdot \sin(n\alpha)}{n} + \frac{\sin\left[(n+1)\alpha\right]}{n+1} + \frac{\sin\left[(n-1)\alpha\right]}{n-1} \right\} \qquad (10\text{-}18)$$

Equation (10-18) can be simplified to

$$\hat{I}_{Ln} = \frac{2\hat{U}_L}{\pi \cdot \omega L \cdot n} \left[\frac{\sin(n-1)\alpha}{n-1} - \frac{\sin(n+1)\alpha}{n+1} \right] \qquad (10\text{-}19a)$$

or alternatively to

$$\hat{I}_{Ln} = \frac{4\ \hat{U}_L}{\pi \cdot X_L \cdot n(n^2-1)} \left[\cos\alpha \cdot \sin(n\alpha) - n \cdot \sin\alpha \cdot \cos(n\alpha) \right] \qquad (10\text{-}19b)$$

The following expression will thus be derived for the instantaneous value of the n^{th}- harmonic:

$$i_{Ln} = \hat{I}_{Ln} \cdot \cos(n\omega t) \qquad (10\text{-}20)$$

The corresponding instantaneous values are derived for the other two phases by replacing ωt by $\omega t - 2\pi/3$ and $\omega t + 2\pi/3$, respectively, in equation (10-20). From this it is obvious, that odd harmonics, where $n = 6m + 1$, have a positive phase-sequence character and, where $n = 6m - 1$, have a negative phase-sequence character. All harmonics, where $n = 6m - 3$, are of zero phase-sequence character ($m = 1,2,3$ etc). Harmonics being odd multipliers of three, i.e. harmonics of order $n = 3, 9, 15$ can, because of that, be eliminated by a Δ-connection when the ac-voltages are symmetric.

It should be noted, that it is not possible to obtain a symmetric alternating current of an asymmetric ac-voltage for a thyristor controlled reactor in a similar way as for a current-source convertor. To make the time intervals between succeeding firings equally large, i.e. equidistant firing, would only increase the asymmetries between the currents for a thyristor controlled reactor. The

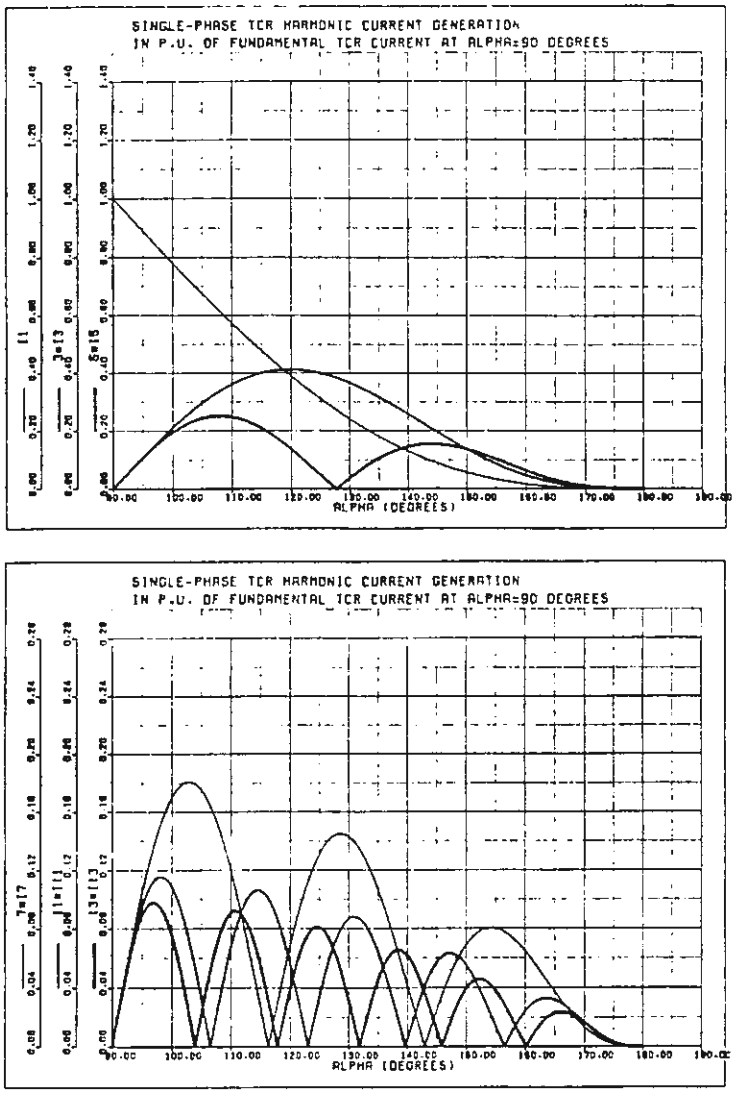

Figure 10-6 Single-phase TCR. Fundamental and harmonic current in p.u. of the fundamental TCR current at α=90°.

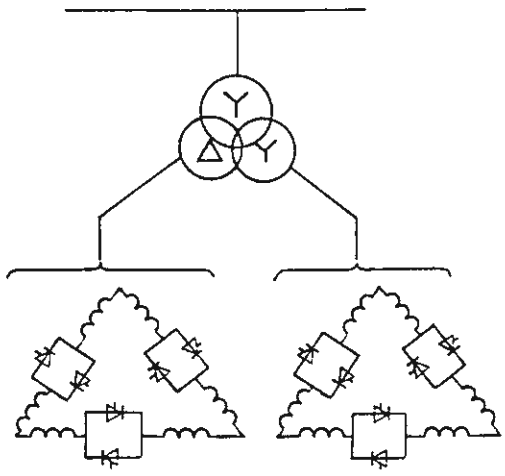

Figure 10-7 12-pulse TCR.

phase-position of the current will be fully determined by the phase position of the voltage. Different values of the firing angles α would give different magnitudes of the currents in the three phases.

The relationships according to the equations (10-16) and (10-19), for the fundamental current component and the harmonics respectively, are illustrated in the figure 10-6. The currents are shown in p.u of the fundamental current at $\alpha = 90°$, i.e., $\hat{U}_L/\omega_1 L$.

It should be noted, that while the harmonic currents of a convertor decrease inversely proportional to the order of the harmonic number n, they will for a TCR unit decrease approximately inversely proportional to the harmonic number square $\left(\frac{1}{n^2}\right)$.

The harmonics generated and injected into the ac-network can be limited by installation of harmonic filters in a similar way as for HVDC convertors. This is specially feasible, when the TCR is combined with a fixed capacitor bank for generation of reactive power. The capacitor unit can then partly or completely be designed as a filter.

The amount of harmonics can also be decreased by the splitting of the TCR in two units of which one is connected to the ac-network through a Y - Y connected transformer and the other through a Y - Δ connected transformer as shown in figure 10-7. The primary winding could be common as shown in the figure. This results in a 12-pulse connection resulting in the harmonics of the order 5, 7, 17, 19 being eliminated at symmetrical operation. An alternative way of reducing the amount of harmonics for two TCR units is to only use one of the units for the control of reactive power, while the other unit is either operating at $\alpha = 90°$, i.e., maximum current, or at 180°, i.e., no current.

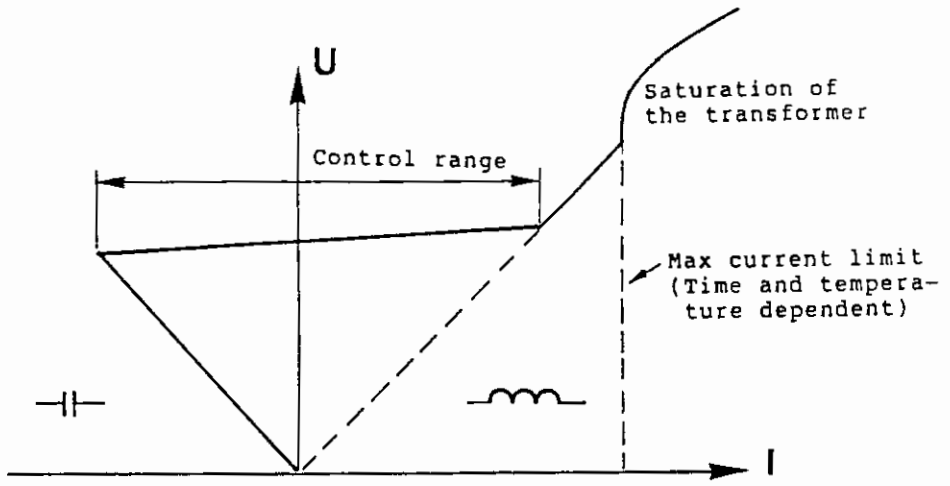

Figure 10-8 Voltage-current characteristics for a thyristor controlled reactor with a capacitor bank.

Voltage-current characteristic

Figure 10-8 shows a typical voltage-current characteristic for a static var compensator consisting of a thyristor controlled reactor (TCR) combined with a fixed capacitor. The capacitor can be connected via a circuit switch and is mainly only switched in, when reactive power has to be generated (left part of the diagram). In order to obtain a continuous control of the reactive power around zero and to avoid many switching operations the capacitor will even at increased absorption of reactive power not be immediatly switched out, when the SVC units starts to absorb reactive power.

The slope of the characteristics within the range for continuous control of reactive power is set within the range of 0 - 5%.

The control can, theorectically, be designed to be very fast as the firing angle values for each phase can be set twice per cycle. However, in practice some limitations in the control speed have to be included in order to get a stable system. Typical response times are of the order of 3-10 cycles. The ac-impedance is a critical parameter for the setting of the speed of the control systems as the amplification of the control depends upon the network impedance. Temporary disconnection of ac-lines can result in a corresponding temporary increase of the ac-network impedances and can thus be critical for the stability of the control system. This will be treated further in section 10.6

A thyristor controlled reactor usually has a short-time overload capability outside the normal control range, as

illustrated in figure 10-8. This is an important feature for the limitation of temporary overvoltages, e.g., caused by sudden load rejections. However, at overload currents, which can give stresses which are too high on the thyristors and the reactors, the current can be limited by increasing the firing angle α. This causes the steep increase in the voltage characteristic of currents above the maximum overcurrent limit.

Thyristor valves

The same type of thyristor valves could be used for thyristor controlled reactors as for thyristor switched capacitors. Snubber circuits have to be connected across each thyristor to attenuate the voltage transients at the current extinction and to obtain a proper voltage distribution between thyristors connected in series. The current stresses on the thyristors at the turn-on of the thyristors will be smaller than for thyristors in valves for HVDC, since the TCR thyristor valves are always connected in series with reactors and since the voltage level is much lower resulting in less influence of stray-capacitances.

There is also no risk for high short-circuit currents for thyristor controlled reactors comparable to what could be obtained for HVDC valves, as each valve is connected in series with reactors. Because of that a higher operating temperature of the thyristor could be used for the TCR valves than for HVDC valves.

The thyristors can be protected against overvoltages which are too high by protective firing since two thyristors with opposite polarity are always connected in parallel. In contrast to the valves for thyristor switched capacitors there are no disadvantages in firing the valves at

SVC CONTROL SYSTEM

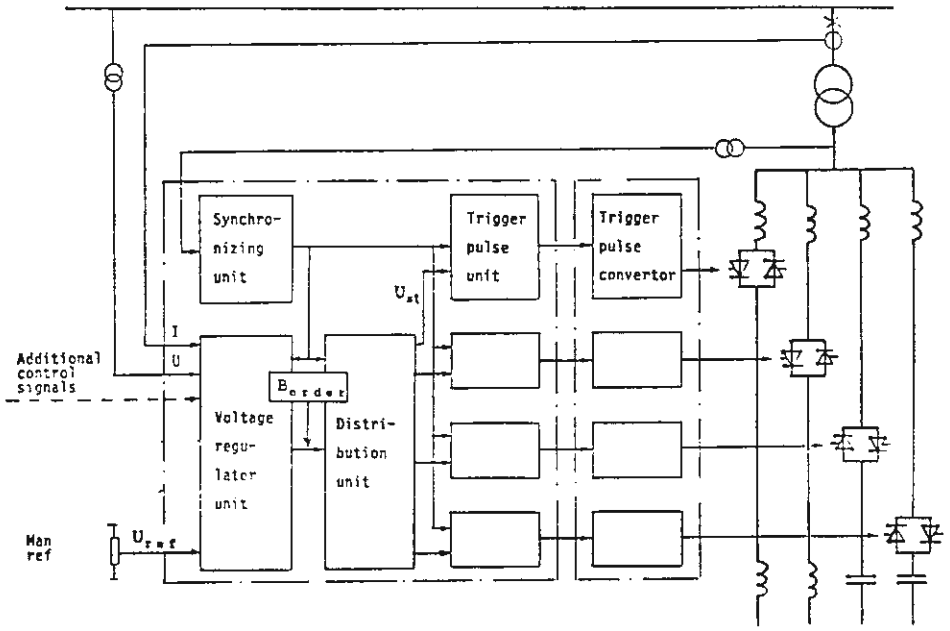

Figure 10-9 SVC control system.

overvoltages of limited duration since connection of the reactor will decrease the overvoltage.

Thyristor controlled reactors are usually connected to the ac-network via transformers. This makes it possible to choose an optimal voltage on the reactor side, which often turns out to be 10-20 kV. The electrical gate pulse to the thyristors can for this voltage be transmitted via pulse transformers (magnetic firing). When no transformers are used and the voltage turns out to be too high for magnetic firing optical fibres are used for the transmission of the firing pulses as for HVDC valves. The thyristors might then be either electrically triggered or directly triggered with light. In the former case an optical firing pulse is transformed to an electrical pulse in thyristor control units in a similar way as described for HVDC valves.

10.5 Control system

The basic principles for a commonly used control system of a static var compensator will be described shortly in this section. The dynamic characteristics will be described in the following section.

The control system is nowadays usually realized with micro-processors. The basic principles will be described based on figure 10-9, which shows a static var compensator with two thyristor switched capacitor units and two thyristor controlled reactor units. It is assumed that one of the thyristor controlled reactor units is used to obtain continuous control of the reactive power, while the other is controlled either at $\alpha = 90°$ or at $\alpha = 180°$. We will make the simplified assumption that the three phases are controlled independently.

The voltage regulator unit can be regarded as the higher

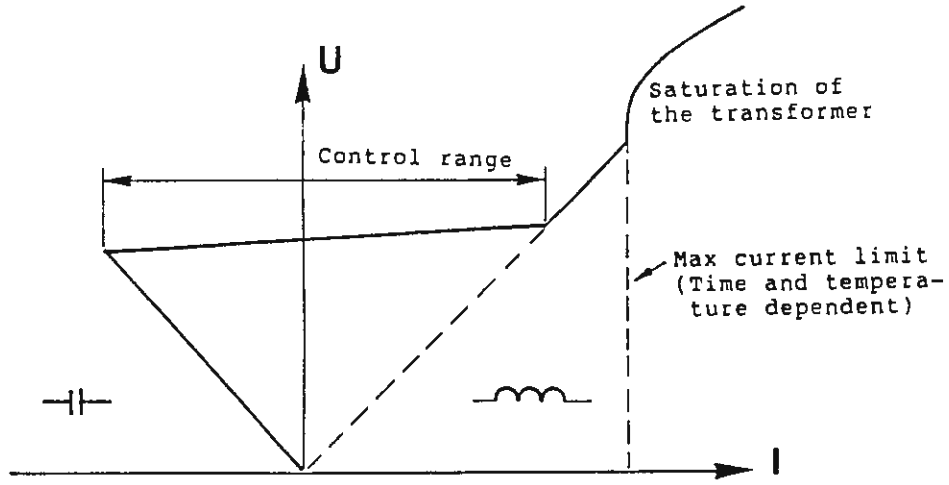

Figure 10-8 Voltage-current characteristics for a thyristor controlled reactor with a capacitor bank.

order control unit. The value of the desired reference voltage U_{ref} is assumed to be manually set. It is of course also possible to set the desired reference voltage in a dispatch center and transmit the U_{ref} order to the SVC unit as a coded telephone signal. The U_{ref} signal could also be made dependent upon some other signals and, for instance, controlled to improve the damping in the ac-network. The measured ac-bus voltage and the static var compensator current are fed to the voltage regulator units.

A continuous controllable static var compensator, as previously described, has a steady-state voltage-current characteristic, as shown in figure 10-8. This is defined by the reference voltage and slope. The linear part between maximum capacitive current and maximum inductive current when the firing angle reaches $\alpha = 90°$, can be described by the following expression:

$$U = U_{ref} + X_{SL} \cdot I_s \qquad (10\text{-}21)$$

The slope reactance X_{SL} determines how the static var compensator current I_s depends on the measured ac-bus voltage U. The slope in per unit is usually of the order 0 - 0.05. The current I_s is defined positive for inductive current, i.e., when the static var compensator absorbs reactive power.

The regulation is mainly of the integrating type with the ordered susceptance as an output signal. This results in the following Laplace expression for the ordered susceptance B_{order}

$$B_{order} = (U_{ref} + X_{SL} \ I_S - U) \ K_s/s \qquad (10\text{-}22)$$

Since the switching of the TSC units are always made at the peak value of the ac-voltage and since the firing of the thyristors for the TCR units at the earliest can be

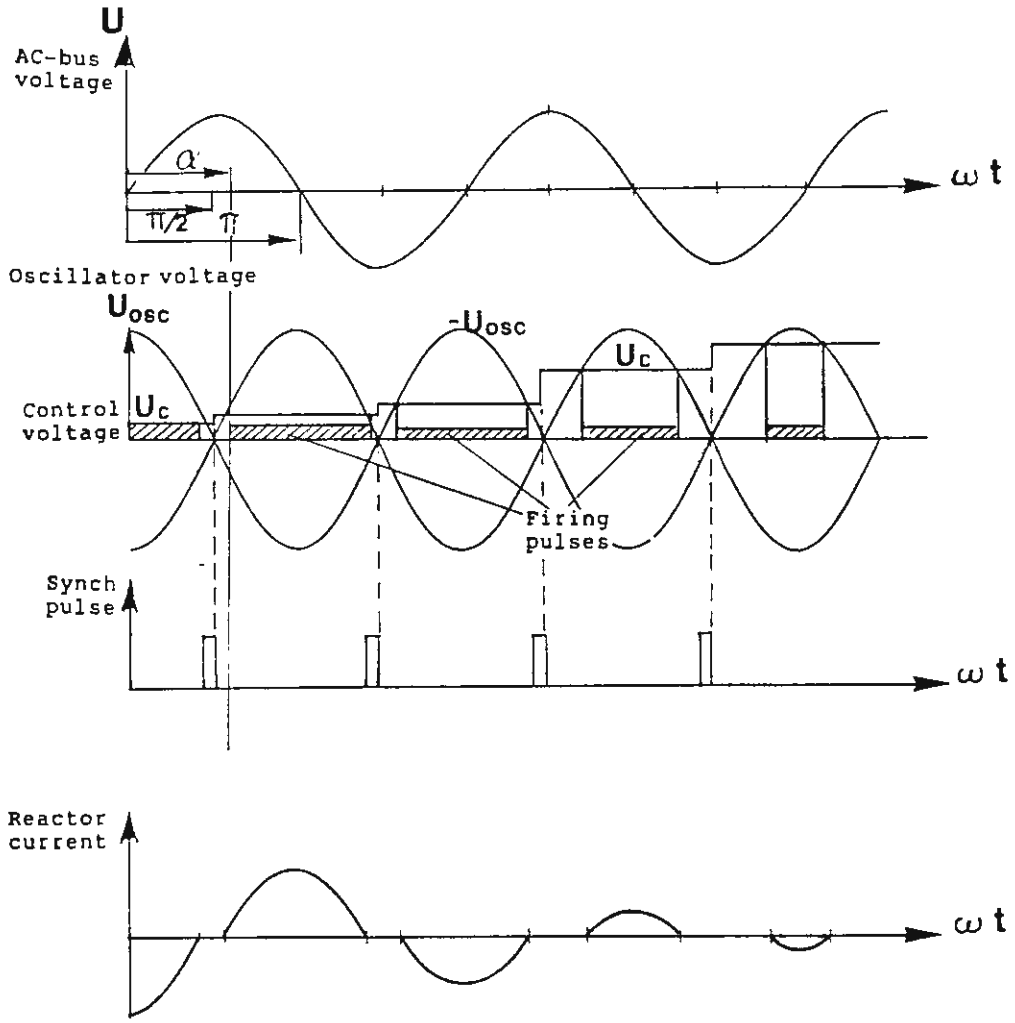

Figure 10-10 AC-bus voltage, oscillator-voltage, synchronizing pulses, control voltage, firing pulses and reactor current.

performed at this point, decision about control actions for the following half cycle will be taken just before the voltage peak will occur. The operation of the control system will, because of that, be synchronized from a synchronizing unit. The basic unit of the synchronizing unit is a phase-locked oscillator. It generates an ac-voltage with fixed amplitude, $\hat{U}_{osc}$, which is phase-locked 90° after the ac-voltage U (See figure 10-10). The sychronizing unit will also generate short synchronizing-pulses immediately before the zero crossings of the oscillator voltage.

The output value from the voltage regulator, i.e., a new ordered value for the susceptance, is fed to the distribution unit when a new synchronizing pulse is received. The distribution unit now determines, which static var unit that shall be switched in during the next half-cycle and sets the value of the ordered susceptance on the active TCR unit (B_{Lorder}). The distribution unit also has to keep track of the energization states of the thyristor switched capacitors to avoid the possibility of seeing energized at the opposite polarity of the voltage.

The output signal (U_{st}) from the distribution unit to the trigger pulse unit for the TCR is not directly proportional to B_{Lorder}, but is determined by the following relationship.

$$U_{st} = \frac{B_{Lmax} - B_{Lorder}}{B_{Lmax}} \cdot \hat{U}_{osc} \qquad (10\text{-}23)$$

B_{Lmax} is the susceptance of the TCR unit at $\alpha = 90°$ and $\hat{U}_{osc}$ is the amplitude of the oscillator voltage. This shows that $U_{st} = 0$ for $B_{Lorder} = B_{Lmax}$ ($\alpha = 90°$) and $U_{st} = \hat{U}_{osc}$ for $B_{Lorder} = 0$ ($\alpha = 180°$). A comparison is made in the triggering unit between voltages U_{st} and U_{osc} and a firing pulse is generated to the valves, when $U_{osc} > U_{st}$ and U_{osc}

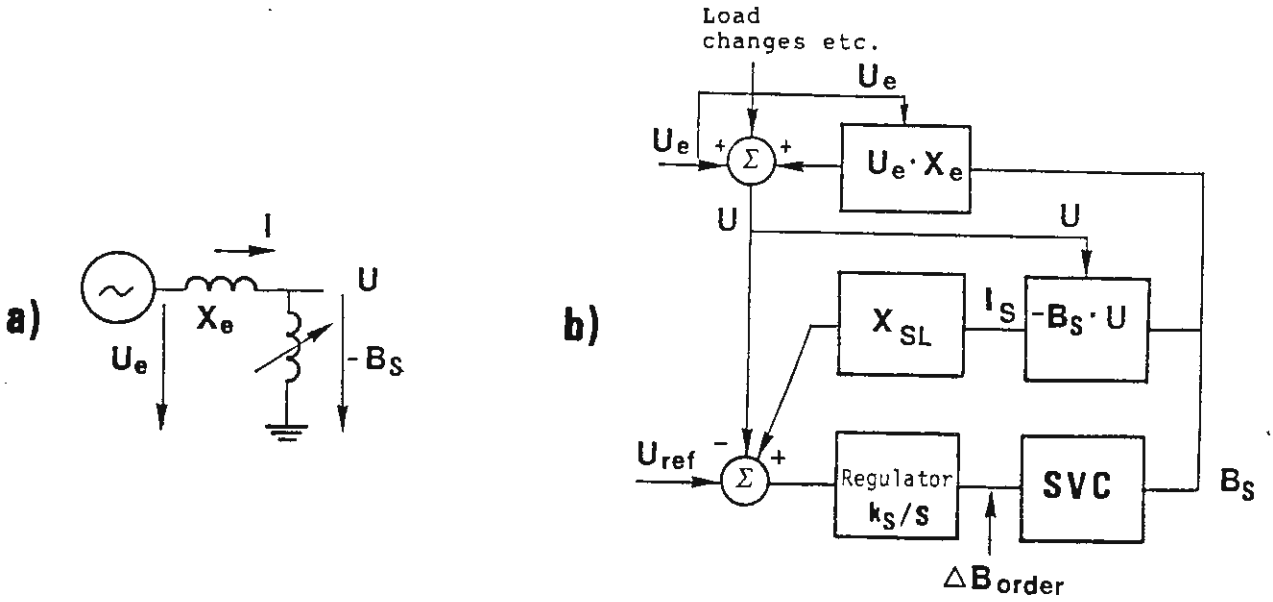

Figure 10-11 Simplified circuit-diagram and block-diagram for voltage control with a static var compensator
a) Circuit diagram
b) Block diagram

$< -U_{st}$, respectively, as illustrated in figure 10-10.

This shows that the firing pulses are generated at $\alpha = 90°$, or $\pi/2$ rad for $U_{st} = 0$, which gives $B_L = -1/X_L$, and at $\alpha = 180°$ or π rad for $U_{st} = U_{osc}$, which gives $B_L = 0$. The control principle described above would, for a pure sinusoidal voltage from the oscillator, give a firing angle determined by the following relationship:

$$\frac{U_{st}}{U_{osc}} = \sin(\alpha - \frac{\pi}{2}) \qquad (10\text{-}24)$$

The susceptance of the TCR unit for the fundamental frequency is, on the other hand, determined by equation (10-17). A comparison between equations (10-23), (10-24) and (10-17) shows, that the presented control principle will not give a linear relationship between B_{Lorder} and B_L. B_{Lorder} will only be equal to B_L for two points, which here were chosen to be at $\alpha = 90°$ and at $\alpha = 180°$. For the intermediate points we find that $|B_L| < |B_{Lorder}|$. One way to improve this could be by including a certain distortion in the voltage from the oscillator making the crest of the wave-shape flatter. Modern control systems are, on the other hand, realized with microprocessors, which makes it possible to calculate the correct firing angle based on the equation (10-17).

10.6 The dynamic characteristics of the voltage control system

The dynamic characteristics of the voltage control system can be analyzed based on the simple circuit diagram according to figure 10-11a. We will assume that the ac-network, as seen from the static var compensator, can be represented by a Thevenin-equivalent consisting of the internal voltage U_e and the reactance X_e which is assumed

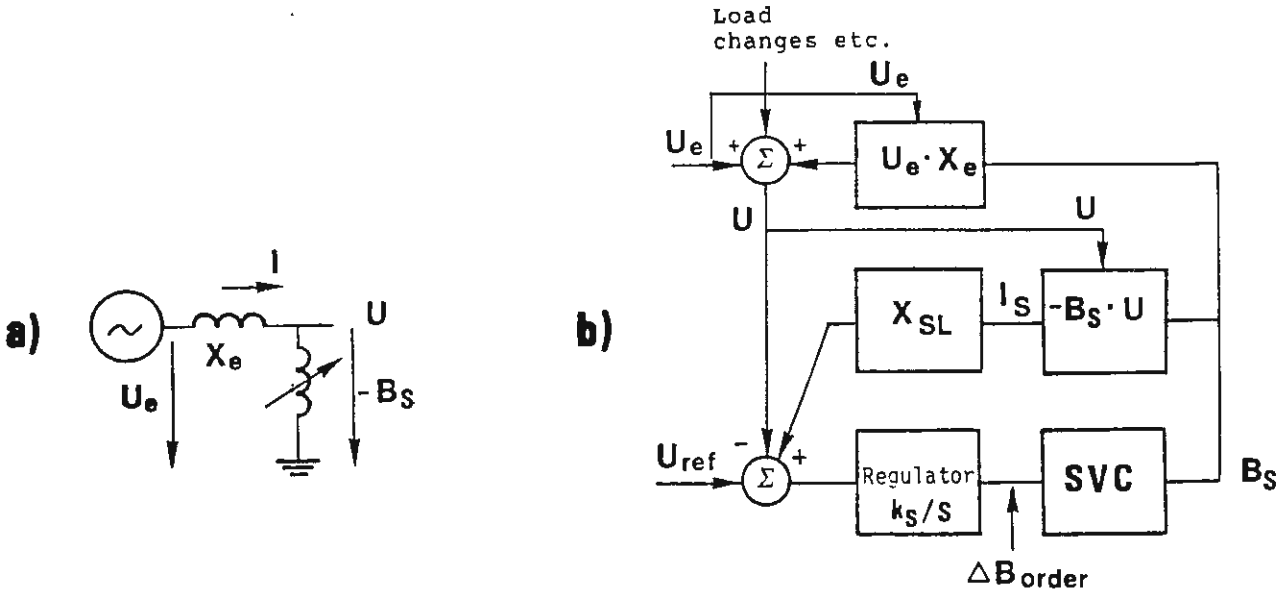

Figure 10-11 Simplified circuit-diagram and block-diagram for voltage control with a static var compensator
a) Circuit diagram
b) Block diagram

to be purely inductive. The static var compensator is represented with the variable negative susceptance $- B_s$.

The voltage U will now be determined by the following expression:

$$U = \frac{U_e}{1 - X_e \cdot B_s} \qquad (10\text{-}25)$$

Usually $|X_e \cdot B_s| << 1$, which shows that equation (10-25) can be approximately rewritten as

$$U \simeq U_e(1 + X_e \cdot B_s) \qquad (10\text{-}26)$$

The dynamic characteristic of the static var compensator is partly determined by the characteristic of the voltage regulator, which is described by equation (10-22), and partly by the transfer function from the ordered susceptance B_{order} to the actual susceptance B_s. The influence from possible delays and filtering at the measurements of the current and the voltage also has to be considered.

Equation (10-22) can be rewritten by using the fact that $I_s = - B_s \cdot U$. The negative sign is obtained as I_s is defined positive for an inductive current. This then gives:

$$B_{order} = (U_{ref} - X_{SL} \cdot B_s \cdot U - U)\, K_s/s \qquad (10\text{-}27)$$

Equations (10-26) and (10-27) are illustrated as a blockdiagram in figure 10-11b.

We will now study how a small change in U_{ref} (ΔU_{ref}) via a small change in B_{order} (ΔB_{order}) and B_s (ΔB_s) will affect the voltage U (ΔU). We differentiate equations (10-26) and (10-27), set $\Delta B_{order} = \Delta B_s$, eliminate ΔB_s and approximately set $U = U_e$. This results in the desired transfer function

from ΔU_{ref} to ΔU

$$\frac{\Delta U}{\Delta U_{ref}} = \frac{X_e}{\left(1+\frac{X_{SL}}{X_e}+X_{SL}B_S\right)\left[1+\frac{s}{K_s \cdot U_e\left(X_e+K_L+X_e \cdot K_L \cdot B_s\right)}\right]} \qquad (10\text{-}28)$$

However, the assumption $\Delta B_{order} = \Delta B_s$ made above, is not quite correct during transients. New order settings are calculated once each half cycle, when the synchronization pulses are generated as described above. It will then take at least one half cycle until an ordered change in susceptance can be executed and result in a change of the measured ac-voltage. As a result the average time delay from a change in ΔB_{order} until it can result in a change in voltage will be at least 3/4 T, where T is the time of one cycle of the ac-network frequency.

One way to take this delay into account is to set:

$$\Delta B_s = e^{-s\frac{3T}{4}} \cdot \Delta B_{order} \qquad (10\text{-}29)$$

The sampling character of the control of a static var compensator will usually have a much more dominating influence upon the performance, than the corresponding sampling character of a convertor for HVDC. This is also obvious from a comparison of equation (10-29) with equation (7-18). For a twelve pulse convertor T_p is only one twelfth of T, which shows that the corresponding delay in the control system can usually be disregarded. The delay caused by the sampling character of the control for a static var compensator can, on the other hand, be a decisive factor, which limits the maximum possible amplification in the control system. One approximate way to take this into

account at the analysis of the control system is to replace s in equation (10-28) with

$$s \cdot e^{s\frac{3T}{4}}$$

Now we will study the dynamics of the system first without considering the influence of the sampling and the other delays as discussed above and then also discuss how these delays could influence the dynamic characteristics. If we first assume that the system can be described by equation (10-28), we will get the following expression for the time response to a step change in U_{ref}:

$$\Delta U = \Delta U \cdot \frac{\left(1 - e^{-\frac{t}{T_s}}\right)}{1 + \frac{X_{SL}}{X_e} + X_{SL} \cdot B_s} \qquad (10\text{-}30)$$

where:

$$T_s = \frac{1}{K_s \cdot U_e\left(X_e + X_{SL} + X_{SL} \cdot B_s \cdot X_e\right)} \qquad (10\text{-}31)$$

The time-constant T_s will thus be determined by the amplification factor K_s, the slope reactance X_{SL}, the susceptance of the static var compensator B_s and the ac-network reactance X_e. Equation (10-31) implies that a high amplification K_s has to be chosen to get a small time-constant T_s and by that a fast control system.

However, as pointed out above, we have made the assumption that $\Delta B_{order} = \Delta B_s$ to arrive at equation (10-28) and thus also at equation (10-30). The fact that the system, in reality, has a sampled character with additional delays sets certain limitations on the maximum amplification that can be used. This could be understood from the following

simple analysis. Assume that the operator s in equation (10-28) can be replaced by:

$$s \cdot e^{s \frac{3T}{4}}$$

The system will be unstable, when the denominater in equation (10-28) approaches zero. If the operator s is replaced with $j\omega$, where ω is the angular frequency for a self-oscillation, we will get the following condition for self-oscillation:

$$1 + j\omega T_s \cdot e^{j\omega \frac{3T}{4}} = 0$$

This condition is met when

$$\omega T_s = 1 \text{ and } \frac{\omega 3T}{4} = \frac{\pi}{2}$$

which results $T_S = \frac{3T}{2\pi}$

The time constant T_s should be at least twice as large as this value, i.e. $T_s > 3T/\pi$. It must also be taken into account that the voltage measurement has to be performed with some filtering.It is because of that reasonable to choose a slightly larger T_s e.g. T_s equal to twice the cycle time T.

The speed of the voltage control will also depend on the reactance of the ac-network since the time-constant T_s depends on X_e. Optimization of the amplification K_s at the minimum short-circuit capacity (maximum X_e) will show that T_s will increase at higher short-circuit capacities. Because of that he amplification K_s has to be automatically adjusted (adaptive control) for applications, where it is essential that the speed of the control is optimized and the short-circuit capacity of the ac-network can vary

within a large range.

The voltage control system has been treated as a continuous control system with a time-delay in the analysis presented above. It might also be of interest to compare this analysis with a treatment, where the state of the system is analysed at the discrete time instants when the synchronization pulses are generated. For this analysis we will assume that the conditions, according to equation (10-21) are fullfilled at time t-1. The reference voltage U_{ref} is assumed to be increased with the amount ΔU_{ref} (t) during the time interval between t-1 and t. This results in a change of the ordered susceptance with the amount ΔB_{order}, which is active during the time interval t to t+1. We will now assume that we have a control algoritm, which corresponds to equation (10-27). The control algoritm is derived through differentiation of equation (10-27), which results:

$$\Delta B_{order}(t) = K_s[\Delta U_{ref}(t)-X_{SL}\cdot B_s(t)\Delta U(t)-X_{SL}\cdot U\cdot \Delta B_s(t)-\Delta U(t)] \qquad (10-33)$$

Differentiation of equation (10-26) gives:

$$\Delta U(t) = U_e \cdot X_e \cdot \Delta B_s\ (t) \qquad (10-34)$$

Insertion of equation (10-34) into (10-33), with the approximation $U \simeq U_1$, results:

$$\Delta\ B_{order}(t) = K_s\cdot[\Delta U_{ref}(t)-(X_{SL}\cdot B_s(t)+X_{SL}/X_e+1)\Delta U(t)] \qquad (10-35)$$

Insertion of $\Delta U(t) = 0$, and $\Delta B_s(t+1) = \Delta B_{order}(t)$ gives:

$$\Delta B(t+1) = K_s \cdot \Delta U_{ref}(t) \qquad (10-36)$$

We assume that $\Delta U_{ref}(t+1) = \Delta U_{ref}(t)$ and choose K_s such that we will obtain $\Delta B_{order}(t+1) = 0$. Insertion of equation (10-36) and (10-34) into equation (10-35) results:

$$K_{sopt} = \frac{1}{U_e(t+1)\left[X_e + X_{SL} + X_e \cdot X_{SL} \cdot B_s(t+1)\right]} \qquad (10\text{-}37)$$

The ordered change U_{ref} will, under these assumptions, be executed during the succeeding sampling interval (compare equation (10-31) with the time-constant $T_s = 1$). We then have obtained a dead beat control system.

It is now of interest to find out what the result would be if the optimization of K_s is based on an impedance that is different from the real impedance. Assume that the ac-network impedance is thought to be X_{eo} and that this impedance is used for optimization of K_s according to equation (10-37). The real impedance X_e is, however, k times X_{eo}, i.e., $X_e = k \cdot X_{eo}$. Insertion in the modified equation (10-35) gives the following expression for $\Delta B_{order}(t+1)$

$$\Delta B_{order}(t+1) = K_{sopt} \cdot \frac{(1-k)(1+X_{SL} \cdot B_S)X_{eo}}{X_{eo} + X_{SL} + X_{eo} \cdot X_{SL} \cdot B_s} \cdot \Delta U_{ref}(t) \qquad (10\text{-}38)$$

We will now find that $\Delta B_{order}(t+1) = 1$ is only obtained for $k = 1$. The case $k < 1$, i.e. when the real impedance is smaller than the impedance for which the optimization was made, will show that the control will be performed with an infinite large number of steps with decreasing magnitudes. The decrease of the ac-network impedance will thus give a slower voltage control system.

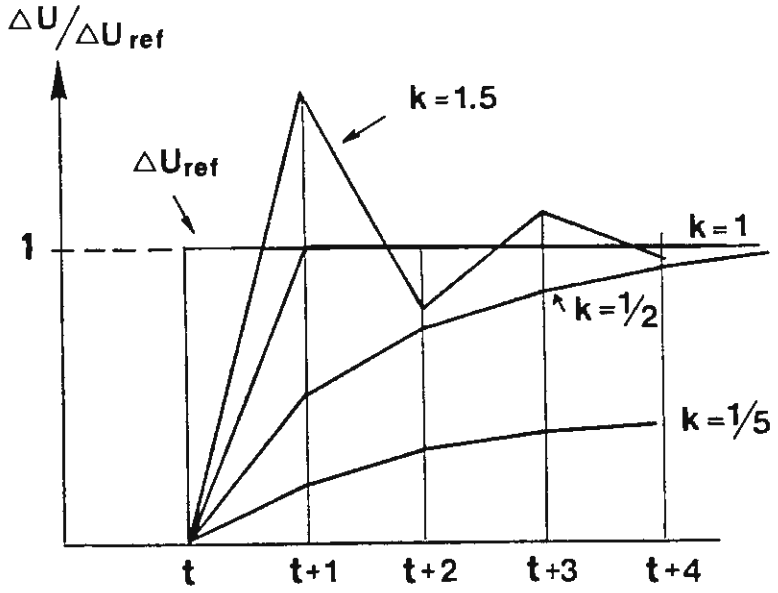

Figure 10-12 Voltage-response curves at a step change in U_{ref} and different values of the ac-network impedance $X_e = k \cdot X_{eo}$. Control optimized for k=1. Dead beat control. Static voltage-current slope reactance $X_{SL}=0$. No delay in voltage measurement.

The case k > 1, i.e. when the real ac-network impedance is larger than the impedance for which optimization was made, will result that ΔB_{order} (t+n) will be interchangeable positive and negative. This is illustrated in figure 10-12 for the case $K_L = 0$. This can be compared with the result from the previously treated continuous control case.

Equation (10-31) shows then that for $X_{SL} = 0$ and no time delay:

$$T_s = \frac{1}{K_s \cdot U_e \cdot X_e}$$

It should be noted, that the time-discrete treatment above is also idealized, as it has been assumed, that the voltage can be measured without any additional time delay (optimal estimation).

11 FORCED-COMMUTATED CONVERTORS FOR HVDC AND SVC

11.1 General

The principle differences between a line-commutated and a forced-commutated convertor as well as between a current--source and a voltage-source convertor were treated in chapter 2. Theoretically, four different types of convertor are possible. However, the line-commutated voltage-source convertor is not usable and can be disregarded.

The line-commutated current-source convertor offers substantial advantages for HVDC applications and is the only type that has been used until now. The major advantages are that a current-source convertor make it easy to limit overcurrents, and in case of faults on the dc-side, can control the direct voltage and the direct current to zero. The line-commutated convertors have simple convertor circuits and make it feasible to use conventional thyristors without turn-off capability.

As described in chapters one and ten static var compensators with thyristor valves are mainly used as thyristor switched capacitors or thyristor controlled reactors. In principle it would be possible to use a line-commutated current-source convertor controlled at $\alpha \simeq 90°$ to absorb reactive power instead of using a thyristor controlled reactor. However, this would result in a more expensive solution without offering any special advantages and it is not used.

The fast development of semi-conductor technology during the latest years has resulted in the forced-commutated convertors now being more widely used for other applications such as motor drive systems and traction.

The fast development of thyristors, which can turn-off the current by signals to the gate (Gate Turn Off thyristors, GTO thyristor), have been very important for the further development of the forced-commutated convertor technology. It is expected that this development will continue towards components for higher voltage and current ratings and with better turn-off capabilities. The combination of the MOS-technology and the thyristor technology will probably result in the new and better components, the so called MOS Controlled Thyristors, MCT. These thyristor are excepted to result in lower power losses and reduced gate currents at turn-off than for GTO thyristors.

The idea to use forced-commutated convertors for HVDC is not new, but was presented long before thyristors with turn-off capabilities were invented at the end of the 1960s. However, the fast development of the semi-conductor technology has now stimulated a new interest for forced-commutated convertors also for HVDC and SVC applications.

The basic advantages, which are expected to be achieved with forced-commutated convertors used for HVDC as compared to line-commutated convertors are:

- Possibility to generate reactive power to the ac-network by the convertor. This could decrease the size of the filters to an absolute minimum only determined by the filtering requirement, which would result in advantages, both, with regard to temporary overvoltages and resonance frequency.

- Possibility for inverters to operate on very weak ac-networks with minimum risks for commutation failures also operating on networks having no synchronous machines connected, at all.

Modern types of forced-commutated convertors will also make it possible to control reactive power independently of active power and voltage level on the dc-side.

The possibility to, both, generate and absorb reactive power with a forced-commutated convertor makes it also attractive to use forced-commutated convertors for static var compensators instead of thyristor switched capacitors and thyristor controlled reactors. One expected advantage is that forced-commutated convertors might offer a cheaper solution, where it is required that reactive power shall both be generated and absorbed, since the same equipment is used for both operation modes. A forced-commutated convertor will further make it possible to generate reactive power without installation of large capacitor banks, which can cause problems with low resonance frequencies. It is also excepted that faster control can be obtained, which can be of great value, when the static var compensator is used for controlling the voltage at special fast varying loads, e.g., at steel arc-furnaces.

Forced-commutated convertors of the voltage-source type have already been used for static var compensators. However, the cost and losses for the valves are still too high and further development of the semiconductor technology is needed to make forced-commutated convertors competitive for static var compensators.

The forced-commutated convertors used in the existing prototype installations are designed for fairly low voltages since series connection of GTO thyristors still have additional problems and higher costs. This has often made it neccessary to use a number of parallel units which have increased the cost. It is expected, that the further development of the semi-conductor technology will make it more easy in the future to connect thyristors with turn-off capability in series. This is of course of special

importance for HVDC applications and therefore justifies a closer study of different types of forced-commutated convertors.
For the sake of completeness forced-commutated convertors, which are not using valves with current turn-off capabilities will also be presented.

The following types of forced-commutated convertors will be treated.

- current-source convertors with valves which can not turn-off the current,

- current-source convertor with valves which can turn-off the current,

- voltage-source convertors with valves which can turn-off the current,

The current-source and voltage-source convertors have different characteristic features as already described in chapter two. Important advantages of the current-source type of convertors are, that it is easier to limit fault currents and to control the dc-voltage with this type of convertors. The voltage-source convertor seems on the other hand, to give advantages with regard to the control of reactive power and cooperation with the ac-network as they behave, as seen from the ac-network, fairly similar to a synchronous compensator. They seem to be especially well suited for back-to-back stations and also for multiterminal stations.

The specific merits of the different types of convertors will be treated in more detail in the following.

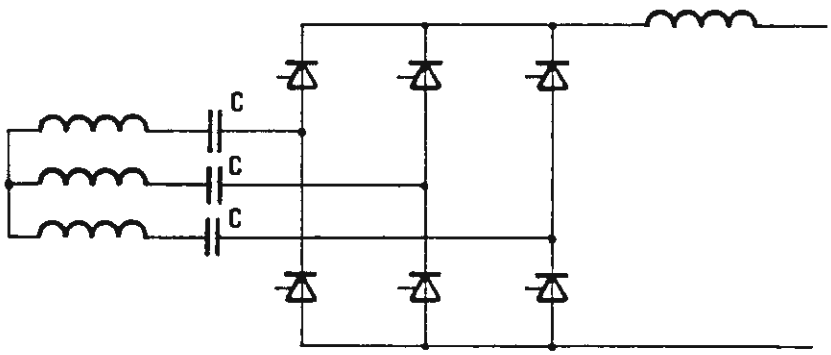

Figure 11-1 Current-source series capacitor commutated converter.

11.2 Current-source forced-commutated convertor with valves not having current turn-off capability

The different types of current-source forced-commutated convertors, which will be presented below, have in common, that it is not required, that the valves must not have the capability to turn-off the current. The commutation between the valves can take place also at time instants where the corresponding line-to-line voltages are negative with assistance of precharged capacitors. These types of convertors have been studied for many years for HVDC applications and have also been used for low voltage applications but are now usually replaced by forced-convertor circuits with GTO thyristors.

Series capacitor commutated convertor

Figure 11-1 shows a modification of the conventional line-commutated current-source two-way six-pulse bridge convertor, which sometime is classified as a forced-commutated convertor. The commutation voltages on the valve side of the capacitors connected in series with the transformer reactances will be phase-shifted relative to the line-to-line voltages of the transformer. Firing of the valves can, due to the voltages across the capacitors, be obtained at firing angles α less than zero in rectifier operation and at commutation margins γ less than zero in inverter operation provided α and γ are defined relative to the zero crossing of the line-to-line voltage on the transformer side of the capacitors. This offers the possibility of operating at firing angles, which gives generation of reactive power instead of absorption of reactive power.

However, the convertor circuit, according to figure 11-1 has a number of important limitations. One is that the charging of the capacitors depends on the magnitude of the

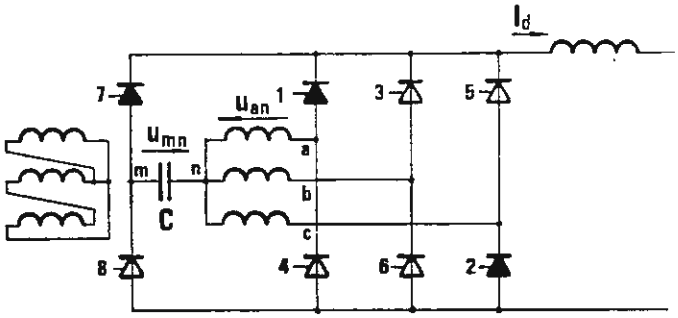

Figure 11-2 Current-source forced-commutated converter with commutation in two steps.

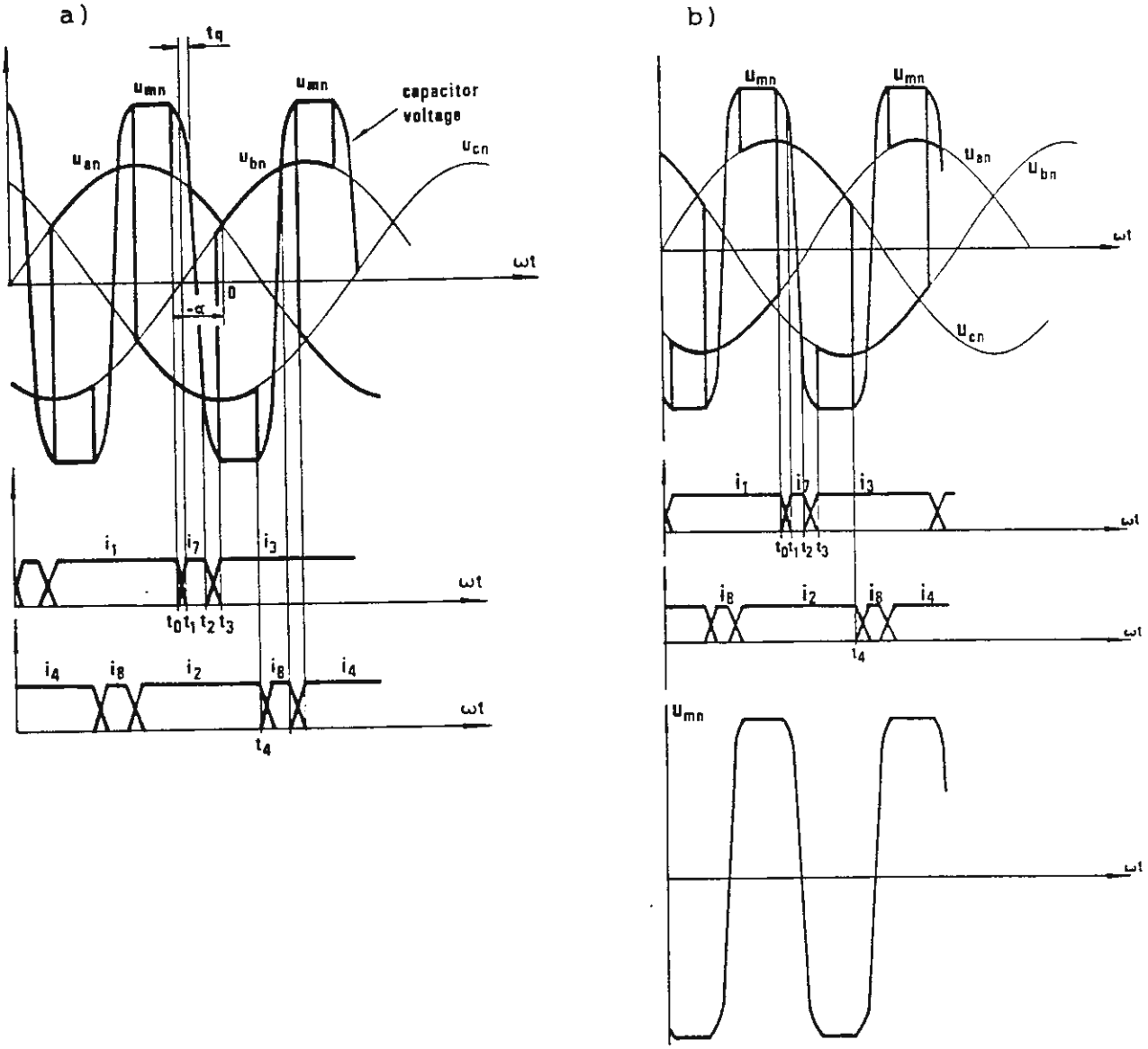

Figure 11-3 a) Commutation between the valves 1→7→3 and 2→8→4 in a converter, circuit according to fig 11-2, with commutation in two steps. Rectifier operation $\alpha \approx -40°$.

b) Commutation between the valves 1→7→3 and 2→8→4. Inverter operation $\alpha \approx 185°$.

current. This results in that the capacitor voltages will be small at small currents resulting in only small negative values of α and γ then being possible. The circuit further show hardly any advantages with regard to reduced risk for commutation failure as compared to a conventional line-commutated convertor or any additional freedom to control reactive power independent of active power.

Forced-commutated convertor with commutation in two steps

Figure 11-2 shows a forced-commutation convertor with two auxiliary valves 7 and 8 and one additional capacitor C. In case the line winding is Y-connected an additional delta connected tertiary winding has to be provided in the convertor transformer. The commutation between two valves in the main bridge (1-6) will not take place directly but in two steps via one of the auxiliary valves (7,8) and the precharged capacitor C.

The commutation between valves 1 and 3 will thus be achieved with assistance of capacitor C and valve 7. If we assume that valve 1 is conducting, valve 7 can be turned-on as soon as the voltage $u_{mn}-u_{an}$ is sufficiently positive to provide a safe commutation from valve 1 to valve 7.

The commutation sequence from valve 1 to 7 and later from 7 to 3 is illustrated by figure 11-3 for a rectifier operation with $\alpha = -40°$, and by figure 11-3 b for inverter operation with $\alpha \simeq 185°$. We have here defined α as the angle between the zero crossing of voltage u_{ba} and the firing of valve 7, which occurs at time t_0. The commutation between valves 1 and 7 is completed at a time t_1. The capacitor C begins to be recharged with opposite voltage polarity as soon as valve 7 is turned on.

Valve 3 is turned on at the time t_2, when the capacitor is almost fully charged in the opposite direction and the

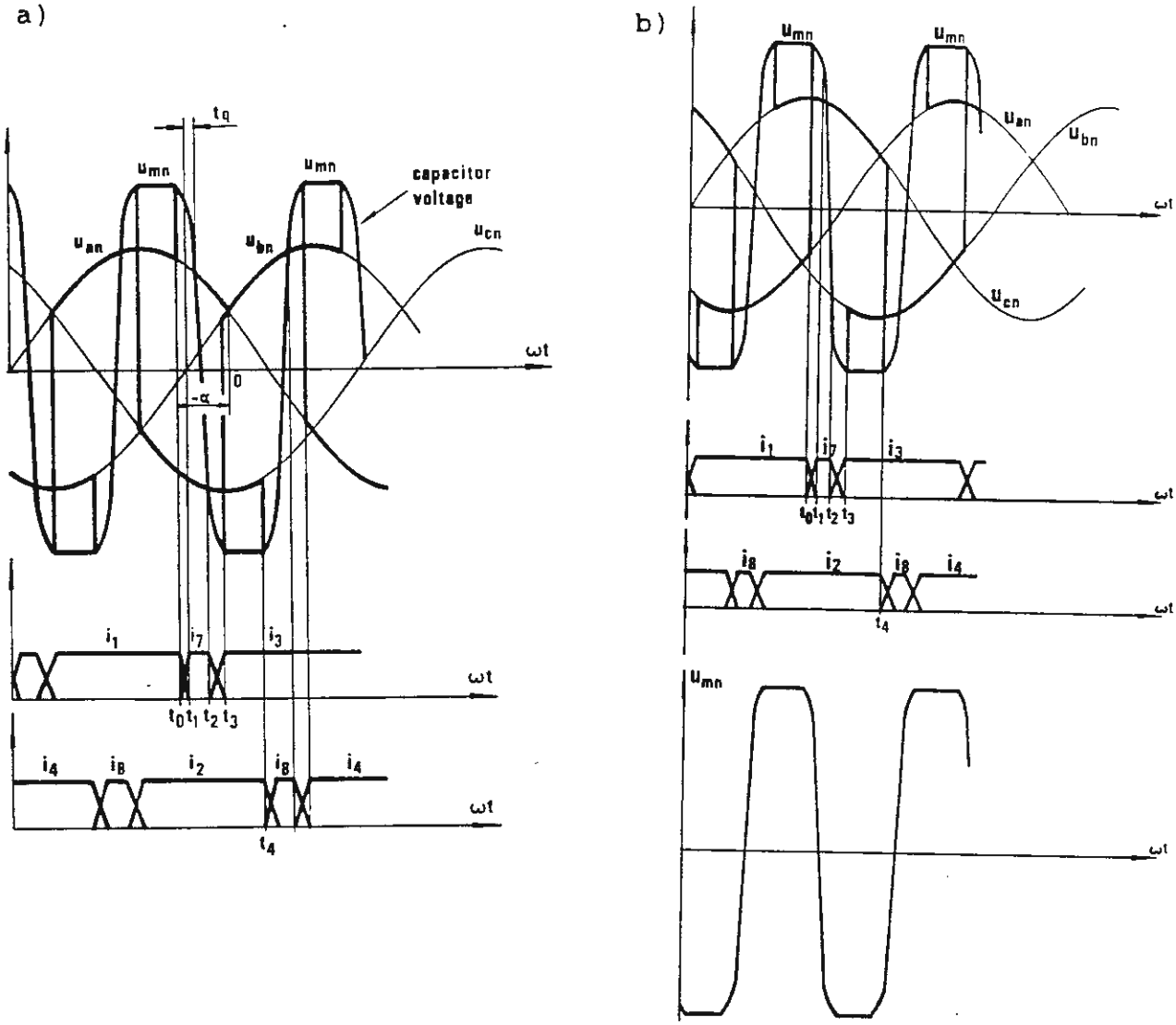

Figure 11-3 a) Commutation between the valves 1→7→3 and 2→8→4 in a converter, circuit according to fig 11-2, with commutation in two steps. Rectifier operation α≈-40°.

b) Commutation between the valves 1→7→3 and 2→8→4. Inverter operation α≈185°.

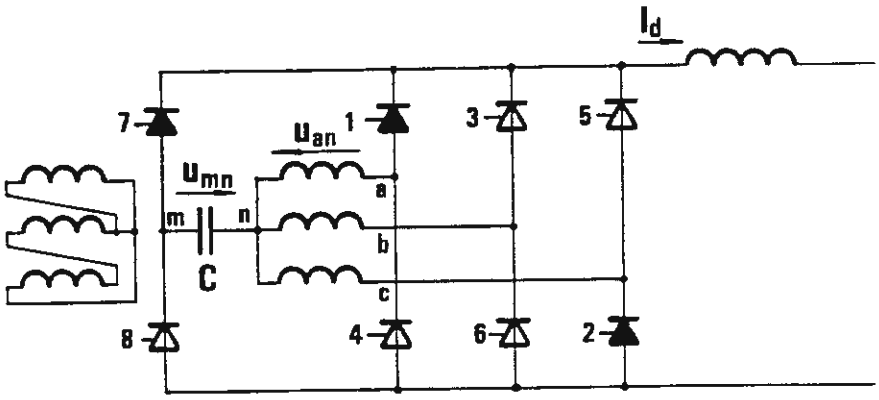

Figure 11-2 Current-source forced-commutated converter with commutation in two steps.

commutation of the current between valve 7 and 3 starts. The commutation is finished at time t_3. The capacitor is now charged in the opposite direction and prepared to assist in the commutation of the current from valve 2 to 4 via valve 8, which is turned on at time t_4.

It should be noted, that the control of the valves have to be chosen so that there will be a proper margin between the voltage across the capacitor u_{mn} and the phase voltages, as otherwise the commutation of the current might fail.

The capacitor C will be recharged six times per cycle of the ac-network frequency. This results in a large third harmonic current of zero-phase sequence in the convertor transformer winding. Because of that, the convertor transformer has to be provided with Δ-connected windings as shown in the figure 11-2.

This forced-commutated convertor circuit has a number of drawbacks, which are rather typical for forced-commutated circuits using auxiliary capacitors for the commutations. One is that the bridge voltage will be substantially more distorted than for line-commutated convertors, as can be seen from figure 11-3 b (difference between the thick curves). Further, the convertor circuit requires the installation of two auxiliary valves and a capacitor. All the valves will be more stressed than for an ordinary line commutated convertor and are often required to recover very quickly (compare the time interval t_q in figure 11-3a). This would probably also result in that valves with faster thyristors and higher losses have to be used.

The major advantage with this convertor circuit is that it can also generate reactive power into the ac-network, although it probably will not be possible to control active and reactive power independently. However, it is not to be expected that this circuit will ever be used for HVDC as

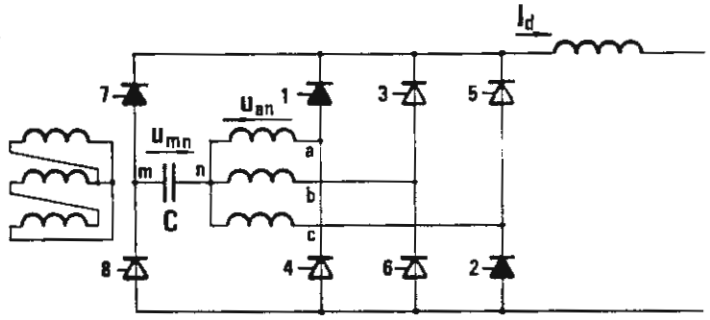

Figure 11-2 Current-source forced-commutated converter with commutation in two steps.

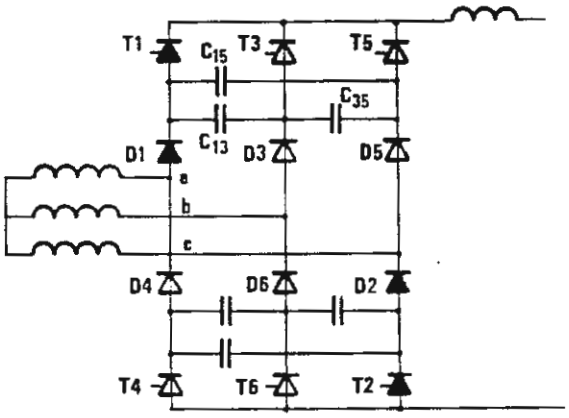

Figure 11-4 Forced-commutated current-source converter with capacitors and diodes.

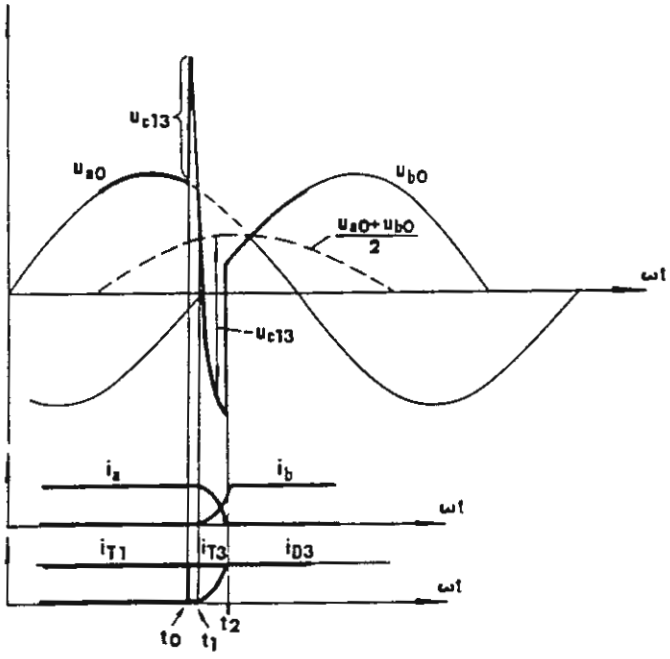

Figure 11-5 Commutation between the valves T1→T3 and D1→D3 in a forced-commutated converter according to figure 11-4.

the circuits requiring valves with turn-off capabilities presented later seem to be more attractive.

Forced-commutated current-source convertor with capacitors and diodes

An alternative to the above described circuit according to figure 11-2 with commutation in two steps is shown in figure 11-4. The commutation between the valves will also occur here in two steps as the current is first commutated between two thyristor valves in a commutating group and that the commutation of the current between the corresponding convertor transformer phases will follow later. The neutral point of the valve windings of the convertor transformer does not have to be accessible and there is no need for a Δ-connection of the transformer windings. These are two advantages as compared to the previously discussed circuit according to figure 11-2. Further the circuit requires six capacitors and six auxiliary diode valves, D1 - D6, but no auxiliary thyristor valves.

The commutation of the current between the thyristor valves T1 and T3 will be obtained with the assistance of the precharged capacitor C_{13} in parallel with C_{15} connected in series with C_{35}. The precharged capacitors will make it possible to commutate the current also when the voltage $u_{bo} - u_{ao}$ is negative, as illustrated in figure 11-5, for rectifier operation with $\alpha < 0$.

The thyristor valves T1 and T2 and the diode valves D1 and D2 are conducting and the voltage across C_{13} is positive, when valve T3 is turned-on at time t_o. It is assumed that voltage u_{13} is sufficiently high to give a positive voltage across valve T3. The commutation of the current from thyristor valve T1 to T3 will occur very quickly, as it is only limited by the valve reactors and the leakage

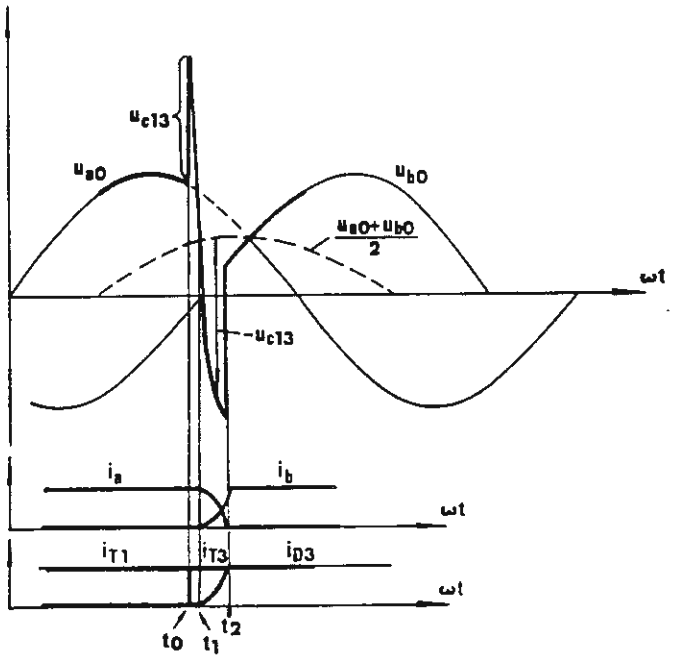

Figure 11-5 Commutation between the valves T1→T3 and D1→D3 in a forced-commutated converter according to figure 11-4.

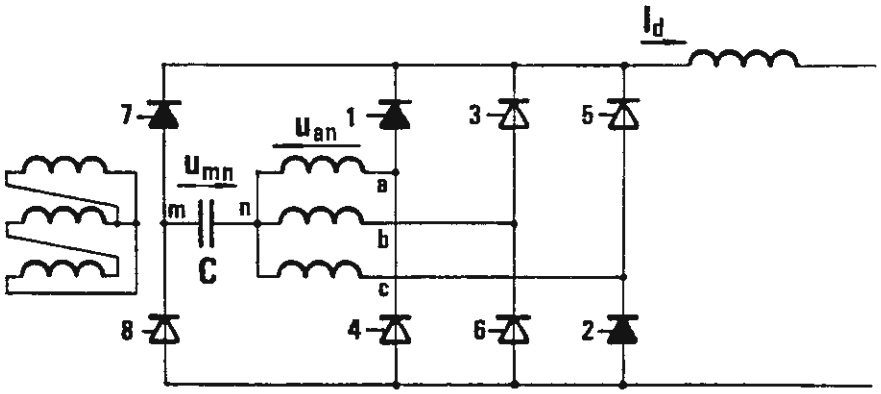

Figure 11-2 Current-source forced-commutated converter with commutation in two steps.

inductances in the circuit. The direct current will, during the time interval $t_0 - t_1$ flow through thyristor valve T3, capacitors C_{13} in parallel with C_{15} and C_{35} and diode valve D1.

This current will quickly recharge the capacitors. Diode valve D3 will start to conduct the current at the time t_1, when $u_a + u_{C13} = u_b$. The commutation of the current from phase (a) to phase (b) in the convertor transformer will now start. The commutation is completed at time t_2. The diode-valve D1 will then prevent the current from flowing in the reverse direction. The sequence of events is illustrated for rectifier operation in figure 11-5a. This forced-commutation circuit will also, as the previously described circuit according to figure 11-2, give a substantially more distorted voltage across the bridge and more severe stresses on the valves than the current-source line-commutated circuit. The commutation of the current between two successive thyristor valves will occur very fast as the commutation is only limited by the leakage reactances in the circuit and possible valve reactors. This causes the turn-on stresses on the valves to be substantially higher than for line-commutated convertors.

The circuit will make it possible to operate at firing angles less than 0° in rectifier operation and larger than 180° in inverter operation. However, the circuit does not permit control of the reactive power independent of the active power at a given ratio between the direct voltage and the no-load direct voltage. Also taking into account the above listed drawbacks with regard to stresses and distortion it is not very likely that this circuit will ever be used for HVDC.

11.3 Forced-commutated current-source convertor with thyristor valves having current turn-off capability

The turning-on of thyristor valves for line-commutated convertors can be directly controlled with a valve firing control pulse, while the turning-off is indirectly controlled by the turning-on off the next succeeding valve. This also applies to the forced-commutated convertors presented above. The commutation of the current at time intervals with negative commutation voltages between the two commutating convertor transformer phases can for these convertors be obtained due to capacitors, which are precharged with suitable voltages. The circuit arrangement and the control can be simplified if the thyristor valve to be turned-off can generate a suitable voltage and force the current to commutate over to the next succeeding valve.

Thyristors with turn-off capabilities were already designed during the 1960s. However, it was not until the end of 1970s, when gate turn-off thyristors (GTO) were designed for sufficiently high voltage and current capabilities, that they began to be of interest for application for higher power ratings. The GTO thyristors available today however still have certain limitations, which make it questionable, whether they are adequate for HVDC applications. They require high gate currents for the turn-off (up to 1/3 of the convertor current) and the spread in turn-off time delays between the thyristors can cause problems at series connection. We will in the following assume that these limitations will be eliminated with the future thyristors.

Application of thyristor valves with current turn-off capabilities will require a convertor circuit with a very low impedance in series with each thyristor valve, so that

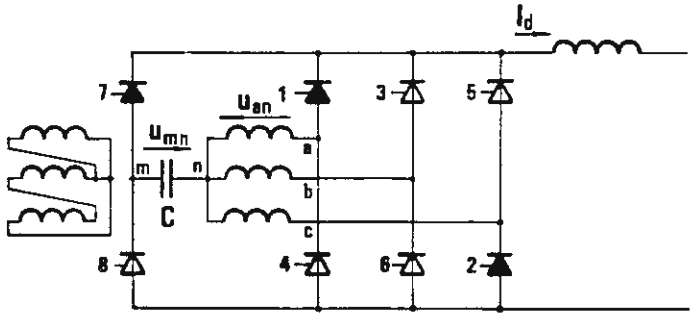

Figure 11-2 Current-source forced-commutated converter with commutation in two steps.

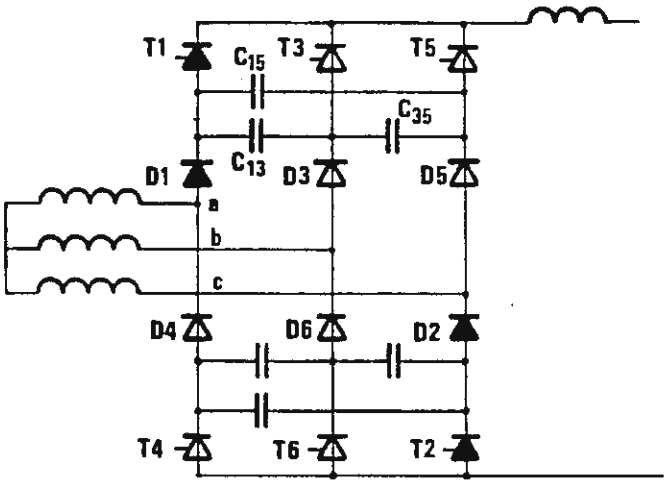

Figure 11-4 Forced-commutated current-source converter with capacitors and diodes.

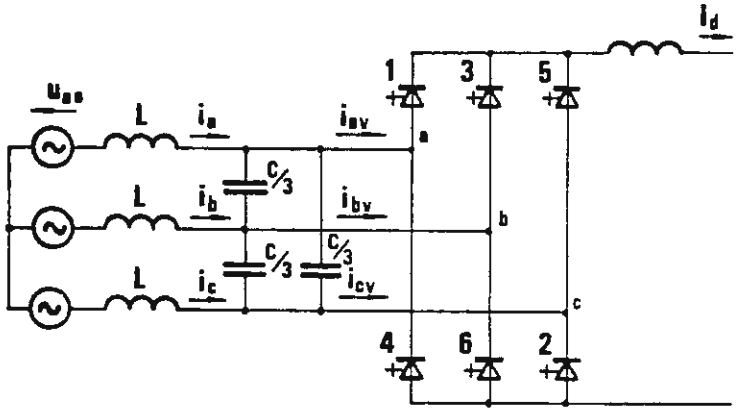

Figure 11-6 Forced-commutated current-source converter with gate turn-off thyristor valves (GTO).

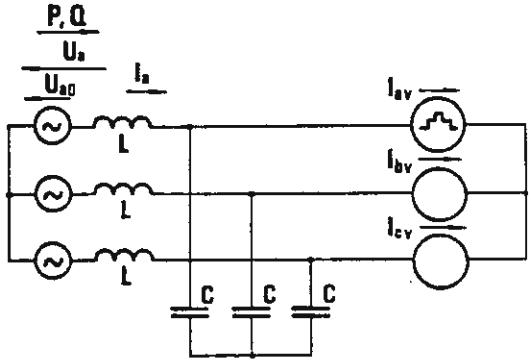

Figure 11-7 Equivalent circuit for the converter according to figure 11-6.

the current can be forced to zero in a very short time, as otherwise the dissipated energy in the valve would be too high. This implies that a GTO-valve cannot be used in the circuit, according to figure 11-2 but that GTO valves could replace the thyristor valves in the convertor circuit, according to figure 11-4.

The convertor circuit according to figure 11-4 can be simplified when the thyristor valves have turn-off capabilities, as precharged capacitors no longer are needed for the commutations. This means that the diode valves can be deleted and the capacitors can be located between the ac-phases as shown in figure 11-6. The gates in the thyristor symbol are drawn here as a cross to indicate, that it is also possible to turn-off the thyristor with a gate pulse.

The commutation of the current between succeeding valves will take a very short time, while the commutation of the current between the ac-phases of the convertor transformer will take a considerably longer time. Because of that fairly large capacitors have to be chosen to avoid overvoltages, which are too high at each commutation. The negative voltage-notches occurring at each commutation for a line-commutated convertor is here replaced by positive voltage notches. It should also be noted, that the valves will be stressed with both forward and reverse blocking voltages as for other current-source convertors.

The convertor circuit according to figure 11-6 can be represented by an equivalent circuit as shown in figure 11-7.

The mathematical analysis of the convertor circuit will be rather simple, as the commutation of the current between the thyristor valves will take place with zero angle of overlap. The current in each phase of the convertor bridge

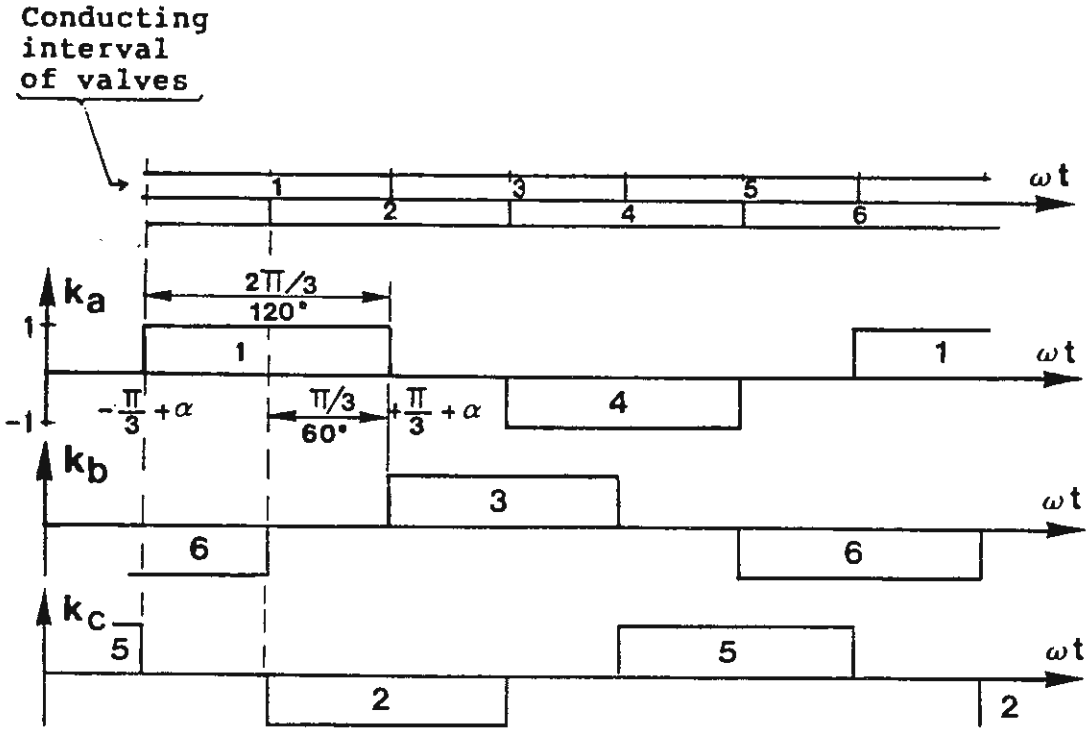

Figure 4-5 Conversion function at two-way six-pulse converter.

can be represented by a current generator. The currents are determined by the previously derived conversion functions k_a, k_b and k_c, according to figure 4-5, multiplied by the convertor current i_d as described by the equations (4-5) to (4-7). This gives the following expression for the instantaneous value of the fundamental frequency component of the current in phase (a) to the bridge, which we denote i_{av1}

$$i_{av(1)} = \frac{2\sqrt{3}\ I_d}{\pi} \cos(\omega t - \alpha) \qquad (11\text{-}1)$$

Here we have assumed that the instantaneous value of the sinusoidal source voltage in phase (a) is:

$$u_{a0} = \hat{U}_0 \cos \omega t \qquad (4\text{-}1)$$

The fundamental frequency components of the current and the voltage can also be obtained as the complex r.m.s quantities, which gives:

$$I_{av(1)} = \frac{\sqrt{6}}{\pi} I_d \cdot e^{-j\alpha} \qquad (11\text{-}2)$$

and

$$U_{ao} = U_o \qquad (11\text{-}3)$$

Pulse-width modulation (PWM)

We have so far assumed that the number of commutations is equal to the pulse number. However it has often been found to be suitable to use the turn-off capability of the GTO thyristors to commutate the current more often and apply so called pulse-width modulation (PWM). This will make it possible to control the ratio between the direct current and the fundamental component of the ac-current, which otherwise is constant, as can be seen from the equations

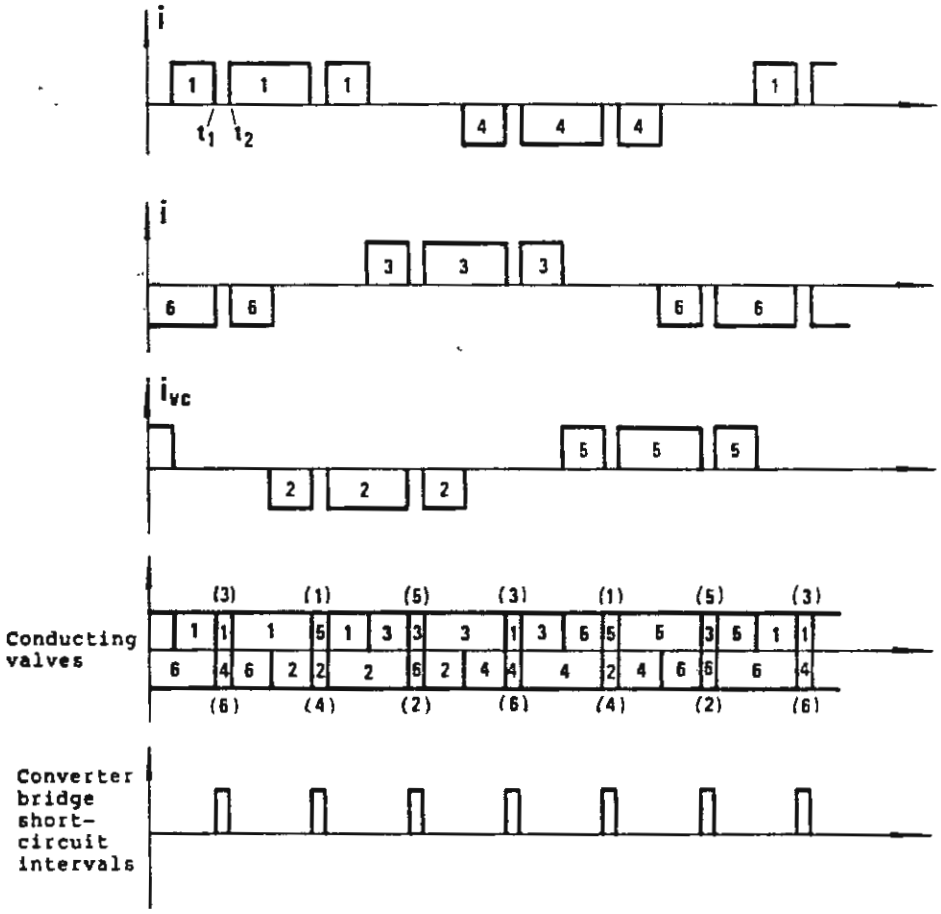

Figure 11-8 Example of phase-currents, conducting valves and converter bridge short-circuit intervals for a forced-commutated current-source converter.

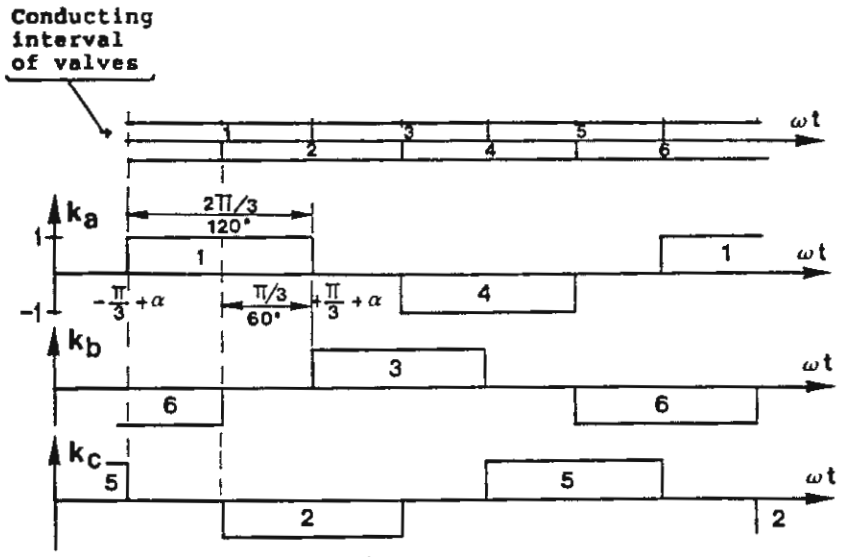

Figure 4-5 Conversion function at two-way six-pulse converter.

(11-1) and (11-2).

A possible way of arranging the pulse-width modulation for a current-source convertor is illustrated in figure 11-8, which shows the waveshape of the currents i_{av}, i_{bv} and i_{cv} to the valve bridge, as well as the valves which are conducting. A comparison with figure 4-5 shows that the waveshapes of the ac-current are almost the same as for an ordinary line-commutated convertor with zero angle overlap, except for short periods, when two valves connected to the same ac-phase are conducting and give a short circuit across the convertor bridge. These short-circuit intervals will reduce both the fundamental component of the ac-current I_{av1}, I_{bv1}, and I_{cv1} as well as the direct voltage component across the bridge.

The short circuit of the bridge at time t_1 can either be obtained by turning-on valve 4 and turning off valve 6, or turning on valve 3 and turning off valve 1. At time t_2 the direct current is commutated back to valve 1 or 6. Pulse-width modulation will thus give the possibility of controlling the ratio between the ac-current and the dc-current. This will be considered by multiplying equations (11-1) with a factor k_λ, which is called the control ratio. This gives:

$$i_{av1} = \frac{2\sqrt{3} \cdot k_\lambda \cdot I_d}{\pi} \cos(\omega t - \alpha) \qquad (11\text{-}4a)$$

and

$$I_{av1} = \frac{\sqrt{6}}{\pi} k_\lambda \cdot I_d \cdot e^{-j\alpha} \qquad (11\text{-}4b)$$

Calculation of the ac-current of the convertor

The convertor circuit, according to figure 11-6, can as

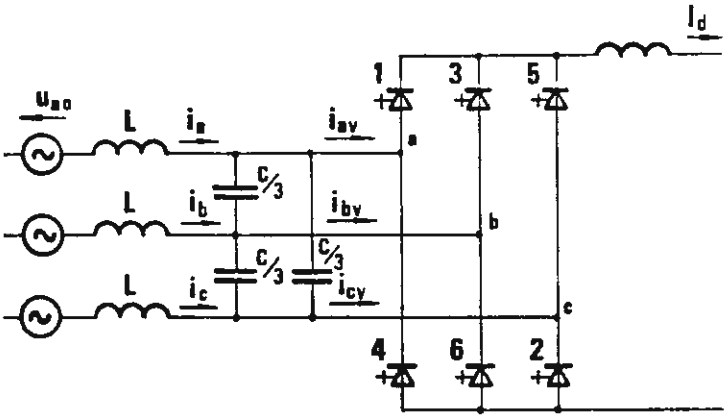

Figure 11-6 Forced-commutated current-source converter with gate turn-off thyristor valves (GTO).

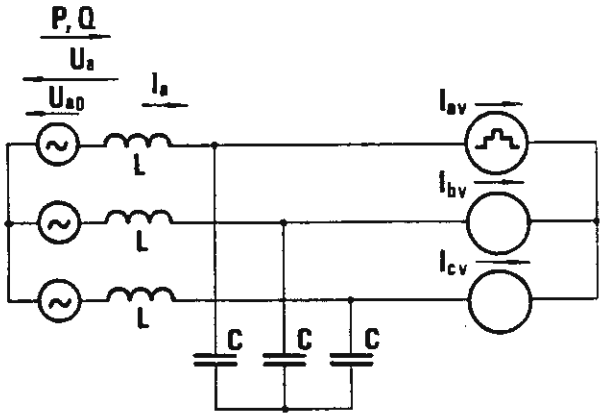

Figure 11-7 Equivalent circuit for the converter according to figure 11-6.

mentioned above be represented by an equivalent circuit as shown in figure 11-7. The valve bridge is substituted by three current- source generators. The fundamental frequency current in phase (a) is described by the equations (11-4a) or (11-4b) and the current in the other phases are obtained by replacing ωt by $(\omega t - 2\pi/3)$ and $(\omega t - 4\pi/3)$, respectively.

The fundamental of the current in the convertor transformer phase a, I_{a1}, is obtained by adding the current generated by the voltage U_{ao} to the current I_{av1}. This gives:

$$I_{a1} = \frac{\sqrt{6} \cdot k_\lambda \cdot I_d}{(1-\omega^2 LC)} \cdot \frac{e^{-j\alpha}}{\pi} + \frac{j\,\omega C \cdot U_o}{1 - \omega^2\, LC} \qquad (11\text{-}5)$$

The denominator in the first term is caused by the current distribution between L and C.

The total supplied fundamental complex power from the ac-network is given by:

$$P + jQ_{(1)} = 3\,\bar{U}_o \cdot \bar{I}_{(1)}^{*}$$

The subscript (a) has been deleted, as it is assumed, that the ac-system is symmetric supplying equal contribution from all phases.
This gives

$$P+jQ_{(1)} = \frac{3\sqrt{6}}{\pi} \cdot \frac{U_o \cdot I_d \cdot k_\lambda}{(1-\omega^2\, LC)} \cos\alpha + j\left[\frac{3\sqrt{6}}{\pi} \cdot \frac{U_o\ I_d\ k_\lambda}{\left(1-\omega^2\, LC\right)} \sin\alpha - \frac{3\omega C \cdot U_o^{\,2}}{1 - \omega^2\, LC}\right] \qquad (11\text{-}6)$$

The equation (11-6) result in the following expression for the active power:

$$P = \frac{3\sqrt{6}}{\pi} \frac{U_o \cdot I_d \cdot k_\lambda \cdot \cos \alpha}{1 - \omega^2 LC} \qquad (11\text{-}7)$$

The absorbed reactive power for the fundamental frequency will be:

$$Q_{(1)} = \frac{3\sqrt{6}}{\pi} \frac{U_o \cdot I_d \cdot k_\lambda \cdot \sin \alpha}{(1 - \omega^2 LC)} - \frac{3 \omega C \cdot {}^2U_o}{1 - \omega^2 LC} \qquad (11\text{-}8)$$

It should be noted that U_0 is the r m s value of the phase voltage.

The expressions for the active power and the first term for reactive power are very similar to the corresponding expression for a line-commutated convertor with zero angle of overlap. The capacitance C will result in a slight increase of, both, the active and reactive power due to the corresponding increase of the bridge voltage. The control ratio k_λ will of course effect both the active and the reactive power. The second term for the reactive power absorption is caused by the generation of reactive power from the capacitors.

The active powers on, both, the ac- and the dc-side of the convertor have to be equally large. The relation $P = U_d \cdot I_d$ and equation (11-7) result in:

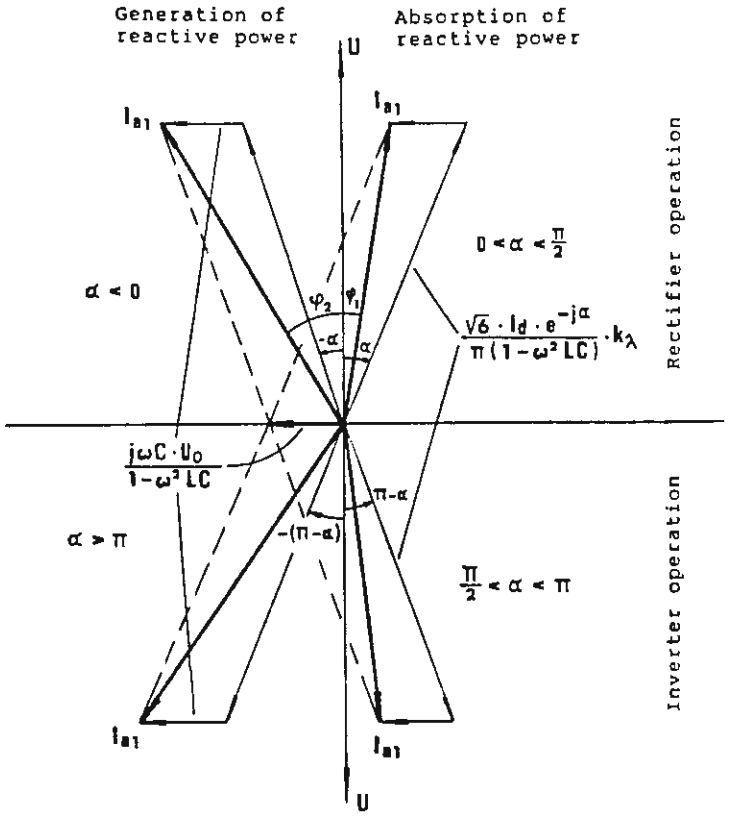

Figure 11-9 Phasor-diagram for fundamental components of the ac-currents of a forced-commutated current-source converter according to figure 11-6 and 11-7.

$$U_d = \frac{3\sqrt{6}}{\pi} \frac{U_o \cdot k_\lambda \cdot \cos \alpha}{1 - \omega^2 LC} \qquad (11\text{-}9)$$

or expressed as a function of the line-to-line voltage U_h:

$$U_d = \frac{3\sqrt{2}\, U_h \cdot k_\lambda \cdot \cos \alpha}{\pi \left(1 - \omega^2 LC\right)} \qquad (11\text{-}10)$$

A comparison between equation (11-10) and equation (4-35c) for a line-commutated current source convertor shows that the capacitance C gives a certain increase in the voltage and that the direct voltage can also be controlled with the pulse-width modulation factor k_λ. However, the commutation reactance will not give any additional voltage drop for the forced-commutated convertor.

Equations (11-9) and (11-10) show that cosα determines the ratio between the dc- and ac-voltage for a convertor without pulse width modulation ($k_\lambda = 1$). This shows that the absolute values of α and $(\alpha-\pi)$ are given for rectifier and inverter respectively with given dc- and ac-voltages and that only two operational points are possible for each operation mode, as illustrated in the phasor-diagram according to figure 11-9. From this it is obvious that some kind of pulse-width modulation has to be introduced, if we have to meet the requirement, that it shall be possible to control active and reactive power independently.

Operation at $\alpha = \pm 90°$ implies, that the direct voltage will be zero and the convertor will act as a static var compensator giving the possibility for a continuous control of the reactive power by control of the current I_d within the operating range $0 < I_d < I_{dmax}$.

One advantage with this convertor circuit compared with the forced-commutated voltage-source convertor, which will be presented in the next paragraph, is that it probably will

be more easy to limit fault currents with the current-source convertor.

One drawback is that the valves might be stressed with fairly high overvoltages in both forward and reverse blocking direction. Further, it is recommended to use a fairly low resonance frequency defined as $\omega_0 = 1/\sqrt{LC}$, e.g., $\omega_o = 3\ \omega$. This will probably make it possible to limit the voltages at commutations without introducing additional damped filters, which would increase the losses. However, it should be noted that a resonance frequency of $\omega_0 = 3\omega$ would give a fairly large capacitance. If we assume that $\omega L \cdot I_{alN} \leq 0.2 \cdot U_{oN}$ we find that a resonance frequency $\omega_0 = 1/\sqrt{LC} = 3\omega$ would give $\omega C \cdot U_{oN} \geq I_{aN}/1.8$. The installed capacitance would be of the same order of magnitude as for the complete filters and capacitor banks used for existing line-commutated convertors. Since additional filters also have to be installed for the forced-commutated convertor, this would, both, result in high cost and problems to control the reactive power specially at light loads.

11.4 Forced-commutated voltage-source convertor

The forced-commutated voltage-source convertor with GTO thyristors have turned out to be very suitable for many low and medium voltage applications, e.g., for motor drives and electrical tractions. They are very often designed for pulse-width modulation (PWM). One advantage with the voltage-source type is that the valves only have to withstand forward blocking voltages, as they are connected in parallel with diode valves conducting current in the reverse direction. The voltage across the valves will also be better controlled as the valves are directly connected to the dc-side, where the voltage should be essentially constant. On the other hand the voltage-source convertor causes higher fault currents.

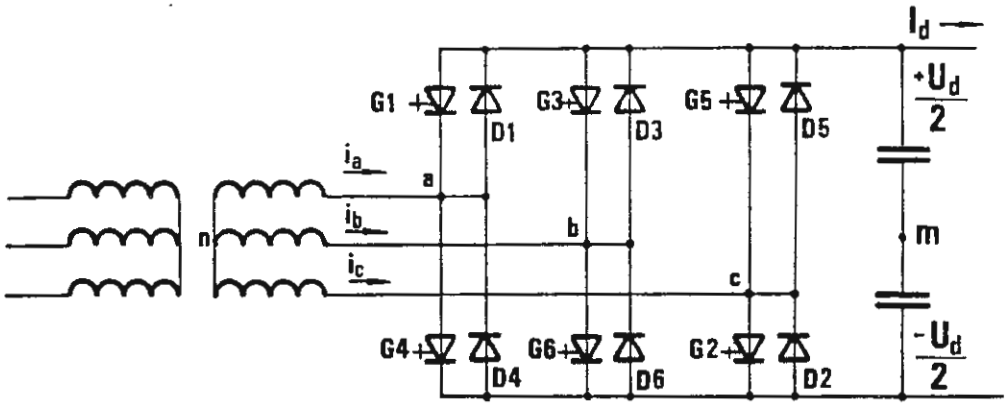

Figure 11-10 Forced-commutated voltage-source converter.

Square-wave operation

The basic convertor circuit for a forced-commutated voltage-source convertor is illustrated in figure 11-10. The most simple operation mode is when the number of commutations is equal to the pulse number and is often called square-wave operation. Each bridge arm consists of one thyristor valve with current turn-off capability and a diode valve, which is connected in parallel with the thyristor valve but with reversed polarity. The diode valves show that the bridge voltage can only have one polarity but that the current can flow in both directions in a bridge-arm with a turned-on thyristor valve. A change of the power direction will, because of that, be obtained by a change of current direction as the current can flow through the bridge in both directions. The voltage across the bridge is assumed to be stiff. This type of convertor is, because of that, sometimes called voltage-stiff convertor instead of a voltage-source convertor.

It should be noted that we, in figure 11-10, have defined the positive current direction for rectifier operation, i.e., when power is transmitted from the ac-side to the dc-side. However, the most common practice is to define the positive current direction in the reverse direction as voltage-source convertors are usually mainly operating in inverter mode and then also called voltage-source inverters (VSI).

The need to have, both, thyristor valves and diode valves might be considered to be a disadvantage for this type of convertor. However, as previously mentioned, this results in the advantage, that the thyristor valves only have to be designed for forward blocking voltage, which will make it possible to design the thyristor wafers thinner and obtain lower losses.

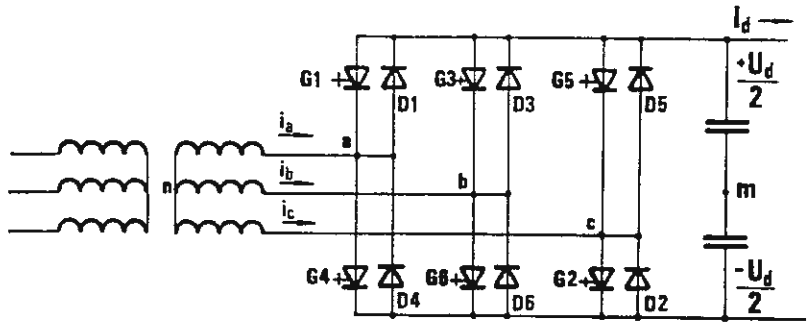

Figure 11-10 Forced-commutated voltage-source converter.

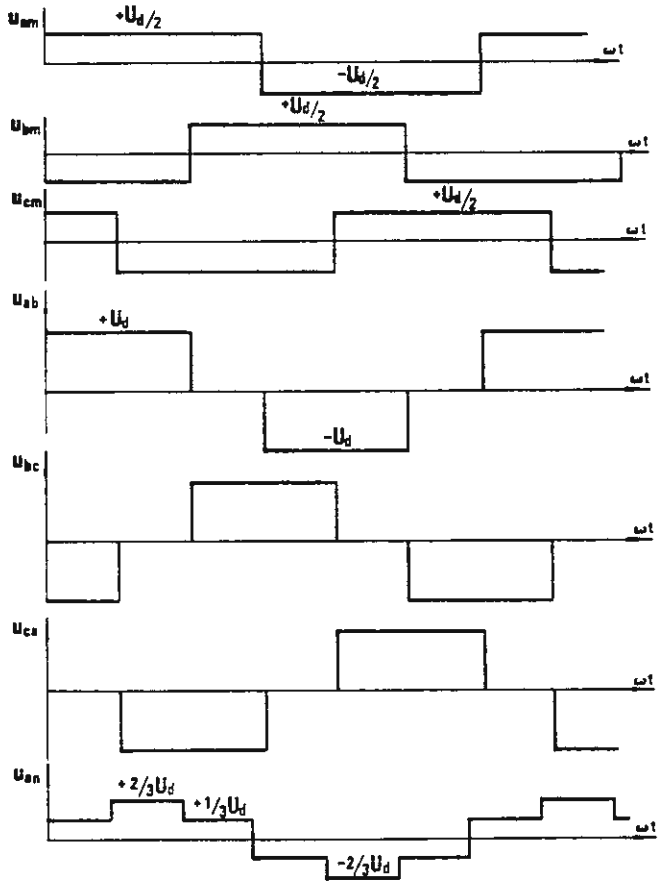

Figure 11-11 Voltages between the ac-phase terminals and the midpoint m, phase-to-phase voltages and phase voltage u_{an} at the valve side of the converter transformer. Forced-commutated voltage-source converter with square wave operation.

The basic operating principle for the convertor is rather simple. The control of the valves is arranged so that at least one of the two thyristor valves connected to each phase during normal operation is always prepared to conduct the bridge current. This shows that for phase a either the thyristor valve 1 or 4 (here denoted G1 and G4 as they have gate turn-off capability) is always turned on. Since the diodes D 1 and D 4 are connected in parallel with the thyristors, either one of the thyristors or one of the diodes will always conduct the current. The combination of a thyristor valve and of a diode valve will function as a switch, which connects the phase to either the positive or the negative pole of the bridge. If we assume that valve G1 is conducting and that the current I_d is flowing in the negative reference direction when a turn-off-signal is applied to valve G1, the turn off of valve G1 will force the current to commutate to valve D4. It should be noted that the transformer leakage inductance will prevent the transformer current from changing quickly, but that due to the low inductance in the external dc-circuit via the capacitor across the bridge the current can change quickly in this circuit. The thyristor valve G4 will, on the other hand, start to conduct immediately if valve D1 is conducting, when a firing pulse is given to valve G4. This shows that the GTO-valves and the diode valves will alternate to conduct current.

The terminal voltage of the bridge will be $\pm U_d/2$ with the midpoint (m) used as reference.

The voltage of the ac-terminals of the bridge, u_{am}, u_{bm} and u_{cm} will then get the waveshape, as illustrated in the figure 11-11. The differences between these voltages give the line-to-line voltages u_{ab}, u_{bc} and u_{ca}. The voltage at the neutral point (nt) of the transformer is determined by $1/3\ (u_{am} + u_{bm} + u_{cm})$. The phase-voltages can now be determined, as illustrated for u_{an} in figure 11-11.

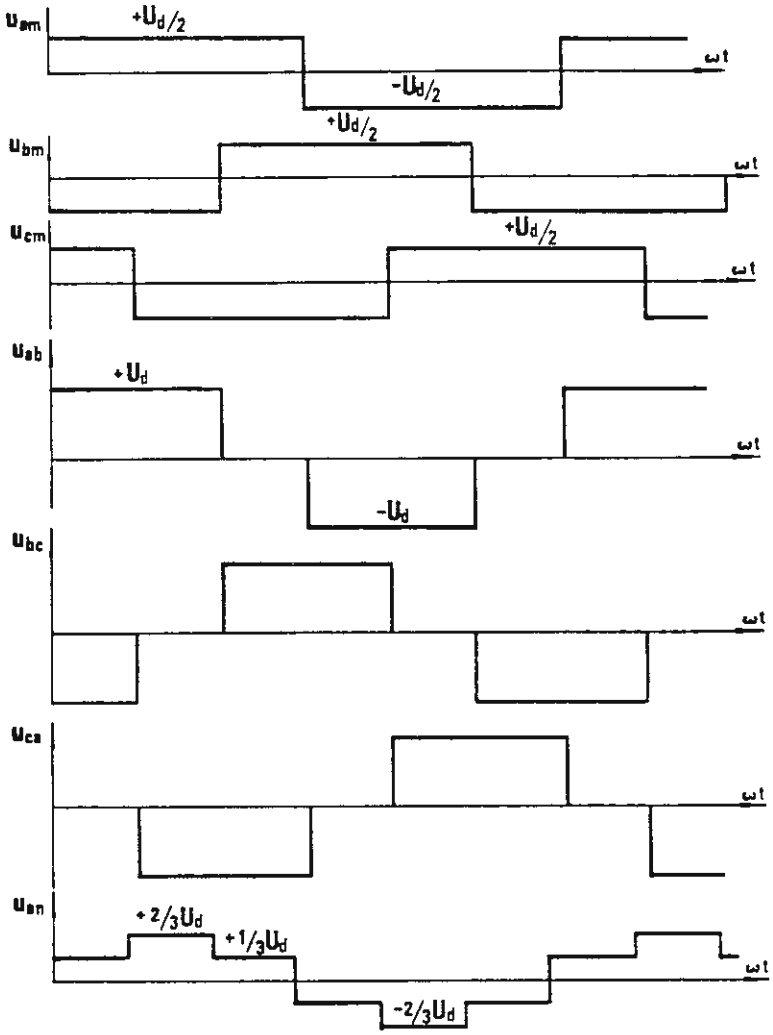

Figure 11-11 Voltages between the ac-phase terminals and the midpoint m, phase-to-phase voltages and phase voltage u_{an} at the valve side of the converter transformer. Forced-commutated voltage-source converter with square wave operation.

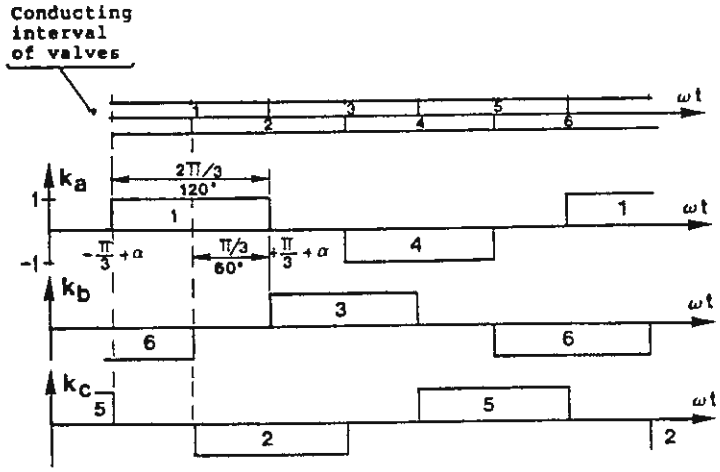

Figure 4-5 Conversion function at two-way six-pulse converter.

The wave-shape of the ac-voltages can for an arbitrary form of the convertor bridge voltage $U_d(t)$ be derived by multiplications of $u_d(t)$ by a conversion function.

A comparison between figure 11-11 and figure 4-5 shows that the conversion function from convertor bridge voltage to the ac-line-to-line voltage for the voltage-source square-wave convertor is the same as for the convertor current to the ac-current for a current- source convertor with zero angle of overlap.

We will thus obtain the following expression for the instanteous value of the line-to-line voltage on the valve side of the convertor transformer.

$$u_{ab} = \frac{2\sqrt{3}}{\pi} U_d \sum_{n=1}^{\infty} \pm \frac{\cos n\left(\omega t - \delta + \frac{\pi}{6}\right)}{n} \qquad (11\text{-}11)$$

where $n = 6\,m \pm 1$ and m is an integer 1, 2, 3, etc., and δ is the firing angle defined relative the source voltage.

It has here been assumed that the bridge voltage is a pure direct voltage U_d.

The following expression is derived for the phase voltage u_{an} as the conversion function is symmetric between the phases.

$$u_{an} = \frac{2}{\pi} \cdot U_d \sum_{n=1}^{\infty} \pm \frac{\cos n(\omega t - \delta)}{n} (-1)^m \qquad (11\text{-}12)$$

The complex r.m.s value of the fundamental voltage is obtained from equation (11-12):

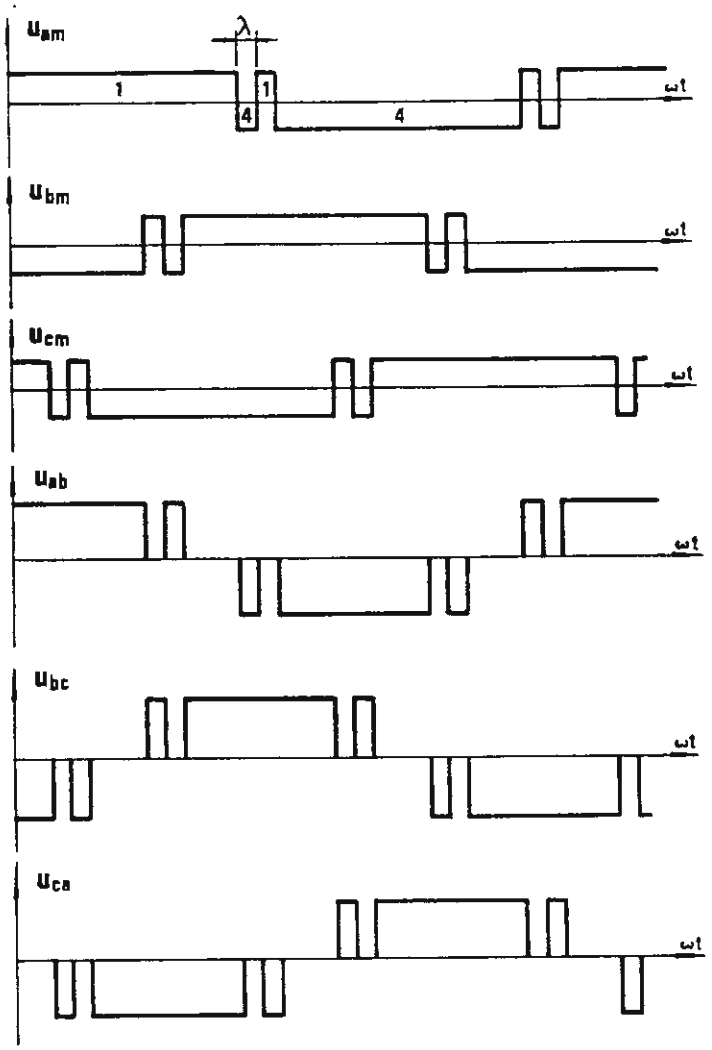

Figure 11-12 Phase-to-midpoint and phase-to-phase voltages on the valve side of the converter transformer. Voltage-source converter with end-pulse modulation.

$$U_{a(1)} = \frac{\sqrt{2}}{\pi} U_d \cdot e^{-j\delta} \qquad (11\text{-}13a)$$

The indeces (n) and (m) can be deleted, since the fundamental of the voltage between the terminal (a) and the neutral point n, u_{an}, is equal to the fundamental of the voltage between the terminals (a) and (m).

Equation (11-13a) can also be compared with equation (2-4), in which the notation U'_{L1} has been used instead of U_{a1}. The r.m.s value of the fundamental component of the phase-voltage on the valve side of the convertor transformer will, in the following, be denoted $U_{v(1)}$ i.e.,:

$$U_{v(1)} = \frac{\sqrt{2}}{\pi} U_d \cdot e^{-j\delta} \qquad (11\text{-}13b)$$

Pulse width modulation, PWM

The square-wave convertor, as described above, has the characteristic feature of having a fixed relationship between the voltage across the bridge and the ac-voltage on the valve side of the convertor transformer as described by equation (11-12). It was previously described how the similar relationship between the convertor current and the ac-current could be controlled by pulse-width modulation for the current-source convertor. A similar technique could be used for the voltage-source convertor, although this must not result in temporary short-circuits across the convertor bridge. A possible way of pulse-width modulation resulting in three times more commutations per cycle is illustrated in figure 11-12. As can be seen from the figure a single commutation from the bridge arm 1 ⇒ 4 is replaced

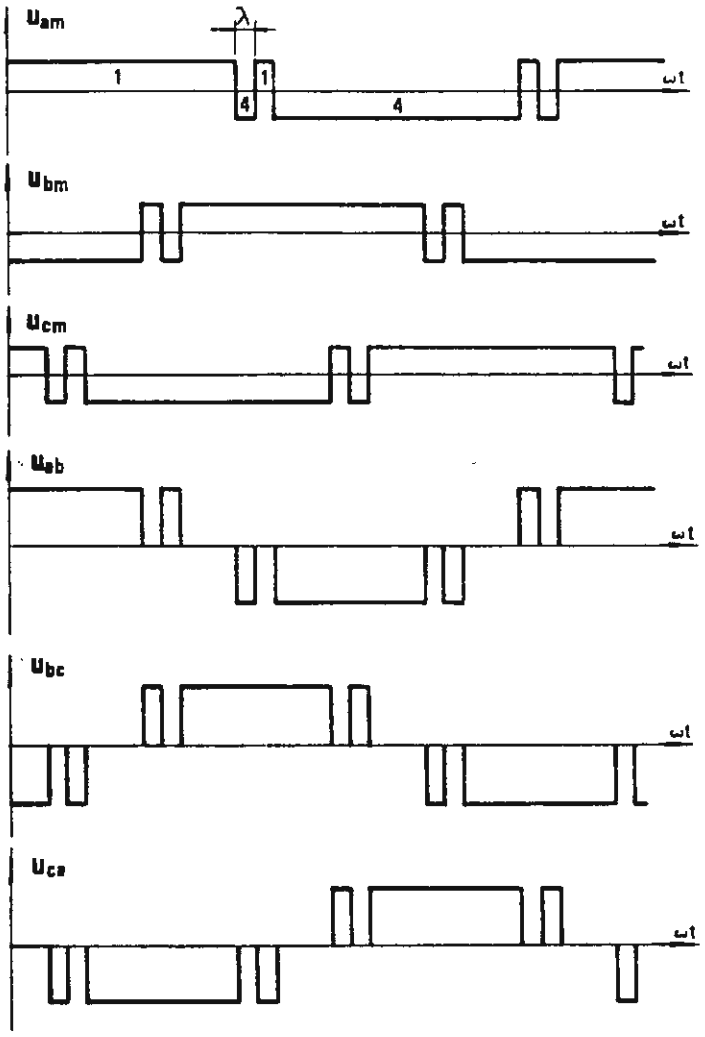

Figure 11-12 Phase-to-midpoint and phase-to-phase voltages on the valve side of the converter transformer. Voltage-source converter with end-pulse modulation.

here by two additional commutations, i.e., 1 ⇨ 4, 4 ⇨ 1 and 1 ⇨ 4. The distance between the additional commutations at the end of the conductive period has here been denoted with the angle λ. This type of pulse-width modulation is also called end-pulse modulation.

The pulse-width angle λ will determine both the amplitude of the fundamental and of the harmonics.

A Fourier expansion results in the following r m s values for the fundamental and harmonic components of the phase voltage on the valve side of the convertor transformer.

$$U_{v(n)} = \frac{\sqrt{2}}{\pi \cdot n} (2 \cos n\lambda - 1) \cdot U_d \qquad (11\text{-}14)$$

Harmonics will only be obtained for odd n, which are not multiples of three.

We will call the ratio between the fundamental at voltage components with modulation and without modulation the control ratio and denote it with k_λ, as for the previously treated current source convertor. Equation (11-14) then gives:

$$k_\lambda = 2\cos\lambda - 1 \qquad (11\text{-}15)$$

Equation (11-15) shows that k_λ will decrease fairly slowly with increased values of λ. Equation (11-14) shows that this type of modulations will decrease the magnitude of the harmonics for small values of λ, but increase them with a factor of up to three for larger values of λ.

The slow decrease of the control ratio k_λ and the fast increase of the magnitude of the harmonics with increased pulse-width angle makes this modulation methods less suitable, when the primary objective is to control the

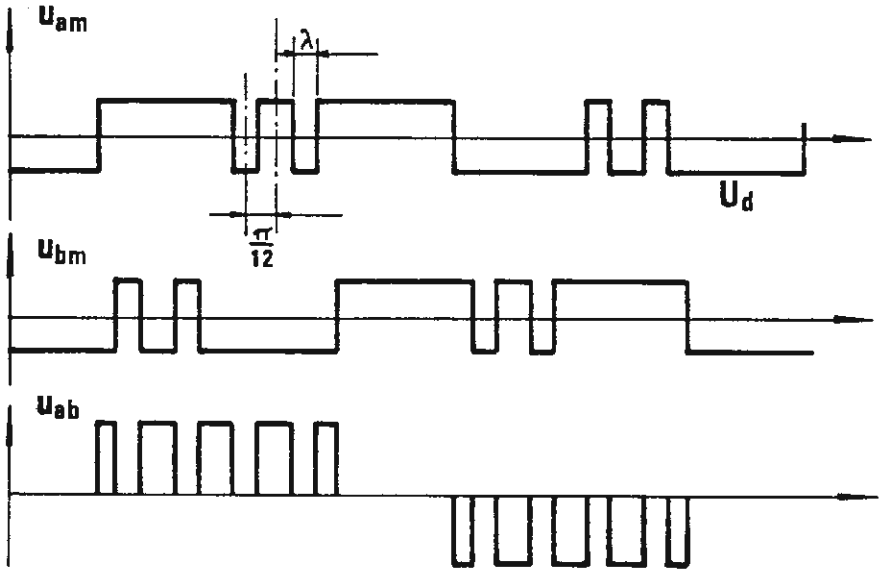

Figure 11-13 Phase-to-midpoint and phase-to-phase voltages on the valve side of the converter transformer. Voltage-source converter with centre-pulse modulation with two notches per half cycle.

ac-voltage amplitude.

Another modulation method with four additional commutations in the middle of the conductive period for the square-wave convertor seems to be more attractive. The modulation method, which is illustrated in figure 11-13, can be called centre-pulse modulation. A Fourier expansion result in the following r m s values of the phase voltages of order n:

$$U_{v(n)} = \frac{\sqrt{2}}{\pi \cdot n} \left(1 - 4 \cdot \cos(n \cdot \frac{\pi}{12}) \cdot \sin(n \frac{\lambda}{2})\right) \quad (11\text{-}16)$$

This results in the following expression for the control ratio:

$$k_\lambda = 1 - 4 \cdot \cos(\frac{\pi}{12}) \cdot \sin(\frac{\lambda}{2}) \quad (11\text{-}17)$$

A comparison between equations (11-16) and (11-14) shows that this modulation method has the advantage, as compared to the previous one, of being able to vary k_λ in the range 1 - 0.8 without getting a too high increase of harmonics of the order of $n \leq 13$.

However, the number of commutations have to be increased by a factor of five as compared to the square wave convertor, which will give additional losses in the thyristors and the snubber circuits and may turn out to make the circuit prohibitive for high power applications until better thyristors have been developed.

<u>The fundamental of the ac-current, active and reactive power</u>

Both, the voltage-source convertors of the square-wave type

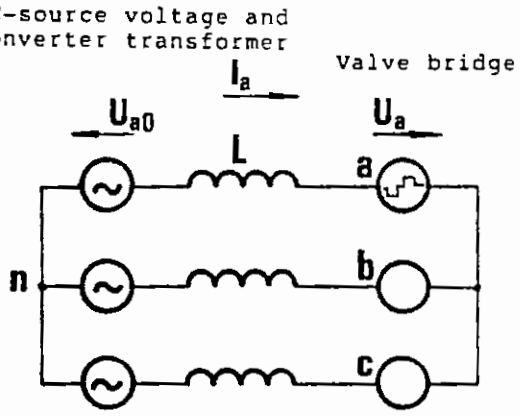

Figure 11-14 Equivalent circuit for a voltage source converter.

and the pulse-width modulated types treated above can be represented with the equivalent circuit, according to figure 11-14. The fundamental component of the stiff phase to neutral voltages is, for the square-wave convertor, determined by equation (11-13 a). For the pulse-width modulated convertors the ac-voltage on the bridge side has to be multiplied with the control ratio factor k_λ. This results in for phase (a):

$$I_{a(1)} = \frac{U_{oa} - \frac{\sqrt{2}}{\pi} \cdot k_\lambda \cdot U_d \cdot e^{-j\delta}}{j\omega L} \qquad (11\text{-}18)$$

Corresponding expressions are obtained for the other phases. It should be noted that the current can flow in both directions in a bridge arm with a firing pulse on the thyristor valve since diode valve is connected in parallel 1, which can conduct current in the reverse direction. The fundamental apparent power of the convertor in complex form is for a symmetrical system

$$P + jQ = 3\bar{U}_o \cdot \bar{I}_{(1)}^*$$

Insertion of $I_{(1)} = I_{a(1)}$, according to equation (11-18)

gives:

$$P+jQ = \frac{3\sqrt{2}}{\pi} \frac{U_d \cdot U_o \cdot k_\lambda}{\omega L} \sin\delta + j \frac{3U_0 \left(U_0 - \frac{\sqrt{2}}{\pi} U_d \cdot k_\lambda \cdot \cos\delta\right)}{\omega L}$$

(11-19)

It is usually convenient to express the power as a function of the phase-to-phase voltages, which, on the ac-line side, is denoted by U_{oh} and on the valve side by $U_{vh(1)}$. The r.m.s. value of the fundamental component of the phase-to-phase voltage on the valve side can be written as:

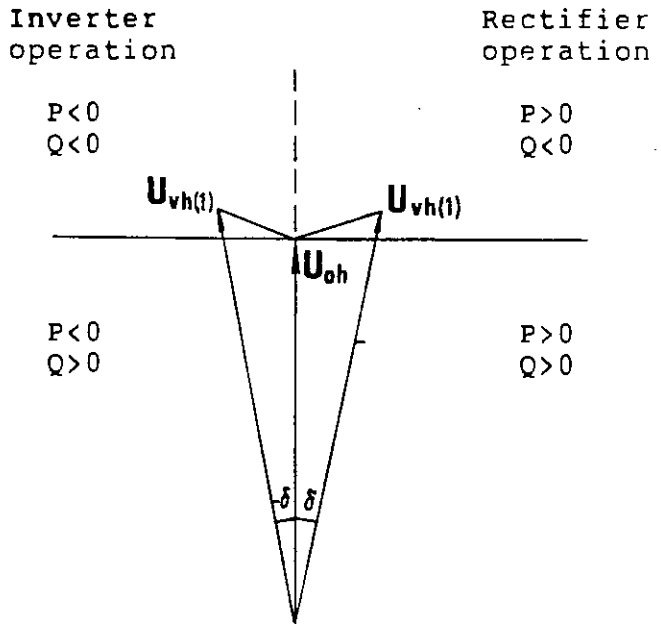

Figure 11-15 Phasor diagram for a forced-commutated voltage-source converter, according to the figures 11-10 and 11-14. Positive P and Q indicates absorption of active and reactive power from the ac-network. Phase-to-phase voltage on the ac-line side of the converter transformer, U_{Oh}, and on the valve side, $U_{vh(1)}$ (fundamental component).

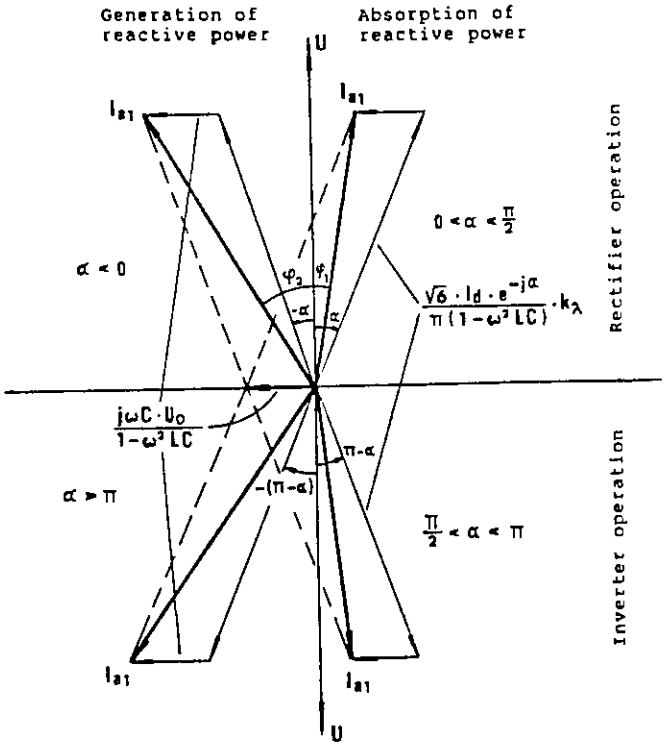

Figure 11-9 Phasor-diagram for fundamental components of the ac-currents of a forced-commutated current-source converter according to figure 11-6 and 11-8.

$$U_{vh1} = \frac{\sqrt{6} \cdot k_\lambda}{\pi} U_d \qquad (11\text{-}20)$$

Insertion of U_{vh1} in equation (11-19) results in:

$$P+jQ_{(1)} = \frac{U_{oh} \cdot U_{vh(1)} \cdot \sin\delta}{\omega L} + j \frac{U_{oh}\left(U_{oh} - U_{vh(1)} \cdot \cos\delta\right)}{\omega L} \qquad (11\text{-}21)$$

The direct current of the convertor bridge I_d can now be determined from equation (11-20) and (11-21) since
$P = U_d \cdot I_d$

$$I_d = \frac{\sqrt{6} \cdot k_\lambda \cdot U_{oh}}{\pi \quad \omega L} \sin\delta \qquad (11\text{-}22)$$

Equation (11-21) corresponds to equation (1-3) for the apparent fundamental power fed to an ac-line according to figure 1-3. The voltage at the feeding end U_a corresponds to U_{oh} and the voltage at the receiving end U_b to $U_{vh(1)}$, which is phase-displaced by the angle δ relative the voltage in the feeding (sending) end.

The equation can also be represented in a phasor diagram as shown in figure 11-15. Equation (11-21) and the phasor diagram illustrate, that the active power mainly is determined by the control angle δ, while the reactive power is determined by the difference in voltages $(U_{oh} - U_{vh(1)} \cdot \cos\delta)$.

A comparison between the phasor diagram 11-15 for the voltage-source convertor and the phasor diagram figure 11-9 for the current-source convertor shows that the voltage-source convertor offers certain advantages with regard to the control of reactive power. The reactive power for the voltage-source convertor is mainly determined by the magnitude of the voltage $U_{vh(1)}$, which at a fixed direct voltage can be controlled with the control ratio

factor k_λ, if pulse-width modulation, is applied, or by the tap-changer setting. This is similar to the control of reactive power for a synchronous machine, in which the reactive power is controlled by the magnitization of the machine.

The reactive power to the current-source convertor is controlled by the delay-angle α and is proportional to the direct current. However, as the direct voltage is also proportional to $\cos \alpha \cdot k_\lambda$ the freedom to change α is limited. The control of the reactive power for a current-source convertor might especially be critical at low values of the direct current as previously mentioned.

However, the control of reactive power is for both the voltage-source and the current-source convertor much easier, if the convertor is only utilized for the control of reactive power, i. e. for static var applications. The voltage-source convertor is then operated at $\delta = 0°$ and the current-source convertor at $\alpha = 90°$. The reactive power can then be controlled with the direct voltage for the voltage-source convertor and with the direct current for the current-source convertor.

Current harmonics from the square wave convertor

The harmonics in the ac-phase currents can easily be determined, when the harmonics of the phase-voltages on the valve side of the convertor transformer are given, since the line side voltage is pure sinusoidal voltage. For the square-wave convertor the phase voltage is given by equation 11-12, where n is an odd number not divisable by three i.e., n= 1, 5, 7, 11, 13 etc. This results in the following equation for the r m s values of the harmonic currents of the order n:

$$I_{(n)} = \frac{\sqrt{2} \cdot U_d}{\pi \cdot n^2 \cdot \omega_1 L} \qquad (11\text{-}23)$$

The magnitude of the harmonic current will thus only be determined by the inductance of the transformer and is independent from the actual load, which is in contrast to the situation for a current-source convertor.

We will get the following expression for the relative short-circuit voltage of the transformer, if we denote the r.m.s value of the phase-current at rated operation by I_{rmsN} and the rated phase-voltage on the line side by U_{oN}

$$e_k = \frac{I_{rmsN} \cdot \omega_1 L}{U_{oN}} \qquad (11\text{-}24)$$

Setting $U_{oN} = U_{v1}$ and using the relationships, according to equations (11-13b) and (11-24) in equation (11-23) gives:

$$I_n = \frac{I_{rmsN}}{e_k \cdot n^2} \qquad (11\text{-}25)$$

For a line-commutated current-source convertor we will get the corresponding equation by using equations (6-1), (6-6), (4-21b) and (4-33c), which give

$$I_n \approx \frac{3}{\pi} \cdot \frac{K_n}{n} \cdot I_{rms} \qquad (11\text{-}26)$$

If we assume that $e_k = 0.12$ for the current-source convertor, we will, at the rated operation for the 5th and 11th harmonic, get $K_5 = 0.91$ and $K_{11} = 0.62$. A comparison between the magnitude of the harmonic currents for the voltage-source square-wave convertor according to equation (11-25) with the line-commutated current-source convertor according to equation (11-26) shows thus, that the magnitudes of the 5th and the 11th harmonic currents will

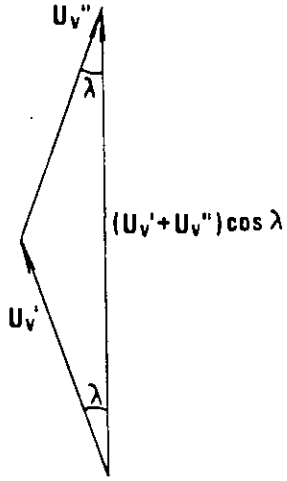

Figure 11-16 Superposition of the ac-voltages from two phase-displaced square-wave voltage source converters.

be 92% and 28 % higher respectively for the voltage-source convertor. This indicates that it might be favourable to choose a higher e_k than 12% for the voltage-source square-wave convertor.

The magnitude of the harmonics can also be decreased if pulse-modulation is used. However, it should be noted that it is not usually possible to reduce the harmonics and control the fundamental voltage component by pulse-width modulation. Pulse-width modulation, as described above, will also increase the number of commutations and by that the valve losses.

Cooperation between two square-wave voltage source converters

The generation of the 5th and 7th harmonic to the ac-network can be drastically reduced by a twelve-pulse connection in a similar way as for line-commutated convertors. The line windings might then be connected in series to avoid high 5th and 7th harmonic currents in the transformer. This connection is often used for low voltage applications with low e_k-values.

The application of two square-wave convertors will alternatively make it possible to continuously control the factor k_λ without increasing the commutation number. If the convertor circuit is arranged so that each convertor is fed with equally large direct voltages U_d and one of the convertor is fired 2λ rad before the other convertor, we will get the total added internal ac-voltage on the valve side to (See figure 11-16) be:

$$U_{v1} = 2 \cdot \frac{\sqrt{2}}{\pi} \cdot \cos \lambda \cdot U_d \qquad (11\text{-}27a)$$

Using equation (11-12) we get the following equation for

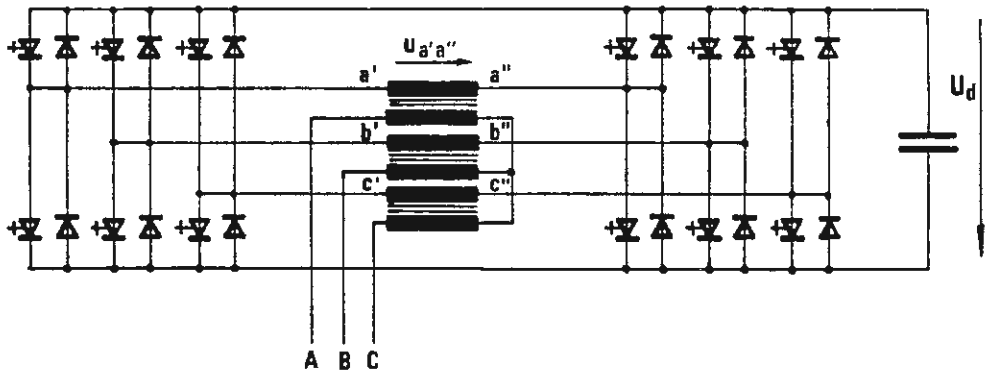

Figure 11-17 Two square-wave converters with phase-shift control.

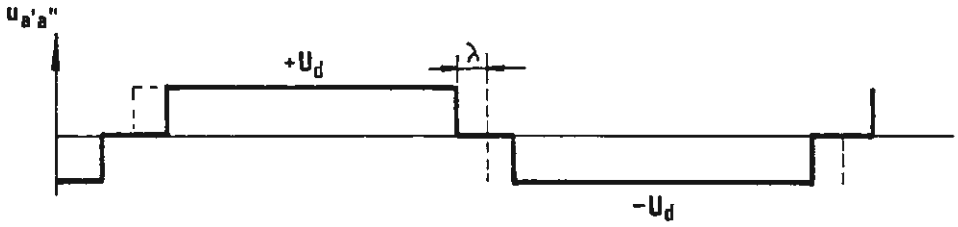

Figure 11-18 Wave-shape of the phase voltage on the valve side of the converter transformer for two phase shifted square-wave converters connected to the same direct voltage Ud.

the voltage harmonics of order n:

$$U_{v(n)} = \frac{2\sqrt{2}}{\pi \cdot n} \cdot \cos(n \cdot \lambda) \cdot U_d \qquad 11\text{-}27b)$$

We find from equation (11-27a), that the expression for the control ratio for the fundamental voltage will be:

$$k_\lambda = \cos \lambda \qquad (11\text{-}28)$$

From equations (11-27b) and (11-27a) we get the following ratio between the harmonic voltages and the fundamental voltage:

$$\frac{U_{vn}}{U_{v1}} = \frac{\cos n\lambda}{n \cdot \cos \lambda} \qquad (11\text{-}29)$$

A value of $\lambda = 15°$ will, for instance, result in a reduction of the magnitudes of the 5th and the 7th harmonic to 27 % of the values valid for a square wave convertor.

Figure 11-17 shows an example of a convertor circuit working according to this principle. This circuit consists of two convertor bridges, which are connected in parallel on the dc-side. The voltage in each ac-phase is determined by the sum of or the difference between the voltages from two bridges depending on the definition of positive voltage directions. The phase voltage between the terminals a' and a" on the valve side is illustrated in figure 11-18. The magnitude of the fundamental component as well as the harmonic components are given by equations (11-27a) and (11-27b). It should be noted, that the phase-voltage also contains odd harmonics, which are multiples of three e.g. 3, 9, 15 etc., which not will appear in the phase-to-neutral voltage of the square wave convertor. The line windings must because of that not be connected in Δ in order to avoid high 3rd harmonic currents in the

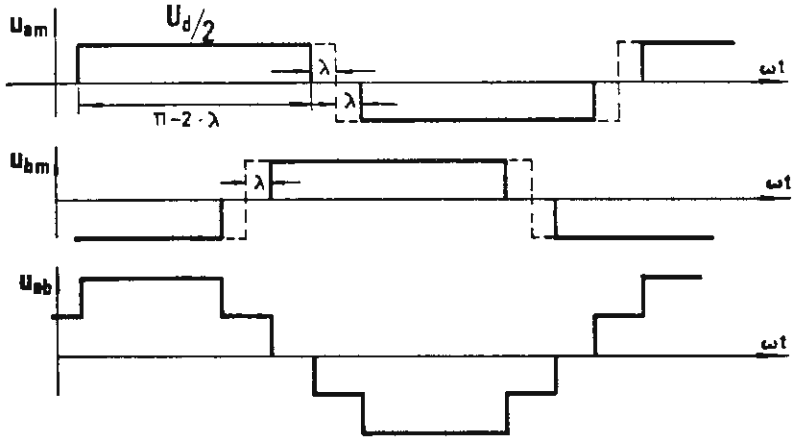

Figure 11-20 Phase-to-midpoint voltages u_{am} and u_{bm} and phase-to-phase voltage u_{ab} on the valve side of the converter transformer for the NPC circuit according to figure 11-19.

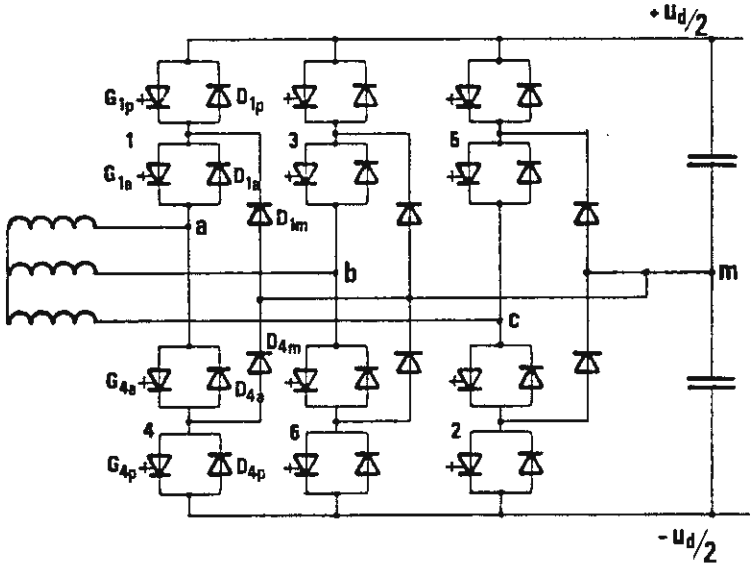

Figure 11-19 Forced-commutated voltage-source converter with a bridge connection to the midpoint (neutral point) of the dc-bridge (Neutral Point Clamping, NPC).

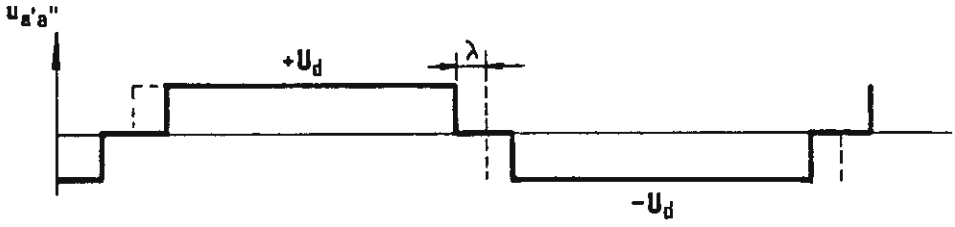

Figure 11-18 Wave-shape of the phase voltage on the valve side of the converter transformer for two phase shifted square-wave converters connected to the same direct voltage Ud.

transformer, or the neutral of a Y-connected windings must not be directly grounded, as the 3rd harmonics will otherwise be transmitted to the ac-network. These limitations make a twelve pulse connection by this convertor circuit in order to cancel 6-pulse harmonics (n = 5, 7, 17 and 19), fairly complicated.

NPC-converter

The convertor circuit shown in figure 11-19 offers an interesting alternative to the circuit with two phase shifted square wave convertors, since it in many respects results in equal performance. The convertor circuit is called NPC convertor (Neutral Point Clamping), as the valve bridge via the six additional diodes is connected to the midpoint or neutral point of the bridge. It is also refered to as a three level converter as the phases can be connected to three voltage levels.

The voltages between the phase terminals of the bridge and the midpoint can, because of the diodes, be controlled to the values $\pm U_d/2$ and 0 as shown in figure 11-20. Phase a is connected to the positive pole of the bridge, when the valves $G_{1p} + G_{1a}$ or $D_{1p} + D_{1a}$ are conducting. Phase a will obtain the same potential as the midpoint, when both valves G_{1a} and G_{4a} are turned on. Valve G_{1p} has to be turned-off before the valve G_{4a} is turned on. Valve G_{1a} is turned-off before valve G_{4p} is turned-on since this will provide the terminal (a) with the same potential as the negative pole of the bridge.

A comparison between the figures 11-18 and 11-20 shows, that the voltage between the ac-terminals of the bridge and the midpoint of the bridge for the NPC convertor will have the same wave-shape as the phase-voltages for the phase-shifted convertor. However, since the harmonic voltages, being multiples of three in the three phases,

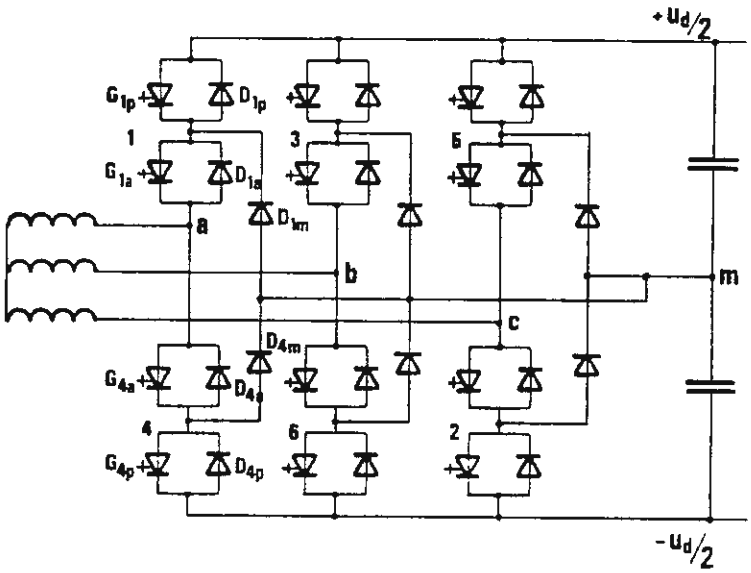

Figure 11-19 Forced-commutated voltage-source converter with a bridge connection to the midpoint (neutral point) of the dc-bridge (Neutral Point Clamping, NPC).

will be in phase, these voltage harmonics will also appear at the neutral point of the transformer but not in the phase-to-neutral voltages. It is, because of that, possible to connect the windings on the valve side in either Y or Δ and to ground the neutral point on the line side, which is often desirable when the convertor is connected to high voltage ac-networks.

The valve arrangement for the NPC convertor might seem to be more expensive than for the square-wave convertor. However, it should be noted, that it is only the six additional diode valves that gives additional costs. The series connection of the thyristor valves (GTO) will reduce the voltage per valve to half of the bridge voltage. This fact has been used to increase the bridge voltage for low voltage applications without having to connect any GTO thyristors in series in the individual valves as shown in figure 11-19.

Harmonic bridge currents

The convertor bridge current will, besides the direct current component, also contain harmonic current components. The order of the harmonics will be multiplied by the pulse-number for a six-pulse convertor i.e., 6, 12, 18 etc. The magnitude of the harmonic currents is proportional to the ac-current and can be obtained by multiplying each phase-current with a conversion function and adding up the contribution from the three phases, as described by the following equation

$$i_d(t) = i_a(t) \cdot k_a(t) + i_b(t) \cdot k_b(t) + i_c(t) \cdot k_c(t) \qquad (11\text{-}29)$$

The conversion function $k_a(t)$ is equal to one when the bridge arm between phase a and the positive terminal of the bridge is conducting and equal to zero when the other

bridge arm is conducting. Equation (11-29), for the voltage-source convertor can be compared with equation (4-4) for the line-commutated current-source convertor with the angle of overlap equal to zero.

The previous analysis of the operation of the voltage-source convertor was based on the assumption that the bridge voltage was completely smoothed and equal to U_d. To obtain this it is essential that the bridge current $i_d(t)$ meets a low impedance for the harmonics generated. This could be obtained either with a large capacitor on the dc-side or a capacitor combined with some filters giving low impedances for the dominating harmonics, e.g., 6, 12, 18 and 24 for a six-pulse convertor or 12 and 24 for a twelve pulse convertor. The advantages of using tuned filter are, that this will probably be less expensive since the total capacitance will be smaller and the inductances will limit the high fault currents, which could be critical for voltage-source convertors.

11.4 Future use of forced-commutated convertors for HVDC and SVC

The previously presented survey of different types of forced-commutated convertors of both the current-source type and the voltage-source type has shown that forced-commutated convertors can offer both possibilities and difficulties when used for HVDC and SVC applications. However, it is to be expected that only forced-commutated convertors based on the application of valves having current turning-off capability will offer sufficient advantages to be of interest.

The voltage-source convertors seem to offer greater flexibility with regard to the control of reactive power and also seem to be more suitable with regard to cooperation with the ac-network since they, in many ways, behave like synchronous machines. The major advantage with

the current-source convertor is that the dc-smoothing reactor in the dc-circuit makes it more easy to limit fault currents on the dc-side and that it is easier to control the voltage on the dc-side to zero. Both features are essential for HVDC transmission systems with overhead lines.

It is to be expected that the first applications for HVDC applications will be for back-to-back stations, cable transmission and small inverter terminal schemes, on multiterminal schemes for which the voltage-source convertor seems to offer the greatest advantages. The decreased risk for commutation failures and the possibility of operating at extremely weak ac-systems will be essential factors here besides the possibility of controlling the reactive power and by that the ac-voltage.

The expected advantages for SVC applications are mainly the possibility for fast control, the ability to both generate and absorb reactive power with the same equipment, and the possibility to generate reactive power without connection of large capacitor banks. As described earlier in chapter 5 installation of capacitor banks, which are too large, can result in a resonance frequency too low in the ac-system.

Small SVC installations based upon the use of, both, phase-shifted and NPC-connected forced-commutated voltage-source convertors are already in operation. However, further improvements in the thyristor technology are still needed, until solutions can be offered, which are competitive with regard to cost and losses with the conventional technique using thyristor switched capacitors and thyristor controlled reactors.